ASEAN-USAID
Buildings Energy Conservation Project
FINAL REPORT

VOLUME II: TECHNOLOGY

Series Editors: M.D. Levine and J.F. Busch
Editor: J.F. Busch

Energy Analysis Program
Energy and Environment Division

June 1992

Association of
South East Asian Nations

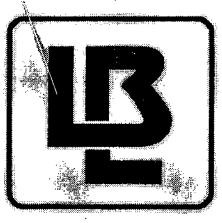

Lawrence Berkeley
Laboratory

DISCLAIMER

LBL-32380
Vol. II
UC-350

ASEAN-USAID
Buildings Energy Conservation Project
FINAL REPORT

VOLUME II: TECHNOLOGY

Series Editors: M.D. Levine and J.F. Busch
Editor: J.F. Busch

June 1992

Association of
South East Asian Nations

Secretariat:
Jakarta, Indonesia

Energy Analysis Program
Energy and Environment Division
Lawrence Berkeley Laboratory
University of California
Berkeley, CA 94720 USA

This work was supported by the U.S. Agency for International Development through the U.S. Department of Energy under Contract No. DE-AC03-76SF00098.

Table of Contents

PREFACE

THE ASEAN-USAID BUILDINGS ENERGY CONSERVATION PROJECT

Technology is the second in a series of three volumes that culminate an eight-year effort to promote building energy efficiency in five of the six members of the Association of Southeast Asian Nations (ASEAN). The Buildings Energy Conservation Project was one of three energy-related sub-projects sponsored by the United States Agency for International Development (USAID) as a result of the Fourth ASEAN-US Dialogue on Development Cooperation in March 1982. It was conceived as a broad and integrated approach to the problem of bringing about cost-effective energy conservation in Indonesia, Malaysia, the Philippines, Singapore, and Thailand (Brunei was the one ASEAN member nation that did not participate).

This volume is a compilation of papers that report on specific energy efficiency technologies in the ASEAN environment. Further findings of the ASEAN-USAID Project are collected in the remaining two volumes of this series, which cover the following topics in depth:

- Volume I - *Energy Standards*, summarizes intensive efforts that have resulted in new commercial building standard proposals for four ASEAN countries and revision of the existing Singapore standard.
- Volume IV - *Audits* presents the results of audits that were performed on a large sample of ASEAN commercial buildings. This information was used to create an ASEAN-wide energy use database. The research was largely conducted by ASEAN analysts and professionals in local universities and government institutions.

PROJECT PHILOSOPHY AND CONTEXT

Underlying every aspect of the ASEAN-USAID Buildings Energy Conservation Project was a recognition that there were significant social, economic, and environmental benefits to be gained through enhanced energy efficiency. For the ASEAN nations, as for developing countries all over the world, the processes of modernization and industrialization have been accompanied by rapid growth in energy consumption. In the ASEAN region, commercial energy consumption grew from 27 to 85 million tons of oil equivalent (Mtoe), a factor of 3.15, during the period from 1970 to 1987. Electricity consumption increased from 20 to 101 billion kilowatt hours (kWh), or by a factor of five. Both growth rates were substantially in excess of the growth of economic productivity in the region; gross domestic product (GDP) increased by a factor of 2.5 during the same period.

While energy consumption has traditionally been regarded, and encouraged, as a vital input and stimulant of economic growth, the experiences of many of the industrialized nations recently have demonstrated the potential for decoupling economic growth rates from energy consumption growth rates. The benefits of this decoupling in an era of expensive energy sources, limited financial and natural resources, and critical global and local environmental stresses are also increasingly recognized. By supporting efforts toward improved energy efficiency through the ASEAN-USAID Project, the larger hope was to realize the potential for:

- Reduced growth of electricity demand to free capital for other uses, while avoiding the environmental externalities associated with power generation,
- Lower oil imports for many ASEAN countries to reduce balance of payments problems, and
- Money saved on electricity bills to be put to more productive uses.

The ASEAN-USAID Project targeted energy conservation in buildings because growth of electricity consumption in this sector has been particularly rapid throughout the region. In 1970, residential buildings in ASEAN consumed approximately 3.5 billion kWh and commercial buildings, 4.3 billion kWh. By 1987, these figures had grown to 22 billion kWh and 23 billion kWh, respectively. Thus, buildings in ASEAN—residential and commercial—currently make up 45% of the demand for electricity in the region. Their consumption has grown almost six-fold during this 17-year period, or at an annual rate of 10.9%.*

One of the immediate implications of increasing energy consumption is financial expense. The total annual cost of electricity for buildings in ASEAN (45 billion kWh) is about $4 billion (U.S.), and if industrial buildings, self-generation, and "public consumption" are counted, the total annual bill may be as high as $5 billion (U.S.). Since electricity consumption in buildings has grown rapidly and is likely to continue to do so, utility costs in the sector are likely to increase markedly over time. Because buildings represent such a significant fraction of electricity consumption in the region, they represent an important target sector for national efforts aimed at reaping the economic and environmental benefits of increased energy efficiency.

The ASEAN-USAID Project focussed on commercial buildings because of the magnitude of potential savings in this energy use sector. As described in greater detail elsewhere in this series, the potential for electricity savings in commercial buildings is significant:

- 10% savings achievable in the near term,
- 20% savings achievable in the intermediate term (5 to 10 years), and
- 40% or more savings achievable in the longer term.

A 10% reduction in commercial building energy use in ASEAN represents $200 million (U.S.) savings in fuel bills per year. Deducting the costs of investments needed to achieve these savings yields net annual savings to ASEAN of $100 to $150 million (U.S.).

A BRIEF HISTORY OF THE ASEAN-USAID BUILDINGS ENERGY CONSERVATION PROJECT

The first phase of the Project was initiated in 1982 with a collaboration by U.S. researchers at Lawrence Berkeley Laboratory (LBL) and the Singapore government. This first effort had several purposes, namely:

- to transfer to Singapore a computer code (DOE-2) to analyze the energy performance of buildings,
- to analyze measures to increase the energy efficiency of buildings in Singapore,
- to use the analysis results to extend and enhance Singapore's standards on energy efficiency in buildings, and
- to establish a process whereby the other ASEAN members can benefit from the experience in Singapore, including the use of DOE-2, the analysis to support energy standards, and the process of adapting and implementing building energy standards.

Detailed results of this first phase were presented at a conference in Singapore in May 1984. The proceedings from this conference are available in a separately bound volume. They include

* Indeed, these consumption estimates underestimate the actual electricity demand attributable to buildings for at least three reasons: (1) a sizeable portion of industrial electricity consumption is for building services, (2) electricity generated on site, either as backup power or for normal use, is counted as self-production even if it is used in buildings, and (3) the category "public electricity consumption" may include considerable use of electricity in buildings. Thus, it is likely that buildings in ASEAN account for considerably more than 45% of total electricity demand—probably in the range of 55 to 60%.

technical studies supporting recommended overall thermal transfer value (OTTV) refinements as well as energy performance simulation results, descriptions of existing energy conservation activities within ASEAN, and papers on several topics related to energy conservation in commercial buildings.

With the initiation of a second phase in 1985, the focus of the ASEAN-USAID Project was expanded to include the other participating ASEAN nations. Its purpose remained to promote the development and implementation of policies to improve the energy efficiency of commercial buildings. In pursuit of this goal, the Project funded 22 different research sub-projects within the five participating ASEAN countries. The current series represents a compilation and synthesis of several of the many research papers that grew out of the overall Project.

Since its inception, the ASEAN-USAID Project has provided training to ASEAN participants, supported research projects throughout ASEAN, conducted research at LBL, and engaged U.S. consultants to work with ASEAN governments and private sector participants to design programs and policies. Within the Project, a key policy focus has been the application of technical tools to the development and assessment of efficiency standards and guidelines. The Project has stressed training (especially in computer simulation of building energy use and energy auditing) and the enhancement of research and development capabilities in ASEAN. Much of the data gathering, analysis, and research activity conducted under Project auspices was directed toward the eventual implementation of energy efficiency standards for ASEAN commercial buildings.

CHAPTER 1: INTRODUCTION

This volume reports on research in the area of energy conservation technology applied to commercial buildings in the Association of Southeast Asian Nations (ASEAN) region. Unlike Volume I of this series, this volume is a compilation of original technical papers prepared by different authors in the project. In this regard, this volume is much like a technical journal.

The papers that follow report on research conducted by both U.S. and ASEAN researchers. The authors from within the ASEAN region, representing Indonesia, Malaysia, Philippines, and Thailand, come from a range of positions in the energy arena, including government energy agencies, electric utilities, and universities. As such, they account for a wide range of perspectives on energy problems and the role that technology can play in solving them.

This volume is about using energy more intelligently. In some cases, the effort is towards the use of more advanced technologies, such as low-emittance coatings on window glass, thermal energy storage, or cogeneration. In others, the emphasis is towards reclaiming traditional techniques for rendering energy services, but in new contexts such as lighting office buildings with natural light, or cooling buildings of all types with natural ventilation.

Used in its broadest sense, the term "technology" encompasses all of the topics addressed in this volume. Along with the more customary associations of technology, such as advanced materials and equipment and the analysis of their performance, this volume treats design concepts and techniques, analysis of "secondary" impacts from applying technologies (i.e., unintended impacts, or impacts on parties not directly involved in the purchase and use of the technology), and the collection of primary data used for conducting technical analyses.

The papers that follow cover a broad range of technologies, impacts, and approaches. Chapter 2, authored by Busch, compares the subjective responses of Thai office workers to the thermal conditions of air-conditioned and naturally ventilated spaces. In Chapter 3, Bauman *et al.*, use wind tunnel experiments to analyze the natural ventilation potential of various building geometries in densely settled urban areas. In Chapter 4, Boon-Long *et al.*, use the ESP building energy simulation model to estimate how effectively thermal comfort can be achieved through natural ventilation in typical small public buildings found in the provinces of Thailand. In Chapter 5, Soegijanto *et al.*, describe an effort to compile and measure general weather data, including solar radiation data, in Indonesia for use in energy analysis. Busch in Chapter 6 performed a parametric energy simulation exercise using the DOE-2 model, comparing the energy and economic performance of prototypical office, hotel, and retail buildings in Thailand. Chapter 7, by Sullivan *et al.*, looks at the effect of fenestration characteristics on the energy use of offices in Singapore. Huang *et al.*, in Chapter 8, develop regression equations, based on DOE-2 simulations, for predicting the savings from daylighting offices in Singapore. In Chapter 9, Busch and Warren analyze air-conditioning systems of varying types and configurations under different operating conditions for the Malaysian climate. In Chapter 10, Soriano studies the feasibility of cogeneration technology applied to Philippine hotels and hospitals. Wyatt, in Chapter 11, assesses the economics of applying thermal storage technology in office buildings in each of the ASEAN countries using current electricity tariffs. In the final chapter, Sairan and Azit evaluate the (hypothetical) use of thermal storage technology in the office sector from the point of view of the Malaysian electric utility.

J.F. Busch
Berkeley, CA USA
June 24, 1992

CHAPTER 2: THERMAL RESPONSES TO THE THAI OFFICE ENVIRONMENT

J.F. Busch
Energy Analysis Program
Applied Science Division
Lawrence Berkeley Laboratory
Berkeley, CA 94720 USA

ABSTRACT

This paper reports on a field study of over 1100 Thai office workers in which a questionnaire survey and simultaneous physical measurements were taken. Both air-conditioned and non-air-conditioned buildings were included. The data are compared to those from other field studies from both temperate and tropical climates. We analyzed Thai subjective responses on the ASHRAE, McIntyre, and other rating scales, relating them to Effective Temperature, demographics, and to rational indices of warmth, such as PMV and TSENS. Selected results are as follows: the neutral temperature of the whole sample was 25 °C and in rough agreement with several empirical model predictions; the ASHRAE Scale category widths determined through probit analysis exceed by several degrees previously published findings; and Thai conditions of thermal acceptability exist over a broad range of Effective Temperature, from 22 to 30.5 °C, pushing the summer comfort zone outwards by 4 °C. These findings suggest that without sacrificing comfort, significant energy conservation opportunities exist through the relaxation of upper space temperature limits.

INTRODUCTION

To date the majority of studies of human response to the thermal environment in building interiors have been carried out in the temperate climates of industrialized countries. In this paper, findings of a field study of thermal comfort in offices in Bangkok, Thailand, are presented. The field study is part of a larger study of energy conservation potential in Thai commercial buildings.

It is important to examine thermal comfort in the context of tropical developing countries because of the concentration of world population and growth there. Currently, air-conditioned buildings in the tropics and elsewhere are designed according to criteria based on comfort studies of white, male, college-age respondents from the West. Because the conditions of race, age distribution, climatic experience, and perhaps expectation are so different in most developing countries, these criteria may be inappropriate. Specifically, there may be opportunities to save energy and capital investment in air-conditioning equipment should there be a preference for or higher tolerance of thermal environmental factors, such as temperature, humidity, and airflow.

The objectives here are to place the data collected in Thai offices in context by comparison with results of other researchers, particularly those from tropical countries, and to contrast the results from different subgroupings of the data, such as between seasons, between conditioned and un-conditioned buildings, between men and women, and other comparisons where appropriate. Ultimately, the goal of this thermal comfort research is to define the limits of tolerance or acceptability of conditions for the purpose of determining energy conservation potential in buildings. The rest of the paper contains a section on the methods used for gathering and processing the data, followed by discussion of the results, conclusions, and recommendations for future work.

METHODOLOGY

In the following section we describe the buildings and how we chose them. We then discuss our methods for conducting the field survey and carrying out the analysis.

Building Selection

The criteria for selecting buildings for the field study were as follows:

1. Located in Bangkok, the capital city of Thailand, where the majority of commercial buildings are;
2. Modern buildings not more than ten years old;
3. Both air-conditioned (AC) and non-air-conditioned (non-AC) or naturally ventilated (NV) buildings;
4. Regular office desk work of a majority of the building occupants;
5. A variety of ages and sexes.

Building Descriptions

The two air-conditioned buildings are of modern high-rise design. One is a head office for a bank; the other is a multiple-client building. The two naturally ventilated buildings are contemporary medium-rise government buildings housing ministerial and departmental offices. All buildings are located within ten kilometers of one another in downtown Bangkok.

Data Collection

Thailand experiences three distinct seasons in a year. The studies reported in this paper were carried out in each of two seasons: during the hot season (in April) and the wet season (in July) of 1988. Each of the four buildings mentioned above were visited in both seasons. Data were typically collected over one work-week at each site per season.

Questionnaire:

The questionnaire consisted of a section of subjective ratings on a variety of thermal scales, followed by a section on recent food and beverage consumption, then separate clothing lists for men and women, and concluded with a section on demographic factors. Subjective ratings employed the seven-point ASHRAE Thermal Sensation Scale shown in Figure 2-1. Respondents were asked to mark the scale at any one of the seven points or the mid-points in between them (i.e., at any "tick mark"). Another seven-point scale, the Bedford Scale, was not used in this study because, though semantically different from the ASHRAE Scale, earlier studies using both produced similar results. The respondents were also asked the question, "I would like to be ..... warmer (1), no change (0), cooler (-1)", otherwise known as the three-point McIntyre Scale. Two further seven-point scales specifically addressing perceptions of airflow and humidity conditions were also used. The questionnaire was translated into the Thai language and scrutinized for semantic accuracy by Thai social scientists with facility in both English and Thai.

Physical Measurements:

The measured quantities were dry-bulb temperature, relative humidity, globe temperature, and air velocity. The globe thermometer was fashioned from a thermister and a 38-milimeter diameter ping pong ball painted flat grey. The dry-bulb thermister was shielded by a cylinder of reflective foil. Air velocity was measured with a hot-wire anemometer. All readings were gathered using a datalogger that stored ten-second readings on magnetic tape. The datalogger, tape recorder, and battery (for the hot-wire anemometer) were all contained within, and the temperature and humidity sensors were attached to a wooden box with a handle, similar in size and shape to a standard tool box (see Figure 2-2). The hot-wire anemometer was detached from the "tool box," but connected by a two-meter cord. As is evident from Figure 2-2, the sensors were attached vertically to maximize exposure to room air and far enough apart to minimize interference with each other. Data for outdoor weather conditions were gathered from measurements made in the city center by the Royal Thai Meteorological Department.

Conduct of the Survey

Teams of two or three typically carried out the survey, with one member taking the physical measurements and one or two handing out and collecting the questionnaire survey forms. The latter would approach prospective respondents and ask if they had been seated at that spot for at least 15 minutes. Those who replied affirmatively received the form; the others did not. The questionnaire came with a cover letter explaining the project and the auspices under which it was being carried out, along with general directions for filling out the form. Confidentiality was confirmed and disclosure of respondent's name was optional. An attempt to avoid gathering multiple responses from the same individual in a given season, but there was no corresponding effort to exclude people from participating in both seasons. Survey teams sought the participation from a roughly equal proportion of men and women in a range of age and job positions and, to the extent possible, those from different zones and floors of each building.

Measurements of the thermal environment were taken at each workstation following, or in some cases during, the completion of the questionnaire survey form, but usually within five minutes of one another. The "tool box" was placed on or very near the desk where the respondent was seated for at least one minute prior to starting a data sweep. A unique code number for each response was entered into the datalogger and also written on the survey form, along with the starting time of the data sweep to assure proper matching of data sets later. The hot-wire anemometer wand was held at the subject's torso level, as close to the respondent as decorum allowed (i.e., 0.5 meters at a minimum) on the side that intercepted the strongest discernible air flow impinging on the subject. A tell-tale made of thread was used to determine air flow direction. After four minutes of data collection, the "tool box" was shifted to the next workstation. Care was taken to allow the equipment to equilibrate when moving to zones with different temperatures.

Data Processing and Archival

Questionnaire data were numerically coded to facilitate statistical analysis. Individual clothing articles indicated in the survey responses were converted into their respective thermal insulation values (I_{comp}) in units of clo (1 clo = 0.155 $m^{2°C/W}$) as tabulated in McIntyre [1]. The overall clo value for each subject's entire clothing ensemble was then determined using the following empirical formulae, also from McIntyre [1],

$$I_{clo,men} = 0.113 + 0.727 \sum I_{comp}$$

$$I_{clo,women} = 0.05 + 0.77 \sum I_{comp}$$

Metabolic heat production was not directly measured, but since respondents were carefully pre-screened to have been seated for at least 15 minutes, their metabolic rate was assumed to be 1.1 met (1 met = 58 W/m^2), the typical level given for light office activities [2]. Later computation of various comfort indices required determining the body surface area (A_{Du}) of each subject in square meters based on their reported weight (W) and height (H) (in kilograms and meters, respectively) using the Dubois formula: [1],

$$A_{Du} = 0.202\, W^{0.425}\, H^{0.725}$$

Mean radiant temperature (MRT) was calculated as prescribed in the 1984 ASHRAE Systems [3]. A program was adapted from the Doherty and Arens [4] model for calculating environmental indices such as ET* and SET* and comfort indices such as PMV*, HSI, DISC, and TSENS. Predicted Mean Vote (PMV) and Predicted Percentage Dissatisfied (PPD) were calculated using the method specified in the International Standards Organization Standard 7730 [5].

Physical measurements were transferred from cassette tape to microcomputer files. Then non-linear analog sensor outputs were converted into physical units and all outputs processed into averages of three minutes' data for each workstation. These physical measurement data, along with the questionnaire data, were entered into microcomputer databases for subsequent analysis

and archival purposes.

RESULTS

Profile of the Sample

The total sample of responses drawn from office workers in four buildings* during each of two seasons numbered 1146. Of these, 669 were women and 476 were men. Six hundred responses were obtained in the hot season and 546 in the wet season. In each season nobody was surveyed more than once, but some portion† of the respondents participated in both seasons. Two-thirds of the sample comes from the AC buildings (757); the rest (389) were taken from NV buildings. The distribution of ages in the sample are shown in Figure 2-3. The age of the sample ranges from 18 to 75 years and has a mean of 32. The highest education attained was the Thai equivalent of high school for 431 of the respondents, a bachelor's degree for 586, and a post-graduate degree for 122. The overwhelming majority (1003) of respondents listed themselves in the lower category of job positions, with 127 in middle positions and only nine in upper positions. Because the sample included people from private sector businesses and professional firms, government civil services, and universities, the survey question dealing with job rank was necessarily general and subject to interpretation in each situation. It is also possible that customary Thai modesty has skewed the choice of job rank lower.

The distribution of measured physical data is broken down by building and season in Tables 2-1 and 2-2. Clo values ranged from 0.24 to 1.19, and averaging 0.53 in both seasons. Figure 2-4 shows two histograms depicting the clo values for men (in the foreground) and women (in the background). Women had much more varied thermal insulation in their attire. The average Dubois body surface area (not shown in Table 2-1) for the entire Thai sample was 1.56 m^2, with a standard deviation of 0.17 and a range from 0.62 to 2.58 m^2. Air temperatures ranged from a low of 19.5°C in an AC building to a high of 34.2°C in a NV building, averaging around 26°C for the sample with little difference between the hot and wet seasons. Vapor pressures reached a high of 28.4 Torr and went as low as 6.9 Torr, averaging 16.9 Torr, again with little seasonality. AC buildings had an average air-velocity of 0.13 m/s, while NV buildings experienced higher airflows of 0.33 m/s on average. Because the latter buildings also utilized local fans, air velocities at the workstation went up as high as 2.25 m/s. From these data, we calculated the ASHRAE Effective Temperature (ET*), defined as that temperature at 50% relative humidity, mean radiant temperature equal to air temperature, and air-velocity of 0.1 m/s that would produce the same thermal sensation as the actual environment. The resultant ET* averaged 27.5°C for the entire sample extending up to 36°C and down to 20.5°C. Figure 2-5 is a frequency distribution of ET* with the hot and wet seasons depicted. The bi-modal separation of the data between AC and NV buildings in each season is clearly evident.

Distribution of ASHRAE and McIntyre Scale Responses

The survey participants cast their votes on the seven-point ASHRAE Thermal Sensation and three-point McIntyre scales in response to the immediate conditions at their desks. The distribution of votes for both scales is shown in Figures 2-6 through 2-8. Almost 35% of the votes were cast in the ASHRAE Scale zero category (e.g., "neutral") and three-quarters voted within the central three categories (between "slightly cool" and "slightly warm" or -1 and 1 on the scale). Few people chose to indicate their thermal sensation in the half-steps between whole-numbered categories. The ASHRAE Scale votes were not appreciably different between the hot or wet seasons, as shown in Figure 2-6 where they are juxtaposed. However, the distribution of votes is quite different for AC versus NV buildings, as shown in Figure 2-7. Almost 90% of the

* One additional building served in a single-day pilot study in the hot season and the 25 responses from that building are included in the analysis.

† For reasons of confidentiality, participant names were not tracked and therefore an exact figure of multiple-season respondents cannot be calculated.

respondents in AC buildings selected between "slightly cool" and "slightly warm," whereas only about 57% of the NV building respondents did so. Responses to the McIntyre Scale (graphed in Figure 2-8) overall were 42% preferring "no change," 52% for "cooler," and 6% for "warmer." In the hot season, slightly more shifted their votes from the other two categories to "cooler" for a total of 58%. "Cooler" and "no change" had an equal percentage of the votes in the wet season (45%), with slightly more preferring it warmer. Again, the greatest contrast exists between the samples in AC and NV buildings. Seventy-eight percent of the NV votes fell into the "cooler" category, whereas the fraction was 38% in the AC case. "No change" was the stated preference of 52% in the AC buildings, where only 20% chose similarly in the NV buildings. A surprising 2% voted to be warmer in the NV buildings where temperatures never fell below 25.9°C. Misinterpretation of the question, however, cannot be ruled out.

The scale votes are, of course, taken in response to thermal conditions and therefore are most meaningfully displayed in juxtaposition with relevant environmental variables. In Tables 2-3 and 2-4, ET* is cross-tabulated with the ASHRAE and McIntyre scales, respectively. These tables show the percentage of votes at each scale category within 0.5°C ET* ranges (i.e., row-wise percentages). The bi-modal character of the data is clear here, with the AC and NV samples overlapping only at ET* of 28°C. The pattern of voting on both the McIntyre and ASHRAE scales alludes to two populations whose thermal sensations (or tolerances or expectations) are distinct from one another.

Mean Responses:

The mean of all of the ASHRAE Scale votes is 0.37, or slightly warmer than neutral. On the McIntyre Scale, the mean response is 0.45. Humphreys [6] regressed such mean responses versus mean air or globe temperatures from 34 field studies worldwide encompassing some two-hundred thousand observations and got the following relation:

$$\text{Standardized Mean Response} = -0.244 + 0.0166\, T_m$$

where the mean response is standardized by dividing the absolute mean response by the number of positive categories on the scale. For the Thai sample, the standardized mean ASHRAE scale response is 0.12 (the McIntyre Scale requires no standardization). The above equation predicts 0.19, which is quite close to the mean ASHRAE response but much less so for the mean McIntyre response.

Regression Analysis

Simple linear regression was performed of the mean ASHRAE Scale responses (calculated at 0.5°C ET* intervals) versus ET* to determine the strength of the relationship between them. All of the fits are weighted by the number of votes making up each mean response. Table 2-5 shows the slope, y-intercept, goodness of fit (R^2), and the number of points going into the fit for various aggregations of the data. The aggregations begin with the entire sample and move toward increased differentiation by season, gender, and space conditioning. For the whole sample, the resultant regression coefficient (slope) is 0.176/°C, with an intercept of -4.406 and a high R^2 of 0.91. The regression coefficient is lower than the value of 0.23 found by Humphreys. Schiller's [7] recent study of air-conditioned environments near San Francisco yielded regression coefficients of 0.328 and 0.308 over winter and summer seasons, respectively. Selecting the Thai data coming only from AC buildings results in a comparable 0.324/°C regression coefficient. Though not true in every case, there is a general tendency for the NV samples to have a lower regression coefficient than their AC counterparts. This is particularly true during the wet season, reflecting perhaps some measure of adjustment or accommodation to prevailing outdoor conditions. The wet season directly follows the hot season in Thailand, giving the people in NV buildings longer exposure to hot and humid weather, and possibly more opportunity to acclimatize than workers in AC buildings. It is also true, however, that the correlations are less strong and based on fewer points in the NV disaggregations. There is a slight difference in the responses of men and women in relation to ET*, with women showing a higher tendency to change their vote due to changes in ET* (i.e., a higher regression slope).

In Table 2-6 mean ASHRAE Scale responses are regressed against Standard Effective Temperature (SET*), which is defined similarly to ET* but with clothing and activity also standardized. For the Thai data set in particular, because respondents were pre-screened for "standard" activity levels (seated for at least 15 minutes at desk), SET* differs from ET* due to nonstandard clo levels only. Only a subset of the cases regressed on ET* are repeated with SET* and they differ from the ET* results mainly on the slope terms of AC and NV buildings; they are lesser by a factor of two with SET* the independent variable than with ET*. This suggests that voting distinctions between office workers in conditioned and nonconditioned buildings are explained at least in part by differences in clothing. This result confirms our qualitative observation of more informal dress in the NV buildings than in AC buildings and the roughly 0.5 clo calculated difference between them (see Tables 2-1 and 2-2).

It is customary in reporting on thermal comfort field studies to analyze the mean responses as a function of temperature, as has been done above, but regressions were also performed for four disaggregations of the data using all of the points, and these are shown in Table 2-7. With ET* the independent variable, the regression results are essentially identical to those obtained from mean responses except for lower R^2 values.

Neutral Temperatures

The expected temperature at which a given group would vote "neutral" can also be estimated from the regression of mean ASHRAE Scale response as a function of ET*. This neutral temperature (T_n) is the temperature at which the regression line crosses the x-axis. Computationally, it is obtained by taking the ratio of the y-intercept and the regression coefficient. The neutral temperatures are shown in the last column of Tables 2-5 through 2-7. The full Thai sample produces a T_n of 25.0°C. This compares with other field studies in the tropics, notably those of Ellis [8],[9] in Singapore at 26.1°C and 26.7°C and Webb [10] 27.2°C and Rao [11] with 26.0°C, although substantially lower than Nicol's [12] work in Iran and India during their hot seasons which had T_n of 32.5°C and 31.1°C. Since these are all taken in unconditioned environments, perhaps a better comparison with the above is the subgroup of NV buildings whose neutral temperature is 28.5°C, placing the Thai NV result well within the tropical study range. Auliciems [13] found the neutral temperature of AC building occupants in Northern Australia to be 24.2°C, very close to the Thai AC T_n of 24.5. Other studies done in AC buildings in temperate climates generally find lower thermal neutralities, such as Schiller's average of 22.3°C over two seasons.

Auliciems [13] developed relations for predicting group neutrality based on either the mean indoor air temperature, mean outdoor temperature, or both, recorded over a field study. They are, respectively,

$$T_{n,i} = 5.41 + 0.73\, T_i$$

$$T_{n,o} = 17.6 + 0.31\, T_o$$

$$T_{n,i\&o} = 9.22 + 0.48\, T_i + 0.14\, T_o$$

Results comparing group neutralities predicted by the above equations with those determined by regression are in Table 2-8. For the sample as a whole, $T_{n,i}$ is the best predictor of group neutrality, coming within 0.5°C. Over the sample of disaggregated results, though, $T_{n,i\&o}$ more reliably matches the regression results, averaging within 0.7°C of the latter. Not surprisingly, mean outdoor temperature alone does not anticipate the neutral temperature of AC building occupants. $T_{n,o}$ also poorly predicts group neutrality in the hot season but improves substantially for the wet season. This, again, may be evidence of seasonal acclimatization. With the hot season coming on the heels of the cool season, followed immediately by the wet season (which is hot as well as humid), extended exposure to hot outdoor weather, even for occupants of AC office buildings, could possibly cause group neutrality to increasingly reflect outdoor conditions.

Humphreys [6] had his own empirical equation for predicting neutral temperature based on mean indoor temperature, namely,

$$T_{n,i} = 2.6 + 0.831\ T_i$$

Table 2-8 shows this equation to bear similar results to Auliciems' $T_{n,i}$, though with slightly lower values.

Thermal Acceptability

The concept of thermal acceptability has been widely debated in the literature but in practice is difficult to determine experimentally. The convention arrived at assumes that votes within the central three categories of the seven-point scales (i.e., from -1 to 1) connote satisfaction with the thermal environment. ASHRAE [14] uses this criterion, along with the objective of satisfying 80% of building occupants (thermally speaking), to establish their comfort standard. The McIntyre Scale represents an alternative method for determining thermal acceptability by assuming that any desire for change is tantamount to dissatisfaction. One can look at the interplay of the two scales by examining the cross-tabulations shown in Tables 2-9 and 2-10 for AC and NV buildings, respectively. While 52% of the respondents in AC buildings indicated "no change," a much higher 89% voted within the central three categories on the ASHRAE Scale. Similarly, only 22% wanted "no change" on the McIntyre Scale in NV buildings, but by the ASHRAE Scale thermal acceptability criteria, 58% were satisfied. Figure 2-9 is a relative frequency plot of the percentage of votes at "neutral" (ASHRAE = 0), at "thermal acceptability" (ASHRAE between -1 and 1), and at "no change" (McIntyre = 0), at each 0.5°C ET* bin over the range temperatures. The smooth curves are fits of these data weighted by the number of votes in each ET* bin. The "thermal acceptability" curve (by ASHRAE criteria) crosses the 80% line at roughly 22°C and 30.5°C, the latter going 4°C beyond the warm boundary of the ASHRAE summer comfort zone. The percentage of ASHRAE Scale votes strictly within the "neutral" category is much lower, at 45% or less over a broad range of ET*. Where Schiller's study showed the ASHRAE "neutral" category to be a stricter standard than the McIntyre "no change," here this is true only at ET* less than 25°C, and there is virtual consonance between them especially at temperatures above 30°C.

The ASHRAE Standard 55-81, "Thermal Environmental Conditions for Human Occupancy," depicts a summer thermal comfort "zone" bounded by loci of ET* 22.8°C to 26.1°C and dew-point temperatures of 1.7°C to 16.7°C. This thermal comfort zone is shown in Figure 2-10 along with bars indicating the range and mean of dew-point temperatures experienced by Thai respondents who voted within the central three ASHRAE Scale categories. Below each bar is printed the number of "acceptable" votes, and the percentage of votes these make up within each 1.0°C temperature bin. Roughly three-quarters are satisfied over a wide range of conditions, much wider in fact than the standard allows. If the "acceptable" criteria were constructed of 75% of a population voting within the central three categories (instead of 80%), the Thai thermal comfort zone would stretch from 21°C to 32°C ET*. Mean dew-point temperatures for those voting acceptable are either just under or well above the Standard 55-81 upper dew-point threshold. Other considerations besides comfort play a part in ASHRAE's choice of upper dew-point temperature boundary, health especially. Yet in view of the tremendous savings potential in relaxed comfort standards, it would be fruitful to reassess the upper dew-point boundary, along with the 80% satisfied criteria.

Correlations between Variables

Reviewed were a number of Pearson product-moment correlations among the four rating scales and among the ASHRAE Scale responses and other potential explanatory variables.

Comfort Scales:

Tables 2-11 and 2-12 show correlations among the ASHRAE, McIntyre,* Air Flow, and Humidity scales for each season and for each of the AC and NV buildings. As might be expected,

* For the purpose of interpreting the signs in the McIntyre Scale, a response of "cooler" is coded as -1, "warmer" as 1, and "no change" as 0.

there is a rather high correlation between the ASHRAE and McIntyre scales, except for the NV buildings where it drops off. Ratings on the air velocity are somewhat correlated to those on the ASHRAE and McIntyre scales in the wet season and in AC buildings. This is interesting since the air velocities are higher and more varied in NV buildings. Responses from NV buildings on the ASHRAE and McIntyre Scales are mildly correlated with perceptions of humidity levels. Other correlations are extremely weak or statistically insignificant.

ASHRAE Scale and Other Indicators:

In Table 2-13 the correlations between responses on the ASHRAE Scale of selected subgroups to various physical and demographic factors are depicted. Indoor dry-bulb and mean radiant temperature, ET* and SET*, and vapor pressure correlate fairly well with votes on the ASHRAE Scale for both seasons. The correlations are generally lower, however, when disaggregated by space conditioning type for these same factors. Air velocity has a mixed correlation with ASHRAE for the sample subgroupings; that is, there is a weak yet significant relation between increased air velocity and *higher* ASHRAE Scale votes (counter to intuition) in the two seasons, but *lower* ASHRAE Scale votes (as one would expect) in AC buildings. Air velocity is apparently unrelated to thermal sensation (as measured by the ASHRAE Scale) for NV buildings. In fact, one would expect that the conditions in NV buildings (e.g., higher and more variable airflow) would produce a stronger linkage with thermal sensation. One possible explanation for this is that among the occupants of the NV buildings studied, there were some who were accustomed to the high airflows from fans at their desks from habitual use and perhaps these respondents just incorporated high airflows into their normal thermal expectations. The negative correlation between air velocity and ASHRAE scale vote in the AC buildings is undoubtably influenced by the higher airflows coinciding with cool air emerging from supply-air diffusers. Conversely, air movement in NV buildings is usually associated with warm or hot air and may not provide much cooling sensation. Clo values are mildly negatively correlated with ASHRAE Scale votes. Other factors, such as gender, age, and expressed sensitivity to several environmental parameters, have insignificant relationships to ASHRAE Scale responses.

Respondents were asked to indicate the level of use of home air-conditioning, whether they never used it (coded 0), seldom (1), usually (2), or always (3). This question was intended as a rough proxy for indicating the thermal context of the respondent's time away from the office. Their answers produced no simple direct correlation with their responses on the ASHRAE Scale as shown in Table 2-13. But because responses to the ASHRAE Scale should reflect a combination of the state of the *immediate* thermal environment as well as that to which the respondent is normally accustomed, the differences of the office thermal environment were factored out by binning responses by ET*. Table 2-14 shows the correlation between home air-conditioning and ASHRAE votes binned by 1°C ET*. The correlations are generally insignificant with the exception of a few ET* bins, and for those the correlations are not particularly strong. Obviously it would be more informative to have a more quantitative description of the domestic thermal environment than our rather imperfect indicator.

Probit Analysis

Probit analysis [15] is a technique whereby data are sorted into two categories: those that possess some quality and those that do not, often at different levels (or bins) of some explanatory variable. These binary sets are transformed into percentages within each explanatory variable bin. The resulting percentages can also be thought of as relative frequencies within each bin. These relative frequencies, done over the range of bins, are, in effect, a cumulative relative frequency distribution. The technique was originally developed for use in analyzing the effectiveness of pesticides. In that particular case, the binary sets were percentage of insect kills versus non-kills at different insecticide dose levels. Probit analysis has been used to evaluate thermal comfort responses on rating scales as a function of temperature [16], [6]. The binary sets are percentages of votes greater than or equal to—versus less than—a given vote category. A family of curves results when done over the range of comfort scale categories. For example, using the ASHRAE Scale, one binary grouping would be the percentage of the votes equal to or greater

than "neutral" and those less than "neutral," done at 0.5°C ET* intervals. The result is a set of curves, each depicting the transition to higher voting categories. This technique tells one the temperatures at which the majority of the sample population would change their votes from one category to the next (i.e., the transition temperatures) as well as the category widths of the scales in question. The chief feature of probit analysis is that it circumvents the assumption of equal scale category widths embedded in regression analysis.

Figures 2-11 and 2-12 show probit analysis of ASHRAE and McIntyre Scale votes, respectively, for the Thai data binned by ET*. The number of curves is always the number of categories minus one, so in Figure 2-11 there are six curves and in Figure 2-12 just two. For reasons of visual clarity, only the curves (and not the actual data points) have been plotted in Figure 2-11. The transition temperature is a value often quoted in the literature and is defined as that temperature at which the majority (i.e., 50% or more) of the respondents would change their votes to the next higher category. In the ideal case, a sufficient temperature range would allow the plotting of each curve from 0 to 100% of the votes. However, in this study only three of the six curves of the ASHRAE Scale probit analysis pass across the 50% line. This allows determination of transition temperatures. The transition from "slightly cool" (-1) to "neutral" (0) takes place at approximately 22.5°C; from "neutral" to "slightly warm" (1) at 27.5°C; and from "slightly warm" to "warm" (2) at 33.5°C. These transition temperatures imply category widths of 5°C and 6°C, respectively, for the "neutral" and "slightly warm" categories. The ASHRAE Scale categories from the Thai sample are considerably wider as compared to those of McIntyre [1] who used a large data set collected at a state university and found corresponding transition temperatures of 3.8°C and 3.1°C, respectively. Ballantyne [16] presented results of a study of Melanesians in Papua New Guinea and found the transition temperature from "cool" to "neutral" to fall at 24.4°C and from "neutral" to "warm" at 30.0°C, implying an even wider 5.6°C central category width.*

On the McIntyre Scale, only the transition temperature from "no change" to "cooler" is defined, and it is about 25.5°C. It is not possible to determine any category width for the McIntyre scale with these data.

It is interesting to note that the point at which 20% of the Thai respondents changed their votes from one or below to higher than one (i.e., 80% retained their choice) is 30.5°C, identical to the earlier finding of the upper bound of thermal acceptability. In fact, Figure 2-11 is useful for determining the Thai comfort zone under different criteria of "thermal acceptability." For instance, suppose the transition temperature were used as the criteria (i.e., 50% shifting their votes). The rightmost boundary of the comfort zone would slide over to 33.5°C ET*!

Other Comfort Indices

In the results reported so far, we have used Effective Temperature (ET*) for combining the thermal effects of the four environmental variables—temperature, radiant temperature, humidity, and air velocity—into a single index. Other comfort indices exist, however, and in this section distinctions between some of the more widely used indices and their relative merits in the Thai context are explored.

Rational Indices:

The Standard Effective Temperature (SET*) is an extension of ET* in that it also normalizes for the two personal variables, clothing insulation and metabolic rate. Standard clothing insulation values are based on metabolic rate. Thus, SET* is defined as the value of an isothermal enclosure with radiant temperature equal to the air temperature, at 50% relative humidity, and air-velocity of 0.1 m/s, in which a person with standard clothing for the actual activity level would have the same heat loss at the same mean skin temperature and the same skin wettedness as he or she does in the actual environment with the actual clothing insulation after one hour of exposure.

* Note that Ballantyne employed at five-point scale instead of the usual seven-point scale. Other studies have shown that scales using fewer points have wider categories. This makes the Thai results surprisingly close to those using subjects in a similar climate yet with a "broader" scale.

Like ET*, SET* is an index based on analysis of the thermoregulatory response of the body to thermal stress, which is represented in a two-node heat transfer model [17]. The key physiological determinants of human comfort used in the model are skin temperature in cooler than neutral exposures and skin wettedness in warmer than neutral exposures. Skin wettedness is the fraction of the skin surface covered with sweat and is related to the ability of the body to lose heat through evaporation in the given environment. Numerous experiments in warm, humid environments have confirmed a strong relationship between skin wettedness and thermal discomfort. TSENS is a comfort index calculated with the J.B. Pierce model analogous to, and used for, predicting votes on the ASHRAE seven-point scale. TSENS is based on the mean body temperature, which, in turn, is related to skin wettedness when body temperature is regulated by sweating [4].

Fanger [18], the pioneer in developing rational methods for predicting thermal comfort responses, produced two linked indices with his Comfort Equation: Predicted Mean Vote (PMV) and Predicted Percentage Dissatisfied (PPD). Fanger's central premise is that thermal sensation relates to the state of the body rather than the environment. The original Comfort Equation he devised performed a heat balance between the body and the environment, coupled with two key empirical observations: that both the skin temperature and evaporative heat loss *at comfort* are linearly proportional to metabolic rate. PMV is an expression of the difference between the actual metabolic rate and that required to maintain "comfort" as determined by the heat balance calculation. PMV is essentially a rational prediction of the population mean vote on the ASHRAE seven-point scale (same as used in this study). PPD is derived from the the distribution of votes from thermal comfort laboratory experiments as a function of temperature that were related to PMV and the ASHRAE acceptability criteria (that votes outside the central three categories are votes of dissatisfaction).

A criticism of Fanger's method is that the results become increasingly inaccurate at conditions away from comfort, e.g., at high temperatures, humidities, or metabolic rates. Further, the data upon which it is based come from a fairly homogeneous group of white, college-aged subjects whose responses may not be representative in all possible contexts.

The mean PMV and mean TSENS are plotted with the mean ASHRAE Scale vote from the sample of Thai office workers as a function of ET* in Figure 2-13 and SET* in Figure 2-14. TSENS overpredicts the average Thai ASHRAE vote below 24°C ET* but is generally within 0.5 Scale units in warmer conditions. Surprisingly, PMV is within 0.5 scale units of average Thai ASHRAE votes over most of the range and *underpredicting* it below 33°C ET*. When plotted versus SET* (Figure 2-14), all of the curves smooth out. TSENS and the average ASHRAE vote show remarkable agreement over the range, much more so than with ET*. PMV, on the other hand, diverges from the average ASHRAE vote below 25°C SET* by over one scale unit. PMV, TSENS, and the Thai votes agree quite well above 28°C SET*. This suggests that either the Gagge or Fanger models can be used to predict the average Thai office worker response in NV buildings. Thus, while Fanger's method is theoretically lacking in relatively extreme situations away from comfort, in the Thai context it is apparently vindicated. For Thai AC environments, however, the Gagge model is preferred.

Figure 2-15 compares the percent dissatisfied (those voting *outside* the central three ASHRAE scale categories) of the Thai sample and the PPD calculated using the Fanger model. These are plotted as a function of the average ASHRAE scale vote. Each PPD point represents the average of all the PPDs calculated for each individual *within a given 0.5°C ET* bin.* Similarly, the percent dissatisfied from the Thai data are taken from ET* bins. For each series we show a second-order polynomial fit to the data weighted by the number of data points behind each plotted point. The y-axis scale is logarithmic to facilitate comparison with Fanger's [18] classic PPD versus PMV plot also using this format. The PPD fit grossly overpredicts Thai dissatisfaction below thermal neutrality by as much as 25%, but is quite accurate in the region above about 0.3 on the ASHRAE scale. Figure 2-15 is consistent with Figure 2-13, and this is to be expected since PPD and PMV are linked. One final point worth noting is that the minimum point in the percent dissatisfied curve occurs slightly below the zero scale point. It has been suggested that people accustomed to a hot climate might find a slightly cool environment preferable to a neutral one. To

the extent that minimal dissatisfaction connotes "preference," the small offset of the curve may demonstrate this effect on the part of the Thai sample.

Empirical Indices:

Field studies performed in the tropics have yielded numerous empirical indices for predicting the response to thermal conditions. Most of these empirical indices are simple to compute using commonly measured variables. A disadvantage of this class of comfort index is that the applicability of the index is limited to the conditions found in the data set from which the index is derived. For field studies, where the researcher exercises little or no control over the environmental conditions (the usual case), the range of applicability can be rather narrow. Comparisons of empirical indices applied to the Thai data set are beyond the scope of this work.

CONCLUSIONS

A sample of thermal comfort responses and environmental data was collected for 1146 Thai office workers. Preliminary findings from analyzing two seasons of data gathered in four Bangkok buildings are as follows:

- There is little apparent gender or seasonal bias in the responses, although different clothing insulation between men and women could be masking real differences, and the weather differences between the hot and wet seasons in Bangkok in 1988 were more subtle than usual.
- Two distinct populations emerged from our analysis: those who worked in AC offices and those who worked in NV offices. The latter group expressed satisfaction with temperatures and humidities well above those deemed acceptable in the HVAC industry.
- Regression of the mean ASHRAE Scale responses produced a rather shallow slope term indicating less sensitivity on the part of the Thais to thermal environment change, relative to other populations studied in the literature. This finding is also supported by an analysis showing the ASHRAE Scale category widths to be substantially wider than other studies have found using the seven-point scale.
- The Thai neutral temperature of 25°C is in agreement with other field studies done in the tropics but above most from temperate climates.
- This sample registered thermal acceptability (as defined by ASHRAE Standard 55-81) over a broader effective temperature range than previous work, from 22°C to 30.5°C. This extends the hot and humid boundary of the summer comfort zone 4°C outward. The implications of this finding, if put into practice, could have a profound impact on energy use in commercial buildings located in the tropics. Relaxing the criteria for defining the comfort zone boundaries (on the humidity or temperature "edges") even slightly from the present choice could push the savings significantly further.
- Gagge's TSENS model predicts the average Thai thermal sensation well over the range of temperatures experienced in this study. Fanger's PMV does less well at lower temperatures but at temperatures above 28°C is quite accurate.

REFERENCES

1. McIntyre, D.A., *Indoor Climate*, Applied Science Publishers, Ltd., London, 1980.
2. American Society of Heating, Refrigerating, and Air-Conditioning Engineers, Inc., *ASHRAE Handbook — 1989 Fundamentals*, Altanta, GA, 1989.
3. American Society of Heating, Refrigerating, and Air-Conditioning Engineers, Inc., *ASHRAE Handbook — 1984 Systems*, Altanta, GA, 1984.
4. Doherty, T.J. and Arens, E., "Evaluation of the Physiological Bases of Thermal Comfort Models," *ASHRAE Transactions*, Vol. 94, Part 1, pp. 1371-1385, 1988.
5. International Standards Organization, "International Standard 7730: Moderate Thermal Environments - Determination of the PMV and PPD Indices and Specification of the

Conditions for Thermal Comfort," Geneva, 1984.

6. Humphreys, M.A., "Field Studies of Thermal Comfort Compared and Applied," *Building Services Engineer*, Vol. 44, pp. 5-27, 1976.
7. Schiller, G.E., Arens, E.A., Bauman, F.S., Benton, C., Fountain, M., and Doherty, T., "Thermal Environments and Comfort in Office Buildings," *ASHRAE Transactions*, Vol. 94, Part 2, 1988.
8. Ellis, F.P., "Thermal Comfort in Warm, Humid Atmospheres—Observations in a Warship in the Tropics," *Journal of Hygiene*, Vol. 50, pp. 415-432, Cambridge, 1952.
9. Ellis, F.P., "Thermal Comfort in Warm, Humid Atmospheres—Observations on Groups and Individuals in Singapore," *Journal of Hygiene*, Vol. 51, pp. 386-404, Cambridge, 1953.
10. Webb, C.G., "An Analysis of Some Observations of Thermal Comfort in an Equatorial Climate," *British Journal of Industrial Medicine*, Vol. 16, pp. 297-310, 1959.
11. Rao, M.N., "Comfort Range in Tropical Calcutta—A Preliminary Experiment," *Indian Journal of Medical Research*, Vol. 40, No. 1, pp. 45-52, 1952.
12. Nicol, J.F., "An Analysis of Some Observations of Thermal Comfort in Roorkee, India and Baghdad, Iraq," *Annals of Human Biology*, Vol. 1, No. 4, pp. 411-426, 1974.
13. Auliciems, A. and deDear, R., "Air Conditioning in a Tropical Climate: Impacts upon European Residents in Darwin, Australia," *International Journal of Biometeorology*, Vol. 30, No. 3, pp. 259-282, 1986.
14. American Society of Heating, Refrigerating, and Air-Conditioning Engineers, Inc., "ASHRAE Standard 55-1981: Thermal Environmental Conditions for Human Occupancy," Atlanta, GA, 1981.
15. Finney, D.J., *Probit Analysis*, The University Press, Cambridge. 1971.
16. Ballantyne, E.R., Hill, R.K., and Spencer, J.W., "Probit Analysis of Thermal Sensation Assessments," *International Journal of Biometeorology*, Vol. 21, No. 1, pp. 29-43., 1977.
17. Gagge, A.P., Nishi, Y., and Gonzalez, R.R., "Standard Effective Temperature - A Single Temperature Index of Temperature Sensation and Thermal Discomfort," *Thermal Comfort and Heat Stress, Proceedings of the CIB Commission W45 (Human Requirements) Symposium,* held at the Building Research Station, His Majesty's Stationary Office, 13-15 September, 1972.
18. Fanger, P.O., *Thermal Comfort*, Danish Technical Press, Copenhagen, 1970.

ACKNOWLEDGEMENTS

Many people assisted on various aspects of the project and without them it never would have gotten off the ground. Among those gratefully acknowledged are Ed Arens for his overall guidance on the project; Rick Diamond and Richard deDear for their advice on the survey instrument; Tawachai Prathuangsit and Vimolsiddhi Horayangkura for translating the survey into Thai; Marc Fountain for significant help in setting up the instrumentation; Boonpong Kijawatanachai for help in selecting, gaining access to, and later surveying the buildings; Surapong Chirarattananon for enthusiasm and logistical support in the data collection phase; Jinda Kaewkeaw and Patana Rugkwamsook who facilitated student participation and helped with measurements; Thai graduate students Kuskana Kubaha, Nuansri and Chutima Kitsuwannawong, Pichai Paromadilok, Surapong Wangsupakitakosol, Paritas Aramwanich, Jomjai Siriporn, Pucharee Chantabuppa, and Chaiyoot Sripadet who helped carry out the surveys. And last, but certainly not least, the Thailand - U.S. Educational Foundation is gratefully acknowledged for its financial support during the year in Bangkok.

Figure 2-1.
Subjective Rating Scales

ASHRAE Scale: "Rate how you feel at this moment"

-3	-2	-1	0	1	2	3
cold	cool	slightly cool	neutral	slightly warm	warm	hot

McIntyre Scale: "I would like to be ..."

Warmer
No Change
Cooler

Humidity Scale: "Rate the immediate environment at this moment in terms of humidity"

-3	-2	-1	0	1	2	3
much too dry	too dry	slightly dry	just right	slightly humid	too humid	much too humid

Air Flow Scale: "Rate the immediate environment at this moment in terms of air movement"

-3	-2	-1	0	1	2	3
much too still	too still	slightly still	just right	slightly breezy	too breezy	much too breezy

Figure 2-2.
Data Acquisition System for Physical Measurements

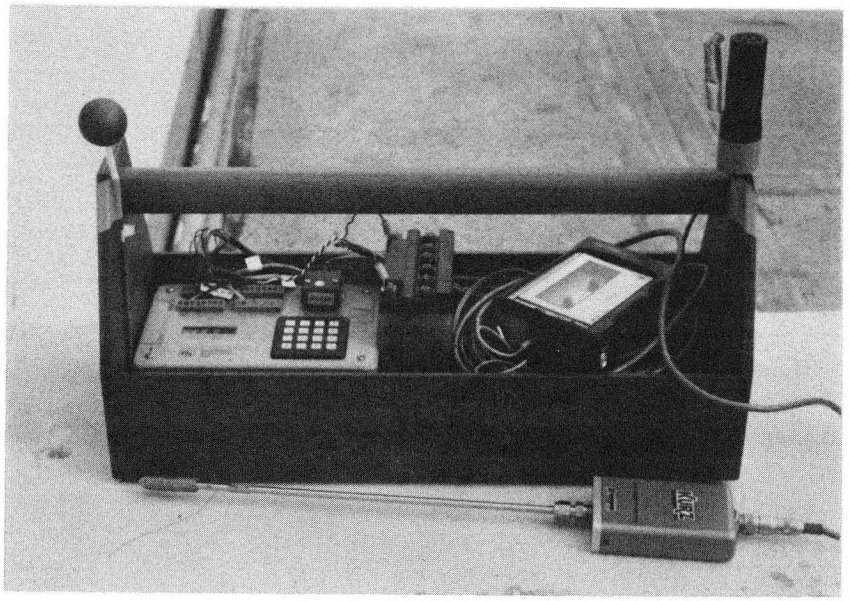

Figure 2-3.
Age Frequency Distribution

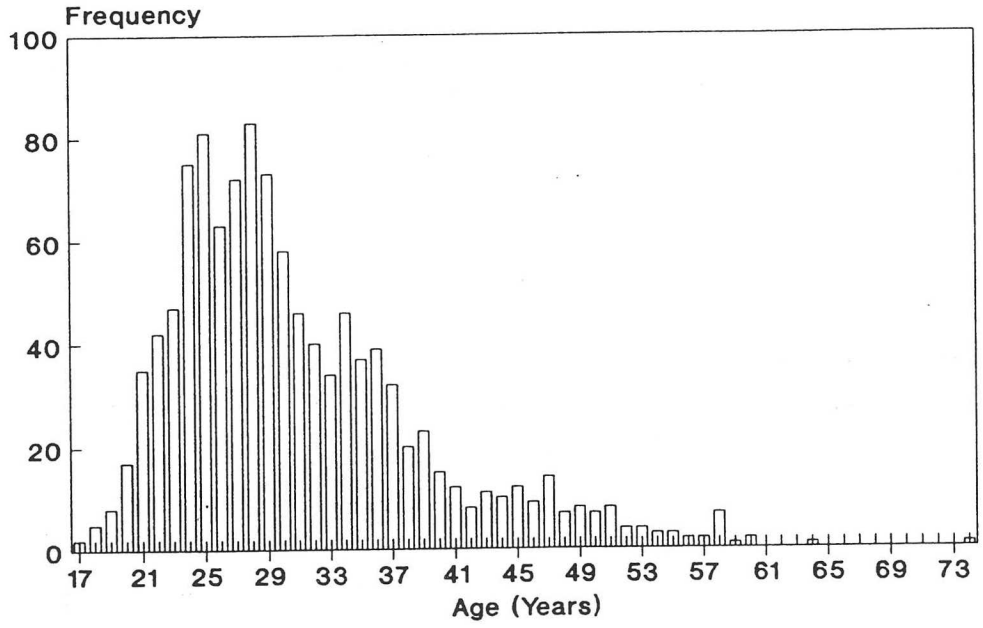

Figure 2-4.
Clo Value Frequency by Gender

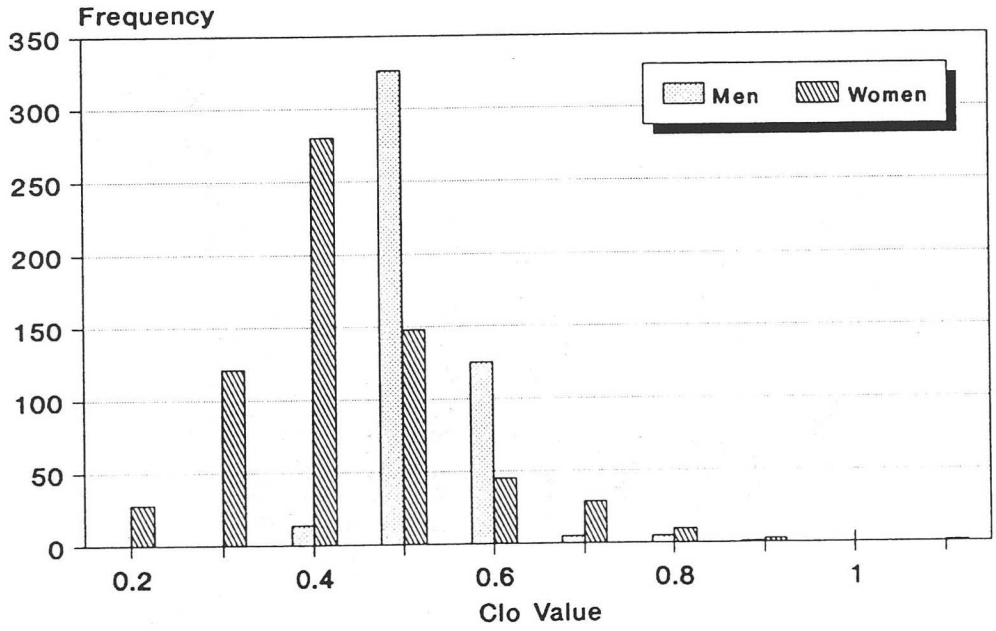

Figure 2-5.
ET* Frequencies by Season

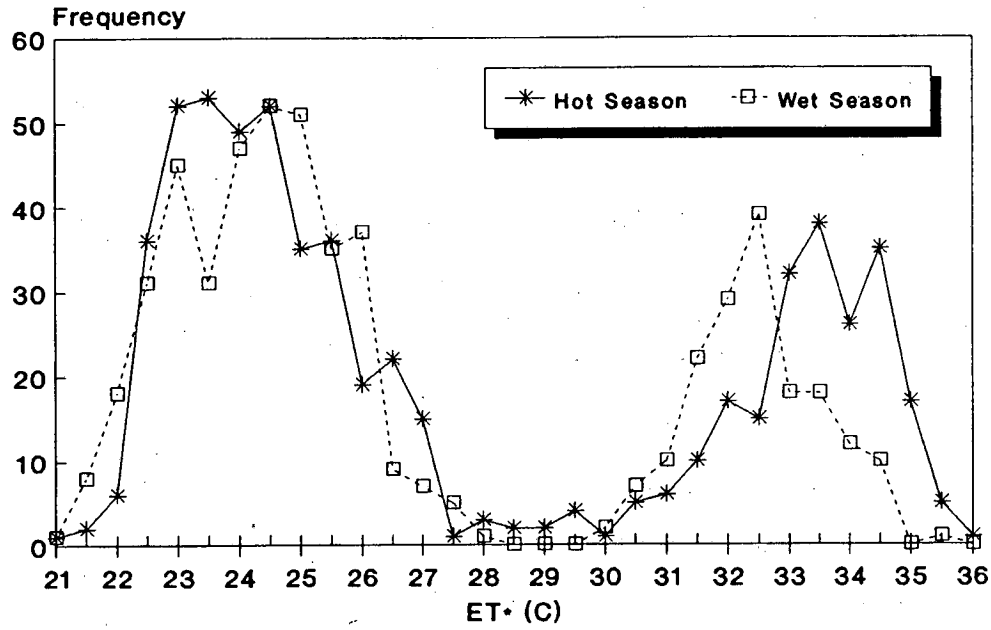

Figure 2-6.
Relative Frequency of ASHRAE Votes

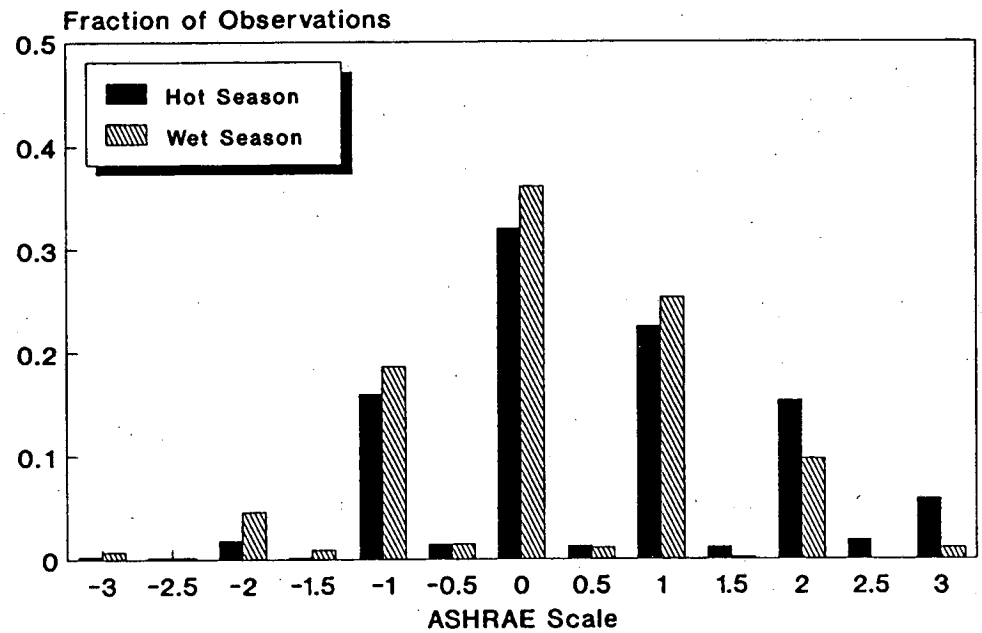

Figure 2-7.
Relative Frequency of ASHRAE Votes

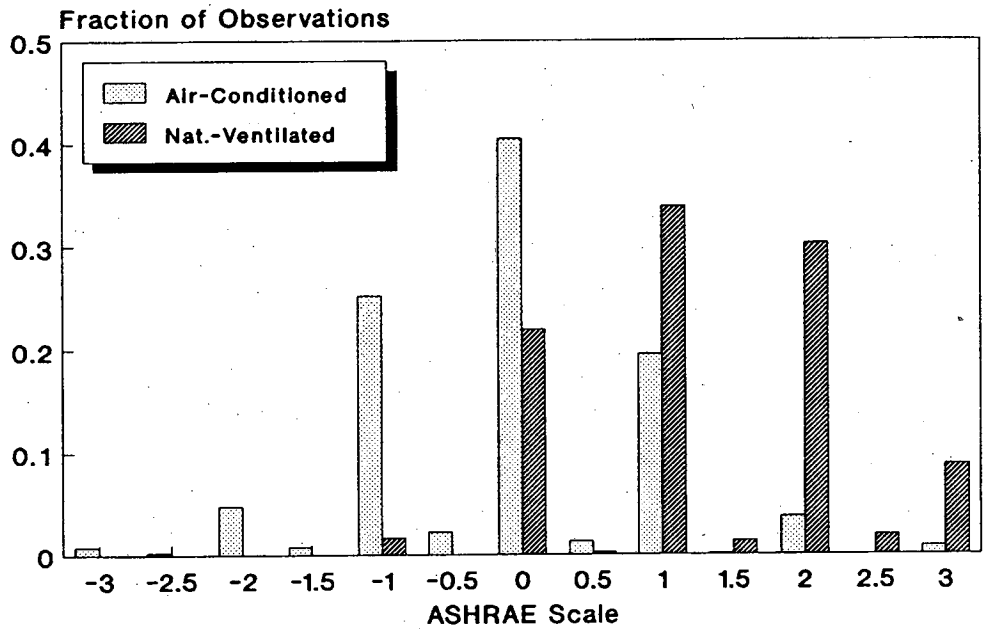

Figure 2-8.
Relative Frequencies of McIntyre Votes

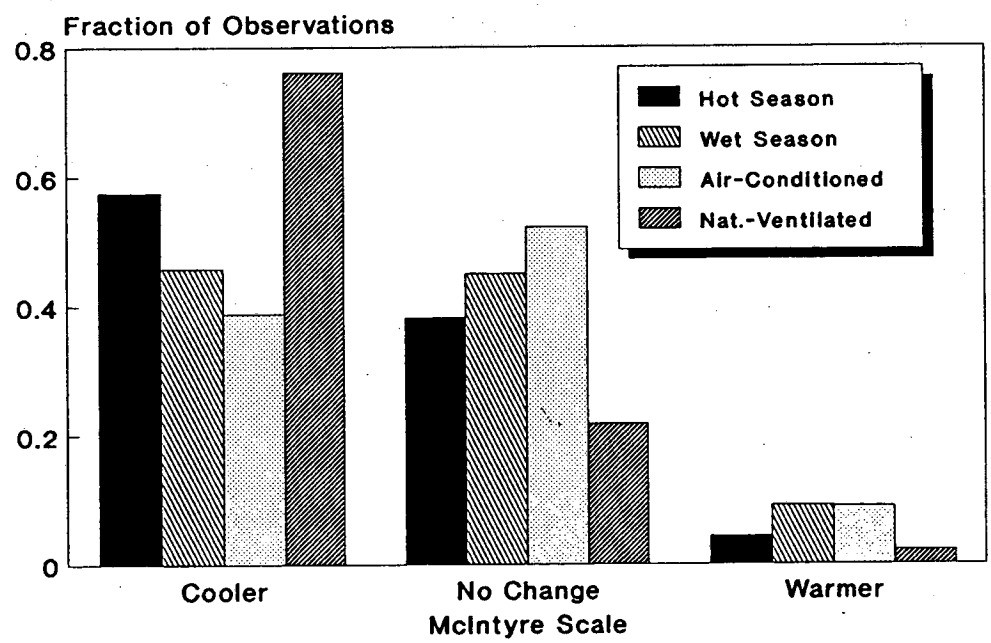

Figure 2-9.
Thermal Acceptability

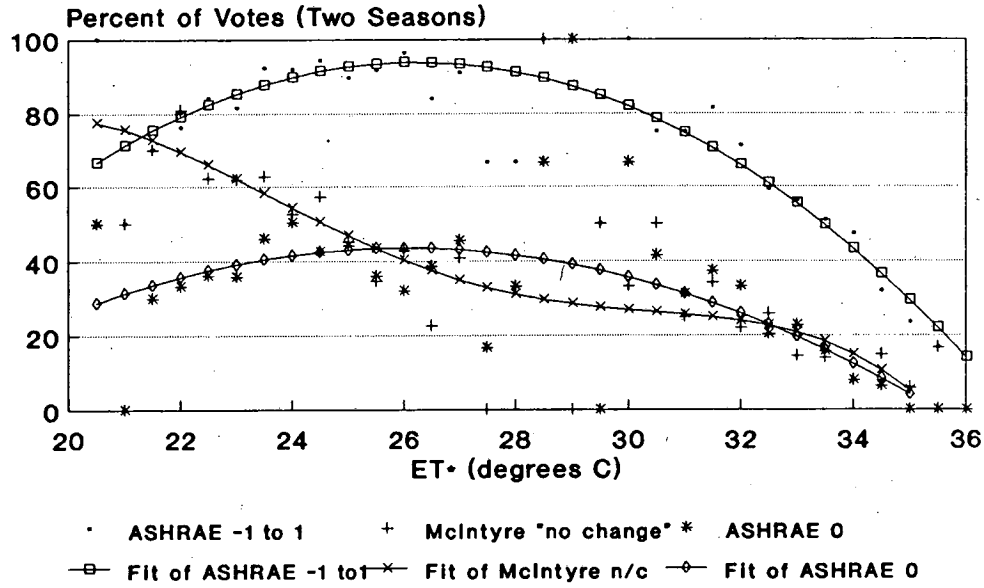

Figure 2-10.
"Acceptable" Votes vs. ASHRAE Standard

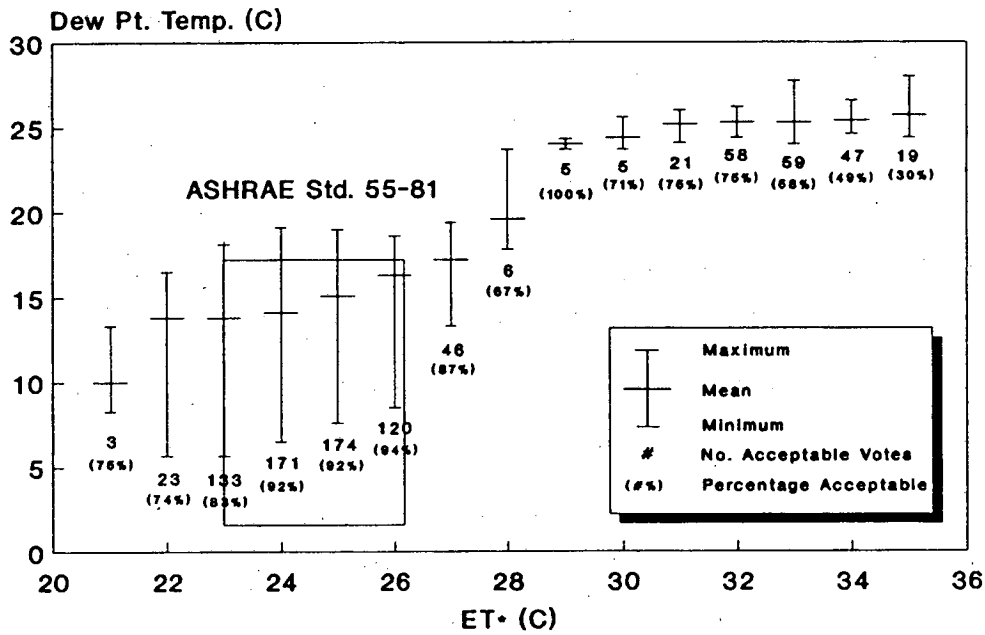

Figure 2-11.
Probit Analysis of ASHRAE Scale Votes

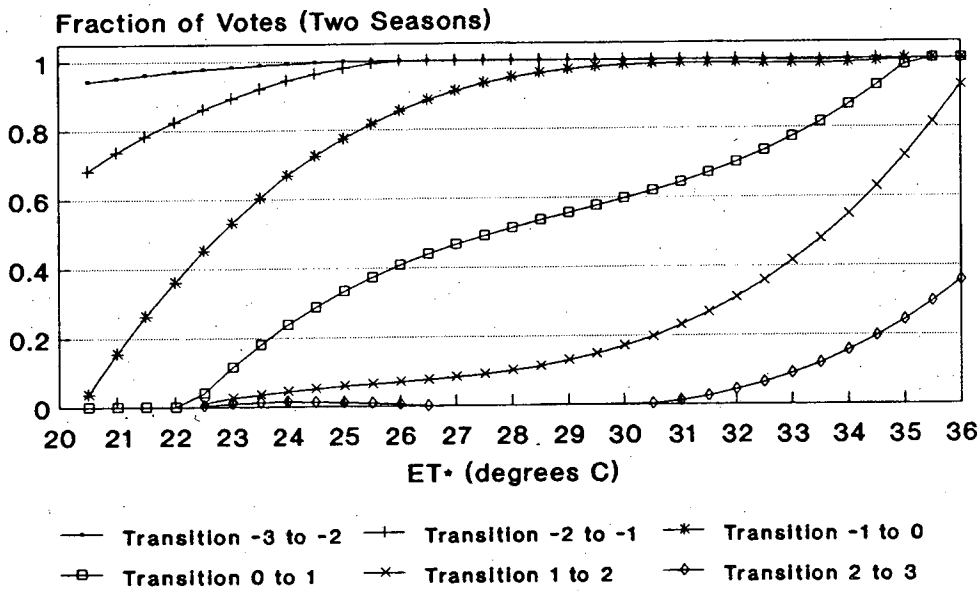

Figure 2-12.
Probit Analysis of McIntyre Scale Votes

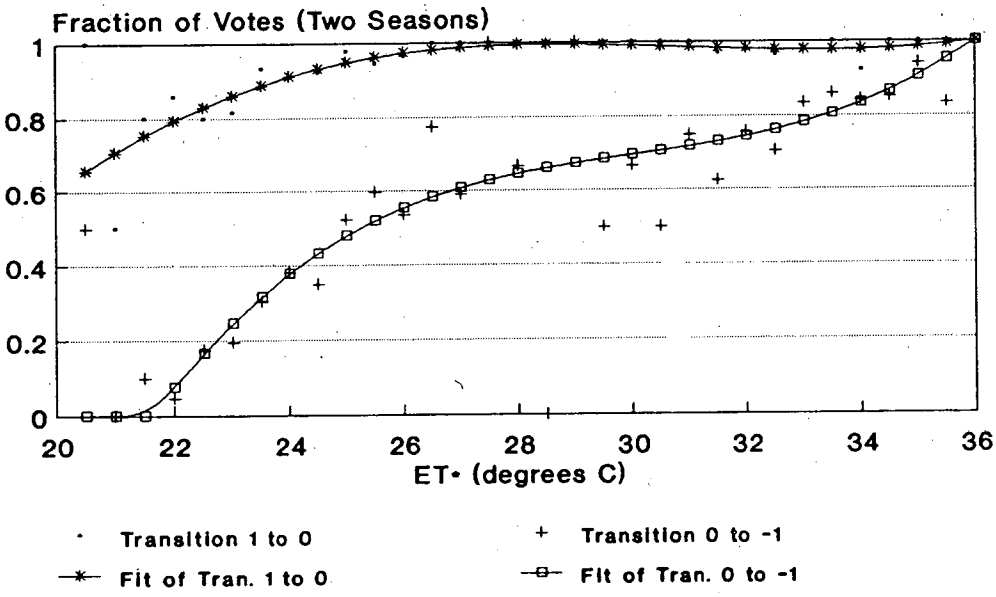

Figure 2-13.
ASHRAE Vote, TSENS, and PMV vs. ET*

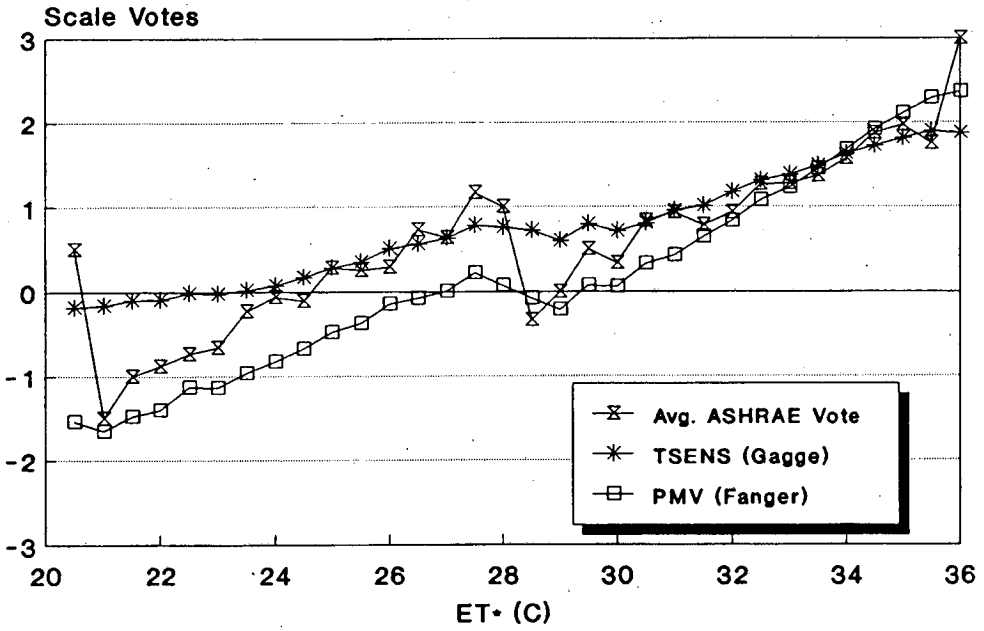

Figure 2-14.
ASHRAE Vote, TSENS, and PMV vs. SET*

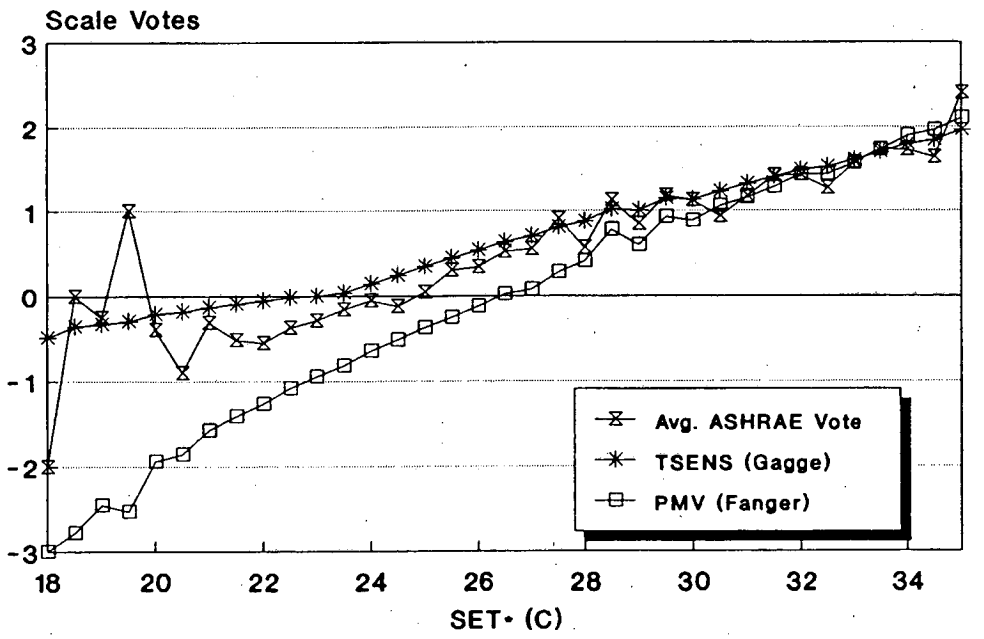

Figure 2-15.
Percent Dissatisfied vs. ASHRAE Vote

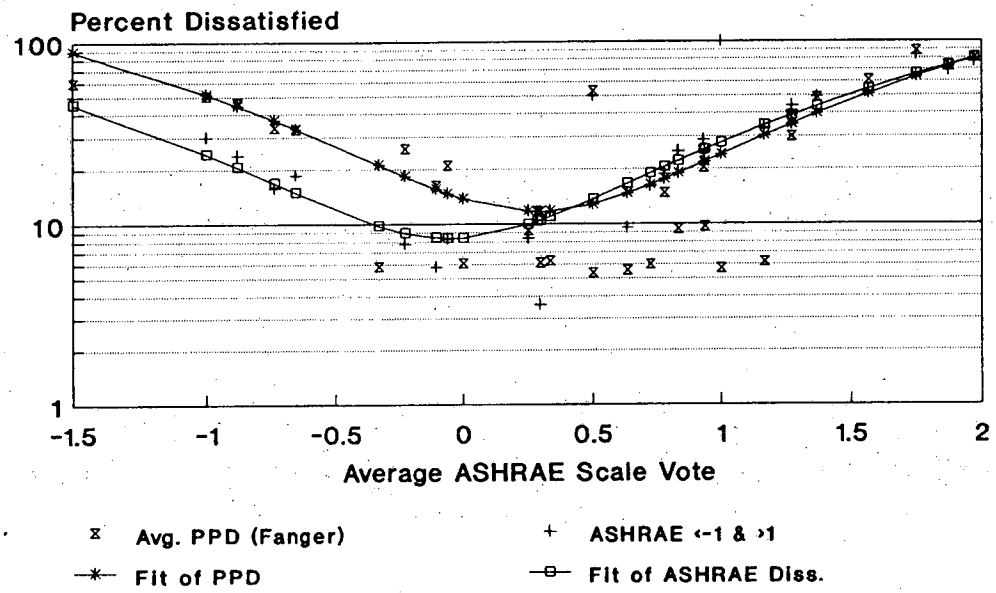

Table 2-1.
Distribution of Physical Data
Hot Season Study

Building*	D	M	P	S	T	All
Sample Size	99	97	25	195	196	600
Clothing (clo)						
average	.49	.50	.50	.55	.56	.53
std dev	.09	.09	.10	.12	.12	.12
min	.24	.28	.24	.25	.24	.24
max	.72	.68	.65	.89	.95	.95
Air Temperature (^{o}C)						
average	30.0	32.6	30.2	23.2	24.0	26.3
std dev	1.5	0.8	1.5	1.1	1.4	4.0
min	25.9	31.4	24.0	19.5	19.7	19.5
max	32.1	34.1	31.3	25.8	26.5	34.1
Vapor Pressure (Torr)						
average	24.1	24.8	23.7	12.2	13.4	17.1
std dev	1.1	0.8	4.0	2.9	1.1	5.9
min	18.9	23.1	9.1	6.9	11.4	6.9
max	26.4	26.2	26.3	16.6	15.7	26.4
Air Velocity (m/sec)						
average	0.33	0.31	0.26	0.13	0.12	.20
std dev	0.26	0.18	0.21	0.03	0.02	.16
min	0.11	0.12	0.10	0.09	0.09	.09
max	1.68	1.20	0.83	0.31	0.19	1.68
ET* (^{o}C)						
average	32.3	34.6	32.6	24.1	24.9	27.8
std dev	1.5	0.5	2.0	1.1	1.4	4.5
min	28.5	33.5	25.5	20.5	20.7	20.5
max	34.3	36.0	34.0	27.3	27.5	36.0

* Buildings D, M, and P are naturally ventilated while S and T are air-conditioned.

Table 2-2.
Distribution of Physical Data
Wet Season Study

Building*	D	M	S	T	All
Sample Size	95	73	181	197	546
Clothing (clo)					
average	.50	.46	.55	.57	.53
std dev	.10	.11	.11	.11	.12
min	.27	.24	.27	.31	.24
max	.71	.65	.91	1.19	1.19
Air Temperature (^{O}C)					
average	30.6	30.5	22.7	24.6	25.8
std dev	1.3	1.2	1.0	.95	3.4
min	28.3	28.1	20.5	22.7	20.5
max	34.2	32.4	25.3	26.9	34.2
Vapor Pressure (Torr)					
average	24.5	24.1	12.0	14.2	16.6
std dev	.9	.9	2.3	.7	5.4
min	22.5	22.1	7.0	12.7	7.0
max	27.9	28.4	16.7	18.0	28.4
Air Velocity (m/sec)					
average	.35	.32	.13	.12	.19
std dev	.38	.22	.02	.02	.21
min	.09	.11	.09	.09	.09
max	2.25	1.63	.25	.20	2.25
ET* (^{O}C)					
average	32.9	32.6	23.5	25.4	27.0
std dev	1.0	1.1	1.0	1.0	4.0
min	30.7	30.1	21.2	23.5	21.2
max	35.5	34.6	26.0	28.2	35.5

* Buildings D and M are naturally ventilated while S and T are air-conditioned.

Table 2-3.
Crosstabulation of ET* vs. ASHRAE Scale
All Buildings (Two Seasons)

	% ASHRAE Scale Thermal Sensation Votes[1,2]													Row Totals	
ET*	-3	-2.5	-2	-1.5	-1	-0.5	0	0.5	1	1.5	2	2.5	3		
20.5	0	0	0	0	0	0	50	0	50	0	0	0	0	.2	(2)
21	0	0	50	0	50	0	0	0	0	0	0	0	0	.2	(2)
21.5	0	10	10	10	40	0	30	0	0	0	0	0	0	.9	(10)
22	0	0	23.8	0	38.1	4.8	33.3	0	0	0	0	0	0	1.8	(21)
22.5	5.8	0	7.2	1.4	42.0	4.3	36.2	0	1.4	0	1.4	0	0	6.0	(69)
23	2.2	1.1	12	1.1	38.0	3.3	35.9	0	4.3	0	2.2	0	0	8.0	(92)
23.5	0	0	3.4	1.1	33.7	1.1	46.1	1.1	10.1	0	1.1	0	2.2	7.8	(89)
24	0	0	5.2	0	19.6	3.1	50.5	1.0	17.5	0	2.1	0	1.0	8.5	(97)
24.5	0	0	2.9	1	27.2	1.9	42.7	2.9	19.4	0	1.9	0	0	9.0	(103)
25	0	0	1.2	0	15.1	2.3	44.2	1.2	26.7	0	8.1	0	1.2	7.5	(86)
25.5	0	0	1.4	1.4	16.7	1.4	36.1	1.4	36.1	1.4	4.2	0	0	6.3	(72)
26	0	0	0	0	19.6	1.8	32.1	3.6	39.3	0	1.8	0	1.8	4.9	(56)
26.5	0	0	0	0	3.2	0	38.7	3.2	38.7	0	12.9	0	3.2	2.7	(31)
27	0	0	0	0	0	0	42.9	0	47.6	0	9.5	0	0	1.9	(22)
27.5	0	0	0	0	0	0	16.7	0	50	0	33.3	0	0	.5	(6)
28	0	0	0	0	0	0	0	0	0	0	100	0	0	.3	(3)
28.5	0	0	0	0	33.3	0	66.7	0	0	0	0	0	0	.3	(3)
29	0	0	0	0	0	0	100	0	0	0	0	0	0	.2	(2)
29.5	0	0	0	0	50	0	0	0	0	0	50	0	0	.3	(4)
30	0	0	0	0	0	0	66.7	0	33.3	0	0	0	0	.3	(3)
30.5	0	0	0	0	0	0	41.7	0	33.3	8.3	8.3	8.3	0	1.0	(12)
31	0	0	0	0	0	0	31.3	0	43.8	0	25	0	0	1.4	(16)
31.5	0	0	0	0	3.1	0	37.5	0	40.6	0	15.6	0	3.1	2.8	(32)
32	0	0	0	0	2.2	0	33.3	2.2	33.3	0	24.4	2.2	2.2	3.9	(45)
32.5	0	0	0	0	0	0	20.4	0	38.9	0	33.3	1.9	5.6	4.7	(54)
33	0	0	0	0	2.1	0	22.9	0	31.3	0	31.3	4.2	8.3	4.2	(48)
33.5	0	0	0	0	1.8	0	15.8	3.5	29.8	3.5	35.1	0	10.5	5	(57)
34	0	0	0	0	0	0	7.9	2.6	36.8	2.6	34.2	2.6	13.2	3.3	(38)
34.5	0	0	0	0	0	0	6.4	0	25.5	0	40.4	4.3	23.4	4.1	(47)
35	0	0	0	0	0	0	0	0	23.5	11.8	29.4	17.6	17.6	1.5	(17)
35.5	0	0	0	0	0	0	0	0	16.7	16.7	66.7	0	0	.5	(6)
36	0	0	0	0	0	0	0	0	0	0	0	0	100	.1	(1)
Column Totals	.5 (6)	.2 (2)	3.1 (36)	.5 (6)	17.3 (198)	1.5 (17)	33.9 (389)	1.2 (14)	23.8 (273)	.7 (8)	12.7 (145)	1.0 (11)	3.6 (41)	100	(1146)

1. Percentages are calculated by row, e.g. within each ET* category.
2. Numbers in parentheses are the total number of votes in the respective column or row.

Table 2-4.
Crosstabulation of ET* vs. McIntyre Scale
All Buildings (Two Seasons)

ET*	% McIntyre Scale Votes[1,2,3] "Cooler"	"No Change"	"Warmer"	Row Totals	
20.5	50	50	0	.2	(2)
21	0	50	50	.2	(2)
21.5	10.0	70.0	20.0	.9	(10)
22	4.8	81.0	14.3	1.8	(21)
22.5	17.4	62.3	20.3	6.0	(69)
23	19.6	62.0	18.5	8.0	(92)
23.5	30.3	62.9	6.7	7.8	(89)
24	38.1	52.6	9.3	8.5	(97)
24.5	35.0	57.3	7.8	9.0	(103)
25	52.3	45.3	2.3	7.5	(86)
25.5	59.7	34.7	5.6	6.3	(72)
26	53.6	42.9	3.6	4.9	(56)
26.5	77.4	22.6	0	2.7	(31)
27	59.1	40.9	0	1.9	(22)
27.5	100	0	0	.5	(6)
28	66.7	33.3	0	.3	(3)
28.5	0	100	0	.3	(3)
29	100	0	0	.2	(2)
29.5	50	50	0	.3	(4)
30	66.7	33.3	0	.3	(3)
30.5	50	50	0	1.0	(12)
31	75	25	0	1.4	(16)
31.5	62.5	34.4	3.1	2.8	(32)
32	75.6	22.2	2.2	3.9	(45)
32.5	70.4	25.9	3.7	4.7	(54)
33	83.3	14.6	2.1	4.2	(48)
33.5	86	14	0	5.0	(57)
34	84.2	7.9	7.9	3.3	(38)
34.5	85.1	14.9	0	4.1	(47)
35	94.1	5.9	0	1.5	(17)
35.5	83.3	16.7	0	.5	(6)
36	100	0	0	.1	(1)
Column Totals	51.9 (595)	41.4 (475)	6.6 (76)	100	(1146)

1. McIntyre Scale indicates responses to the question, "I would like to be ...."
2. Percentages are calculated by row, e.g. within each ET* category.
3. Numbers in parentheses are the total number of votes in the respective column or row.

Table 2-5.
Regression of *Mean* ASHRAE Scale responses and ET*

	Slope	Intercept	R^2	Nr. Pts.	T_n (°C)
All	0.176	-4.406	.91	32	25.0
Hot Season	0.187	-4.586	.91	16	24.5
Wet Season	0.154	-3.959	.85	32	25.7
Air-Conditioned	0.324	-7.952	.88	26	24.5
Nat.-Ventilated	0.289	-8.247	.87	17	28.5
Men	0.175	-4.313	.84	28	24.6
Women	0.179	-4.553	.90	32	25.4
Hot Sea., Men	0.181	-4.391	.84	27	24.3
Hot Sea., Women	0.192	-4.743	.88	31	24.7
Wet Sea., Men	0.164	-4.111	.73	23	25.1
Wet Sea., Women	0.153	-4.032	.88	25	26.4
Hot Sea., AC	0.235	-5.746	.80	21	24.5
Hot Sea., NV	0.237	-6.321	.69	19	26.7
Wet Sea., AC	0.329	-8.185	.88	15	24.9
Wet Sea., NV	0.157	-4.147	.63	12	26.4
Hot, Men, AC	0.200	-4.847	.58	18	24.2
Hot, Men, NV	0.224	-5.858	.61	15	26.2
Hot, Women, AC	0.264	-6.475	.77	18	24.5
Hot, Women, NV	0.246	-6.627	.58	18	26.9
Wet, Men, AC	0.324	-8.004	.77	14	24.7
Wet, Men, NV	0.157	-4.006	.17	10	25.5
Wet, Women, AC	0.322	-8.061	.83	14	25.0
Wet, Women, NV	0.170	-4.627	.71	11	27.2

Table 2-6.
Regression of *Mean* ASHRAE Scale responses and SET*

	Slope	Intercept	R^2	Nr. Pts.	T_n (°C)
Hot Season	0.194	-4.632	.92	33	23.9
Wet Season	0.157	-3.932	.84	33	25.0
Air-Conditioned	0.171	-4.178	.71	22	24.4
Nat.-Ventilated	0.161	-3.787	.70	21	23.5

Table 2-7.
Regression of *All* ASHRAE Scale responses and ET*

	Slope	Intercept	R^2	Nr. Pts.	T_n (°C)
Hot Season	0.187	-4.636	.48	599	24.8
Wet Season	0.154	-4.001	.32	545	26.0
Air-Conditioned	0.326	-8.090	.20	756	24.8
Nat.-Ventilated	0.289	-8.298	.19	363	28.7

Table 2-8.
Comparison of Neutral Temperatures (T_n)*

	T_i	T_o	Regression T_n	Auliciems $T_{n,i}$		$T_{n,o}$		$T_{n,i\&o}$		Humphreys $T_{n,i}$	
All	26.1	29.9	25.0	24.5	(-.5)	26.9	(1.9)	25.9	(.9)	24.3	(-.7
Hot Season	26.3	30.7	24.5	24.6	(.1)	27.1	(2.6)	26.1	(1.6)	24.5	(0)
Wet Season	25.8	29.1	25.7	24.2	(-1.5)	26.6	(.9)	25.7	(0)	24.0	(-1.7
Air-Conditioned	23.6	30.5	24.5	22.6	(-1.9)	27.1	(2.6)	24.8	(.3)	22.2	(-2.3
Nat.-Ventilated	30.9	28.7	28.5	28.0	(-.5)	26.5	(-2.0)	28.1	(-.4)	28.3	(-.2
Men	25.4	30.1	24.6	24.0	(-.6)	26.9	(2.3)	25.6	(1.0)	23.7	(-.9
Women	26.5	29.8	25.4	24.8	(-.6)	26.8	(1.4)	26.1	(.7)	24.6	(-.8

* Numbers in parentheses are the differences between the neutral temperatures using regression and given equation.

Table 2-9.
Crosstabulation of ASHRAE Scale vs. McIntyre Scale
Air-Conditioned Buildings (All Seasons)

ASHRAE Scale	% McIntyre Scale Votes[1,2,3] "Cooler"	"No Change"	"Warmer"	Row Totals	
-3	0	0	100	.8	(6)
-2.5	0	0	100	.3	(2)
-2	5.6	38.9	55.6	4.8	(36)
-1.5	0	50	50	.8	(6)
-1	7.9	74.9	17.3	25.2	(191)
-0.5	29.4	64.7	5.9	2.2	(17)
0	29.1	70.3	.7	40.4	(306)
0.5	90	10	0	1.3	(10)
1	94.6	4.7	.7	19.6	(148)
1.5	100	0	0	.1	(1)
2	96.4	3.6	0	3.7	(28)
2.5	0	0	0	0	(0)
3	100	0	0	.8	(6)
Column Totals	38.8 (294)	52.2 (395)	9 (68)	100	(757)

1. McIntyre Scale indicates responses to the question, "I would like to be ....."
2. Percentages are calculated by row, e.g. within each ASHRAE Scale category.
3. Numbers in parentheses are the total number of votes in the respective column or row.

Table 2-10.
Crosstabulation of ASHRAE Scale vs. McIntyre Scale
Naturally-Ventilated Buildings (All Seasons)

ASHRAE Scale	% McIntyre Scale Votes "Cooler"	"No Change"	"Warmer"	Row Totals	
-3	0	0	0	0	(0)
-2.5	0	0	0	0	(0)
-2	0	0	0	0	(0)
-1.5	0	0	0	0	(0)
-1	0	66.7	33.3	1.6	(6)
-0.5	0	0	0	0	(0)
0	40	60	0	22	(80)
0.5	100	0	0	.3	(1)
1	78.9	18.7	2.4	33.8	(123)
1.5	80	0	20	1.4	(5)
2	94.5	3.6	1.8	30.2	(110)
2.5	100	0	0	1.9	(7)
3	100	0	0	8.8	(32)
Column Totals	76.1 (277)	21.7 (79)	2.2 (8)	100	(364)

Table 2-11.
Simple Correlations between Comfort Scales

Naturally-Ventilated → ↓ Air-Conditioned	ASHRAE Scale	McIntyre Scale	Air Flow Scale	Humidity Scale
ASHRAE Scale		-.47***	-.12*	-.21***
McIntyre Scale	-.69***		.14**	.21***
Air Flow Scale	-.25***	.23***		.13*
Humidity Scale	-.09*	.07*	.19***	

Table 2-12.
Simple Correlations between Comfort Scales

Wet Season → ↓ Hot Season	ASHRAE Scale	McIntyre Scale	Air Flow Scale	Humidity Scale
ASHRAE Scale		-.67***	-.25**	.02
McIntyre Scale	-.67***		.23***	.05*
Air Flow Scale	-.10*	.12**		.10*
Humidity Scale	-.13***	.09*	.21***	

* = significant beyond .05; ** = significant beyond .01; *** = significant beyond .001.

Table 2-13.
Simple Correlations between ASHRAE Scale and various Indices

	Hot Season	Wet Season	Air-Conditioned	Naturally-Ventilated
Outdoor Temperature	.70***	.58***	.44***	.44***
Mean Radiant Temperature	.69***	.57***	.42***	.42***
Vapor Pressure	.65***	.51***	.26***	.14**
Air Velocity	.33***	.19***	-.13***	-.06
Clo	-.27***	-.20***	-.16***	.02
ET*	.69***	.56***	.45***	.43***
SET*	.66***	.53***	.29***	.34***
Gender	.08*	-.03	-.09*	-.05
Age	.13*	.16***	.03	.09
Use of Home AC	-.06	-.02	.06	.07
Temperature Sensitivity	.03	-.03	-.01	.08
Humidity Sensitivity	.02	0	-.02	-.05
Air Flow Sensitivity	.01	-.03	.02	-.04

* = significant beyond .05; ** = significant beyond .01; *** = significant beyond .001.

Table 2-14.
Correlation between ASHRAE Scale and Use of Home AC (binned by ET*)

ET*	Correlation	Significance	Nr. Points
21	.26	.742	4
22	.40	.024	31
23	.02	.755	161
24	-.04	.595	186
25	.20	.005	189
26	.06	.491	128
27	-.01	.953	53
28	.24	.540	9
29	.41	.495	5
30	-.50	.257	7
31	-.12	.553	28
32	.20	.076	77
33	.19	.062	102
34	-.14	.172	95
35	.11	.402	64
36	.36	.426	7

CHAPTER 3: THE EFFECTS OF SURROUNDING BUILDINGS ON WIND PRESSURE DISTRIBUTIONS AND NATURAL VENTILATION IN LONG BUILDING ROWS

F.S. Bauman, D. Ernest, and E.A. Arens
Building Science Laboratory
Department of Architecture
University of California
Berkeley, CA 94720 USA

ABSTRACT

To predict the performance of a naturally ventilated building, estimates of the wind-induced surface pressure distribution are needed. In urban environments, where buildings are grouped closely together, these surface pressures will be strongly influenced by the surrounding structures. In addition, the sheltering effect of the surrounding built-up environment can make it more difficult to obtain large enough pressure differences across a building necessary to produce adequate natural ventilation airflow rates. This paper describes the results of a wind tunnel investigation of wind pressure distributions over an attached two-story shop or housing unit contained in long building rows of the variety that are commonly found in densely populated commercial centers of Southeast Asia (shophouse) and other urban settings (British row house). Surface pressure measurements were made on a 1:125 scale model as a function of wind direction, spacing between adjacent building rows, and building geometry. Simplified correlations are developed to predict the measured surface pressure coefficients. The jack roof, a roof-level ventilation device, is a key architectural feature of the test model. Using the developed correlations, the characteristics of the ventilation performance of the jack roof are discussed and compared to those for other flow configurations. The jack roof demonstrates significant potential to be an effective natural ventilation design for densely built-up urban areas.

INTRODUCTION

Buildings in hot and humid climates have traditionally been cooled by ventilation. Ventilative air movement in the building interior acts to cool the occupants in two ways. First, it cools the occupant directly by increasing the convective and evaporative heat transfer from the body surface. Second, it cools the occupant indirectly by removing heat stored in the building structure. Traditional buildings are operated in either or both modes, depending on the climate. Internal airflows in such naturally ventilated buildings can be (1) wind-driven, resulting from the external wind pressure field; and (2) buoyancy-driven, resulting from the temperature differences between the building interior and exterior. Even in relatively light winds and under typical interior-exterior temperature differences, wind pressure forces, rather than buoyancy forces, are the dominant cause of naturally driven ventilation.

In urban environments, where buildings are grouped closely together, the wind-induced surface pressure distribution on a building, as well as the local wind velocity field around a given building, will be strongly influenced by the surrounding structures. In addition, the sheltering effect of the surrounding built-up environment can make it more difficult to obtain large enough pressure differences across a building necessary to produce adequate ventilation airflow rates.

Previous related studies have looked at the effect of vegetation windbreaks and fences on wind pressures and the resulting air infiltration energy losses/gains in residential housing. The studies were done at small scale in a wind tunnel [1] and at full scale in the field [2]. Peterka and Cermak [3] performed a wind tunnel study of wind velocities in the wakes of freestanding buildings. The effect of a single adjacent upwind building on wind pressures on a rectangular building was the subject of a wind tunnel study by Peterka *et al.* [4]. Aynsley described the influence of a single upwind row of houses on the mean windward and leeward surface pressures of a house for a limited number of wind directions and building spacings [5]. A thorough review of recent wind

tunnel studies of wind loads on low-rise buildings was reported by Holmes [6].

The effect of a group of surrounding buildings has been studied in a series of wind tunnel experiments performed in the United Kingdom. Soliman studied a cuboid [7] and Lee *et al.*, studied a rectangular model at several geometric aspect ratios [8]. In both studies, the test model was surrounded by various arrays of identically shaped models. The results of Lee *et al.* give reductions in surface pressures on the test model as a function of building alongwind spacing, the layout of the buildings in the crosswind direction (two grid patterns were examined), and the wind approach direction over either layout. The results of the study show wind pressure reductions of up to 90% resulting from wind blockage by upwind buildings. However, there is a variability of 80%, depending on the configuration of the buildings. Hussain and Lee present additional wind tunnel results on the surface pressure fields and airflow regimes between buildings for rectangular blocks representative of low-rise buildings in suburban areas [9].

Wiren has performed an extensive wind tunnel study of the wind pressure effects on a 1 1/2-story single-family house surrounded by identical models in various regular arrays. Measurements were made for an isolated model, a model with one upwind model, a model with two adjacent models, and a model within a large group of models. Unlike the previous flat-roofed models, the models used in Wiren's study had a roof pitch angle of 45 degrees. His tests indicated that the maximum reduction in ventilation airflow rate, obtained with three rows of houses surrounding the test house, was about 40% [10]. The above wind tunnel study was recently repeated for two-story terrace houses [11].

Given a set of pressure distribution data for a building, simplified calculation techniques exist for estimating the amount of infiltration airflow through cracks or other small leakage areas or ventilation airflow through larger wall openings. The internal airflow is driven by the pressure difference between surfaces containing flow inlets and outlets. Ventilation airflow equations have been described by Aynsley for a series of openings without internal flow branching [12] and by Vickery for multiple openings with significant internal flow branching [13]. The models make use of discharge coefficients derived from ventilation duct studies, obviously an approximation for typical building ventilation openings. As with the current wind tunnel study, the vast majority of available surface pressure data have been collected for solid models. The presence of flow inlets and outlets will influence the surface pressure in the vicinity of the opening. However, investigations by Vickery *et al.* have shown that the effect of small openings (less than 20% of total wall area) on solid-building pressure data does not significantly affect the accuracy of the above flow models, if the openings are in walls. Vickery did find that the model predictions (based on solid-building pressure data) significantly overpredicted the measured internal airflow for small roof-level outlets [14]. More work is needed to fully understand the performance of roof-level ventilation openings.

Wind pressure will vary over a given building surface, particularly near the edges. But for low-rise buildings these variations will not have a significant effect on ventilation airflow predictions. As a result, a single average pressure over an entire building surface is typically used in the above airflow models. Swami and Chandra found that the error produced by using average vs. local pressure data was about 5% [15]. Similarly, Wiren indicated an error of less than 10% [10].

Correlations of the type reported in the current study, along with the appropriate airflow models, can be usefully incorporated into ventilation design manuals using manual methods or small computer calculation techniques. Manual design procedures for natural ventilation have been reported by Chandra [16], Arens and Watanabe [17], and Swami and Chandra [15]. Pressure coefficient correlations can also be added to large hourly simulation programs (e.g., ESP) containing more sophisticated internal airflow calculation subroutines [18].

PRESENT INVESTIGATION

The building to be studied is a narrow attached shophouse, commonly found in the densely populated commercial centers of Southeast Asian towns and cities, as well as other urban settings (e.g., the British row house). Figure 3-1A shows a perspective cut-away drawing of the shophouse model, which consists of two identical two-story units separated by a central walled courtyard. In the figure, the facing building and courtyard walls are removed. Each unit has a gable

roof with a small raised roof vent structure (jack roof) at the roof peak. Shophouses are contained in long rows of identical units, each separated from its adjoining units by roof parapets (Figure 3-1B).

As described above, previous wind tunnel experiments on the influence of surrounding obstructions have largely focused on three-dimensional models (typically cubical in shape) surrounded by elements of identical size and shape in some sort of grid pattern. The present study will address a configuration in which the test building unit is located near the middle of a long building row, surrounded by other parallel building rows of identical size and shape. In this arrangement, wind effects in the immediate vicinity of the test model will be largely independent of the ends of the building rows. In other words, the position of the unit within the building row will not be a significant parameter, which is expected to be the case for a large majority of such shophouses.

A key architectural feature of the shophouse design is the jack roof, designed to promote ventilation airflow through the building. The positioning of the jack roof at the roof peak is crucial to its ventilation performance, particularly in built-up urban environments where surrounding buildings can have significant shielding effects. Proposed correction factors based on generalized shielding indicate that the ventilation airflow rates can be reduced by a factor of two to three in typical urban settings, compared to those for the same building in exposed, rural terrain [19].

As shown in the schematic flow diagrams of Figure 3-2, the jack roof can be operated in several different modes. With both sides of the jack roof open, wind-driven airflow through the jack roof will induce air to be extracted from the building (Figure 3-2A). The performance of roof ventilators using this principle has been studied by Wannenburg [20]. If wind entering the windward side of the jack roof is diverted down into the building (Figure 3-2B), its ventilation principle will resemble that of wind towers commonly found in Middle Eastern architecture [21]. If only the leeward side of the jack roof is allowed to be open, the strong negative pressures will promote the suction of air out through this surface (Figure 3-2C). One jack roof design of this type has been described by Fairey and Bettencourt [22]. A model of a full-scale laboratory building incorporating a jack roof has been the subject of a wind tunnel investigation by Cermak *et al.* [23]. Vickery *et al.* performed wind tunnel experiments to compare the measured ventilation airflow rates through a ridge vent (located on the leeward side of a standard gable roof) with those predicted by a simplified model for cross-flow ventilation. When little or no winds are present, all jack roof configurations are effective at promoting stack-driven ventilation (Figure 3-2D) [14].

The objectives of the current study are to:

1. Determine average wind pressures on the external surfaces of a shophouse located in a typical urban environment;
2. Develop simplified correlations to predict the average surface pressure coefficients as a function of building spacing, wind direction, and building geometry; and
3. Study the potential ventilation performance of the jack roof design.

EXPERIMENTAL METHODS

Boundary Layer Simulation

The study was conducted in an open circuit, boundary layer wind tunnel (BLWT) located in a university laboratory (see Figure 3-3). The building configuration under investigation in the current experiments can be characterized as a low urban environment with long rows of relatively closely spaced two- to three-story buildings extending for large distances in any direction. The approaching boundary layer flow was simulated in the wind tunnel using techniques similar to those described by Cook [24].

Velocity and turbulence intensity profiles were measured in the wind tunnel at the front edge of the turntable to document the approach wind conditions. These measured profiles are presented in Figures 3-4A and 3-4B. The velocity data were used to produce a regression fit with the logarithmic velocity profile for a thermally neutral atmosphere given below:

$$U(z) = (u^*/k) \ln [(z-d) / z_0] \quad \text{(Eq.3-1)}$$

where

U(z)	= mean velocity at height z (m/s)
u^*	= friction velocity (m/s)
k	= von Karman's constant (0.4)
z_0	= roughness length (m)
d	= displacement height (m)

The regression fit in Figure 3-4A produced a roughness length (z_0) of 0.19 in (4.8 mm) (full-scale z_0 = 2.0 ft [0.6 m]) for a displacement height (d) of 2.0 in (50 mm) (full-scale d = 20.5 ft [6.25 m]), well within the accepted range of values prescribed by Engineering Sciences Data Unit for low urban terrain [25, 26]. In Figure 3-4B the measured turbulence intensities correspond well to values recommended by ESDU for the lower region of the atmospheric boundary layer [27]. The power spectrum was measured at a height of 5.9 in (150 mm) and matched to that recommended by ESDU [26]. Using the method described by Cook [28], the simulated turbulence scale, and therefore the most appropriate model scale, was calculated to be 1:130, an excellent match with the model scale used.

Building Models

A model containing two identical building units was fabricated out of 1/8 in (3 mm) acrylic sheet at a scale of 1:125, based on the typical shophouse configuration shown in Figure 3-1A. The two model units were connected by a central courtyard area and, together, represent a single attached shophouse unit located within a long double row of similar building units. Each double row is separated from adjacent identical double rows by a space representative of a street or alley (Figure 3-1B). The key architectural features of the shophouse model are as follows:

- The overall dimensions of each model unit are H = 3.1 in (80 mm), L = 3.1 in (80 mm), and W = 1.6 in (40 mm), representative of a two-story shophouse, 33 ft (10 m) high to the top of the jack roof, 33 ft (10 m) long, and 16.5 ft (5 m) wide.
- The roof pitch angle (a) is fixed at 20 degrees. A 0.24 in (6 mm) high jack roof (2.5 ft [0.75 m] full scale) is located at the roof peak and covers the top third of the roof.
- Parapets, equal in height to the jack roof, extend along both sides of the pitched roof, separating each adjacent shophouse unit.
- Both the jack roof and parapets are removable, allowing alternate roof configurations to be investigated.
- Each central courtyard is separated from adjacent courtyards by walls of variable height.

The surrounding building models were all constructed from extruded polystyrene foam board. The 1:125 scale model produced a maximum wind tunnel blockage of 4.9%. No corrections were made to the pressure measurements obtained with this configuration.

When the height of the surrounding environment (adjacent structures, trees, etc.) is on the same order as the height of the subject building, as in the current study, then the surrounding buildings must also be modeled in detail. For low-rise suburban terrain, the extent of this modeling is recommended to be a radius of ten building heights [29]. In the current model setup, surrounding buildings were modeled to the edge of the turntable, having a radius of 3.3 ft (1 m). Further upwind of the turntable, general roughness elements on the wind tunnel floor were used to simulate the characteristics of the approaching boundary layer flow.

No ventilation inlets and outlets (e.g., windows or jack roof openings) was included in the models. Rather, pressure taps were installed at the appropriate locations on the solid model surfaces. Figures 3-5A and 3-5B are exploded plan views of the two models showing the pressure measurement (tap) locations for the standard roof and the jack roof designs. During all tests the models were configured such that Model #1 was the upwind model and Model #2 was the downwind model. For each model unit 18 taps were monitored for the standard gable roof model,

and for the jack roof design, an additional 4 taps for a total of 22 taps were monitored. Tap locations were selected to allow the measured pressures to represent averages over areas of equal size on a given model surface.

Pressure Measurements

Pressure measurements were made with two differential pressure transducers. One transducer monitored the pressure taps on the model surfaces. The taps were connected via equal lengths of 0.063 in (1.6 mm) O.D. vinyl tubing to a pressure switch that allowed up to 48 pressure lines to be connected to a single transducer. The second transducer monitored the dynamic pressure at the reference location. A pitot tube suspended from the ceiling (see Figure 3-3) was used to measure the reference conditions. With a mean reference velocity at the pitot tube of 1710 fpm (8.7 m/s), each pressure measurement consisted of simultaneous readings from the two pressure transducers. The transducers were sampled at a rate of 30 readings per second for a duration of 30 seconds. Upon switching to a new port location of the fluid switch wafer, a delay of 15 seconds was implemented to allow the line pressure to stabilize at its new mean value.

In the current study, the pressure coefficients were normalized by the dynamic pressure at the equivalent 33-foot (10-meter) height, the most common weather station height. This allows the results to be related to full-scale conditions. Since simultaneous measurements at the 10-meter full-scale reference height (80mm at wind tunnel scale) could not be made without disturbing the model measurements, the pressure coefficient was determined in two stages, as defined below:

$$C_p = \frac{(P-P_s)}{0.5\rho U_{10}^2}$$

$$C_p = \frac{(P-P_s)}{P_d} * \frac{P_d}{0.5\rho U_{10}^2}$$

$$C_p = C_{p,ref} * D \qquad \text{(Eq.3-2)}$$

where

C_p = mean pressure coefficient normalized by dynamic pressure at equivalent 10-meter height
$C_{p,ref}$ = mean pressure coefficient normalized by dynamic pressure at stationary reference pitot tube
P = mean pressure at building surface (Pa)
P_s = mean static reference pressure (Pa)
P_d = mean dynamic reference pressure = $P_t - P_s$ (Pa)
P_t = mean total reference pressure (Pa)
ρ = density of air (kg/m^3)
D = dynamic pressure height correction factor (9.47)
U_{10} = mean velocity at equivalent 10-meter height (m/s)

In Equation 3-2, $C_{p,ref}$ was measured directly as described above. The dynamic pressure height correction factor, D, was determined from a separate measurement with a hot-film anemometer placed at the equivalent 10-meter height (3.1 in [80 mm]). The static pressure was assumed to be constant at both the reference and 3.1 in heights, and no static pressure correction factor was applied in the equation. All mean surface pressure coefficients presented in this paper are of the form defined by Equation 3-2.

Full details of the experimental methods are described in Bauman *et al.* [30].

PROGRAM OF STUDY

Building surface pressures were measured in response to a number of parameters varied over the ranges defined below. Refer to Figures 3-6A, 3-6B, and 3-6C for illustrations of the typical model layout, roof configurations, and courtyard configurations.

1) wind direction (Θ):	0°, 15°, 30°, 45°, 60°, 75°, 90°, from normal
2) spacing between double rows (s):	S = s/H = 0.5, I, 2, 3, 4, 5
3) courtyard spacing (s_c):	$S_c = s_c / H$ = 0.25, 0.5, 1
4) courtyard wall height (h_c):	$H_c = h_c / H_e$ = 0, 0.5, 1
5) roof configuration	a) with jack roof, without parapet (NJ,NP)
	b) with jack roof, without parapet (J,NP)
	c) with jack roof, with parapet (J,P)

where

H = building height

H_e = eave height (maximum courtyard height)

For each of the above three roof configurations, seven wind directions and six row spacings were investigated for a total of 42 measured pressure distributions. During each series of tests, the courtyard was held at a fixed configuration. For the standard gable roof (without jack roof, without parapet), this was S_c = 0.5 and H_c = 0. For the two jack roof configurations, this was S_c = 1, H_c = 1. Variations in the courtyard spacing and geometry were studied only for a fixed upwind row spacing of S = 1 and for the jack roof with parapet roof configuration. These procedural simplifications were justified (1) due to the observed insensitivity of courtyard surface pressures to variations in row spacing (S), (2) due to the relatively small effect of roof configuration on courtyard surface pressures, (3) due to the very repeatable dependence of courtyard surface pressures on wind direction, and (4) in the interest of reducing the number of wind tunnel tests to a manageable number.

In the current study, for each of the major ventilation surfaces (i.e., surfaces where ventilation inlets and outlets would typically be located), a single surface averaged pressure measurement is reported. Due to the largely two-dimensional geometry of the long building models, pressures showed little variation laterally across the front and back facades of the models. For these surfaces, a representative average pressure could be obtained from the two centrally located taps. In addition, localized pressure coefficients on both vertical surfaces facing the central courtyard were found to be very similar in magnitude for all model configurations tested. For this reason a single average courtyard pressure coefficient is reported. The individual taps used to produce the average pressure for each surface are identified in Table 3-1.

RESULTS AND DISCUSSION

Correlation Development

The pressure measurement results have been analyzed using a PC-based data analysis and graphics program. Using a step-wise multiple linear regression fitting routine, simplified correlations have been developed as a function of wind direction and row spacing. These predict the average pressure coefficients for many of the surfaces with a high degree of accuracy. All correlation equations took the same general form that is given below:

$$C_p = C_0 + \sum_{i=1}^{N} C_i \cdot F_i \qquad \text{(Eq.3-3)}$$

where

$C_i (i=0,1,...,N)$ are constants defined in Tables 3–2 and 3–3

$F_i (i=1,2,...,N)$ are functions defined in Tables 3–2 and 3–3

Table 3-2A presents the correlations for the standard gable roof building (NJ,NP); Table 3-2B presents the results for the two jack roof buildings ((J,NP) and (J,P)); and Table 3-3 presents the results for the variable courtyard configuration. It was found that for most building surfaces, the pressure coefficients could be correlated with only three or fewer terms in the above equation (all significance levels were $< 10^{-4}$). One term (C_0) was a constant. The "$\cos^2\Theta$" term was used to

account for wind angle dependence. The "$\cos\Theta * S$" and "$\cos\Theta * \ln(S)$" terms account for the decreasing effect of spacing at larger wind angles, when the wind is channeled down the streets. The "$\cos^2(\Theta - \pi / 4)$" term reflects the observed peak pressures on the front jack roof near a wind angle of 45°. The "$H_c * S_c$" term in Table 3-3 accounts for the increased sensitivity to courtyard wall height with increasing courtyard spacing. In the correlation tables and following figures, the model configurations are identified according to the key shown in Table 3-4.

Pressure Distribution on Model #1

Figures 3-7A and 3-7B illustrate the characteristics of the pressure distribution over Model #1 (upwind model) for one model configuration: jack roof with parapet and upwind spacing of S = 2. Figure 3-7A shows mean pressure coefficients as a function of tap location for the front of Model #1, and Figure 3-7B shows the results for the back of the model. The results are shown for three wind directions (0°, 45°, and 90°). Note that the lines on both figures do not represent measured data but are shown only to illustrate the trends in the results. The observations are as follows:

1. Pressures on the windward side of the model exhibit large differences between individual surfaces. This is due to the strong incident winds on some of the surfaces, along with flow separation at several locations (front edge of lower roof, top of jack roof, and, for wind angles of 45° and 90° top of parapets).
2. In contrast, the pressures on the leeward side of the model are nearly constant at all tap locations, for a given wind angle. This clearly demonstrates how the wake region encompasses the entire leeward side of the model.
3. At 90° wind angle, the pressure coefficients for both sides of the model are very nearly equal and approach zero. This is an expected result as the wind is channeled between building rows on both sides of the model.
4. The largest pressures on the windward side of the model are obtained for a wind direction of 45° on the lower front roof (taps #8 and #9), and on half of the front jack roof (tap #12). In both cases, the presence of the parapets strongly influences the pressures at these locations. These roof pressures will be influenced by changes in the roof slope (a = 20° in current study).
5. The largest negative pressures on the leeward side of the model occur on the jack roof, due to its close proximity to the strong separation from the roof peak.
6. For the 0° wind angle, all pressure coefficients on the windward side of the model are negative or zero. This indicates that even at an upwind row spacing of S = 2, the front of the model lies in the wake region of the upwind model.

Measurement and Correlation Results

Figures 3-8A and 3-8B present two examples of measured data and their comparison to the correlation predictions of Table 3-2. Figure 3-8A presents results for the front facade of Model #1 with the jack roof but without parapets (J,NP). The observations are as follows:

1. The results follow similar trends for all three roof designs.
2. Pressure increases with increasing spacing. At small spacings and small wind angles, the front facade falls in the wake region of the upwind building row, as indicated by the large negative pressure coefficients.
3. As expected, as the wind direction approaches 90°, the wind is channeled down the streets between the building rows, resulting in similar surface pressure coefficients for all three model configurations. The results approach zero at 90° for all spacings.
4. For the two models with the jack roof, the existence of the parapet had very little effect, as a single correlation in Table 3-2B was used to fit both sets of data.
5. The model with the standard gable roof (NJ,NP) showed slightly higher pressures compared to the two jack roof models. This was particularly evident at small wind angles, where the shielding effect of the taller upwind building row (with the jack roof)

was strongest.

6. Excellent agreement (R^2 = 0.95) was obtained between the measured data and correlation predictions.

Figure 3-8B presents the measured results and the correlation predictions for the front jack roof for Model #1 (J,NP). The observations are as follows:

1. The results are much less sensitive to upwind spacing than the front facade, as the jack roof is more consistently exposed to the ambient winds.
2. At 0° wind angle, the pressure coefficients are either negative or close to zero, demonstrating the sheltering effect of the upwind building row.
3. The figure indicates that for spacings in the range of 2 to 3, the measured pressures are approaching their maximum values at a wind angle of around 45°. Increasing the upwind spacing any further does not produce a significant increase in pressure on this surface. If a design objective is to maximize pressure on the front of the jack roof (presumably to increase the induced volume of airflow from the building interior out the back of the jack roof [see Figure 3-2A]), a spacing of S = 2 to 3 may be close to an optimum choice in urban areas where large spaces between buildings are not an option.
4. A comparison of the data in Figure 3-8B with results for the front jack roof from the model having parapets (J,P) found the surprising result that, although local pressures were strongly influenced, the surface-averaged pressure coefficients were quite similar in magnitude. A single correlation for the front jack roof (with and without parapets) is reported in Table 3-2B.
5. The influence of the more complex geometry of the jack roof made it more difficult to achieve as accurate of a correlation fit (R^2 = 0.84), although reasonable agreement was obtained between a single correlation and the results of both jack roof model tests (with and without parapets).

Measurement results for the other three surfaces (back jack roof, back facade, and courtyard) are not presented here, but the correlation equations in Table 3-2 indicate similar trends for all of them. Since these surfaces were within the wake region of the immediate upwind building, all experienced large negative pressures at normal wind incidence, making them good choices as ventilation outlets. Pressure coefficients increased with increasing wind angle, approaching zero at 90°. Pressures were found to be virtually independent of upwind row spacing (S) for both the back jack roof and back facade, as excellent correlation fits (dependent only on wind direction) were obtained. Courtyard pressures were only very weakly dependent on spacing.

Table 3-3 presents the correlation equation for the courtyard pressure coefficient in response to variations in courtyard wall height (H_c) and courtyard spacing (S_c). The results were obtained for an upwind row spacing of S = 1 and were found to be only weakly dependent on the courtyard geometry. A full-height courtyard wall (H_c = 1) does provide some amount of protection in the courtyard, slightly reducing the pressure coefficients for all wind directions, especially for larger-sized courtyards.

All measurement results and further discussions are contained in Bauman *et al.* [30].

Use of Correlation Tables

The correlation equations contained in Tables 3-2 and 3-3 can be used to predict average pressure coefficients on similar full-scale long building rows. The predictions are applicable to building units located away from the influence of the ends of the building rows. For all surfaces except the courtyard, average pressure coefficients can be calculated directly from Table 3-2 for the given building configuration. For small row spacings, $0.25 \leq S \leq 1$, use the appropriate correlation with S = 1.

Example 1: Find the average pressure coefficient for the front facade of a building with a jack roof (with or without parapets) for a wind angle of 45° and an upwind row spacing of 2.

From Table 3-2B:

$$C_p = 0.062 - 0.945\ (\cos 45°)^2 + 0.237\ (\cos 45°)\ (2)$$

$$C_p = -0.075$$

The combined effects of courtyard configuration (S_c, H_c) and upwind spacing (S) can be computed using both Tables 3-2 and 3-3 as explained below. In performing this calculation, it is assumed that these effects are additive. (1) Use Table 3-3 to determine the value of C_p for the given values of S_c and H_c. (2) Add the additional contribution due to the effect of upwind row spacing (S) from Table 3-2. This corresponds to only the one term in Table 3-2 dependent on S and only for the contribution for S > 1, the value of S for which Table 3-3 was derived. (3) Add the results from steps 1 and 2.

Example 2: Find the average courtyard pressure coefficient for the following configuration:

$$\Theta = 25°\ ,\ S = 2.5\ ,\ H_c = 0.5\ ,\ S_c = 0.75.$$

(1) From Table 3-3:

$$C_p(3) = -0.471\ (\cos 25°)^2 - 0.147\ (0.5)\ (0.75)$$

$$C_p(3) = -0.442$$

(2) From Table 3-2 (spacing contribution only):

$$C_p(2) = -0.057\ (\cos 25°)\ (2.5 - 1)$$

$$C_p(2) = -0.077$$

(3) Total pressure coefficient:

$$C_p = C_p(3) + C_p(2) = -0.52$$

Wind Pressure Differences: Ventilation Potential

Given a set of pressure distribution data for a building, simplified models can be used to estimate the amount of cross-ventilation airflow through inlets and outlets located on the building walls. The equation for calculating the airflow through a cross-ventilated building with one effective inlet and one effective outlet is given below [15].

$$Q = C_d\ A_e\ U_{ref}\ (\Delta\ C_p)^{1/2} \qquad \text{(Eq.3-4)}$$

where

Q	= airflow (m^3/sec)
C_d	= discharge coefficient
A_e	= effective area of inlet and outlet (m^2)
ΔC_p	= pressure coefficient difference across the inlet and outlet

Using Equation 3-4 as a guide, the relative ventilation effectiveness of various combinations of surfaces has been compared by calculating the square root of the mean pressure coefficient differences between the selected surfaces. Although the specific values of the discharge coefficient, inlet and outlet areas, and reference velocity will directly influence the obtained airflow volume, an analysis of $(\Delta C_p)^{1/2}$ helps to clarify the characteristic performance of the ventilation configuration. In the following series of figures, the quantity $(\Delta C_p) / |\Delta C_p|^{1/2}$, based on the developed correlation predictions, is plotted for selected pairs of surfaces on the front and back jack roof, and the front and back facades of Model #1. By using this quantity, negative values represent a reversal of the flow direction through the building. Note that the back facade of Model #1 is part of the courtyard.

Figure 3-9 presents the pressure difference coefficients between the front and back facades of the model with the standard gable roof (NJ,NP). Without a ventilation opening on the roof, this

is the most appropriate wind-pressure difference to drive cross-ventilation of the building. As expected, the pressure difference increases with increasing spacing. At upwind spacings of $S \leq 1$, the ventilation potential is negligible due to the strong sheltering effect of the adjacent buildings.

Since the back of the jack roof tends to have the largest negative pressures for all leeward building surfaces, using this surface as the ventilation outlet will improve the potential ventilation airflow (see Figure 3-2C). Figure 3-10A shows pressure difference results between the front facade and back of the jack roof. The pressure differences are quite comparable to the previous results for front to back facade (Figure 3-9), although larger values are obtained at the smallest spacing (S=1). Figure 3-10B shows pressure difference results between the back facade and the back of the jack roof. The lower pressure differences are indicative of the fairly uniform pressure distribution over all leeward surfaces of the building, although some ventilation potential does exist.

In the above flow configurations, as well as others incorporating the jack roof, it must be kept in mind that the accuracy of Equation 3-4 for roof-level openings may be unreliable [14]. In addition, the smaller size of the jack roof compared to typical windows in the building walls could reduce the effective inlet/outlet areas. However, in the example discussed above (Figures 3-10A and 3-10B), both the front and back facades of the building can act as flow inlets.

If the front of the jack roof is used as a ventilation flow inlet (Figures 3-2A and 3-2B), generally higher pressure differences will be produced at small row spacings, as this surface experiences higher pressures than the more sheltered front facade of the building. Figure 3-11A presents the pressure difference results between the front jack roof and the back facade, and Figure 3-11B presents results between the front jack roof and the front facade. In both figures, it is seen that higher pressure differences exist at small spacings compared to the previous flow configurations discussed above. In fact, the pressure differences between the front jack roof and the front facade attain their maximum values at the smallest row spacings, when the front facade is heavily sheltered (Figure 3-11B). For the jack roof to be used effectively as a flow inlet, the roof slope must be large enough (20^{o} in the present study) to produce positive pressure differences between the front (windward) jack roof surface and the surface(s) containing ventilation outlets.

Figure 3-12 shows the pressure differences between the front and back of the jack roof. A strong airflow directly through the jack roof could be used to promote ventilation of the building by entraining air from the spaces below the jack roof (Figure 3-2A). If air is diverted down into the building, the ventilation principle would resemble that of a wind tower (Figure 3-2B). The cross-ventilation flow model (Equation 3-3) would clearly have limitations if applied to either of these two flow configurations. Nevertheless, an important performance characteristic of the jack roof design can be identified, as the results of Figure 3-12 are very insensitive to building spacing. This has important implications for use of the jack roof design in urban environments where buildings are often located quite close to each other. If an adequate ventilation airflow can be achieved for this configuration, the jack roof may be quite consistent in its ability to provide ventilation over a wide range of building spacings.

CONCLUSIONS

Wind tunnel measurements have been made of the wind pressure distributions over an attached two-story shop or housing unit contained in long building rows for a range of wind directions, building spacings, and building geometries. Simplified correlations have been developed, which quite accurately predict the average pressure coefficients for the configurations tested. The results have been analyzed to assess the nature of wind pressure effects caused by surrounding building rows of the same size. The jack roof along with the choice of inlet and outlet locations have been discussed in an effort to identify promising naturally ventilated designs in closely spaced buildings typical of urban environments. The major conclusions are as follows:

1. The jack roof has the potential to be an effective ventilation design for urban settings.
2. Compared to standard cross-ventilation designs, the jack roof demonstrates improved ventilation potential at the small building spacings typically found in urban areas.
3. At small building spacings ($S \leq 1$), cross-ventilation designs showed no potential for providing airflow through the building.
4. Since the jack roof element is located at the top of the building, it is more consistently exposed to stronger wind conditions for the building configurations tested. As a result, the performance of the jack roof is less dependent on variations in building spacing.
5. Strong negative pressures were consistently obtained on the back of the jack roof, making it a good choice for a ventilation flow outlet.
6. The results indicate that to achieve optimal performance of a ventilation design incorporating a jack roof, different operating modes may be necessary. In other words, the best choices of flow inlets and outlets may be dependent on building spacing and wind direction.
7. The entire courtyard area was found to consistently fall within the wake flow region of the upwind building row. This was because the largest courtyard spacing tested was $S_c = 1$.
8. Pressure coefficients on all leeward surfaces and the courtyard were found to be practically independent of upwind row spacing and dependent only on wind direction.

Future related work is needed to address the following important areas:

1. Development of algorithms to predict internal ventilation airflow for configurations using roof-level inlets and outlets.
2. Investigations of the effect of internal partitions and obstructions on internal airflows, and incorporation of these results into airflow prediction algorithms.
3. Measurement of building surface pressure distributions for other important building configurations for natural ventilation design.
4. Determination of microclimatic effects on ambient wind conditions.
5. Development of design methods, tools, and guidelines for natural ventilation design.

REFERENCES

1. Mattingly, G.E., and Peters, E.F., "Wind and Trees: Air Infiltration Effects on Energy in Houses," *Journal of Industrial Aerodynamics,* Vol. 2, No. 1., 1977.
2. Mattingly, G.E., Harrje, D.T., and Heisler, G.M., "The Effectiveness of an Evergreen Windbreak for Reducing Residential Energy Consumption," *ASHRAE Transactions,* Vol 85, Part 2., 1979.
3. Peterka, J., and Cermak, J., "Turbulence in Building Wakes." *Proceedings: 4th International Conference on Wind Effects on Building and Structures,* London, Cambridge University Press, September 1975.
4. Peterka, J.A., Zambrano, T.G., and Cermak, J.E., "Effect of an Adjacent Building on Wind Pressures," *ASCE Annual Convention and Exposition Proceedings,* Atlanta, GA, 1979.
5. Aynsley, R.M., "Wind Generated Natural Ventilation of Housing for Thermal Comfort in Hot Humid Climates," *Fifth International Wind Engineering Conference Proceedings,* Pergamon Press, 1979.
6. Holmes, J.D., *Wind Loads on Low Rise Buildings - A Review,* Commonwealth Scientific and Industrial Research Organization, Division of Building Research, Victoria, Australia, 1983.

7. Soliman, B.F., "The Effect of Building Grouping on Wind Induced Natural Ventilation," University of Sheffield, Department of Building Science, Report BS 14, 1973.

8. Lee, B.E., Hussain, M., and Soliman, B.F., "A Method for the Assessment of the Wind Induced Natural Ventilation Forces Acting on Low Rise Building Arrays," Department of Building Science, University of Sheffield, Report No. BS50, 1979.

9. Hussain, M., and Lee, B.E., "A Wind Tunnel Study of the Mean Pressure Forces Acting on Large Groups of Low-Rise Buildings," *Journal of Wind Engineering and Industrial Aerodynamics,* Vol. 6, pp. 207-225, 1980.

10. Wiren, B.D., "Effects of Surrounding Buildings on Wind Pressure Distribution and Ventilation Heat Losses for Single-Family Houses, Part 1: 1 1/2-Storey Detached Houses," The National Swedish Institute for Building Research, Gævle, Sweden, Report No. M85:19, 1985.

11. Wiren, B.D., "Effects of Surrounding Buildings on Wind Pressure Distribution and Ventilation Heat Losses for Single-Family Houses, Part 2: 2-Storey Terrace Houses." The National Swedish Institute for Building Research, Gævle, Sweden, March 1987.

12. Aynsley, R.M., "Natural Ventilation Model Studies," International Workshop on Wind Tunnel Modeling Criteria and Techniques for Civil Engineering Applications Preprints, Timothy A. Reinhold, ed., pp. V.1-1 - V.1-22, April 14-16, 1982.

13. Vickery, B.J., "The Use of the Wind Tunnel in the Analysis of Naturally Ventilated Structures," *AS/ISES International Passive/Hybrid Cooling Conference Proceedings,* Miami Beach, FL, pp. 728-742, November 1981.

14. Vickery, B.J., Baddour, R.E., and Karakatsanis, C.A., "A Study of the External Wind Pressure Distributions and Induced Internal Ventilation Flow in Low-Rise Industrial and Domestic Structures," Boundary Layer Wind Tunnel Laboratory, University of Western Ontario, Canada, Report No. BLWT-SS2-1983, 1983.

15. Swami, M.V., and Chandra, S., "Procedure for Calculating Natural Ventilation Airflow Rates in Buildings," ASHRAE, Final Report, FSEC-CR-163- 86, 1987.

16. Chandra, S., "A Design Procedure to Size Windows for Naturally Ventilated Rooms," *ASES Passive Solar Conference Proceedings,* Glorieta, NM, September 1983.

17. Arens, E.A., and Watanabe, N., "A Method for Designing Naturally Cooled Buildings Using Bin Climate Data," *ASHRAE Transactions,* Vol. 92, Pt. 2, 1986.

18. Clarke, J.A., *Energy Simulation in Building Design,* U.K.: Adam Hilger Ltd, 1986.

19. Sherman, M.H., and Grimsrud, D.T., "Wind and Infiltration Interaction for Small Buildings," *Annual Meeting of the American Society of Civil Engineers Proceedings,* New Orleans, LA, October 23-29, 1982.

20. Wannenburg, J.J., "Performance Testing of Roof Ventilators," *Heating, Piping & Air Conditioning (ASHRAE Journal Section),* pp. 147-154, March 1957.

21. Bookhash, F.M., "Windtower Houses of Bastakeya in Dubai," *AS/ISES International Conference on Passive and Hybrid Cooling Proceedings,* Miami Beach, FL, pp. 75-79, 1981.

22. Fairey, P.W., and Bettencourt, W., "'La Sucka' - A Wind Driven Ventilation Augmentation and Control Device," *AS/ISES International Conference on Passive and Hybrid Cooling Proceedings,* Miami Beach, FL, pp. 196-200, 1981.

23. Cermak, J.E., Peterka, J.A., Ayad, S.S., and Poreh, M., *Passive and Hybrid Cooling Developments: Natural Ventilation - A Wind Tunnel Study,* Fluid Dynamics and Diffusion Laboratory, DOE Contract No. DE-AC03-80CS11510, Colorado State University, Fort Collins, CO, 1981.

24. Cook, N.J., "Simulation Techniques for Short Test-Section Wind Tunnels: Roughness, Barrier and Mixing-Device Methods," International Workshop on Wind Tunnel Modeling Criteria and Techniques for Civil Engineering Applications Preprints, Timothy A. Reinhold, ed., pp. II.3-1 - II.3-12, April 14-16, 1982.

25. Engineering Sciences Data Unit, *Strong Winds in the Atmospheric Boundary Layer,* Item No. 82026, ESDU, London, 1982.

26. Engineering Sciences Data Unit, *Characteristics of Atmospheric Turbulence Near the Ground,* Item Nos. 74030, 75001, and 85020, ESDU, London, 1974, 1975, and 1985.

27. Engineering Sciences Data Unit, *Longitudinal Turbulence Intensities Over Terrain with Roughness Changes for Flat or Hilly Sites,* Item No. 84030, ESDU, London, 1984.

28. Cook, N.J., "Determination of the Model Scale Factor in Wind Tunnel Simulations of the Adiabatic Atmospheric Boundary Layer," *Journal of Industrial Aerodynamics,* Vol. 2, pp. 311-321, 1978.

29. Aynsley, R.M., "Modeling Parameters for Boundary Layer Wind Tunnel Studies of Natural Ventilation," *ASHRAE Transactions,* Vol. 91, Part 2A, 1985.

30. Bauman, F., Ernest, D., and Arens, E., *ASEAN Natural Ventilation Study: Wind Pressure Distributions on Long Building Rows in Urban Surroundings,* Center For Environmental Design Research, University of California, Berkeley, CA, 1988.

ACKNOWLEDGMENTS

The authors wish to thank Mark Levine and Hashem Akbari of Lawrence Berkeley Laboratory for their financial support and technical assistance with this research. We also wish to acknowledge Davide Garda of the UC Berkeley Architecture Department for his help with preparation of model construction drawings and figures for the final report. The IBM personal computer equipment used for data acquisition and analysis throughout this study was provided through an IBM DACE Grant.

Figure 3-1A.
Shophouse Test Model

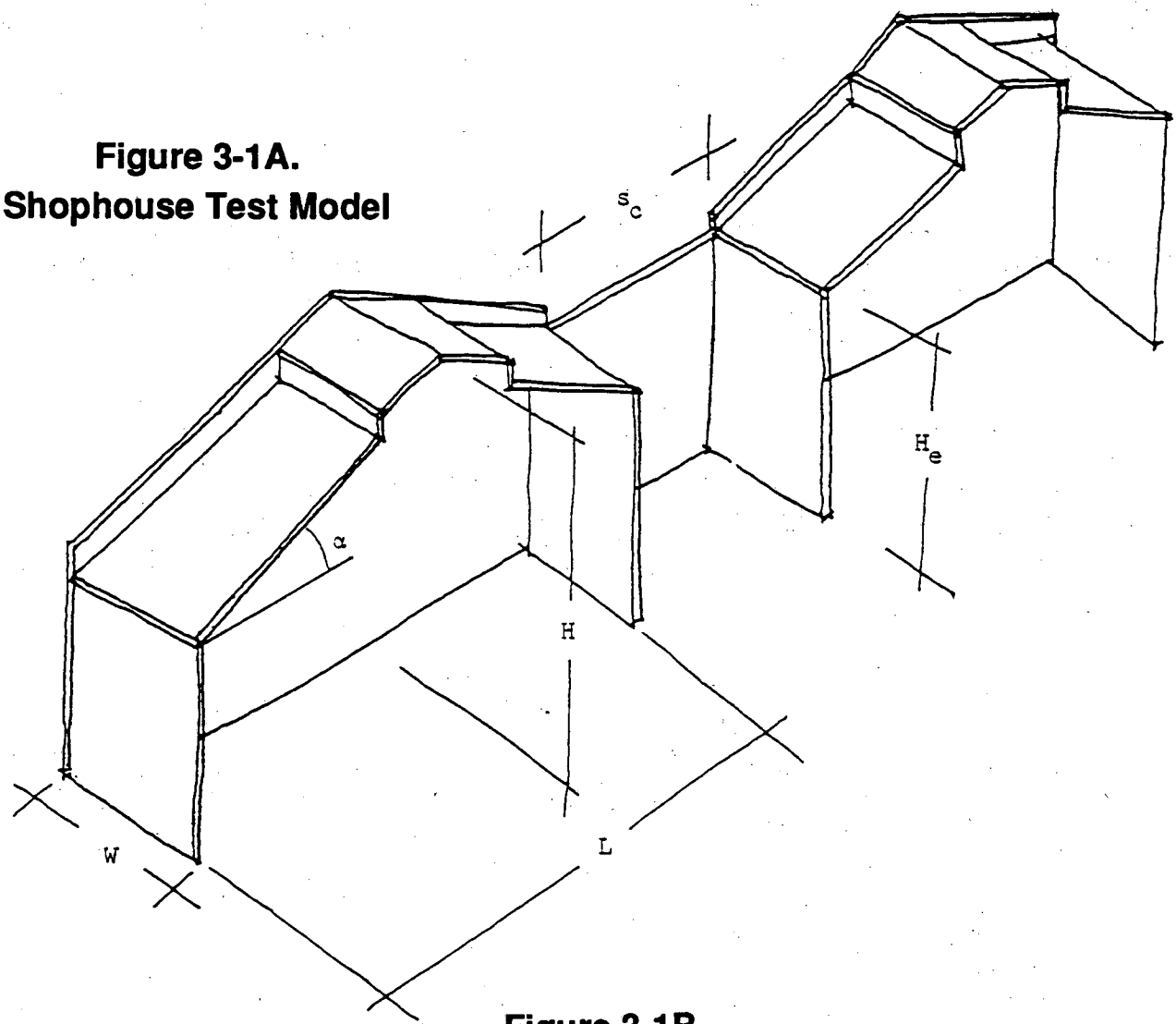

Figure 3-1B.
Test Unit in Row

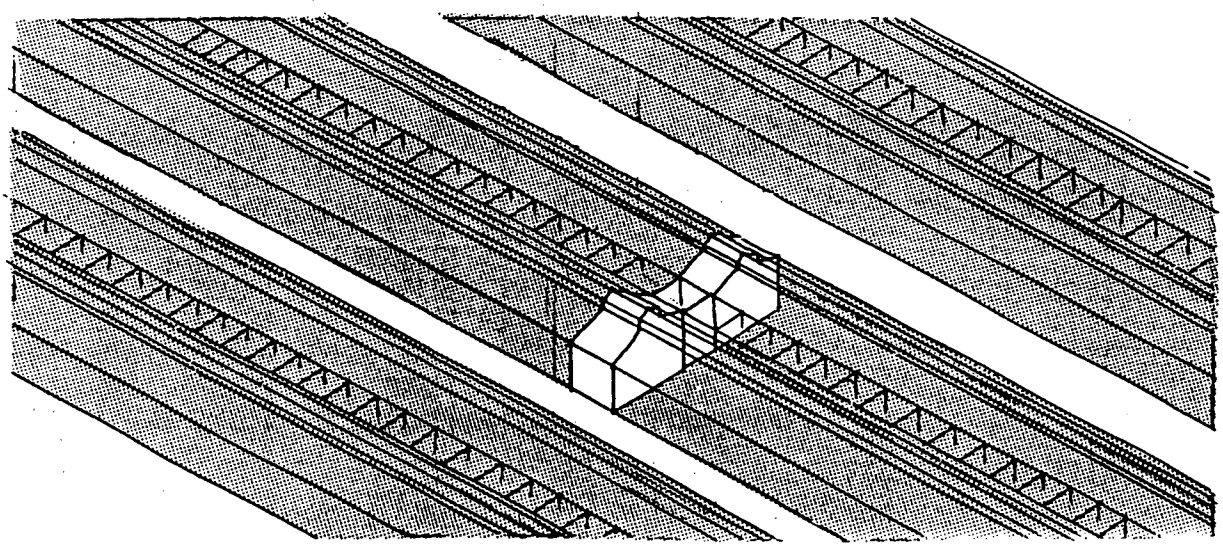

Figure 3-2.
Jack Roof Flow Configurations

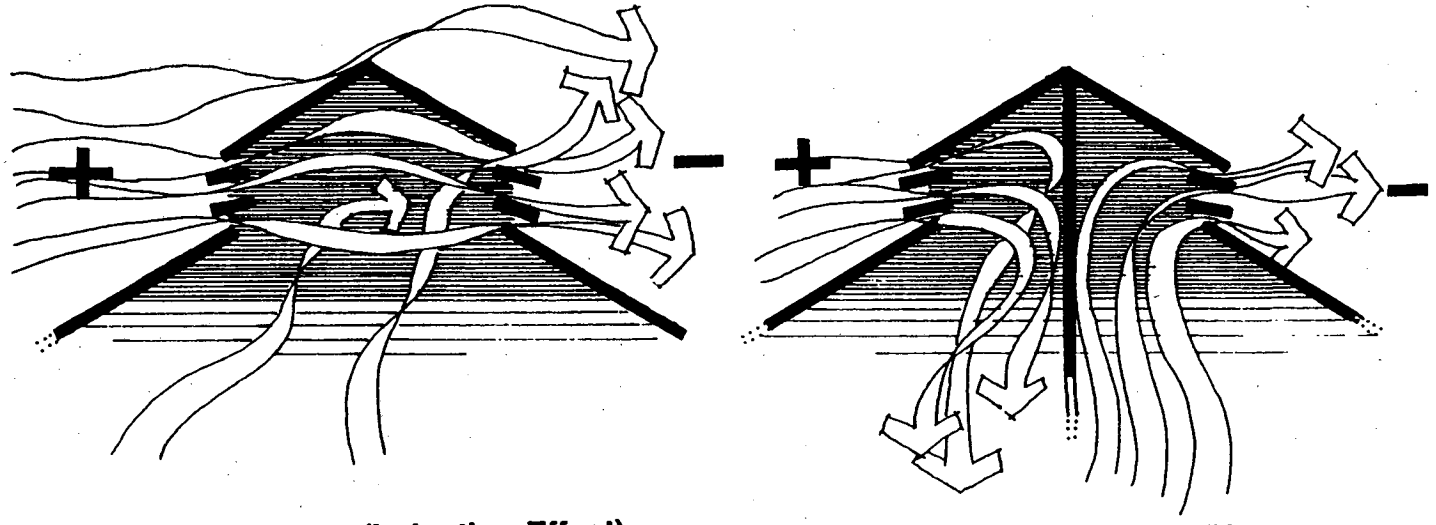

A) Through-Flow (Induction Effect)

B) Diverted Through-Flow

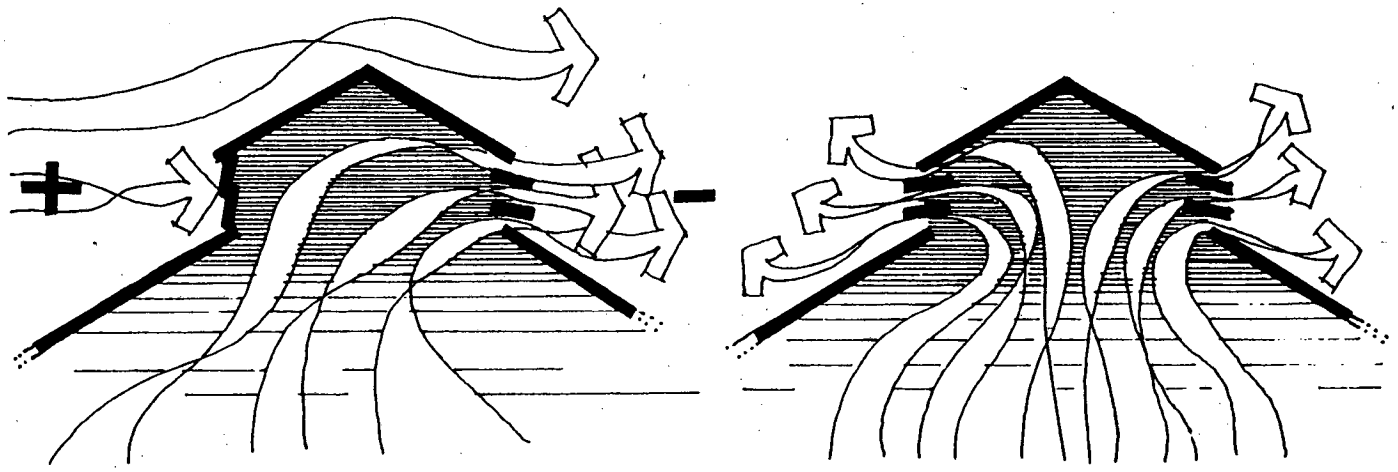

C) Suction Effect

D) Stack Effect

Figure 3-3.
Boundary Layer Wind Tunnel Configuration

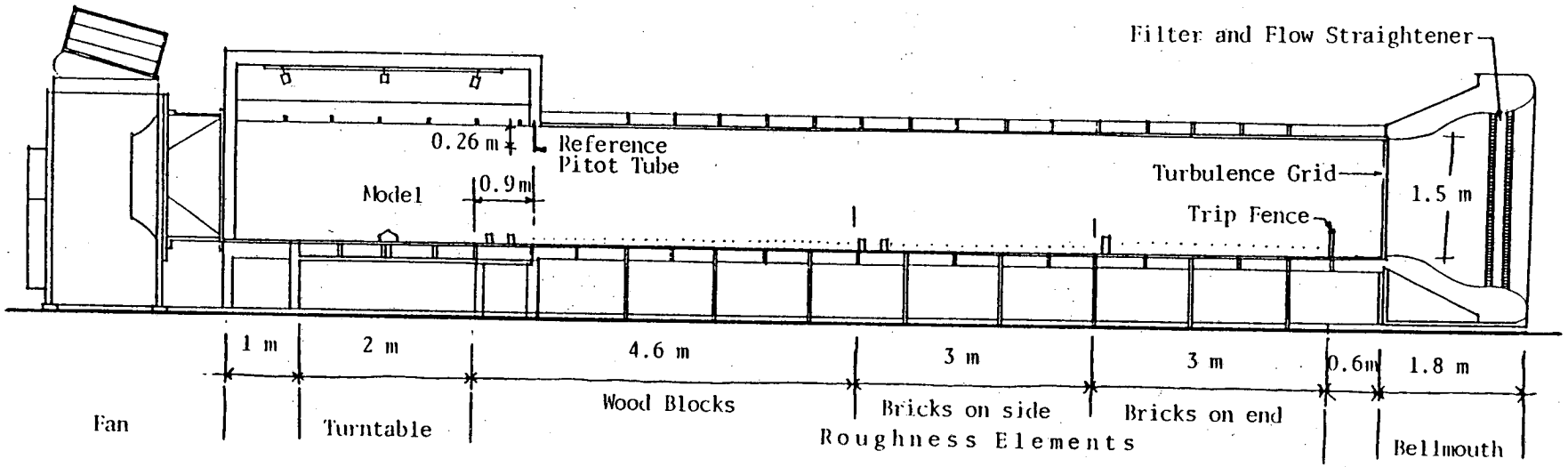

Figure 3-4A.
Wind Tunnel Boundary Layer Profile: Mean Velocity Profile

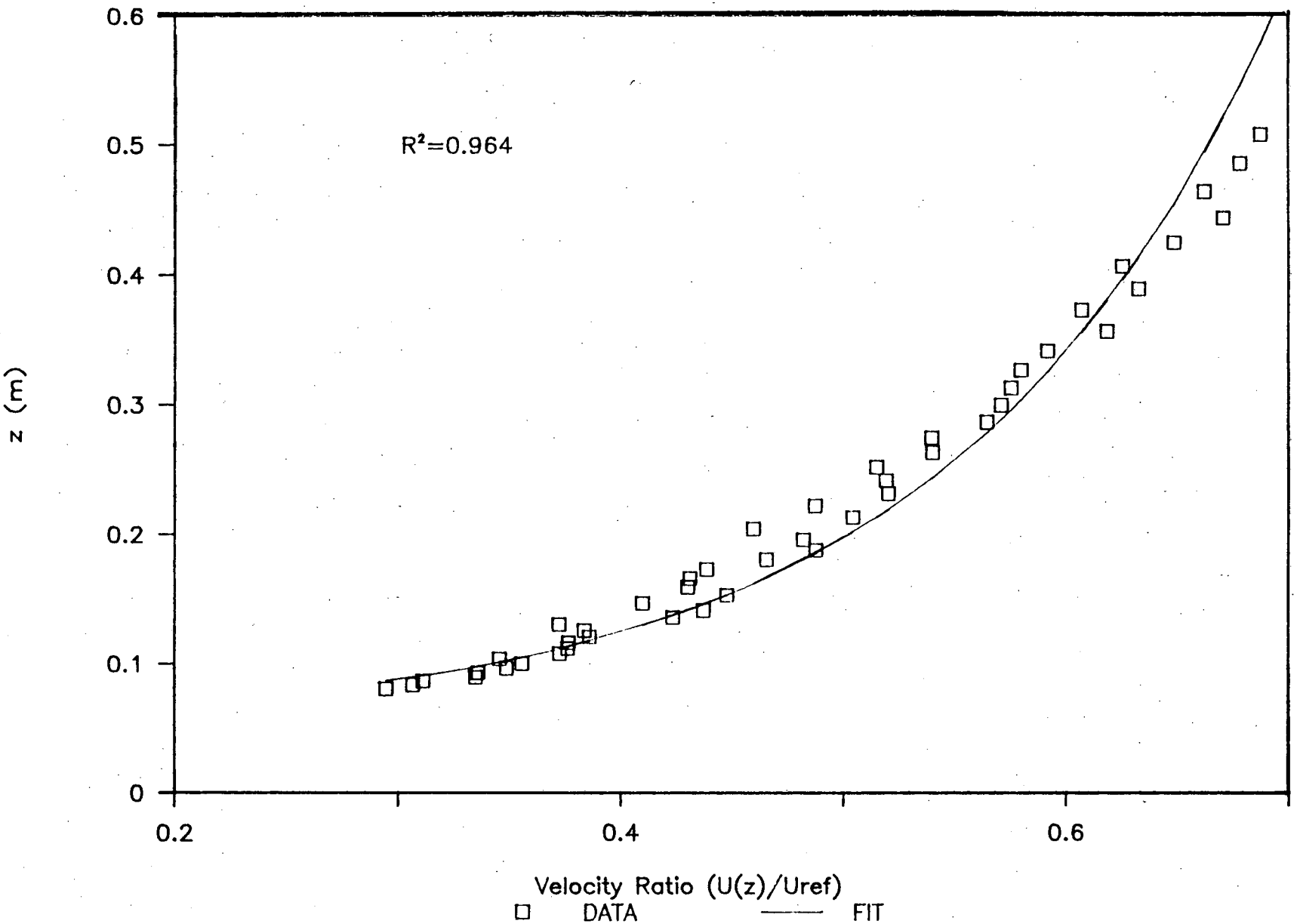

Figure 3-4B.
Wind Tunnel Boundary Layer Profile: Turbulence Intensity Profile

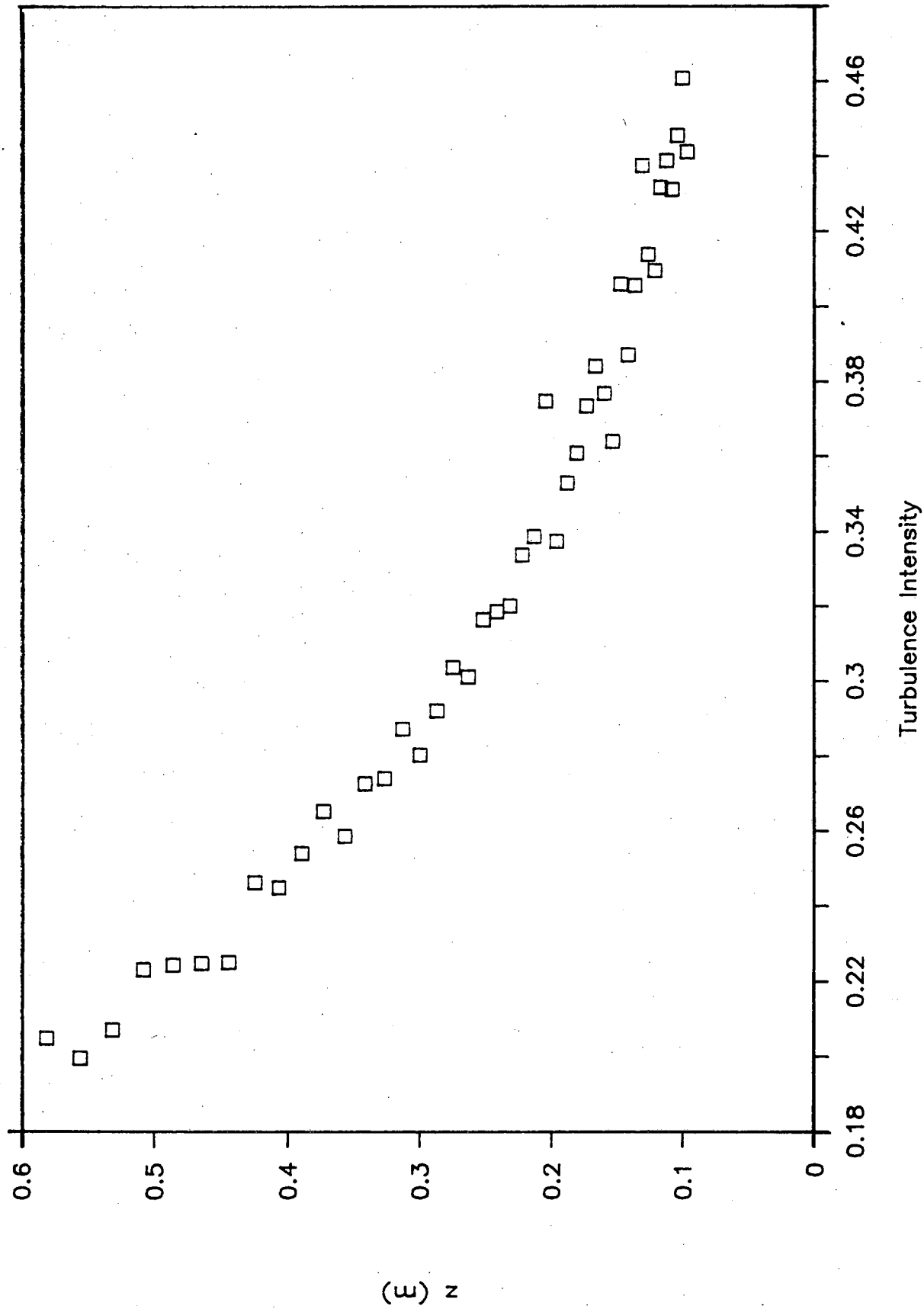

Figure 3-5A.
Tap Locations for Model #1 (dimensions in mm)

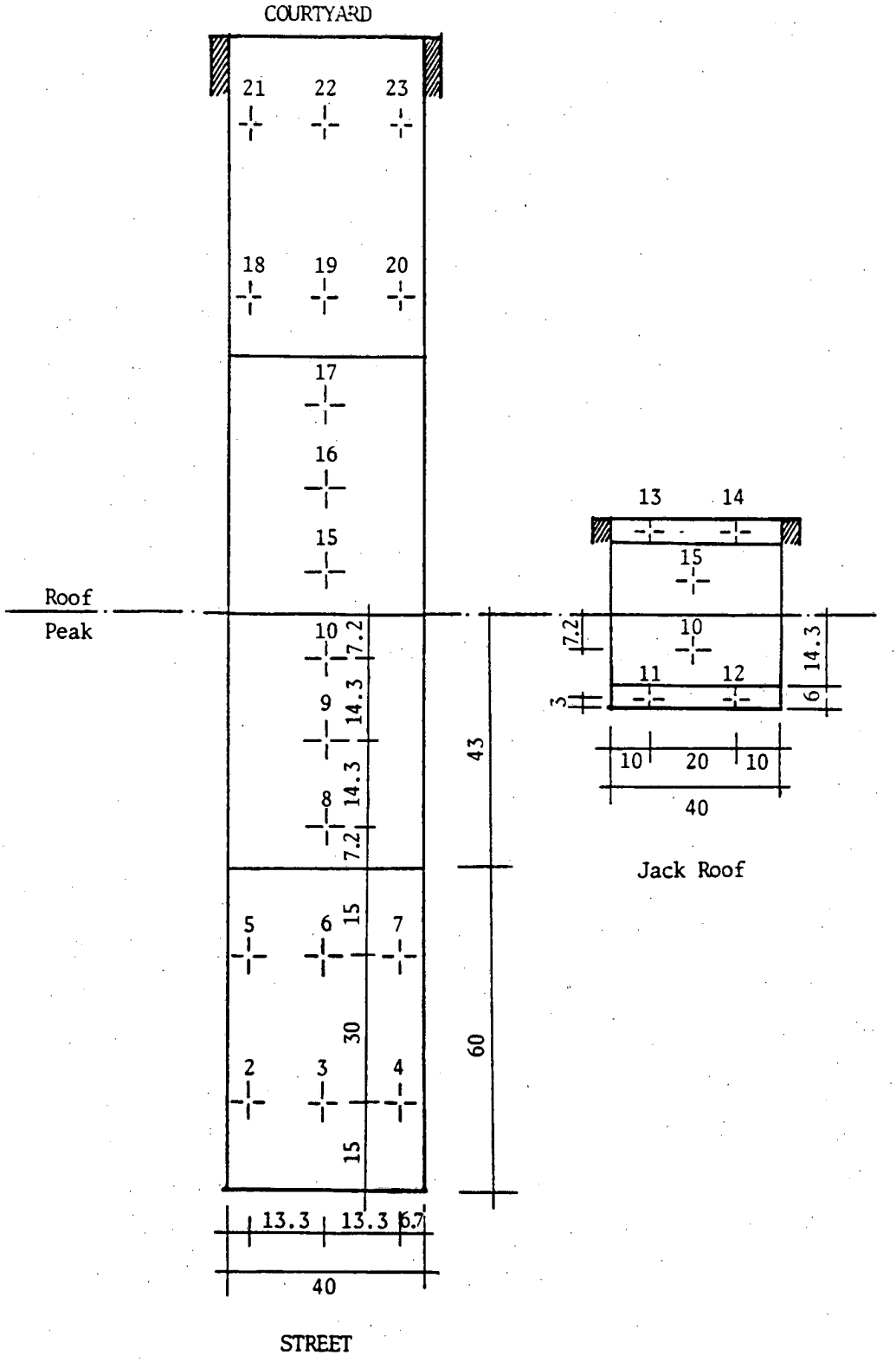

Figure 3-5B.
Tap Locations for Model #2 (dimensions in mm)

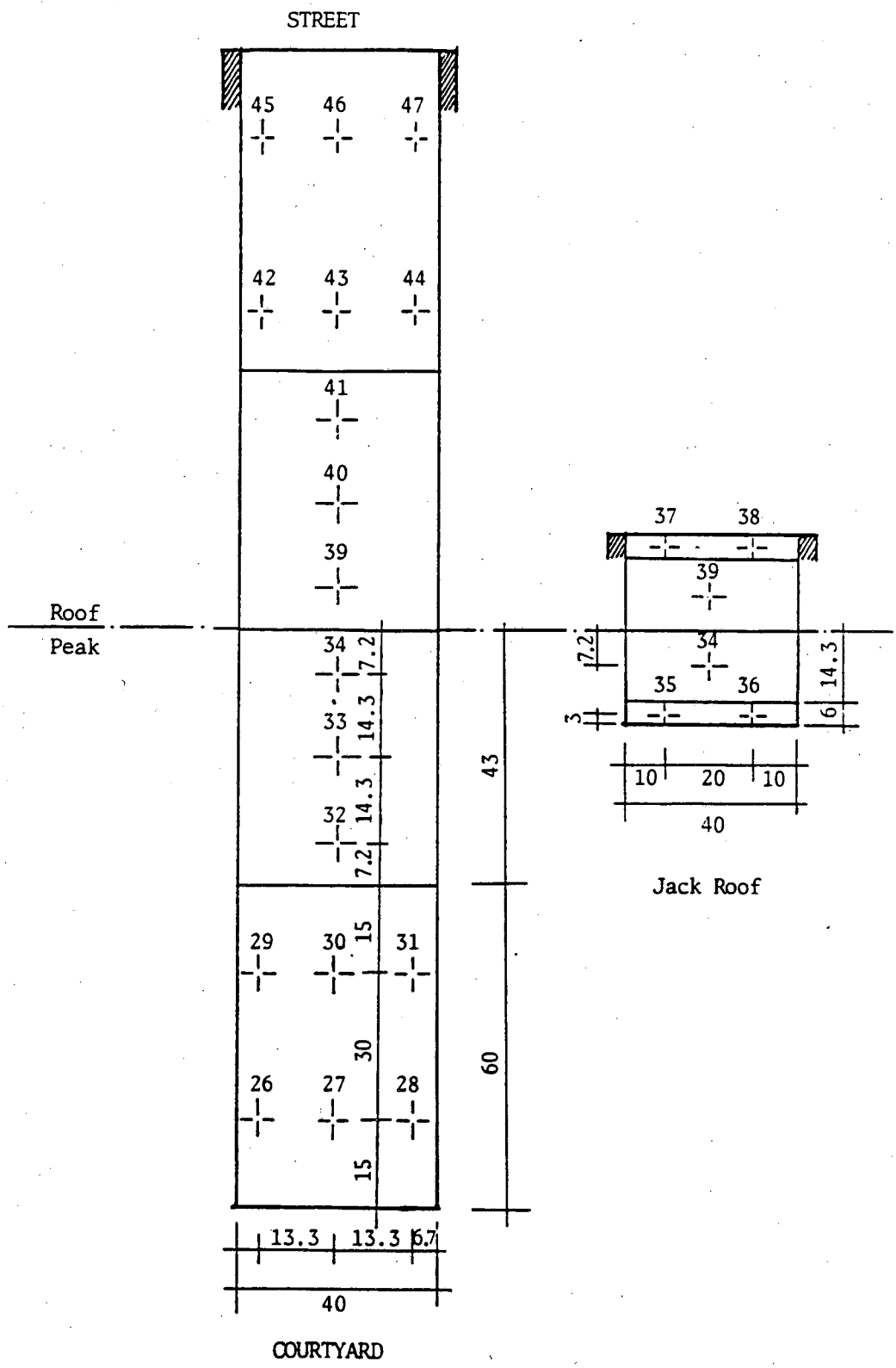

Figure 3-6A.
Model Spacing Configuration and Wind Direction

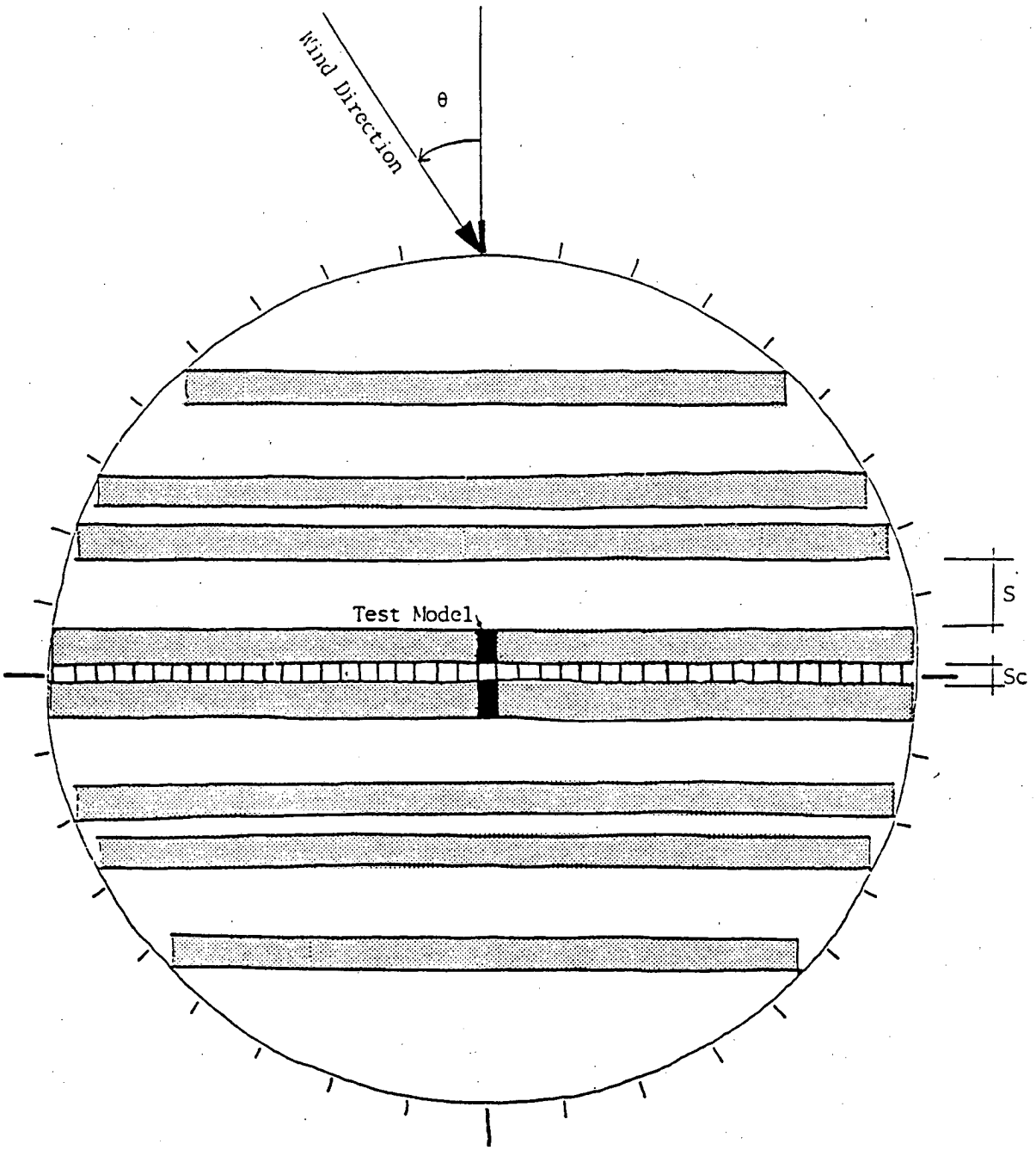

Figure 3-6B.
Roof Configurations

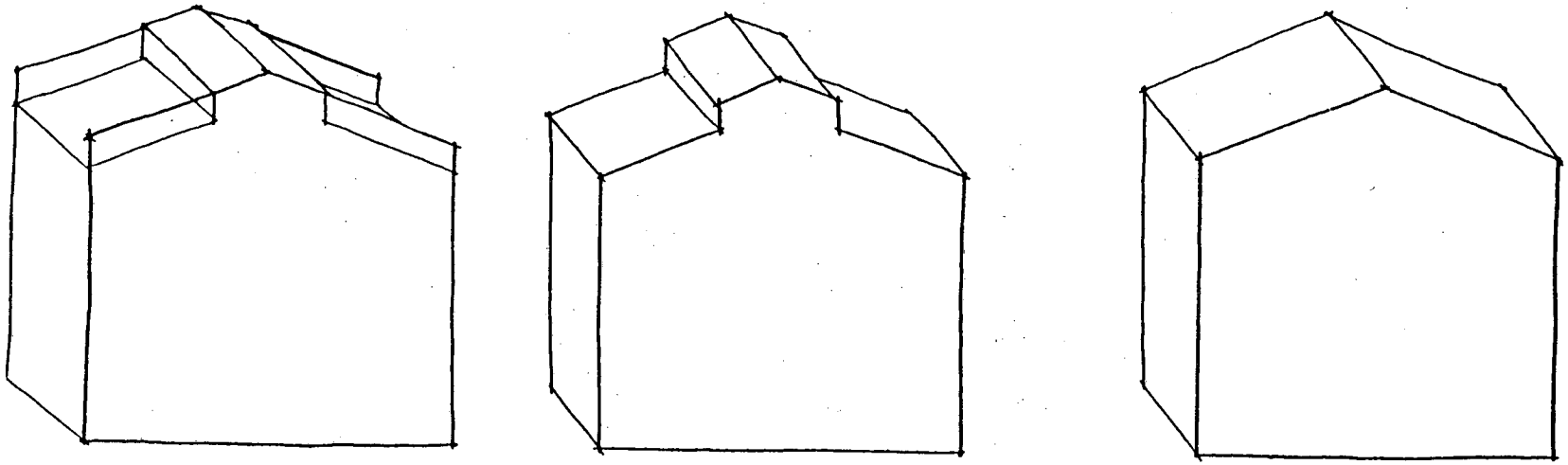

A) With Jack Roof and Parapets B) With Jack Roof, Without Parapets C) Without Jack Roof, Without Parapets

Figure 3-6C.
Courtyard Configurations

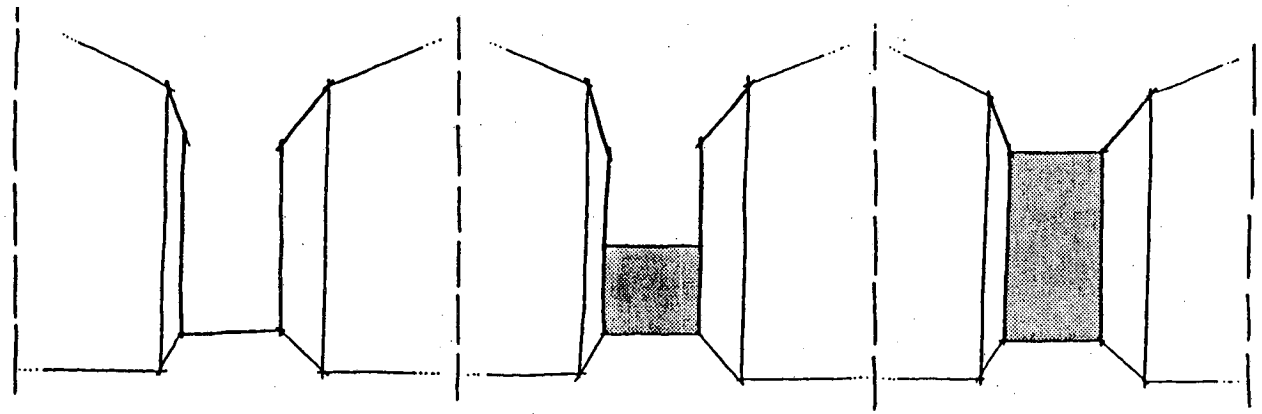

A) No Wall ($H_c = 0$) B) Half Height Wall ($H_c = 0.5$) C) Full Height Wall ($H_c = 1$)

Figure 3-7A.
Mean Pressure Distributions: Front of Model #1, J,P for S = 2

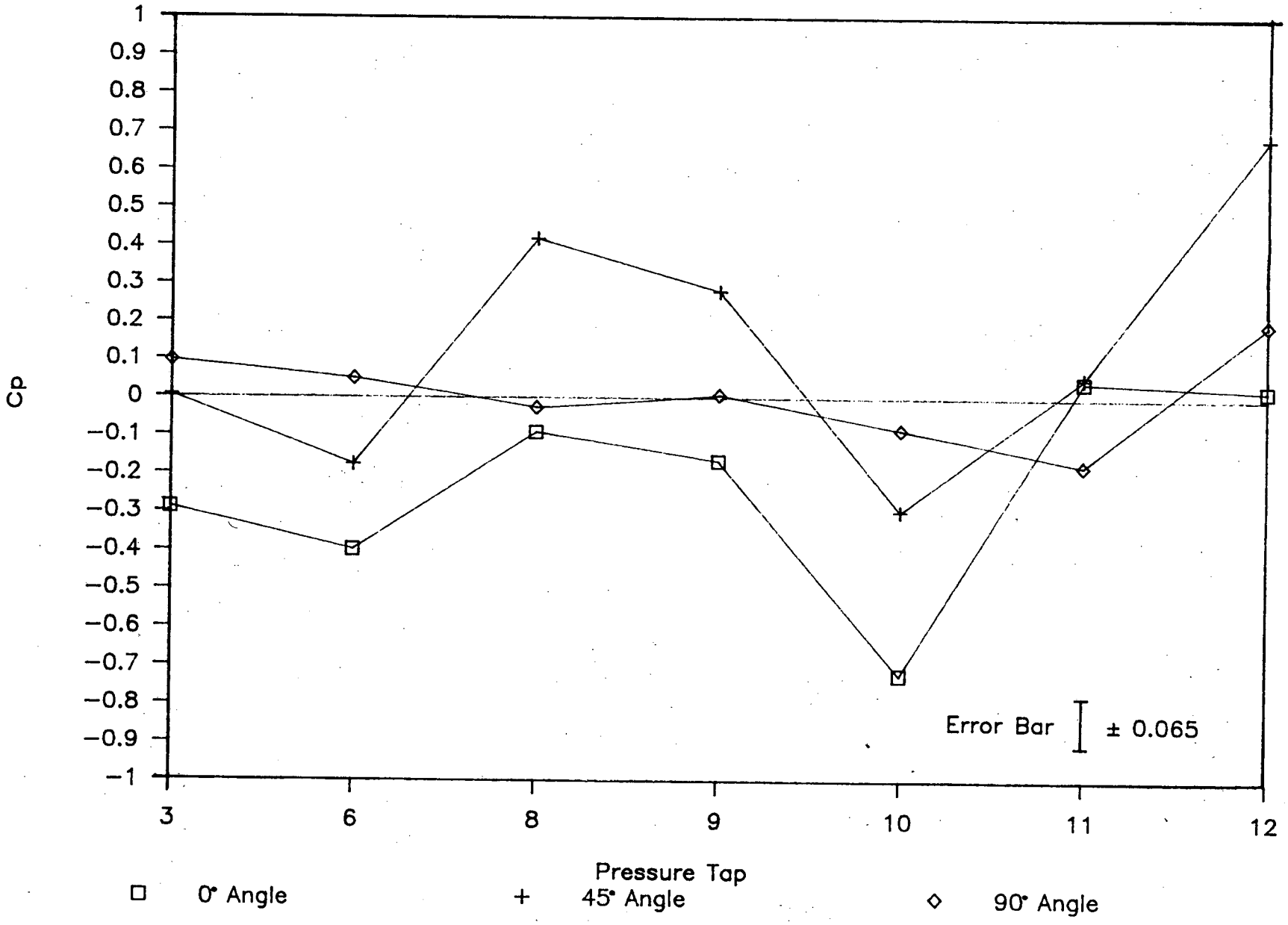

Figure 3-7B.
Mean Pressure Distributions: Back of Model #1, J,P for S = 2

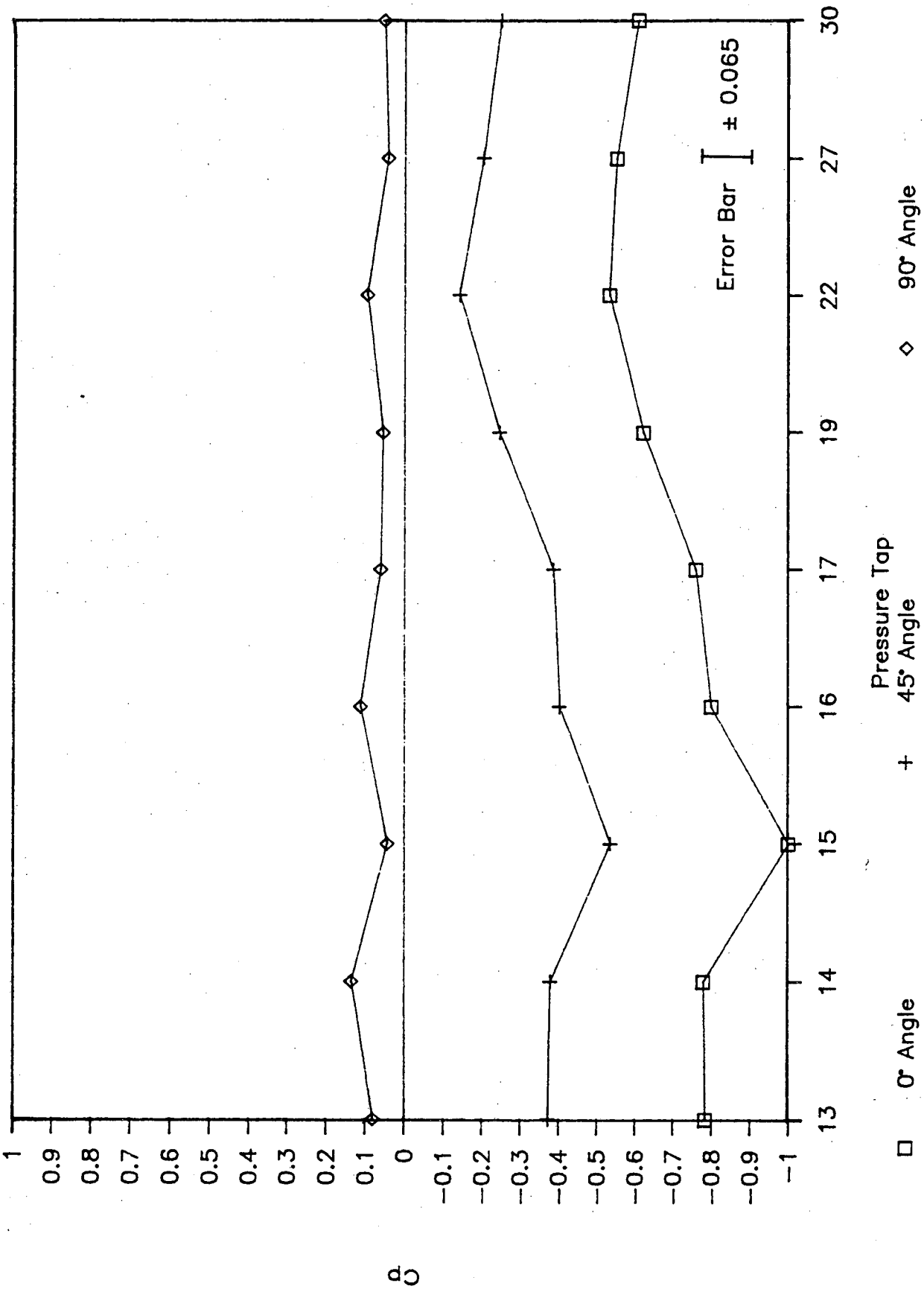

Figure 3-8A.
Measurements vs. Predictions: Front Facade Average, #1, J,NP

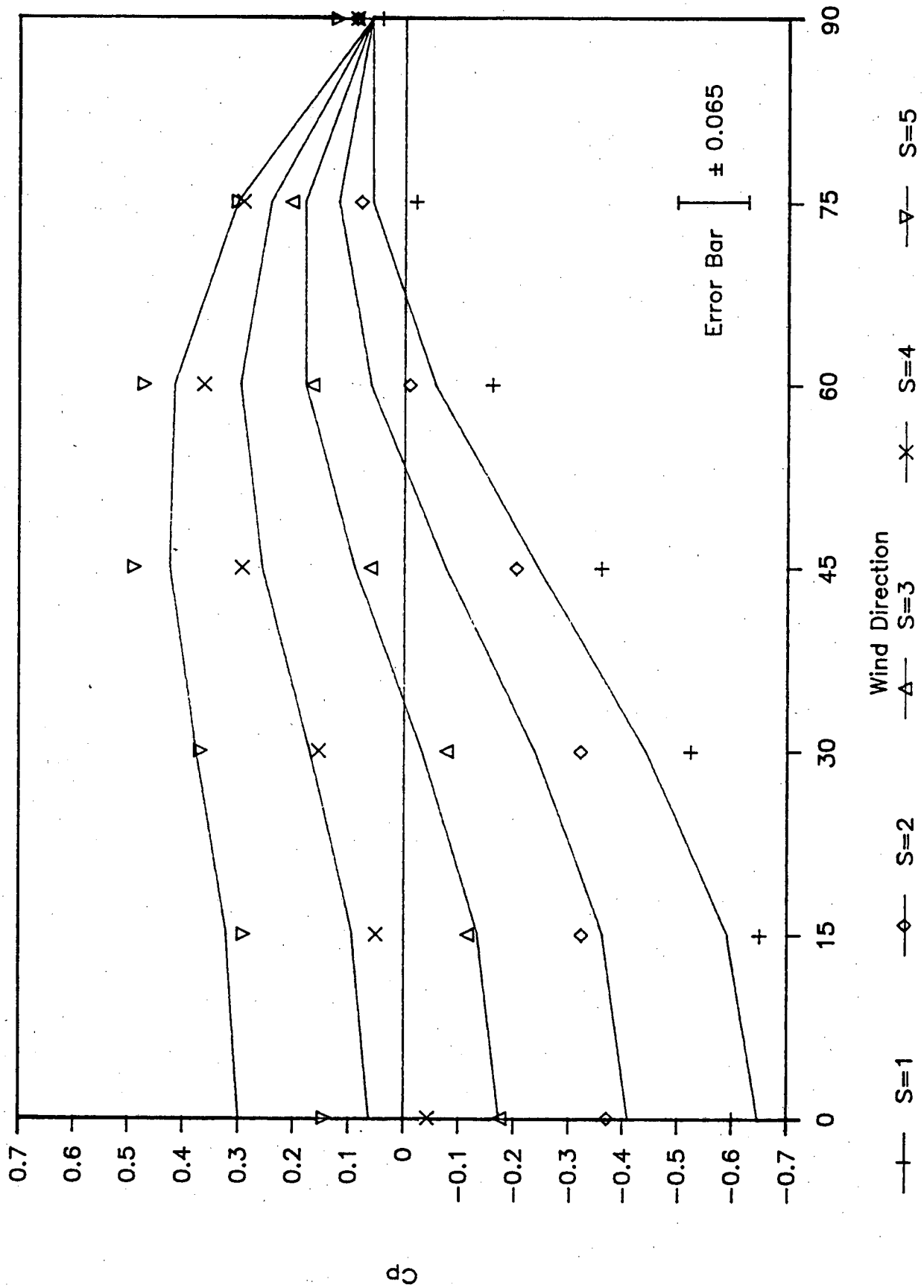

Figure 3-8B.
Measurements vs. Predictions: Front Jack Roof Average, #1, J,NP

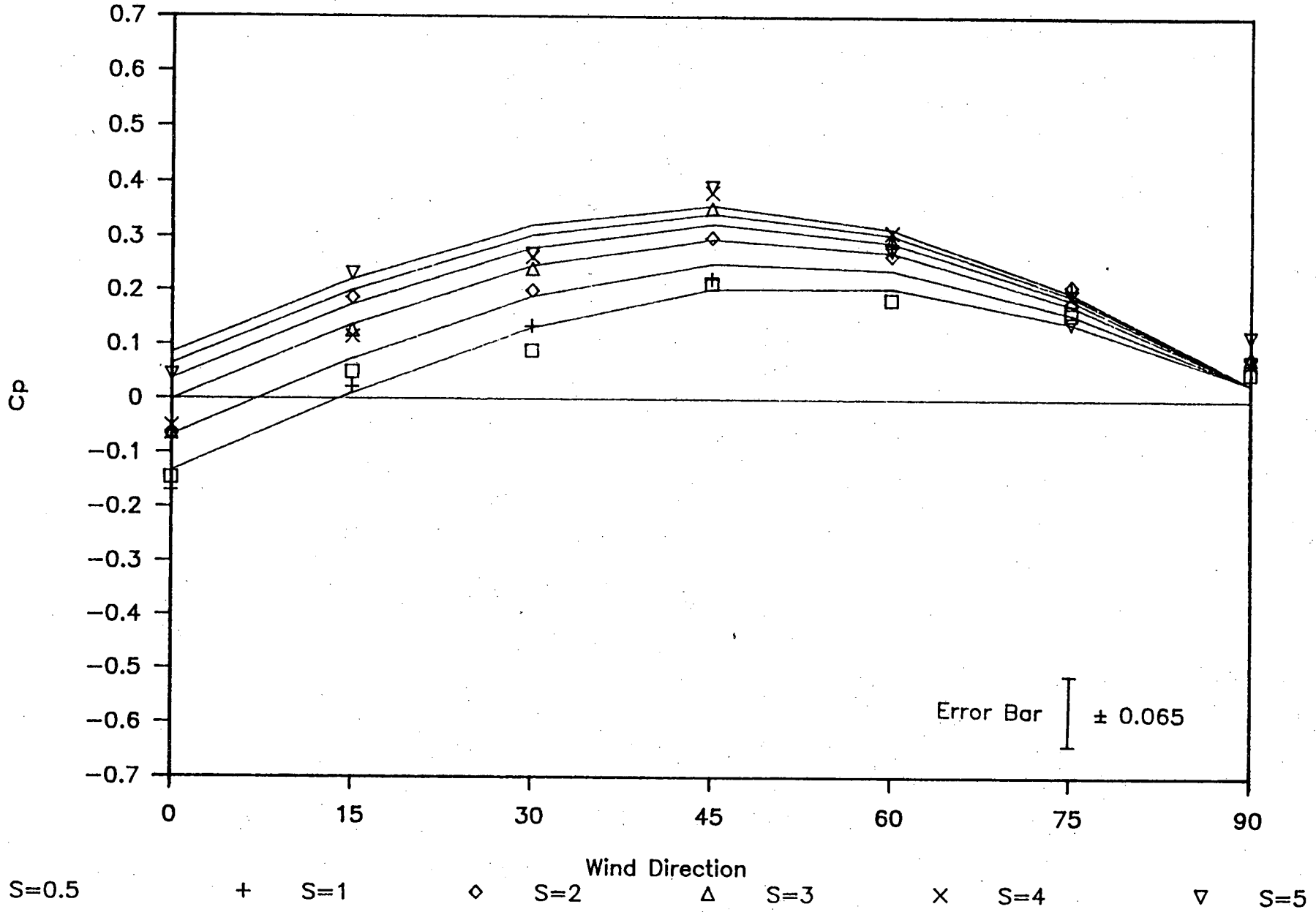

Figure 3-9.
Mean Pressure Differences: Front Facade to Back Facade, #1, NJ,NP

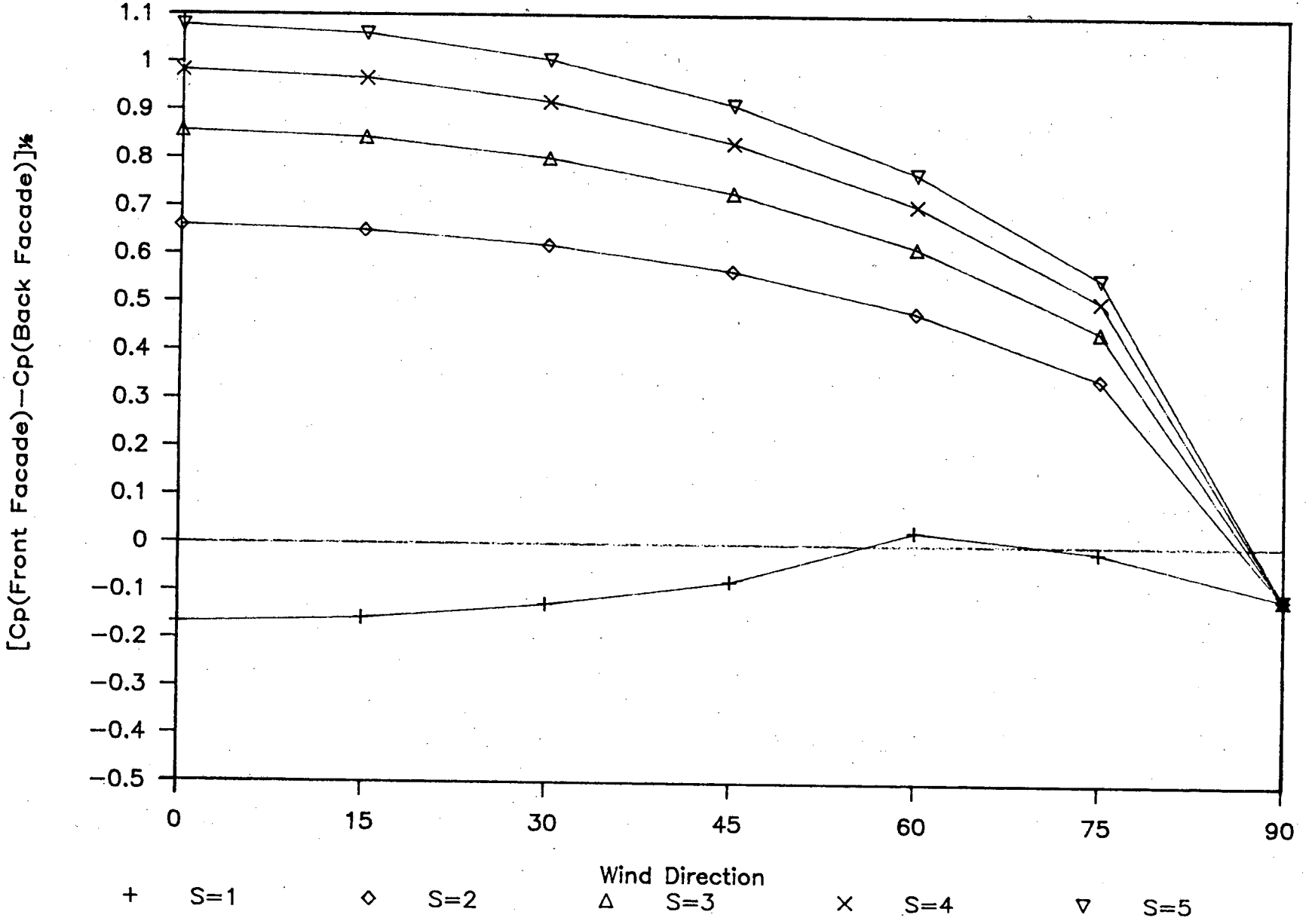

Figure 3-10A.

Mean Pressure Differences: Front Facade to Back Jack Roof, #1, J

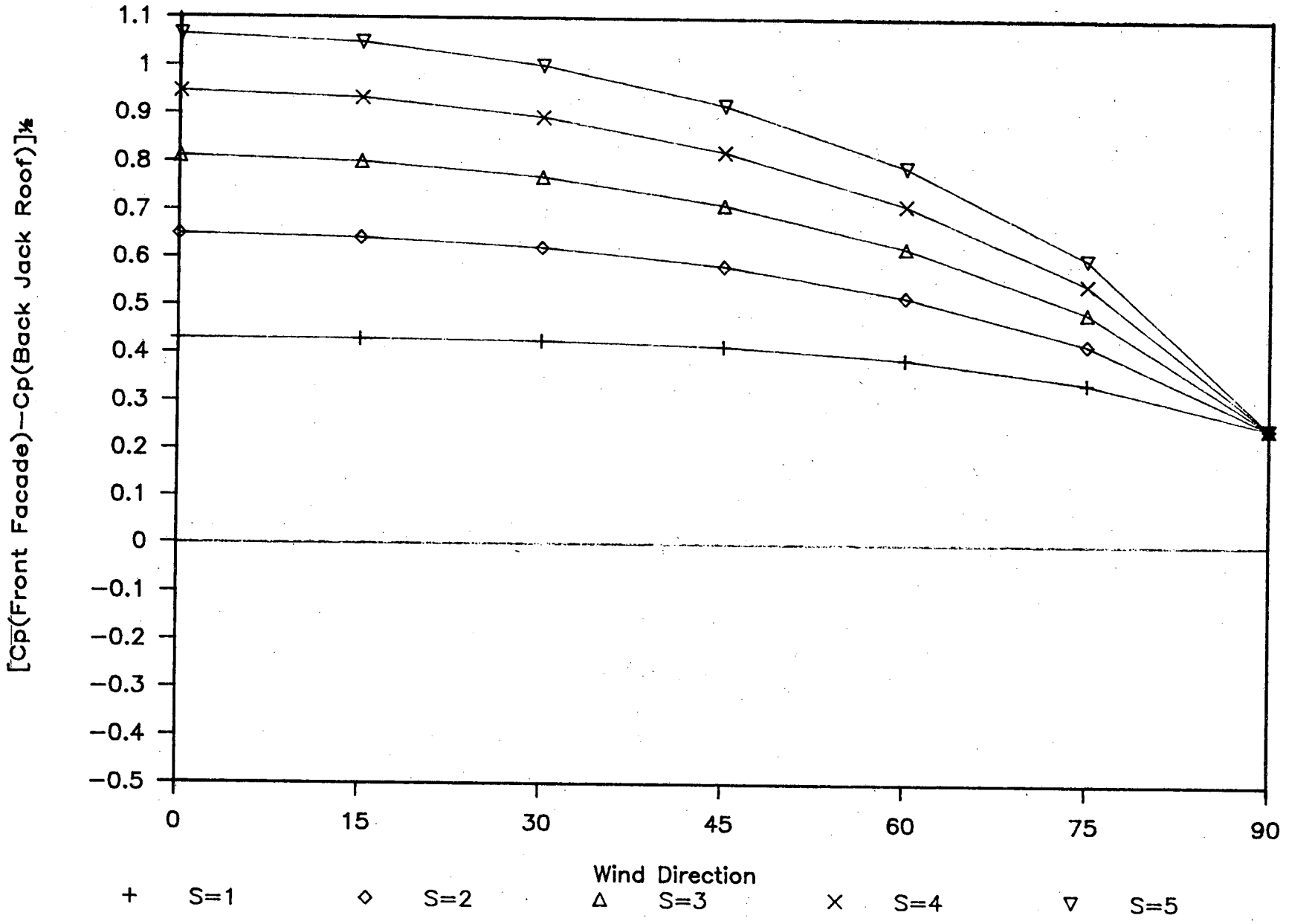

Figure 3-10B.
Mean Pressure Differences: Back Facade to Back Jack Roof, #1, J

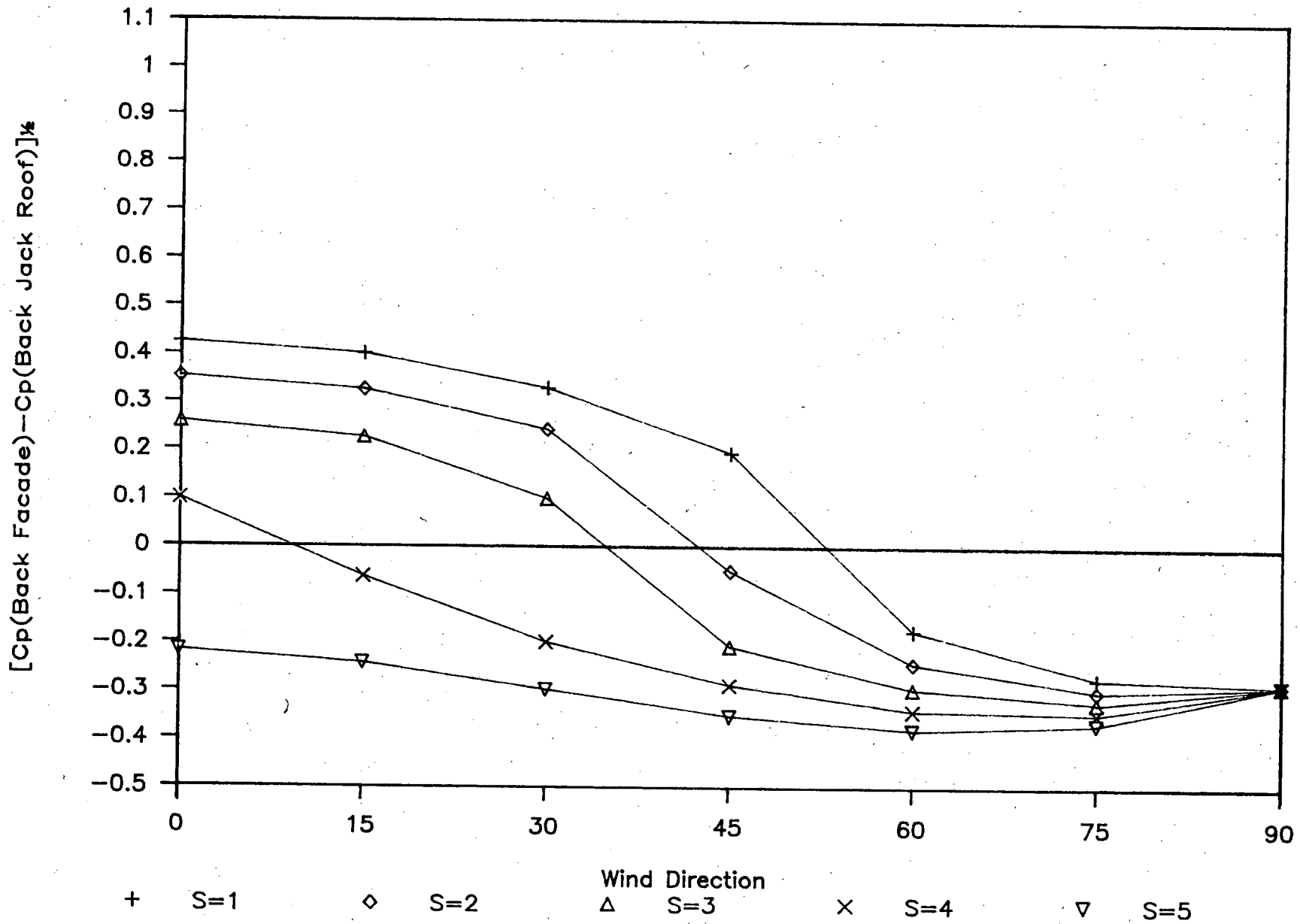

Figure 3-11A.

Mean Pressure Differences: Front Jack Roof to Back Facade, #1, J

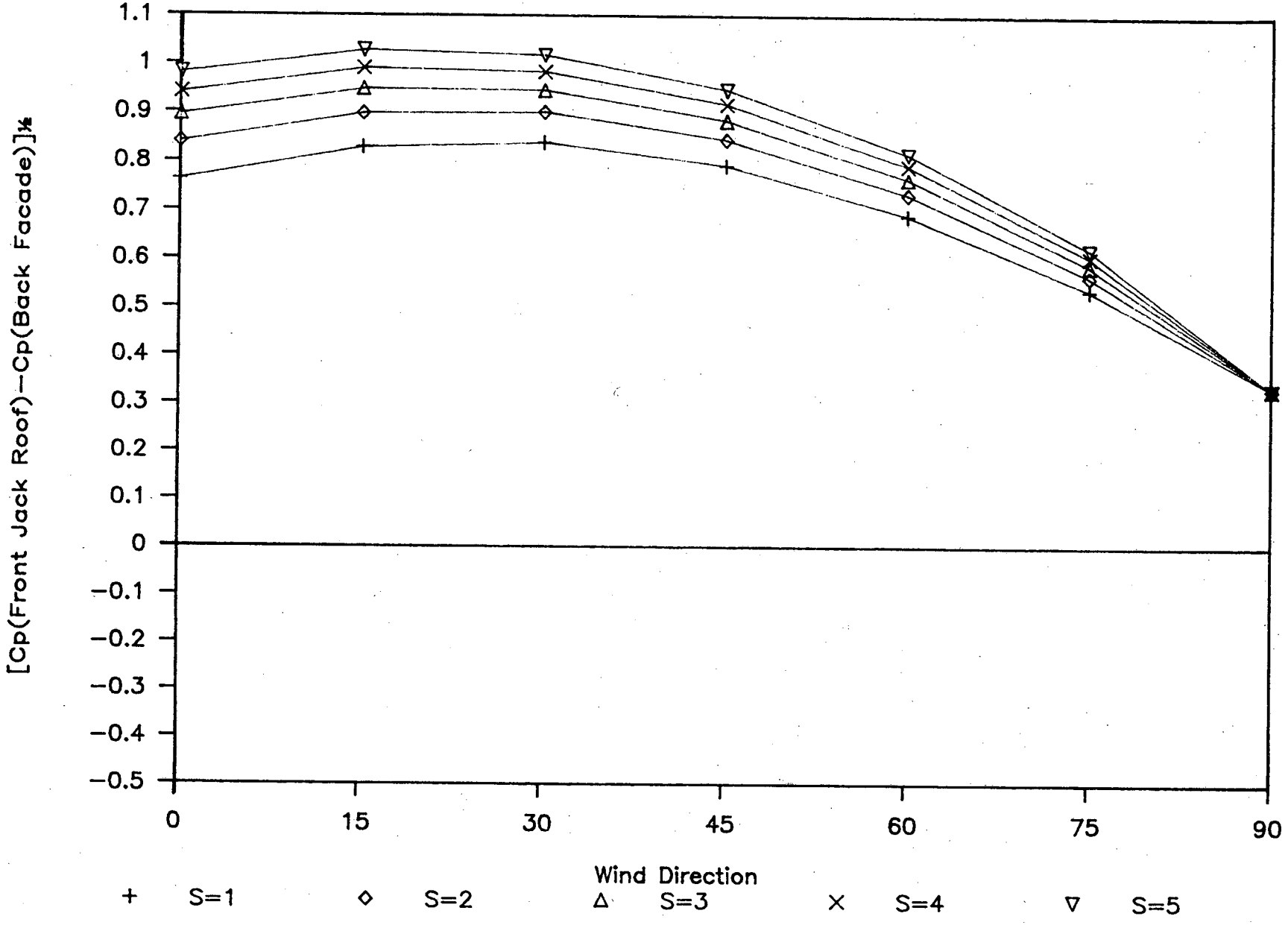

Figure 3-11B.
Mean Pressure Differences: Front Jack Roof to Front Facade, #1, J

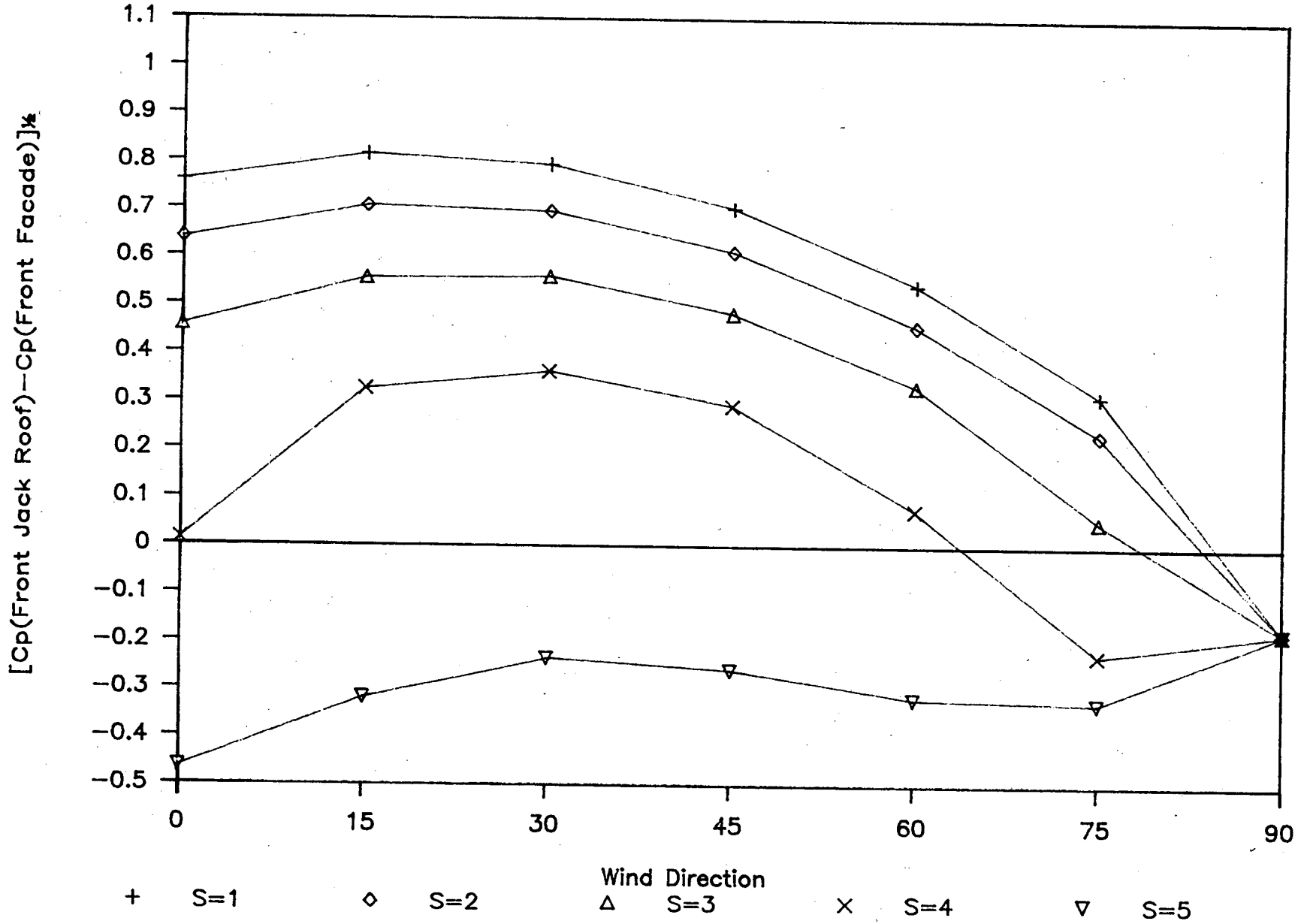

Figure 3-12.
Mean Pressure Differences: Front Jack Roof to Back Jack Roof, #1, J

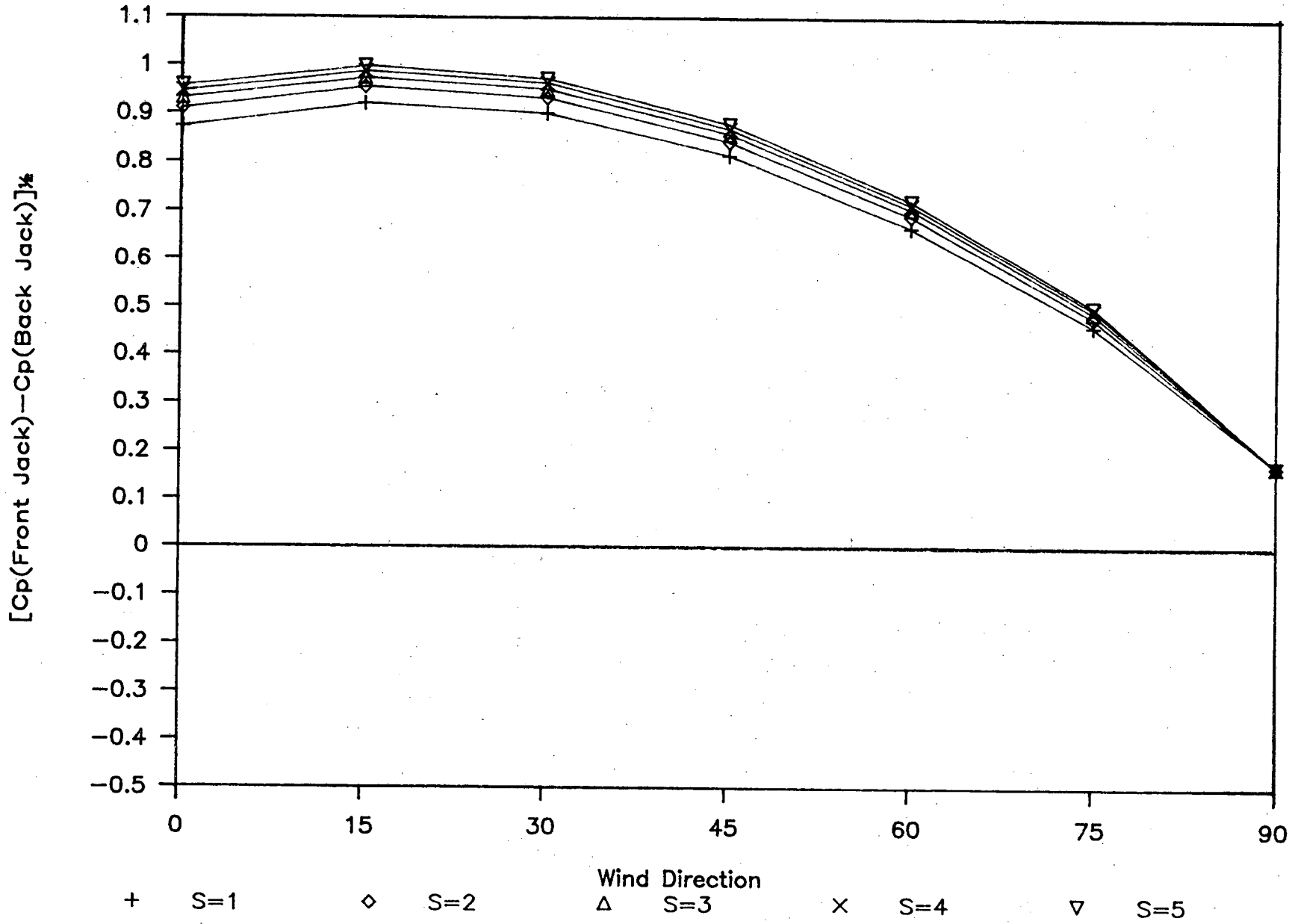

Table 3-1

Tap Locations for Average Pressure Measurements

Surface	Tap Locations Model #1	Model #2
Front Facade	3 + 6	27 + 30
Back Facade	19 + 22	43 + 46
Front Jack Roof	11 + 12	35 + 36
Back Jack Roof	13 + 14	37 + 38
Courtyard	19 + 22 + 27 + 30	

Table 3-2

Correlations For Average Surface Pressure Coefficients *

Correlation Equation: $C_p = C_o + \sum_{i=1}^{N} C_i.F_i$

A) Model Configuration: No Jack Roof and No Parapet (NJ,NP); $S_c = 0.5$; $H_c = 0$

Independent Variables (F_i)	Front Facade (C_i)	Courtyard (C_i)	Back Facade (C_i)
Constant	0.095	0.107	-
$Cos^2\Theta$	-0.519	-0.436	-0.602
$Cos\ \Theta * S$	-	-0.067	-
$Cos\ \Theta * ln(S)$	0.571	-	-
R^2 (ADJ)	0.980	0.982	0.990

B) Model Configuration: Jack Roof (J,NP) and (J,P); $S_c = 1$; $H_c = 1$

Independent Variables (F_i)	Front Facade (C_i)	Front Jack (C_i)	Back Jack (C_i)	Courtyard NP (C_i)	Courtyard P (C_i)	Back Facade (C_i)
Constant	0.062	-0.240	-	0.091	-0.082	-
$Cos^2\Theta$	-0.945	-0.098	-0.832	-0.512	-0.512	-0.690
$Cos\Theta * S$	0.237	-	-	-0.057	-0.057	-
$Cos\Theta * ln(S)$	-	0.095	-	-	-	-
$Cos^2(\Theta - 45^o)$	-	0.539	-	-	-	-
R^2 (ADJ)	0.954	0.843	0.985	0.958	0.986	0.993

* NOTES:

1) Roof slope is $\alpha = 20^o$.
2) Refer to Table 3-1 for definitions of surface tap locations.
3) Correlations for Front Facade and Front Jack, are reported for Model #1 only.
4) Correlations for Back Jack are reported for Models #1 and #2.
5) Correlations for Back Facade are reported for Model #2 only.
6) Ranges of applicability for these correlations are:

$0 \le \Theta \le 90^o$;
$0 \le S \le 5$.

Table 3-3

Correlation For Average Surface Pressure Coefficients: Courtyard Effects *

Correlation Equation: $C_p = C_o + \sum_{i=1}^{N} C_i \cdot F_i$

Model Configuration: Jack Roof and Parapets (J,P); S = 1

Independent Variables (F_i)	Courtyard (C_i)
Constant	-
$Cos^2\Theta$	-0.471
$H_2 * S_c$	-0.147
R^2 (ADJ)	0.989

* NOTES

1) Roof slope is $\alpha = 20^o$.
2) Refer to Table 3-1 for definitions of surface tap locations.
3) Ranges of applicability for this correlation are:

$0 \leq \Theta \leq 90^o$;
$0.25 \leq S_c = 1$;
$0 \leq H_c \leq 1$.

Table 3-4

Key to Figures and Correlations

#1 -	Model #1 or Windward Model
#2 -	Model #2 or Leeward Model
P -	with Parapets
NP -	without Parapets
J -	with Jack Roof
NJ -	without Jack Roof

CHAPTER 4: SIMULATION OF NATURAL VENTILATION IN THREE TYPES OF PUBLIC BUILDINGS IN THAILAND

P. Boon-Long, T. Sucharitakul, C. Tantakitti, T. Sirathanapanta,
P. Ingsuwan, S. Pukdee, and A. Promwangkwa
Department of Mechanical Engineering
Chiang Mai University
Chiang Mai, Thailand

ABSTRACT

The potential effects of ventilative cooling on occupant comfort in three standard-design public buildings in Thailand are studied, using the ESPAIR computer simulation program. Simulations were performed for four climate regions (north, northeast, central, and south) and parametric studies on building design and orientation were also completed. The study has concluded that in general the designs are already good; that comfort in these buildings is not very sensitive to building orientation (except at one location); and that further simulation work should be conducted using the main ESP package, which accounts for the building's thermal loads. If thermal loads are included, natural ventilation and building orientation appear to have much more significant effects on occupants' comfort. These results have been incorporated into a natural ventilation design guidebook which will be used by Thai architects, practitioners, energy analysts, and researchers.

INTRODUCTION

There are many passive or low-energy methods of cooling a building for occupants' comfort. Of these methods, natural ventilation is one of the most effective, and lowest cost, options, and has been used particularly in warm, humid climates like that of Thailand and most other ASEAN countries. Natural ventilation is incorporated in the design of traditional houses, like the native Thai house, which has a high roof, high floors, generous shading, and large window and door areas, all of which allow maximum ventilation. Unfortunately, modern architecture has tended to follow Western models, which often have closed, tight designs requiring expensive and energy-consuming mechanical air-conditioning.

Recently, there has been a growing interest in incorporating natural means of cooling into building designs in Thailand. Shading windows from direct sunlight, for example, is becoming a popular and inexpensive method to lower indoor air temperatures. However, other potentially effective passive cooling methods are still not widely used, mainly because of a lack of awareness among local architects, or lack of the necessary data for climate-appropriate designs. Many architects recognize the potential benefits of such designs, but do not have the knowledge and design tools to create them. Most publications and design data available in Thailand were produced in the West, and are mainly appropriate for temperate-zone climates, in which both heating and cooling are needed (frequently with emphasis on the former). This information is not directly applicable to Thailand's warm, humid climate.

METHODOLOGY

The best way to learn about the effect of natural ventilation cooling for a building is to monitor the actual flow of air into that building. Monitoring is costly, however, and possible only in existing buildings. Furthermore, owners may be reluctant to invest in any modifications to the building that the monitoring shows will make it more climate responsive. Putting a building model in a wind tunnel is another way to study the air flow into the building. This method is also time-consuming and requires expensive wind tunnel facilities. The least time-consuming and least expensive method for studying air flow into buildings is by using computer simulation based on local climate data. We use this method in this study; the program used is called ESPAIR.

ESPAIR

The computer program ESPAIR simulates air flows and evaluates human comfort in ventilated buildings. The program is one of several components of the ESP system, which is intended for dynamic simulation of energy and mass transfer in buildings. The ESPAIR program requires hourly weather data, pressure coefficients that describe the wind-induced pressure field around a building, and a user-input description of the zones and openings that make up the airflow network of a building. Zones in a building may be connected in parallel and/or series, and each opening may be one of a few types. The solution algorithm iteratively balances the air mass flow rate into and out of each zone in the network, during each hour of the simulation period. The resulting file of zone airflow rates may be analyzed to determine human comfort under user-specified conditions of occupant activity and clothing levels, and the ventilation airflow rate in each zone may be summarized either in tabular or graphic format.

The program as used here requires hourly weather data (consisting of dry-bulb air temperature, wind speed, wind direction, and relative humidity) for analysis of human comfort. It also needs a file of pressure coefficient data for selected points on the building's surface. (A pressure coefficient is defined as the ratio of the dynamic pressure on the building's surface to the dynamic pressure of the wind in the free stream at a reference height.) These pressure coefficients are usually estimated from published data for similar buildings with similar surroundings.

The user of the program also has to describe the building under consideration in terms of size and type of ventilation openings, and the type of occupancy (time during which the building is in use, temperature and relative humidity ranges, occupant activity and clothing levels).

The output of the program is air flow rates, or, if coupled with specified temperature and relative humidity, comfort levels in a designated space. Comfort is defined by ASHRAE, and is divided into three levels: Predicted Mean Vote (PMV): acceptable (score 0); slightly warm (score 1.0); and warm (score 2.0). Division into sublevels is also possible, for example 0-0.5, 0.5-1.0, 1.0-1.5 and 1.5-2.0. These calculated results are available for hourly intervals, and can be summed to determine the percentages of human comfort in the observed space over specified periods (e.g., monthly or year-round).

Building Types Studied

Three types of buildings were studied. They were:

a) government schools,

b) district medical clinics, and

c) houses (built by the National Housing Authority of Thailand).

The above buildings were selected because they are all standardized designs, and there are many built all over the country. Hence, improvements in them will have a large impact on comfort and energy conservation nationwide. Details of each are described below.

i) Government Schools. The design, conceived by the Ministry of Education, is shown in Figure 4-1. The building is long and one room deep, with large windows and doors on opposite sides. Each room is approximately 9 x 9 meters, designed for 50 students. Each room has six windows and two doors.

ii) Subdistrict medical clinics. The design is shown in Figure 4-2. The clinic consists of an examination room, a dispensary, an office, a restroom, and a store room. There are no in-patient beds. This type of building is found in most subdistricts, especially in rural areas. In the Chiang Mai province alone, for example, 258 buildings of this type are scattered among 21 districts.

iii) Government houses. These are designed and built by the National Housing Authority for the low-and middle-income population. The design we considered is shown in Figure 4-3. Each house has two bedrooms, a kitchen, a living room, and a bathroom. This design is quite typical of the numerous townhouses built by the private sector as well.

Weather Data Used

The weather data used in the ESPAIR program were obtained from the Royal Meteorological Department in Bangkok for the years 1981-1986. They are three-hourly data, and contain, in addition to the items required by ESPAIR, information on atmospheric pressure, cloud amount and types, visibility, water evaporation rate, and rainfall.

As the data available were in three-hourly form, linear interpolation was used to obtain the hourly data required by ESPAIR. Interpolation causes errors, especially for wind information, but we had no better way to deal with this problem.

The main data items needed in ESPAIR calculations—wind speed and direction—were analyzed for magnitude, frequency, and direction over an entire year, for the four cities of interest.

Simulation Input

1. Building type
   - Government schools as shown in Figure 4-1.
   - Subdistrict medical clinics as shown in Figure 4-2.
   - Government house as shown in Figure 4-3.
2. Weather Year and Site
   - Weather Year 1984.
   - Sites: Chiang Mai, Bangkok, Khon Kaen, and Song Khla (locations shown in Figure 4-4.).
3. Schedule each building type for Comfort Index determination and other specifications:
   i) The temperature and relative humidity inside the observed space was the same as the outside conditions;
   ii) The maximum wind velocity allowed inside was 1 m/s;
   iii) Clothing level was 0.5 (summer clothing);
   iv) Activity level was 1.0 (seated, quiet);
   v) Pressure coefficients after Vickery *et al.*, [1] were used; and,
   vi) Four orientations were tested: N, S, E, W.

In addition, conditions specific to each building type were:

i) For government schools, time in use was 8:00-17:00, Monday-Friday only;
ii) For subdistrict medical clinics, time in use was 8:00-17:00, seven days a week, observed spaces were examination room, dispensary, office room;
iii) For houses time in use was (living room) 8:00-21:00, seven days a week, and (bedrooms) 21:00-07:00, seven days a week.

RESULTS AND DISCUSSION

In general, comfort level in the buildings studied ranged from a high of almost 100% in the winter (December - February) to a low of less than 10% in April - May (hot season). (Figure 4-5 shows a typical comfort profile for Bangkok.) This range reveals the need for buildings to be seasonally adjustable. That is, we should be able to fully open the building during the cool season, to take maximum advantage of natural ventilation. We also should be able to close them tightly during times when air-conditioning is needed.

Table 4-1 shows the comfort level in the three buildings in one of the least comfortable months (May). In this table, two things are apparent. First, there are significant differences in comfort levels among different rooms that have different openings. Second, at three locations (Bangkok, Chiang Mai, and Khon Kaen), comfort level practically does *not* depend on building orientation, and in each case the discomfort percentage is high (more than 2.0). This may have been because the ambient temperature in this month is already so high that it is mostly outside the

comfort zone, regardless of wind speed. An exception is at Song Khla in the south, where there is a strong and almost uni-direction wind from the east. The comfort level changes significantly when the buildings are rotated, and the discomfort percentage is much lower than at other locations.

In other months, the dependence of comfort on building orientation is very small, and believed to be within the limits of the simulation errors.

Note that the above results were based on consideration of only natural ventilation in the building (i.e., assuming that interior air temperature and ambient temperature are the same), without including the effects of thermal loads such as radiant ceilings, heat capacity of walls, and direct solar gain through openings. If such thermal loads are considered, the significance of ventilation—and the importance of building orientation relative to the direction of prevailing winds—would substantially increase. In such a case, ventilation would cool down the interior air temperature significantly, in addition to directly cooling occupants' skin, thus reducing discomfort. These effects can be considered by using another simulation program, ESPSIM.

CONCLUSION

Further work should be conducted, using more comprehensive programs which take into account thermal loads on occupied space.

REFERENCE

1. Vickery, B.J., Baddour, R.E. and Karakatsanis, C.A., "A Study of the External Wind Pressure Distributions and Induced Internal Ventilation Flow in Low-Rise Industrial and Domestic Structures," Florida Solar Energy Center Report BLWT-552-1983, January, 1983.

Figure 4-1.
Government School

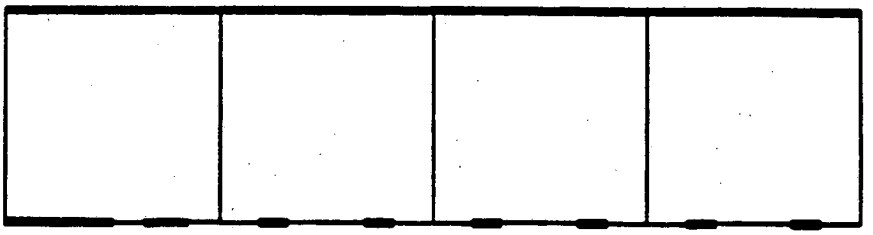

Floor Plan

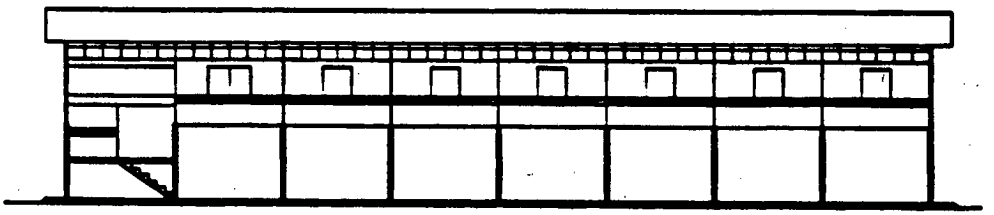

Front Elevation

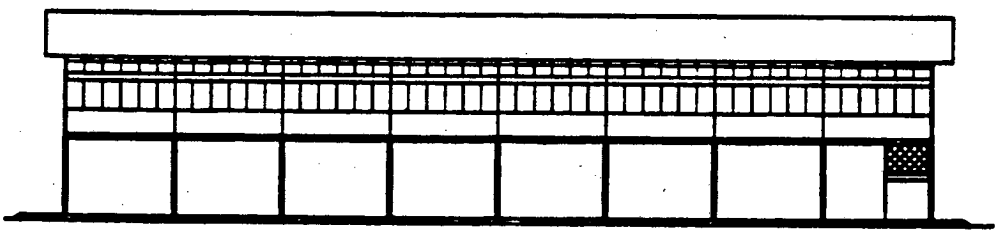

Back Elevation

Scale 1 : 300

Figure 4-1. (cont'd)
Government School

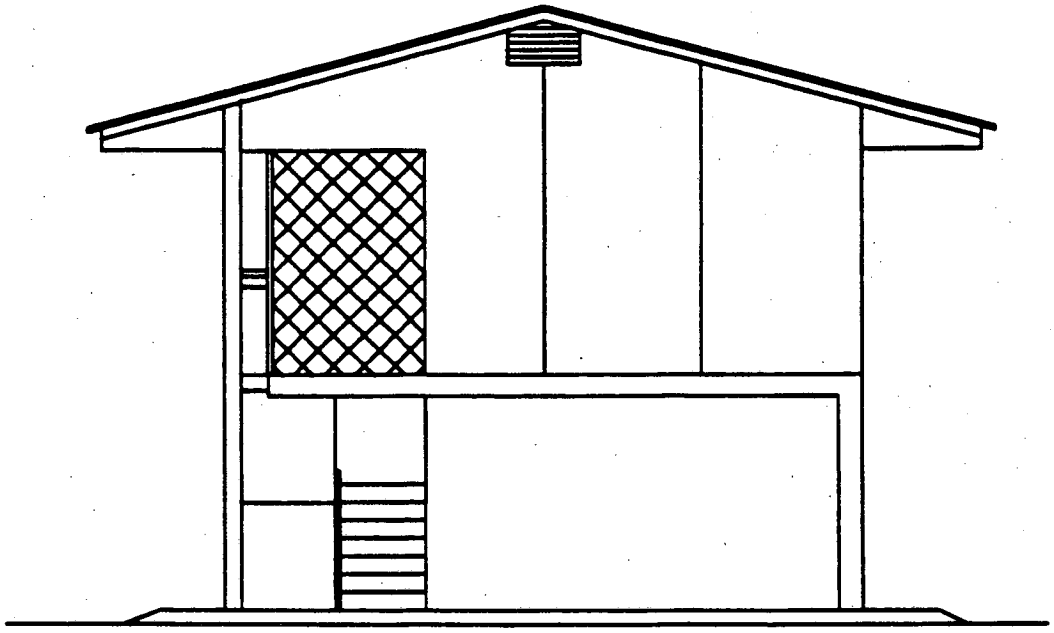

Left Elevation

Scale 1 : 100

Figure 4-2.
Subdistrict Medical Clinic

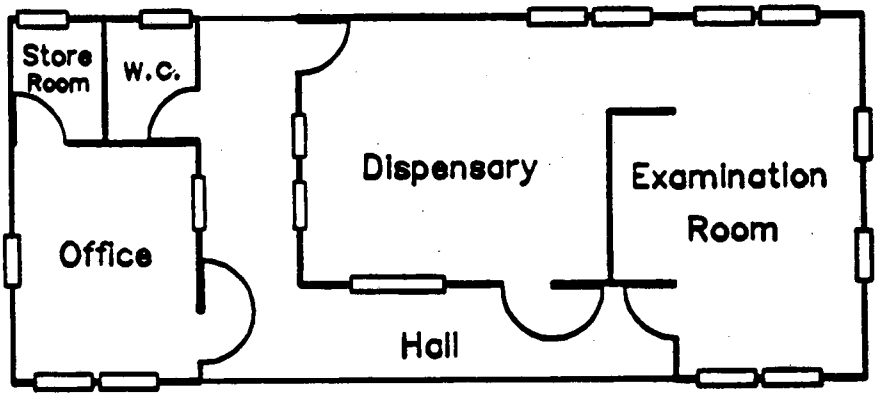

Floor Plan

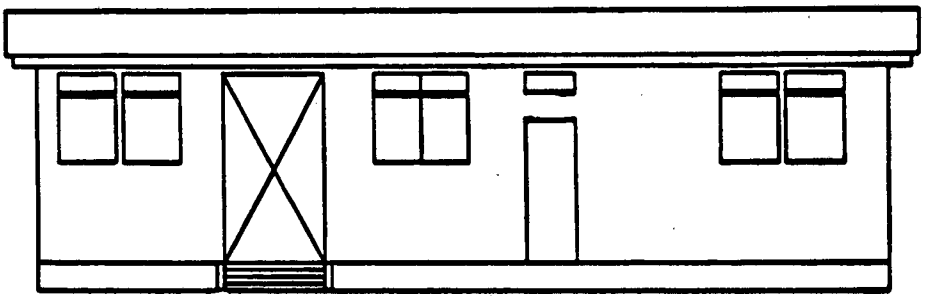

Front Elevation

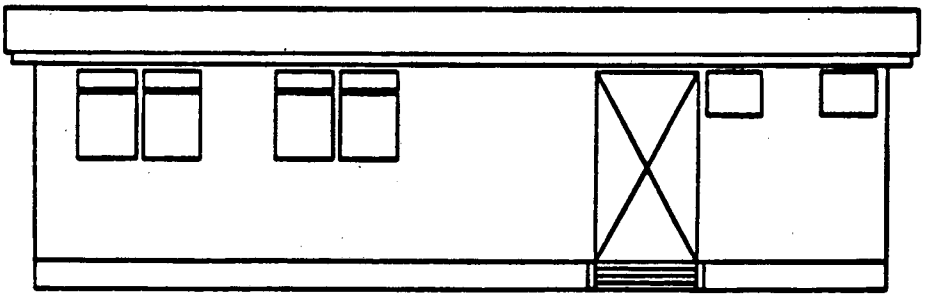

Back Elevation

Scale 1 : 100

Figure 4-3.
Government House

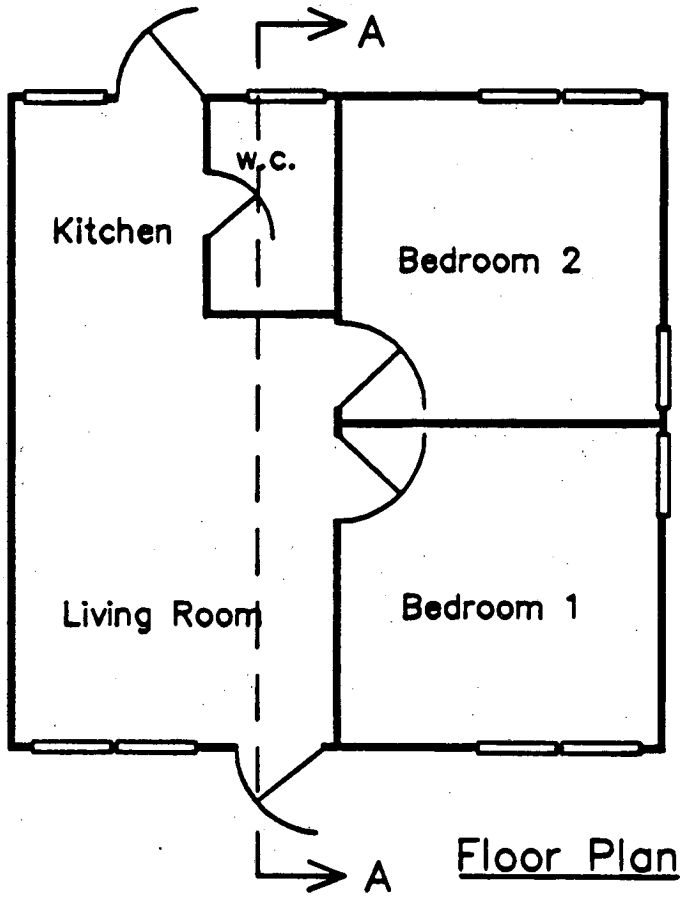

Floor Plan

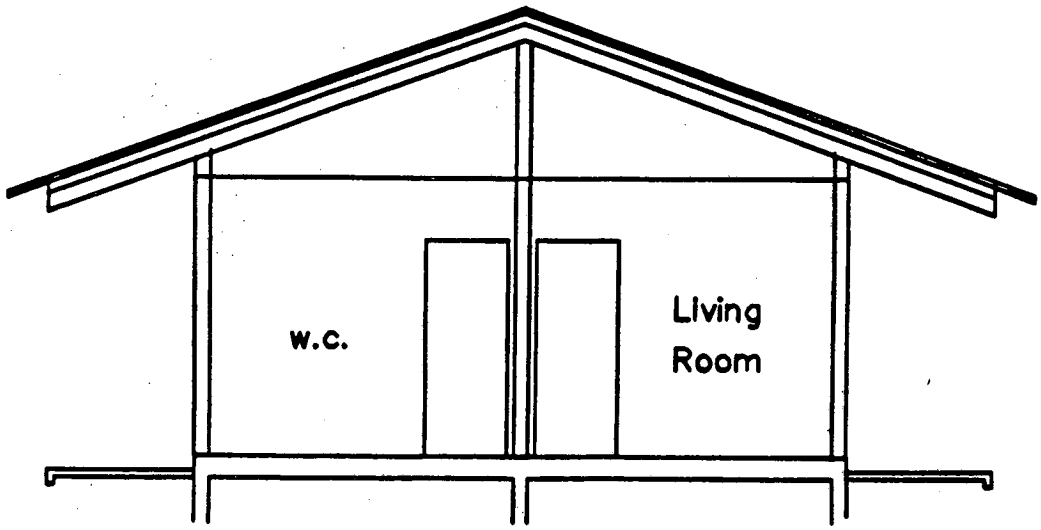

cross section AA

Scale 3 : 200

Figure 4-3. (cont'd)
Government House

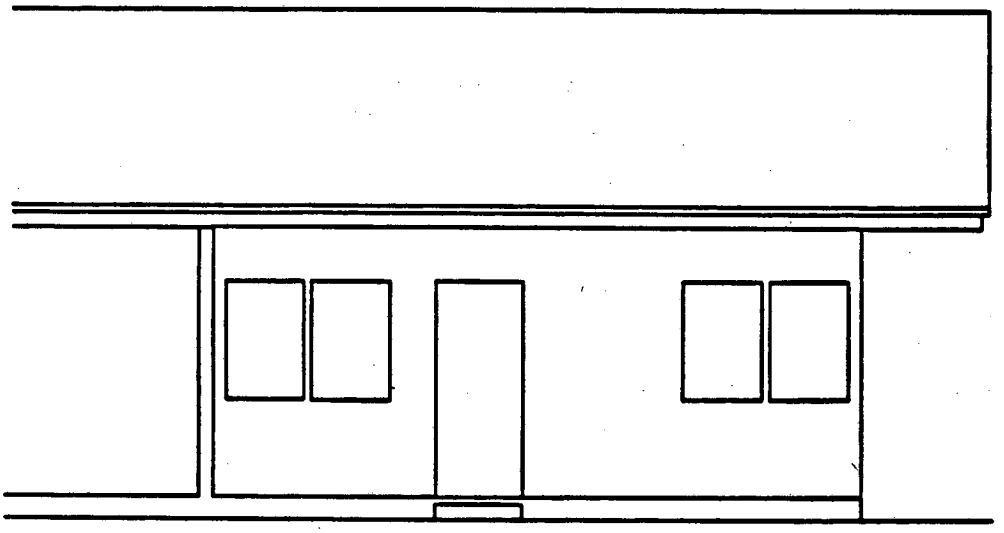

Front Elevation

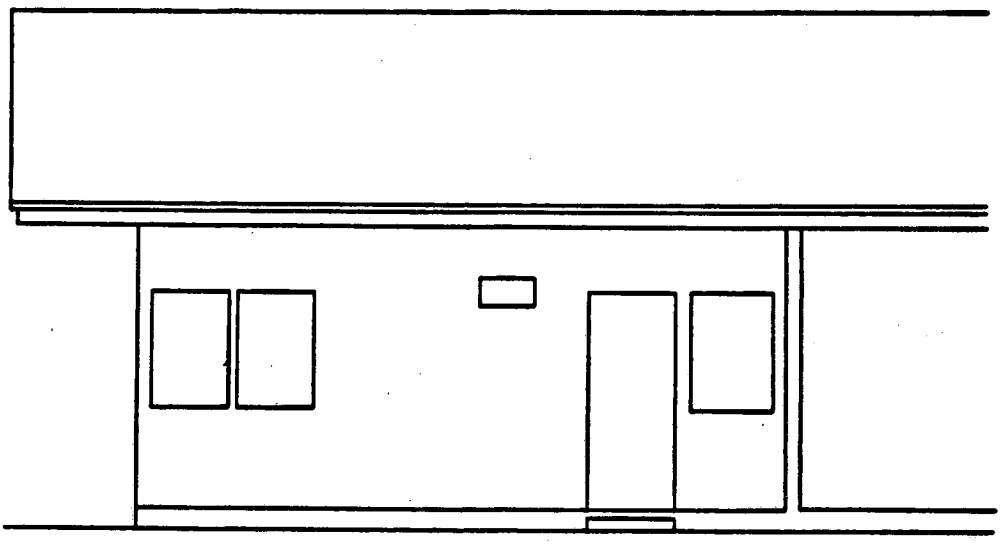

Back Elevation

Scale 3 : 200

Figure 4-4.
Map of Thailand

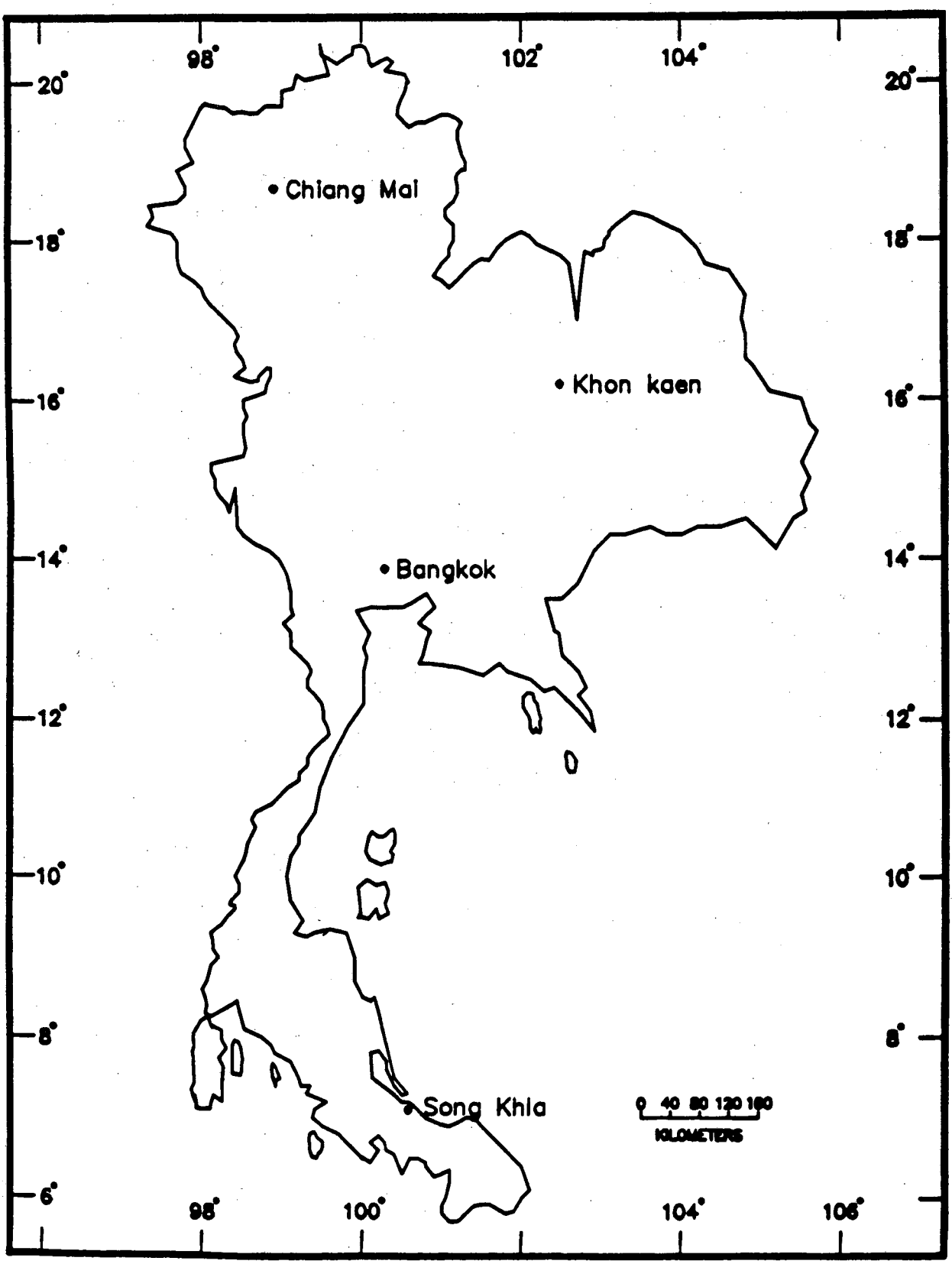

Figure 4-5.
A Comfort Profile for Bangkok

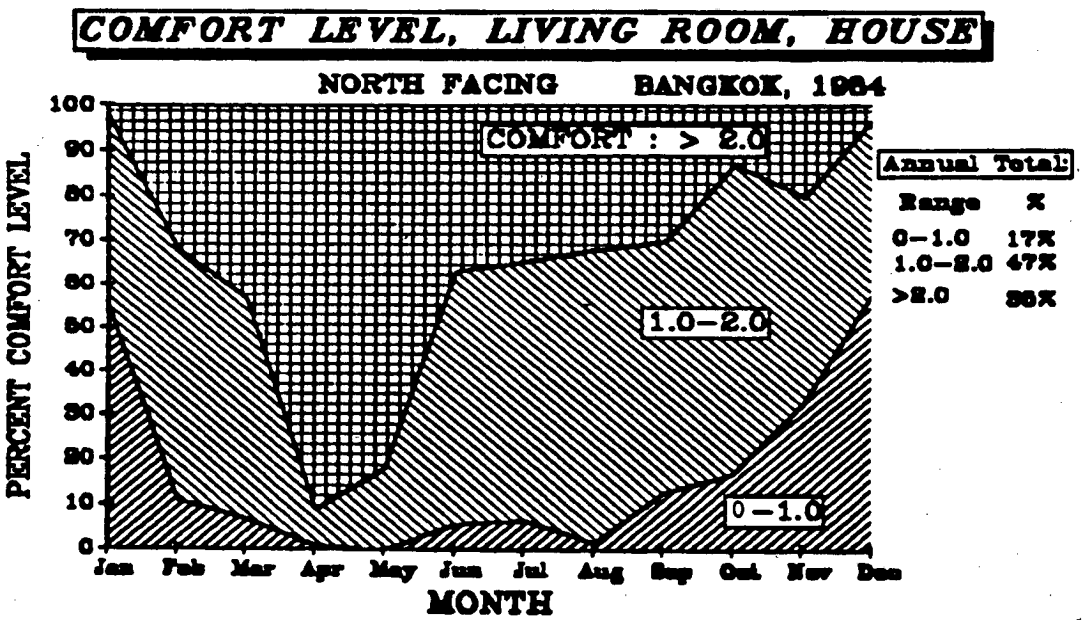

Table 4-1: Comfort Levels for May 1984

		N			E			S			W			Prevailing Wind	
		0-1	1-2	>2	0-1	1-2	>2	0-1	1-2	>2	0-1	1-2	>2	Direction	Speed
Bangkok	School:														
	Classroom	2	10	88	2	11	87	2	10	88	2	12	86		
	Hospital:														
	Office	1	9	90	1	8	91	1	9	90	1	17	83	W	<5m/s
	Dispensary	0	8	92	1	11	88	1	9	90	1	13	86		
	Exam Room	2	14	84	2	15	83	1	15	84	2	17	81		
	House:														
	Living Room	0	18	82	1	23	76	0	17	83	1	23	76		
	Bedroom 1														
Chiang Mai	School:														
	Classroom	11	32	58	11	32	58	11	32	58	11	32	58		
	Hospital:													W and SW	<5m/s
	All rooms	13	31	56	13	31	56	13	31	56	13	31	56		
	House:														
	Living Room														
	Bedroom 1														
Khon Kaen	School:														
	Classroom	2	16	82	2	17	81	2	16	82	2	17	81		
	Hospital:														
	Office	2	27	71	2	27	71	2	27	71	3	27	70	W and SW	<5m/s
	Dispensary	2	27	71	3	26	71	3	26	71	2	26	72		
	Exam Room	3	29	68	3	29	68	4	29	67	3	29	68		
	House:														
	Living Room	4	30	66	3	32	65	4	30	66	4	30	66		
	Bedroom 1														
Song Khla	School:														
	Classroom	9	71	20	14	79	8	10	72	19	14	78	8		
	Hospital:														
	Office	11	82	7	7	78	15	7	78	15	15	78	7	E	>10m/s
	Dispensary	8	70	22	9	82	9	6	73	21	9	84	7		
	Exam Room	14	80	6	15	80	5	14	81	5	15	81	4		
	House:														
	Living Room	20	64	15	21	72	7	21	60	19	22	71	7		

CHAPTER 5: SOLAR RADIATION AND WEATHER DATA FOR INDONESIA

Ir. Soegijanto,
R. Triyogo, I.B. Ardhana Putra, and I.G.N. Merthayasa
Teknik Fisika
Institut Teknologi Bandung
Bandung, Indonesia

INTRODUCTION

This report presents a brief history of the collection and recording of weather data in Indonesia. Solar and weather data have been recorded in Indonesia ever since the period of Dutch administration. At present, the Meteorological and Geophysical Center in Jakarta coordinates these activities.

Weather measurements have been taken at the approximately 150 meteorological stations located throughout Indonesia. The station farthest to the north and west is located at longitude 5°31′ N and latitude 95°25′ E, the southernmost at 10°10′ S and 123°40′ E, and the easternmost at 2°34′ and 140°29′ E. The area covered ranges about 4800 km from east to west and 1600 km from north to south.

Measurements are taken chiefly to supply data for agricultural and air transportation purposes. Factors measured include air temperature (mean, maximum, and minimum), relative humidity, wind speed, barometric pressure, rainfall, and sunshine duration. Most of the measurements are taken only three times a day.

Global solar radiation measurements have been collected since 1928 in Jakarta, although the measurements have been taken intermittently at a few other places.*

OBJECTIVES

- To collect hourly solar and weather data in Bandung and Jakarta.
- To perform solar and weather data analysis.
- To put weather data into a format compatible with the DOE-2 building energy simulation computer program.

DATA COLLECTION

The data collection project consisted both of collecting existing data and of field measurements.

The Existing Data

Solar Radiation Data:

The solar radiation data collected in Jakarta (6°11′ S, 106°50′ E) consist of:

- Mean monthly and average values of the intensity of solar radiation at normal incidence (in gr. cal/cm^2-min) for the period 1915 to 1924. The intensity at normal incidence was measured as a function of the sun's altitude, ranging from 15° to 90°, at 5° intervals. A silver disk pyrheliometer was used to measure the data [1].
- Monthly averages of total† hourly radiation (in gr. cal/cm^2-hr), calculated from data collected from 1928 to 1941 [1].

* Until about 1980 the Meteorological and Geophysical Center issued official publications of weather and global solar radiation data, but no official publication has been issued recently. A request must be submitted to obtain the compiled data.

† "Total" includes both direct beam and diffuse sky radiation.

- Hourly global solar radiation data (in cal/cm^2) collected from 1964 to 1968 [2].
- Hourly global radiation (in cal/cm^2) for the period 1969 to 1971 [3].
- Hourly global radiation (in cal/cm^2) for the period 1972 to 1976 [4].

Data from other locations are very limited:

- Hourly global solar radiation in Lembang for the period 1964 to 1968. Lembang (6°50′ S, 107°37′ E, 1300m above sea level) is situated about 20km north of Bandung (6°54′ S, 107°36′ E, 770 m above sea level) [5].
- Hourly global solar radiation in Denpasar for the period 1969 to 1973. Denpasar (8°45′ S, 115°10′ E, 1 m above sea level) is situated on the island of Bali [6].

Currently, the Bandung office of the Indonesia National Institute of Aeronautics and Space is measuring hourly global and diffuse solar radiation on a continuous basis. Diffuse radiation has been measured only since mid-1985, but the global radiation data collection goes back to 1977.

Weather Data:

Data on Jakarta's weather for the period 1968 to 1977 were issued in a series of publications entitled *Observations Made at Jakarta Observatory*. Measurements were taken of hourly barometric pressure, dry and wet bulb temperature, relative humidity, wind direction and speed, cloudiness, sunshine duration, and rainfall. Jakarta's data are more complete than those taken anywhere else in Indonesia.

Data for other locations were issued in two series. The first contains climatological data taken from about 155 stations, for the period 1971 to 1979. The data consist of monthly averages of mean temperature, maximum temperature, minimum temperature, rainfall, sunshine duration, barometric pressure, wind speed, highest wind speed and prevailing wind direction [7]. The second series, running from 1954 to 1960 and 1964 to 1970, contains monthly averages of every other hour of air pressure, temperature, relative humidity, and duration of sunshine for some of the climatological stations [8].

The meteorological station in Bandung has taken daily hourly measurements (from 7:00 A.M. to 7:00 P.M.) of air temperature, relative humidity, and wind speed and direction.*

The Collection of Existing Data:

We currently have data on solar radiation and weather for Jakarta, Bandung, and a few other places.

Solar Radiation. For Jakarta we have:

- Hourly global solar radiation data for the periods 1964 to 1979 and 1984 to 1987.
- Mean monthly average of direct solar radiation as a function of solar radiation for 1915 to 1924.
- A monthly average of hourly global radiation for the period 1928 to 1941.

For Bandung we have:

- Hourly global solar radiation data for the periods 1977 to 1980 and 1984 to 1987.
- Hourly diffuse solar radiation data for 1986 and 1987.

For Lembang and Denpasar we have:

- Data on hourly global solar radiation in Lembang for the period 1964 to 1968.
- Data on hourly global solar radiation in Denpasar for 1969 to 1973.

* The station does not publish the data, but will provide it on request. However, since the data needs to be prepared first by the station, obtaining it takes some time.

Weather Data. For Jakarta we have:

- Hourly data taken the period 1968 to 1977 on dry and wet bulb temperatures, relative humidity, barometric pressure, wind speed and direction, cloudiness, sunshine, and rainfall.
- Hourly data on temperature, relative humidity, and wind speed for 1984 to 1988.

For Bandung we have:

- Hourly data (7:00 A.M. to 7:00 P.M.) on temperature, relative humidity, and wind speed for the period 1978 to 1987.

From other locations we have:

- Two monthly averages of barometric pressure, air temperature, relative humidity, wind speed, and sunshine duration measured at about 50 meteorological stations during the periods 1954 to 1959 and 1964 to 1970.
- A monthly average of the mean, minimum, and maximum temperature, rainfall, sunshine duration, barometric pressure, wind speed, highest wind speed, and prevailing wind direction for 1971 to 1979.

Data Storage:

All the data received were printed in paper format. Eventually, all of the existing hourly solar and weather data on Jakarta and Bandung will be stored on diskettes.

The data already stored consists of:

- Hourly global solar radiation data for Jakarta for the years 1972, 1973 (no data for January to June), 1974, 1975 (no data for August), 1976, 1984 (no data for April), 1985 (no data for February and March), 1986, and 1987.
- Hourly global solar radiation data for Bandung for the years 1977 (no data for January, February, July, August), 1978 (no data for March, August, September), 1979, 1980 (no data for August), 1984, 1985, 1986, and 1987.
- Hourly diffuse solar radiation data for Bandung for the years 1985 (no data for August, November, December), 1986, and 1987.
- Hourly weather data for Jakarta consisting of temperature, relative humidity, and wind speed for the years 1972, 1973, 1975 to 1977, and 1984 to November 1988. Only data on wind speed for November 1985 was missing.
- Hourly weather data for Bandung consisting of temperature, relative humidity, and wind speed for the years 1978 and 1987. The data for 1978 were taken from 7:00 A.M. to 7:00 P.M., and that for 1987, for 24 hours.

Conclusions Drawn About the Existing Data:

- Inadequate data made it impossible to produce data for a "typical year," as was planned.
- Jakarta has the most complete hourly weather and global solar radiation data, but no diffuse radiation data.
- Only Bandung has both global and diffuse radiation data available for three years or more, but hourly weather data for 24 hours a day is only available for 1987.
- Very limited weather data and almost no solar radiation data exist for places outside Jakarta and Bandung.
- In order to run an hourly energy simulation program, a complete one year set of data on (at least) hourly air temperature, relative humidity or wet bulb temperature, wind speed and direction, and global and diffuse solar radiation must be available. For Bandung, a complete set of data was available for 1987. To make a complete set of data for Jakarta, diffuse solar radiation was calculated by correlating global and diffuse radiation for Bandung in 1987.

Measurement of Solar Radiation and Weather

Solar Radiation and Weather Measuring Instruments:

In February, 1988, a set of solar and weather measuring instruments was acquired (see Table 5-1 for a list of the equipment).

The Variables Measured:

- Diffuse solar radiation (W/m^2)
- Global solar radiation (W/m^2)
- Terrestrial radiation (W/m^2)
- Global illuminance (lux)
- Relative humidity (%)
- Air temperature ($^{\circ}C$)
- Wind speed (mps)
- Wind direction (degrees)

Although terrestrial radiation and global illumination are not required for the energy simulation program, we measured both variables because the instruments were already in place and the data may be useful for further research.

Measurement Procedures:

The instruments were preliminarily set up in Bandung on the roof of an Institut Teknologi Bandung laboratory building (see Attachment 1 of [9] for photographs of the installation of the instruments).

The data initially collected was reviewed, and the measurement procedures were subsequently readjusted several times. The needed adjustments consisted of changing the measuring ranges and adding multiplier settings.

We moved the instruments from Bandung to Jakarta in mid-October of 1988. The measurement needed to be taken in the middle of an urban area of Jakarta where no surrounding buildings were higher than the measuring sensors. We choose Jalan Asem Baris Raya No. 158, Tebet Timur, Jakarta, a two-story house located in a residential area. The instruments were set up on the roof (see photograph in Attachment 2 of [9]).

The measurements in Jakarta were taken from mid-October to December 31, 1988. From January 1, 1989 to March 30, 1989, however, no data were recorded on the tape because we made the mistake of not adjusting the recording program on December 31, 1988. From March 31, 1989 on there was no trouble with the instruments. A whole year of data was obtained by the end of March, 1990 (a sample of the data measured at Jakarta can be seen in Attachment 3 of [9]).

SOLAR RADIATION

Solar Radiation Data Analysis

Global solar radiation data for Jakarta and Bandung for the period 1984 to 1987 was analyzed, even though data from the 1970s was available for Jakarta.

Solar Radiation Data for Jakarta:

The hourly averages of global solar radiation for each year and for the whole period of 1984 to 1987 are shown in Figures 5-1 and 5-2 respectively. The maximum hourly average for the four years occurred at 12:00 P.M., but for the years 1986 and 1987, the maximum occurred between 1:00 to 2:00 P.M. 1987 had the highest hourly average.

The monthly average of global radiation for the period 1984 to 1987 and the monthly average of each year during that same period are shown in Figures 5-3 and 5-4, respectively.

The highest monthly average during the four years occurred in September (1600 Joules/cm^2), and the lowest in January (300 Joules/m^2). Since September is in the dry season

and January is in the rainy season, these results make sense.

Solar Radiation Data for Bandung:

Figures 5-5 and 5-6 show the hourly average of global solar radiation for Bandung during 1984 and 1987 and the hourly average for each year of that same period. The maximum hourly average for all four years, as well as the maximum hourly average for each year, occurred at 11:00 A.M. Thus, sky conditions before noon must be clearer than those in the afternoon.

The monthly average of global radiation for the period 1984 to 1987 and the monthly average for each year of that period are shown in Figure 5-7 and 5-8.

The month with the highest average over the four-year period was February (1950 Joules/cm^2), while the lowest was June (1600 Joules/cm^2). February is still the rainy season, but the sun is much closer to Earth than in June when the sun is at its most distant position. In Bandung, the difference between the rainy and dry seasons is not always significant.

A Comparison of Global Solar Radiation Between Jakarta and Bandung:

Both Bandung's hourly average and its monthly average of global radiation were higher than Jakarta's. The monthly average in Bandung was 1700 Joules/cm^2 while Jakarta's was 1500 Joules/cm^2. The daily average for Bandung was 393 W/m^2 and for Jakarta, 347 W/m^2.

Weather Data Analysis

Jakarta's weather data from 1984 to 1987 were analyzed, but only Bandung's 1987 data on temperature, relative humidity, and wind speed were used.

Jakarta's Weather:

Air Temperature. Average diurnal variation was around 7° to 8°C, as shown in Figure 5-9, with an hourly average maximum of 32°C and an average minimum of 24°C. The hourly maximum temperature occurred around 2:00 P.M., and the hourly minimum temperature around 6:00 A.M.

Figure 5-10 shows that the average maximum temperature in May through October was slightly higher than the average maximum temperature, and that the maximum temperature in December to March slightly lower than the average maximum temperature. The monthly variation was around 2°C. The seasons influenced the maximum air temperatures; May through October is the dry season, and December through April is the rainy season.

It is interesting to note that during the four years there was a trend towards increasing temperatures.

Relative Humidity. Figure 5-11 shows that average diurnal variation was around 35%, with the hourly average maximum between 85% to 90%, and the average minimum between 60% and 65%. The monthly average relative humidity was between 68% and 87%. Higher relative humidity occurred during the rainy season, while lower relative humidity occurred during the dry season (see Figure 5-12).

There was also a trend towards decreasing relative humidity over the four years.

Wind Speed. The average daily wind profile can be seen in Figure 5-13. The wind speed gradually increased before noon, with the maximum occurring in the afternoon around 12:00 to 3:00 P.M. Then, the wind gradually decreased until it reached its minimum sometime between 2:00 and 6:00 A.M. The maximum hourly average was around 7 to 8 knots, and the minimum was less then 1 knot.

The monthly average for a year was around 3 knots. Very little month-to-month variation occurred during the four years. (See Figure 5-14).

Bandung Weather:

Air Temperature. Average diurnal variation in 1987 was around 8°C, as shown in Figure 5-15, with the hourly average maximum temperature of 28°C occurring at around 2:00 P.M, and the hourly average minimum of 20°C occurring around 6:00 A.M.

The average maximum temperatures in August (29°C), October (30°C), and November (29°C) were higher than the yearly average maximum (28°C), while the average minimums in January (26°C), February (27°C), and April (27°C) were lower (see Figure 5-16). The higher maximum temperature occurred during the dry season, and the lower during the rainy season.

Relative Humidity. The hourly average maximum was around 90%, and the minimum was around 60%, so there was a 30% diurnal variation. The maximum monthly average relative humidity (84%) occurred in December (the rainy season), and the minimum (66%) occurred in August (the dry season) (see Figures 5-17 and 5-18).

Wind Speed. Figure 5-19 shows the average daily wind profile. From 7:00 A.M. to 3:00 P.M., the wind speed gradually increased to its maximum (9 knots), and then gradually decreased to its minimum (3 knots) sometime between 11:00 P.M. and 7:00 A.M.

The average monthly maximum was 8 knots (January), the minimum was 3.5 knots (June), and the average was 5 knots (see Figure 5-20).

Correlation of Global and Diffuse Radiation at Bandung

Global and diffuse radiation data were available for Bandung for three years, but no diffuse radiation data were available for Jakarta, since the measurements were still in progress at the time the analysis was performed. Based on the assumption that the correlation between global and diffuse radiation found in Bandung applies throughout Indonesia, diffuse radiation was calculated for Jakarta. The correlation was derived using global and diffuse solar radiation data for 1987. The method of calculation used can be found in the literature, such as Duffie & Beckman [10] and Hawlader [11].

First, the hourly extraterrestrial radiation (I_o) for Bandung was calculated for the whole year, generating 4380 data points (12 x 365). The ratio of global radiation to extraterrestrial radiation (I/I_o) and the ratio of diffuse radiation to global radiation were then calculated (I_d/I), each generating 4380 data points.

The correlation was derived by plotting corresponding I_d/I and I/I_o in a rectangular coordinate system, with I/I_o as the abscissa and I_d/I as the ordinate. The plots can be seen in Figures 5-21 and 5-22 (each covers a six month period). The correlation yields:

Range I : $I_d/I = 0.7943 - 0.1767\ I/I_o$ for $I/I_o < 0.225$

Range II : $I_d/I = 0.9997 - 1.1454\ I/I_o$

for $0.225 < I/I_o < 0.725$

Range III : $I_d/I = 0.1693$ for $I_o > 0.725$

The percentages of the data within Ranges I, II and III was 25.89%, 73.18%, and 0.93%, respectively (see Figure 5-23).

Calculation on Diffuse Radiation in Jakarta for 1987

Calculations were performed to find:

- extraterrestrial radiation (I_o) in Jakarta for the whole year;
- the ratio of global solar radiation to extraterrestrial radiation (I/I_o) (using global solar radiation data for Jakarta 1987);
- the ratio of diffuse to global solar radiation (I_d/I) (using the correlation already derived for Bandung); and
- I_d (found from the ratio of I_d/I).

PUTTING SOLAR AND WEATHER DATA INTO DOE-2 FORMAT

All of the solar and weather data will eventually be formatted to suit the DOE-2 building energy simulation program. In this case, the modified TRY format is being used. Jakarta 1987 data on global and calculated diffuse radiation, air temperature, relative humidity, and wind speed have been coded into this format. Bandung's 1987 data has also been put into the modified TRY format.

The Jakarta data for 1987 has been processed and the following results presented below:

- A summary of Jakarta's 1987 monthly data (see Table 5-2).
- A summary of measured solar data (Table 5-3a - f), which includes:
  - Insolation on surfaces of various orientations (kWh/m^2).
  - Power insolation on surfaces with varying orientations (W/m^2).

    Power was determined for:
    - All hours of daylight
    - between 8:00 A.M. and 6:00 P.M.
    - between 9:00 A.M. and 5:00 P.M.
    - between 8:00 A.M. and 5:00 P.M.
    - between 9:00 A.M. and 6:00 P.M.
- Solar factor calculations for Jakarta for 1987 (see Table 5-4).

CONCLUSION

The following parts of the project have been or remain to be completed:

- An overview of the availability of solar and weather data in Indonesia has been presented. Several years' worth of hourly solar and weather data for Jakarta and Bandung have been filed.
- The 1987 solar and weather data for Jakarta and Bandung have been put into the modified TRY format, which can be used as input for the DOE-2 building energy simulation program.
- The measurement of solar and weather data in Jakarta is still in progress, and measured data will be added the database.
- Solar and weather data are not available for other large cities in Indonesia such as Surabaya, Medan, Ujung Pandang, and Semarang, and measurements should be conducted in these cities.

REFERENCES

1. Boerema, J., and Berlage, Jr., H.P., "Solar Radiation Measurements in the Netherlands Indies," Verhandelingen No. 34, Departement Van Verkeer, Energie en Mynwezen, Meteorologische en Geophysische Dienst, Koninklyk Magnetisch en Meteorologisch Observatorium te Batavia.
2. Lembaga Meteorologi dan Geofisika, Departemen Perhubungan, "Solar Radiation Data No. 1, Total Radiation Observations at Jakarta, 1964 - 1968." Jakarta, 1969.
3. _____. "Solar Radiation Data No. 3, Global Solar Radiation Observations at Jakarta, 1969-1971," Jakarta, 1971.
4. _____. "Solar Radiation Data No. 5, Global Solar Radiation Observations at Jakarta, 1972-1976," Jakarta, 1978.
5. _____. "Solar Radiation Data No. 2, Global Radiation Observations at Lembang (Bandung), 1964-1968," Jakarta, 1971.

6. _____. "Solar Radiation Data No. 4, Global Solar Radiation Observations at Denpasar, 1969-1973," Jakarta, 1978.

7. Pusat Meteorologi dan Geofisika, Departemen Perhubungan, Jakarta, "Data Iklim di Indonesia, 1971, 1972, 1973, 1974, 1975, 1976, 1977, 1978, 1979."

8. Lembaga Meteorologi dan Geofisika, Departemen Perhubungan, Jakarta, "Climatological Data of Indonesia – A continuation of observations made at secondary station," Vol. XXIII A, 1954-1955; Vol. XXIII B, 1956-1957; Vol. XXIX, 1958-1960; Vol. XXXII, 1964-1965; Vol. XXXII, 1966-1967; Vol. XXXV, 1970.

9. Soegijanto, Ir., Triyogo, R., Ardhana Putra, I.B. and Merthayasa, I.G.N., "ASEAN-US Project on Energy Conservation in Buildings - Project I-3: Solar Radiation and Weather Data," Institut Teknologi Bandung, Bandung, Indonesia, December 1989.

10. Duffie, J. and Backman, W., "Solar Engineering and Thermal Processes," John Willey & Sons, 1980.

11. Hawlader, "Diffuse, Global and Extraterrestrial Solar Radiation for Singapore," *International Journal of Ambient Energy,* Vol. 5, 1984.

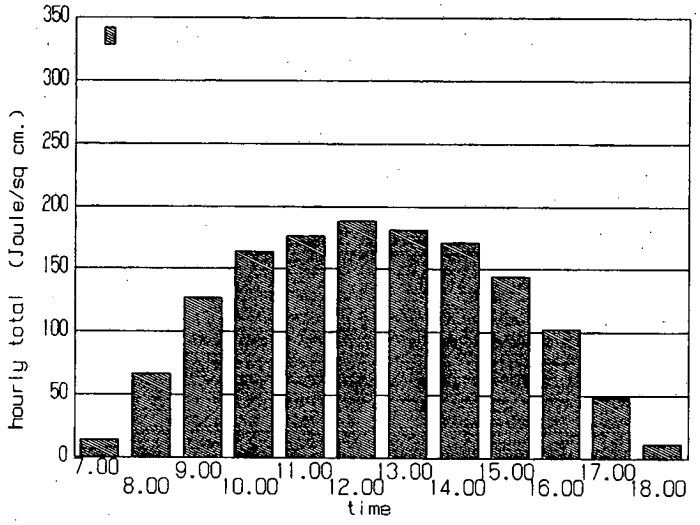

Figure 5-1. Hourly Average Global Solar Radiation for Jakarta for the Period 1984 to 1987.

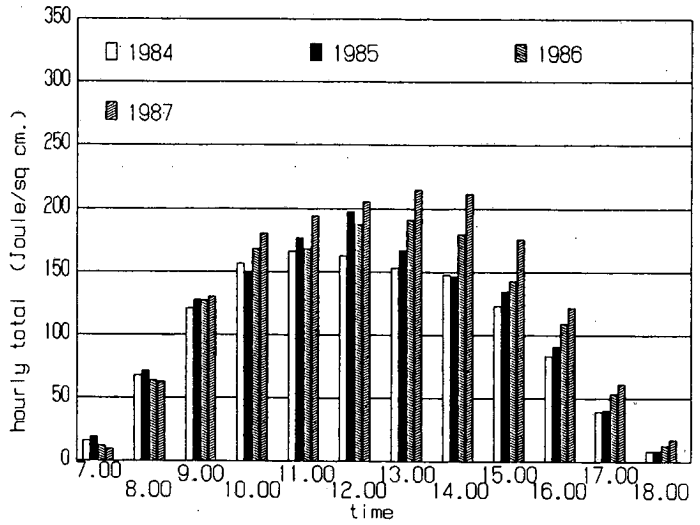

Figure 5-2. Hourly Average Global Solar Radiation for Jakarta by Year, for 1984 to 1987.

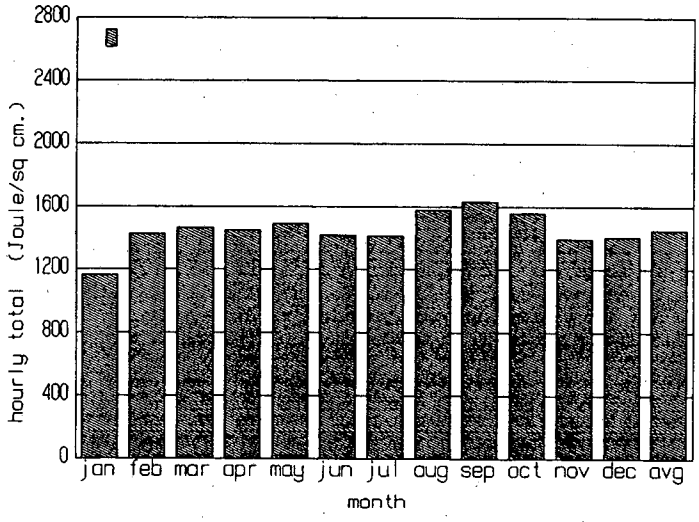

Figure 5-3. Monthly Average Global Solar Radiation for Jakarta for the Period 1984 to 1987.

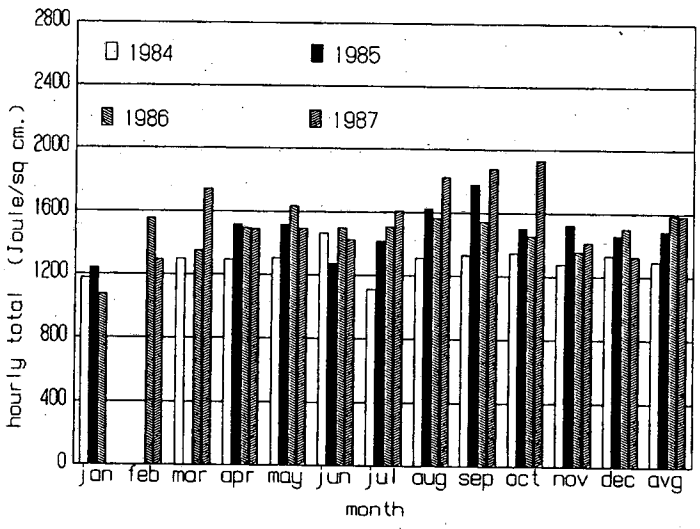

Figure 5-4. Monthly Average Global Solar Radiation for Jakarta by Year, for 1984 to 1987.

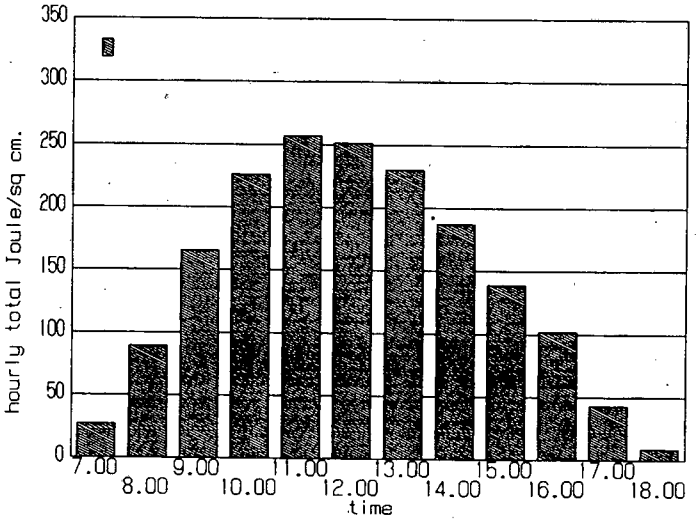

Figure 5-5. Hourly Average Global Solar Radiation for Bandung for the Period 1984 to 1987.

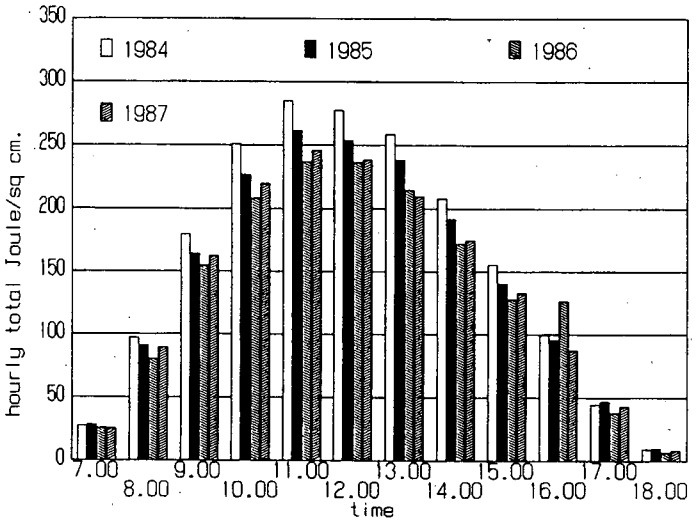

Figure 5-6. Hourly Average Global Solar Radiation for Bandung by Year, for 1984 to 1987.

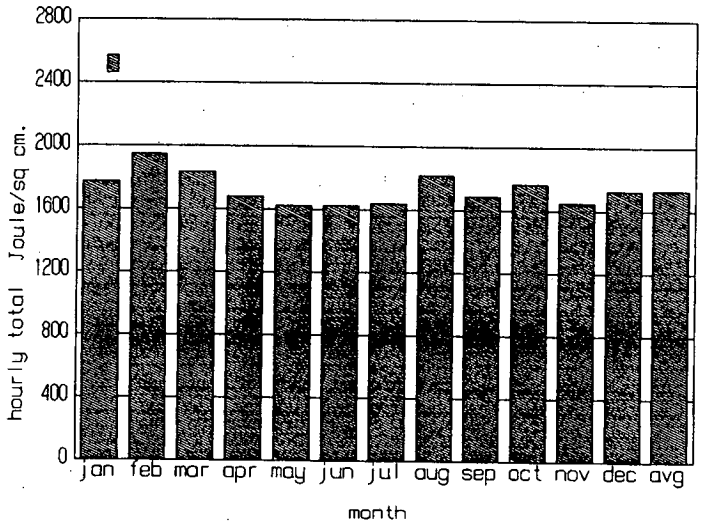

Figure 5-7. Monthly Average Global Solar Radiation for Bandung for the Period 1984 to 1987.

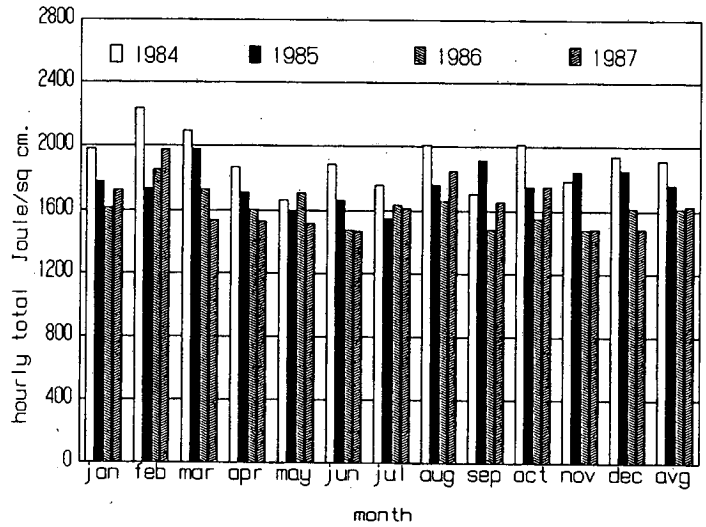

Figure 5-8. Monthly Average Global Solar Radiation for Bandung by Year, for 1984 to 1987.

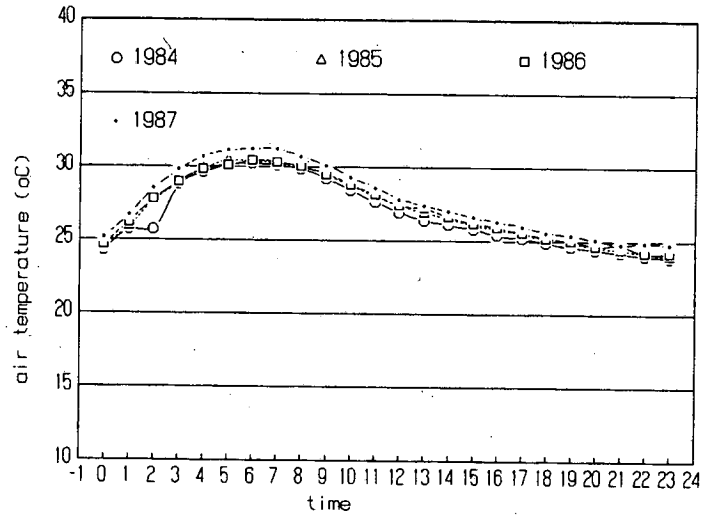

Figure 5-9. Hourly Average Air Temperature for Jakarta by Year, for 1984 to 1987.

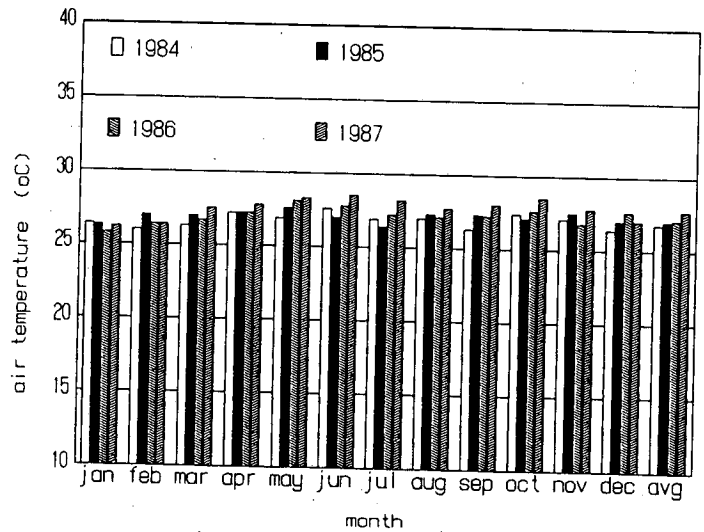

Figure 5-10. Monthly Average Air Temperature for Jakarta by Year, for 1984 to 1987.

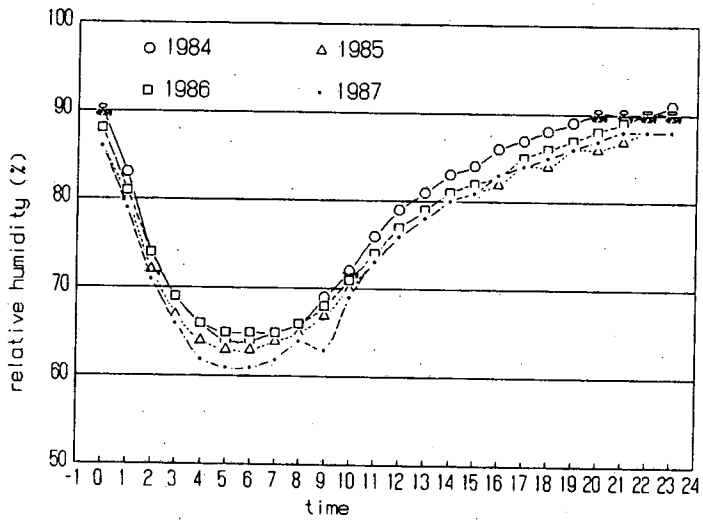

Figure 5-11. Hourly Average Relative Humidity for Jakarta by Year, for 1984 to 1987.

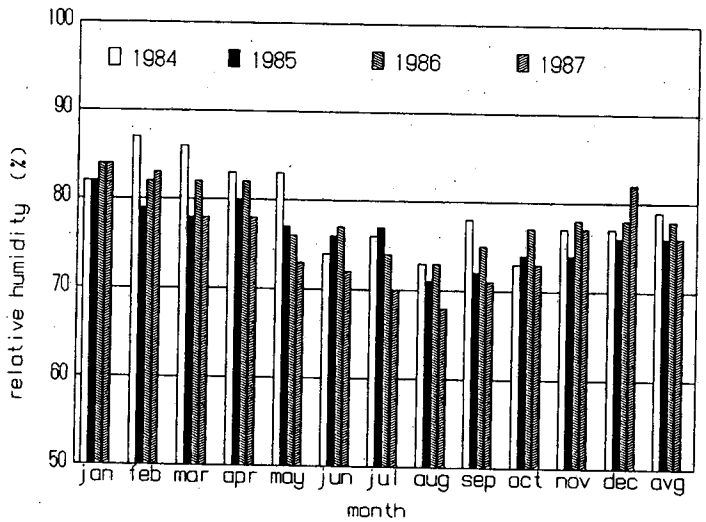

Figure 5-12. Monthly Average Relative Humidity for Jakarta by Year, for 1984 to 1987.

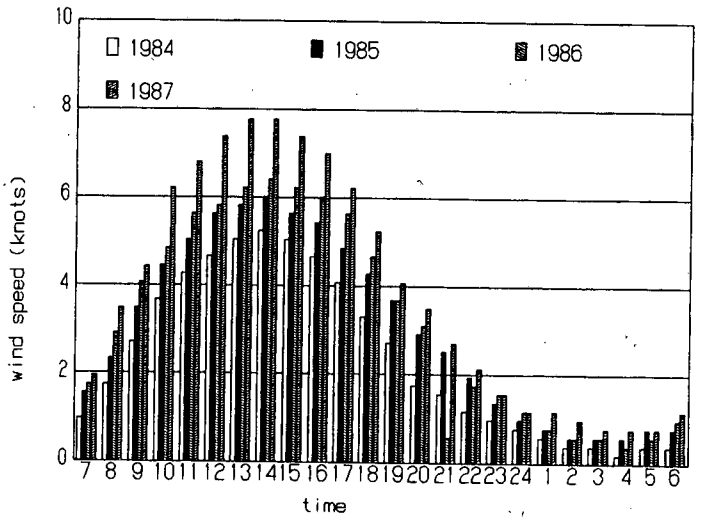

Figure 5-13. Hourly Average Wind Speed for Jakarta by Year, for 1984 to 1987.

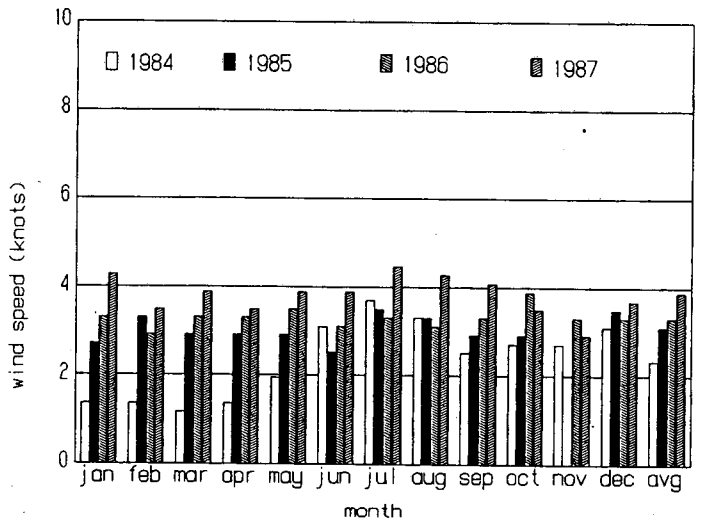

Figure 5-14. Monthly Average Wind Speed for Jakarta by Year, for 1984 to 1987.

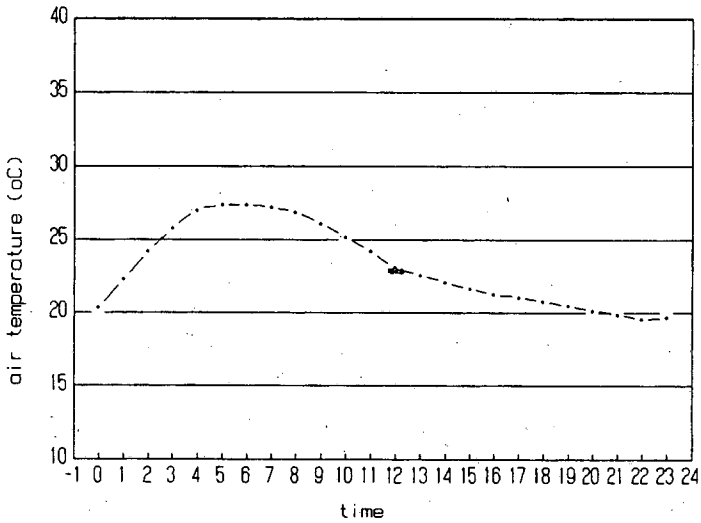

Figure 5-15. Hourly Average Air Temperature for Bandung in 1987.

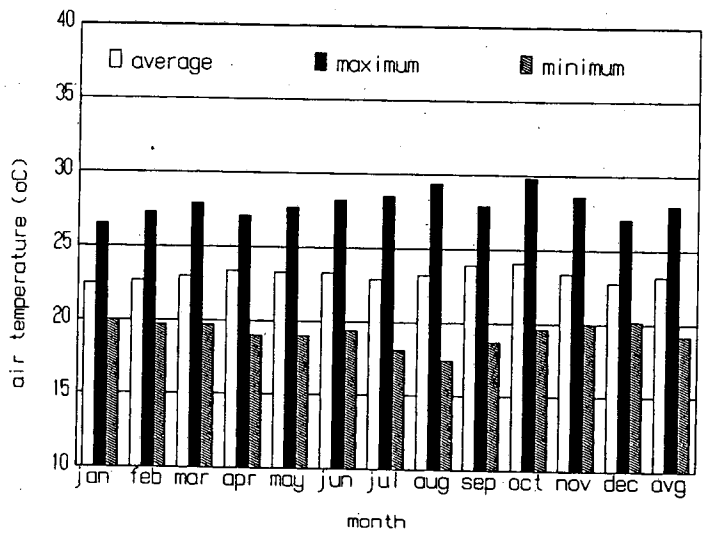

Figure 5-16. Monthly Average Air Temperature for Bandung in 1987.

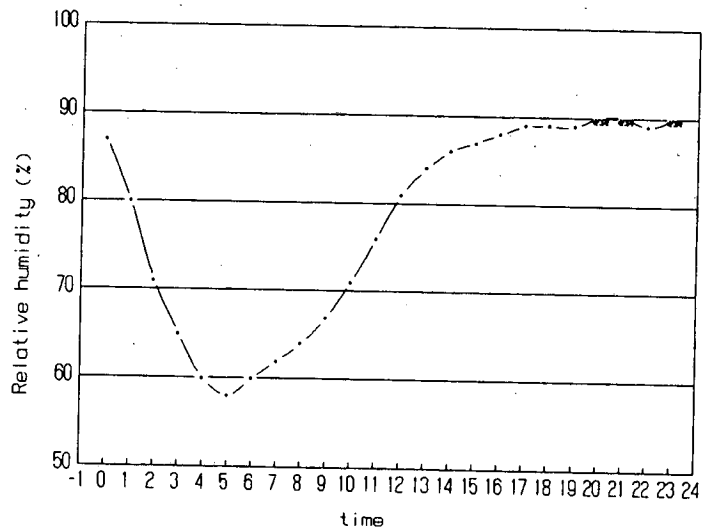

Figure 5-17. Hourly Average Relative Humidity for Bandung in 1987.

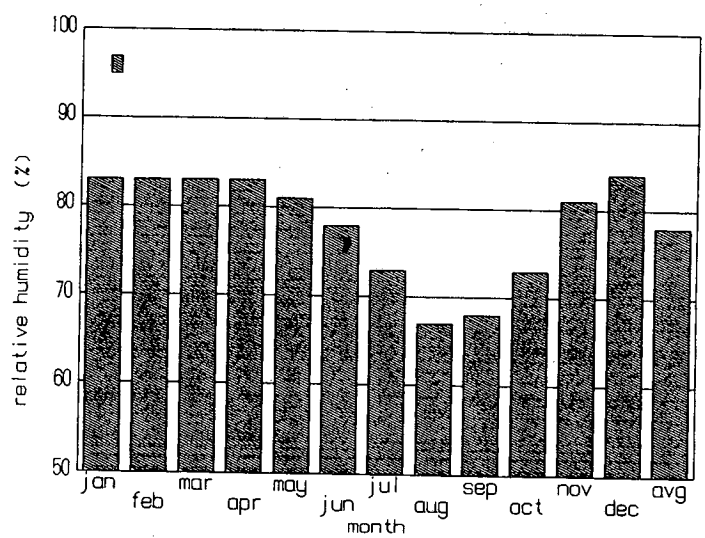

Figure 5-18. Monthly Average Relative Humidity for Bandung in 1987.

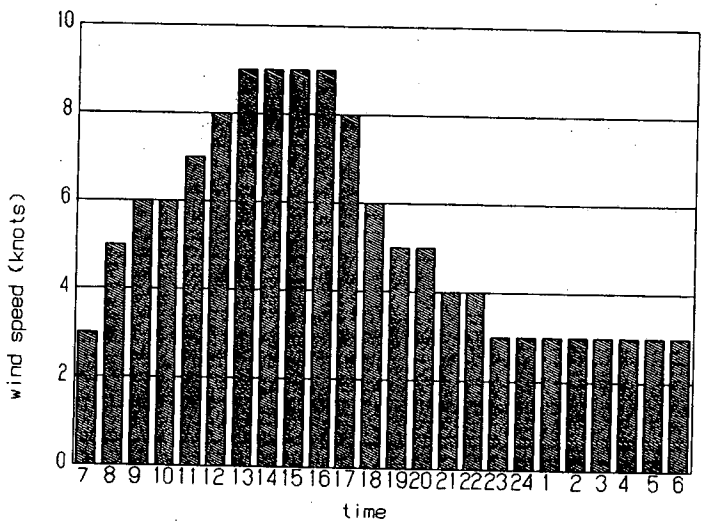

Figure 5-19. Hourly Average Wind Speed for Bandung in 1987.

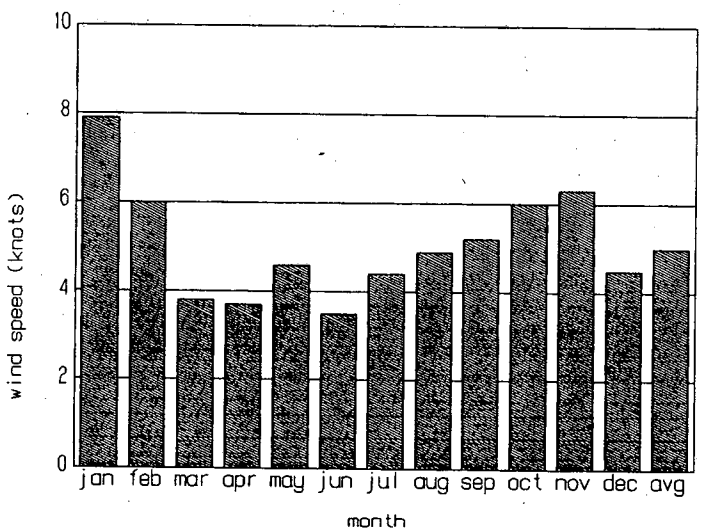

Figure 5-20. Monthly Average Wind Speed for Bandung in 1987.

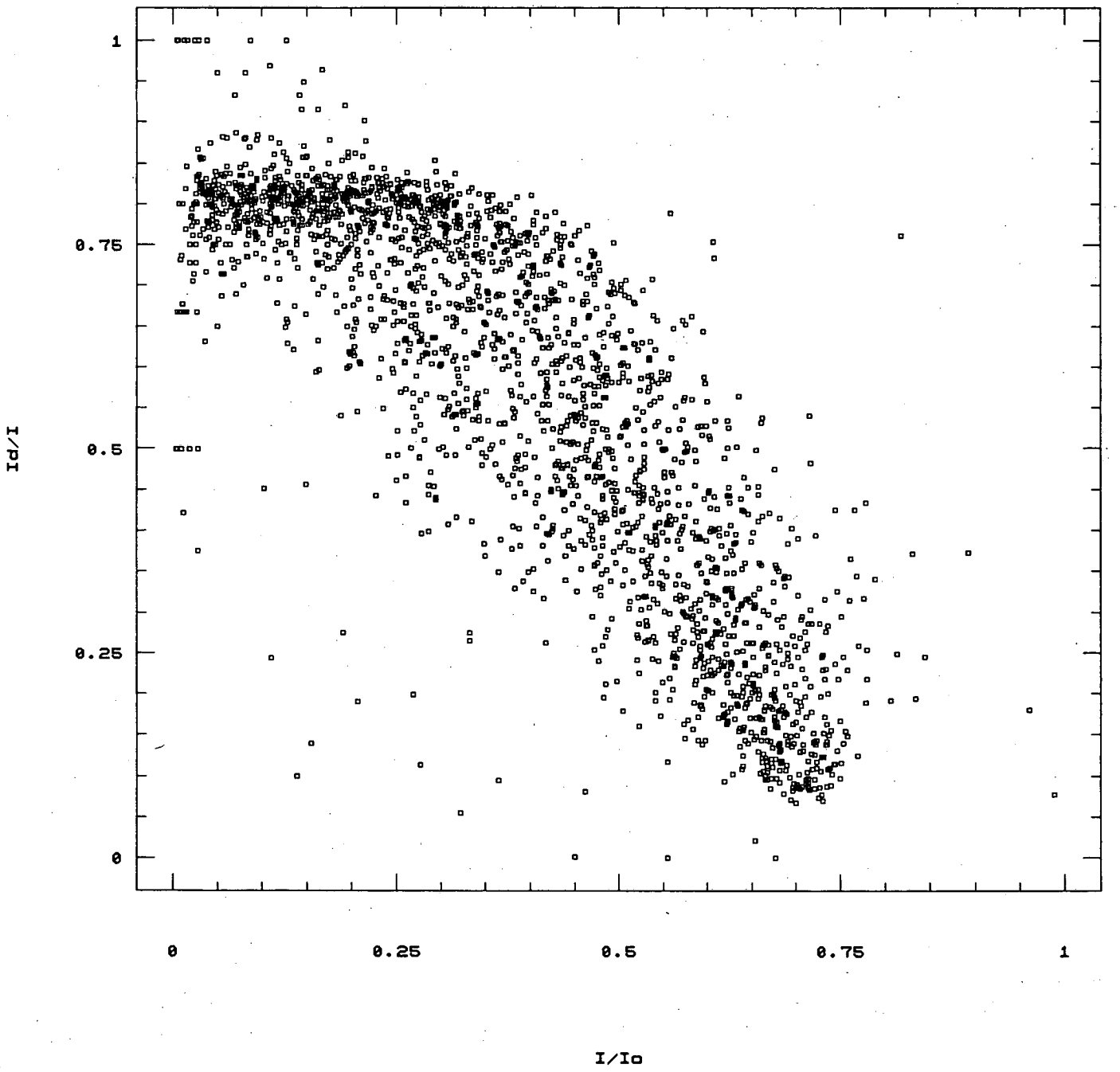

Figure 5-21. Relationship Between I/Io and Id/I, Bandung, During the Wet Season (Nov. to Apr.)

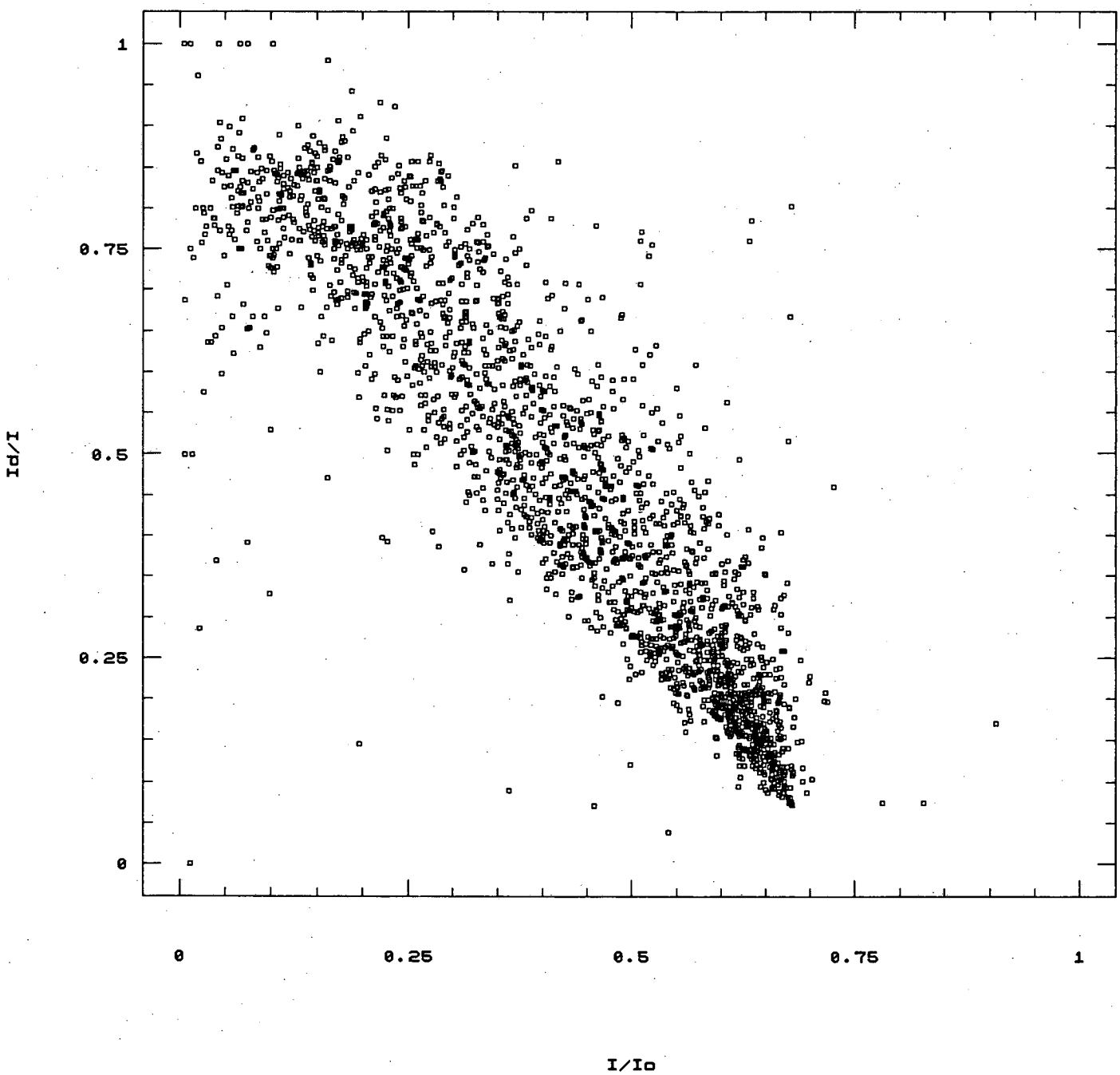

Figure 5-22. Relationship Between I/Io and Id/I, Bandung, During the Dry Season (May to Oct.)

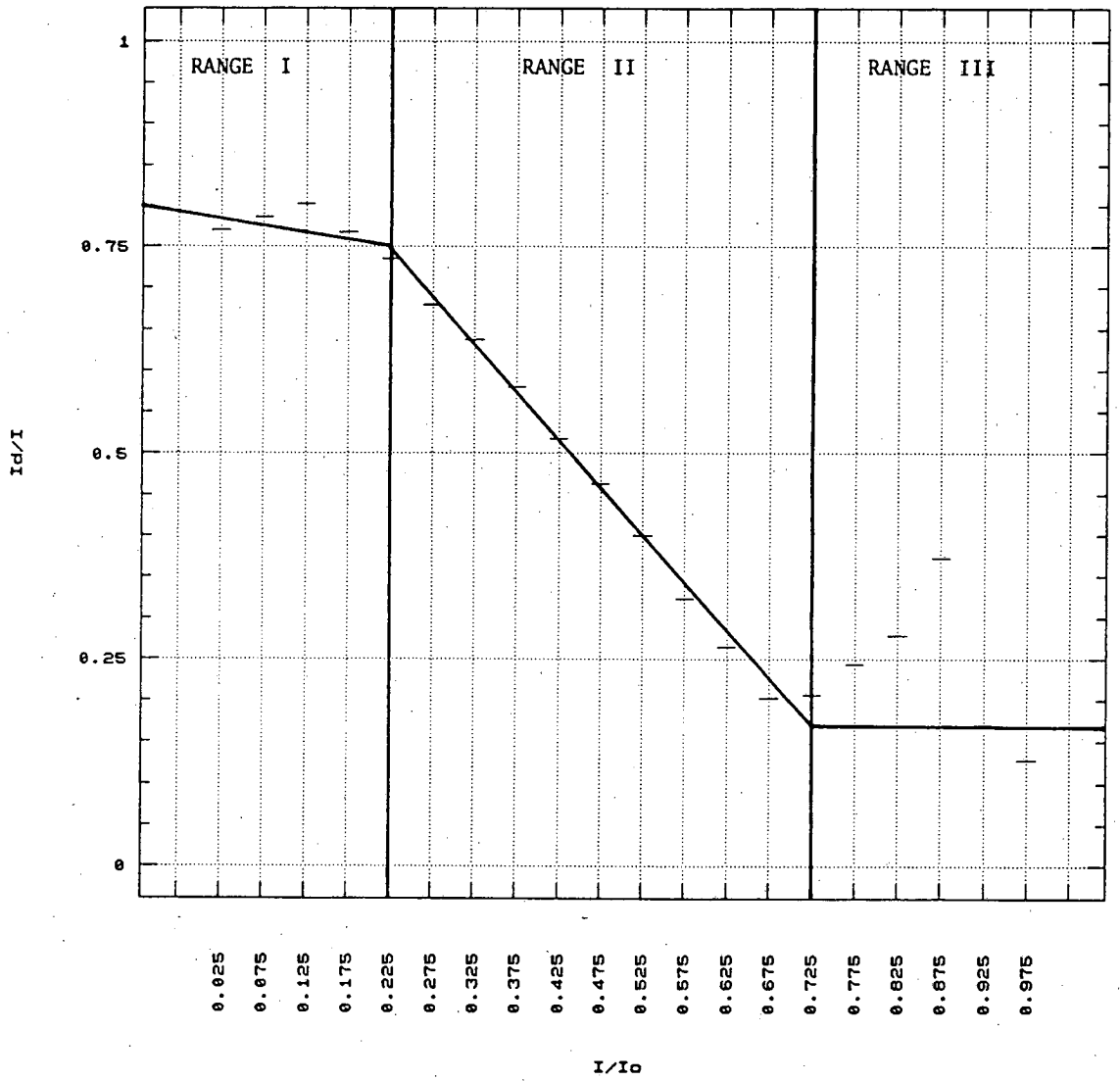

$$Id/I = 0.7943 - 0.1767\ I/Io \quad ; \quad I/Io < 0.225$$

$$Id/I = 0.9997 - 1.1454\ I/Io \quad ; \quad 0.225 < I/Io < 0.725$$

$$Id/I = 0.1693 \quad ; \quad I/Io > 0.725$$

Range	Number of Data
I	1148 (25.89 %)
II	3527 (73.18 %)
III	41 (0.93 %)

Figure 5-23. Correlation of I/Io and Id/I

Table 5-1. Solar and Weather Measuring Equipment

No.	Name of Instrument	Quantity
1.	Precision Spectral Pyranometer, Eppley, model PSP, serial number 26473F3 and 26474F3	2
2.	Shadow Band, Eppley, Model SBS	1
3.	Precision Infrared Radiometer, Eppley, model PIR, serial number 26877F3	1
4.	Cable for Radiometer	50 feet
5.	Illumination probe, Licor model 210 SA	1
6.	Sensor base for level mounting, Licor model LI 12003s	2
7.	Thin film humidity sensor, Weathermeasure 5134E	1
8.	Sintered filter, Weathermeasure 51140	1
9.	Conductor 20 AWG shielded cable, Weathermeasure T 600507	1
10.	Self-aspirating radiation shield, Weathermeasure 8140-A	1
11.	Combination windspeed/direction sensor, including 100 feet 5 conductor cable, Weathermeasure	1
12.	Tripod tower 10 feet, Weathermeasure	1
13.	Vertical mast 1.66 ODX 5 feet with 0.84 in. reducer for 2132, Weathermeasure 85007	1
14.	Campbell 21X Micrologger, serial number 4928 LBL/DOE 6033960	1
15.	Cassette Recorder, Campbell RC36	1
16.	Recorder interface, Campbell SC92	1
17.	Clock SI/O tape reader card for IBM-PC, Campbell, model PC-201, serial number 1953, including PC-201 software recorder cable, ribbon cable and relay box	1

TABLE 5.2. 1987 JAKARTA W/SOLAR MONTHLY WEATHER DATA SUMMARY

LATITUDE = -6.20 LONGITUDE = -106.80 TIME ZONE = -7

	JAN	FEB	MAR	APR	MAY	JUN	JUL	AUG	SEP	OCT	NOV	DEC	YEAR
AVG. TEMP. (F) (DRYBULB)	79.3	79.5	81.6	82.2	82.9	83.3	82.8	81.9	82.4	83.4	81.5	80.5	81.8
AVG. TEMP. (F) (WETBULB)	74.8	75	75.1	75.7	74.8	74.7	73.4	71.4	73.7	75	75.2	75.4	74.5
AVG. DAILY MAX. TEMP.	84.6	84.9	89.6	89.6	91.1	91.5	91.4	90.8	90.7	90.9	89.1	86.8	89.3
AVG. DAILY MIN. TEMP.	75	74.9	75.8	76.7	77	77.1	75.9	74.5	75.5	76.9	76.1	75.3	75.9
HEATING DEG. DAYS (BASE 65)	0	0	0	0	0	0	0	0	0	0	0	0	0
(BASE 60)	0	0	0	0	0	0	0	0	0	0	0	0	0
(BASE 55)	0	0	0	0	0	0	0	0	0	0	0	0	0
(BASE 50)	0	0	0	0	0	0	0	0	0	0	0	0	0
COOLING DEG. DAYS (BASE 80)	13	9	85	94.5	125.5	129.5	112.5	82	93.5	120.5	80.5	49	994.5
(BASE 75)	149.5	137.5	239	244.5	280.5	279.5	267.5	236.5	243	275.5	228	191	2772
(BASE 70)	304.5	277.5	394	394.5	435.5	429.5	422.5	391.5	393	430.5	378	342	4593
(BASE 65)	459.5	417.5	549	544.5	590.5	579.5	577.5	546.5	543	585.5	528	497	6418
HEATING DEG. HRS./24 (BASE 65)	0	0	0	0	0	0	0	0	0	0	0	0.5	0.5
(BASE 60)	0	0	0	0	0	0	0	0	0	0	0	0.1	0.1
(BASE 55)	0	0	0	0	0	0	0	0	0	0	0	0	0
(BASE 50)	0	0	0	0	0	0	0	0	0	0	0	0	0
COOLING DEG. HRS./24 (BASE 80)	37.2	35.7	92.5	91.9	114.2	118.5	115.5	102.8	104	125.7	82.2	63	1083.2
(BASE 75)	133.4	128	207	216.3	245.7	250.3	241.6	216.7	223	260.4	196.1	172.2	2490.7
(BASE 70)	286.9	265.4	361	366.1	400.7	399.6	395.6	368.8	372.1	415.4	345.5	326.2	4303.2
(BASE 65)	441.9	405.4	516	516.1	555.7	549.6	550.6	523.7	522.1	570.4	495.5	480.5	6127.5
MAXIMUM TEMP.	88	91	93	93	95	95	94	93	95	95	92	92	95
MINIMUM TEMP.	73	72	73	74	75	73	73	69	70	75	69	58	58
NO. DAYS MAX. 90 AND ABOVE	0	1	18	16	22	25	30	23	17	27	15	8	202
NO. DAYS MAX. 32 AND BELOW	0	0	0	0	0	0	0	0	0	0	0	0	0
NO. DAYS MIN. 32 AND BELOW	0	0	0	0	0	0	0	0	0	0	0	0	0
NO. DAYS MIN. 0 AND BELOW	0	0	0	0	0	0	0	0	0	0	0	0	0
AVG. WIND SPEED (MPH)	5	4.3	4.6	4.3	4.7	4.8	5.2	4.9	5	4.2	3.4	4.5	4.6
AVG. WIND SPEED (DAY)	6.6	6.4	6.9	6	7.2	7.2	7.4	7.2	7.2	6.2	5.1	6	6.6
AVG. WIND SPEED (NIGHT)	3.2	2.1	2.4	2.5	2.1	2.4	3.1	2.7	2.6	1.8	1.4	2.7	2.5
AVG. TEMP. (DAY)	80.7	81.2	84.4	84.5	85.7	86	85.6	84.7	85.1	85.9	83.7	82.5	84.2
AVG. TEMP. (NIGHT)	77.7	77.8	78.9	79.9	80.2	80.7	80	79.1	79.5	80.6	78.9	78.3	79.3
AVG. SKY COVER (DAY)	2	2	2	2	2	2	2	2	2	2	2	2	2
AVG. REL. HUM. AT 4AM	91.6	91.8	89.5	87.7	84.4	83.3	83.1	80.9	84.9	86.1	89	91.4	86.9
10AM	79.5	78.9	68.9	69.7	65.5	64.7	63.6	59.3	61.3	62.6	69.2	75.8	68.2
4PM	70.4	69.9	59.7	62.2	55.3	51.8	47.5	43.3	51.1	55.2	62.8	69.6	58.2
10PM	85.2	86.5	83.5	81.2	76.5	74.4	69.7	66.7	72.9	73.8	82.6	85.5	78.2

TABLE 5.2 (cont)

LATITUDE = -6.20 LONGITUDE = -106.80 TIME ZONE = -7

1987 JAKARTA W/SOLAR MONTHL	JAN	FEB	MAR	APR	MAY	JUN	JUL	AUG	SEP	OCT	NOV	DEC	YEAR
AVG. DAILY DIRECT NORMAL SOLAR	1014.2	830.5	1288.7	1051.2	1163.5	1158.4	1344.2	1523.6	1364.7	1578.8	1143.8	936.7	1203.1
AVG. DAILY TOTAL HORIZNTL SOLAR	1239.9	1117.7	1506.1	1250.6	1275.8	1241.3	1399	1615.3	1552.4	1685.8	1380	1166	1371.4
MAX. DAILY DIRECT NORMAL SOLAR	1919	1444	2120	1824	1791	1643	1903	1919	1902	2088	1877	2223	2223
MAX. DAILY TOTAL HORIZNTL SOLAR	1896	1583	2066	1805	1762	1573	1739	1864	1886	2072	1874	2082	2082
MIN. DAILY DIRECT NORMAL SOLAR	284	231	318	419	372	354	472	1134	797	869	523	107	107
MIN. DAILY TOTAL HORIZNTL SOLAR	544	549	616	753	579	613	795	1216	1096	1160	829	225	225
MAX. HRLY DIRECT NORMAL SOLAR	342	318	337	324	316	297	296	322	322	330	321	342	342
MAX. HRLY TOTAL HORIZNTL SOLAR	313	298	324	298	317	251	251	269	280	302	284	309	324
AVG. MAX. HRLY DIRECT NORML SOLAR	211.8	181	254.5	222.5	238.5	216.5	224.2	238.8	243.4	289.7	238.8	193.3	229.8
AVG. MAX. HRLY TOTAL HRZNTL SOLAR	225.2	208.1	265.4	225.8	219.5	206.8	219.8	236.7	230.8	257.5	244.4	198.2	228.4
AVG. DAILY TOTAL VERTICAL SOLAR													
JAKARTA													
N	387.3	399	565.5	768.1	1006.3	1092	1161.8	1066.3	727.2	520.2	419.1	372.7	709.2
E	574.5	547	658.2	578.4	543.5	551.5	633.7	695	661.3	676.8	621.4	539.3	607.2
S	805.9	603.3	488.2	389.4	386.3	378.7	404.8	446.4	489.4	697.3	812.9	803.8	559
W	1030.6	994	1215.7	1084.4	1145.5	1084.2	1178.7	1355.9	1415.3	1576.2	1125.2	992.1	1184.8
MAX. DAILY TOTAL VERTICAL SOLAR													
AZIMUTH													
N	501.8	483.3	843.9	1029.1	1358.6	1343.6	1379.3	1202.5	986.6	587	494.7	551.1	1379.3
E	769.7	770	823.4	702.1	642.8	649.9	720.7	755.9	749.7	749.9	750.4	948.4	948.4
S	1217.5	812.7	632.3	522.5	450.6	438.9	442.4	472.6	554	892	1034	1359	1359
W	1713.4	1483.5	1761.9	1713.2	1523.1	1439.2	1414.1	1593.7	1701.7	1785.1	1704.6	1834	1834
MAX. HRLY TOTAL VERTICAL SOLAR													
AZIMUTH													
N	78.3	71.3	110.1	167.1	193.8	194	184.1	160.3	126.7	96.1	81.8	75.5	194
E	158.8	148.6	170	138.2	119	113	131	138.9	149.5	145.8	174.7	177.9	177.9
S	169.9	106.9	94.1	76	65.9	61.6	67.5	71.5	88	111.5	143.6	181.3	181.3
W	373.9	373.9	403.6	439.4	365.6	341.3	330.2	346.1	371.8	397.8	369.8	385.1	439.4

TABLE 5.2 (cont)

DESIGN TEMPERATURES ---------- SUMMER ---------- WINTER

PER CENT	T(DRY)	T(WET)	T(DRY)
1.0	91 80	73	
2.5	90 78	74	
5.0	88 78		

MONTHLY AVERAGE TEMPERATURES AS A FUNCTION OF HOUR OF THE DAY

HOUR	JAN	FEB	MAR	APR	MAY	JUN	JUL	AUG	SEP	OCT	NOV	DEC	YEAR
0	77.3	77.6	78.2	79.4	79.3	79.9	79.4	78.4	79.1	79.7	78.4	77.7	78.7
1	76.9	76.9	77.8	78.8	78.9	79.7	78.6	77.5	78.4	79.2	77.9	77.3	78.2
2	76.6	76.1	77.3	78.5	78.5	79	78	76.9	77.5	78.6	77.3	76.8	77.6
3	76.2	75.8	76.8	78	78.2	78.5	77.4	76.2	77.2	78	77.1	76.5	77.2
4	75.7	75.5	76.6	77.7	77.7	78.1	76.7	75.5	76.4	77.5	76.9	75.9	76.7
5	75.7	75.4	76.5	77.2	77.5	77.8	76.5	75.1	76.1	77.2	76.6	75.8	76.5
6	75.4	75.5	76.7	77.1	77.6	77.7	76.1	74.9	76	77.1	76.7	75.7	76.4
7	76.2	76.1	77	77.9	78	78.1	77.1	75.4	76.9	78.8	77.7	77.4	77.2
8	77.8	78.3	80	80.6	80.5	80.6	79.9	78.3	80.4	82.6	80.9	80.2	80
9	80	80.5	83.6	84	84.4	84.4	83.2	82.2	84.3	85.8	83.3	82.1	83.1
10	80.9	81.9	86.1	86	86.9	86.7	86.5	85.8	86.8	88	85.1	83.9	85.4
11	81.9	82.4	87.5	87.8	88.9	89.1	88.3	88	89.1	89.7	87.4	85	87.1
12	82.7	82.9	88.3	88.5	89.8	90.3	89.5	89.5	89.4	89.9	88.1	85.6	87.9
13	83.3	83.6	88.3	87.9	90.2	90.6	90.8	90.2	89.8	89.8	87.8	85.5	88.2
14	83.6	84.1	88.1	87.3	90	90.3	90.7	89.6	89.1	89.6	87.2	85.1	87.9
15	83.6	83.9	87.1	87	88.5	89.3	89.6	88.8	88.3	88.6	86.1	84.7	87.2
16	82.6	83.4	86	85.9	87.8	88.3	88.4	87.5	87.2	87.7	84.9	84.3	86.2
17	81.6	82.3	84.7	84.9	86.1	86.2	86.5	86	85.7	86.6	83.8	82.9	84.8
18	80.5	80.9	82.9	83.6	84.6	84.8	84.9	84.5	84.2	85.4	82.6	81.8	83.4
19	79.7	79.9	81.5	82.3	83.2	83.5	83.4	82.8	82.8	84.1	81.4	80.7	82.1
20	79	79.4	80.5	81.4	82.1	82.6	82.4	81.9	81.9	83.1	80.8	79.9	81.2
21	78.6	79	79.9	81	81.2	81.9	81.6	80.7	81.2	82.3	80	79.3	80.6
22	78.4	78.4	79.3	80.4	80.5	81.4	80.7	80.1	80.4	81.5	79.4	78.9	80
23	77.8	78	78.8	79.9	80	80.6	80.1	79.4	79.6	80.7	78.9	78.5	79.4

Table 5.3A 1987 JAKARTA W/SOLAR

Insolation on surfaces of various orientations (kWh/sqm) Measured insolation

	Jan	Feb	Mar	Apr	May	Jun	Jul	Aug	Sep	Oct	Nov	Dec	Year
Hor													
Direct	63.2	45.7	86.4	62.5	67.7	63.1	78.2	94.9	81.7	97.5	71.2	57.7	869.8
Diffuse	56.2	51.5	58.2	54.1	55.3	52.6	56.5	60.8	63.2	65.2	57.5	54.5	685.6
Total	119.4	97.2	144.6	116.5	123	115.7	134.7	155.7	144.9	162.8	128.7	112.2	1555.4
Total Transmitted	97.8	79.3	119.4	95.1	100	93.9	109.7	127.6	118.4	133.2	105.5	91.6	1271.3
Vert-N													
Direct	0	0	6.2	23.3	42.4	47.7	53.7	43.7	14.8	0.4	0	0	232.1
Diffuse	32.2	29.5	38.7	37.6	42.1	43.4	48.1	47.3	40	37.5	33.2	29.7	459.3
Total	32.2	29.5	44.9	60.9	84.5	91.1	101.8	91	54.8	37.9	33.2	29.7	691.4
Total Transmitted	25.7	23.6	32.6	42.8	63.7	70.9	78.2	65	37.3	30	26.5	23.7	519.9
Vert-E													
Direct	10.6	7.9	14	10.4	8.6	9.6	14.6	15.6	10.7	11.4	11.8	9.8	134.8
Diffuse	36.6	31.9	39.2	34.2	33.7	33.4	38.2	41	38.5	40.2	37.3	33.1	437.2
Total	47.1	39.7	53.2	44.6	42.3	43	52.8	56.6	49.2	51.6	49.1	42.9	572
Total Transmitted	37.2	31.6	42	35.1	33	33.6	41.4	44.4	38.6	40.6	38.5	33.8	449.8
Vert-S													
Direct	27.1	10.9	1.5	0	0	0	0	0	0.1	12.9	24.7	27.6	104.7
Diffuse	40.9	33.6	37.3	29.8	29.3	28.5	31.9	34.7	35.1	40	40.7	39	420.8
Total	68	44.5	38.7	29.8	29.3	28.5	31.9	34.7	35.2	52.8	65.5	66.6	525.5
Total Transmitted	48.8	31.3	30	23.9	23.4	22.8	25.5	27.7	28	36	45.7	48.5	391.5
Vert-W													
Direct	46	37.7	58.6	48.9	56.1	50.7	58.3	69.6	68.9	85.2	49.1	42.8	672
Diffuse	44.7	41.2	53	42	42	40.5	45.9	49.7	47.4	48.2	45.6	43.2	543.2
Total	90.7	78.9	111.6	90.9	98.2	91.2	104.2	119.3	116.3	133.3	94.7	86	1215.2
Total Transmitted	73.9	64.6	91.1	74.6	80.4	74.4	85.1	97.6	96	110.4	77.7	70.2	995.9
Vert-NE													
Direct	3.5	4.1	11.3	12.9	15.9	19.4	25.3	21.9	10.9	7	4.2	2.8	139.1
Diffuse	33.7	30.3	38.4	35.5	37	37.6	42.5	43.7	38.8	38.4	34.6	30.8	441.4
Total	37.2	34.4	49.7	48.4	52.9	57	67.8	65.6	49.7	45.5	38.8	33.6	580.5
Total Transmitted	28.8	26.9	38.6	37.9	41.3	44.6	53.3	51.3	38.6	35.1	29.8	26	452.1
Vert-SW													
Direct	47.7	32.9	39.5	23.7	19.6	14.7	18.2	29.2	41.7	68	48	45.6	428.8
Diffuse	45.7	39.8	47.2	35.4	33.8	32.1	36.4	40.8	41.6	45.9	45.9	44.5	489.1
Total	93.4	72.7	86.7	59.1	53.3	46.8	54.6	70	83.2	113.9	93.9	90.2	917.9
Total Transmitted	75.8	58.8	68.5	45.8	39.9	34.5	40.5	53.2	65.7	92.2	76.1	73.4	724.5
Vert-SE													
Direct	13	7.1	8.6	3.5	1.2	1.1	2.3	4.1	4.9	9.3	14	12.6	81.7
Diffuse	37.9	31.9	37.3	31.3	30.4	29.6	33.6	36.7	36.1	39.5	38.3	34.6	417.3
Total	50.9	39	45.9	34.8	31.6	30.7	35.8	40.8	41	48.8	52.3	47.2	499
Total Transmitted	39.9	30.7	35.6	27	24.8	24.1	27.8	31.5	31.8	37.8	40.6	37.1	388.9
Vert-NW													
Direct	18.9	20.6	43.6	47.2	64.8	63.9	71.1	73.1	56.4	52.6	22.9	16.5	551.5
Diffuse	37.5	35.5	48	42.4	45.4	45.2	50.5	51.9	45.9	43.4	38.7	35.1	519.4
Total	56.3	56	91.6	89.6	110.2	109.1	121.6	125	102.4	96	61.6	51.5	1070.9
Total Transmitted	42.5	43.6	72.7	72.8	90.1	89.3	99.3	101.7	82.6	75.4	47.2	38.6	855.9

Table 5.3B 1987 JAKARTA W/SOLAR
Power of Insolation on surfaces various orientations (W/sqm)
Measured insolation
Power determined for all hours of daylight.

	Jan	Feb	Mar	Apr	May	Jun	Jul	Aug	Sep	Oct	Nov	Dec	Year
Hor													
Direct	176.2	140.2	244.7	192.8	208.2	197.9	229.5	278.2	249.1	286.9	219	167.6	216.1
Diffuse	156.4	157.9	164.9	166.9	170.1	164.9	165.7	178.3	192.8	191.8	177	158.5	170.3
Total	332.6	298.1	409.6	359.7	378.3	362.8	395.1	456.6	441.9	478.7	396	326.1	386.4
Total Transmitted	272.4	243.2	338.3	293.5	307.7	294.2	321.6	374.1	361.1	391.7	324.5	266.2	315.8
Vert-N													
Direct	0	0	17.7	71.8	130.4	149.4	157.5	128.1	45.1	1	0	0	57.7
Diffuse	89.8	90.5	109.5	116.1	129.6	136.1	141.1	138.7	121.9	110.3	102	86.3	114.1
Total	89.8	90.5	127.2	188	260	285.5	298.6	266.8	166.9	111.3	102	86.3	171.8
Total Transmitted	71.7	72.3	92.3	132	195.9	222.1	229.2	190.7	113.8	88.2	81.5	68.9	129.2
Vert-E													
Direct	29.4	24.1	39.6	32.2	26.5	30.1	42.9	45.7	32.5	33.5	36.2	28.4	33.5
Diffuse	101.9	97.8	111.1	105.5	103.6	104.7	111.9	120.3	117.5	118.2	114.8	96.3	108.6
Total	131.3	121.9	150.6	137.6	130.1	134.8	154.9	165.9	150	151.7	150.9	124.7	142.1
Total Transmitted	103.7	97	118.9	108.2	101.7	105.5	121.3	130.2	117.6	119.3	118.4	98.3	111.7
Vert-S													
Direct	75.5	33.3	4.1	0	0	0	0	0	0.3	37.8	76.1	80.1	26
Diffuse	114	103	105.6	92.1	90.1	89.3	93.5	101.7	106.9	117.6	125.4	113.4	104.5
Total	189.5	136.4	109.8	92.1	90.1	89.3	93.5	101.7	107.2	155.4	201.5	193.5	130.6
Total Transmitted	136	95.9	85	73.6	72	71.4	74.7	81.2	85.5	105.9	140.6	141	97.3
Vert-W													
Direct	128.1	115.8	166.1	151	172.7	159	171	204	210	250.4	151.1	124.4	167
Diffuse	124.6	126.3	150	129.5	129.3	126.9	134.6	145.7	144.5	141.6	140.2	125.5	135
Total	252.8	242.1	316.2	280.5	302	285.9	305.7	349.7	354.6	392.1	291.3	249.9	301.9
Total Transmitted	205.8	198	258.1	230.3	247.2	233.1	249.5	286.1	292.6	324.8	239.2	204	247.4
Vert-NE													
Direct	9.7	12.7	31.9	39.9	49.1	60.7	74.2	64.2	33.2	20.7	12.8	8.1	34.6
Diffuse	94	93	108.9	109.6	113.7	117.9	124.5	128.1	118.3	113.1	106.5	89.6	109.7
Total	103.7	105.6	140.8	149.5	162.8	178.6	198.7	192.3	151.5	133.7	119.3	97.6	144.2
Total Transmitted	80.4	82.5	109.3	116.8	127.2	139.7	156.4	150.4	117.6	103.2	91.7	75.7	112.3
Vert-SW													
Direct	132.9	101	111.8	73.2	60.2	46.2	53.4	85.5	127.1	200.1	147.8	132.6	106.5
Diffuse	127.4	122.1	133.7	109.4	103.9	100.5	106.8	119.8	126.8	134.9	141.1	129.5	121.5
Total	260.3	223.1	245.5	182.6	164.1	146.7	160.2	205.3	253.8	334.9	289	262.1	228.1
Total Transmitted	211.1	180.4	194.1	141.5	122.7	108.3	118.8	155.9	200.4	271.2	234.2	213.3	180
Vert-SE													
Direct	36.1	21.8	24.3	10.8	3.8	3.5	6.6	11.9	14.9	27.4	43	36.7	20.3
Diffuse	105.6	97.7	105.8	96.7	93.6	92.9	98.4	107.7	110.2	116.2	117.7	100.6	103.7
Total	141.8	119.5	130.1	107.5	97.4	96.4	105	119.7	125.1	143.6	160.8	137.3	124
Total Transmitted	111.1	94.3	100.9	83.3	76.3	75.5	81.6	92.5	96.9	111.3	125	107.8	96.6
Vert-NW													
Direct	52.6	63	123.4	145.6	199.3	200.2	208.5	214.4	172.1	154.8	70.5	47.9	137
Diffuse	104.4	108.9	136.1	130.8	139.8	141.6	148.1	152.1	140	127.6	119	101.9	129
Total	156.9	171.9	259.5	276.4	339.1	341.9	356.6	366.5	312.1	282.3	189.5	149.8	266.1
Total Transmitted	118.5	133.8	206	224.6	277.3	279.9	291.2	298.3	251.9	221.7	145.3	112.3	212.7

Table 5.3C 1987 JAKARTA W/SOLAR
Power of Insolation on surfaces various orientations (W/sqm)
Measured insolation
Power determined between 8 to 18

	Jan	Feb	Mar	Apr	May	Jun	Jul	Aug	Sep	Oct	Nov	Dec	Year
Hor													
Direct	185.1	147.9	253.2	189.3	198.5	191.3	229.5	278.2	247.6	286	215.7	169	216.6
Diffuse	161	163.3	168.9	163.8	162.1	159.4	165.7	178.3	191.6	191.2	174.3	158.1	169.8
Total	346	311.2	422.1	353.1	360.6	350.7	395.1	456.6	439.2	477.3	390	327.1	386.4
Total Transmitted	283.7	254.2	348.7	288.2	293.2	284.4	321.6	374.1	358.9	390.6	319.6	267.1	315.9
Vert-N													
Direct	0	0	18.3	70.5	124.3	144.4	157.5	128.1	44.8	1	0	0	57.8
Diffuse	94.6	96.3	114.1	114	123.5	131.6	141.1	138.7	121.1	110	100.5	87.8	114.6
Total	94.6	96.3	132.5	184.6	247.8	276	298.6	266.8	165.9	111	100.5	87.8	172.4
Total Transmitted	75.6	77	96.2	129.6	186.7	214.7	229.2	190.7	113.1	87.9	80.3	70.2	129.6
Vert-E													
Direct	31	25.5	41	31.6	25.3	29.1	42.9	45.7	32.3	33.4	35.6	28.7	33.6
Diffuse	107.4	104.1	116.9	103.6	98.7	101.2	111.9	120.3	116.8	117.8	113	97.9	109.2
Total	138.3	129.7	157.9	135.1	124	130.3	154.9	165.9	149.1	151.2	148.7	126.6	142.8
Total Transmitted	109.3	103.2	124.6	106.3	96.9	101.9	121.3	130.2	116.9	118.9	116.6	99.8	112.3
Vert-S													
Direct	73.4	31.2	3.5	0	0	0	0	0	0.3	37.7	75	78.6	25
Diffuse	119.6	109.2	109.2	90.5	85.8	86.4	93.5	101.7	106.3	117.2	123.5	114.7	104.8
Total	193	140.5	112.7	90.5	85.8	86.4	93.5	101.7	106.6	155	198.4	193.3	129.8
Total Transmitted	138.7	99.6	87.7	72.3	68.6	69	74.7	81.2	84.9	105.6	138.5	141	96.9
Vert-W													
Direct	117.9	105	162.1	148.3	164.6	153.7	171	204	208.8	249.7	148.8	120.1	163.3
Diffuse	129.8	132.3	142.3	127.1	123.3	122.7	134.6	145.7	143.7	141.2	138	126.4	134
Total	247.8	237.4	304.4	275.4	287.9	276.4	305.7	349.7	352.4	390.9	286.9	246.4	297.2
Total Transmitted	200.8	193.2	248.1	226.1	235.6	225.3	249.5	286.1	290.9	323.9	235.6	200.9	243.4
Vert-NE													
Direct	10.2	13.4	33.1	39.2	46.8	58.6	74.2	64.2	33	20.6	12.6	8.1	34.7
Diffuse	99.1	99	114.7	107.6	108.4	114	124.5	128.1	117.6	112.7	104.9	91.1	110.2
Total	109.3	112.4	147.8	146.8	155.1	172.6	198.7	192.3	150.6	133.3	117.5	99.3	144.9
Total Transmitted	84.7	87.8	114.7	114.7	121.2	135.1	156.4	150.4	116.9	102.9	90.3	76.9	112.8
Vert-SW													
Direct	123.6	91.7	108.2	71.8	57.4	44.6	53.4	85.5	126.3	199.5	145.6	128.3	103.2
Diffuse	132.8	128.2	129.1	107.4	99	97.2	106.8	119.8	126	134.5	139	130.4	120.8
Total	256.3	219.9	237.3	179.2	156.4	141.8	160.2	205.3	252.3	334	284.6	258.7	224
Total Transmitted	207	176.9	187	138.9	116.9	104.6	118.8	155.9	199.2	270.4	230.7	210.3	176.5
Vert-SE													
Direct	38	23.1	25.2	10.6	3.6	3.4	6.6	11.9	14.9	27.3	42.4	37	20.3
Diffuse	111.4	104.1	111.5	94.9	89.2	89.8	98.4	107.7	109.5	115.9	116	102.3	104.2
Total	149.4	127.1	136.7	105.5	92.8	93.1	105	119.7	124.4	143.2	158.4	139.3	124.6
Total Transmitted	117.1	100.3	106.1	81.8	72.8	73	81.6	92.5	96.3	110.9	123.1	109.4	97.1
Vert-NW													
Direct	47.7	57.2	121.3	143	190	193.6	208.5	214.4	171	154.3	69.4	46.1	135.2
Diffuse	109.4	114.8	132.9	128.4	133.2	136.9	148.1	152.1	139.2	127.2	117.2	103.2	128.6
Total	157	171.9	254.3	271.4	323.2	330.5	356.6	366.5	310.2	281.5	186.6	149.2	263.9
Total Transmitted	118.6	133.5	201.4	220.5	264.3	270.5	291.2	298.3	250.4	221.1	143.1	112	210.9

Table 5.3D 1987 JAKARTA W/SOLAR
Power of Insolation on surfaces various orientations (W/sqm)
Measured insolation
Power determined between 9 to 17

	Jan	Feb	Mar	Apr	May	Jun	Jul	Aug	Sep	Oct	Nov	Dec	Year
Hor													
Direct	218.3	173.7	302.6	226.2	238.6	229	274	333	296.4	343.5	258.8	199.8	258.6
Diffuse	184.4	188.1	194.2	186.7	183.3	180.8	187.5	200.2	214.9	210	199.6	179.9	192.5
Total	402.7	361.8	496.8	412.9	421.9	409.9	461.5	533.2	511.3	553.5	458.4	379.7	451.1
Total Transmitted	333.1	298.3	413.7	339.8	345.6	335.1	378.9	440.7	421.4	456.5	378	312.7	371.8
Vert-N													
Direct	0	0	21.7	77.7	137	156.7	171.9	142.3	51	1.3	0	0	63.7
Diffuse	109.6	111.3	134	136.8	152.9	159.6	167.6	165.9	148.7	136.2	120.1	105.6	137.5
Total	109.6	111.3	155.7	214.4	289.9	316.3	339.5	308.2	199.7	137.5	120.1	105.6	201.3
Total Transmitted	87.6	88.9	113	152.4	220.1	247.3	262	222.5	137.8	108.9	96	84.4	152.2
Vert-E													
Direct	33.5	29.3	47.7	37.4	30.7	34.2	49.4	53.3	38.9	39.2	41.2	30.5	38.9
Diffuse	123.5	120.5	137.6	124.8	122.4	122.3	132.4	143.1	143.1	144.7	134.3	116.9	130.5
Total	157.1	149.8	185.4	162.2	153.1	156.5	181.7	196.4	182	183.9	175.5	147.4	169.4
Total Transmitted	123.7	119	146	127.4	119.6	122.3	142	153.9	142.6	144.5	137.4	115.9	133
Vert-S													
Direct	76.8	30.6	2.8	0	0	0	0	0	0.1	37.7	80.2	80.8	25.8
Diffuse	136.5	124.9	127.7	109.1	106.6	104.9	111.3	121.5	130.8	146	147.2	134.6	125.1
Total	213.4	155.4	130.5	109.1	106.6	104.9	111.3	121.5	130.8	183.7	227.4	215.5	150.9
Total Transmitted	153.5	111.1	102.3	87.1	85.2	83.8	89	97.1	104.5	127.9	159.3	157.3	113.2
Vert-W													
Direct	111.7	94.9	156.9	136.5	157.7	142.3	159.5	194.8	196.9	248.3	146.9	112.4	155.4
Diffuse	144.1	146.1	161.2	148	152.5	148.7	158.4	172.9	178.8	182.1	164.1	143.9	158.5
Total	255.7	241	318	284.6	310.2	291	317.9	367.7	375.7	430.5	311	256.2	313.9
Total Transmitted	205.6	194.5	256.9	231.4	251.7	234.9	257	297.9	307	353.7	253.7	207.2	254.8
Vert-NE													
Direct	10.6	15.3	38.8	46.9	57	70.2	87.5	76.1	39.8	24.2	14.2	8	40.9
Diffuse	114.4	114.5	135.1	129.8	134.2	137.9	147.7	152.8	144.2	138.7	125	109.2	132.1
Total	124.9	129.8	173.9	176.7	191.1	208.1	235.2	229	184	162.9	139.2	117.2	173
Total Transmitted	96.8	101.3	134.8	138	149.3	162.7	184.9	178.8	142.7	125.6	107	91	134.6
Vert-SW													
Direct	120.1	83.3	102.6	62.1	49.8	35.9	43.9	75.6	115.5	197.8	145.6	123	96.4
Diffuse	148.1	142.4	147.2	126.4	122.7	117.9	126.2	142.2	156.5	172.2	165.4	149	143
Total	268.2	225.7	249.8	188.5	172.5	153.8	170.1	217.8	272.1	370	311.1	272	239.5
Total Transmitted	214.9	180	194.8	144.8	128.9	114	126.2	164	212.7	297.1	250.4	219.4	187.4
Vert-SE													
Direct	42.3	26.6	29.1	12.3	4.3	3.6	6.8	13.3	17.8	32.1	49.6	40.8	23.2
Diffuse	128.4	120.5	131.2	114.5	110.7	108.8	116.7	128.4	134.3	142.5	138	122.3	124.7
Total	170.7	147.1	160.2	126.8	115	112.4	123.6	141.8	152	174.6	187.6	163.1	148
Total Transmitted	133.3	115.9	124.1	98.3	90.2	88.2	96.1	109.5	117.7	135.2	145.5	127.7	115.2
Vert-NW													
Direct	43.2	51.3	119.6	137.3	191	190.8	206.3	214	165.5	154.3	67.6	41.5	132.4
Diffuse	123.7	128.9	152.3	150.7	164.8	166.1	174.9	181	172.4	161.9	139.7	120.6	153.2
Total	166.9	180.2	271.9	288	355.8	357	381.1	395	337.9	316.2	207.3	162.1	285.7
Total Transmitted	125.7	139.1	213.6	232.2	288.9	290	308.9	319.2	270.5	246.8	158.6	121.7	226.9

Table 5.3E 1987 JAKARTA W/SOLAR
Power of Insolation on surfaces various orientations (W/sqm)
Measured insolation
Power determined between 8 to 17

	Jan	Feb	Mar	Apr	May	Jun	Jul	Aug	Sep	Oct	Nov	Dec	Year
Hor													
Direct	198.3	157.1	273.2	204	214.8	206.6	247.7	300.6	267	309.9	234.1	181.8	233.6
Diffuse	168.1	170.7	176.6	169.5	165.6	164	170.9	183	194.8	191.7	182.4	163.9	175.1
Total	366.3	327.7	449.8	373.5	380.4	370.6	418.6	483.6	461.9	501.6	416.6	345.7	408.7
Total Transmitted	302.7	270.1	374.4	307.4	311.6	302.9	343.4	399.4	380.6	413.6	343.4	284.5	336.7
Vert-N													
Direct	0	0	19.6	70.1	123.4	141.6	155.9	128.7	46	1.2	0	0	57.6
Diffuse	100.2	101.1	121.9	124.1	137.9	144.7	152.9	151.4	134.7	124.3	109.9	96.5	125.1
Total	100.2	101.1	141.4	194.3	261.3	286.4	308.8	280.2	180.7	125.5	109.9	96.5	182.7
Total Transmitted	80	80.8	102.7	138.1	198.4	223.9	238.3	202.3	124.7	99.4	87.8	77.1	138.2
Vert-E													
Direct	34	28.1	45.1	34.7	27.8	32	47.2	50.2	35.5	36.7	39.2	31.6	36.9
Diffuse	114.2	109.9	125.7	113.8	110.5	111.5	121.9	131.7	129.7	132.6	123.7	107.6	119.5
Total	148.3	138	170.7	148.5	138.3	143.5	169.1	182	165.3	169.3	162.9	139.2	156.4
Total Transmitted	117.1	109.8	134.7	116.8	108.1	112.3	132.5	142.8	129.6	133.2	127.8	109.7	123
Vert-S													
Direct	70.6	27.9	2.6	0	0	0	0	0	0.1	34.1	72.9	74.3	23.6
Diffuse	125	113.4	116.2	99.1	96.3	95.2	101.7	111.2	118.6	133.2	134.6	123	114
Total	195.6	141.3	118.8	99.1	96.3	95.2	101.7	111.2	118.6	167.3	207.5	197.3	137.5
Total Transmitted	140.7	101	93.1	79.2	76.9	76.1	81.2	88.8	94.7	116.7	145.5	144.1	103.2
Vert-W													
Direct	100.5	85.4	141.2	122.9	141.9	128.1	143.6	175.3	177.2	223.5	132.2	101.2	139.8
Diffuse	131.1	132.4	146.2	134.2	137.6	134.7	144	157.3	161.8	165.6	149.5	130.9	143.9
Total	231.7	217.8	287.4	257	279.6	262.7	287.5	332.7	339	389.1	281.7	232	283.7
Total Transmitted	186.2	175.7	232.2	209	226.8	212.1	232.5	269.5	277	319.7	229.8	187.6	230.3
Vert-NE													
Direct	11.2	14.7	36.4	43.1	51.4	64.5	81.6	70.6	36.3	22.7	13.8	9	38.1
Diffuse	105.1	104.3	123.2	118.2	121.1	125.6	135.7	140.3	130.7	127	114.8	100.1	120.6
Total	116.3	119	159.6	161.3	172.5	190.1	217.4	210.9	167	149.6	128.6	109.1	158.7
Total Transmitted	90.1	92.9	123.8	126.1	134.8	148.7	171.1	164.9	129.6	115.5	98.8	84.6	123.6
Vert-SW													
Direct	108.1	74.9	92.3	55.9	44.8	32.3	39.5	68	104	178	131.1	110.7	86.8
Diffuse	134.8	129.1	133.7	114.7	110.8	106.9	115	129.8	141.8	156.7	150.6	135.5	130
Total	242.9	204	226	170.6	155.6	139.2	154.5	197.8	245.7	334.7	281.7	246.2	216.8
Total Transmitted	194.6	162.7	176.3	131	116.3	103.2	114.7	149	192.1	268.7	226.8	198.6	169.6
Vert-SE													
Direct	41.8	25.4	27.7	11.7	4	3.7	7.3	13.1	16.3	30	46.6	40.7	22.4
Diffuse	118.6	109.9	119.7	104.3	100	99	107	117.9	121.8	130.4	126.9	112.4	114
Total	160.4	135.2	147.4	115.9	104	102.7	114.3	131.1	138.1	160.5	173.6	153.2	136.4
Total Transmitted	125.7	106.7	114.3	89.9	81.5	80.5	88.8	101.3	107	124.4	134.9	120.3	106.3
Vert-NW													
Direct	38.9	46.2	107.6	123.6	171.9	171.8	185.6	192.6	149	138.8	60.9	37.4	119.2
Diffuse	112.8	116.9	138.2	136.5	148.7	150.3	158.8	164.7	156	147.4	127.5	110	139.1
Total	151.7	163.1	245.9	260.1	320.5	322.1	344.5	357.3	305	286.2	188.3	147.3	258.3
Total Transmitted	114.3	125.9	193.2	209.7	260.3	261.6	279.2	288.6	244.2	223.5	144.1	110.7	205.1

Table 5.3F 1987 JAKARTA W/SOLAR
Power of Insolation on surfaces various orientations (W/sqm)
Measured insolation
Power determined between 9 to 18

	Jan	Feb	Mar	Apr	May	Jun	Jul	Aug	Sep	Oct	Nov	Dec	Year
Hor													
Direct	201.8	162	277.7	207.8	218.2	210	251.4	305.2	272.1	313.9	236	183.9	237.3
Diffuse	174.9	178.3	184	178.7	177.7	174.1	180.1	193.4	209.3	207.6	188.9	171.9	184.9
Total	376.7	340.3	461.7	386.5	396	384.1	431.5	498.5	481.4	521.5	425	355.8	422.3
Total Transmitted	309.1	278.1	381.6	315.5	322	311.6	351.3	408.7	393.4	426.8	348.4	290.7	345.3
Vert-N													
Direct	0	0	20.1	77.4	136.7	158.2	172	140.3	49.2	1.2	0	0	63.3
Diffuse	102.6	105	124.3	124.4	135.5	143.6	153.2	150.4	132.4	119.2	108.8	95.2	124.7
Total	102.6	105	144.4	201.8	272.2	301.8	325.2	290.7	181.6	120.4	108.8	95.2	188
Total Transmitted	82	83.9	104.8	141.6	205.1	234.8	249.6	207.7	123.7	95.3	86.9	76	141.4
Vert-E													
Direct	30.2	26.4	43	33.7	27.7	30.7	44.4	48	35	35.3	37.1	27.5	35
Diffuse	115.1	113.1	126.9	112.5	108.2	109.8	120.4	129.4	127.5	127.3	121.5	105.3	118.1
Total	145.3	139.4	169.8	146.1	135.9	140.6	164.8	177.4	162.5	162.5	158.6	132.8	153.1
Total Transmitted	114.5	110.8	133.8	114.8	106.2	109.9	128.8	139	127.3	127.7	124.2	104.3	120.2
Vert-S													
Direct	79.3	34	3.7	0	0	0	0	0	0.3	41.3	81.8	84.9	27.1
Diffuse	129.5	119.1	118.8	98.5	94.1	94.2	101.4	110	116	127.1	133.7	124.4	113.9
Total	208.7	153.1	122.6	98.5	94.1	94.2	101.4	110	116.4	168.5	215.4	209.3	141
Total Transmitted	150	108.6	95.4	78.7	75.2	75.2	81	87.9	92.7	114.7	150.2	152.6	105.2
Vert-W													
Direct	129.7	115.5	178.3	163.1	181.1	169.1	188.1	224.4	229.6	274.7	163.7	132.1	179.6
Diffuse	141.3	144.7	155.3	138.9	135.2	134.1	146.6	158.6	157.2	153.6	150.1	137.6	146.1
Total	271.1	260.2	333.6	302	316.3	303.2	334.8	382.9	386.8	428.3	313.8	269.7	325.7
Total Transmitted	219.7	211.8	272	248	258.9	247.2	273.3	313.3	319.2	354.9	257.7	219.8	266.8
Vert-NE													
Direct	9.5	13.8	34.9	42.2	51.3	63.2	78.8	68.5	35.8	21.8	12.8	7.2	36.8
Diffuse	106.8	107.7	124.6	117	118.9	123.9	134.1	138.1	128.4	121.9	113.1	98.4	119.5
Total	116.3	121.4	159.5	159.2	170.1	187.1	212.9	206.6	164.3	143.7	126	105.6	156.3
Total Transmitted	90.2	94.8	123.7	124.3	132.9	146.2	167.4	161.4	127.4	110.7	96.8	81.9	121.7
Vert-SW													
Direct	135.9	100.8	119	79	63.1	49.1	58.8	94.1	138.9	219.4	160.2	141.2	113.5
Diffuse	144.6	140.1	140.8	117.2	108.6	106.1	116	130	137.7	146.2	151.1	142	131.7
Total	280.5	240.9	259.8	196.2	171.7	155.2	174.8	224	276.6	365.7	311.3	283.2	245.1
Total Transmitted	226.5	193.9	204.8	152	128.4	114.5	129.6	170	218.5	296	252.4	230.2	193.1
Vert-SE													
Direct	38.1	23.9	26.2	11.1	3.9	3.3	6.2	12	16	28.9	44.6	36.7	20.9
Diffuse	119.5	113.1	121	103.2	97.8	97.7	106.2	116.2	119.6	125.3	124.8	110.1	112.9
Total	157.5	137	147.2	114.3	101.7	101	112.4	128.2	135.5	154.2	169.4	146.9	133.8
Total Transmitted	123.1	108	114.1	88.5	79.7	79.2	87.4	99	104.9	119.3	131.5	115	104.1
Vert-NW													
Direct	52.4	62.9	133.4	157.3	209	212.9	229.4	235.9	188.1	169.8	76.4	50.7	148.8
Diffuse	118.8	125.3	145.1	140.3	146.2	149.8	161.5	165.5	152.2	138.2	127.2	112.1	140.3
Total	171.2	188.2	278.5	297.6	355.2	362.7	390.8	401.4	340.4	308	203.5	162.7	289
Total Transmitted	129.3	146.2	220.6	241.8	290.5	296.9	319.2	326.7	274.7	241.8	156	122	231

Table 5.4 Solar Factor Calculation for Jarkarta, 1987

All Daylight Hours (W/m2)

Orientation	Direct	Diffuse	Total	ASHRAE Algorithm Total	% Diff.	Total Transmitted	Implied Transmittance
Horizontal	216.1	170.3	386.4				
North	57.7	114.1	171.8	185.4	7%	129.2	75%
East	33.5	108.6	142.1	161.2	12%	111.7	79%
South	26.0	104.5	130.5	153.7	15%	97.3	75%
West	167.0	135.0	302.0	294.7	-2%	247.4	82%
NE	34.6	109.7	144.3	162.3	11%	112.3	78%
SW	106.5	121.5	228.0	234.2	3%	180.0	79%
SE	20.3	103.7	124.0	148.0	16%	96.6	78%
NW	137.0	129.0	266.0	264.7	-1%	212.7	80%
AVERAGE			188.6	200.5	6%	148.4	78%

Hours 7 am to 6 pm (W/m2)

Horizontal	216.6	169.8	386.4				
North	57.8	114.6	172.4	185.2	7%	129.6	75%
East	33.6	109.2	142.8	161.0	11%	112.3	79%
South	25.0	104.8	129.8	152.4	15%	96.9	75%
West	163.3	134.0	297.3	290.7	-2%	243.4	82%
NE	34.7	110.2	144.9	162.1	11%	112.8	78%
SW	103.2	120.8	224.0	230.6	3%	176.5	79%
SE		20.3	104.3	127.4	18%	97.1	93%
NW		135.2	128.6	127.4	-1%	210.9	164%
AVERAGE			168.0	179.6	6%	147.4	91%

Hours 8am to 5 pm (W/m2)

Horizontal	258.6	192.5	451.1				
North	63.7	137.5	201.2	191.1	-5%	152.2	76%
East	38.9	130.5	169.4	166.3	-2%	133.0	79%
South	25.8	125.1	150.9	153.2	2%	113.2	75%
West	155.4	158.5	313.9	282.8	-11%	254.8	81%
NE	40.9	132.1	173.0	168.3	-3%	134.6	78%
SW	96.4	143.0	239.4	223.8	-7%	187.4	78%
SE	23.2	124.7	147.9	150.6	2%	115.2	78%
NW	132.4	153.2	285.6	259.8	-10%	226.9	79%
AVERAGE			174.1	199.5	13%	164.7	78%

Table 5.4 Solar Factor Calculation for Jarkarta, 1987

Orientation	Direct	Diffuse	Total	ASHRAE Algorithm Total	% Diff.	Total Transmitted	Implied Transmittance
				All Daylight Hours (W/m2)			
				Hours 7 am to 5 pm (W/m2)			
Horizontal	233.6	175.1	408.7				
North	57.6	125.1	182.7	185.0	1%	138.2	76%
East	36.9	119.5	156.4	164.3	5%	123.0	79%
South	23.6	114.0	137.6	151.0	9%	103.2	75%
West	139.8	143.9	283.7	267.2	-6%	230.3	81%
NE	38.1	120.6	158.7	165.5	4%	123.6	78%
SW	86.8	130.0	216.8	214.2	-1%	169.6	78%
SE	22.4	114.0	136.4	149.8	9%	106.3	78%
NW	119.2	139.1	258.3	246.6	-5%	205.1	79%
AVERAGE			191.3	193.0	1%	149.9	78%
				Hours 8 am to 6 pm (W/m2)			
Horizontal	237.3	184.9	422.2				
North	63.3	124.7	188.0	190.7	1%	141.4	75%
East	35.0	118.1	153.1	162.4	6%	120.2	79%
South	27.1	113.9	141.0	154.5	9%	105.2	75%
West	179.6	146.1	325.7	307.0	-6%	266.8	82%
NE	36.8	119.5	156.3	164.2	5%	121.7	78%
SW	113.5	131.7	245.2	240.9	-2%	193.1	79%
SE	20.9	112.9	133.8	148.3	10%	104.1	78%
NW	148.8	140.3	289.1	276.2	-5%	231.0	80%
AVERAGE			204.0	205.5	1%	160.4	78%

CHAPTER 6: ENERGY AND ECONOMIC ANALYSIS OF ENERGY CONSERVATION IN THAI COMMERCIAL BUILDINGS

J.F. Busch
Energy Analysis Program
Applied Science Division
Lawrence Berkeley Laboratory
Berkeley, California 94720 USA

ABSTRACT

Commercial buildings consume one-quarter of the electricity in hot-and-humid Bangkok, yet the best means for conserving electricity in this fast-growing sector is unclear. To investigate this issue, we performed a series of parametric simulations using the DOE-2.1D computer program on three commercial building prototypes: an office, a hotel, and a shopping center. These buildings are based on actual buildings in Bangkok, Thailand, and benchmarked to actual electricity consumption. We investigated a wide range of energy conservation measures appropriate for each building type, from architectural measures to HVAC equipment and control solutions. Conservation measures applied individually reduce total electricity consumption in the modeled buildings in the range of 5 to 10%, but go as high as 35%. The best measures applied in combination can generate savings of 50%. Savings in peak power and energy generally followed one another. Thermal cool storage and cogeneration, evaluated for their potential to reduce peak demands on the power sector, each looked favorable under some operating regimes.

INTRODUCTION

In the last few years, Thailand has witnessed a boom in both general economic growth and commercial building construction in Thailand. Accompanying these two phenomena has been a commensurate growth in the demand for electricity. Most of these new buildings are designed for a high level of amenity, including air-conditioning (AC), and thus, are contributing significantly to the 15% annual peak demand growth for the country. Designing and retrofitting buildings to use less energy is a way to avoid both high energy bills for building owners, and strains of rapid growth on the nation's electricity infrastructure. While some energy conservation measures are well understood by Thai designers and engineers, the extent of the potential savings, particularly in the Thai climate, is not always known. Techniques applied elsewhere also may hold conservation promise in Thailand. In this paper, we evaluate numerous conservation measures and quantify their energy and economic savings potential in Thai commercial buildings. We focus primarily on commercial buildings that utilize some form of centralized air-conditioning system, because of the trends in construction of buildings of this type. However, some of the issues raised are also relevant to older and naturally ventilated buildings.

METHODOLOGY

Our general approach was to develop typical building prototypes drawn from actual data and field experience, and to simulate the energy impact of modifications to the base buildings using actual weather data and a computer simulation program. The simulation approach was chosen over an approach using statistical analysis of measured data, for instance, because a simulation program facilitates the exploration of many conservation measures, individually or in combination, particularly ones that have not been tried before in Thailand. Below, we describe the details of the building prototypes, weather data, and simulation model. Following that, we describe several indices used in evaluating the economic performance of conservation measures.

Building Prototypes

We chose to model offices, hotels, and retail buildings on the basis of a survey of installed air-conditioning over 100 tons* because these data include virtually all buildings with central air-

* Except for movie theaters outside of Bangkok where buildings with 50 tons and above were included.

conditioning systems with which this paper is solely concerned [1]. Table 6-1 shows the breakdown of AC type and chiller cooling capacity (expressed in tons of cooling) by commercial building type in Bangkok and the whole kingdom as of 1986. Water-cooled water chillers (WCWC) make up 87% of all central AC capacity, followed by direct-expansion (DX) units with 10%, and air-cooled water chillers (ACWC) with 3%. In the country as a whole, 32% of the AC tonnage is found in offices, 28% in hotels, and 21% in shopping centers, department stores, and other retail outlets (from here on referred to simply as retail buildings). Movie theaters, hospitals, and academic buildings represent 10%, 5%, and 3% of national central AC tonnage, respectively. The total share of AC tonnage in offices, hotels, and retail buildings for the whole country is 82% with 70% found in Bangkok. Thus, understanding how Thai offices, hotels, and retail buildings operate, and which conservation measures are effective in each of them, will give a good indication of the conservation potential available in the Thai commercial sector as a whole.

The following building prototypes are all based on models of actual buildings, first benchmarked to within 10% of actual utility bills, and then modified to reflect typical current construction practice. This point is important. Starting with real buildings has advantages and disadvantages. The advantage is that the model description contains rich detail about a building's construction, geometry, configuration, and use. The disadvantage is that every building is anomalous in some respect, and in the absence of a detailed database on typical buildings characteristics, these anomalies can go unrecognized. Nonetheless, even with these caveats, the use of real building prototypes is frequently used, most notably by the American Society of Heating, Refrigeration, and Air-Conditioning Engineers (ASHRAE) in developing their recommended building standards.

Detailed information was obtained about the prototype precursors from numerous site visits, construction blueprints, and interviews with designers, building engineers, and other building staff. Energy costs were estimated using the current tariff structure in the Large Business category of 1.23 Baht/kWh (U.S.$ .05/kWh) for energy and 229 Baht/kW (U.S.$ 9.16/kW) for monthly peak demand.

Office:

A large bank in Bangkok served as the model building upon which the prototypical office was designed. Schedules, intensity of use, and air-conditioning system configuration were retained from the bank building, while size, shape, and facade were adjusted to reflect the normal practice. Table 6-2 lists a summary of the key characteristics of the prototypical office.

Data were compiled from numerous sources of existing commercial building characteristics and energy use in Thailand. Figure 6-1 shows the distribution of annual electricity consumption normalized by conditioned floor area for six offices in the database, with the office prototype fitted into the distribution. The first bar on Figure 6-2 shows the end-use energy breakdown for the office prototype. Cooling and HVAC (fans and pumps) use 40%, lights 30%, office equipment 20%, and elevators 10% of the total energy.

Hotel:

Key characteristics of the Thai hotel prototype are listed in Table 6-3. A modern hotel in Bangkok, built originally by a major international chain, was the actual building upon which the prototype was based. Guestroom configurations and use, construction, and air-conditioning system were retained from the actual building. The shape of the plan and facade of the prototype were simplified, while the composition of the public spaces (e.g., lobby, restaurants, meeting rooms, offices, and shops) and the patterns and intensity of use were based on detailed audits of similar hotels in Manila, the Philippines. The hotel prototype is shown in Figure 6-3 in a distribution of 14 actual Thai hotels for electricity intensity. The breakdown of energy end-uses for the hotel prototype are shown in the middle bar of Figure 6-2. Cooling and HVAC consume 60% of the electricity, lights 25%, elevators 10%, and miscellaneous equipment 5%.

Retail:

The Thai retail prototype building, whose characteristics are reproduced in Table 6-4, is based on a multi-tenant shopping center in Bangkok. Few of the characteristics were altered from the original building. The actual annual energy consumption for three buildings, along with that

simulated for the retail building prototype, are shown in Figure 6-4. The energy end-use breakdown for the retail prototype building, shown in the last bar of Figure 6-2, reveals lighting as the major category at roughly 55% of the total electricity bill, followed by cooling and HVAC at 40%, and the remaining 5% shared between escalators and miscellaneous uses.

Weather Data

Hourly weather data from Bangkok for 1985 were used in the analysis. The weather data include temperature, humidity, wind speed, and solar data. Figure 6-5 shows average monthly solar and temperature data. All weather data, except the solar data, were gathered within Bangkok proper by the Meteorological Department of the Thai government. Hourly total and diffuse horizontal solar radiation data were collected on location by the Department of Energy and Materials of King Mongkut's Institute of Technology in Thonburi (within metropolitan Bangkok). Compared to 30-year normals [2], the mean monthly, mean daily maximum, and minimum dry-bulb temperatures in 1985 are all within .5 °C of long-term data. Mean monthly relative humidities (RH) for 1985 are within 5 RH percent of the 30-year normals, but are generally lower. There were no long-term solar data available for comparison with 1985.

Temperatures vary within a limited range throughout the year, with the average dry-bulb temperature ranging from 25.5 °C in December to 29.7 °C in April. Similarly, the average total horizontal solar radiation intensity varies only from 324 W/m^2 in October to 406 W/m^2 in March. The direct horizontal component of solar radiation, on the other hand, varys over a relatively wide range, being three times lower in June during the monsoon season than during the dry season in December. Overall, the direct *horizontal* solar radiation is 56% of total horizontal, while direct *normal* is 80% of total horizontal.

Simulation Model

We used the DOE-2.1D building energy program to simulate the response of the building prototypes to the Thai weather and to changes in the buildings' configuration and operation. The DOE-2.1D program is widely recognized as state-of-the-art for this purpose. The program solves, on an hour-by-hour basis, the mathematical relations governing the thermodynamic behavior of a building. It does this in sequential steps through four modules: LOADS, SYSTEMS, PLANT, and ECONOMICS. The LOADS module is based on user input describing the building surfaces, enclosed spaces, internal usage, and schedules. In it, the instantaneous heating and cooling loads are calculated and then modified to incorporate dynamic effects of thermal mass through the use of weighting factors. The SYSTEMS module calculates the heat extraction/addition of the coils from a large menu of system types and operation parameters. Fuel requirements to operate the primary heating and cooling equipment and pumps are determined in PLANT. The ECONOMICS module calculates the energy costs of operating the building, with the capability of handling complex tariff structures. A good description of the program can be found in BESG [3]; for more detailed information on using the program and descriptions of the algorithms, refer to the full set of manuals [4].

Economic Indices

Building operators are often more concerned about saving money than saving energy. Energy cost savings need to be compared to the extra costs incurred to achieve the savings. In the analysis that follows, we employ several indices of economic performance. Simple payback time is the most universal cost-effectiveness indicator. It is calculated as the ratio of the incremental cost of the conservation and the annual energy cost savings.

$$\text{Simple Payback Time} = \frac{\text{Incremental Cost}}{\text{Annual Cost Savings}} \qquad \text{(Eq.6-1)}$$

We also utilize the cost of conserved energy (CCE), an indicator whose chief virtue is that it can be directly compared to the energy prices one expects to face.

$$\text{Cost of Conserved Energy} = \frac{\text{Incremental Cost x Capital Recovery Factor}}{\text{Annual Energy Savings}} \qquad \text{(Eq.6-2)}$$

The capital recovery factor in Equation 6-2 converts the initial investment in energy saving features into an annual payment using a discount rate (d) and conservation feature lifetime (n).

$$\text{Capital Recovery Factor} = \frac{d}{1 - (1 + d)^{-n}} \qquad \text{(Eq.6-3)}$$

A related indicator is the Cost of Avoided Peak Power. This is the quotient of first investment cost and the annual peak demand savings of the building, regardless of when the peak occurs.

$$\text{Cost of Avoided Peak Power} = \frac{\text{Incremental Cost}}{\text{Peak Savings}} \qquad \text{(Eq.6-4)}$$

Because conservation investments are often evaluated in the context of other investment opportunities, it can be helpful to calculate the internal rate of return (IRR). This is the discount rate that results in the conservation investment reaping a net present value of zero.

$$\text{Incremental Cost} = \sum_{i=1}^{i=n} \frac{\text{Annual Cost Savings}}{(1 + d)^i} \qquad \text{(Eq.6-5)}$$

Solving Equation 6-5 for the internal rate of return requires iterating over different discount rates.

RESULTS AND DISCUSSION

In this study we employ the parametric technique of building energy analysis. By varying each parameter one at a time, we can observe its contribution in the overall energy performance of the building. The disadvantage of this approach is that we are unable to account for interactions between parameters that either dampen or accentuate the effect of varying each independently. Therefore, we developed a few cases which combine conservation measures together to illustrate the tradeoffs in an interactive context. The primary basis of comparison used in this study is the percentage annual electricity savings over each prototype's base case. The reader can assume that the peak power and operating cost savings are comparable (in percentage terms) to the energy savings unless otherwise noted. In selected cases, we analyze the cost-effectiveness of conservation measures. The remainder of this section is sub-divided into four: architectural, system control, system equipment energy conservation measures, followed by two illustrative conservation cases (high-efficiency and building energy standard).

Architectural Measures

Architectural measures are those that relate to the building as a whole, to the envelope, or to its interior design and use. Measures relating to systems that maintain control over the indoor thermal environment will be dealt with in later sections.

Orientation:

Building orientation has an effect on energy use mainly through the magnitude and timing of solar radiation gains. If the building is square or highly shaded, orientation is irrelevant. However, if the building has an aspect ratio of greater than 1:1 and if it is not shaded from direct beam solar radiation when the sun is low in the sky in early morning and late afternoon, orientation does have an effect. With the retail and hotel building prototypes, both of which have aspect ratios greater than 1:1, the energy savings from orienting the long axis of the buildings east-west instead of north-south are .7 and 1.1%, respectively. For these buildings, the peak power savings exceed the energy savings, up to 1.4% and 1.7%, respectively. While the office building is square, one of the perimeter zones is unconditioned (as is often found in Thai offices), so we looked at the impact of orientation of the unconditioned zone. In the base case, this zone faces south. Figure 6-6 shows the effect of rotating the building around to face the unconditioned zone in different compass directions. It is most advantageous to face the unconditioned zone west, and least

advantageous to face it north. The effect on total energy consumption is small in both cases, on the order of 1% of total energy. However, because of the role afternoon solar gains play in building peak power loads, orienting the unconditioned zone towards the west saves over 2% of peak power.

Infiltration:

The quality of building construction can effect the amount of unintended outside air that enters the building. Infiltration occurs in commercial buildings principally when the building is not pressurized by the fans. All of the building prototypes assumed one air-change per hour (ach) infiltration rate. Figure 6-7 shows the impact of varying the infiltration from .2 to 3 ach. Hotel and retail buildings show positive energy savings from reducing infiltration while the office does not. This is because infiltration occurs during the daytime in unoccupied hotel guestrooms and prior to shops opening in mid-morning, whereas daytime infiltration in the office occurs only on weekends. The benefit of reducing the infiltration below one ach is minimal, but the penalty for allowing it to rise substantially above that is high: energy use increases 5% to 7% and is accompanied by equally high penalties in peak demand and equipment sizing. It is also possible that these estimates of the implications from increased infiltration are understated: this is because DOE-2 does not model moisture absorbing into, and later evaporating from, building materials and furnishings. Given the high humidity conditions that exist in Bangkok, in an actual situation higher energy expenditures could result from these higher latent cooling loads.

Opaque Walls and Roofs:

The effects of thermal mass in offices and retail buildings are shown in Figure 6-8. This plot differs from the others in this study in that the savings relate to the parametric run with the lowest mass rather than to the base case. Office walls exhibit the largest effect from increasing the thermal mass, with savings of 2.5% of total energy over the wall mass range of 100 to 500 kg/m^2. Hotel walls show only a 1% effect and the office roof effect is negligible, primarily because it is such a small percentage of the overall envelope area in a 12-story building.

Insulating the walls to lower the thermal conductivity saves 3.5% of total energy in hotels, but shows a marginal impact with offices (see Figure 6-9). This is probably due to the 24-hour operation of the hotel and the systems that regulate the heat gains whereas in the office building, some of the heat gains are delayed by the thermal mass and dissipate overnight. Roof thermal conductivity has little impact on energy use for these same reasons. It can, however, have an impact on local comfort if not properly accounted for in the air-conditioning system design.

Light-colored walls absorb less solar radiation than dark-colored walls, resulting in lower surface temperatures and hence lower conduction heat gains. Figure 6-10 plots the percent of total energy savings over the solar absorptance range of .1 to .9. Even though the office has the smaller proportion of opaque wall to gross wall area, it has a greater response to changing solar absorptance. Again, the hours of building operation are the likely explanation.

Windows:

High solar intensity in Thailand results in the potential for high radiation heat gains through building window apertures. Conduction heat gains also occur through the typically single-pane window construction. Therefore, any effective energy conservation design strategy includes provisions for handling heat gains through windows. A primary issue is the amount of glazed area in a building. Figure 6-11 compares the energy savings versus window-to-wall ratio (WWR) for the three building prototypes. Note that the shading coefficient (SC) of the glass influences the amount of solar energy penetration, which in turn differs in each case. The shading coefficient is defined as the ratio of solar heat gain through a window to the solar gain through a reference glass. The office, which has the lowest shading coefficient (SC=.34), nonetheless displays the greatest impact of varying WWR, ranging ± 6% energy savings over .1 to .9 WWR. This is significant because of the current popularity of glass curtain-wall construction for offices in Bangkok. The office is more susceptible than the hotel or retail buildings to SC as well, as shown in Figure 6-12. This latter plot shows that even with a modest WWR of .5, choosing a glazing with a high SC for an office building will be costly in operating expenses. Hotels and retail buildings by

virtue of typically lower WWR and different operating schedules are not impacted as much either in relative or absolute energy savings terms.

Shading:

Besides attenuating solar gains by selecting glass with a higher SC, shading devices can be attached to window systems. These shading devices may be either external or internal. External shading devices are in fact part of the vernacular design, and often are a major aesthetic expression of a building, taking on complex shapes, geometries, or colors. But typically, external shades take the form of horizontal overhangs and/or vertical fins. In the prototypical office building, already "shaded" with .34 SC glass, large fins and overhangs can provide up to an additional 5% energy savings, as shown in Figure 6-13. In this plot, the shade dimension is given in percent of the window height for overhangs and in percent of window width for fins. The plot also shows that little energy savings benefit is derived from sizing fins larger than 10% of the window width, and averages about 1% overall. Specific orientations could potentially benefit more from larger fin depths but this effect is not explored here. Overhangs or fins were simulated on the hotel and retail buildings. At a depth of 100% of the window height, overhangs show roughly 2% energy savings for both building types as shown in Figure 6-14. Fins show about .5% savings over the range of fin depths.

Internal shading devices were also simulated. The three building prototypes all assumed that venetian blinds were present and that occupants closed them when incident solar radiation exceeded a threshold intensity (126 W/m^2), thereby reducing solar gains by 25%. The results show that less than 1% savings accrue when shades are triggered by half the solar intensity of the base case. Conversely, little is lost by not using them at all. Occupants may want to pull the blinds for other reasons, such as to reduce glare or enhance privacy.

Lighting and Internal Process Loads:

Lighting is a significant end-use in commercial buildings for two reasons: 1) it uses energy directly to provide light; and 2) it generates waste heat that must be removed by the air-conditioning system. Internal process loads are those from any device that uses energy and generates heat, including appliances such as refrigerators in guestrooms or photo-copying machines, computers, and electric typewriters in offices. Particularly as offices environments become more automated, internal process loads will rise, creating the impacts shown in Figure 6-15. Different schedules of usage explain the different energy savings seen between lighting and equipment in offices. Cutting the lighting power density by half yields a total energy savings of roughly 18%. Many options exist for installing lighting systems that use less than 10 W/m^2, while still maintaining adequate luminance levels [5], [6]. Although there is currently no apparent market for energy-efficient models of office equipment, it is included in our analysis simply to illustrate the magnitude of the impact of automating offices. Figure 6-16 depicts how much total energy is saved by implementing lighting power density reductions in hotel and retail buildings. The diversity of lighting in each of these buildings dictates that lighting power reductions through any means be considered in terms of a floor-weighted average. The savings for the retail building are nothing short of dramatic; total energy savings equal three-quarters of the percentage reduction in lighting. For instance, a 20% reduction in lighting results in a total 15% energy savings. Hotel savings from lighting efficiency improvements are comparable to those for offices.

Daylighting:

The use of natural light to augment or replace electric light in offices has the potential to realize some the savings discussed above. In fact, most buildings admit natural light already. Daylighting technology consists of controls for the electric lighting to reduce their energy consumption when natural lighting is sufficient. To fully realize the benefits of daylighting, however, the building ideally is designed to exploit the natural light resource through proper fenestration design, interior design and layout of spaces, and through advantageous placement and wiring of overhead electric lighting. It is beyond the scope of this study to discuss techniques for designing a daylit building. We will instead concern ourselves with potential savings in Thai offices.

There are two basic types of daylight control systems: stepped and continuous control. Both are actuated by a luminance sensor that is calibrated to maintain the light levels at desk height (75 cm), 3 meters back from the window, at 500 lumens. Only perimeter zones (with a depth of 6 meters) are equipped with daylighting controls; the core zone retains the base lighting configuration. The energy savings from stepped controls as a function of the number of steps is shown in Figure 6-17. Simple on/off controls (i.e., one-step) achieve only 3% energy savings in the office prototype. In addition to showing only modest savings, on/off controls can be distracting or even irritating to building occupants when they switch between being on and off. Three steps or greater yield much higher savings: up to 9%. Continuous dimming controls are a more refined version of the stepped controls, providing more visual comfort to building occupants through smooth transitions between all electric light and all natural light regimes. The energy savings from daylight utilization with continuous dimming devices is depicted in Figure 6-18. Depending on the manufacture, these devices can consume different amounts of power even when the lights are fully dimmed: the plotted curve shows the total energy savings from continuous dimming devices that consume from 0 to 50% of full lighting power.

The optical and thermal properties of window glass are also important for daylighting. The ideal glazing material is one that selectively repels all but the visible portion of the solar radiation spectrum. No such product yet exists, but there are commercially available glasses with low-emittance coatings that do admit proportionally more visible than thermal gains. To explicitly account for the tradeoff between heat and light gains through glass with different properties, we plot the savings potential vs. the ratio of the shading coefficient and the visible transmittance (called K_e) in Figures 6-19 and 6-20. Figure 6-19 shows results using a shading coefficient of .34 (base case) whereas Figure 6-20 uses a SC of .70. The family of curves in each figure correspond to different overhang depths. Note that these data reflect the use of continuous dimming controls with 30% minimum power draw. Energy savings are twice as high with a K_e of 1.3 as with a K_e of .3. Overhangs increase the savings a few percent with SC=.34 glass. However, as can be seen in Figure 6-20 with less tinted glass (e.g., SC=.70), overhangs make a significant difference in the energy savings from daylighting. Maximum savings range from less than 6% to almost 12% depending on the depth of the overhang. It is clear that even with a high ratio of visible light to heat gain (e.g., 1.3), the heat gains associated with unshaded relatively high SC glass (e.g., .70) erode the daylighting savings significantly. Good daylighting design in Thailand must include provisions for reducing the solar heat gains through the windows.

Summary:

Figures 6-21 through 6-23 summarize the savings potential for individual architectural conservation measures applied over each measure's parameter range expressed in earlier figures for offices, hotels, and retail buildings, respectively. It is immediately apparent which architectural measures have the greatest influence over energy use in the building prototypes. The reader should refer to earlier discussion and related figures for information on the parameter end points and a more complete depiction of the relationship between the measures and energy savings.

Air-Conditioning System Control Measures

Zone Air Temperature:

Few measures affect energy use in a commercial building as much as the setpoint temperature of the conditioned space. Figure 6-24 illustrates this point over the range of 20 to 30 °C for the three building prototypes. This temperature range was chosen to reflect observed values at the low end [7] and a thermally acceptable temperature level as determined through a field survey of thermal comfort in Thai offices [8] at the high end. The hotel is most sensitive to changes in the thermostat setting, ranging from more than -40% to 20% total energy savings. This is almost certainly due to the constant (as opposed to intermittent) operation, and also because guestrooms, unoccupied and uncooled during parts of the day, require larger systems to cool down the accumulated heat gains when guests return and turn on the fan coil units in their rooms. The resulting equipment oversizing means that it operates at most other times in a less efficient manner. Offices are nearly as sensitive as hotels, going from -20% to 15% savings. It is interesting to note

that while the peak demand savings lag behind energy savings for the hotels and retail buildings, in offices it is the opposite—peak demand is conserved up to 1% more than energy conserved at a zone air temperature setting of 30 °C.

Certainly a factor in explaining the large negative savings shown at the low end of the temperature scale is that fan sizes are hugely increased to meet the peak cooling loads (by a factor of 5 in the office and 10 in the hotel). Given that the air-system operates at constant volume, the fans continuously push that much more air at all times. A more conservative scenario would have the supply-air temperature reduced along with the setpoint temperatures, to take advantage of the better chiller part-load performance characteristics. We take a closer look at supply-air temperature next.

Supply-Air Temperature:

The supply-air temperature is an interesting parameter because it embodies important trade-offs. First of all, fans are generally sized to meet peak cooling loads based on a particular supply-air temperature. Lower supply-air temperatures require less air-flow (and therefore lower fan capacity) to meet cooling loads, but demand more capacity (and energy) from the chillers. The converse is true of higher supply-air temperatures. Thus, supply-air temperature affects whether more AC energy is expended by fans or chillers. The optimal supply-air temperature depends on the relative efficiencies between them [5]. The supply-air temperature also affects the amount of latent cooling that occurs. In Thailand, with its high humidity levels, that is an important consideration for human comfort and health, and the preservation of documents and fabrics.

Figure 6-25 shows the energy savings as a function of supply-air temperature. Each of the buildings with their respective systems behave differently. The office building achieves energy savings up to 2% at low supply-air temperatures, whereas at the same 8 °C, the hotel consumes 6% more energy than the base case. This contrast can be explained as follows: the office air-distribution system, with low static pressure but also low-efficiency fans, is apparently less efficient to operate than the chiller, hence the energy savings. The hotel, on the other hand, has most of its fan capacity in fan coil units, which also are inefficient, but which operate at such low static pressure, that little offsetting savings occur through reduced operation as compared to the increased chiller usage. The result is that only negative savings are achieved for the hotel. The retail building yields different results altogether, where the system configuration seems to dominate the result. There, the central water chiller system provides only 20% of the cooling, while individual split-system units cool the bulk of the building. Overall, roughly comparable efficiencies appear to exist between the cooling and air-distribution sides, as seen in Figure 6-25, where savings are essentially zero over the supply-air temperature range, and the tradeoffs cancel each other out. The lesson here is that careful examination of relative equipment efficiencies and system-type is needed to ascertain optimal supply-air temperature and also that simulation is probably the best way to do this because of part-load operation considerations.

Supply-air temperature can be controlled in different ways. It can be fixed to a constant level (as assumed for the three Thai building prototypes), or it can respond to the cooling needs of the warmest zone, or it can be set by a pre-determined schedule according to outside temperature. Under the conditions treated with these buildings, however, the control type had little or no effect on energy consumption.

Fan Control:

All of the base case systems are constant volume systems. We did explore the use of variable air volume (VAV) systems in place of these. VAV systems differ from one another mainly in how the fan speed is modulated. There are three main technologies for doing this: discharge dampers, inlet vanes, and variable speed drives. Figure 6-26 shows the energy savings over the respective constant volume base cases when the three Thai building prototypes employ these fan control techniques. Discharge dampers are the least desirable; savings are in fact negative when the retail building uses them. The offices and hotels save 4% and 2%, respectively. Inlet vanes are the intermediate fan control technique in terms of energy savings, with offices and hotels saving nearly 8%. Variable speed drives save the most; offices conserve 9% and hotels 10%.

Because of the system configuration in the retail building, it does not seem to exploit the advantages of a VAV system.

Outside Air:

Human health requires that some fresh air be brought into the building and mixed with recirculated air. This is done for dissipating odors and diluting air-borne contaminants from furnishings, smoking, cooking, etc. Because outdoor air is generally hot and humid in Thailand, there are energy implications in choosing the quantity of outdoor air to be brought in. Figure 6-27 plots the energy savings for different amounts of outdoor air in terms of cubic feet per minute (cfm) per person. The hotel shows the most substantial savings, reaching 15% if outdoor air is reduced to 5 cfm/person. The office and retail building respond similarly, saving up to 5% at the 5 cfm/person level. For the office, a 5 cfm/person ventilation level extends to a 7.5% peak power savings, and for the retail building, to a 6% savings in peak power.

In some climates it can be advantageous to increase the amount of outdoor air beyond the minimum level when temperatures and humidities are below those of the return air. This is the so-called economizer cycle. The base case design in each of the building prototypes assumed a fixed outdoor air damper (i.e., no economizer capability). Simulations were performed with an economizer cycle activated when 1) the outdoor temperature was below the return air; and 2) when the outdoor air enthalpy was below return air enthalpy. Neither case generated any savings of any sort with any of the building prototypes, and in fact led to negative savings in the office when activated by temperature.

Pre-Cooling:

Studies have shown that pre-cooling the building prior to occupancy can reduce peak loads and the needed air-conditioning system capacity at the expense of increases in energy use [9], [7]. In that sense, it is not an energy conservation technique per se, but rather a load-management strategy. We ran the Thai office prototype AC system for one, two, and three hours prior to office hours to assess the relative energy losses and peak savings. These results are shown in Figure 6-28. We looked at pre-cooling before every working day (all days except Sundays), and at pre-cooling on Monday mornings only, on the theory that peak days tend to occur on Mondays after a weekend of heat gains have gathered within the building thermal mass. The plot shows that energy penalties run about 2.5% per extra hour of pre-cooling, whereas the peak savings approach only 1% after 3 hours of pre-cooling and are less for shorter pre-cooling durations. Interestingly, though, there is no difference in the peak savings between pre-cooling all days and pre-cooling on Mondays only. This confirms the hypothesis that building electricity demand peaks tend to occur on Mondays in hot climates. So, it obviously it is not efficient to pre-cool the building on all days, and though the savings are very modest, peak demand can be trimmed slightly by pre-cooling on Mondays or on the day after a holiday. However, under the current utility rate structure for large businesses, this strategy does not result in operating cost savings.

Night Fans:

Night ventilation of the building under certain circumstances can help to reduce daytime cooling loads, and thereby reduce AC system design capacity and peak demand. The building fans are turned on to circulate outside air through the interior spaces under different control strategies. This technique is not applicable to hotels which require 24-hour conditioning (except when running the economizer cycle which, as mentioned above, is unattractive). We chose to look at the use of fans at night in the office prototype. We looked at control logic that turned on the fans when both the outdoor temperature was below a threshold value (29 through 31 °C) and the indoor-outdoor temperature difference was greater than some given values (1 through 4 °C). We also examined simple pre-scheduled fan usage. None of the simulations revealed any savings potential using this measure. In fact, in most cases the peak demand savings were actually negative and 2 to 3 times higher on a percentage basis than the expected negative energy savings. There is no apparent justification for running fans at night in daytime-occupied Thai commercial buildings.

Air-Conditioning System Equipment Measures

Chillers:

Within the cooling end-use, which as we have seen comprises from 40 to 60% of the total energy budget, chillers are the major piece of energy-consuming equipment. Scale economies exist with chillers. The larger units tend to use the more efficient technology, (i.e., centrifugal chillers coupled with a cooling tower for lowering condenser temperatures). In the smaller sizes (for commercial applications), one typically sees air-cooled reciprocating chillers with lower efficiencies. Coefficient of performance (COP) is the usual figure of merit in comparing chiller efficiencies and is calculated as the ratio of cooling output to electrical input. Energy savings by COP are shown in Figure 6-29. At a COP of 3.5, we modeled reciprocating chillers, but at higher COPs we used water-cooled centrifugal chillers. The hotel shows the most promise in the application of an efficient chiller, saving 10% with a 5.5 COP unit. The office follows with a savings of 7%, while the retail building shows a 5% savings. Likewise, a large energy cost is associated with using an inefficient chiller on the hotel, losing 12% when dropping the COP from 4.0 to 3.5. As we have seen elsewhere, the base case building operation and system configuration have a large effect on the size of total savings. In the case of the hotel, the day-night operation of the system means that efficiency improvements in energy-using equipment translate into large savings. For the retail building, the use of split-system air-conditioning units in the shops limits the benefits from improvements to the central system serving the circulation zones where more efficient options exist.

Fans:

Fan equipment is also available in a range of technologies and efficiencies. The types are airfoil and backward inclined at the high end and forward-curved and vaneaxial fans at the low end. Scale economies exist in fan technology as well, with large built-up systems using the more efficient technologies. Larger, more efficient motors are also more prevalent in the large fan sizes. One of the tradeoffs involved in the choice of fan size is that a larger fan usually implies a longer duct run resulting in an increase in the static pressure that, in turn, increases the energy consumption of the fan. We look at both fan efficiency and static pressure for potential energy savings in Figure 6-30 and 6-33. Using fans that are 70% efficient (over the base 40%) can save close to 8% in hotels, 6% in offices, and 2% in retail buildings. Conversely, using 30% efficient fans can result in 6%, 5%, and 1% energy consumption increases in the hotel, office, and retail buildings, respectively. The relationship between static pressure and energy savings is plotted in Figure 6-31. Doubling the static pressure from 2 to 4 inches causes negative energy savings of 17% in the hotel, 15% in the office, and 8% in the retail building. The energy penalty for increases in static pressure is high.

Because some engineering designers put in large safety factors when sizing equipment, we looked at how much more energy fans use if they are oversized. This can be especially costly for a constant volume system because there is no mechanism for reducing flow (and hence energy consumption) when zone cooling loads are already met. Figure 6-32 displays the fan oversizing penalties. Oversizing of 10% has a 2% total energy increase in the hotel and office, and 1% increase in the retail building; fan oversizing of 50% results in 10% and 4%, respectively. Careful cooling load analysis to avoid the need "to be extra sure" can save energy.

Pumps:

Pumps circulate chilled water around the building to provide a cooling effect to the coils in air handling units and then back to the chiller. Generally, these pumps are run at constant speed, but can be outfitted with variable speed drives, thereby saving pumping energy. Although chilled water pumping energy makes up only a small portion of the total energy expenditure in a building (i.e., between .5% and 2.5%), the savings for using variable speed pumps in the hotel were almost 2%, and 1.5% in the office, and less than .5% in the retail building.

Thermal Storage:

Electricity load management is an issue for both building owners who are interested in controlling their demand payments, and utility planners who are trying hard to keep up with demand

growth and maintain system load factor. The air-conditioning system contributes significantly to the building peak demand and is therefore an attractive target for load shifting to a period when other electricity-using equipment is dormant. Thermal cool storage is one technique for shifting the electrical AC load by storing chilled water, ice, or some other phase-change material, that can be used later used to meet part or all of the cooling load. The economic climate for cool storage in Thailand and the other ASEAN countries was examined in earlier work and found to be attractive [10]. A general explanation of the technology can be found in Piette [11] and more detailed design information in EPRI [12].

We looked at the use of a chilled-water cool storage system in the Thai office prototype under a few different control strategies. The partial storage strategy runs the chiller continuously, to store "coolth" during unoccupied hours, and to augment the cooling output of the storage during occupied periods. Full storage seeks to supply all of the cooling from storage during the building's occupied period and to run the chiller only during the unoccupied period to recharge storage. The demand-limited strategy is a hybrid of the two: the chiller runs to either recharge storage or meet cooling load directly until some pre-determined, threshold building electrical load is reached, whereupon the chiller switches off and cooling is provided solely by storage. Table 6-5 shows the results of thermal storage by strategy.

One can see the implications of operating strategy in storage and chiller sizing. Partial storage requires the smallest capacity of each because neither is used to meet the whole load. Full storage, on the other hand, needs a large storage tank in order to satisfy the entire cooling load during the peak cooling day, and also needs a large chiller to be able to charge the storage in the remaining off-hours. The table shows the resultant electricity purchases and savings in terms of energy, demand, and cost, assuming chiller cost at United States at $ 400/ton and storage cost at U.S.$ 75/ton-hr.

Demand-limited storage saves the most peak power, saving 37%, while full storage is next, saving 32%, and partial storage saves 18%. Cooling energy purchases are the same for all three. The investment cost for the storage tank and peripherals are traded off against chiller capacity and operating cost savings, expressed as a simple payback period. Partial storage has the shortest payback at 4.3 years, followed by the demand-limited strategy at 6.3 years, and full storage at 9.5 years.

Cool storage could be used in lieu of new power plant capacity. Some electric utilities in the U.S. have offered incentives to commercial customers to invest in cool storage. From the point of view of the electric utility, it is important to know the equivalent capacity cost of thermal cool storage in order to be able to compare it with supply alternatives. Cost of avoided peak electricity is shown for the three cool storage strategies in Table 6-5. In order of increasing U.S.$/kW they were 302, 580, and 877, for the partial, demand-limited, and full storage strategies, respectively. Note that these figures indicate nothing about the operating energy or cost savings, only investment. They also take no account of the timing of the building peak load and how much it coincides with that of the utility. In that sense, these figures are prepared from the perspective of the building owner who is not concerned with when the demand occurs, but only with how large it is because no time-of-use tariff is in use for Thai businesses. For the same reason, the full storage strategy looks unattractive in comparison to the others; should a time-of-use demand tariff go into effect and should there be a large differential between the on-peak and off-peak rates, then full storage could very well be more economic than the others. Currently, however, partial storage is the most suitable cool storage strategy to pursue in offices in Thailand.

Analysis of thermal storage using the partial storage strategy in hotel and retail building prototypes was similarly performed. Table 6-6 shows the results. The continuous operation and pattern of loads of the hotel dictate that the storage be sized modestly because of limited daily opportunities for recharging. Peak demand reduction is accordingly modest, saving 12% of the base peak load. Nonetheless, cool storage is so cost-effective in hotels that it has a zero payback time and *negative* cost of avoided peak power. That is, the incremental cost of the storage system is more than offset by savings in installed chiller capacity.

Thermal storage sizing (relative to the cooling load) and cost-effectiveness in the retail building prototype are more similar to the office case. Simple payback time is a shorter 3.1 years, while the cost of avoided peak power is slightly higher at 367 U.S.$/kW.

Cogeneration:

When electricity is generated in a typical thermal power plant, a large amount of heat is rejected unused into the atmosphere. Advocates of increasing the efficiency of society's use of energy have pointed towards coupling the generation of electricity with some productive process requiring heat, thereby squeezing more utility out of the overall energy conversion process. This coupling, known as cogeneration, has been applied primarily in industrial sectors where large process heat requirements exist. Commercial buildings have interesting potential for cogeneration applications because they always have on-site electricity needs, and often have a process heat load for domestic hot water (especially in hotels) and/or for thermal cooling equipment.

The Thai office prototype building was simulated using gas-turbine generators coupled with exhaust heat recovery to a two-stage absorption chiller. The gas turbine was assumed to be 24% efficient in electricity conversion at maximum output, and the exhaust heat recovery maximum was 55%. The absorption chiller had a COP of .8. Since natural gas is not currently sold to commercial customers in Thailand, economic calculations used the price paid by the electric utility, or U.S.$ 2.4/kJ. Without the electrical chiller, the building electricity demand from all the other end-uses was about 500 kW, so we looked at generator sizes less than and in excess of the building's electrical demand. The cogeneration plant was tested in several operating modes: tracking the thermal load, tracking the electrical load, and running at maximum output throughout. Any electricity generated in excess of the building's need was assumed to be sold back to the electric utility at the same effective electricity purchase price of the utility in the base case (i.e., U.S.$ .087/kWh). This price was chosen for illustrative purposes only, since no such buyback provision yet exists in Thailand, but it is part of the country's latest five-year economic plan [13] to develop such an arrangement to encourage private power production in the way it has been in the U.S. under the Public Utilities Regulatory Policy Act legislation.

Table 6-7 shows the cogeneration results. The capacity factor relates the actual electricity production to that which the generator could theoretically produce over the same period. As one moves into the larger capacity units, the capacity factors fall under the thermal and electrical tracking modes. The payback time, calculated by dividing the net operating savings into the investment cost of U.S.$ 1000/kW, generally follows an inverse relationship to the capacity factors. Thermal tracking is the least attractive operating mode because of the low price of natural gas in relation to electricity, and because of under-utilization of the cogeneration system. This is dictated by the structure of thermal and electrical loads in the office building; in a building with a better match of thermal and process heat demands (like a hotel with guest and laundry demand for hot water, for instance) the thermal tracking strategy would be more attractive. In terms of thermodynamic efficiency, however, the thermal tracking is the best because it assures that none of the heat is wasted. Running the cogenerator at full output has the shortest payback time (2 years at every capacity simulated) because of the healthy revenues collected on electricity sales to the utility. Although the utility does not now purchase power from private power producers, this particular scenario of cogeneration in an office building should be of particular interest in Thailand since the evening period when the Thai power system generally experiences its greatest demand is also when all of the cogenerator's output is going back to the utility. When tracking the building's electrical load, the 300 kW cogeneration system has a payback of 3.5 years, increasing to 6.8 years with the 700 kW system. In the absence of a buy-back contract with the utility, this is the best operating mode to use.

Cogeneration and Thermal Storage Combined:

One further configuration using a hybrid of cogeneration and thermal cool storage was simulated. This is interesting because cool storage can help provide a steady process heat load during the storage recharging period. We looked at the same 300 kW cogeneration plant as above with the cool storage sized and operated in the partial storage mode. Table 6-8 shows the results for this system under the three cogeneration operating modes. Payback times are essentially the

same as the cogeneration-only scenario for both electricity tracking and maximum output modes. The payback for the thermal tracking mode increases to 8.1 years, despite the steadier heat demand. To use the thermal tracking mode, this building would need to use a smaller generator whose waste heat capability more closely matched the building thermal needs.

Non-Electric Cooling:

Another strategy for reducing peak electric demands is to utilize thermal cooling technology that runs on fuels other than electricity, or even waste heat [14], [15]. We examined chillers operating on the absorption cycle and engine-driven, vapor compression chillers, both powered by natural gas. Using equipment efficiency assumptions and installed cost data found in Ogden [14], the above gas cooling systems were simulated in the three building prototypes, and their energy and economic performance assessed. The economic calculations used natural gas prices paid by the electric utility and assumed the incremental costs above those for a conventional chiller only (i.e., for new installations and not for replacement of existing equipment). The results are presented in Table 6-9.

Due to higher efficiency, the engine chiller out-performed the absorption chiller; yet both had payback times under 3 years. Non-electric cooling was most advantageous in retail buildings, then hotels, and finally offices. >From an avoided peak power perspective, the engine chiller was slightly superior to the absorption chiller, ranging around U.S.$ 300/kW.

Summary:

Figures 6-33 through 6-35 summarize the savings potential for individual air-conditioning control and equipment conservation measures applied over each measure's parameter range expressed in earlier figures for offices, hotels, and retail buildings, respectively. Thermal storage, cogeneration, and thermal cooling technologies are not shown in the figures because the factors that make them cost-effective are not strictly related to energy savings, but more towards electricity/alternate fuel price, and energy/demand charge differentials.

High Efficiency

To illustrate the potential savings through the use of multiple conservation measures, we have combined the most promising measures (as revealed above) into high-efficiency cases for the office, hotel, and retail building prototypes. Any interactions between measures are embedded in the performance of these cases making them more realistic than simple addition of the savings from individual measures.

We evaluated individual measures for inclusion in the high-efficiency cases, not only for high-efficiency gains, but also for cost-effectiveness. The high-efficiency cases were not strictly optimized for economic performance; instead, measures were chosen for maximum energy performance and screened for cost-effectiveness. In fact, only a few measures were screened out in this way.

Our economic analyses obtained energy, power, and operating cost savings values as compared to the base cases, and on the basis of incremental costs of the conservation measures, calculated several indices of economic performance: cost of conserved energy, simple payback time, and internal rate of return. Costs of conservation measures were obtained from a mix of local sources [1], [16], [17], [18], and U.S. sources [6]. We assumed a 7% real discount rate and, for most measures, 20-year lifetimes. Some conservation measures allow HVAC equipment to be downsized, resulting in potential investment cost savings. We also prepared the economic indices using the incremental investment cost net of the HVAC downsizing "credit." The resultant energy and economic performance of the high-efficiency cases is shown in Table 6-10.

All of the high-efficiency cases used the same basic AC system configuration: a VAV system with variable speed fan and pump drives, 70% efficient fans, chiller COP of 5.5, a temperature set-point of 28 °C, and outside air flow of 10 cfm/person. The architectural measures that were employed in the high-efficiency cases varied by building prototype.

Office:

The following changes from the base case form the high-efficiency office: window overhangs with a depth of 10% of window height, window-to-wall ratio of .3, solar absorptance of .2 for the opaque walls, and lighting power density of 10 W/m^2.

The high-efficiency office saves 45% of total electricity over the base case. The CCE is U.S.$ .016/kWh, well below the average electricity rate of U.S.$ .087/kWh (including demand charges). The simple payback time is 2 years, the IRR is 51%, and cost of avoided peak power U.S.$ 508/kW. When credited with HVAC downsizing, the high-efficiency office becomes twice as attractive economically.

Hotel:

With the AC system configured as above while retaining the fan coil system in guestrooms, the high-efficiency hotel generates savings by overhangs depth of 40% of window height, glass SC of .3, WWR of .3, wall solar absorptance of .2, U-value of the wall of .2 W/m^2-°C, and lighting power reduction of 40%.

The hotel high-efficiency case saves 51% over the base case. The CCE is U.S.$ .015/kWh, the IRR is 44%, the payback time is 2.3 years, and the cost of avoided peak power is U.S.$ 849/kW. A roughly 60% improvement in these economic measures results from the HVAC downsizing credit.

Retail:

This case used glass with a SC of .3, roof solar absorptance of .2, and lighting power reduction of 40%. Note that the VAV system is used throughout the retail building, i.e., that the split-systems in the shops were replaced.

The retail building high-efficiency case saves 56% of total electricity over the base case. This case is the most cost-effective compared to the office and hotel cases. The CCE is U.S.$ .013/kWh, the simple payback is 1.7 years, the IRR is 60%, and the cost of avoided peak power is U.S.$ 453/kW. On the other hand, the improvement in cost-effectiveness due to HVAC downsizing is much more modest in the retail as compared to the office and hotel buildings because of the sizing penalty involved in going from a distributed to a central system.

Building Energy Standard

An energy standard for new commercial construction has been proposed [19]. It is currently under consideration for voluntary compliance only. The Thai standard draws on earlier work in neighboring countries [20], [21], [22]. The standard aims to reduce energy use through provisions for the building envelope, lighting, and space-conditioning systems. Table 6-11 compares some of the key criteria of the standard with those of the base cases of the three prototype buildings (shown in parentheses). The lower half of Table 6-11 shows the results of, and inputs to, the Overall Thermal Transfer Value (OTTV). The OTTV approach attempts to capture the key parameters of the building envelope causing cooling demand on the chiller. The OTTV equation for walls, as formulated in Thailand, follows the approach found in DBCD [20] modified for local solar radiation conditions. The equation has three terms each for different heat transfer pathways: conduction through the opaque wall, conduction through the fenestration, and radiation gain through the fenestration.

$$OTTV = U_w (1-WWR)\, TD_{eq} + U_f (WWR)\, \Delta T + SC\, (WWR)\, SF \qquad \text{(Eq.6-6)}$$

where,

U_w = U-value of the opaque wall (W/m^2-°C);
WWR = Window to wall ratio (dimensionless);
TD_{eq} = equivalent indoor-outdoor temperature difference for the opaque wall (°C);
U_f = U-value of the fenestration (W/m^2-°C);
ΔT = indoor-outdoor temperature difference for the fenestration (°C);
SC = fenestration shading coefficient (dimensionless);

SF = solar factor (W/m^2).

The U_w, WWR, U_f, and SC are all parameters chosen by the building designer. The other terms, TD_{eq}, ΔT, and SF are quantities stipulated by the standard. TD_{eq} varies according to the solar absorptivity of the exterior wall surface, ranging from 14 to 18 °C, while ΔT is a fixed 5 °C. SF has been set at 160 W/m^2 but is corrected for orientation and non-vertical slopes. Thailand has set the OTTV compliance level at or below 45 W/m^2.

The prototype buildings were modified to minimally comply with the standard.* Note that many combinations of parameters can be used to comply with the OTTV standard, but that we illustrate only one here. The energy savings were 23% in the office, 35% in the hotel, and 42% in the retail building. The major contribution to these savings obtained from the standard comes from the lighting power density provisions, saving both lighting energy directly and cooling energy (and capacity) indirectly. No economic analyses were performed for the standard, but are probably as cost-effective as the high-efficiency cases discussed above.

CONCLUSIONS

Energy conservation measures have been evaluated for commercial buildings in Thailand by means of computer simulation. A prototypical office, hotel, and retail building were developed based on actual Bangkok buildings, and simulated in the Thai environment. The best measures combined into high-efficiency cases for each prototype cut energy and peak power usage, and cut electricity bills in half, as compared to typical design practice. When considering the cost of installing the measures that make up the high-efficiency cases, they remain attractive by being highly cost-effective. Compliance with the proposed energy standard for new buildings lowers energy intensity by approximately one-third overall, with substantial variation among the building types. Taken individually, the conservation measures demonstrated the following savings.

Architectural Measures

Architectural measures showing the greatest impact on energy use are those relating to fenestration and lighting.

- Window area, glass shading coefficient, and, for offices, the use of external shading devices, are all critical features that can each result in up to a 5% increase or decrease in total energy consumption.
- Energy conservation in lighting saves both directly in lighting energy and indirectly in cooling load reductions; this leads to dramatic savings potential of 20% to 35% for cutting lighting power density in half.
- Daylighting can cut energy use by 6% to 15%, depending on the design. Lower savings result when the daylighting design fails to limit solar heat gains through windows.
- Insulating the opaque wall section of hotels saves almost 4%, but in offices and retail buildings the savings are negligible.

Air-Conditioning Measures

- In the use of an air-conditioning system, the single most important parameter is the zone thermostat setpoint. Savings reach above 10% for this measure alone within a temperature range proven acceptable to Thai office workers. This is also a no-investment-cost measure.
- The use of a VAV system with variable speed fan drives in place of constant volume can save between 8% and 10% in offices and hotels.
- Efficient chillers and fans each indicate savings potential in the 5% to 10% range.

* Where a base case parameter was equal to or "better" than the level set by the standard, it was left unchanged.

- Reducing outside air quantities in hotels to 10 cfm per person saves 10% of total energy; about 4% could be saved in offices and retail buildings ventilated to the same degree.
- Conversely, high static pressures in the fan duct system, or fan oversizing, or inefficient chillers, or excessive quantities of outside air, all carry large energy penalties.
- Thermal storage employing a partial storage strategy can significantly reduce peak demands and associated charges in a cost-effective manner, particularly in hotels where the chiller cost savings can be greater than the extra cost of the storage system.
- Should natural gas become available to commercial customers in Thailand, cogeneration can be economically attractive, particularly when sized to match the thermal load from the absorption chiller, but operated to track the building electrical load. If excess electricity can be sold back to the utility at a price close to the current retail price of power, operating the generator at maximum output is the best strategy, almost independent of generator size.
- Gas-fired, engine-driven, or absorption chillers are an effective means for reducing peak electrical demands, Engine chillers, by virtue of higher efficiency at comparable cost, are the more cost-effective alternative.

Comparisons Among Building Types

Comparing the building types, the savings potential shown for retail buildings is dominated by the prototype system configuration and lighting power density. Because most of the building area is served by distributed, individual split-system AC units, few of the measures applied to the central systems (where alternative technologies exist) could have a large impact. Lighting should be the overwhelming concern for retail buildings. Careful tradeoffs between the store marketing strategy, the cost of more efficient lighting versus high operating costs of standard lighting, and the quality of light produced, all have to be made. Hotel performance seems most influenced by its 24-hour schedule, and especially the constant operation of the AC system. Air-conditioning conservation measures applied to the hotel prototype had relatively large impacts. Office performance is balanced between internal and external influences, especially lighting and transmitted solar radiation. The office prototype was equally responsive to both architectural and air-conditioning conservation treatments.

REFERENCES

1. Kijwatanachai, Boonpong, Engineer, MITR Technical Consultant Co., Ltd., Bangkok, Thailand. Private communication, December 1989.
2. Meteorological Department, Ministry of Communications, *Climatological Data of Thailand; 30-Year Period (1956-1985)*, Bangkok, Thailand. 1987.
3. Building Energy Simulation Group, "Overview of the DOE-2 Building Energy Analysis Program," Lawrence Berkeley Laboratory Report LBL-19735, 1985.
4. Building Energy Simulation Group, "DOE-2 Reference Manuals," Lawrence Berkeley Laboratory Report LBL-8706-Rev. 5., 1981-1989. Available through the National Technical Information Service, Springfield, VA.
5. Usibelli, A., Greenberg, S., Meal, M., Mitchell, A., Johnson, R., Sweitzer, G., Rubenstein, F., and Arasteh, D., "Commercial-Sector Conservation Technologies," Lawrence Berkeley Laboratory Report LBL-18543, 1985.
6. Piette, M.A., Krause, F., and Verderber, R., "Technology Assessment: Energy-Efficient Commercial Lighting," Lawrence Berkeley Laboratory Report LBL-29032, 1989.
7. Busch, J.F., and Warren, M.L., "Improving the Performance of Air-Conditioning Systems in an ASEAN Climate," *Proceedings of the Fifth Annual Symposium on Improving Building Energy Efficiency in Hot and Humid Climates*, College Station, TX, September 13-14, 1988. Also published as Lawrence Berkeley Laboratory Report LBL-24270.
8. Busch, J.F., "Thermal Responses to the Thai Office Environment." *ASHRAE Transactions*, Vol. 96, Pt. 1, 1990.

9. Eto, J.H., "Cooling Strategies Based on Indicators of Thermal Storage in Commercial Building Mass," Presented at the 2nd Annual Symposium Improving Building Energy Efficiency in Hot and Humid Climates, College Station, TX, September 24-26. 1985. Also published as Lawrence Berkeley Laboratory Report LBL-19912.

10. Wyatt, E., "The Feasibility of Commercial Building Thermal Energy Storage in ASEAN Countries," Lawrence Berkeley Laboratory Report LBL-27920, 1986.

11. Piette, M.A., Wyatt, E., and Harris, J., "Technology Assessment: Thermal Cool Storage in Commercial Buildings," Lawrence Berkeley Laboratory Report LBL-25521, 1988.

12. Electric Power Research Institute, *Commercial Cool Storage Design Guide*, EPRI EM-3981, Palo Alto, CA. 1985.

13. National Economic and Social Development Board, *Energy Issues and Policy Directions in the Sixth National Economic and Social Development Plan (1987-1991)*, Office of the Prime Minister, Bangkok, Thailand, 1985.

14. Ogden, J.M., "Alternative Cooling Technologies for Commercial Buildings: A New Jersey Case Study," Center for Energy and Environmental Studies, Princeton University, Princeton, NJ. 19 October 1988 (Draft).

15. Brodrick, J.R. and Patel, R.F., "Gas-Fired Cooling Systems Create Energy Cost Savings in Commercial Buildings," *Proceedings from the Panel on Appliances and Equipment, ACEEE 1988 Summer Study on Energy Efficiency in Buildings*, American Council for an Energy Efficient Economy, Washington D.C., August 1988.

16. Nimboonchai, Vajrindr, Vice President, Casa Co., Ltd., Bangkok, Thailand. Private communication, July 1988.

17. Chevasutho, Chaivut, Assistant Manager, MITR Technical Consultant Co., Ltd., Bangkok, Thailand. Private communication, July 1988.

18. Seehanath, Rongyuth, Senior Architect, Yon Hong Seng Co., Ltd., Bangkok, Thailand, Private communication, July 1988.

19. National Energy Administration, *Guidelines and Requirements for Energy Conservation in New Buildings*, Bangkok, Thailand, November, 1989 (Draft, in Thai).

20. Development and Building Control Division, Public Works Department, *Handbook on Energy Conservation in Buildings and Buildings Services*, Singapore, 1979.

21. Busch, J.F., and Deringer, J.J., "A Building Energy Envelope Standard for Malaysia," *Proceedings of the ASHRAE Conference on Air Conditioning in Hot and Humid Climates*, Singapore, September 1987. Also published as Lawrence Berkeley Laboratory Report LBL-23280,

22. Deringer, J.J., Busch, J.F., Hall, J., Kannan, K.S., Levine, M.D., Ayub, A.C., and Turiel, I., "Energy and Economic Analyses in Support of Energy Conservation Standards for New Commercial Buildings in Malaysia," *Proceedings of the ASHRAE Conference on Air Conditioning in Hot and Humid Climates*, Singapore, September 1987. Also published as Lawrence Berkeley Laboratory Report LBL-23279,

ACKNOWLEDGEMENTS

This work was supported by the U.S. Agency for International Development through the U.S. Department of Energy, under Contract No. DE-AC03-76SF00098. The author also gratefully acknowledges the support of the Thailand-U.S. Educational Foundation for the fieldwork portion of this project. Useful guidance and insights were shared by Dr. Pibool Hungspreug and Dr. Surapong Chirarattananon, while invaluable logistic support in collecting building data was provided by Boonpong Kijwatanachai.

Figure 6-1.
Thai Office Buildings

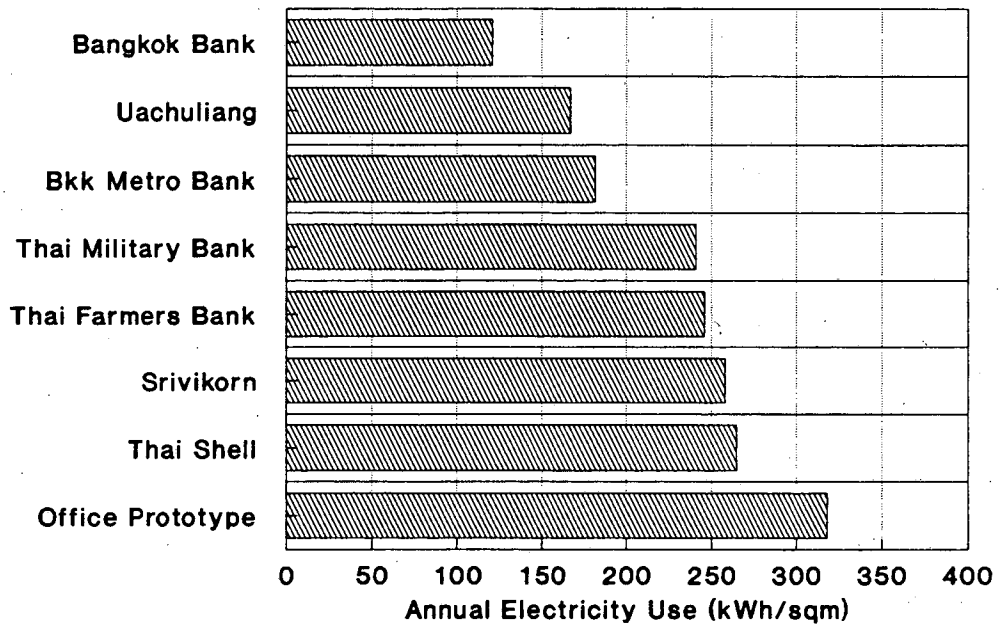

Figure 6-2.
End-Use Breakdown of Thai Buildings

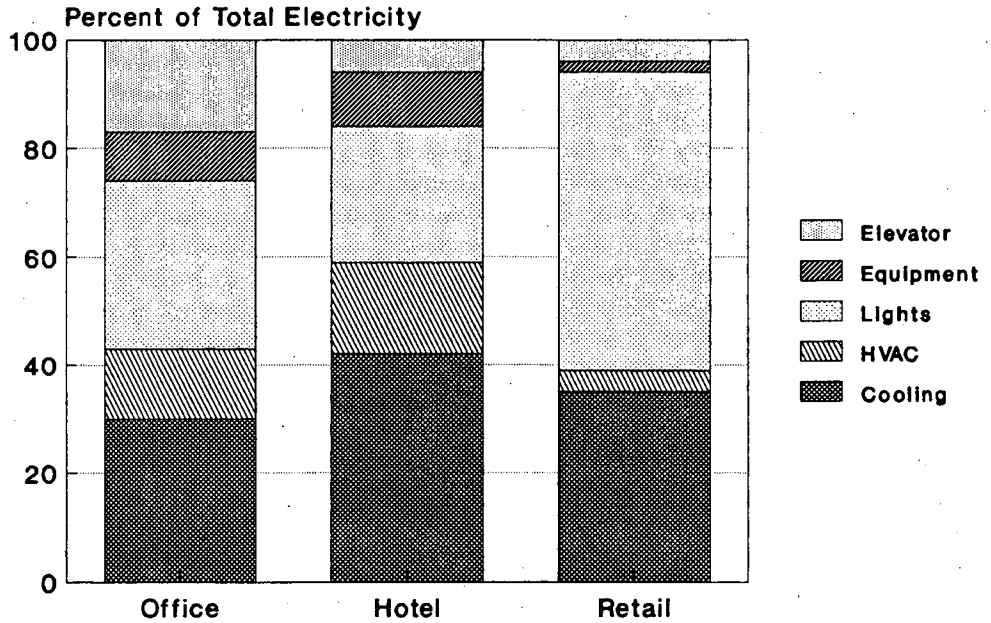

Figure 6-3.
Thai Hotels

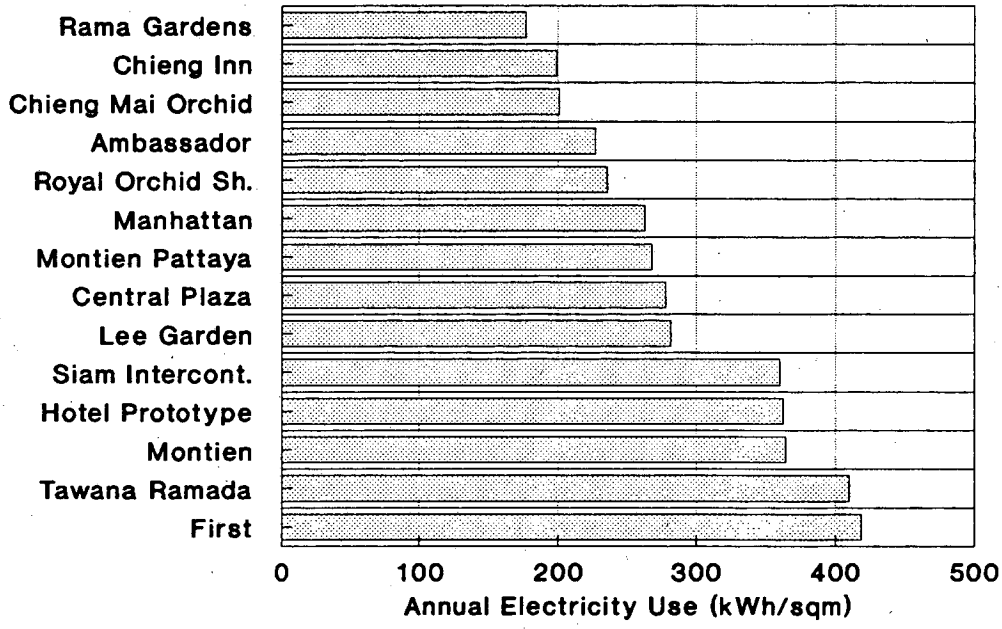

Figure 6-4.
Thai Retail Buildings

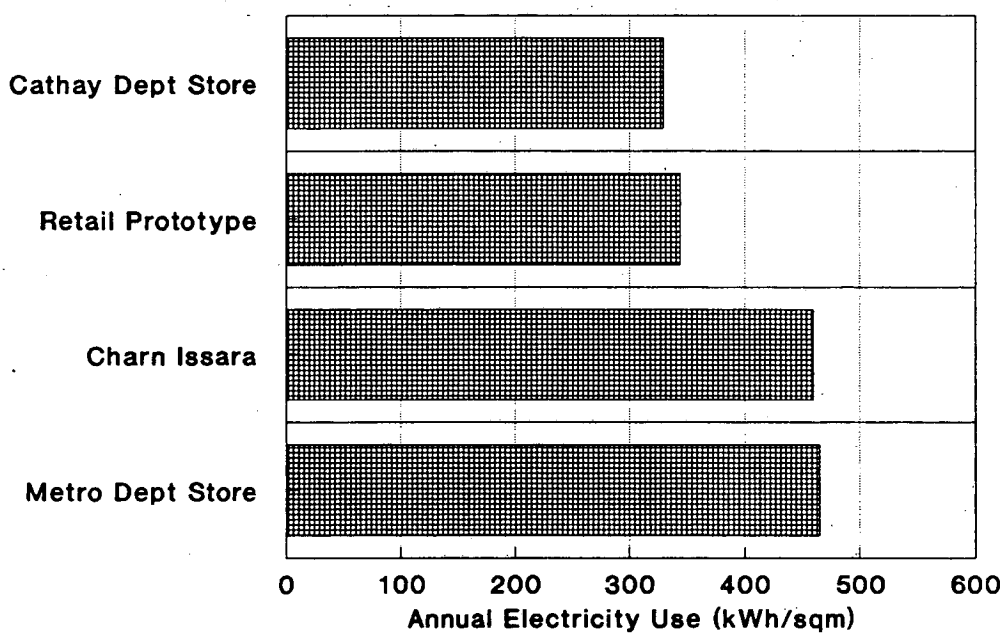

Figure 6-5.
Bangkok Weather (1985)

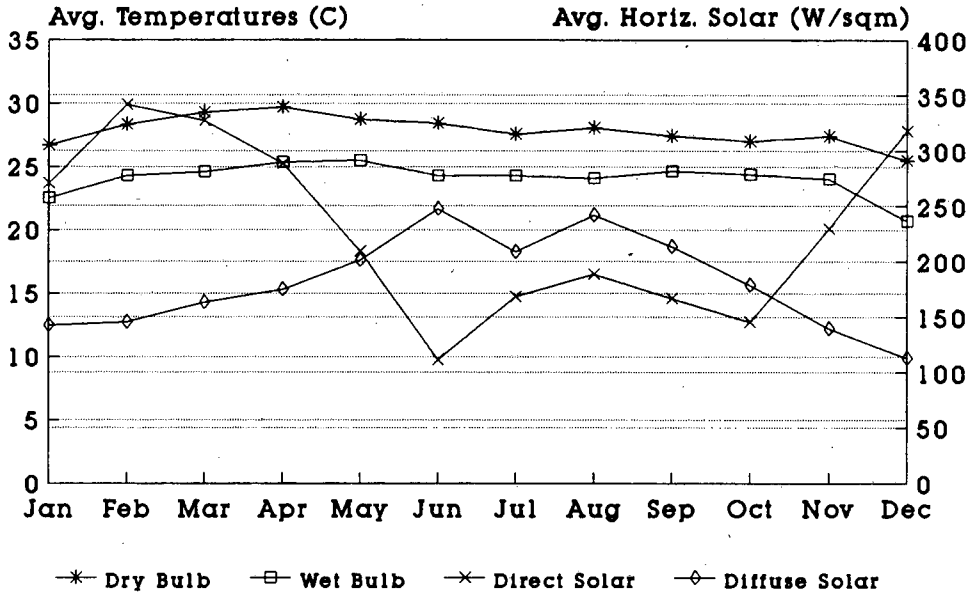

Figure 6-6.
Orientation of
Unconditioned Space of Office

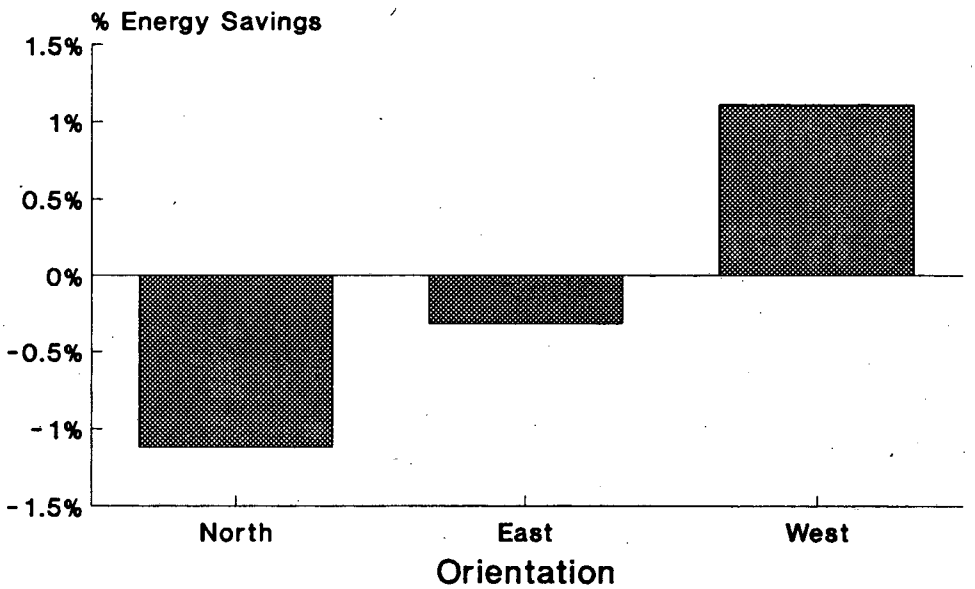

Figure 6-7.
Infiltration

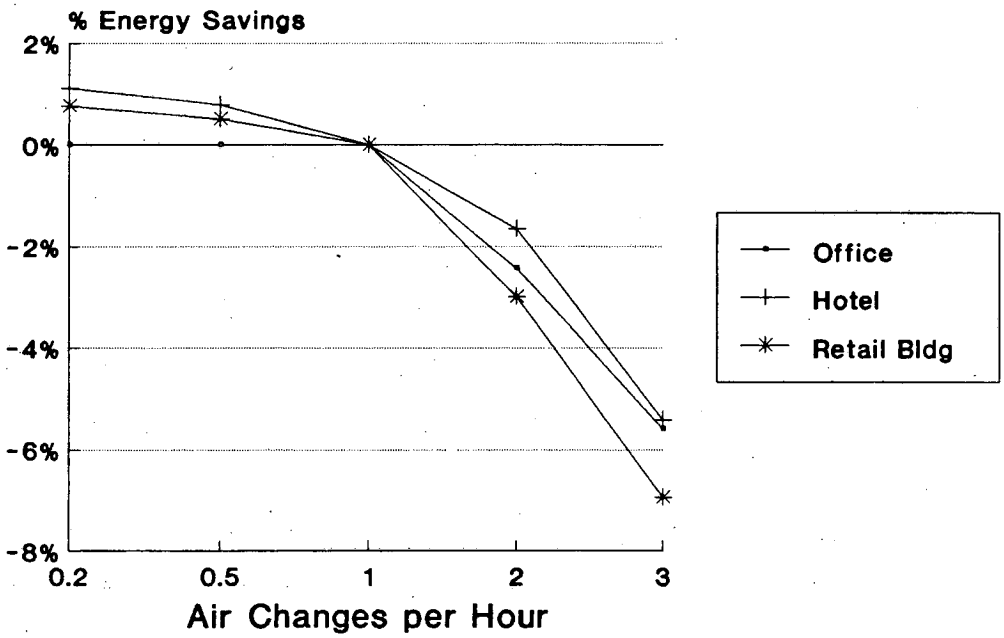

Figure 6-8.
Thermal Mass

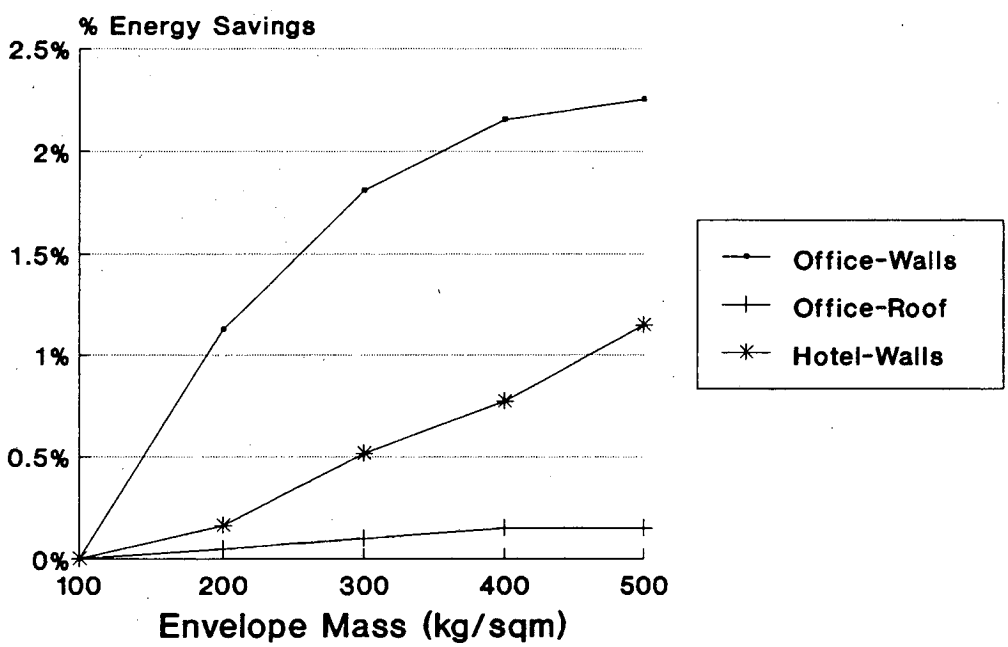

Figure 6-9.
Opaque Wall Conductivity

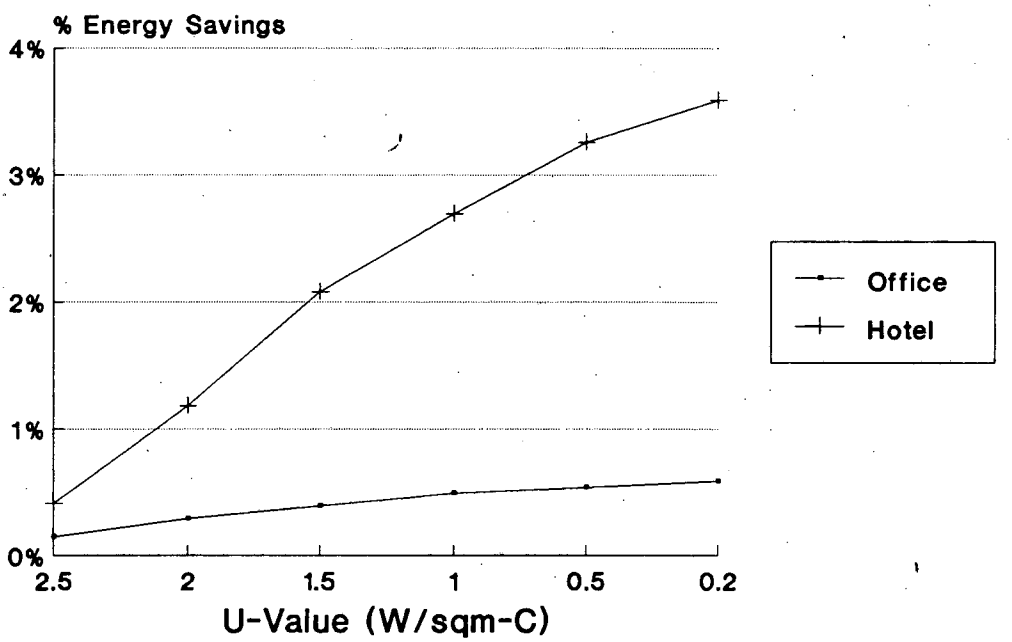

Figure 6-10.
Wall Solar Absorptance

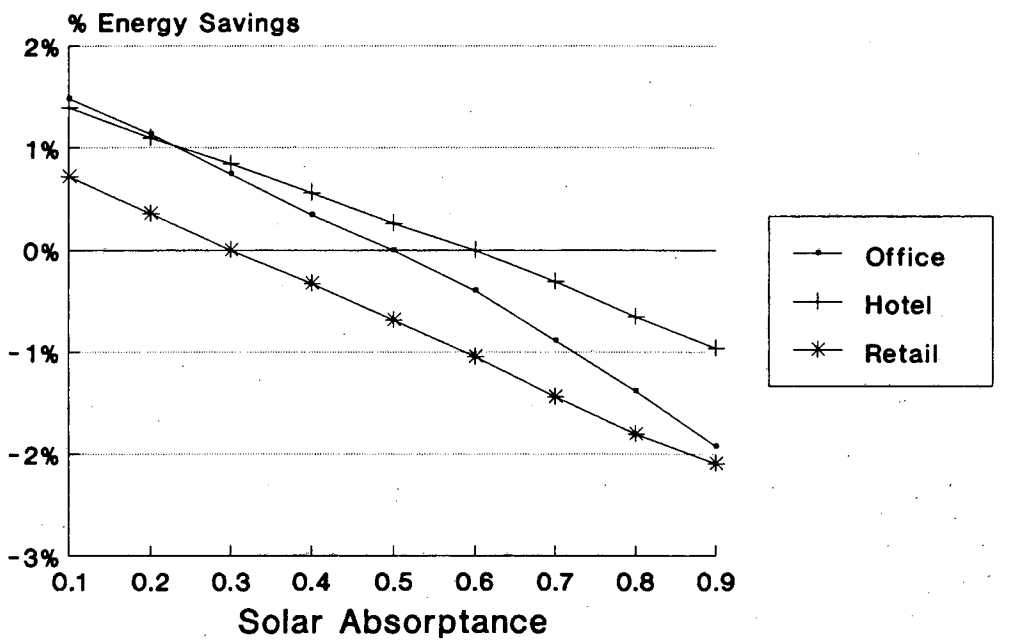

Figure 6-11.
Fenestration Area

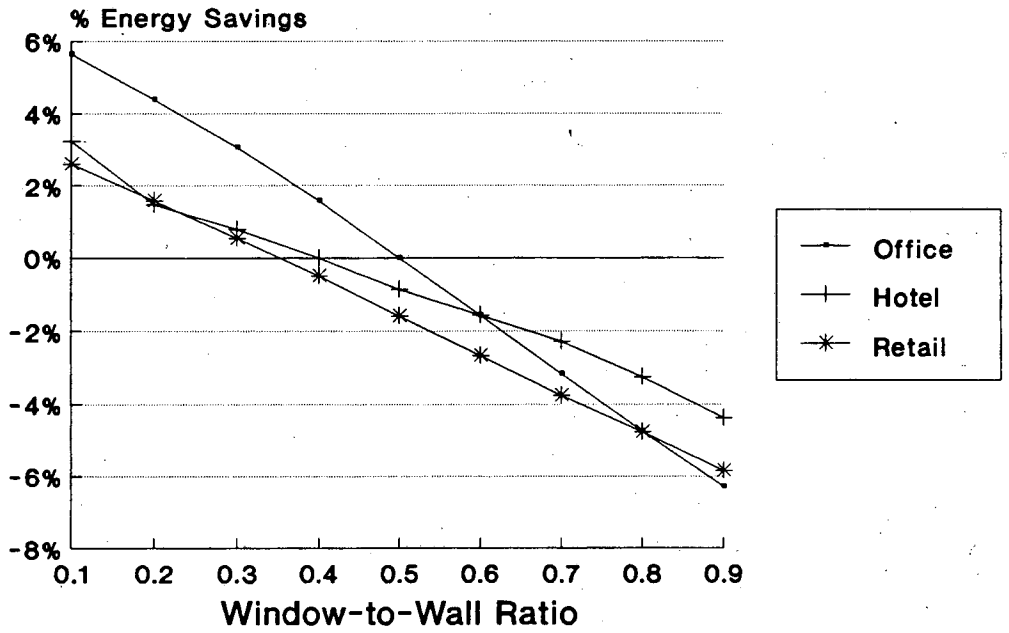

Figure 6-12.
Glass Shading Coefficient

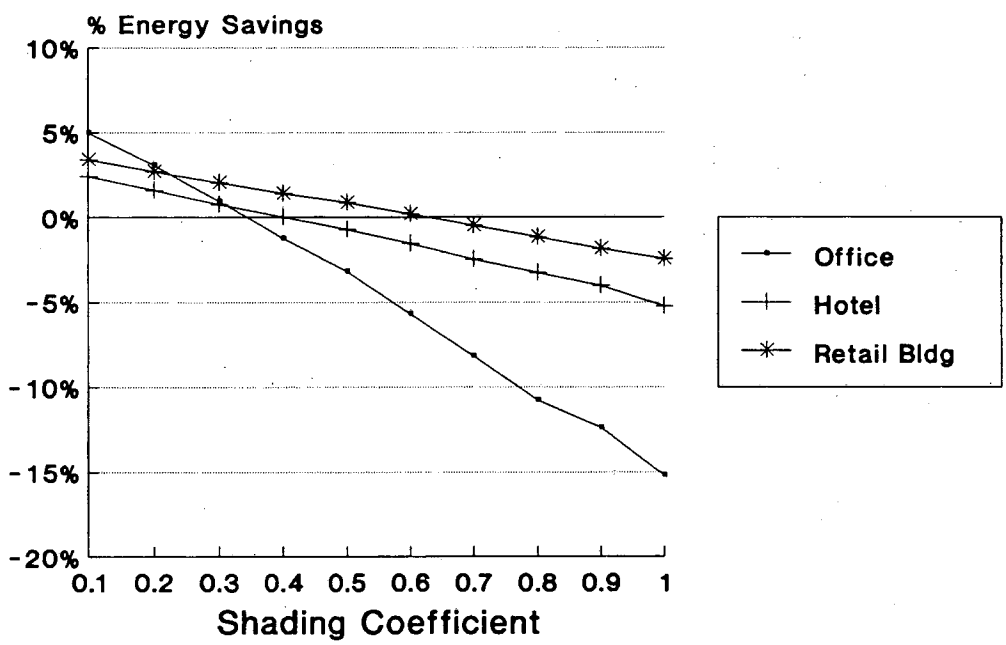

Figure 6-13.
External Shading of Office

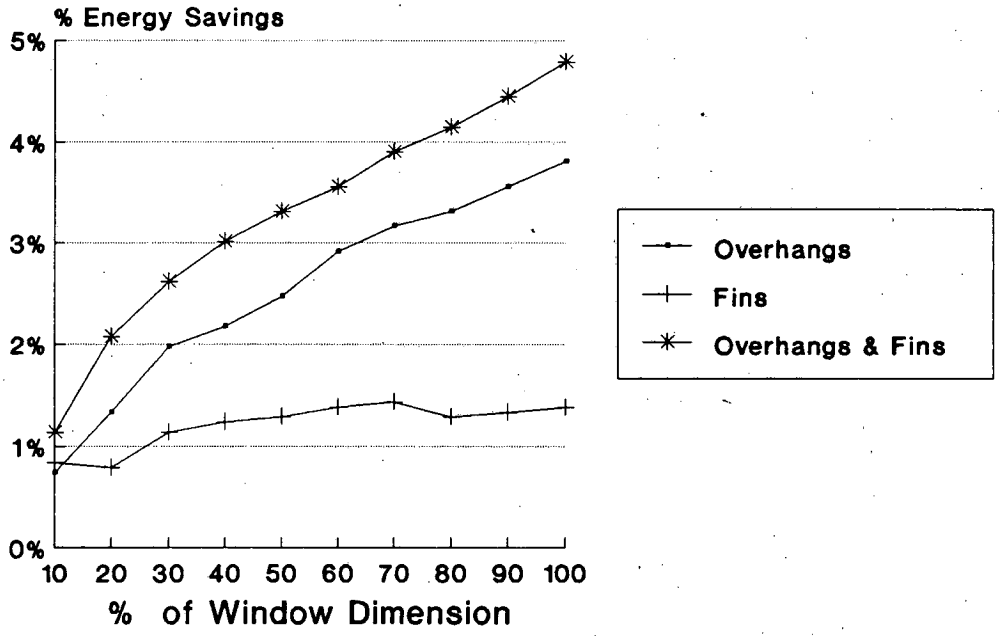

Figure 6-14.
External Shading of
Hotel and Retail Building

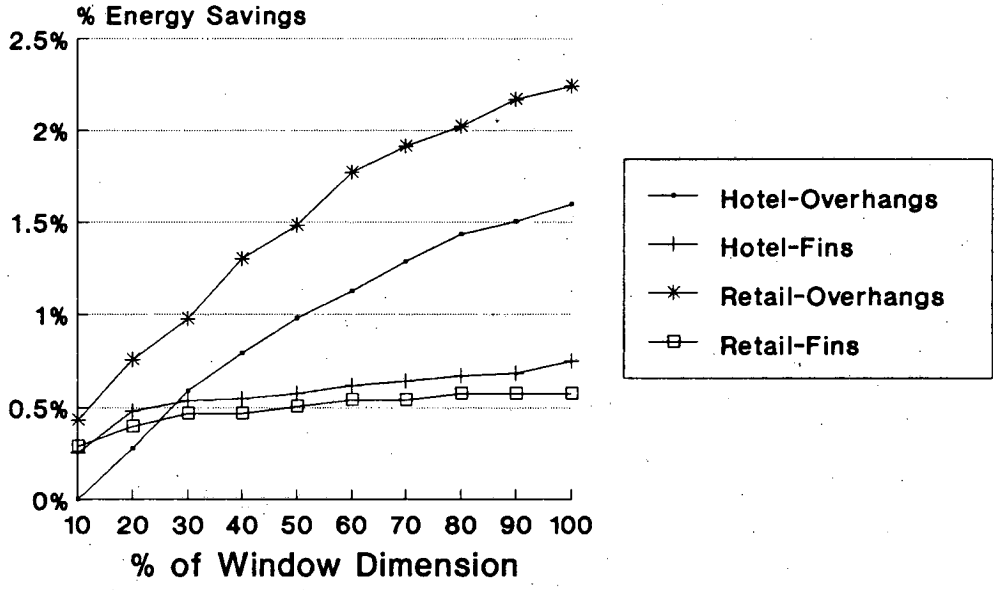

Figure 6-15.
Lights and Office Equipment in Offices

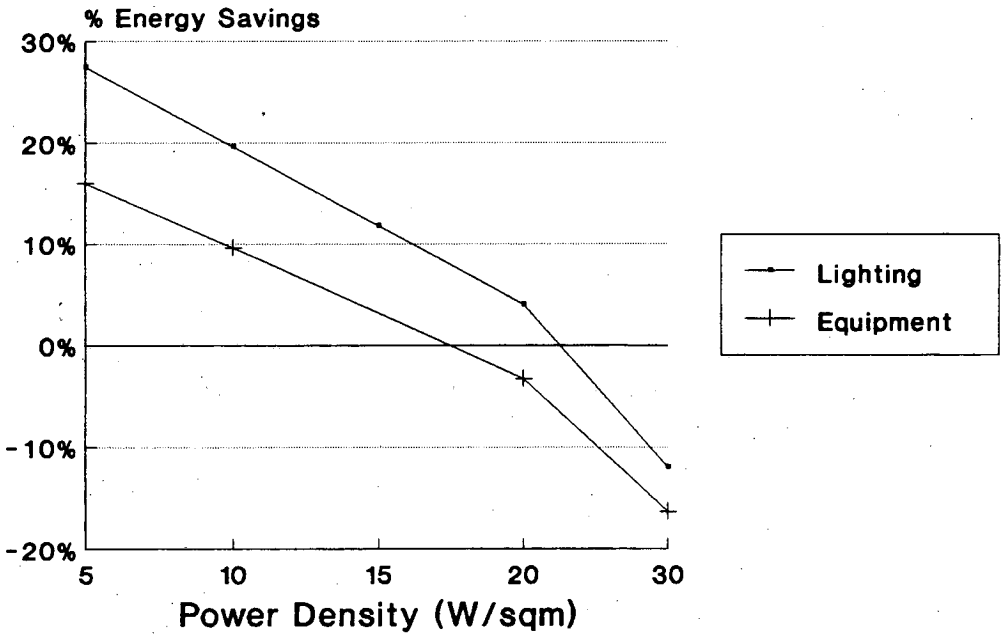

Figure 6-16.
Lighting Power Reduction in Hotel and Retail Building

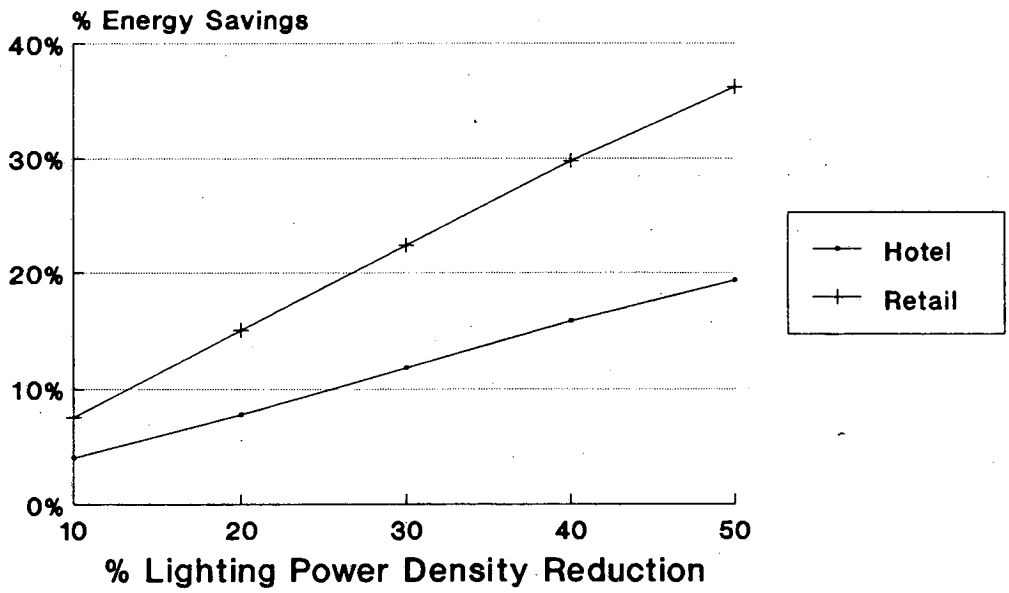

Figure 6-17.
Daylighting in Office Using Stepped Controls

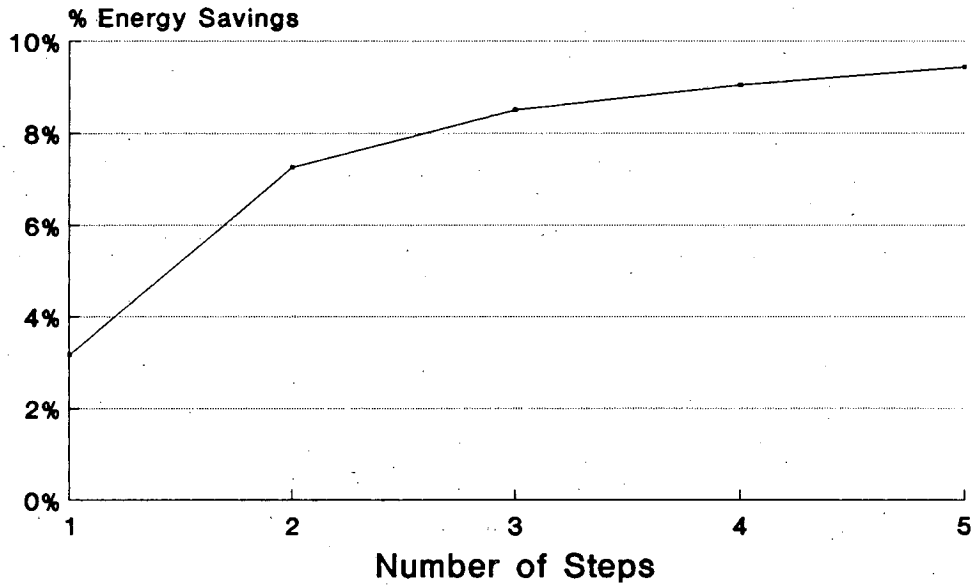

Figure 6-18.
Minimum Power Draw of Continuous Dimming Daylighting Controls

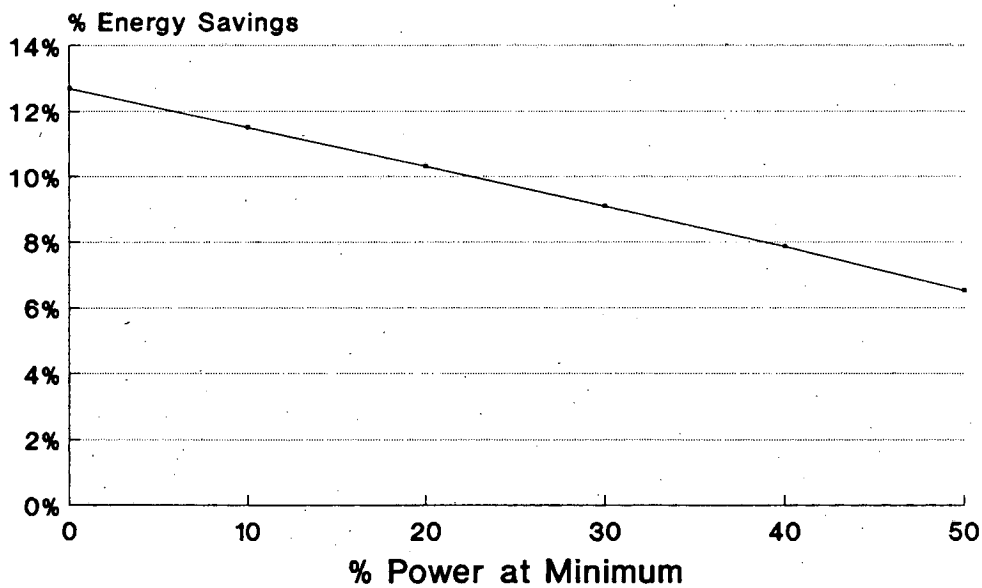

Figure 6-19.
Glass Visible Transmittance
Effect on Daylighting (SC = .34)

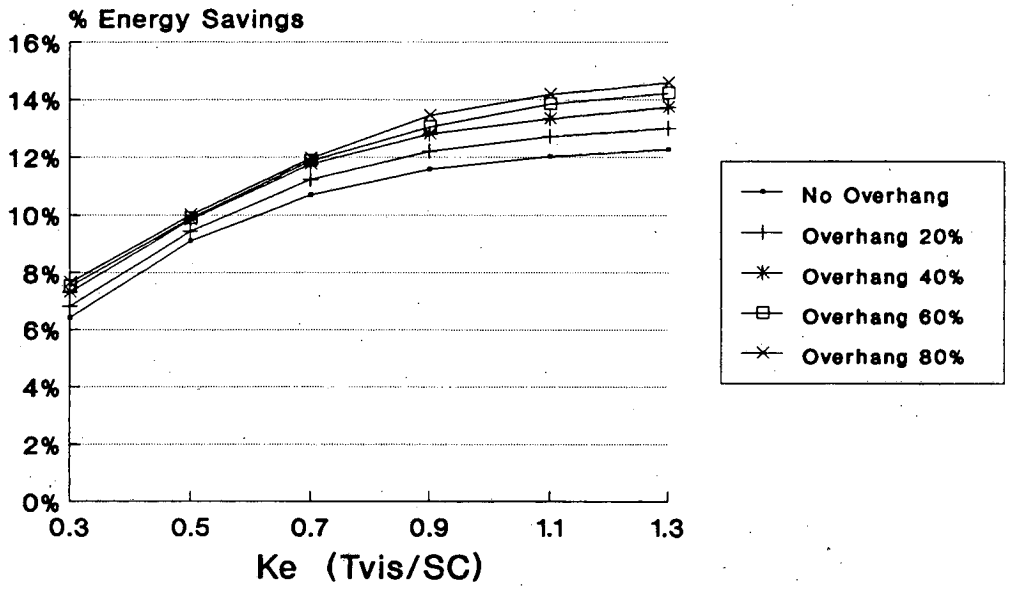

Figure 6-20.
Glass Visible Transmittance
Effect on Daylighting (SC = .70)

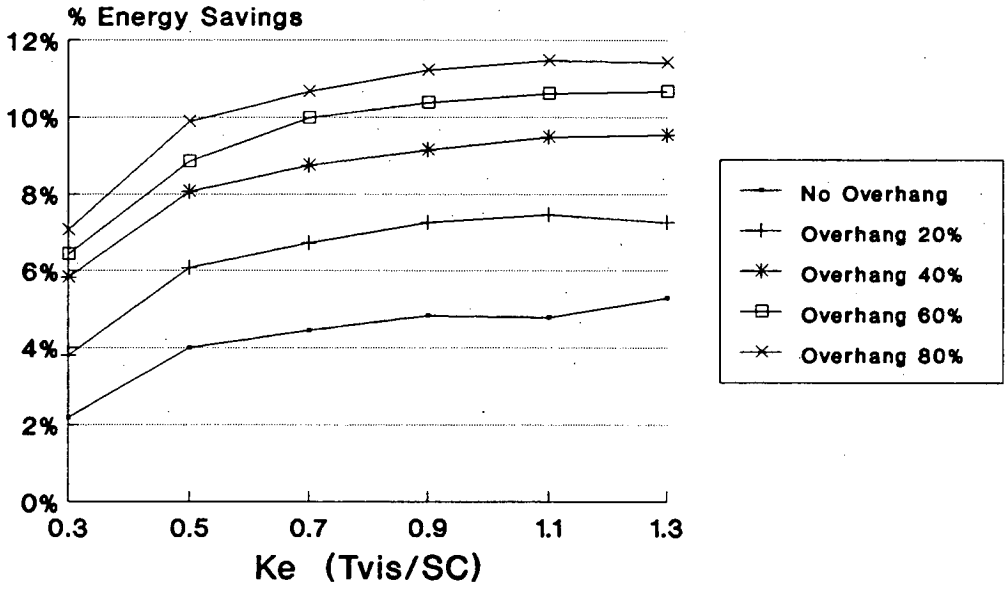

Figure 6-21.
Range of Savings for
Thai Office Architectural Measures

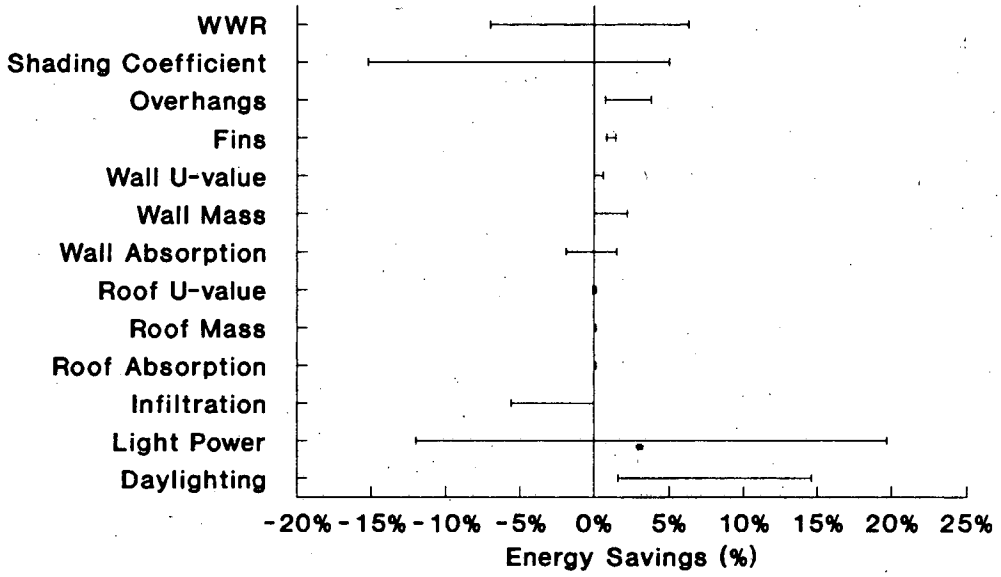

Figure 6-22.
Range of Savings for
Thai Hotel Architectural Measures

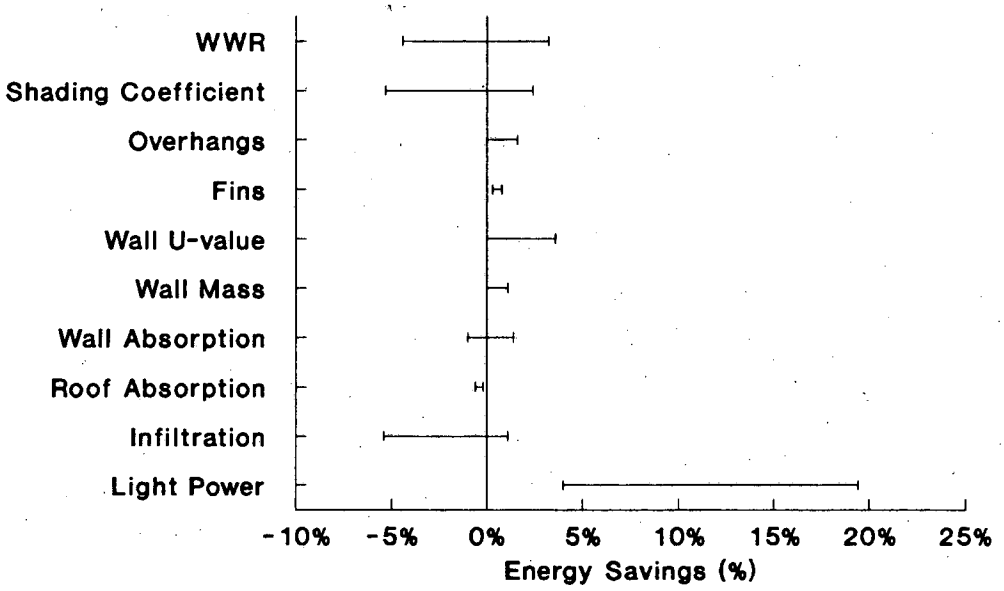

Figure 6-23.
Range of Savings for
Thai Retail Architectural Measures

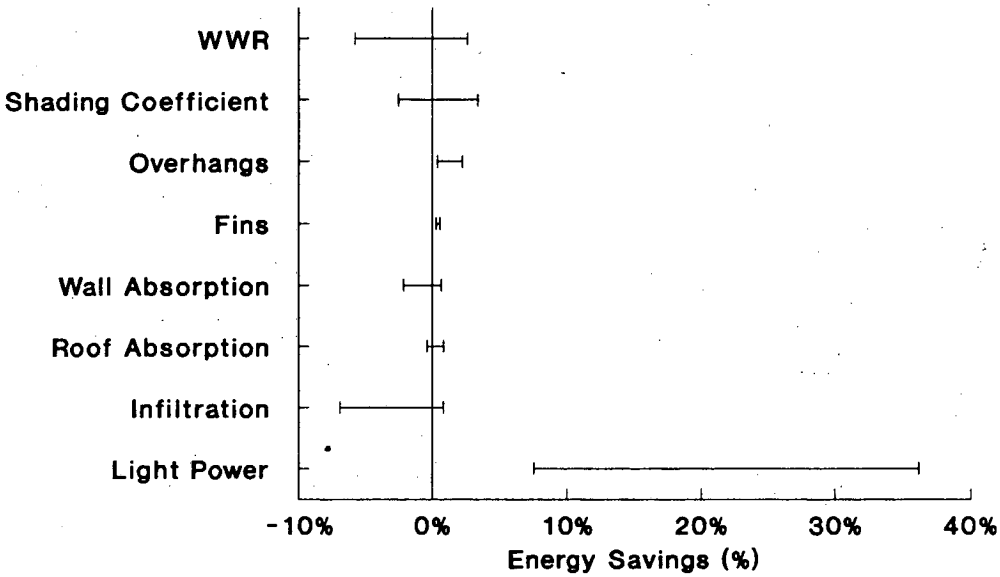

Figure 6-24.
Zone Temperature Setting

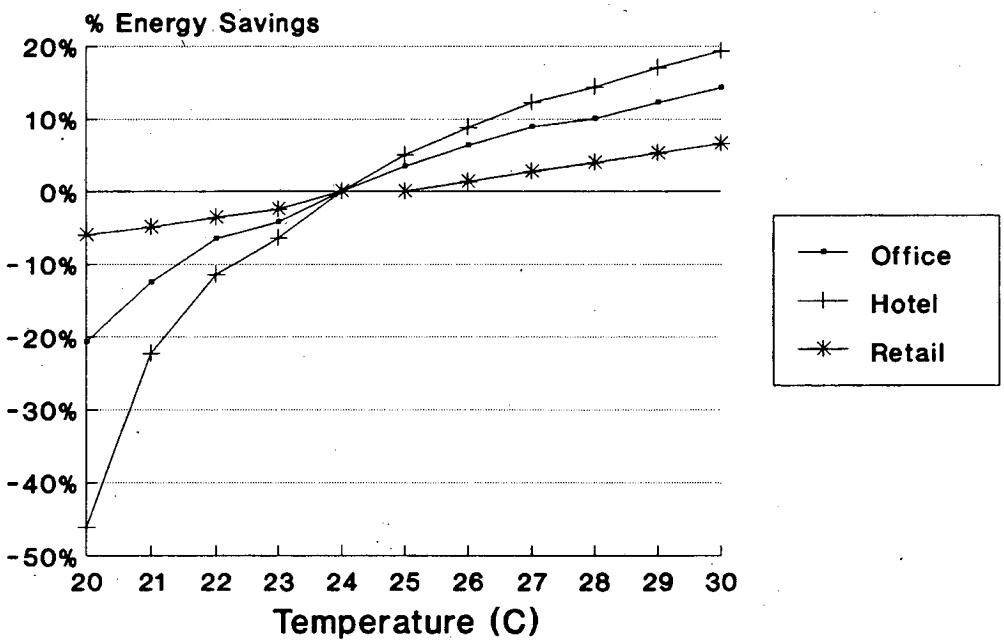

Figure 6-25.
Supply Air Temperature

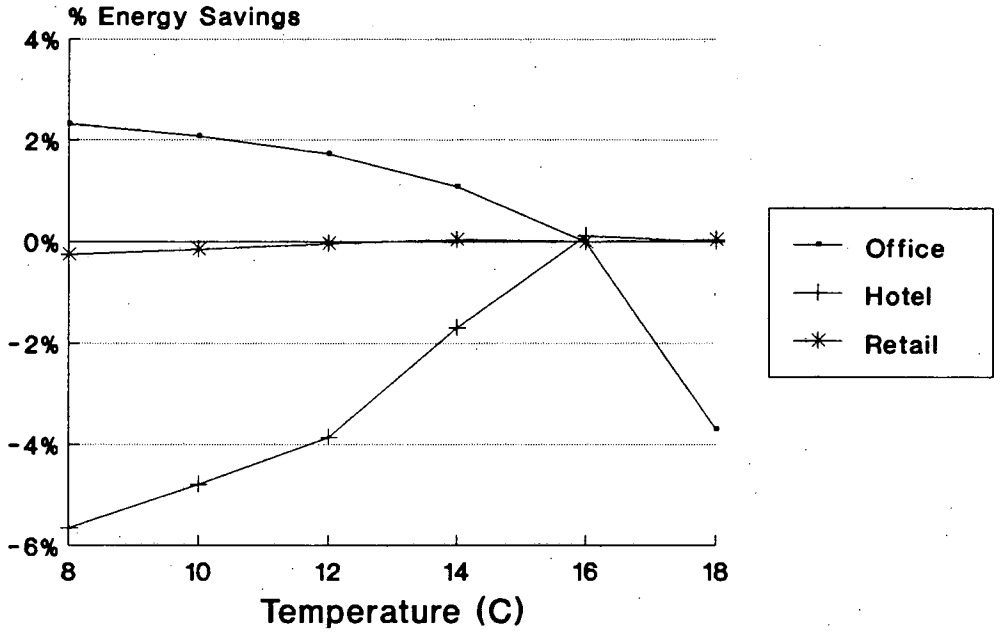

Figure 6-26.
Fan Control for VAV System

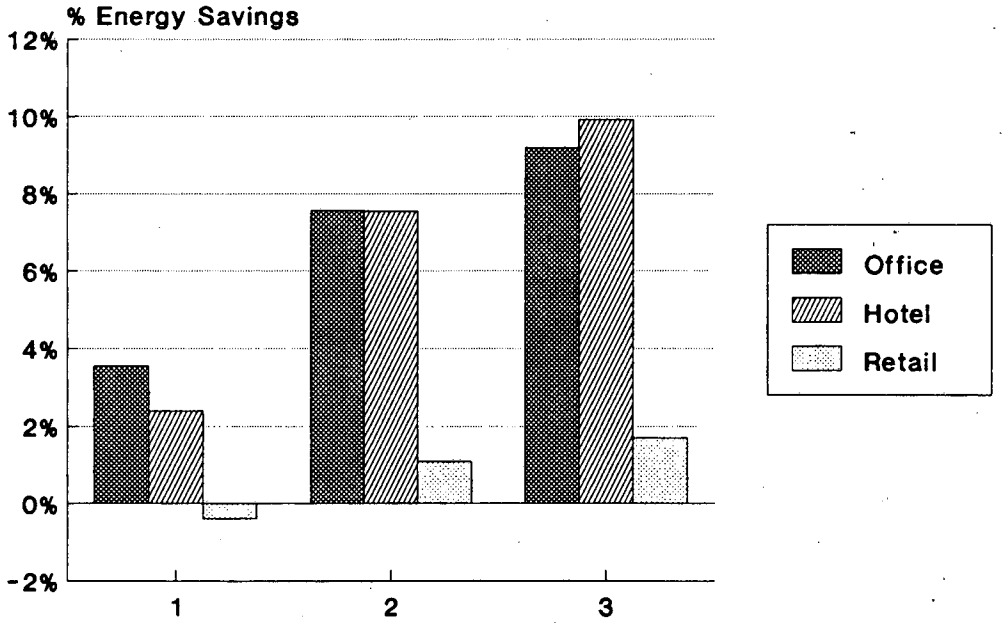

Figure 6-27.
Outdoor Air Quantity

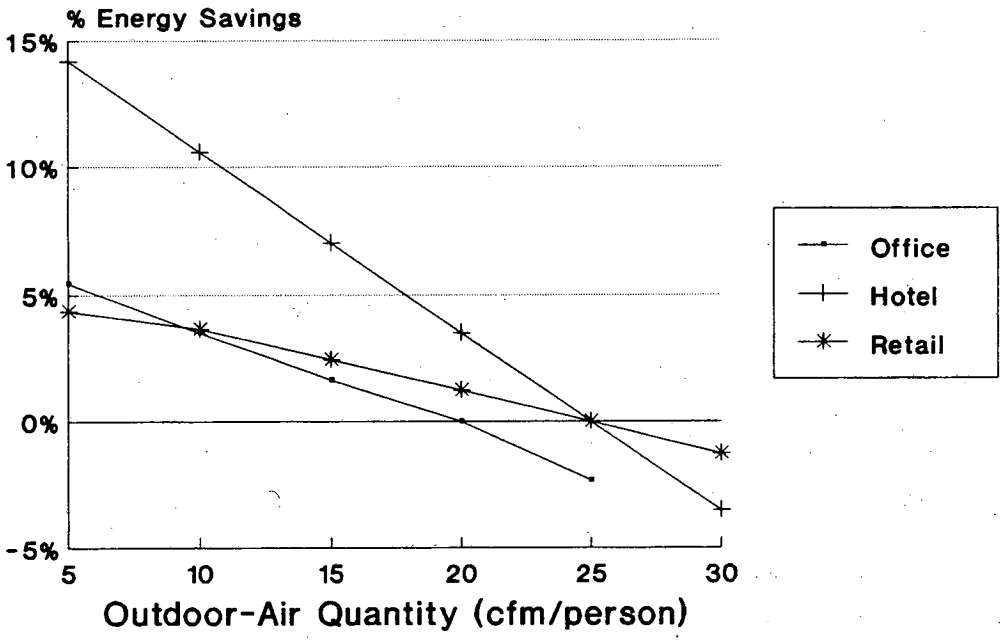

Figure 6-28.
Pre-Cooling of Office

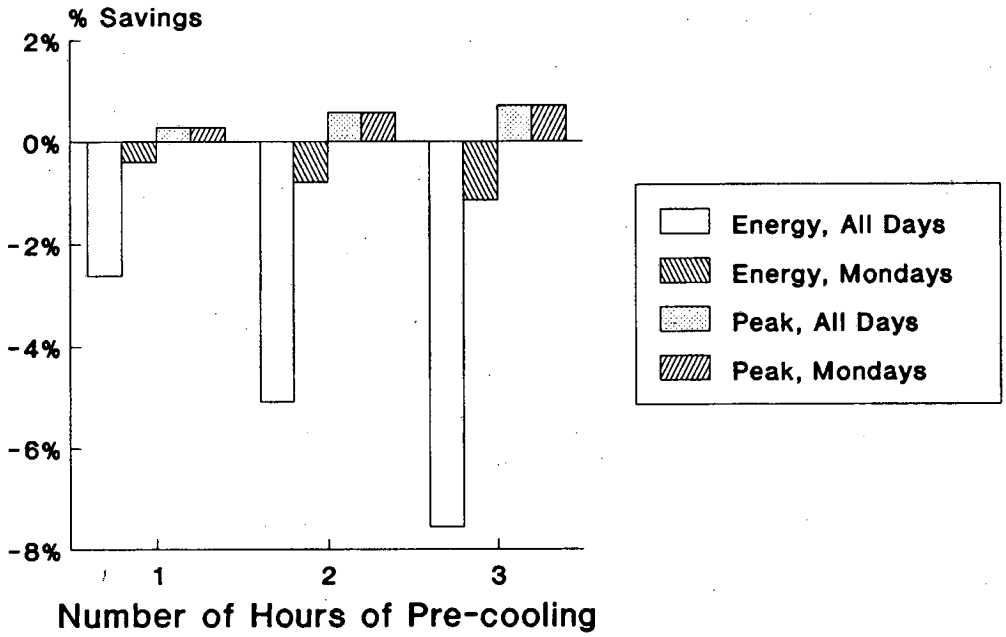

Figure 6-29.
Chiller Efficiency

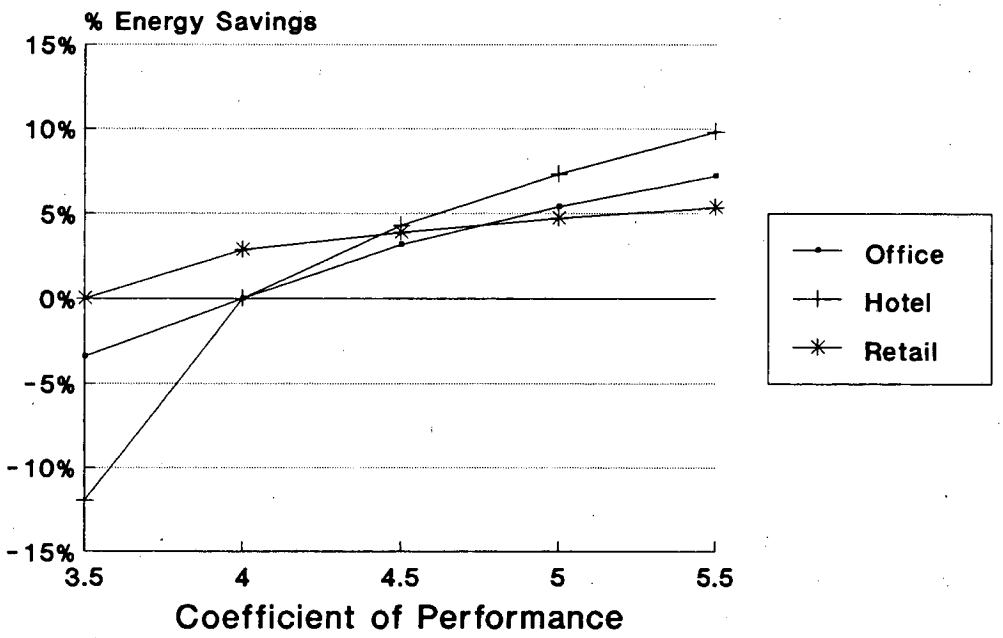

Figure 6-30.
Fan Efficiency

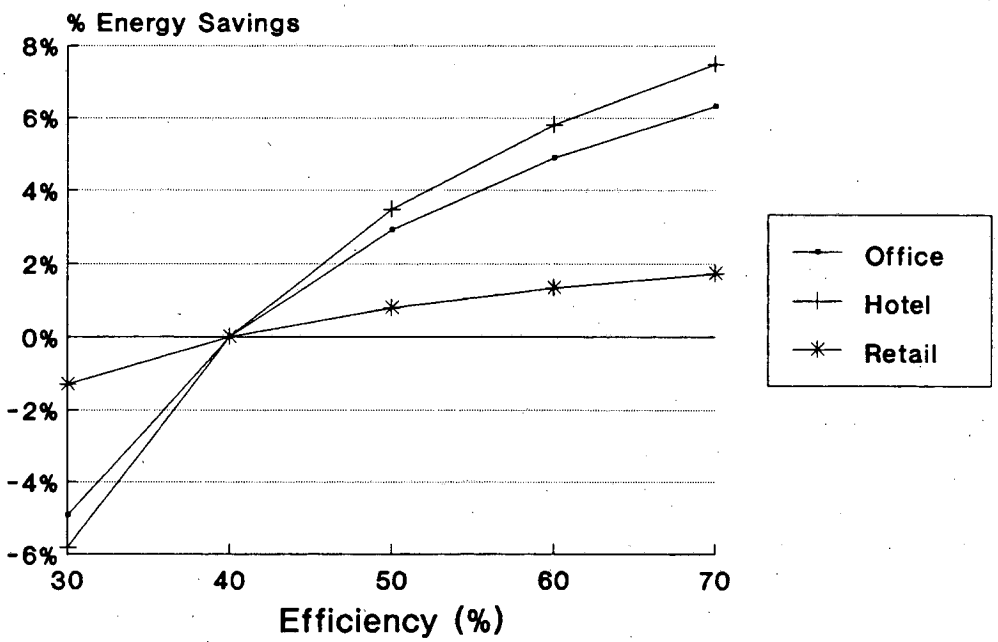

Figure 6-31.
Fan Static Pressure

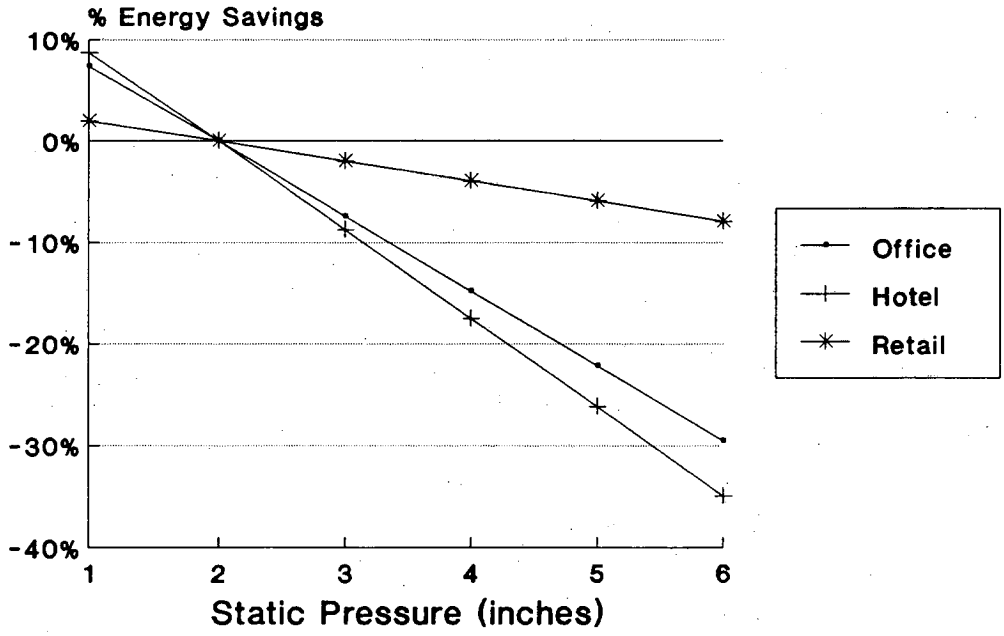

Figure 6-32.
Fan Oversizing Penalty

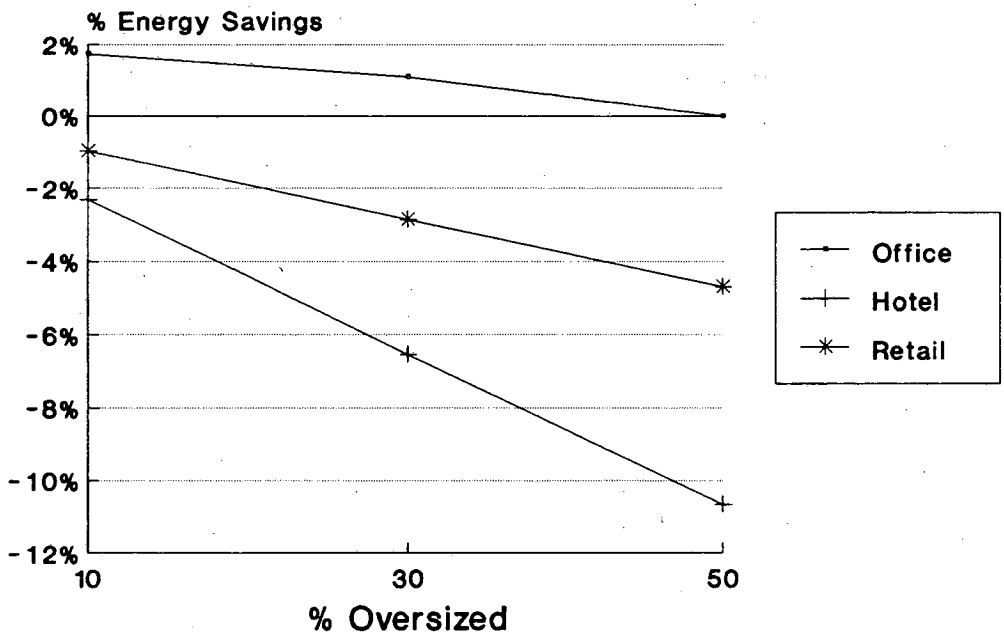

Figure 6-33.
Range of Savings for
Thai Office AC Measures

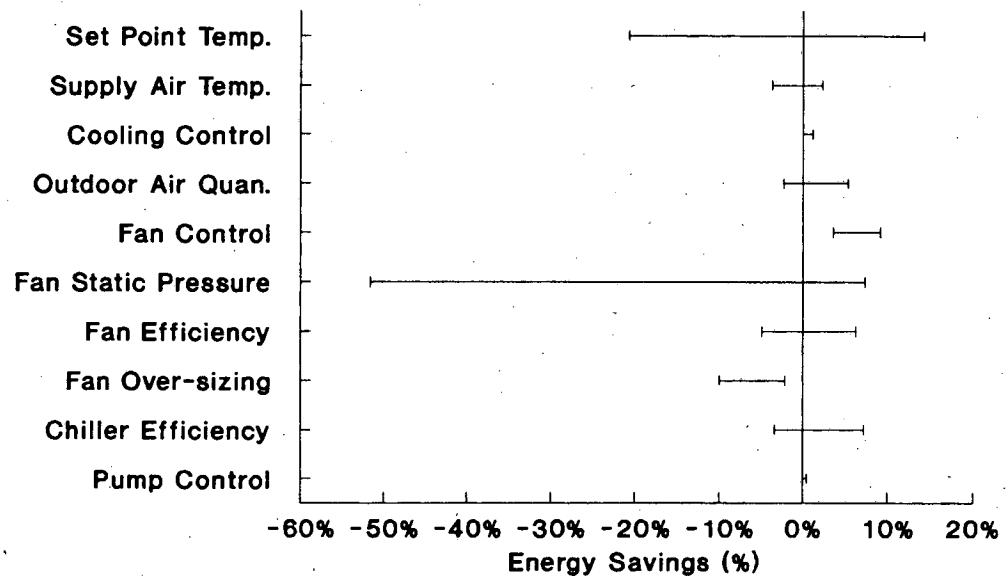

Figure 6-34.
Range of Savings for
Thai Hotel AC Measures

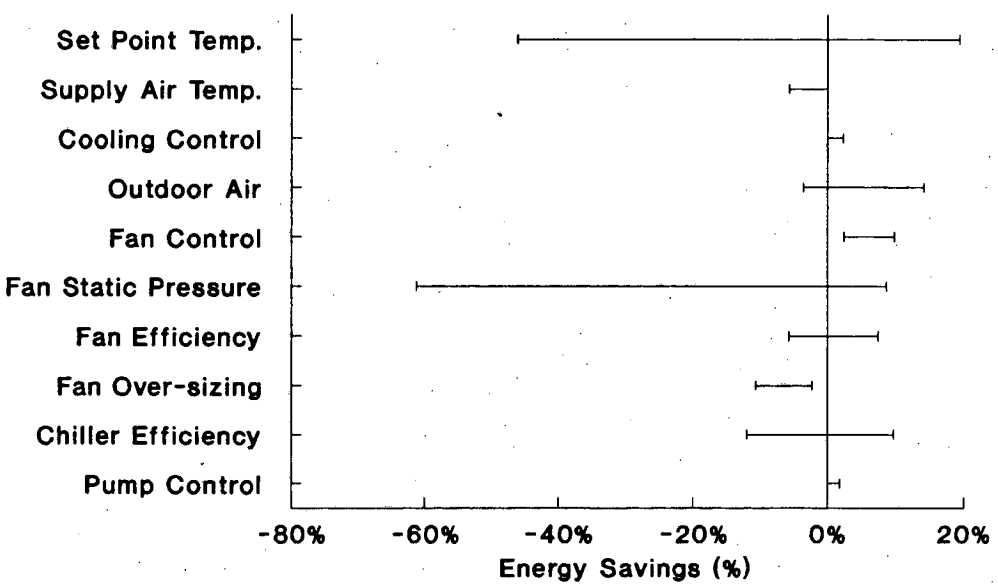

Figure 6-35.
Range of Savings for
Thai Retail AC Measures

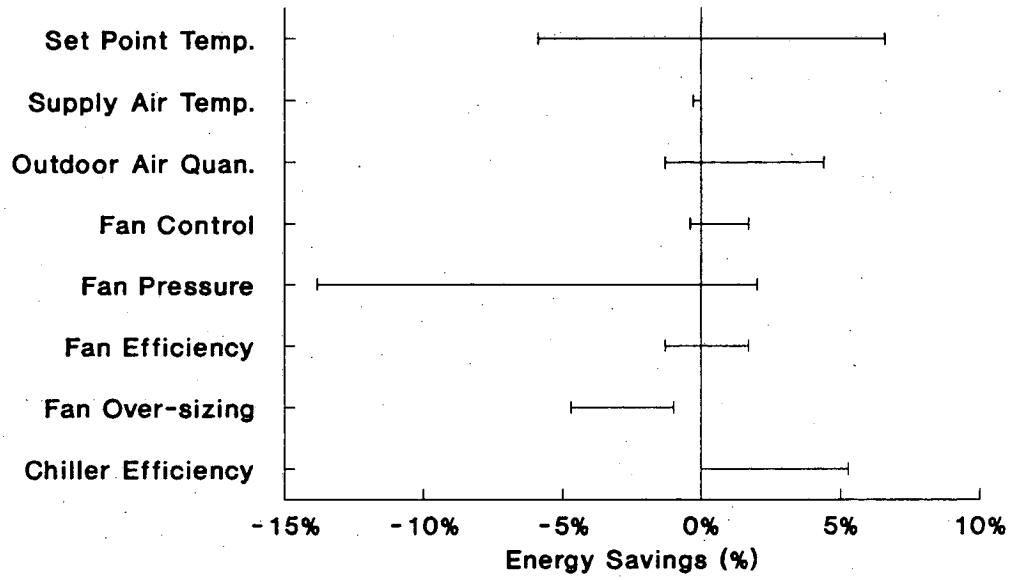

Table 6-1.
Installed Commercial Building Air-Conditioning Over 100 Tons* in Thailand up to 1986

	Whole Kingdom										Bangkok				
Type	# of Bldgs	% Bldgs ACWC	% Bldgs DX	% Bldgs WCWC	% Tons ACWC	% Tons DX	% Tons WCWC	Total Tons	Average Tons	% of WK Tons	# of Bldgs	Total Tons	Average Tons	% of Bkk Tons	% of WK Tons
Office	129	11%	13%	76%	4%	14%	82%	81292	630	32%	115	77003	670	38%	30%
Hotel	144	8%	1%	92%	3%	3%	94%	71626	497	28%	64	48190	753	23%	19%
Shopping Center	51	8%	6%	86%	1%	2%	97%	54491	1068	21%	46	53093	1154	26%	21%
Movie Theater	240	1%	94%	5%	1%	88%	11%	25523	106	10%	84	10320	123	5%	4%
Hospital	27	11%	0%	89%	8%	0%	92%	12830	475	5%	22	9710	441	5%	4%
Academic	24	17%	4%	79%	4%	4%	92%	8077	337	3%	18	6824	379	3%	3%
TOTAL or AVERAGE	615	8%	22%	70%	3%	10%	87%	253839	413	100%	349	205140	588	100%	81%
TOTAL of Office, Hotel, & Shopping Center	324	9%	6%	85%	3%	7%	90%	207409	640	83%	225	178286	792	87%	70%

* Except for movie theaters outside of Bangkok where buildings with 50 tons and above are included.

Source: MITR Technical Consultants, Co., Ltd., Bangkok, Thailand.

Table 6-2.
Characteristics of Thai Office Prototype

Gross Floor Area	7869 m^2
Conditioned Floor Area	6439 m^2
Nr. of Stories	12
Aspect Ratio	1:1
Wall Construction	Reinforced Concrete w/ Brick Infil
Window-to-Wall Ratio	.5
Glazing Type	Single-Pane, Tinted, Reflective Bronze (SC = .34)
Occupancy	Perimeter: 14 m^2/person
	Core: 6.5 m^2/person
Occupied Hours	Mon-Fri: 8am-5pm; Sat: 8am-noon
Lighting Power Density	24 W/m^2
HVAC System	Constant Volume, Distributed AHU
Thermostat Setting	24 °C
Supply Fan Capacity	58228 lit/sec
Outside Air Quantity	9 lit/sec/person
Cooling Plant	2 130-ton Centrifugal Chillers
	Cooling Tower
Chiller COP	4.0

Table 6-3.
Characteristics of Thai Hotel Prototype

Floor Area	20628 m^2
Nr. of Stories	Public Floors: 2
	Guest Floors: 10
Nr. of Guestrooms	280
Aspect Ratio	2.8:1
Wall Construction	Reinforced Concrete
Window-to-Wall Ratio	.4
Glazing Type	Single-Pane, Tinted Blue (SC = .4)
Occupancy	2300 (maximum)
Occupied Period	24 Hours
Lighting Power Density	Public Area: 37 W/m^2 (average)
	Guest Area: 10 W/m^2
HVAC System	Public Areas: Constant Volume
	Guestrooms: Two-Pipe Fan Coil
Thermostat Setting	24 °C
Fan Capacity	154485 lit/sec
Outside Air Quantity	12 lit/sec/person
Cooling Plant	650-ton Centrifugal Chiller, Cooling Tower
Chiller COP	4.0

Table 6-4. Characteristics of Thai Retail Building Prototype	
Floor Area	8062 m^2
Nr. of Stories	4
Aspect Ratio	2.5:1
Wall Construction	Reinforced Concrete
Window-to-Wall Ratio	.35
Glazing Type	Single-Pane, Tinted Grey (SC = .63)
Occupancy	18.5 m^2/person
Occupied Hours	10am-7pm
Lighting Power Density	Circulation: 22 W/m^2 Shops: 74 W/m^2
HVAC System	Circulation: Constant Volume Shops: Split-Systems
Thermostat Setting	25 °C
Supply Fan Capacity	13152 (Circulation)
Outside Air Quantity	12 lit/sec/person
Cooling Plant	2 100-ton Reciprocating Chillers Cooling Tower 144 tons (total) Split-system units
Chiller COP	3.4

Table 6-5.
Thermal Cool Storage in Thai Office Prototype

	Units	Base Case	Partial Storage	Full Storage	Demand-Limited Storage
Storage Size	ton-hours	-	1200	2667	2208
Chiller Size	tons	260	133	260	225
Cooling Electricity	MWh	598	635	625	628
Total Electricity	MWh	2024	2061	2051	2054
Peak Demand	kW	706	577	478	444
Electricity Cost	k$	101	103	103	103
Demand Cost	k$	75	63	52	49
Storage Cost	k$	-	90	200	166
Chiller Cost Savings	k$	-	51	0	14
Operating Cost Savings	k$	-	9	21	24
Simple Payback	years	-	4.3	9.5	6.3
Cost/Avoided Peak Elec.	$/kW	-	302	877	580

Table 6-6.
Thermal Cool Storage in Thai Hotel and Retail Prototypes
(Partial Storage Strategy)

		Hotel		Retail	
	Units	Base	Storage	Base	Storage
Storage Size	ton-hours	-	680	-	1333
Chiller Size	tons	650	450	240	120
Cooling Electricity	MWh	3156	3020	995	949
Total Electricity	MWh	7464	7326	3092	3045
Peak Demand	kW	1393	1223	882	724
Electricity Cost	k$	373	366	154	152
Demand Cost	k$	143	132	94	77
Storage Cost	k$	-	51	-	100
Chiller Cost Savings	k$	-	80	-	42
Operating Cost Savings	k$	-	17	-	19
Simple Payback	years	-	0	-	3.1
Cost/Avoided Peak Elec.	$/kW	-	-171	-	367

Table 6-7.
Cogeneration in Thai Office Prototype

Capacity (kW)	Operating Mode	Capacity Factor	Electricity Generated (MWh)	Electricity Sold (MWh)	Operating Cost (k$)	Revenues (k$)	Net Savings (k$)	Payback (years)
300	Therm.	.52	334	0	122	0	54	5.6
	Elec.	.79	1007	0	91	0	85	3.5
	Max.	.95	2434	1404	138	122	160	1.9
400	Therm.	.58	357	0	118	0	58	6.9
	Elec.	.77	1274	0	78	0	98	4.1
	Max.	.95	3310	2011	146	175	205	2.0
500	Therm.	.40	303	0	124	0	52	9.6
	Elec.	.77	1485	0	66	0	110	4.5
	Max.	.95	4138	2628	156	229	249	2.0
600	Therm.	.27	244	0	130	0	46	13.0
	Elec.	.70	1519	0	67	0	109	5.5
	Max.	.95	4868	3314	175	288	289	2.1
700	Therm.	.15	152	0	140	0	36	19.4
	Elec.	.59	1519	0	73	0	103	6.8
	Max.	.95	5841	4288	211	373	338	2.1

Table 6-8.
Cogeneration & Thermal Storage in Thai Office Prototype

	Units			
Thermal Storage Mode		Partial	Partial	Partial
Cogeneration Mode		Thermal	Electrical	Max. Output
Electricity Generated	MWh	152	1073	2434
Electricity Sold	MWh	0	0	1349
Electricity Bought	MWh	1402	479	467
Natural Gas Bought	MWh	1541	5020	10276
Peak Elec. Demand	kW	462	211	211
Operating Cost	k$	134	89	133
Revenues	k$	0	0	117
Incremental Cost	k$	339	339	339
Simple Payback	years	8.1	3.9	2.1
Cost/Avoided Peak Elec.	$/kW	1400	685	685

Table 6-9.
Non-Electric Cooling in Thai Commercial Buildings

		Office			Hotel			Retail		
	Units	Base	Engine	Absorption	Base	Engine	Absorption	Base	Engine	Absorption
Chiller Size	tons	260	260	260	650	650	650	240	240	240
Cooling Energy	MWh	598	1475	2229	3157	7123	11384	995	1921	2981
Total Electricity	MWh	2024	1536	1559	7465	5067	5230	3092	2117	2288
Peak Demand	kW	706	476	484	1393	845	863	882	586	625
Total Gas	MWh	0	1366	2096	0	6364	10463	0	1901	2790
Electricity Cost	k$	101	77	78	373	253	261	155	106	114
Demand Cost	k$	75	52	53	143	93	95	94	64	69
Gas Cost	k$	0	12	18	0	54	89	0	16	24
Total Energy Cost	k$	176	141	149	516	400	445	249	186	207
Chiller Cost	k$	104	182	182	260	455	455	84	168	168
Incremental Chiller Cost	k$	-	78	78	-	195	195	-	84	84
Operating Cost Savings	k$	-	35	27	-	116	71	-	63	42
Simple Payback	years	-	2.2	2.9	-	1.7	2.7	-	1.3	2.0
Cost/Avoided Peak Elec.	$/kW	-	339	351	-	356	368	-	284	327

Table 6-10.
High Efficiency Cases of Thai Commercial Buildings

	Units	Office	Hotel	Retail	Incl. HVAC Credit Office	Hotel	Retail
Energy Savings	kWh / m^2 / yr	141	185	192	141	185	192
Peak Savings	W / m^2	48	34	57	48	34	57
Operating Cost Savings	\$ / m^2 / yr	12	13	16	12	13	16
Incremental Cost	\$ / m^2	24	29	26	11	18	22
Cost of Conserved Energy	\$ / kWh	.016	.015	.013	.008	.009	.011
Cost/Avoided Peak Power	\$ / kW	508	849	453	241	539	384
Simple Payback	years	2.0	2.3	1.7	.9	1.4	1.4
Internal Rate of Return	%	51%	44%	60%	107%	70%	71%

Table 6-11.
Criteria of Thai Energy Standard for New Commercial Buildings †

Criteria	Units	Offices		Hotel		Retail	
Lighting	W / m^2	16	(24)	15* 20-17**	(10)* (37)**	23	(25)
Thermostat Setting	°C	24	(24)	24	(24)	24	(25)
Cooling Equipment COP							
–Centrifugal Chillers	-	4.5	(4.0)	4.5	(4.0)	-	-
–Reciprocating Chillers	-	-	-	-	-	3.8	(3.4)
OTTV:	W / m^2	45	(67)	45	(65)	42	(74)
U_w	W / m^2–°C	1.5	(3)	1.5	(2.8)	1.5	(2.8)
WWR	-	.4	(.5)	.4	(.4)	.35	(.35)
SC	-	.3	(.34)	.3	(.4)	.3	(.63)
U_f	W / m^2–°C	6.3	(6.3)	6.3	(6.3)	6.3	(6.3)

† Values given in parentheses are from the respective base cases.

* Guestrooms.

** Public areas.

CHAPTER 7: THE INFLUENCE OF GLAZING SELECTION ON COMMERCIAL BUILDING ENERGY PERFORMANCE IN HOT AND HUMID CLIMATES

R. Sullivan, D. Arasteh, G. Sweitzer, R. Johnson, and S. Selkowitz
Windows and Lighting Program
Applied Science Division
Lawrence Berkeley Laboratory
Berkeley, CA 94720 USA

ABSTRACT

This paper presents a comparative study in which commercial building perimeter zone electric energy (cooling, lighting, fan) and peak electric demand are analyzed as a function of window glazing type, with a particular emphasis on the use of glazings with wavelength-selective solar-optical properties. The DOE-2 energy analysis simulation program was used to generate a data base of the electric energy requirements of a prototypical office building module located in Singapore. Algebraic expressions derived by multiple regression techniques permitted a direct comparison of those parameters that characterize window performance in hot and humid climates: orientation, size, and solar-optical properties. Also investigated were the effects of exterior and interior shading devices, as well as interior illuminance level, power density, and lighting controls to permit the use of daylighting. These regression equations were used to compare the energy implications of conventional window designs and newer designs in which the type of coating and substrate were varied. The analysis shows the potential for substantial savings through combined solar load control and lighting energy use reduction with daylighting.

INTRODUCTION

The impact of nonresidential building design on energy conservation in hot and humid climates was the major topic at the ASEAN Conference on Energy Conservation in Buildings, Singapore [1]. Window and daylighting technologies were widely discussed because fenestration has proven to be the most significant envelope design factor affecting energy use in nonresidential buildings. In Singapore and other hot and humid locations, exterior shading and window size have been successfully used to limit solar heat gain. Lately, architects and engineers have been designing buildings with large areas of glass and without exterior shading. Tinted glazing is being specified to reduce solar loads and comply with energy codes.

The benefits of using daylighted perimeter zones in office buildings were also discussed at the ASEAN conference. A large fraction of electric lighting can be saved by dimming or switching electric lights in response to available daylight. The degree to which daylighting can reduce lighting loads depends primarily on the size and visible transmittance of the window. Other studies [2,3,4] have demonstrated the total energy-related benefits of daylighting building perimeter zones.

While daylighting energy savings from windows are a function of window area and visible transmittance, cooling loads from windows are a function of area and shading coefficient. Previous studies, referenced above, have explored the critical relationship between solar transmittance and daylighting benefits if energy performance is to be optimized. From an energy viewpoint, the ideal glazing would have a high visible transmittance, τ_v, and a low shading coefficient, SC. We define a glazing luminous efficacy constant, k_e, the ratio of τ_v to SC, as a relative indicator of glazing performance in this regard. Conventional blue and green glazings have higher k_es than other tinted, reflective, or clear glazings, since they transmit comparatively higher fractions of visible solar radiation than solar infrared radiation. Low-emissivity (low-E) coated glazings, introduced in recent years to reduce glazing conductances and suppress heat losses, also have the property of admitting a higher proportion of visible light relative to the total solar transmittance, thus making them attractive candidates for application in cooling dominated climates.

The energy implications of using glazings with different areas, SCs, τ_vs, and k_es are a function of climate, orientation, and building operating characteristics. In this paper, we discuss these effects in the context of the Singapore climate. We compare the performance of seven different glazing types and demonstrate the viability of new glazing technologies to reduce electric energy consumption and peak electrical demand in a hot and humid climate.

METHODOLOGY

The procedure used in the study involved the use of multiple regression equations that defined the electric energy and peak electric demand of a prototypical single-story office building module. These equations were derived from a large number of DOE-2 [5,6] hour-by-hour simulations that were completed for a variety of configurations using 1979 weather data for Singapore (1.3°N latitude). On an average day in Singapore, the dry bulb temperature varies between 25°C (76°F) and 30°C (85°F), and the relative humidity between 74 and 88%. Sunshine hours are limited to 30 to 48% of the possible hours because of cloud cover that is prevalent during most of the year. The module shown in Figure 7-1 has four perimeter zones consisting of ten offices, each 4.57 m (15 ft) deep by 3.05 m (10 ft) wide, surrounding a central core zone of 929 m^2 (10,000 ft^2) floor area. Floor-to-ceiling height was 2.6 m (8.5 ft) with a plenum of 1.07 m (3.5 ft) height. Work presented at the ASEAN conference [1] also used this module in tabulating daylighting characteristics. A paper by Johnson [7] contains more detailed information on the model.

Continuous-strip windows with no setback were used in the exterior wall of each perimeter zone. Thermal transfers were selectively constrained to isolate the energy effects of interest. That is, the floor and ceiling as well as the walls at each end of the perimeter zones were modeled as adiabatic (i.e., no heat transfer) surfaces. The envelope effects can thus be considered analogous to those in an individual office in a series of contiguous offices. Normal building thermal interactions included heat capacity effects and small convective/conductive transfers between core and perimeter.

A data base of electric energy usage and peak electric demand was generated for changing window and lighting system properties. We calculated system extraction rates for each perimeter zone using a single zone constant volume variable temperature HVAC system. Cooling energy was determined by assuming a fixed COP of 3.0. Daytime operational hours were from 7 A.M. to 6 P.M. weekdays. Cooling thermostat setpoint was 25.5°C (78°F). The design supply air flow rate per square meter of floor area was 0.031 l/s-m^2 (0.7 cfm/ft^2). Minimum amount of outside air per zone occupant was 2.36 l/s (5 cfm). The economizer limit temperature was 16.67°C (62 °F). Air-infiltration was fixed at an equivalent value of 0.6 air changes per hour. Our analysis is presented as a function of orientation. Coincident peak loads for the building module were not analyzed. Rather, we studied each zone's peak independent of other zones. Sensitivity studies completed prior to this work indicate that other HVAC systems will have a small effect on the numerical results.

The glazing characteristics that were varied included solar optical and thermal conductance properties and area. Lighting characteristics investigated included the use of daylighting with continuous dimming controls for varying lighting power densities and lighting levels. External shading was also simulated with continuous, fixed, horizontally projecting, opaque overhangs. Overhang projection width was varied parametrically to a maximum ratio of projection width to window height of 0.6. Shading by adjacent buildings was not considered in the analysis. Interior shading was simulated using shading coefficient and visible transmittance multipliers of 0.6 and 0.35, respectively. These conventional shades were deployed automatically when transmitted direct solar radiation exceeded 63 W/m^2 (20 W/ft^2). Exterior and interior shading were not simulated simultaneously.

A regression analysis was performed on the DOE-2-generated data base, deriving simplified algebraic expressions that accurately reproduced the simulated electric energy and peak demand. Multiple regression is an analytical technique for determining the best mathematical fit for a dependent variable as a function of many independent variables. The resultant regression expression used to predict these quantities was of the form:

$$\Delta E = \beta_1 \cdot U_g \cdot A_g + \beta_2 \qquad \text{(Eq.7-1)}$$

where ΔE is the incremental effect due to the fenestration system. The regression coefficients are denoted by β and the equation has three components chosen to contain the energy effects from a particular building thermal component: conduction ($U_g A_g$), solar radiation ($k_o S C_g A_g$), and lighting ($k_d L A_f$), where U_g is the overall conductance of the glazing, SC_g is the shading coefficient, k_o is a solar correction factor due to overhangs, L is the lighting installed power density, and k_d is a lighting correction term due to daylighting. A_g and A_f are glass and floor areas respectively. Shade management effects are accounted for by revised solar radiation coefficients, β_2.

The regression coefficients are presented in Table 7-1 for each orientation along with the r^2 values to indicate the quality of fit of the expression to the data (an r^2 value of 1.0 represents a perfect fit). The configuration parameters are expressed in SI units, i.e., U_g ($W/m^2 \cdot °C$), A_g (m^2), L (W/m^2), A_f (m^2). An analysis of the regression terms shows that they are reasonably physically consistent with expected performance. For example, the β_3 coefficient is almost constant for all orientations since, in the absence of lighting controls, lighting energy is not affected by external conditions. Also, glazing conductance variations are quite small and can be safely ignored because of the much larger contributions from solar gain and lighting. β_2 coefficients for shade management are presented for east and western orientations, only. The shades were not implemented very often in north and south because the direct solar radiation did not approach the level sufficient for triggering the devices. The diffuse component represents a significant portion of available sunlight in these directions.

Tables 7-2 and 7-3 show the regression coefficients for the solar and lighting correction terms, k_o and k_d. The solar factor from overhangs was a function of the ratio of overhang projection width to window height (R). Two forms are used to show the effects of overhangs: an exponential to predict electric energy usage for all orientations and both exponential (north and south) and linear (west and east) forms for peak demand predictions.

$$k_o = 1.0 - \delta_1[1 - e^{\delta 2^R}] \quad \text{or} \quad k_o = 1.0 - \delta_1 R \qquad \text{(Eq.7-2)}$$

where δ denotes the regression coefficients.

The lighting correction factor due to daylighting was also exponential and a function of desired lighting level (C) in lux, and effective aperture (A_e), which is the product of window-to-wall ratio and visible transmittance, i.e.,:

$$k_d = 1.0 - [\phi_1 + \phi_2(C)][1 - e^{(\phi_3 + \phi_4 C A_e)}] \qquad \text{(Eq.7-3)}$$

where ϕ denotes the regression coefficients, which are shown for four orientations in Table 7-3. North and south are so similar that they can be considered the same.

It was not possible to perform a regression on the DOE-2 simulation results that used shade management because only a limited set of runs was completed. However, changes that occur in the lighting correction factor when shade management is employed are discussed below.

DISCUSSION

The above equations were used to predict the performance of the seven window-glazing products shown in Table 7-4. Clear, tinted, and low-E single and double glazings were investigated. These products are currently available commercially and represent windows used in hot and humid locations and also systems that offer improvements in performance. The improvement is associated with changing proportions of total solar to visible transmittance, since these dominate the thermal variations due to window conductance differences.

Values for glazing luminous efficacy, k_e, range from 1.34 for low-E green-tinted double glazing with shading coefficient of 0.35 and visible transmittance of 0.47, to 0.69, for gray-tinted double pane with SC of 0.55 and τ_v of 0.38. Clear glazings with and without a low-E coating have the highest SCs and τ_vs and are most suitable for use with small window areas. Although green- and gray-tinted double glazings have similar SCs, their τ_vs differ greatly. Other tinted glazings, e.g., bronze, have τ_vs that are between green and gray. Adding a low-E coating decreases the shading coefficient more than the visible transmittance; thus green low-E double glazing is presented as a low-SC option with the highest τ_v. Although the low-emittance glazings are normally used in locations that require heating, this study indicates that they perform well in locations such as Singapore, particularly if combined with a spectrally selective glazing such as green glass.

Figure 7-2 shows the variation of the solar correction factor from overhangs for electric usage and peak demand as a function of the ratio (R) of projection width to window height. Generally, asymptotes are approached as the ratio increases. Peak demand curves for the east and west, however, are more linear than exponential. This is because for these orientations, the peak occurs when the sun is low in the sky. The k_o values at R = 0.6, the maximum ratio used in our work, represent decreases of 30%-35% for annual electricity and 27%-40% in peak demand, depending on window orientation.

Figure 7-3 presents the lighting correction factor from daylighting for four orientations and three lighting levels (323, 538, and 753 lux [30, 50, 70 footcandles]) as a function of effective aperture. Annual lighting energy savings with daylighting drop linearly until the space begins to become saturated with daylight; savings then asymptotically approach the maximum of 69%-74%. Daylighting savings are greatest when the desired interior illuminance is lowest. For small effective apertures, there is approximately a 10%-15% variation due to orientation, with east giving the largest reduction of lighting energy and north/south the smallest. However, the orientation effect is small and becomes insignificant as the asymptote is approached.

We found that there was a very small change in daylight availability when using overhangs. This is probably due to the large fraction of diffuse solar radiation in Singapore. Figure 7-4 shows the change in k_d at a lighting level of 538 lux (50 footcandles) when shade management is employed. Throughout most of the effective aperture range, daylight was reduced by 20%-25% for eastern and western orientations and less than 10% for north and south.

Solar- and lighting-induced electric energy consumption and peak demand are presented in Figures 7-5 and 7-6 as a function of the product of shading coefficient and window area. These figures represent the form expressed by Equation 7-1 with the exception that glazing conductance, a very minimal effect, is ignored. The incremental increase from solar gain and the decrease in lighting from daylighting are shown. Results are for four orientations, at a relatively efficient lighting power density of 18.3 W/m^2 (1.7 W/ft^2), a lighting level of 538 lux (50 footcandles), with and without the largest overhang. Also annotated are the relative positions of the seven glazings for a window area of 50 m^2 (538 ft^2).

These curves demonstrate the importance of orientation. North and south receive very little direct-beam solar radiation and therefore yield the lowest solar gain increments. A western orientation requires twice as much electricity and demand as north and south, with east being between the two. Overhangs with R = 0.6 provide about 30%-35% reduction in solar gain on each orientation, and because the gain is greatest on the west, the absolute benefit of an overhang is greatest on that side. This is particularly important since overhangs can provide substantial benefits without significantly diminishing daylighting potential. On a western orientation, in particular, the

daylighting benefit can be overwhelmed by solar gains. Thus, minimal effective apertures with overhangs are necessary to mitigate the substantial solar load.

Glazing type can also have a substantial impact on solar load reduction but may do so at the expense of daylighting. Table 7-5 shows the percent reduction in solar-gain-induced electric usage for each glazing when using single-pane clear as a base. The solar values given can be used for both usage and demand and for all orientations, with and without overhangs. This is because the percent change in energy or demand shown along the vertical axis in Figures 7-5 and 7-6 is equivalent to the percent change in shading coefficient due to the linearity associated with Equation 7-1. The largest changes occur with low-E tinted double glazing. For the module used in this study, annual cooling energy due to solar gain can be reduced by 63% when using this glazing type. This corresponds to a net cooling energy reduction of 20 MWh and peak demand reduction of 10KW for a western orientation. The monolithic green absorbing glass unit results in a 23% reduction, so the addition of the low-E coating in the double glazed unit provides significant additional benefits.

In addition to the solar gain effects, Figures 7-5 and 7-6 also show some of the changes in daylighting savings. Lighting reduction curves are shown for an eastern orientation for three (two limiting and one midpoint) values of efficacy corresponding to glazings in Table 7-4 (types 3, 5, and 7). For electric energy consumption, the savings due to daylighting can approach the same magnitude as savings from the use of large overhangs. For the 50 m^2 window area, all glazing types have about the same daylight utilization, because the asymptotic values have been approached. One sees, however, that glazing type 7 (low-E green tinted), which has the lowest shading coefficient providing the maximum reduction in solar gain, also has the largest efficacy, k_e=1.34. Glazing type 3 (k_e = 0.95) provides almost the same available daylighting benefits as type 7 but with a large increase in solar gain. Better performance could be achieved by decreasing the glazing area to reduce the solar load without affecting daylight availability significantly.

Figures 7-5 and 7-6 also can be used for predicting the effects due to shade management. It was previously indicated that shade management was most useful for eastern and western orientations because of the large fraction of diffuse radiation present for north and south. The reduction in solar gain is coincidentally approximately the same as the decrease due to overhangs. Thus, for a shading coefficient multiplier of 0.6, about a 30% reduction is seen in both perimeter zone electricity use and peak demand. Note also that this shade management scheme has no effect on glazings with shading coefficients lower than 0.4. With such a low SC, the 63 W/m^2 (20 W/ft^2) direct solar radiation level for shade management is not reached. Using interior shades does influence the savings with daylighting. The lighting curves in Figures 7-3 and 7-4 remain exponential in form and the daylighting reduction is about 25%.

CONCLUSIONS

Many techniques are available for reducing the annual electricity requirements and peak electrical demands of commercial office buildings in hot and humid climates. Several methods that relate to the design of the fenestration system have been documented. The effects of building orientation, external and internal shading devices, and glazing selection have been briefly discussed. A comparative study of several different glazings and the solar-optical properties that contribute to energy efficient design have also been presented. Conclusions are as follows:

- Controlling solar gains from windows should be a major consideration in any new building design in hot climates.
- There is an extremely large variation in direct solar heat gain with orientation. Orientation also affects the level of influence that exterior and interior shading devices have on controlling these gains.
- Lighting energy savings through the use of daylighting is a function of the visible transmittance of the glazing, the window area, desired lighting level, and lighting power density. It is possible to reduce electric lighting requirements by as much as 75% in perimeter zone

offices.

- Selecting the proper glazing type is as critical as orientation. It has been shown that it is possible to reduce electricity and peak demand of perimeter zones by using glazings with high efficacy values. These types of glazings reduce solar heat gain while maintaining a satisfactory level of daylighting utilization.
- The use of exterior and interior shading devices on western and eastern orientations can reduce solar loads to the point that they are equivalent to northern and southern orientations. Shade management, as implemented in this study, gave results similar to an opaque overhang whose projection-width to window-height ratio was 0.6.
- In Singapore, the use of overhangs did not significantly affect daylight availability because of the large fraction of diffuse sunlight. Interior shades, however, reduced daylight effectiveness 20%-25% for eastern and western orientations and less that 10% for north and south throughout most of the effective aperture range.
- Previous studies [2,3,4] indicate that it is possible to have large first-cost savings by using high-efficacy glazings with daylighting controls rather than conventional glazings. The lower chiller and HVAC system first costs will pay for some or all of the increased glazing, solar shading, and lighting-control costs in many cases.

REFERENCES

1. United States Agency for International Development, "Proceedings of the ASEAN Conference on Energy Conservation in Buildings," Development and Building Control Division, Public Works Department, Ministry of National Development, Republic of Singapore, 1984.
2. Arasteh, D., Johnson, R., Selkowitz, S., and Connell, D., "Cooling Energy and Cost Savings with Daylighting in Hot and Humid Climates," Lawrence Berkeley Laboratory Report LBL-19734, 1985.
3. Johnson, R., Arasteh, D., and Connell, D. and Selkowitz, S., "The Effect of Daylighting Strategies on Building Cooling Loads and Overall Energy Performance," Lawrence Berkeley Laboratory Report LBL-20347, 1986.
4. Sweitzer, G., Arasteh, D., and Selkowitz, S., "Effects of Low-Emissivity Glazings on Energy Use Patterns in Nonresidential Daylighted Buildings," *ASHRAE Transactions,* V.93 P.2, 1987.
5. Building Energy Simulation Group, "DOE-2 Supplement, Version 2.1C," Lawrence Berkeley Laboratory Report LBL-8706, 1984.
6. Winkelmann, F.C. and Selkowitz, S., "Daylighting Simulation in the DOE-2 Building Energy Analysis Program," *Energy and Buildings,* 8 (271), 1986.
7. Johnson, R., Sullivan, R., Selkowitz, S., Conner, C., and Arasteh, D., "Building Envelope Thermal and Daylighting Analysis in Support of Recommendations to Upgrade ASHRAE/IES Standard 90," Lawrence Berkeley Laboratory Report LBL-16770, 1983.

ACKNOWLEDGMENT

This work was supported by the Assistant Secretary for Conservation and Renewable Energy, Office of Buildings and Community Systems, Building Systems Division, U.S. Department of Energy under Contract No. DE-AC03-76SF00098.

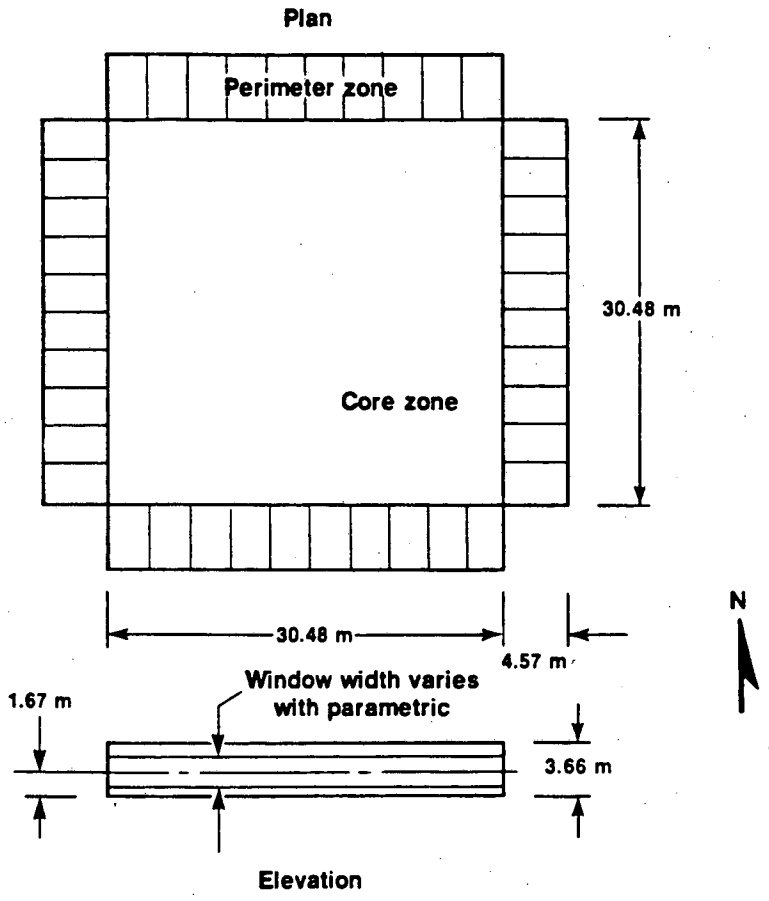

Figure 7-1. Plan of simulated office building showing alternative window-to-wall ratios. Module consists of a 929-m^2 core surrounded by a 4.57-m-deep perimeter zones, each divided into 10 modules 3.05 m wide.

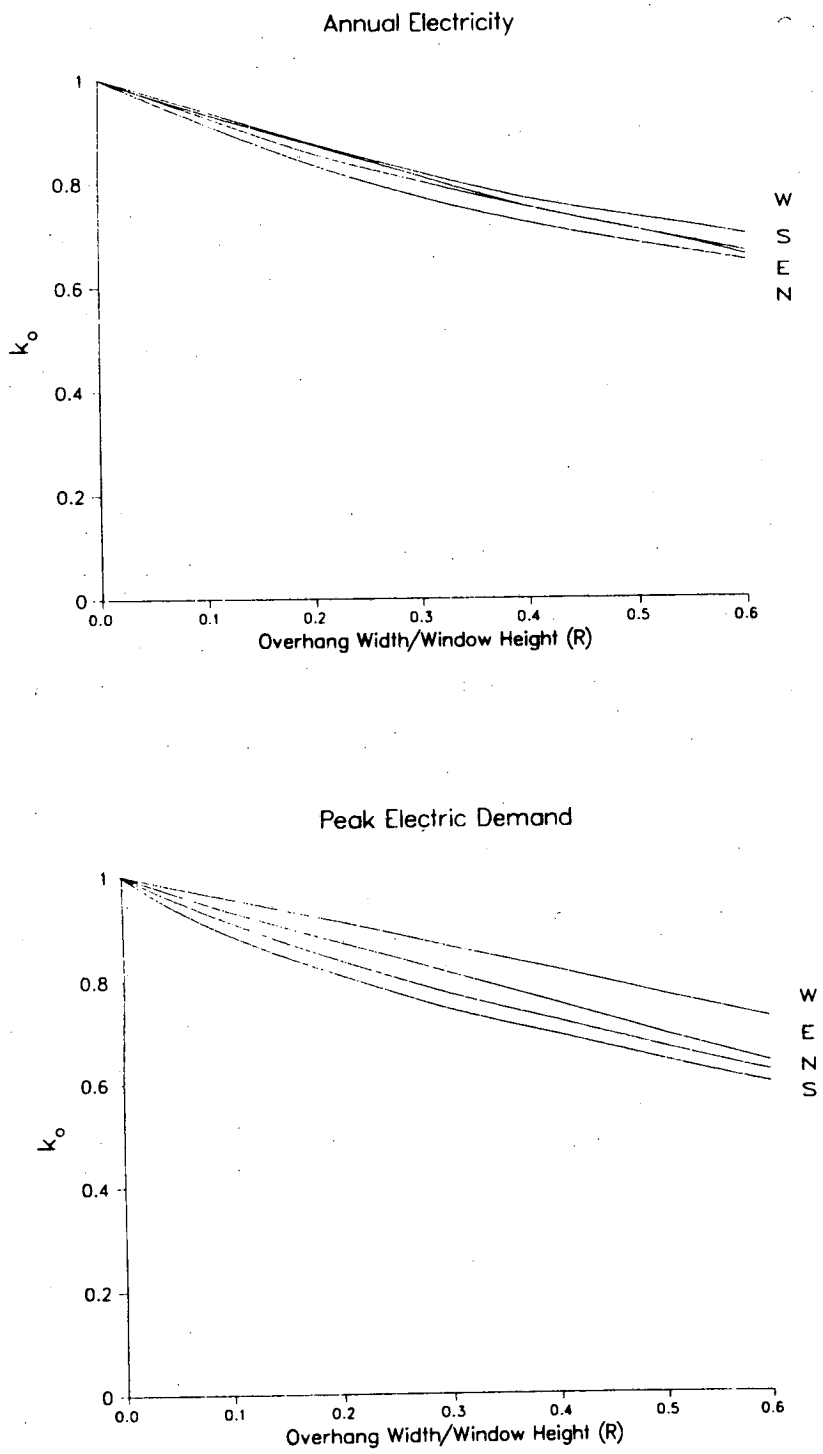

Figure 7-2. Solar correction factor for overhangs for perimeter zone annual electricity consumption and peak demand. The nondimensional factor for each orientation is the ratio of overhang width to window height.

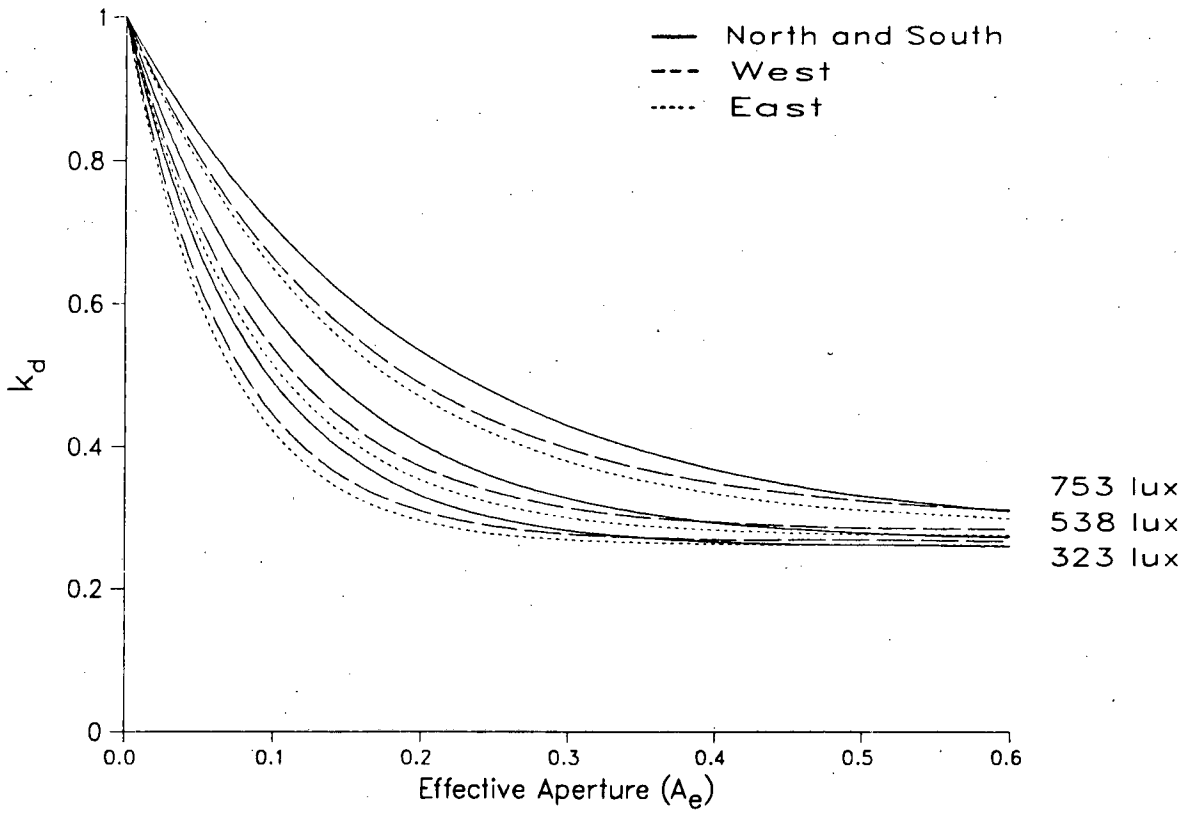

Figure 7-3. The daylighting correction factor, a nondimensional value, is a function of effective aperture at lighting levels of 753, 538, and 323 lux.

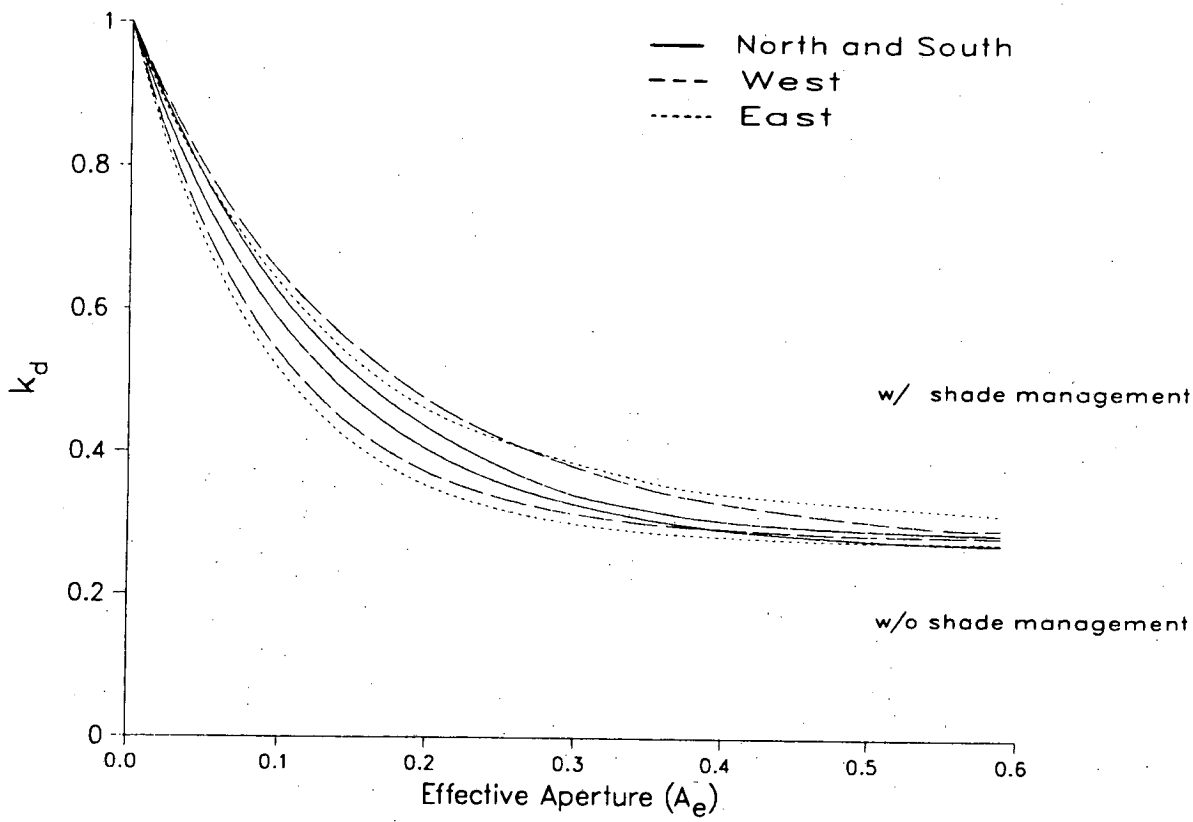

Figure 7-4. This plot shows the effect of shade management on the daylighting correction factor, a non-dimensional value, and a function of effective aperture at a lighting level of 538 lux.

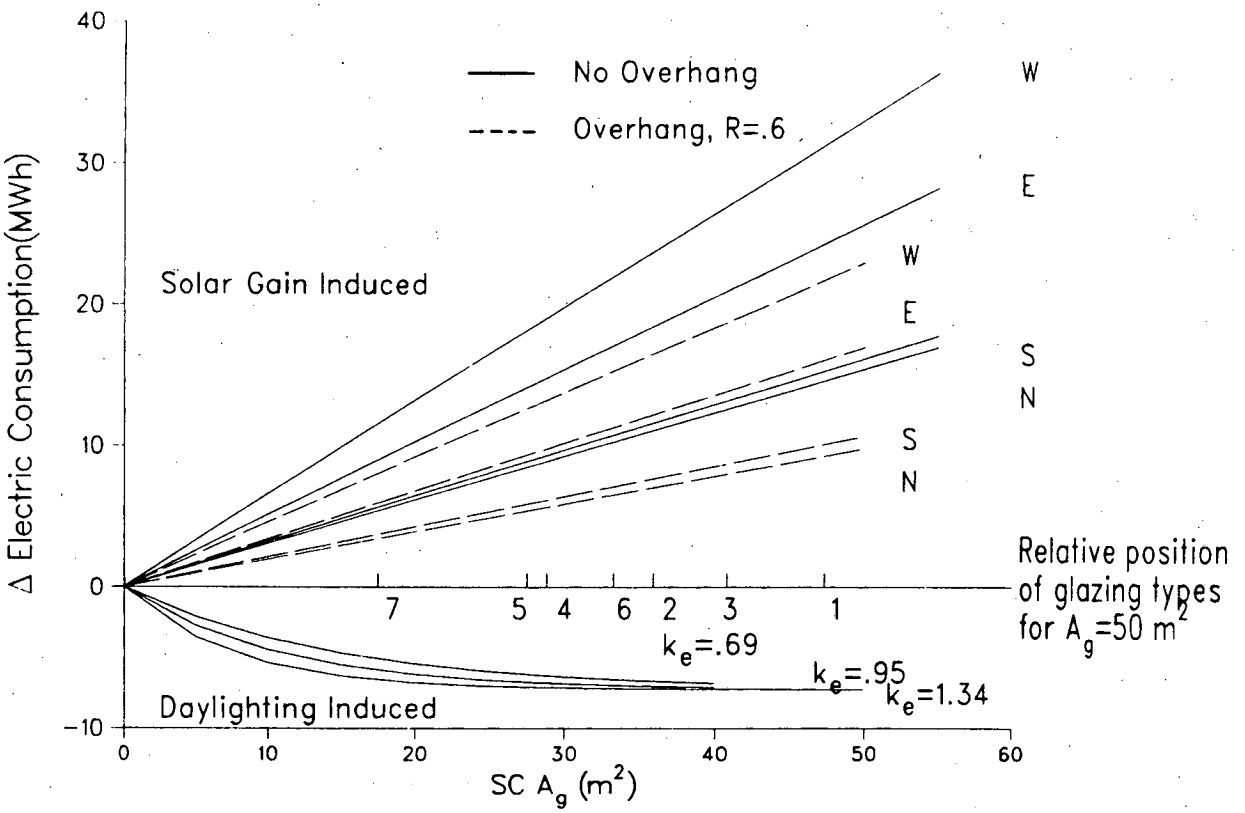

Figure 7-5. Incremental solar-gain- and daylighting-induced electric energy usage for four orientations of a commercial building as a function of the product of shading coefficient and window area. The lighting power density is 18.3 W/m^2 and the interior lighting level is 538 lux. The seven glazing types (from Table 7-1) are plotted at an area of 50 m^2 for comparison. For east and west orientations, the data for overhangs are about the same as for shade management.

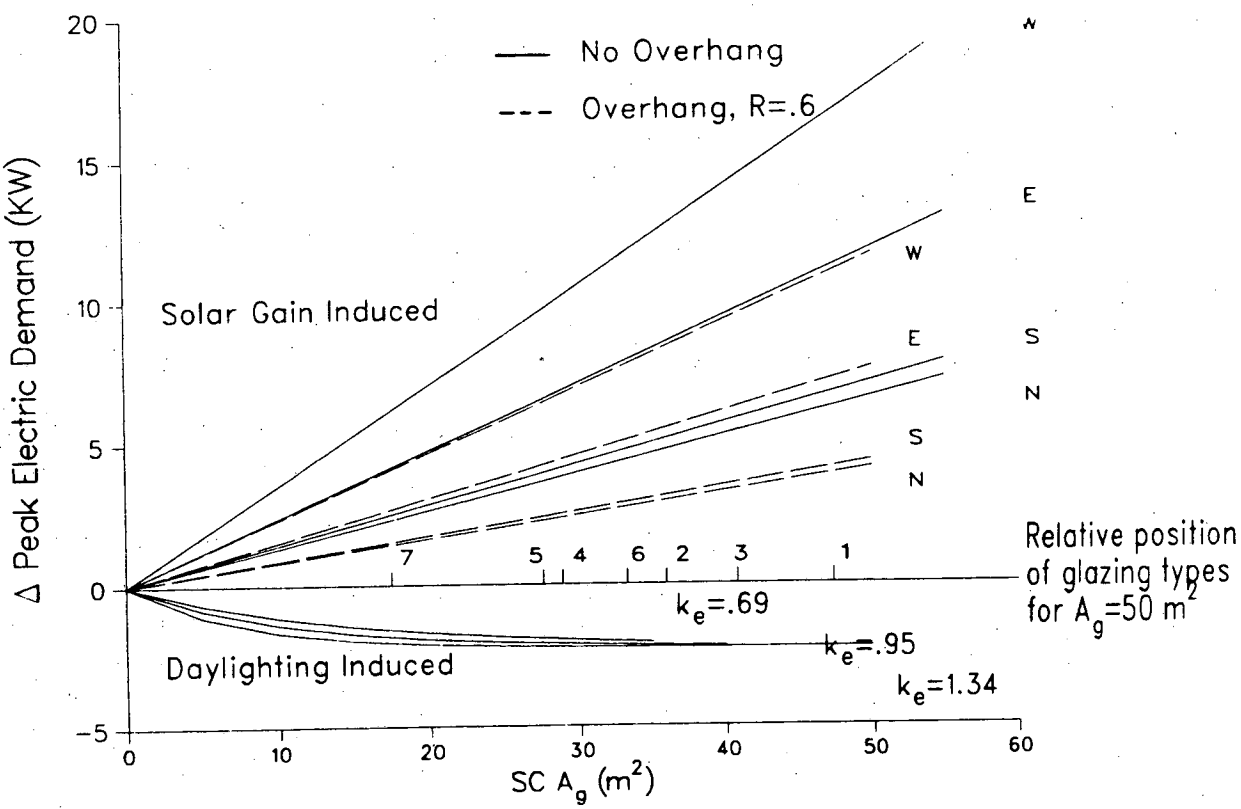

Figure 7-6. Incremental solar-gain- and daylighting-induced peak electric energy demand for four orientations of a commercial building as a function of the product of shading coefficient and window area. The lighting power density is 18.3 W/m^2 and the interior lighting level is 538 lux. The seven glazing types (from Table 7-1) are plotted at an area of 50 m^2 for comparison. For east and west orientations, the data for overhangs are about the same as for shade management.

Table 7-1. Regression Coefficients:
Annual Electricity Usage (kWh) and Peak Electric Demand
(SI units)

		Electricity		Peak Demand	
		w/o SM	w/ SM	w/o SM	w/ SM
β_1	N	2.387		3.733	
	S	3.104		4.494	
	E	-2.069		.439	
	W	-5.411		.409	
β_2	N	306.114		132.180	
	S	319.910		141.214	
	E	514.862	360.403	237.690	144.991
	W	662.550	447.036	324.350	252.993
β_3	N	3.948		1.258	
	S	3.975		1.278	
	E	3.953		1.270	
	W	3.997		1.163	
r^2		.994		.994	

Note: SM = Shade Management

Table 7-2. Regression Coefficients: Overhang Solar Correction Factor

		Electricity (Exponential)	Peak Demand (Exponential)	Peak Demand (Linear)
δ_1	N	.507	.725	-
	S	.534	.576	-
	E	.842	-	-.608
	W	.550	-	-.467
δ_2	N	-2.083	-1.271	-
	S	-1.708	-2.029	-
	E	-.893	-	-
	W	-1.396	-	-
r^2		.992	.991	.998

Note: East and west peak demand curves are linear.

Table 7-3. Regression Coefficients: Daylighting Lighting Correction Factor (SI Units)

ϕ_1	N	.754
	S	.753
	E	.758
	W	.756
ϕ_2	N	-.0000381
	S	-.0000429
	E	-.0000598
	W	-.0000710
ϕ_3	N	-16.325
	S	-16.720
	E	-21.728
	W	-20.003
ϕ_4	N	.0149
	S	.0152
	E	.0198
	W	.0179
r^2		.978

Table 7-4. Window System U-Values and Shading Coefficients Analyzed

Window Type	Summer U-Value	Shading Coefficient (SC)	Visible Transmittance (τ_v)	Efficacy k_e—τ_v/SC
(1) G	6.11 (1.07)	.95	.88	.93
(2) G_g	6.45 (1.13)	.72	.75	1.04
(3) G-G	3.31 (.58)	.82	.78	.95
(4) G_g-G	3.37 (.59)	.58	.66	1.14
(5) G_y-G	3.37 (.59)	.55	.38	.69
(6) GE-G	1.94 (.34)	.67	.74	1.10
(7) G_gE-G	1.83 (.32)	.35	.47	1.34

Notes:

1. U-value units are W/m^2C (Btu/hr-ft^2F).
2. G denotes glazing layer; G_g tinted green; G_y tinted grey; E, a sputtered low-E coating (e = .1 for clear, .07 for green).
3. Glass thickness is 6mm (0.25 in); gap width between layers is 12.7 mm (0.5 in.).

Table 7-5. Percent Reduction in Solar-Induced Annual Electric Usage with Single Pane Clear Glazing as a Base

Window Type	Solar Gain %	Shading Coefficient
(1) G	0	.95
(2) G_g	23	.72
(3) G-G	13	.82
(4) G_g-G	40	.58
(5) G_y	42	.55
(6) GE-G	29	.67
(7) G_g	63	.35

CHAPTER 8: A DAYLIGHTING DESIGN TOOL FOR SINGAPORE BASED ON DOE-2.1D SIMULATIONS

Y.J. Huang, B. Thom, B. Ramadan, and Y.Z. Huang
Energy Analysis Program
Applied Science Division
Lawrence Berkeley Laboratory
Berkeley CA, 94720 USA

ABSTRACT

Daylighting has the potential of reducing the energy use of commercial buildings in the Southeast Asian climates by as much as 30% through reducing lighting as well as air-conditioning electrical use. Effective daylighting design, however, requires balancing the above benefits against the detrimental effects of unwanted solar heat gain through windows. These interactions can best be evaluated through parametric analysis with a detailed hourly computer simulation program. To make such information more readily accessible to architects and engineers, a large data base has been compiled using the DOE-2.1D program to analyze various designs, lighting options, and daylighting strategies for a prototypical office building in Singapore. This data is then transformed into regression equations that will be incorporated into a simplified microcomputer-based daylighting design tool.

INTRODUCTION

Daylighting in commercial buildings refers to the use of electronic sensors in perimeter zones. These sensors measure the availability of natural lighting through windows and skylights, and then reduce the artificial lighting intensity to maintain specified illumination levels. Daylighting is a particularly attractive energy-conservation strategy in hot climates, since it lowers electricity use not only for lighting, but also for air-conditioning, by reducing unwanted heat from the artificial lights. A previous study has estimated that daylighting can reduce overall energy use in a typical Singapore office building by 20% [1].

In a strictly cooling climate such as Singapore, daylighting is always an energy saver. That is, the same building with daylighting will always use less energy than without it. However, proper daylighting design requires careful balancing of the benefits of lighting energy savings against the detrimental effects of increased solar heat gain. Since there are significant costs associated with daylighting controls, designers also need to know the magnitude of energy savings with daylighting so they can analyze it economically as an energy-conservation option.

There are many factors that influence the energy savings from daylighting: the efficiency of the artificial lighting being replaced, desired indoor illumination level, the optical properties of the window glass, size and location of the windows, dimensions and orientation of the perimeter offices, and the existence of shading devices such as building overhangs and fins. The best method to analyze the impact of these factors on building energy use is through a detailed hourly energy simulation program such as DOE-2.1 [2]. However, because of the time and effort required, it is unlikely that architects and engineers can afford to do custom DOE-2 daylighting analysis on a building-by-building basis.

The intent of this study is to provide the groundwork for a Simplified Daylighting Design Tool that can be used by practicing architects and engineers. Since the relationship between a building's design and its daylighting potential is relatively complex, this tool is conceived as a microcomputer program that allows users to vary a number of design options and quickly determine their effects on a building's lighting, air-conditioning, and fan energy use. The analytical basis for the program are sets of regression equations developed through extensive analysis of a large data base of DOE-2.1D daylighting simulations for prototypical office configurations. The program allows users to quickly recreate the results of the data base simulations and extend those results to offices of various sizes and configurations.

MODELING APPROACH

The technique described in this study for estimating the energy impacts of daylighting designs utilizes a set of regression equations developed through analysis of a large data base of DOE-2.1D simulations for a prototype office building located in Singapore (Figure 8-1).

It is important to stress that this prototype is not meant to be typical or representative, but rather a hypothetical construct aimed at capturing the variety of solar and internal heat gain conditions found in typical offices in Singapore. The DOE-2 file has been structured to allow inputs for relevant design parameters to be easily changed to study their influence on building energy use. The methodology is also tailored to allow the data base to be extrapolated to real building designs.

The prototype building is modeled as a symmetrical box with dimensions of 36.6m x 36.6m (120 x 120 ft), divided into 18 thermal zones : nine zones per floor (four perimeter, four corner, and one core zone), and two types of floor conditions (top floor with a roof, and middle floor without a roof). These 18 zones cover the range of thermal and solar conditions found in typical offices. The assumed size and shape of the prototype building is of secondary importance, since the analysis is done using zone-level loads and energies that have been normalized per floor area. The resultant regression coefficients, with some additional terms for whole building interactions, can be extrapolated to buildings of various sizes, shapes, and shell designs.

The operating conditions as well as some basic characteristics of the prototype building have been kept constant for all the data base simulations. The hours of operation and thermostat settings of the building are based on previous studies of ASEAN office buildings and taken to be typical of Southeast Asia (see Table 8-1). The building can be simulated with either concrete or steel construction, although for the current data base only the concrete construction has been simulated. The other physical characteristics of the prototypical building that have been kept fixed are shown in Table 8-2.

To construct the DOE-2 daylighting data base, simulations have been done with the prototype building varying those parameters that affect the performance of daylighting measures. These are listed in Table 8-3. Variations in window area and glazing properties have been treated in particular detail, as shown in Table 8-4. Equal window conditions in all perimeter and corner zones are modeled in nine of the eleven cases. To test interactions when window areas are unequally distributed, two of the cases are highly directional, with large amounts of windows in two opposite orientations, and none in the other two.

Singapore weather data for 1988 has been used in the DOE-2.1D simulations. The weather tape was obtained from the National University of Singapore, and has measured hourly data for dry and wet bulb temperatures, wind velocity, direct and diffuse solar radiation. This data represents the most comprehensive and reliable weather information for Singapore available at the time of this analysis.

The total number of simulations completed for the data base is 819, which is slightly lower than the product of all the parametric variations in Table 8-3, because daylight simulations were unnecessary for the zero window area condition.

The prototype building has been modeled with individual packaged VAV systems in each zone so that cooling loads and energy use can be determined at the zone level. This zone-level approach permits the data to be aggregated differently for buildings of various sizes and shapes, and makes the results less dependent on the assumed geometry of the prototype building.

ANALYSIS

From each simulation, the annual cooling loads, and cooling, fan, and lighting electrical use per zone have been saved and analyzed.* The purpose of the analysis is to develop simple algebraic expressions that can replicate the information in the data base, as well as extend this data to

* Data on annual latent cooling loads, as well as peak cooling loads and energies were also saved, but not used for the Simplified Design Tool analysis.

differing building design conditions. The approach taken in the regression analysis incorporates the findings from several previous efforts on the same topic [3], [4], along with techniques developed in the course of this work.

Since the ultimate aim of the analysis is to utilize the regression equations in a microcomputer-based tool, there is no need to reduce the data beyond where they can be easily handled by a typical microcomputer. A stepwise approach has been taken whereby sets of equations are developed that accounted for the impacts of single design variables, which are then combined into more complex expressions if relatively straightforward correlations were identified. For example, the preliminary regression equation for lighting energy savings expresses the savings only as a function of the zone daylighting aperture, thus requiring 432 sets of coefficients, 54 per zone for differences in office size, lighting powers, lighting levels, and overhang conditions. Subsequent analysis revealed relatively simple linear or quadratic relationships between these parameters and lighting savings, so that the number of equations can be reduced to 24, three per zone that give lighting energy savings as functions of lighting power and overhang ratio, as well as the daylighting aperture.

Separate regression equations have been developed for the base case zone loads and electrical use, as distinct from the load reductions and energy savings due to daylighting. The reasons for this separation are that (1) the functional forms of the equations are different, and (2) it maintains better accuracy for predicting the energy savings from daylighting, one of the major objectives for the Simplified Design Tool.

The regression equations cover six parameters: base case cooling load; cooling and fan energy use; lighting energy savings; and cooling and fan energy savings. Base case cooling load and lighting energy savings are considered to be primary parameters whose values depend on the interactions between the building, its operations, and the climate. Cooling and fan energy use, cooling load reduction, and cooling and fan energy savings are considered secondary parameters dependent on one of the two primary parameters. This distinction is made because it clarifies the approach taken in the analysis.

For example, lighting energy savings is a primary parameter, and analyzed as a function of the zone's window-to-wall ratio, lighting wattage, lighting level, etc. Cooling energy savings, however, is a secondary parameter and analyzed not directly in terms of zone conditions, but as a function of the lighting energy savings.

Base Case Cooling Loads

The base case refers to the loads and energy use of a zone without the use of daylighting. The first step in the analysis is to develop simple regression equations for cases that varied only in their solar aperture, which is defined as the zone's window-to-wall ratio (WWR) times the glass shading coefficient. This term indicates the proportion of incident solar that enters the zone as heat gain. A set of 486 linear coefficients have been developed in the form :

$$CL_{base} = \alpha_1 + \alpha_2 \cdot WWR \cdot SC \qquad \text{(Eq.8-1)}$$

where:

CL	= Cooling Load (MJ/m^2·year)
WWR	= Window-to-wall ratio (dimensionless)
SC	= Shading coefficient (dimensionless)
α_1,α_2	= Regression coefficients

Figure 8-2 shows typical results for the Middle Floor South zone at a lighting power of 21.5 W/m^2. The x-axis represents the solar aperture and the y-axis the base case cooling load of the zone. The lines are for differing combinations of office depth and overhang ratio. Office depth is defined as the distance from the wall to the opposite wall. Overhang ratio is defined as the length of the overhang projection divided by the vertical distance from the overhang to the window sill. As evident from the plot, the linear fits are very good, with R^2's in the range of .996 -.999. After these

equations have been derived, comparisons of the coefficients show that lighting power has a linear effect on the intercept (α_1), while the overhang ratio has a nonlinear effect on the slope (α_2). Consequently, it is possible to reduce the 486 preliminary equations into 54 equations of the following form with little loss of accuracy:

$$CL_{base} = \beta_1 + \beta_2 \cdot LP \qquad \text{(Eq.8-2)}$$

where:

LP	= Lighting power (watts/m^2)
OHR	= Overhang ratio (dimensionless)
$\beta_1,\beta_2,\beta_3,\beta_4$	= Regression coefficients

These regression coefficients for the base case cooling loads are shown in Table 8-5. For each of the 18 zone conditions, there are three equations for different office depths. For the core zones, office depth is substituted with the Core Area Ratio, or fraction of the floor area per floor that comprise the core zone. There is no advantage to further collapsing these equations, since it will only make the equations more complex and non-intuitive, as well as introduce more errors. These equations can be used to estimate the base case cooling loads per zone for a variety of office conditions. Loads for intermediate office depths and orientations can be estimated by linear interpolation between the closest conditions.

Base Case Cooling and Fan Energy Use

The cooling and fan energy uses of each zone are estimated as linear functions of the zone cooling load. These lines in essence show the variations in the average seasonal efficiency of the equipment as a function of the zone solar aperture, since other building parameters have been kept constant throughout the data base. Because the hourly pattern of cooling load differ significantly zone to zone depending on their orientation, these efficiency slopes also vary, as evident in Figure 8-3. There are some slight non-linearities because of changing sensible load ratios over different solar apertures, but the effects are not significant.

To calculate cooling and fan energy use, the Simplified Design Tool will rely on 54 sets of linear coefficients which will be applied to the base case cooling load calculated earlier (Table 8-6):

$$CE_{base} \text{ or } FE_{base} = \beta_1 + \beta_2 \cdot CL \qquad \text{(Eq.8-3)}$$

where:

CE	= Cooling energy use (kWh/m^2·year)
FE	= Fan energy use (kWh/m^2·year)
CL	= Cooling load (MJ/m^2·year, from Eq. 2)
β_1,β_2	= Regression coefficients for CE and FE

Lighting Energy Savings

The characteristic shape of the lighting energy savings curve due to daylighting is an inverse exponential in respect to a zone's daylighting aperture (Figure 8-4). *Daylighting aperture* is defined here as the zone's window-to-wall ratio times the Total Visible Transmittance (TVIS) of the window glass. The concept is the same as for Solar Aperture, except that here it is applied to the amount of light, rather than heat, that enters the zone. At small daylighting apertures, the capacity of daylight to displace artificial lighting is high. However, as the aperture increases, this capacity progressively degrades until it becomes nil at the point where additional daylight will not reduce lighting energies (while still contributing to the zone's cooling loads). This exponential asymptote is less than one since there are always hours when lighting is required but daylight is unavailable, such as at night.

The preliminary functional form used to describe lighting energy savings is similar to that found in earlier studies [4], [1]:

$$\Delta LE = \alpha_1 \cdot (1 - e^{\alpha_2 \cdot DA}) \qquad \text{(Eq.8-4)}$$

where:

ΔLE = Lighting energy savings (kWh/m^2·year)
DA = Daylighting Aperture (WWR x TVIS)
α_1, α_2 = Regression coefficients

This expression has been used to develop 432 equations for cases where the zones differ only by their daylighting aperture (8 perimeter zones x 3 depths x 3 lighting powers x 2 lighting levels x 3 overhang conditions). The number of zones is less than half that considered for the cooling calculations because there are no differences in lighting energy savings between top and middle floors, and no savings at all for the core zones.

Lighting energy savings from daylighting depend only on the zone's daylight characteristics and installed lighting wattage, and are not affected by other aspects of the zone or building, as is the case for cooling or fan energy use. Consequently, these lighting energy saving curves are very well-behaved and easy to interpret. Figure 8-5 is a set of preliminary plots showing lighting energy savings plotted against Daylighting Aperture for the Middle Floor South Zone. Each plot represents a different office depth, with the solid lines indicating three lighting powers at a lighting level of 323 lux (30 foot-candles), and the dotted lines at a lighting level of 538 lux (50 foot-candles). It is apparent from the plots that lighting power has a multiplicative effect on the asymptote, while lighting level, office depth, and overhang length (shown on Figure 8-4, but not on Figure 8-5) all affect only the curvature of the line.

>From these observations, it is possible to reduce the number of equations to 24 (8 perimeter zones times 3 depths):

$$\Delta LE = \beta_1 \cdot LP \cdot (1 - e^{(1 + \beta_2 \cdot OHR + \beta_3 \cdot OHR^2) \cdot (\beta_4 + \beta_5 \cdot LL) \cdot DA}) \qquad \text{(Eq.8-5)}$$

where:

LP = installed Lighting Power (watts/m^2)
LL = required Lighting level (lux)
β_1,β_2,β_3,β_4, and β_5 = Regression coefficients

These exponential regression coefficients are shown in Table 8-7.

Cooling Load Reductions

The cooling loads reductions from daylighting are due to the reduced heat gain from those electric lights that have been dimmed or shut off. In this study, cooling load reductions have been defined as the difference in loads due to daylighting between identical zones with the same window and lighting conditions. Since increasing window size will also increase the base case cooling loads (re: Equations 8-1 or 8-2), the load savings estimated here must be added to the base case loads to properly derive the net impact of any daylighting design.

The dependent nature of the cooling loads reductions on the lighting energy savings can be seen in comparing Figure 8-6 to Figure 8-5. Figure 8-6 shows the cooling load reductions corresponding to the lighting energy savings shown in Figure 8-5. Note that the daylighting, rather than solar, aperture is used for the x-axis because the cooling load *reductions* are dependent on the lighting energy savings, which in turn are dependent on the daylighting aperture. In contrast, the *base case* cooling loads in Figure 8-2 have been plotted against the solar aperture.

The general shapes of the cooling load reduction curves clearly follow those of the lighting energy saving curves. However, whereas the asymptotes on the lighting curves are perfectly flat, indicating constant savings once the maximum daylighting potential is reached, those on the

cooling curves have slight but noticeable upward slopes, indicating degradation of cooling savings at unnecessarily high daylighting apertures. This sloping asymptote can be interpreted as due to interactions between the load reduction and zone configuration unrelated to the lighting energy savings. One possible explanation is that lighting energy savings may lower the number of cooling hours at smaller solar apertures,* but not so when there is a great amount of solar gain.

Based on the above observations, the regression expressions for cooling load reductions assume a linear relationship to the lighting energy savings, with a smaller linear term related to the zone solar aperture to account for the interactive effect. The second assumption is reasonable since the data base covers only differences in solar and daylighting apertures.

$$\Delta CL = \alpha_1 \cdot \Delta LE + \alpha_2 \cdot \Delta LE \cdot SA \qquad \text{(Eq.8-6)}$$

where:

ΔCL = Cooling load reductions ($MJ/m^2 \cdot year$)
ΔLE = Lighting energy savings ($kWh/m^2 \cdot year$)
SA = Solar Aperture (WWR x SC)

The data base results also show that lighting energy savings in the perimeter zones produce small but noticeable cooling load reductions in the core zones (Figure 8-7). Without the benefit of a detailed study, this reduction has been attributed to the lowered balance point of the entire building due to daylighting. Although the load reduction trends are similar to those in Figure 8-6, note that the x-axes now show the daylighting apertures of the building rather than the zone, and that the plots are for differing Core Area Ratios rather than office depths. The Core Area Ratio (Core floor area/ Total floor area) indicates how much effect the perimeter has on the core based on their relative sizes. Since the load reduction curves for the core zone are also exponential, Equation 8-6 can still be used, although building-level lighting energy savings and the Core Area Ratio have been substituted for the two independent variables.

This analysis of cooling load reductions has produced 54 sets of linear coefficients (18 zones x 3 depths), that can be used to estimate the cooling load reductions for a zone dependent on its lighting energy savings and solar aperture. These are shown on Table 8-8.

Cooling and Fan Energy Savings

Comparisons of cooling loads reductions to the corresponding cooling energy savings show that their relationship was even more straightforward than that between lighting energy savings and cooling load reductions. Figure 8-8 shows the results for four typical zones (middle floor south and southwest, and top floor north and northeast). These show that a simple linear correlation of loads to energies, i.e., the use of an effective seasonal efficiency, corresponds very closely to the DOE-2 simulation results. The reason for this constant efficiency is that the loads reductions are always sensible and occur during the same hours of the day, i.e., daytime hours with ample sunshine, so that the COP of the equipment stays about the same.

For fan energy savings, the relationship to cooling load reductions is not as precise as for cooling energy, although a basically linear relationship is still evident (Figure 8-9). The larger scatter is because fan energy efficiencies vary more with loads than does the COP of the cooling equipment. Without reliance on binned or hourly data, it will be difficult to predict this variation. Since fan energy savings are typically less than 30% that of cooling energy savings, it is felt that simple linear equations relating the fan energy savings to cooling load reductions are adequate.

For the Simplified Design Tool, the data consist of two coefficients per zone, one for the cooling energy savings and the other for the fan energy savings as linear functions of the cooling

* Note from Table 8-4 that the simulation data base assumes a rough parallel relationship between daylighting and solar apertures, since it is physically impossible due to glass properties or window geometries to have diametrically different daylighting and solar apertures.

loads reductions. Although the current data base assumes a VAV system, the same approach can be used to develop different coefficients for other air-conditioning systems types, such as constant volume systems.

APPLICATIONS

The equations discussed in this paper can be used to calculate the changes in base case cooling and fan energy, as well as the savings in lighting, cooling, and fan energy use to daylighting, in an office zone depending on the following zone characteristics :

- Floor Area (m^2)
- Orientation (azimuth)
- Floor Condition (middle or top floor)
- Office Depth (distance from exterior to interior wall, m)
- Lighting Power (W/m^2)
- Lighting Level (lux)
- window-to-wall ratio
- Overhang ratio
- Glass shading coefficient
- Glass visible transmittance

As an example, Figure 8-10 shows the results for a middle floor zone with an office depth of 6.1 m, a lighting power of 21.5 W/m^2, and a required lighting level of 538 lux. The left plot shows the base case energy uses per m^2 for cooling, fan, and lights as a function of the solar aperture of the zone. The dotted line indicates the effects of an overhang ratio of 1 (i.e., an overhang extending out 1.5 m above a 1.5 m high window). The right plot shows the modified energy uses once the energy savings from daylighting have been subtracted. Note that although cooling and fan energy use still increase with zone solar aperture, the reductions in lighting energies more than compensate for these increases, so that there is a minimum total energy use at a solar aperture of 20. Beyond that aperture, increases in lighting energy savings become progressively smaller, while cooling energy uses continue in linear fashion, so that total energy use again rises.

The case shown in Figure 8-10 is made more dramatic by the relatively high lighting wattage. The optimum daylighting design for a particular building or zone depends heavily on the zone characteristics, as well as economic trade-offs between the saved energy costs and the increased first costs for daylighting controls. The intent behind this work is not to make specific guidelines, but to provide architects and engineer with a simplified calculation tool to make those decisions.

TEST OF REGRESSION MODEL

The above methodology can be used to estimate the base case cooling loads and energy use, as well as the savings in lighting, cooling, and fan energy use for office buildings of various configurations and conditions. To test the reliability of the procedure, DOE-2 simulations were done for two test office buildings that differed markedly from the symmetrical prototype floors, and the results then compared to estimates using the described methodology.

The first test building is a ten-story high-rise office with a rectangular floor plan and a high aspect ratio of 2.5 to 1. The second is a low-rise L-shaped building of four stories, with two wings facing south and west (Figure 8-11). For the test DOE-2 simulations, the operating conditions and simulation methodology were kept identical to those used for the prototype building. To test the reliability of the simplified methodology for various solar load conditions, three different window-to-wall ratios were used for the test rectangular building and five for the L-shaped building. These include a low solar aperture of 0.20 window-to-wall ratio and a shading coefficient of 0.40 (i.e., tinted glass), an average solar aperture of 0.40 window-to-wall ratio and a shading coefficient of 0.80 (i.e., double glazing or slightly tinted glass), and a high unsymmetrical distribution with a 0.60

window-to-wall ratio and a shading coefficient of 1.00 on the north and south walls, but no windows at all on the east and west walls. For the L-shaped building, the effects of 1.67 m (5 ft.) overhangs were also tested.

Tables 8-9 and 8-10 give the results for this comparison. Compared to the detailed DOE-2 results, the simplified regression method show almost no error for the lighting energy savings, except for the 9% difference in the L-shaped building with large overhangs over small windows. The maximum differences in total cooling loads are 5% for the rectangular and 12% for the L-shaped building, in both bases at small solar apertures. The differences in cooling and fan energies are higher, averaging 7-8% for the nine test cases but up to 18% in several instances. In the more critical areas of cooling load reductions and energy savings, the simplified approach on average give results within 6% for the rectangular and 12% for the L-shaped buildings. The differences in fan energy savings are often large in percentages, but comparable to those for cooling energy in absolute terms.

The lack of any significant error in the estimation of lighting energy savings is to be expected, since these are dependent only on the zone solar loading and installed wattage, and hence independent of building configuration once they have been properly adjusted by the floor area, size, and orientation of each zone. The errors in the other parameters are due to interactions among building zones that are impossible to address without detailed hourly simulations. For a simplified tool to provide design guidance to architects and engineers, the level of accuracy found, < 10%, is quite acceptable. Since this level applies to both totals as well as the estimated savings, the procedure will not be giving the wrong signals or lead to improper designs.

CONCLUSIONS

A data base of DOE-2 simulations of the energy impacts of daylighting in Singapore office buildings has been created, and a simplified methodology developed for extrapolating that data to office buildings of different configurations. This methodology estimates the base case cooling load and energy, and the savings in lighting, cooling, and fan energy use on a zone-by-zone basis, which are then aggregated to give the totals for a particular building of any size and shape. A test of this method for two very different building designs show that it is accurate to well within 10%.

This regression procedure is designed for use in a microcomputer-based daylighting design tool. Such a tool will give architects and engineers a quick and reliable method for assessing the energy benefits of different daylighting designs, and assist them in developing designs that utilize daylighting to its full potential. The prospective tool can also incorporate some simple economic calculations that can encourage users to consider daylighting from an economics point of view, and weigh its cost-benefits compared to other conservation strategies.

REFERENCES

1. Levine, M.D., Turiel, I., and Curtis, R., "Towards a Practical Daylighting Analysis Tool for Singapore," in *Proceedings of the ASEAN Conference on Energy Conservation in Buildings*, Singapore, 29-31 May 1984, pp. 277-308.
2. Building Energy Simulation Group, *DOE-2 BDL Summary, Version 2.1D*, Lawrence Berkeley Laboratory Report LBL-8688-Rev. 4, 1984.
3. Arasteh, D., Johnson, R., Selkowitz, S., and Connell, D., "Cooling Energy and Cost Savings with Daylighting in Hot and Humid Climates," Lawrence Berkeley Laboratory Report LBL-19734, 1985.
4. Sullivan, R., Arasteh, D., Sweitzer, G., Johnson, R., and Selkowitz, S.D., "The Influence of Glazing Selection on Commercial Building Energy Performance in Hot and Humid Climates," *ASHRAE Far East Conference on Air Conditioning in Hot Climates*, Singapore, 1987.

Figure 8-1. Sketch of Prototypical Office Modules

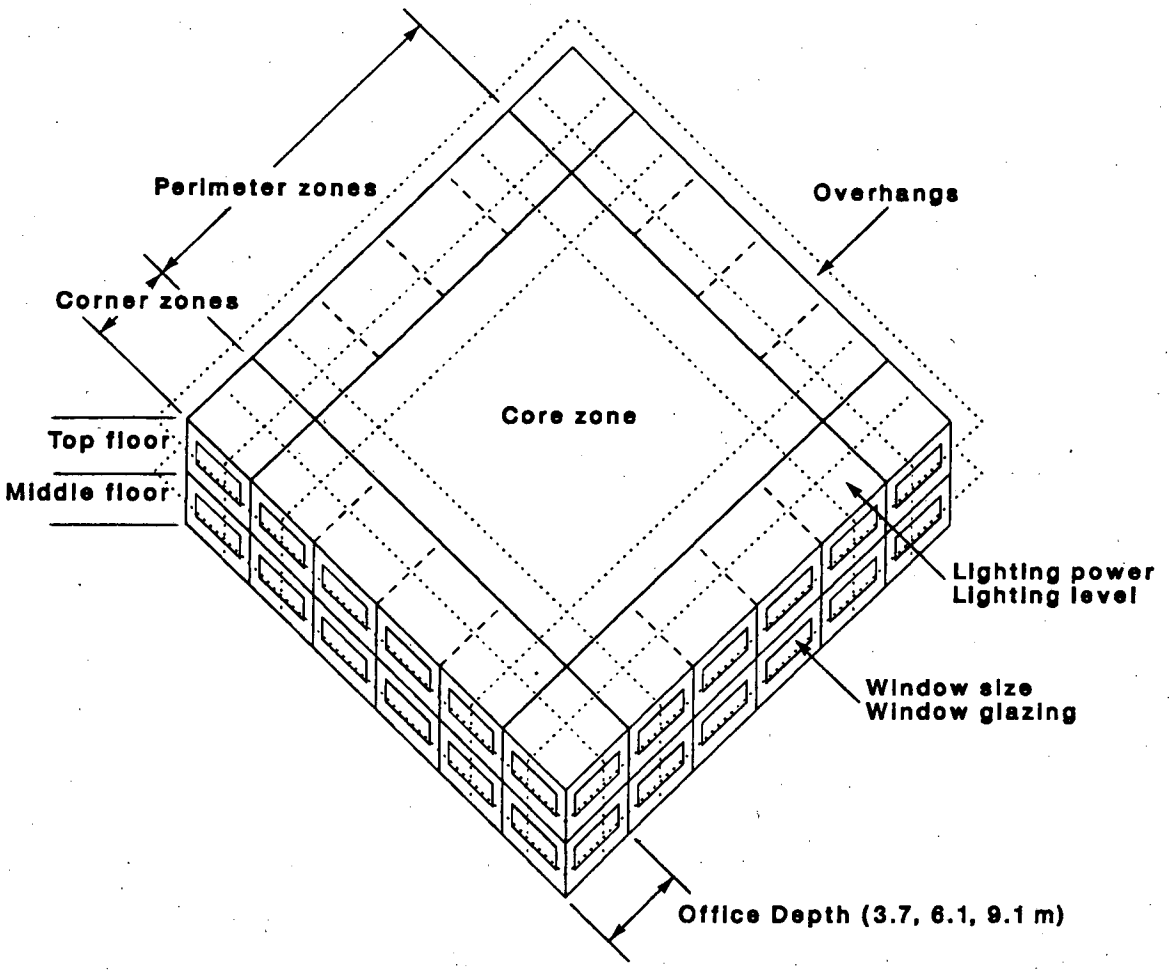

Figure 8-2. Base Case Cooling Loads for Middle Floor South Zone (Lighting Power 21.53 W/m^2)

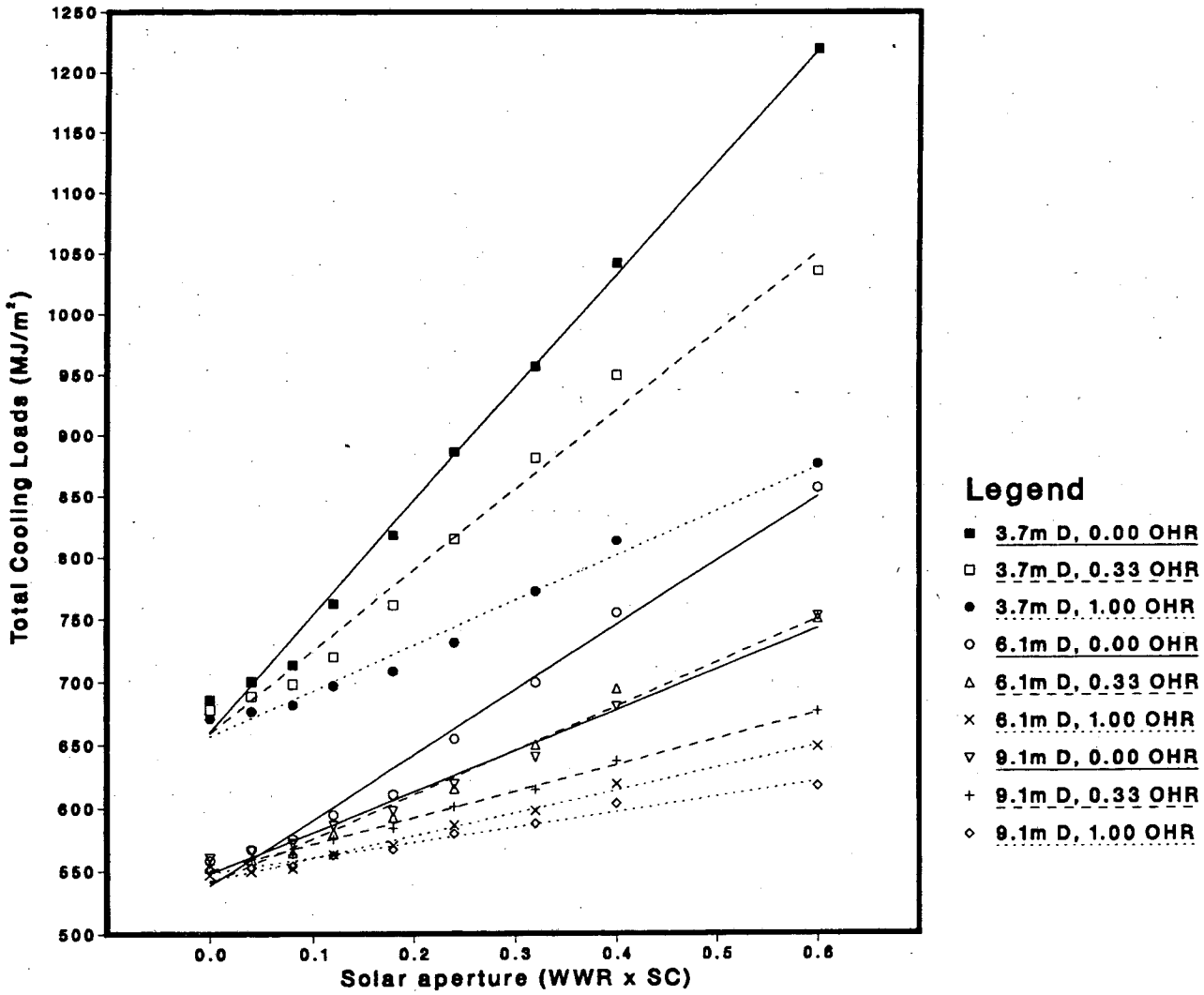

Figure 8-3. Base Case Cooling Energy Use Compared to Cooling Loads

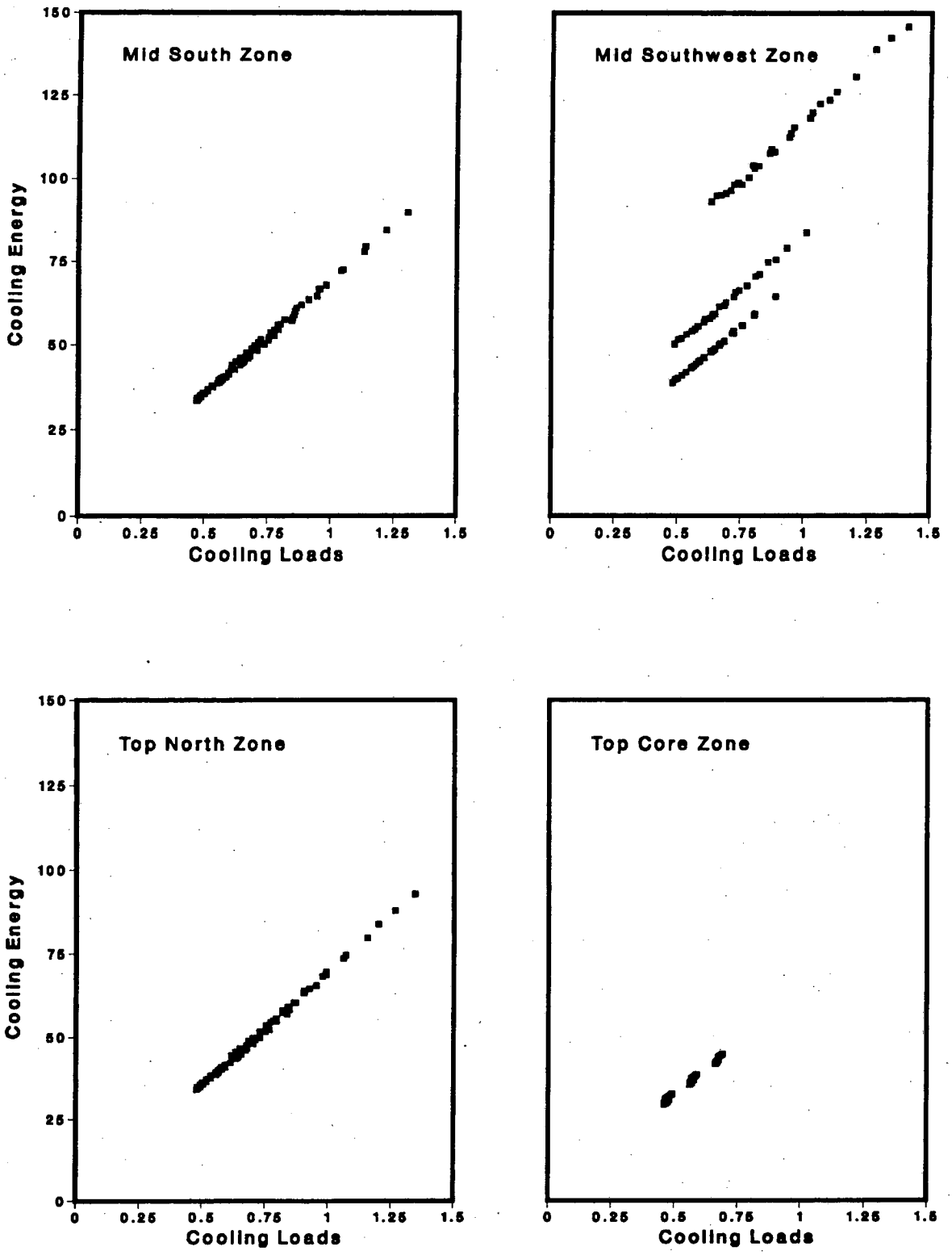

Figure 8-4. Lighting Energy Savings for Middle Floor South Zones with Lighting Power of 21.5 W/m^2 and Lighting Level of 538 lux

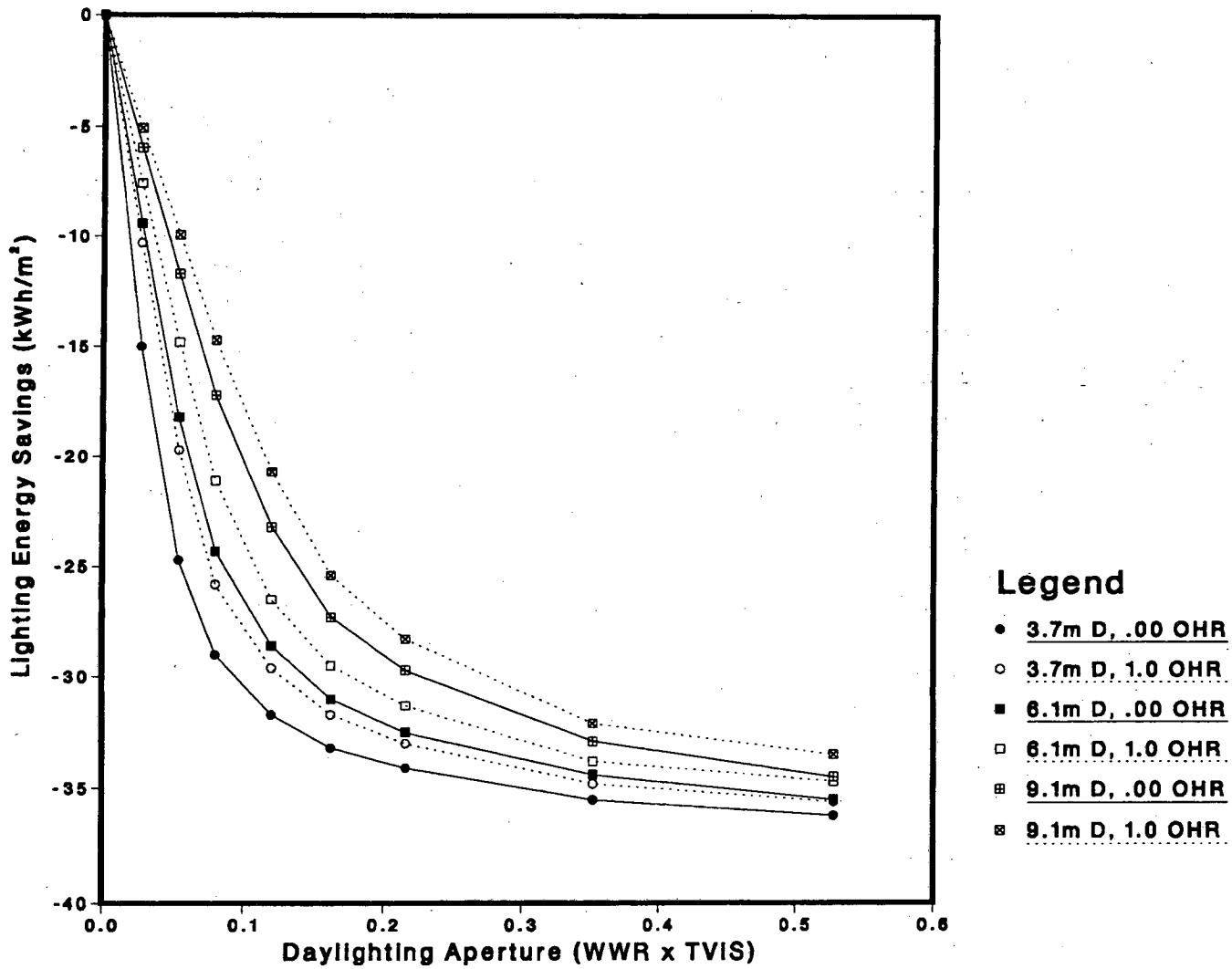

Figure 8-5. Lighting Energy Savings from Daylighting for Middle Floor South Zone (0.33 Overhang Ratio)

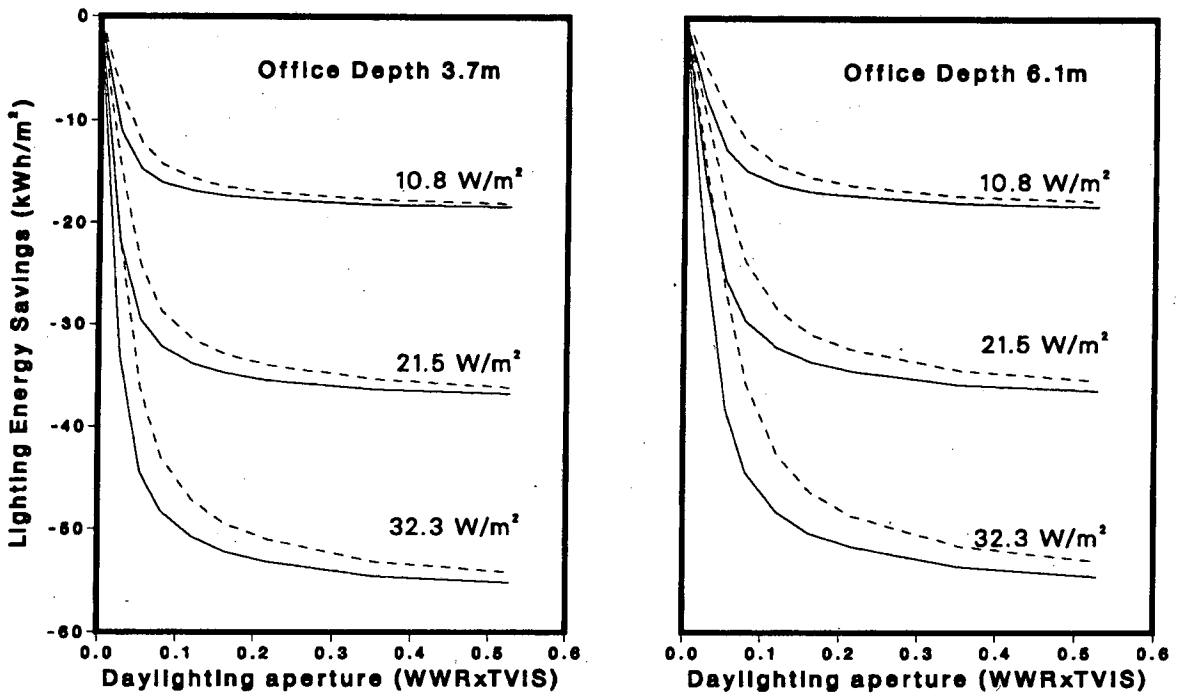

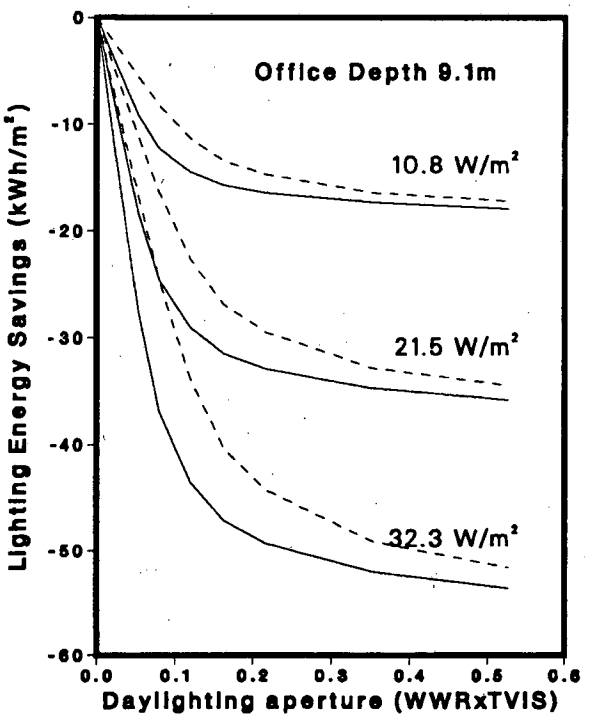

Legend

Lighting level 323 lux

Lighting level 538 lux

Figure 8-6. Cooling Load Reductions from Daylighting for Middle Floor South Zone (0.33 Overhang Ratio)

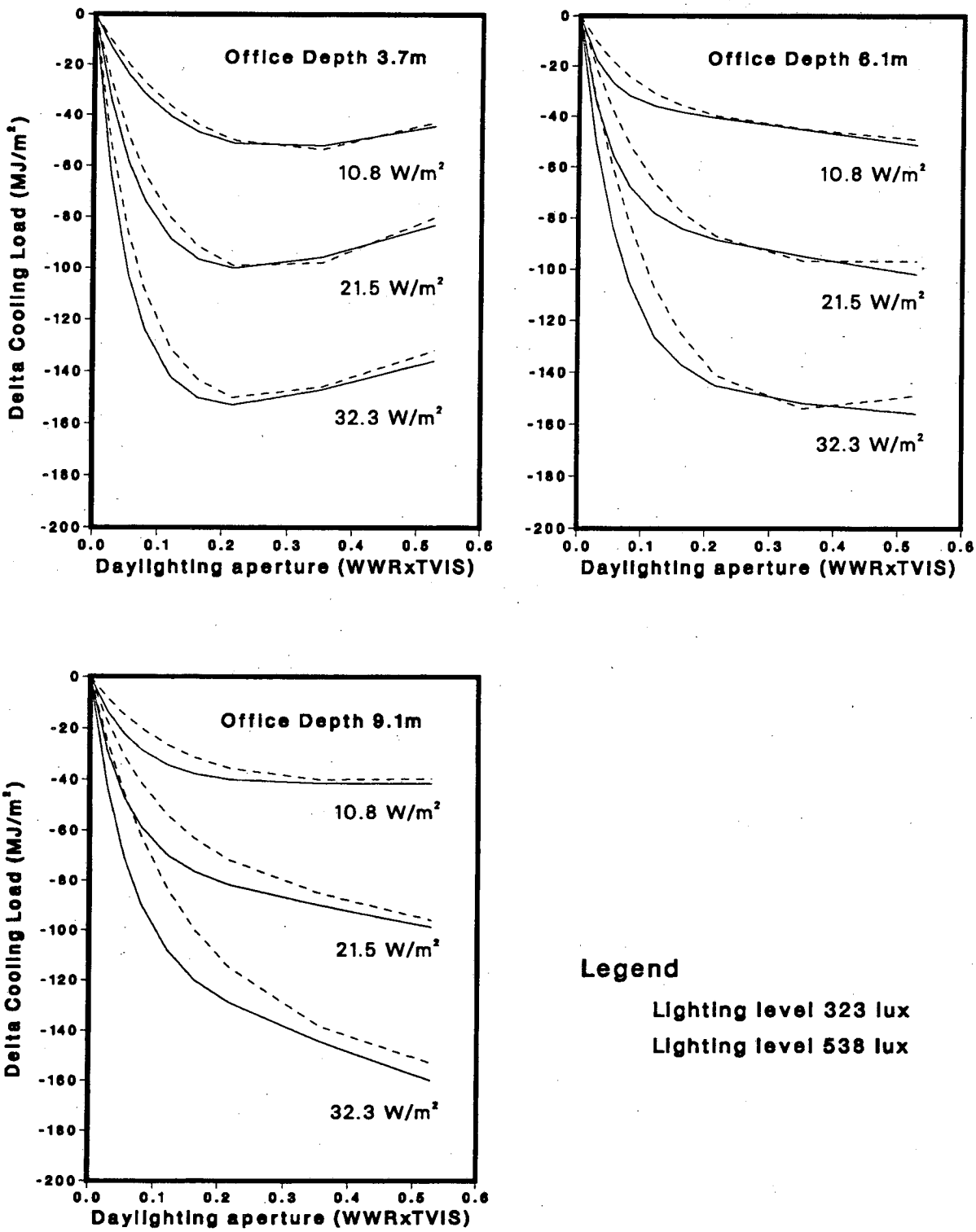

Figure 8-7. Cooling Load Reductions from Daylighting for Middle Floor Core Zones (0.0 Overhang Ratio)

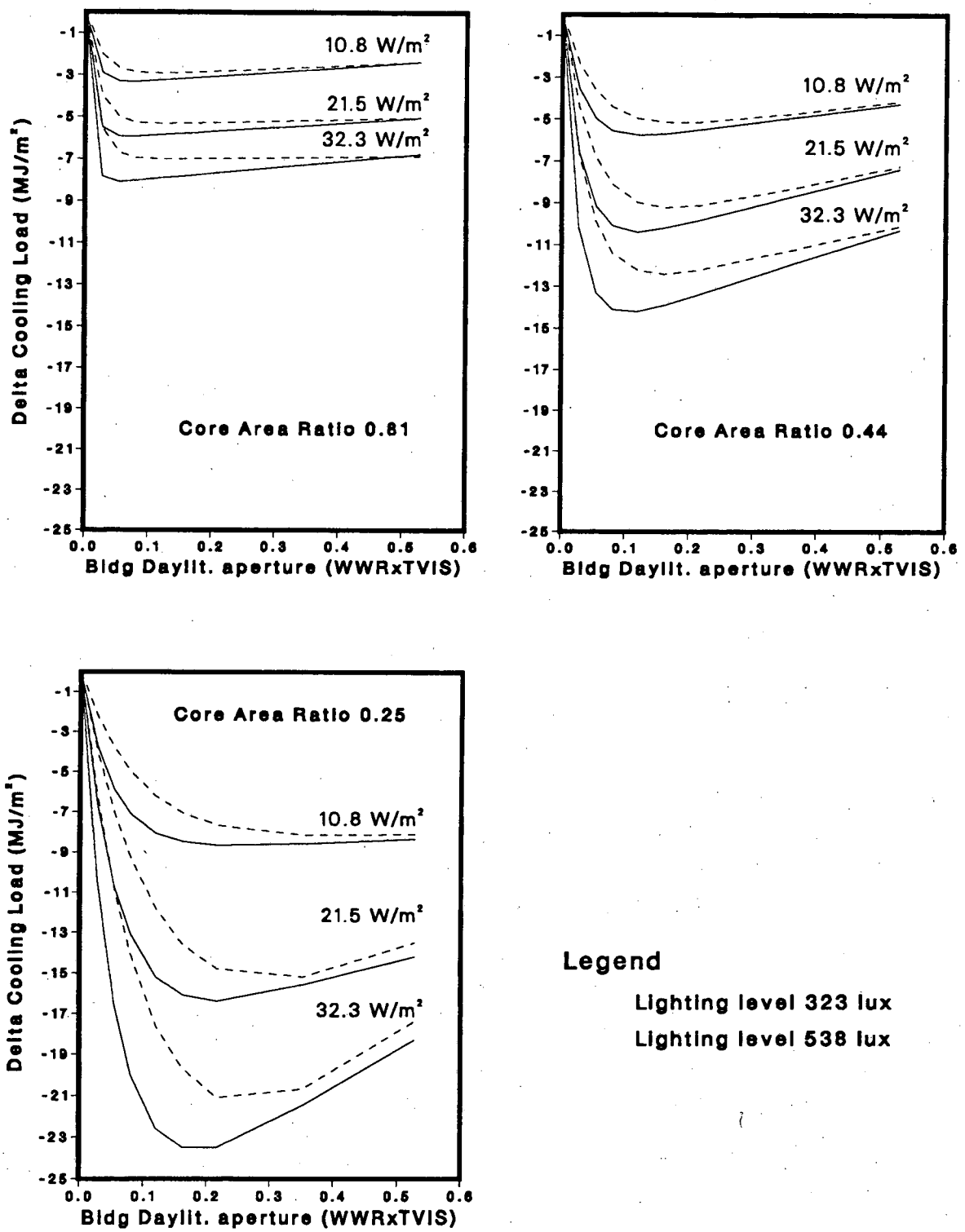

Figure 8-8. Cooling Energy Savings Compared to Cooling Load Reductions

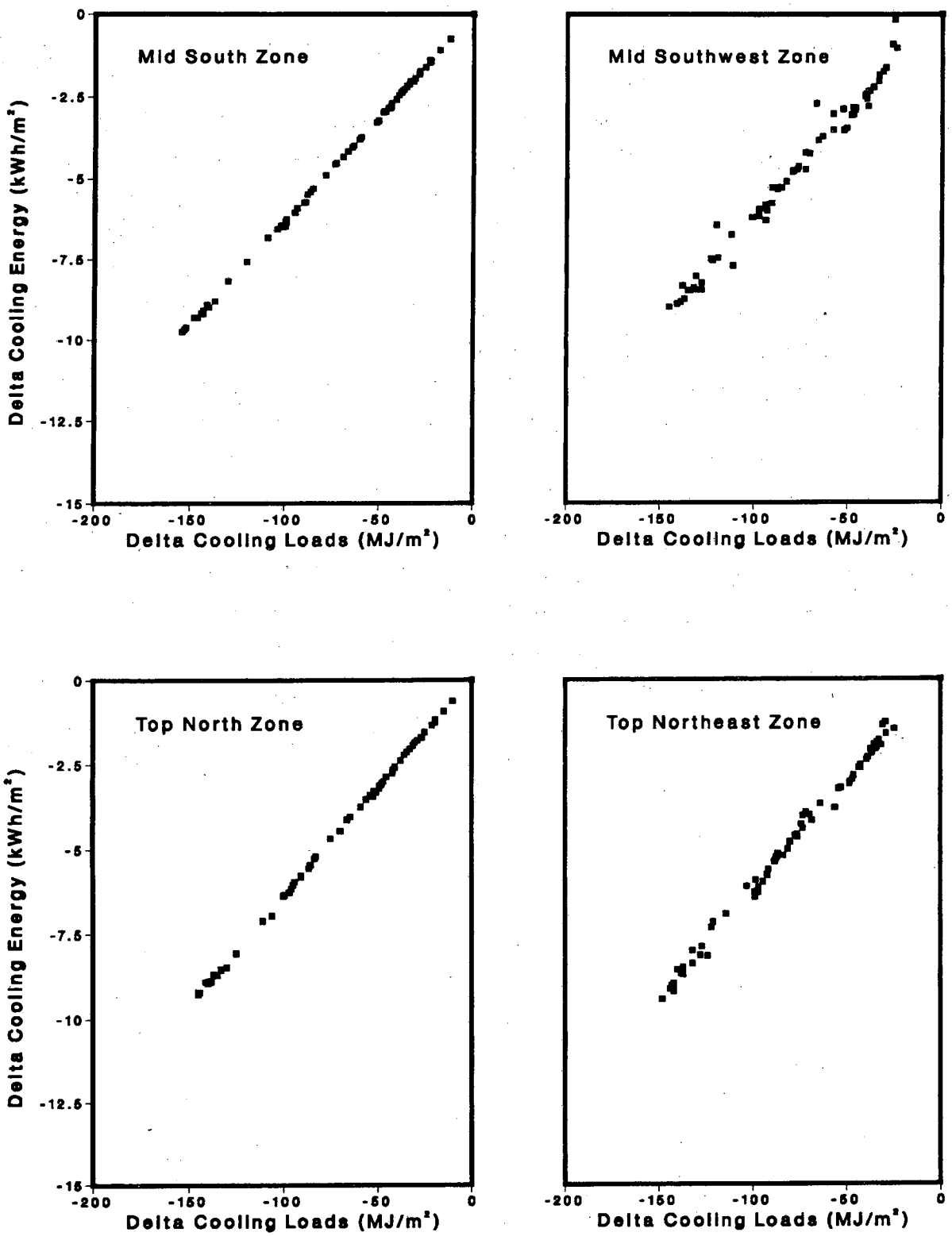

Figure 8-9. Fan Energy Savings Compared to Cooling Load Reductions

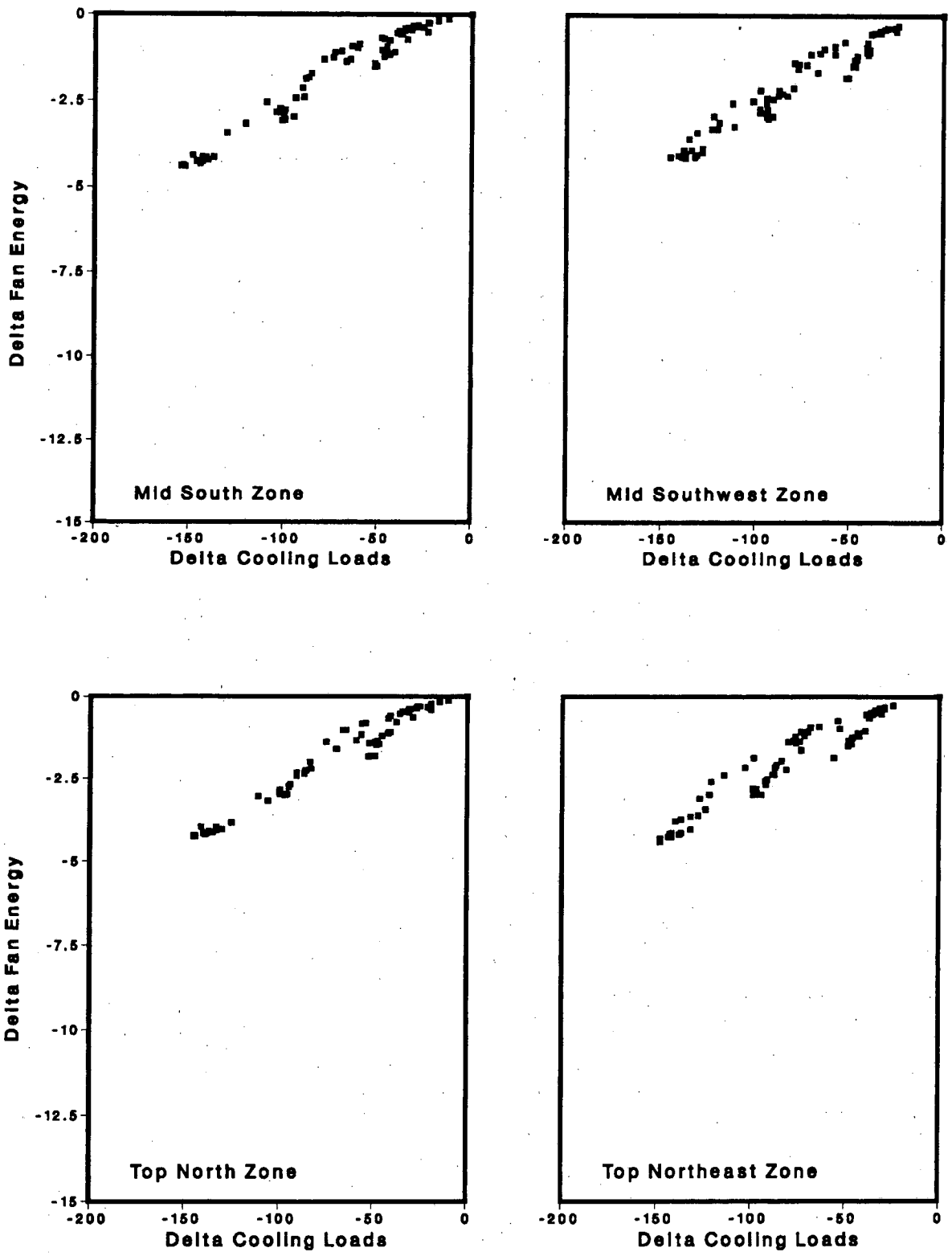

Figure 8-10. Net Energy Use in Middle Floor South Zone with Daylighting
(Depth 6.1 m, Lighting Power 21.5 W/m^2, Lighting Level 538 lux)

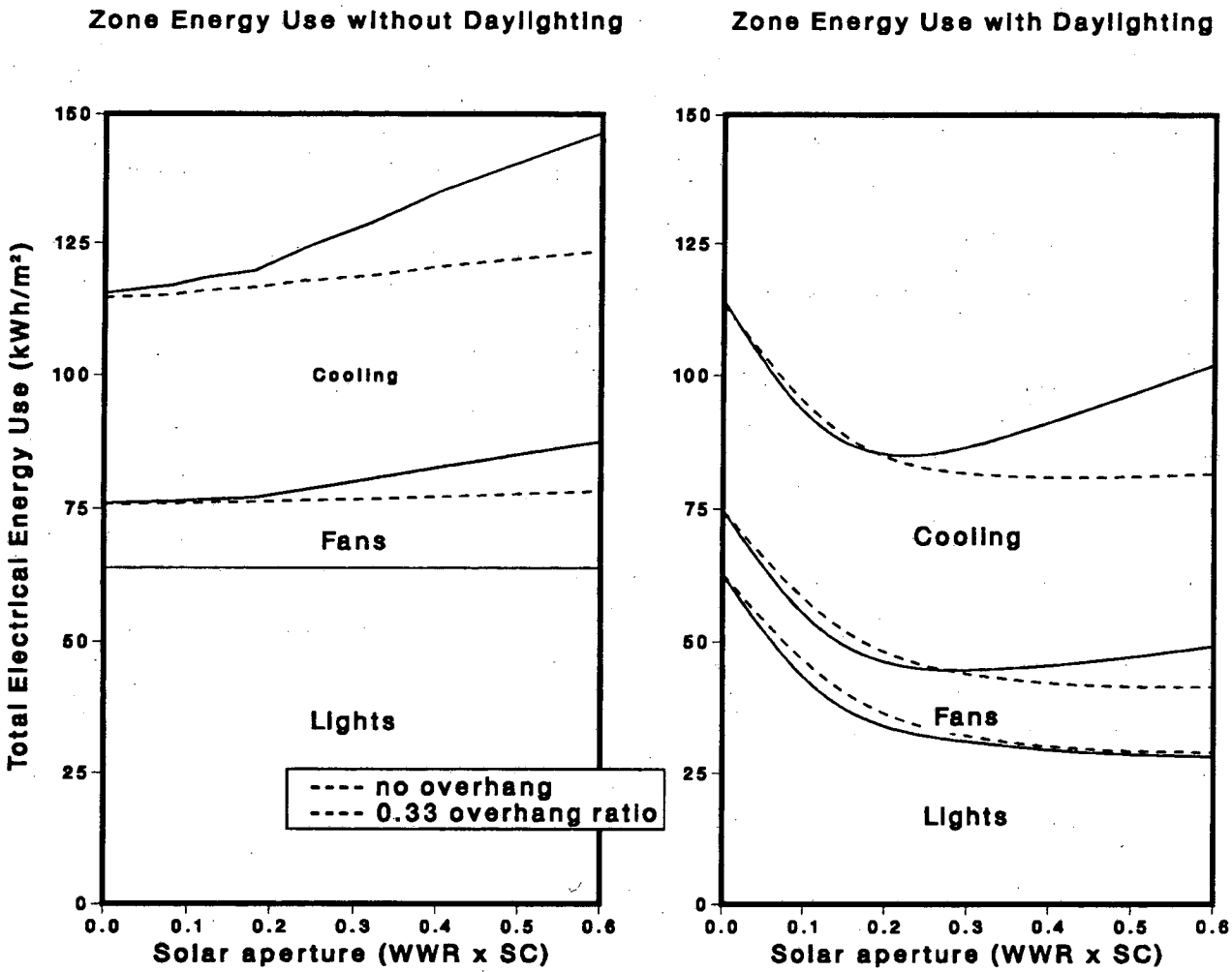

Figure 8-11. Test Buildings to Verify Daylighting Analysis Methodology

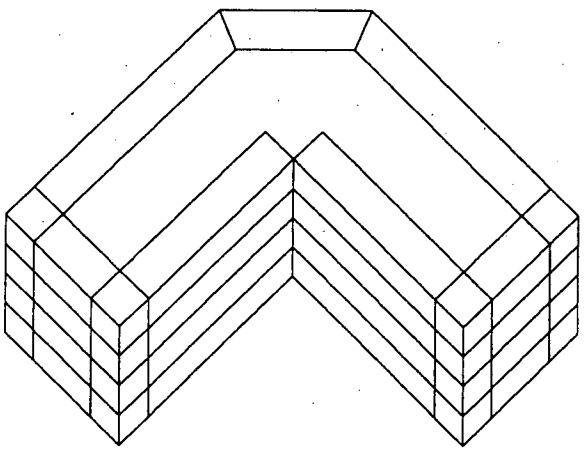

L-shaped office
(4 stories, 5050 m²)

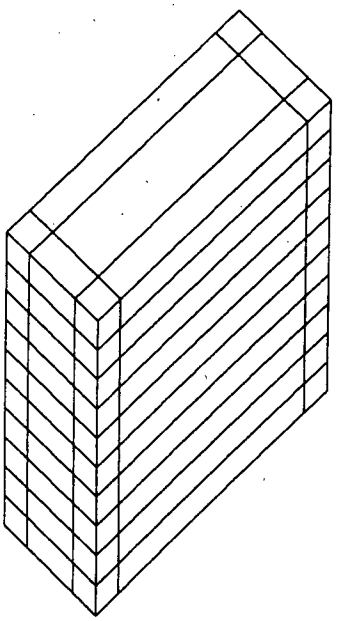

Rectangular office
(10 stories, 4816 m²)

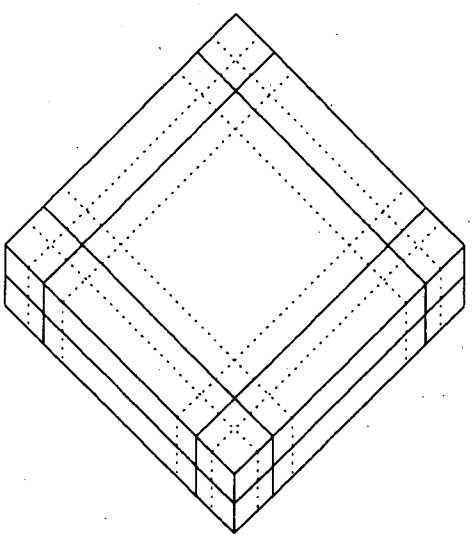

Prototype office
(top & mid floor, 1340 m² each)

Table 8-1. Operating Conditions of Prototype Office Building

Hour	Infiltration *	Occupancy **	Lighting **	Cooling Setpoint(°C)	Fans *
MONDAY-FRIDAY					
1-5	1	0.00	0.05	37	0
6	1	0.00	0.10	37	0
7	0	0.10	0.10	25	1
8	0	0.20	0.30	25	1
9-12	0	0.95	0.90	25	1
13	0	0.50	0.80	25	1
14-17	0	0.95	0.90	25	1
18	1	0.30	0.50	37	0
19	1	0.10	0.30	37	0
20	1	0.10	0.30	37	0
21	1	0.10	0.20	27	0
22	1	0.10	0.20	37	0
23	1	0.05	0.10	37	0
24	1	0.05	0.05	37	0
SATURDAY					
1-5	1	0.00	0.05	37	0
6	1	0.00	0.05	37	0
7	0	0.10	0.10	25	1
8	0	0.10	0.10	25	1
9-12	0	0.90	0.90	25	1
13-17	1	0.10	0.15	37	0
18	1	0.05	0.05	37	0
19	1	0.05	0.05	37	0
20-24	1	0.00	0.05	37	0
SUNDAY					
1-6	1	0.00	0.05	37	0
7-18	1	0.05	1.00	37	0
19-24	1	0.00	0.05	37	0

* 1 = on, 0 = off.

** Decimal indicates percentage of maximum occupancy or lighting power.

Table 8-2: Physical Characteristics of Prototype Office Building

Walls :	
External (structural) :	0.8 cm (0.3 in) blackened glass, 1.9 cm (0.75 in) air layer, 25 cm (9.75 in) brick, 1.3 cm (0.5 in) plaster. Total R = 0.54 $m^2 \cdot °K/W$ (3.1 $hr \cdot ft^2 \cdot °F/Btu$)
External (infill) :	0.8 cm (0.3 in) blackened glass, 1.9 cm (0.75 in) air layer, 10 cm (4 in) brick, 1.3 cm (0.5 in) plaster. Total R = 0.55 $m^2 \cdot °K/W$ (3.1 $hr \cdot ft^2 \cdot °F/Btu$)
Internal :	1.6 cm (0.6 in) gypsum board, 4 in air layer, 1.6 cm (0.6 in) gypsum board. Total R = 0.49 $m^2 \cdot °K/W$ (2.7 $h.ft^2$ °F/Btu)
Roofs :	1.27 cm (0.5 in) roof gravel, .95 cm (0.38 in) built up roofing, R5 polystyrene insulation, 15.2 cm (6 in) concrete 10.2 cm (4 in), air layer, 1.3 cm (0.5 in) acoustic tile. Total R = 1.62$m^2 \cdot °K/W$ (9 $hr \cdot ft^2 \cdot °F/Btu$)
Floors :	20 cm (8 in) concrete floors. Total R = 0.5$m^{2} \cdot °K/W$ (2.8 $h.ft^2$ °F/Btu)
Absorptivity	Walls: 0.45 Roofs : 0.30
Infiltration:	0.6 air changes per hour when fans off.
Windows:	
No. of panes:	single glazing
Glass conductance:	6.13 $W/m^2 \cdot °K$ (1.1 $Btu/h.ft^2$ °F)
Window setback:	none
Systems:	
Outside air:	2.9 lit/sec (7 cfm) per person
Cooling setpoint:	25.6°C (78°F)
Night setback:	37°C (99°F)
Economizer:	None
Chiller COP:	4.17 (not including fans and pumps)

Table 8-3. Design Variations Analyzed in Creating the DOE-2 Daylighting Data Base

Building parameter	Range
3 Perimeter Zone Depths	: 3.66, 6.10, and 9.14 m (12, 20, and 30 ft)
11 Window Conditions	: WWR from .00 to 60, SC from 0.2 to 1.00, TVIS from 0.02 to 0.80 (see Table 8-4)
3 Window Overhang Ratios *	: .0, .33, and 1.0
3 Lighting Powers	: 10.8, 21.5, and 32.3 watts/m^2 (1, 2, and 3 watt/ft^2)
3 Lighting Levels	: none (no daylighting), 323 and 538 lux (30 and 50 foot-candles)

* overhang ratio = overhang projection/vertical distance from overhang to bottom of window sill.

Table 8-4. Glazing Conditions Analyzed in DOE-2 Daylighting Data Base

Case	Window/ Wall Ratio (WWR)	Shad. Coef (SC)	Vis.Trans. (TVIS)	Glazing distrib.	Solar aperture (WWRxSC)	Daylighting aperture (WWRxTVIS)
1	0	*	*	equal	.00	.000
2	10	0.40	0.27	equal	.04	.027
3	20	0.40	0.27	equal	.08	.054
4	20	0.60	0.40	equal	.12	.080
5	30	0.60	0.40	equal	.18	.120
6	30	0.80	0.54	equal	.24	.162
7	40	0.80	0.54	equal	.32	.216
8	40	1.00	0.90	equal	.40	.360
9	60	1.00	0.90	equal	.60	.540
10	0 EW, 60 NS	1.00 NS,	0.90 NS,	unequal	.00 EW, .60 NS	.00 EW, .54 NS
11	0 NS, 60 EW	1.00 EW,	0.90 EW,	unequal	.00 NS, .60 EW	.00 NS, .54 EW

* SC and TVIS are not applicable when WWR is 0.

Table 8-5. Regression Coefficients for Base Case Cooling Loads

Zone	Off. Depth (m)	β_1	β_2	β_3	β_4
MIDN	3.66	499.54	7.496	993.12	-0.979
	6.10	377.51	7.617	555.77	-1.073
	9.14	378.32	7.934	351.27	-1.021
MIDS	3.66	497.69	7.528	930.77	-0.921
	6.10	378.07	7.565	517.74	-1.017
	9.14	378.87	7.907	325.22	-0.951
MIDE	3.66	507.50	7.202	934.92	-0.900
	6.10	385.38	7.451	522.18	-0.976
	9.14	382.10	7.950	332.33	-0.927
MIDW	3.66	493.43	8.100	1886.85	-0.763
	6.10	371.58	8.110	1050.11	-0.797
	9.14	376.61	8.172	682.23	-0.854
MIDNE	3.66	525.98	5.581	801.53	-0.746
	6.10	396.88	6.014	455.28	-0.868
	9.14	390.76	6.702	289.48	-0.833
MIDNW	3.66	528.03	5.960	1151.55	-0.573
	6.10	394.63	6.317	667.85	-0.748
	9.14	393.86	6.735	432.81	-0.835
MIDSE	3.66	525.75	5.417	784.08	-0.731
	6.10	396.69	5.985	439.40	-0.832
	9.14	390.31	6.715	277.91	-0.792
MIDSW	3.66	523.61	6.058	1114.84	-0.549
	6.10	394.76	6.282	651.46	-0.697
	9.14	394.33	6.705	424.18	-0.802
MIDCO	0.81 *	326.31	10.221	42.79	-0.416
	0.44 *	323.28	10.473	55.39	-0.451
	0.25 *	323.91	10.740	71.23	-0.543
TOPN	3.66	510.58	6.977	1004.54	-1.175
	6.10	391.69	6.821	548.70	-1.379
	9.14	394.80	6.908	334.07	-1.370
TOPS	3.66	512.78	6.796	940.44	-1.164
	6.10	392.75	6.757	505.30	-1.334
	9.14	395.38	6.889	305.18	-1.305
TOPE	3.66	519.09	6.657	978.94	-1.240
	6.10	397.66	6.678	539.35	-1.336
	9.14	398.61	6.878	329.32	-1.283
TOPW	3.66	495.78	7.366	2030.42	-0.875
	6.10	375.81	7.398	1087.84	-0.948
	9.14	385.35	7.265	666.47	-1.015
TOPNE	3.66	528.70	5.552	794.03	-0.924
	6.10	404.73	5.571	448.86	-1.109
	9.14	402.44	5.979	277.08	-1.113
TOPNW	3.66	528.14	5.819	1171.23	-0.667
	6.10	398.37	5.900	659.74	-0.891
	9.14	400.92	6.083	414.75	-1.057
TOPSE	3.66	532.04	5.165	779.02	-0.937
	6.10	404.82	5.527	428.84	-1.103
	9.14	402.04	5.998	262.97	-1.077
TOPSW	3.66	525.17	5.776	1141.34	-0.634
	6.10	397.57	5.919	641.34	-0.813
	9.14	401.26	6.052	406.20	-0.984
TOPCO	0.81 *	359.11	9.305	19.40	-0.526
	0.44 *	357.21	9.478	29.18	-0.572
	0.25 *	358.48	9.669	41.57	-0.736

* = Core Area Ratio.

Table 8-6. Linear Coefficients for Base Case Cooling and Fan Efficiency

Zone	Depth (m)	Cooling Energy		Fan Energy	
		β_1	$\beta_2 * 100$	β_1	$\beta_2 * 100$
MIDN	3.66	3.300	6.634	-13.083	3.710
	6.10	3.327	6.472	-5.422	3.092
	9.14	3.472	6.350	-1.962	2.459
MIDS	3.66	3.476	6.607	-13.034	3.697
	6.10	3.542	6.429	-5.221	3.050
	9.14	3.691	6.304	-1.529	2.380
MIDE	3.66	4.111	6.509	-9.215	3.133
	6.10	4.081	6.333	-2.328	2.541
	9.14	4.259	6.213	-0.009	2.123
MIDW	3.66	1.828	6.808	-21.581	4.796
	6.10	2.082	6.670	-13.304	4.384
	9.14	2.494	6.508	-9.079	3.661
MIDNE	3.66	49.747	6.650	-9.273	3.213
	6.10	19.538	6.170	-2.370	2.597
	9.14	9.006	6.141	0.467	2.068
MIDNW	3.66	45.769	7.270	-16.180	4.166
	6.10	16.383	6.732	-8.120	3.598
	9.14	7.457	6.408	-3.853	2.811
MIDSE	3.66	49.802	6.622	-9.402	3.219
	6.10	19.603	6.150	-2.252	2.568
	9.14	9.130	6.112	0.762	2.012
MIDSW	3.66	45.962	7.198	-16.466	4.194
	6.10	17.057	6.607	-8.500	3.657
	9.14	8.012	6.304	-3.973	2.824
MIDCO	0.81 *	1.726	6.009	4.733	1.236
	0.44 *	2.241	5.978	4.511	1.271
	0.25 *	3.200	5.977	4.197	1.317
TOPN	3.66	2.876	6.703	-14.375	3.916
	6.10	2.857	6.569	-6.772	3.349
	9.14	2.826	6.478	-3.288	2.714
TOPS	3.66	3.040	6.676	-13.920	3.838
	6.10	3.095	6.521	-6.343	3.267
	9.14	3.126	6.420	-2.546	2.583
TOPE	3.66	3.792	6.562	-10.442	3.309
	6.10	3.526	6.442	-3.820	2.814
	9.14	3.523	6.351	-0.724	2.262
TOPW	3.66	1.143	6.914	-23.393	5.104
	6.10	1.097	6.856	-16.176	4.948
	9.14	1.418	6.714	-12.830	4.369
TOPNE	3.66	49.659	6.697	-9.731	3.299
	6.10	19.163	6.249	-2.981	2.721
	9.14	8.552	6.232	-0.065	2.174
TOPNW	3.66	45.052	7.413	-17.722	4.423
	6.10	15.313	6.953	-10.396	4.041
	9.14	6.510	6.597	-6.194	3.258
TOPSE	3.66	49.599	6.672	-9.608	3.260
	6.10	19.304	6.220	-2.615	2.644
	9.14	8.693	6.203	0.466	2.077
TOPSW	3.66	45.411	7.321	-18.312	4.496
	6.10	16.096	6.803	-10.987	4.146
	9.14	6.988	6.501	-6.798	3.361
TOPCO	0.81 *	1.198	6.121	4.039	1.371
	0.44 *	1.921	6.050	4.022	1.368
	0.25 *	2.935	6.038	3.942	1.374

* = Core Area Ratio.

Table 8-7. Regression Coefficients for Δ Lighting Energy

$$\Delta LE = \beta_1 \cdot LP \cdot (1 - e^{(1 + \beta_2 \cdot OHR + \beta_3 \cdot OHR^2) \cdot (\beta_4 + \beta_5 \cdot LL) \cdot DA)})$$

Zone	Depth (m)	β_1	$\beta_2 * 10$	β_3	β_4	$\beta_5 * 10$
North	3.66	-1.655	-0.466	-0.243	-50.29	0.583
	6.10	-1.646	-0.883	-0.106	-32.99	0.384
	9.14	-1.647	-1.617	0.006	-21.28	0.253
South	3.66	-1.641	-0.074	-0.300	-55.18	0.632
	6.10	-1.632	-0.551	-0.157	-35.95	0.415
	9.14	-1.631	-1.354	-0.042	-23.18	0.273
East	3.66	-1.723	-0.110	-0.344	-69.41	0.837
	6.10	-1.732	-0.368	-0.212	-43.03	0.514
	9.14	-1.749	-1.033	-0.108	-26.61	0.318
West	3.66	-1.595	0.250	-0.269	-55.50	0.576
	6.10	-1.573	-0.299	-0.151	-40.42	0.438
	9.14	-1.553	-0.838	-0.067	-27.01	0.299
North-east	3.66	-1.699	0.768	-0.424	-77.18	0.771
	6.10	-1.686	-0.643	-0.220	-61.96	0.764
	9.14	-1.686	-1.477	-0.108	-38.72	0.490
North-west	3.66	-1.633	-0.022	-0.207	-47.41	0.434
	6.10	-1.605	-0.352	-0.150	-39.49	0.412
	9.14	-1.588	-1.182	-0.066	-28.99	0.329
South-east	3.66	-1.691	0.009	-0.286	-61.20	0.612
	6.10	-1.682	-0.366	-0.243	-51.13	0.611
	9.14	-1.702	-1.598	-0.118	-33.72	0.428
South-west	3.66	-1.632	0.149	-0.224	-48.05	0.421
	6.10	-1.602	-0.288	-0.168	-40.98	0.415
	9.14	-1.580	-1.098	-0.092	-30.97	0.347

Table 8-8. Regression Coefficients for Δ Cooling Loads

Zone	Depth	β_1	$\beta_2 * 100$	Zone	Depth	β_1	$\beta_2 * 100$
MIDN	3.66	2.141	0.3066	TOPN	3.66	1.975	0.5753
	6.10	2.293	0.3396		6.10	2.163	0.4278
	9.14	2.414	0.3764		9.14	2.332	0.3052
MIDS	3.66	2.101	0.4795	TOPS	3.66	2.011	0.3954
	6.10	2.268	0.4422		6.10	2.132	0.5769
	9.14	2.384	0.4865		9.14	2.263	0.5050
MIDE	3.66	2.075	0.5844	TOPE	3.66	1.974	0.5585
	6.10	2.193	0.5862		6.10	2.079	0.6293
	9.14	2.285	0.6166		9.14	2.200	0.5870
MIDW	3.66	2.362	-0.1533	TOPW	3.66	2.136	-0.2106
	6.10	2.481	-0.2357		6.10	2.385	-0.4620
	9.14	2.638	-0.3043		9.14	2.556	-0.5364
MIDNE	3.66	1.849	0.6744	TOPNE	3.66	1.745	0.5662
	6.10	2.099	0.3549		6.10	1.935	0.5041
	9.14	2.170	0.4924		9.14	2.039	0.5804
MIDNW	3.66	1.930	0.8329	TOPNW	3.66	1.759	0.8927
	6.10	2.110	0.7182		6.10	1.980	0.6901
	9.14	2.244	0.6131		9.14	2.156	0.5540
MIDSE	3.66	1.884	0.5476	TOPSE	3.66	1.735	0.6427
	6.10	2.070	0.4427		6.10	1.915	0.5217
	9.14	2.132	0.5727		9.14	1.993	0.6362
MIDSW	3.66	1.954	0.7930	TOPSW	3.66	1.770	1.0283
	6.10	2.090	0.8666		6.10	1.959	0.9220
	9.14	2.221	0.8249		9.14	2.131	0.7653
MIDCO	0.81 *	0.267	-19.276	TOPCO	0.81 *	0.193	-11.979
	0.44 *	0.312	-24.818		0.44 *	0.216	-15.173
	0.25 *	0.357	-21.782		0.25 *	0.247	-15.112

* Core Area Ratio.

Table 8-9. Comparison of DOE-2 to Interpolated Loads and Energies for Test Rectangular Building (10 stories, 4816 m^2)

Window-to-Wall Ratio (WWR)	.20	.40	.60/.00
Shad. Coeff (SC)	0.4	0.8	1.0
Total Vis. Trans. (TVIS)	0.27	0.54	0.90
Cooling Loads (GJ)			
DOE-2	2652.1	3494.1	3755.2
Interpolated	2797.6	3567.5	3839.3
Delta	145.5	73.4	84.1
Percent Delta	(5.5)	(2.1)	(2.2)
Cooling Energies (MWh)			
DOE-2	185.81	244.29	262.66
Interpolated	220.68	272.13	289.79
Delta	34.9	27.8	27.1
Percent Delta	(18.8)	(11.4)	(10.3)
Fan Energies (MWh)			
DOE-2	58.12	92.98	106.73
Interpolated	53.07	82.09	90.47
Delta	-5.0	-10.9	-16.3
Percent Delta	(-8.7)	(-11.7)	(-15.2)
Lighting Energy Savings (MWh)			
DOE-2	45.50	52.93	44.50
Interpolated	44.68	51.34	43.79
Delta	-0.8	-1.6	-0.7
Percent Delta	(-1.8)	(-3.0)	(-1.6)
Cooling Load Reductions (GJ)			
DOE-2	100.66	127.81	102.37
Interpolated	99.40	113.33	95.25
Delta	-1.3	-14.5	-7.1
Percent Delta	(-1.3)	(-11.3)	(-7.0)
Cooling Energy Savings (MWh)			
DOE-2	6.73	8.49	6.76
Interpolated	6.60	7.53	6.34
Delta	-0.1	-1.0	-0.4
Percent Delta	(-1.9)	(-11.3)	(-6.2)
Fan Energy Savings (MWh)			
DOE-2	1.59	3.26	2.77
Interpolated	3.59	4.12	3.42
Delta	2.0	0.9	0.6
Percent Delta	(125.8)	(26.4)	(23.5)

Table 8-10. Comparisons of Test DOE-2 Results to Interpolated Values for L-Shaped Building (5050 m^2)

	No Overhang			1.67 m Overhang		
Window-to-Wall Ratio (WWR)	.20	.40	.60/.00	.20	.40	.60/.00
Shad. Coeff (SC)	0.4	0.8	1.0	0.4	0.8	1.0
Total Vis. Trans.(TVIS)	0.27	0.54	0.90	0.27	0.54	0.90
Cooling Loads (GJ)						
DOE-2	2443.5	3100.6	3011.2	2367.3	2804.9	2785.9
Interpolated	2708.2	3382.6	3030.8	2609.2	2986.5	2761.1
Delta	264.7	282.0	19.6	241.9	181.6	-24.8
Percent Delta	(10.8)	(9.1)	(0.7)	(10.2)	(6.5)	(-0.9)
Cooling Energies (MWh)						
DOE-2	176.55	222.49	216.14	171.65	201.98	200.99
Interpolated	208.45	253.20	230.79	201.88	226.93	211.82
Delta	31.9	30.7	14.7	30.2	25.0	10.8
Percent Delta	(18.1)	(13.8)	(6.8)	(17.6)	(12.4)	(5.4)
Fan Energies (MWh)						
DOE-2	58.86	85.19	84.05	57.50	72.98	74.81
Interpolated	53.56	78.81	63.03	49.85	63.99	54.35
Delta	-5.3	-6.4	-21.0	-7.6	-9.0	-20.5
Percent Delta	(-9.0)	(-7.5)	(-25.0)	(-13.3)	(-12.3)	(-27.3)
Lighting Energy Savings (MWh)						
DOE-2	32.83	47.40	22.79	27.94	46.48	22.58
Interpolated	32.95	48.51	23.15	30.56	48.03	22.40
Delta	0.1	1.1	0.4	2.6	1.6	-0.2
Percent Delta	(0.4)	(2.3)	(1.6)	(9.4)	(3.3)	(-0.8)
Cooling Load Reductions (GJ)						
DOE-2	76.87	122.41	56.28	61.42	116.58	55.19
Interpolated	75.95	111.04	51.11	70.46	109.95	49.50
Delta	-0.9	-11.4	-5.2	9.0	-6.6	-5.7
Percent Delta	(-1.2)	(-9.3)	(-9.2)	(14.7)	(-5.7)	(-10.3)
Cooling Energy Savings (MWh)						
DOE-2	5.32	8.06	3.73	3.87	7.68	3.63
Interpolated	4.99	7.30	3.37	4.63	7.23	3.26
Delta	-0.3	-0.8	-0.4	0.8	-0.4	-0.4
Percent Delta	(-6.2)	(-9.4)	(-9.7)	(19.6)	(-5.9)	(-10.2)
Fan Energy Savings (MWh)						
DOE-2	1.12	3.28	1.65	0.78	2.94	1.57
Interpolated	2.64	3.89	1.70	2.46	3.85	1.65
Delta	1.5	0.6	0.1	1.7	0.9	0.1
Percent Delta	(135.7)	(18.6)	(3.0)	(215.4)	(31.0)	(5.1)

CHAPTER 9: IMPROVING THE PERFORMANCE OF AIR-CONDITIONING SYSTEMS IN AN ASEAN CLIMATE

J.F. Busch and M.L. Warren *
Energy Analysis Program
Applied Science Division
Lawrence Berkeley Laboratory
Berkeley, California 94720

ABSTRACT

This paper describes an analysis of air-conditioning performance under hot and humid tropical climate conditions appropriate to the Association of South East Asian Nations (ASEAN) countries. This region, with over 280 million people, has one of the fastest economic and energy consumption growth rates in the world. The work reported here is aimed at estimating the conservation potential derived from good design and control of air-conditioning systems in commercial buildings.

To test the performance of different air-conditioning system types and control options, whole building energy performance was simulated using DOE-2. The 5,100 m^2 (50,000 ft^2) prototype office building module was used in earlier commercial building energy standards analysis for Malaysia and Singapore. In general, the weather pattern for ASEAN countries is uniform, with hot and humid air masses known as "monsoons" dictating the weather patterns. Since a concentration of cities occurs near the tip of the Malay peninsula, hourly temperature, humidity, and wind speed data for Kuala Lumpur was used for the analysis. Because of the absence of heating loads in ASEAN regions, we have limited air-conditioning configurations to two-pipe fan coil, constant volume, variable air volume (VAV), powered induction, and ceiling bypass configurations. Control strategies were varied to determine the conservation potential in both energy use and peak electric power demands. Sensitivities including fan control, pre-cooling and night ventilation, supply air temperature control, zone temperature set point, ventilation and infiltration, daylighting and internal gains, and system sizing were examined and compared with a base case that was a variable air volume system with no reheat or economizer. Comfort issues, such as over-cooling and space humidity, were also examined.

VAV systems clearly have the best performance minimizing energy use while maintaining comfort conditions. Excess outdoor air in this humid climate has a significant energy penalty. Two-pipe fan coil units have the lowest energy consumption due to fan energy savings and low latent cooling capacity, but perform poorly during morning pull-down periods. Large fan energy savings for all systems can be obtained by using supply air temperatures as low as 7°C (45°F). A combination of system conservation measures incorporated into one building saved 14% of annual energy and 16% on peak power. Other results of the analysis will be discussed.

INTRODUCTION

The countries of the Association of South East Asian Nations (ASEAN), Indonesia, Malaysia, the Philippines, Singapore, and Thailand, with over 280 million people, are among the fastest growing regions economically and in terms of energy use. With the elevated standard of living, the number of air-conditioned commercial buildings has increased dramatically. In this hot humid climate, more than 50% of the energy use of Western-style buildings goes for air-conditioning.

Besides increasing the overall energy intensity of commercial buildings, the installation of electric air-conditioning adds to the peak electrical demand of the country's power system for the life of the building. This can place a significant capital burden on the country to provide the

* Formerly with Lawrence Berkeley Laboratory, currently with ASI Controls, San Ramon, CA.

additional generation capacity to meet this demand. Thus, measures that reduce peak cooling loads and electrical demands of new commercial buildings will reduce demands for capital and foreign-exchange for imported energy sources and provide greater opportunities for making effective use of limited indigenous resources. Therefore, energy conservation for air-conditioning in Southeast Asian commercial buildings has public planning and policy significance.

Energy-conserving principles worked out in the developed world are not always relevant because of differences in climate and structure of economies. While a major concern in tropical building design for energy efficiency is the mitigation of cooling loads, either through the envelope or internally-generated, we concern ourselves here only with the performance of the mechanical systems that cope with the loads that do appear. We attempt to identify, through a parametric study, the impact of some air-conditioning operating strategies and equipment choices on energy use and comfort levels in ASEAN climates.

This paper describes issues surrounding air-conditioning use and develops preliminary solutions and guidelines for future work within the context of a larger collaborative research effort between the Lawrence Berkeley Laboratory and researchers, practitioners, and policy makers in the ASEAN countries. The project, which is funded by the U.S. Agency for International Development, seeks to develop workable conservation policies for commercial buildings' energy use in the region. While policy options will not be directly addressed in this study, we are aware that the conditions for realizing the energy-saving potential of the measures suggested here are often lacking and will require skilled attention. For instance, lowest first cost is a powerful driving force for the design of air-conditioning systems, and thus the most efficient and cost-effective options (over the building's life-cycle) are often overlooked. Also, those with responsibility for operating and maintaining air-conditioning equipment may not be rewarded for efficient operation.

What follows is an explanation of our approach and methodology for estimating the air-conditioning conservation potential, some results from an informal survey of installed systems in ASEAN and from our simulation work, and recommendations for further research.

METHODOLOGY

In order to test a number of air-conditioning system types and wide variety of control options, we simulated building energy performance using a state-of-the-art computer model. We chose whole-building analysis over a system-only simulation to give a more comprehensive picture of the energy savings potential. Our analysis consists of three elements: the DOE-2.1C computer model, a prototype office building module used in earlier studies of commercial building energy standards for Malaysia and Singapore, and measured hourly weather for Kuala Lumpur. Each of these is described below. Our approach was to vary the important system configuration and control parameters in individual simulations to determine the conservation potential in energy use and peak power demands and then to compare the performance of these options. We also compared the performance of the different generic system types using comparable input assumptions. Comfort issues such as overcooling and space humidity levels are also discussed. Because of the absence of heating loads in the ASEAN region, we have limited the types of air-conditioning systems. For instance, four-pipe fan coil units, heat pumps, or dual-duct systems are rarely used in the region and were ignored.

DOE-2

The DOE-2.1C program simulates the thermodynamic behavior of a building [1, 2]. It does this by approximately solving the mathematical relations describing the non-linear flows of heat through and among all the building's surfaces and enclosed volumes, driven by a variety of heat sources, both internal and external. Hour-by-hour calculations are performed in four sequential modules, LOADS, SYSTEMS, PLANT, and ECONOMICS. In the LOADS module, the instantaneous heating and cooling loads are calculated and then modified to incorporated dynamic effects of thermal mass through the use of weighting factors. These loads are calculated at a single space temperature setting. The SYSTEMS module calculates the heat extraction/addition of the coils while reconciling the varying temperature set points and humidity levels from actual system operation

and schedules. Fuel requirements of the primary heating and cooling equipment and pumps are determined in PLANT, while annual operating energy and life-cycle building costs are evaluated in ECONOMICS.

The program was employed here not only because of the variety of HVAC systems and control options available, but also because of the demonstrated accuracy of the code in numerous validation efforts and relative ease of use.

ASEAN Weather Data

In general, the weather pattern for ASEAN countries is quite uniform throughout the year, compared to temperate climate zones with distinct summer and winter seasons. Hot and humid air masses known as "monsoons" dictate the weather patterns. The countries closer to the equator receive two different monsoon seasons originating from different compass directions, while those further away from the equator generally only experience one. Therefore, some distinctions can be made between climates in the region. The climate tends to be hot and humid all year long, with monthly average wet-bulb temperature varying from 75.5 °F to 78.4 °F in Singapore and 74.1 °F to 76.9 °F in Kuala Lumpur, Malaysia. Other areas have more seasonal weather patterns that are humid during the wet season but have a cooler, drier season. In Chiang Mai, Thailand, the monthly average wet bulb temperature in the wet season ranges from 73.5 °F to 74.3 °F from April to September, but drops to 63.9 and 62.1 °F in December and January, respectively, and stays below 68 °F through March. The rest of the metropolitan area climates in the ASEAN region fall between these extremes. However, since a concentration of cities occurs near the tip of the Malay peninsula (principally Kuala Lumpur, Singapore, and Jakarta), we selected Kuala Lumpur as our representative site.

For the purposes of this study we used temperature, humidity, and wind-speed data from Kuala Lumpur to represent a typical hot humid climate. Solar gains play an important role in the building cooling loads, and obtaining good solar data was one of the objectives of research undertaken in the ASEAN region.* Earlier research demonstrated the inadequacy of using the DOE-2 cloud-cover model as a substitute for actual measured data in the ASEAN region [3]. Within the region, the only city with reliable and verified solar data consistent with the requirements of DOE-2—at the time this study was conducted (1988)—was Singapore. Because of the close proximity of Kuala Lumpur to Singapore, Singapore solar data was used to simulate the solar loads.

Malaysia Building Module

Simulation of an office building was chosen to provide a basis for evaluation of different types of cooling systems. Office buildings are the most representative commercial building type in ASEAN using central systems. Hence, we used a prototype office building, originally developed for analysis of standards in Singapore [4], but later adapted to Malaysia [5]. Features of the building will be summarized here, but the interested reader can find more detail on the building in the above references.

The building is a ten-floor office complex with a total of 55,000 ft^2 (5,150 m^2). A central chilled water VAV system is used with central fans sized for 70,000 cfm (32.7 m^3/s) with about 230 tons (825 kW of cooling) provided by a centrifugal chiller. Air is supplied to the zones at a minimum of 55 °F (12.8 °C) (the actual supply temperature being that which adequately cools the warmest zone at design flow rates) through VAV boxes with minimum stops at 50% of design flow. Temperatures are controlled by zone thermostats set at 75.2 °F (24 °C) during occupied hours and set-up to 99 °F (37 °C) otherwise. Fans are forward-curved centrifugal design, controlled by means of inlet vanes. No economizer cycle was used, because, unlike temperate climates, economizer cycles are not feasible in hot, humid ones.

These system options were varied both for this and different system types. The systems with central fans include: single-zone, constant-volume; multiple-zone, constant-volume; variable

* See Chapter 5 in this Volume for a discussion of the Indonesian weather data-gathering activities.

air volume; ceiling bypass VAV; powered induction unit; and two-pipe powered induction, all without reheat. A two-pipe fan coil system with no central fan was also modeled.

System-Type General Descriptions

Here we describe the systems modeled, their typical operating strategies and control settings. More complete explanations are found in the *DOE-2 Reference Manual* [2], *ASHRAE Systems Handbook* [6], and McQuiston [7]. We will identify and henceforth refer to the system types with the mnemonic codes used in DOE-2.

Single Zone Reheat (SZRH):

This is a constant volume system with a central fan and cooling coil that responds to meet the cooling load in a specified control zone. All other zones are subordinate to the control zone in terms of the supply-air temperature with no reheat available. Although in the United States, these systems are usually installed with reheat capability, which would undoubtedly enhance zone temperature control and comfort conditions in Southeast Asia, the energy and cost penalty is considered too high for wide application in ASEAN countries. When these systems are installed without reheat, then some overcooling typically occurs.

Reheat Fan System (RHFS):

This system is also a constant volume system with a central fan and cooling coil, but is a multi-zone system. That is, the supply-air temperature is set according the logic of one of several options, including responding to the warmest zone's needs, which will change throughout the day. Again, no reheat is simulated with this system.

Variable Air Volume System (VAVS):

A variable volume central fan and cooling coil provide supply air according to the particular cooling control strategy followed. Zone control is achieved via individually-controlled VAV terminal boxes in each space which control air-flow by throttling the primary supply air down to a specified minimum level.

Ceiling Bypass Variable Volume (CBVAV):

This system is similar to the VAVS system, except that the primary air is supplied at constant volume and the VAV terminal boxes behave somewhat differently. When throttling of the primary air is called for, the correct amount of air is injected into the space and the excess is rejected to the plenum.

Powered Induction Unit (PIU):

The PIU system is yet another variation on the basic VAVS system. There are both parallel and series types, but here we consider only the latter. The terminal box is fitted with a small fan running at constant speed which draws air from two sources, the primary supply air stream and a secondary source. The secondary source is typically a core zone return air stream using standard VAV boxes. The proportion of air drawn from each source is dependent on the cooling demand. The function of this system is to provide warm air from interior zones (thus saving reheat energy) and to increase the air movement in zones normally served by VAV boxes. Obviously, with no reheat being used anyway, the benefits of this system come in increased comfort.

Two-Pipe Fan Coil (TPFC):

This is an all-water terminal system consisting of coil and fan located in the zone. Temperature control is achieved by throttling the flow of water through the coil. The fan operates at constant speed across a low static head.

Fan coil units are commonly used in hotel rooms and other zone cooling applications. Typical fan coil installations include reheat to allow control of both the sensible and latent cooling load for the systems. When the reheat coils are omitted, either the zone temperature is controlled by raising the effective coil temperature, thereby decreasing cooling with lighter loads but losing dehumidification, or the coil is kept cold, thereby maintaining dehumidification but significantly overcooling.

Two-Pipe Induction Unit (TPIU):

This is a zonal air-water system, in which cooling is provided at both the system and zone levels. Primary supply air is cooled and de-humidified and delivered to an induction box located in each space. Room air is induced over a zone coil providing additional sensible cooling and mixed with the primary air. A key parameter is the ratio of induced room air-to-primary air simulated.

SYSTEMS TYPICAL TO THE ASEAN REGION

Efforts were made to identify the types of mechanical system that are commonly used in ASEAN countries. A limited number of questionnaires (~30) were sent to leading building-energy professionals in each country requesting estimates of the types of systems and the configurations commonly used based on the engineering judgment of the respondent. Approximately 65% of the commercial buildings use systems with central fans and ducts. Of these, 35% have VAV systems, and the rest have constant volume air distribution systems. Of the 35% of buildings with VAV systems, a little over half used inlet vane fan control and there is some use of variable speed drives (~8%) with the rest using discharge dampers. Zone control is achieved by on/off controls (38%) and thermostats (62%). Typical thermostat settings are in the range of 75.2 °F (24 °C). Very few buildings use return fans.

Estimates indicate that 35% of the commercial buildings use systems with no central fan. Split-type systems are the most popular air conditioners of this category, and are found in 38% of these buildings, followed by window units (24%) and two-pipe fan coil units (22%), the rest being rooftop units.

Most of the ventilation air is supplied through fixed outside-air dampers, with ventilation rates designed for 12 cfm/person (5.7 liter/s-person) on the average. Economizer cycles and reheat are simply not used.

Packaged air-conditioners are commonly used in retail and small office buildings. Chilled water systems are used for larger buildings. In hotels, central fan systems are used for meeting and common areas and two-pipe fan coil units are used in guestrooms. Older office buildings tend to have single zone constant volume systems, while newer construction utilizes VAV systems in large buildings and packaged units in 5-story and smaller office buildings.

Design trends in the ASEAN region, based on responses to the above questionnaire, are in the area of VAV systems, high-efficiency chillers (centrifugal and screw-type), variable speed drives for pumps and fans, and more sophisticated controls.

SIMULATION RESULTS

We evaluated HVAC system performance under various assumptions to establish the sensitivity of annual energy consumption and comfort provision. These assumptions included: ventilation rate, increase in infiltration, economizer cycle, control strategy to determine supply-air temperature, zone thermostat set point, cooling coil control strategy, system over- and under-sizing, fan control strategy, internal gains and daylighting, precooling, night ventilation, and zoning. We combined several effective measures together to establish a high-performance case. The different system types were then run under various conditions and compared to the base case.

Base Case System Performance

The base case system against which other systems and alternative operating strategies are compared is a VAV system with no economizer cycle or reheat, inlet vane fan control at a static pressure of 11 cm-H_2O (1080 Pa), a minimum fan volume ratio of 0.5, a supply air temperature of 55 °F (12.8 °C), a minimum outside air quantity of 10 cfm/person (4.7 liter/s-person), and thermostat set points of 75.2 °F (24 °C) daytime and 98.6 °F (37 °C) nighttime, and represents "typical" conditions based on questionnaire responses and engineering judgement.

The 376 MWh of chiller cooling energy constitutes over 40% of the total; lighting at 328 MWh uses 36%; fans at 136 MWh use 15%; and the rest is miscellaneous equipment. The building peak electrical demand of 354 kW occurs Monday February 25 at 3 P.M. The control of space

temperatures is good. With a zone thermostat setting of 24 °C and throttling range of 1.1 °C, the average zone temperature during system operating hours was 75.2 °F (24 °C) and only 4% of the time was the temperature beyond the throttling range in some zone. The ability of the VAVS system to handle the high humidity conditions is also quite good (see Table 9-3). More than 99% of the time the relative humidity of the return-air is within 41-50%. Plant loads were met 99.9% of the hours in the one-year simulation period.

Sensitivity Analysis of Base-Case System Performance

The following sensitivities on the assumptions in our base case building are shown in Table 9-1.

Fan Control:

The base case assume inlet vane control of supply fans. Fan control using discharge dampers increases fan energy use by 38% and total energy usage more than 7% over inlet vane control. Consequently, discharge dampers are seldom used in commercial building applications to control fan volume. Application of variable speed fan control saves 13% of fan energy and 3% overall. The new variable-frequency motor drive controllers provide opportunities to take advantage of these energy savings. Building peak power is unchanged for variable-speed fans but increases 2% with discharge dampers.

Pre-Cooling and Night Ventilation:

Pre-cooling the building prior to occupancy one hour earlier than usual raises the total energy budget by 2%, but saves 2% of the peak power. Starting the pre-cooling 2 hours earlier increases total energy by 3% and lowers peak energy both by 3%, while 3 hours of pre-cooling results in a 5.3% energy penalty for a 4.5% peak savings.

An earlier study [8] identified Mondays as the most likely day for a peak load to occur due to the "charging" of building thermal mass over the weekend when cooling systems are normally turned off. Therefore, under a scenario where one hour of pre-cooling was undertaken on Mondays only, peak power went down 2%, with no significant increase in energy use. Lengthening the pre-cooling period on Mondays had little benefit in terms of reducing the building peak but increased total energy penalty.

Starting the fans *alone* prior to occupancy in an "optimal" fashion (that is, by specifying that they be turned on only when there is just enough time to cool the majority of the zones down to their day-time set-points and no sooner) has the identical end result as the one-hour pre-cooling scenario.

Due to the fact that during the fan-off hours, zone temperatures averaged 3.5 °C higher than outdoor temperatures, it seemed that night ventilation might be a viable strategy for reducing peak power due to morning "pull-down" under certain conditions (i.e., provided there was a net enthalpy loss). A control strategy, whereby the building was mechanically ventilated with the system fans when the indoor-outdoor temperature difference was at least 5 °F *and* some zone was above a threshold temperature setting, was simulated. With a threshold temperature of 75.2 °F (the base case cooling set-point), the building peak lowers by 3.3% as does the chiller sizing by 3.6% and cooling energy use by 9%. However, fan energy use increases by 146% leading to 20% greater total energy than the base case. Humidity conditions also increase to 11% of the time in the 51-60% RH range. If, however, the threshold is raised to 85 °F, which is about the average zone temperature during fan-off hours for the base case, peak savings of 3.3% still obtain but at a smaller total energy penalty of 9%.

Supply Air Temperature Control:

The control strategy used in the base case sets the supply-air temperature at the level were the *warmest* zone is adequately cooled at the design air-flow rate. The supply-air temperature was limited to a minimum 55 °F. When the supply-air temperature was controlled at a *constant* 55 °F, the resulting performance was identical to the base case. Therefore, during every operating hour, some zone demanded at least 55 °F air in the base case strategy. In either case, the temperature condition in other zones is maintained by air-flow modulation of each VAV box.

When the supply-air temperature is dictated by the outside-air temperature under *reset* control logic, it is difficult to maintain temperature conditions in the zones. However, out of the many combinations of supply- and outside-air temperatures examined, a few combinations do hold zone conditions within the throttling range *and* save 2% energy and 3% peak power.

Tamblyn [9] describes the advantages of using low supply-air temperatures in hot and humid environments. Lowering the minimum supply air temperature set point to 50 °F and 45 °F Interrupt determines the actual setting, resulted in total energy savings of 2.2% and 3.4%, respectively. At 45 °F, the 28% savings in fan energy is offset by an increase in chiller usage to give an net 3.4% annual energy savings and there is an additional peak power reduction benefit of 5.7%. This is primarily due to reduction in the fan energy that offsets the additional chiller power required to produce the lower temperatures. Return air humidity is also reduced with over half of the hours in the 31-40% RH range. The latent coil capacity increases with lower supply-air temperatures. Since the latent load is relatively high in the ASEAN region, this strategy is promising for reducing humidity levels as well as saving energy. However, as Guntermann [10] points out, this necessarily results in low air motion in spaces served by VAV systems, often leading to comfort complaints. Care must be exercised in balancing the factors that affect human comfort while pursuing energy conservation.

Alternatively, raising the minimum supply-air temperature to 60 °F increases total and peak 4% and 5%, respectively, and leaves loads unmet 25% of the time. In addition, humidity control is lost somewhat, with all hours registering return-air humidity of 51-60% RH.

Zone Thermostat Set-Point:

Increasing the zone thermostat set-point for cooling from 75.2 °F to 77 °F saves 3% total energy and 4% peak power; from 75.2 °F to 79 °F saves 6% and 8%, respectively; and from 75.2 °F to 81 °F saves 8% and 12%.

Internal Gains and Daylighting:

Cooling systems are designed with a particular split between latent and sensible cooling. In ASEAN climates, the latent loads are the primary concern. Internal gains typically make up a large portion of the sensible load in commercial buildings. As measures such as more efficient equipment and lighting are introduced, the sensible cooling load in the zones may be reduced significantly increasing the importance of latent loads. This may adversely affect the performance of certain system types.

For the case of efficient electric lighting, for instance, lowering the lighting power density from 1 to 2 W/ft^2 saves 9% of the cooling energy, 23% of building total energy, and 20% building peak power. Likewise, an increase to 4 W/ft^2 consumes 18% more cooling energy, 47% more total energy, and a 38% higher building peak load. More than a third of the time, loads in some space go unmet.

Daylighting has been identified as a major option of reducing energy use in commercial buildings in tropical climates. When properly controlled, daylighting reduces the electric lighting power requirement, but may increase the sensible heat gain in the perimeter zones. Daylighting can be used to reduce the lighting loads. A continuous-dimming control scheme saves 19% of total energy.

Ventilation and Infiltration:

The latent load in ASEAN buildings is very dependent on the rate of ventilation and infiltration. The various system types have different capabilities for dealing with latent loads. Ducted systems bring all ventilation air past the cooling coil where the supply air is dehumidified to near the dew point temperature of the coil. If the coil temperature is set upward (for instance under the supply-air control scheme responding to the warmest zone), there can be a loss of dehumidification. Fan coil systems, on the other hand, must do their dehumidification in the zones where ventilation and infiltration air mixes with the zone air. This causes the humidity of the air entering the coil to be less. Consequently, there is less dehumidification.

Simulation of the operation of an economizer cycle where outdoor air is used when its temperature or enthalpy is below the return air conditions demonstrated no benefit in the latter case and increased total energy by 5% in the former.

Increasing outside-air quantity during system operating hours from 10 to 30 cfm/person increases total energy by 16%, cooling energy by 37%, fan energy by 6%, chiller size-requirements by 38%, and building peak by 18%.

Infiltration introduces outdoor air directly into the perimeter zones. If infiltration is large, one would expect humidities and zone latent cooling loads to be greater in the perimeter zones. However, in our simulations infiltration occurs only during fan-off hours and actually shows a very small depression in energy usage when increasing the infiltration rate from 1 to 2 air changes per hour (ach).

Impact of System Sizing:

Our base case sizing methodology uses endogenous DOE-2 routines which size fans and coils to meet maximum non-coincident zone loads and chillers to meet the peak load. It has been suggested that it is a grave design error to oversize air-conditioning systems in hot and humid conditions, because of the loss of latent cooling, and that, in fact, slight undersizing is preferable [10]. We tested the liability of oversizing the fans and chiller by 25%. A small (3%) energy penalty results, with little effect on return-air humidity impact. Undersizing the fans and chiller by 25% shows less than 1% savings and a significant loss of temperature control (i.e., over half of the time some zone's temperature is out of its throttling range).

Over-sizing of the air-handling unit (AHU) by *only* 25% has the effect of raising total energy consumption by 2% and shifting the humidity conditions upward such that 7% of the time it is above 50% RH, as opposed to virtually no hours above 50% RH for the base case. Undersizing the AHU behaves similarly as above.

Sizing of the system equipment to meet the maximum coincident building demand (instead of the default assumption of sizing to meet each zone's maximum load regardless of when it occurs) increases consumption only slightly, but leaves loads unmet 10% of the time.

Sensitivity to Zoning:

Separate variable temperature systems have greater flexibility than a single system. As the temperature is set upward, however, there is a loss of dehumidification. The sensitivity to zoning was tested by running simulations with separate systems serving zones with core, east, west, south, and north orientations. Total and building coincident peak energy use falls 5.6% and 7.1%, respectively, mostly due to the 28% reduction in fan power due to the lower static pressure accompanying shorter duct runs. Cooling energy savings were 3.5%. The humidity balance changed, though, with 11% of the operating hours showing return air RH greater than 50%.

High Performance Case:

Combining several of the measures together in one high-performance case shows significant savings. It is usually necessary to run a separate simulation because invariably the savings are less than the sum of the savings for each measure run individually. This is because of interaction among conservation measures. In this case, we combined variable-speed fans with raised space thermostat-settings (81 °F) and supply-air temperature (45 °F) and one hour of pre-cooling on Mondays. All other variables remained as in the base case. Total energy consumption goes down, 14% while the electrical peak is reduced 16%. The total energy savings are achieved through 13% and 58% cooling and fan energy reductions, respectively. Humidity levels are very low, however, with the majority of hours below 40% RH. Building occupants accustomed to high outdoor humidity levels may find these conditions unacceptable.

Comparisons Among System Types

In this section, we compare the performance of the base case VAV system with that of six other generic systems. Table 9-2 shows the annual energy breakdown and peak for the various systems modeled. For the more commonly installed systems in the ASEAN region, we also

discuss sensitivities of the input assumptions, focussing on those instances where the results differed from those of the base case VAV system or where a significant change in performance was exhibited.

Two-Pipe Fan Coil (TPFC):

This system uses 16% less cooling energy, 59% less fan power, and 15% less total energy than the VAVS. Because it is not necessary to move air through long ducts, the pressure drops are much smaller. Chillers are also sized smaller by 13% and building peak electrical load is 18% lower. However, this comes at the cost of a significant loss of humidity control. Only 6% of the time is the relative humidity below 50%; 29% of the time the relative humidity is above 60%. The building electrical peak demand registered on June 10 at 4 P.M. (again on a Monday) and was 291 kW, the lowest of all systems.

The pre-cooling strategy only makes the humidity matters worse. Raising the thermostat set-point only exacerbates the humidity situation. For instance, with a thermostat set-point of 81 °F there is a significant energy savings of nearly 10%, but the relative humidity is always above 50% and 70% of the time it is above 60% RH. Running the coils colder helps to alleviate the high humidity conditions somewhat by increasing dehumidification, however, with no energy penalty. With a 45 °F supply-air temperature, the RH is above 60% only 6% of the operating hours and RH 50% or below 71% of the time.

Single Zone Reheat (SZRH):

This system responds only to one zone specified as the control zone (in this case an east-facing zone on a middle floor), and all other zones are conditioned as the control zone with no reheat capability. It uses 10% more energy than the VAVS system, mostly due to the 50% increase in fan power. Chiller energy use was higher by 4% and the chiller sizing greater by 6%. The peak day in terms of total electrical demand was June 10 at 4 P.M. with 365 kW, though February 22 was a close second. Humidity control is almost as poor as with the TPFC system, with only 89% of the hours above 50% RH and 21% of the hours above 60%. Shifting the control zone to one with a different orientation has the effect of improving the performance of the system. For the case where the control zone was west-facing, a 2.4% overall savings occur with no change in the building peak, improved temperature control, and only a slight degradation in humidity control. When the control zone is shifted to a south-facing zone, a slightly more modest 1.8% savings accrue.

Reheat Fan System (RHFS):

This system under the base control scheme reponds to the warmest zone, and all other zones are similarly supplied with cooling. As with the SZRH system, no reheat was made available. This is the highest energy user of all, 11% more total energy, and 4% higher peak load than VAVS. However, zone temperature control is maintained at all times in the simulations and humidity control is improved over SZRH, though not as well as VAVS.

The strategy of under-sizing the system by 25% by reducing the design air-flow and chiller capacity has a positive impact on energy consumption *and* humidity control. Total energy goes down 6%. Seventy-eight percent of the time the humidity is below 50% RH (as compared to only 11% in the base RHFS strategy). The explanation is that the chiller operates at near capacity, where the efficiency is highest, for a much larger portion of the operating hours (in the 90-100% part load range instead of 70-80% part load range). A particular configuration of the RHFS system, whereby multiple systems each serving zones of a particular compass orientation are run, produces significant savings: total energy 10.4%, peak power 9%, fan energy 31%, and cooling 10%. Although the savings are great compared to the base RHFS, the energy use level is only slightly better than the base VAV system. Humidity conditions were unfavorable too, with 82% of the time the return air over 50% RH, 23% of the time above 60% RH, and 7% of the time above 70%. Variations in other system operating parameters produce similar *savings* (in percentage terms) as the with VAV system but always use more energy than other systems.

Powered Induction Unit (PIU):

This system provides a constant volume of air to each zone, inducing plenum air when less cool primary air is needed to handle the load. This system is used in the perimeter zones with standard VAV boxes in the core zone. The PIU system uses 3% more total energy than the VAV system, 6% more each in the chiller and fans. Peak power demand is 2.5% more as well. Humidity control is comparable to the VAV system.

Ceiling Bypass Variable Volume (CBVAV):

This system throttles zone air-flow when full cooling is not needed by diverting flow into the plenum space above the zone. The energy performance is identical to the RHFS, but with much superior humidity control.

Two-Pipe Induction Unit (TPIU):

This system is a mixed air-hydronic zonal system providing some cooling and humidification at the system level. The constant volume of primary air is mixed with 2.5 times as much induced secondary air at the terminal unit. The energy performance is second only to the other zonal system considered here (e.g., TPFC). It uses 6.7% less total energy, 11.3% less peak power, 32% less fan power, and 4.8% less energy to run the chiller. The primary air supply maintains good dehumidification of the outdoor ventilation air, while the induction unit maintains good mixing of air in the zones and good zone temperature control. What distinguishes this system from the TPFC system is that the return-air relative humidity is virtually always in the 41-50% range.

Hourly Profiles

It is often helpful in interpreting the annual results to look at hourly profiles within the building. In Figures 9-1 through 9-6 we compare the SZRH, VAVS, and TPFC systems on two separate days. August 15 was chosen arbitrarily, whereas February 22 is the peak day for the two central system types. We are primarily interested in the space conditions and cooling loads. Four variables are plotted over the course of the day: air flow, dry-bulb temperature, humidity ratio, and cooling coil load. For the two central system types, the space conditions are actually *return-air* conditions and thus represent a weighted-average of individual-zone conditions across the building, whereas the fan coil results come from an arbitrarily chosen zone. So that systems can be directly compared, the air-flow and energy quantities are expressed on a per unit floor area basis and the ordinate range is the same for each day simulated.

Fan coil systems have trouble handling latent loads. As shown in Figure 9-4, during the morning, humidity ratios reach almost 14 g moisture/kg dry air. As the coil responds to increasing sensible loads throughout the day, the humidity is eventually driven down to acceptable levels.

The SZRH system displays a curious transient response to the morning start-up load by first cooling at near-peak capacity in the first hour, then throttling way back in the second hour, and finally recovering in the third hour and beyond to a more stable climb in coil load response. The VAV system behaves similarly but reduced considerably and with little impact on temperature or humidity. It is unclear whether real buildings with these systems would experience a similar phenomenon or whether this is simply a simulation artifact.

By maintaining lower coil temperatures and by modulating capacity by reducing the air flow through the cooling coils, the VAV system shows superior moisture control, maintaining humidity ratio at or below 9 g/kg.

Temperature control is similar between the system types, although the SZRH system maintains somewhat lower levels. Again, since the central systems report return air conditions, individual zones will exhibit more variable behavior.

Load Shapes

The pattern of electric loads in buildings is of interest both to utilities, which see rising electricity demand on the system, and building operators who must pay demand charges for electricity. One such representation is the load duration curve (LDC) which describes the number of hours

total building electrical demand was at or above a given level. In Figure 9-7, we plot two curves, one is the base case LDC and the other is the earlier mentioned high-performance case. Both buildings have a fairly "flat" load shape at the higher demand level dropping off precipitously at 30% to 35% time fraction. Beyond the 40% time fraction the building is unoccupied and operates at minimal demand. The high-performance case shows less opportunity for peak-shaving due to the flatter slope at high demand.

Cooling load can be similarly plotted and is shown in Figure 9-8. The cooling load never goes below 110 (387 kW) tons during the operating hours. However, only 5% of the time does the cooling load go above 210 tons (739 kW). If conservation measures or load shifting could preempt the need to meet those loads for only 5% of the operating hours, a 12% cooling-peak savings results.

The chronological daily electrical load pattern is helpful for knowing when demand occurs during the day. Figure 9-9 shows an *average day* profile for electrical demand. This is determined by summing the electricity consumption by hour of the day over the whole year and dividing by the total to get the demand frequency. It is curious that the peak demand frequency occurs at noon when the instantaneous peak actually occurs later in the afternoon. This is probably because the plot includes Saturday morning operation over the year. An interesting plot would be the demand profile over the *peak* day but is not shown here.

To be most meaningful to the utility analyst, the coincidence of building loads with the electric utility's system loads has to be established explicitly. This allows a determination of the value of any load reduction (or increase) to the utility. Since our analysis is regionally based (and not focussed on a single utility service area), we have ignored this effect here.

CONCLUSIONS

- Variable air volume systems clearly have the best combination of low energy use and maintenance of comfortable zone temperature and humidity levels.
- Constant volume systems have significantly higher energy use than the other systems, and without reheat can give significant overcooling of the space as well as producing high space humidity conditions.
- Two-pipe fan coil units have the lowest energy consumption primarily due to fan energy savings. The low latent cooling capacity adversely affects humidity control and these systems performed poorly during morning pull-down periods.
- Permitting excess outdoor air into the building either by the use of an economizer cycle or high ventilation rates carries a significant energy penalty.
- The power level for internal gains has a direct impact on total, cooling, and fan electrical energy use.
- The easiest measure for generating savings is to increase the thermostat setting during the daytime. Savings in system equipment sizing, energy, and peak power all accrue at no cost.
- Lower supply-air temperatures have significant benefits in reducing fan and building power requirements.
- Control strategies such as pre-cooling, for operating the system during unoccupied hours can save on peak power at the expense of higher energy costs. The structure of local electricity tariffs will determine whether the trade-off is worthwhile.
- A combination of system conservation measures incorporated into one building saved 14% of total energy and 16% on peak power. Clearly, proper air-conditioning system configuration and operation has comparable savings potential to the more frequently cited envelope and internal gain conservation measures.
- The nature of the savings, be it energy, peak power, or equipment sizes, are different for each measure. Depending on whether one is trying to economize on first cost, energy costs, or demand charges dictates the choice of technologies and control strategies.

FUTURE WORK

In view of the preliminary nature of this work it is fruitful to suggest areas of further research pursuit, namely:

- A careful identification of *actual* air-conditioning practices in ASEAN buildings is needed. Energy audit and survey activities in ASEAN should help in accomplishing this. "Benchmarking" the performance of the stock air-conditioning systems clarifies the conservation potentials indicated here.
- Moisture conditions within the spaces are a large concern in the ASEAN region. The daily cycle of moisture adsorption/desorption is not well understood in buildings. Measurements indicate that the effect may be large [12]. Part of the auditing effort in the ASEAN regions should attempt to characterize the success or failure in dealing with the high ambient humidity levels. Humidity also presents a significant modeling challenge. DOE-2, for instance, does not handle adsorption/desorption processes between room air and furnishings, and this may skew results. Handling the mass transfer processes rigorously entails a large increase in the computational effort. MAD/TARP, developed at the Florida Solar Energy Center, is a model with these capabilities. Analysis of moisture impacts is a current area of research in the United States [13].
- Collection of cost data on system components (including labor costs), and electricity and fuel rates should be gathered in ASEAN countries to facilitate economic analysis. Because of the distribution of costs between capital and labor are different in ASEAN countries from the United States, analysis based on U.S. values can be misleading.
- In this work we analyzed the load impacts of measures which are employed primarily for saving energy. There are situations, however, where it might be advantageous to undertake cooling strategies, such as thermal energy storage, that shift loads to other time periods without saving any energy (or even at the expense of somewhat higher energy use). These situations usually entail either time-of-use electricity rates with significant price differentials between on- and off-peak, or high demand charges with ratcheting clauses.

REFERENCES

1. Curtis, R.B., Birdsall, B., Buhl, W.F., Erdem, E., Eto, J., Hirsch, J.J., Olson, K.H., and Winkelmann, F.C., "The Use of DOE-2 to Evaluate the Energy Performance of Buildings," in *Proceedings of the ASEAN Conference on Energy Conservation in Buildings*, Singapore, 29-31 May 1984, pp. 1-23.
2. Building Energy Simulation Group, *DOE-2 Reference Manual, Version 2.1C,*, Lawrence Berkeley Laboratory Report LBL-8706-Rev. 4, May 1984.
3. Busch, J.F. and Deringer, J.J., "A Building Envelope Energy Standard for Malaysia," *Proceedings of the ASHRAE Far East Conference on Air Conditioning in Hot Climates*, Singapore, September 3-5, 1987. Also published as Lawrence Berkeley Laboratory Report LBL-23280.
4. Turiel, I., Curtis, R., and Levine, M.D., "Parametric Energy Analysis in Support of Singapore Energy Conservation Standards for Commercial Buildings," *Proceedings of the ASEAN Conference on Energy Conservation in Buildings*, Singapore, 29-31 May 1984. pp. 195-265.
5. Deringer, J.J. *et al.*, "Energy and Economic Analysis of Commercial Building Standards in Malaysia," *Proceedings of the ASHRAE Far East Conference on Air Conditioning in Hot Climates*, Singapore, September 3-5, 1987. Also published as Lawrence Berkeley Laboratory Report LBL-23281.
6. American Society of Heating, Refrigeration, and Air-Conditioning, *ASHRAE 1984 Systems Handbook*, Atlanta, GA, 1984.
7. McQuiston, F.C. and Parker, J.D., *Heating, Ventilating, and Air-Conditioning: Analysis and Design*, 2nd ed., John Wiley & Sons, New York, 1982.

8. Eto, J.H., "Cooling Strategies Based on Indicators of Thermal Storage in Commercial Building Mass," Presented at the 2nd Annual Symposium Improving Building Energy Efficiency in Hot and Humid Climates, College Station, TX, September 24-26, 1985. Also published as Lawrence Berkeley Laboratory Report LBL-19912.

9. Tamblyn, R.T., "Wringing the Moisture out of Buildings and Lowering Cost with Low-Temperature Air and Cool Storage," *Proceedings of the ASHRAE Far East Conference on Air Conditioning in Hot Climates*, Singapore, September 3-5, 1987.

10. Guntermann, A.E., "VAV System Enhancements," *Heating, Piping and Air-Conditioning*, August 1986, pp. 67-78.

11. ARMM Consultants Inc., *Air Conditioned Buildings in Humid Climates: Guidelines for Design, Operation, and Maintenance*, Prepared for Southern Division, Naval Facilities Engineering Command, P.O. Box 10068, Charleston, SC 29411, April 1980.

12. Martin, P.C, and Verschoor, J.D., "Investigation of Dynamic Latent Heat Storage Effects of Building Construction and Furnishing Materials," Oak Ridge National Laboratory Report, ORNL/SUB/86X-22016-C, Oak Ridge, TN, 1986.

13. Florida Solar Energy Center, *Five-Year Plan for Solar Cooling Research Project*, Cape Canaveral, FL, April 1987.

ACKNOWLEDGEMENTS

This work was supported by US Agency for International Development, USAID, through the U.S. Department of Energy under Contract Number DE-AC03-76SF00098.

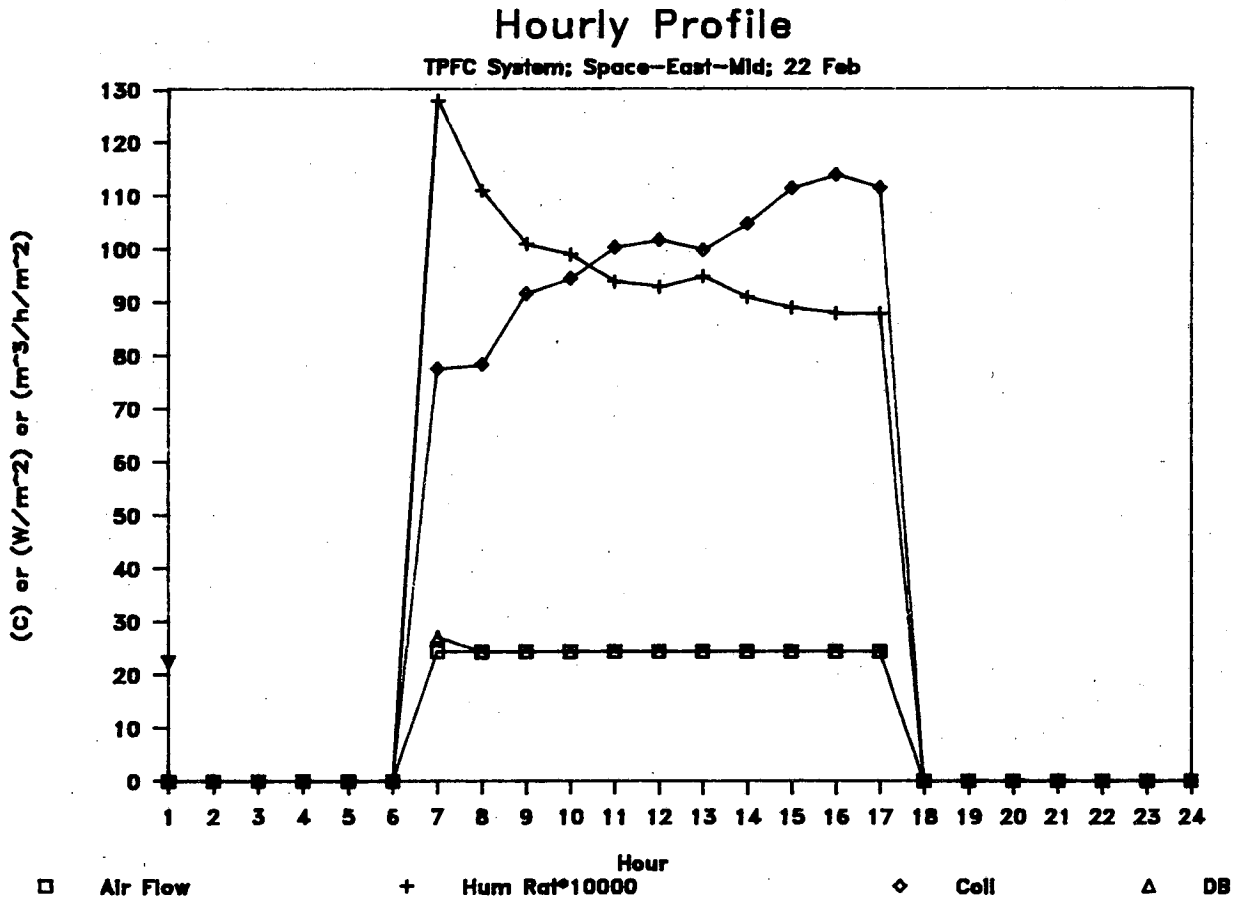

Figure 9-1. Hourly Profile for a Two Pipe Fan Coil (TPFC) System showing zone humidity ratio, temperature, coil air flow, and cooling load on a typical day (22 February 1985).

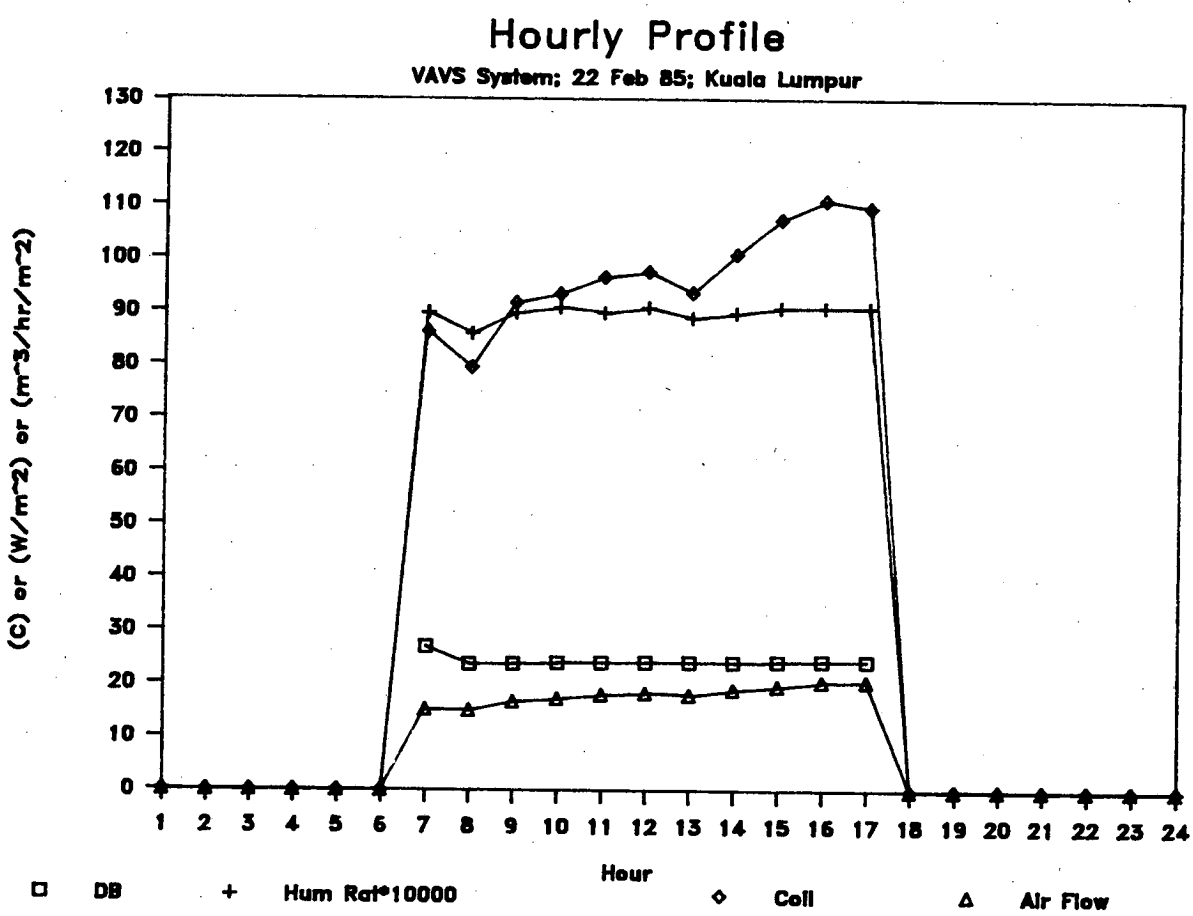

Figure 9-2. Hourly Profile for a Variable Air Volume (VAV) System showing return air humidity ratio and temperature and system air flow and cooling load on a typical day (22 February 1985).

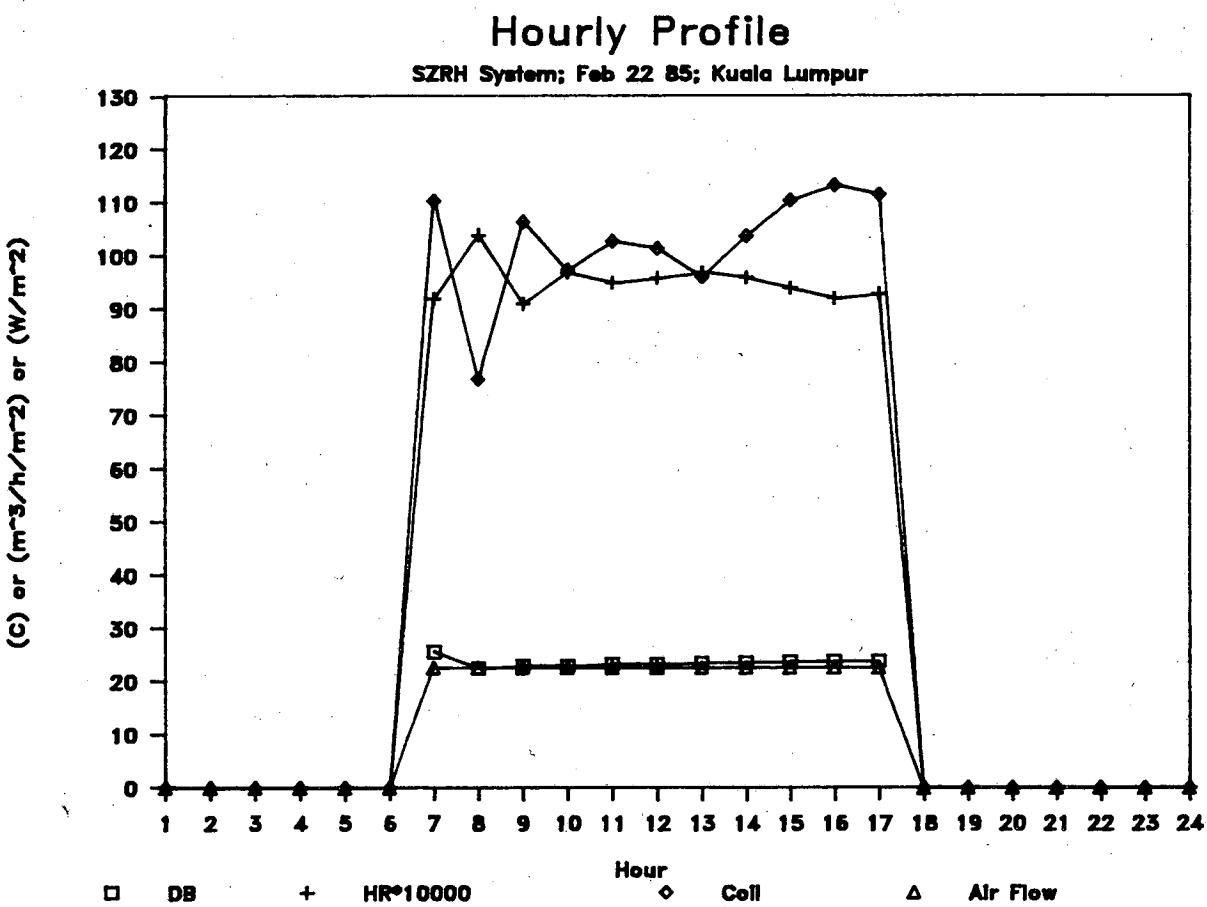

Figure 9-3. Hourly Profile for a Single Zone Reheat (SZRH) System showing return air humidity ratio and temperature and system air flow and cooling load on a typical day (22 February 1985).

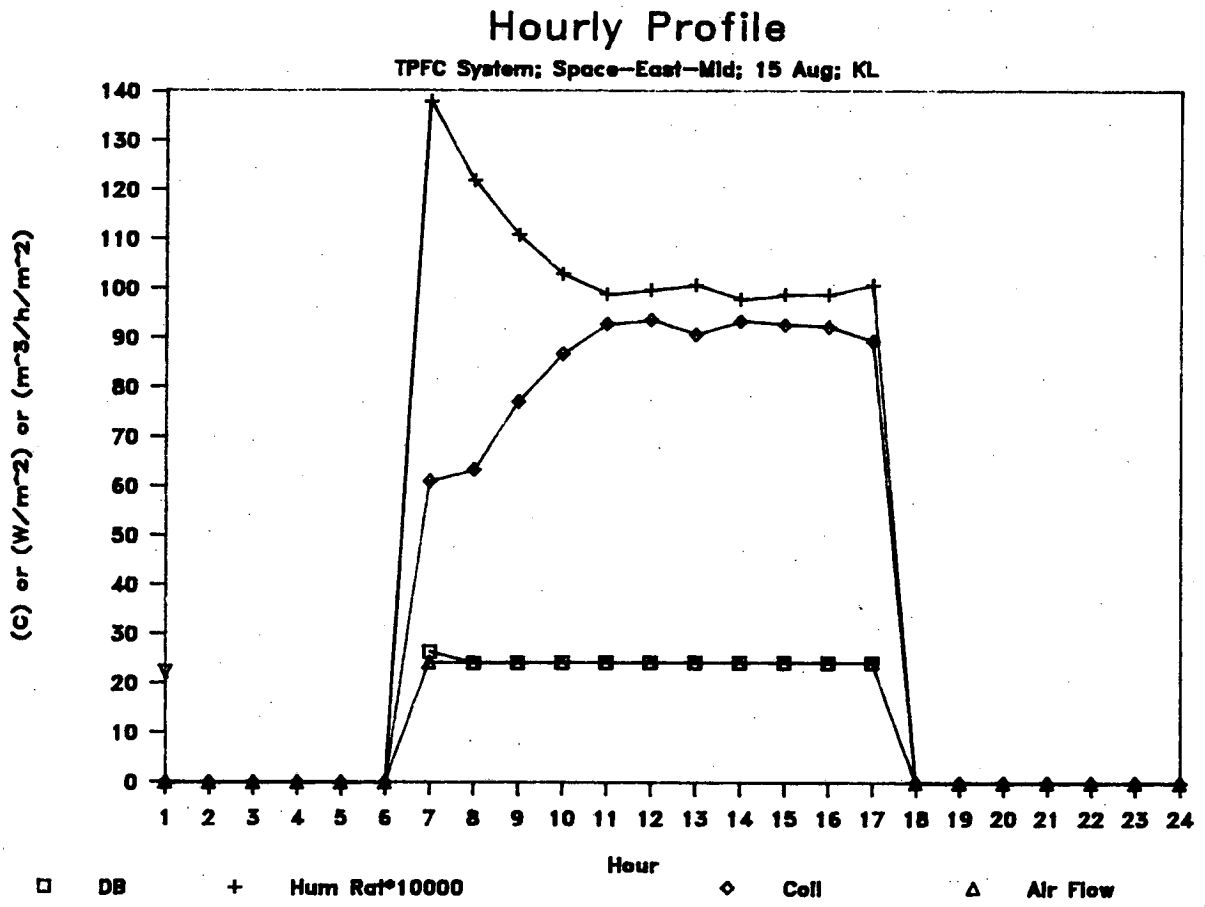

Figure 9-4. Hourly Profile for a Two Pipe Fan Coil (TPFC) System showing zone humidity ratio, temperature, coil air flow, and cooling load on a peak day (15 August 1985).

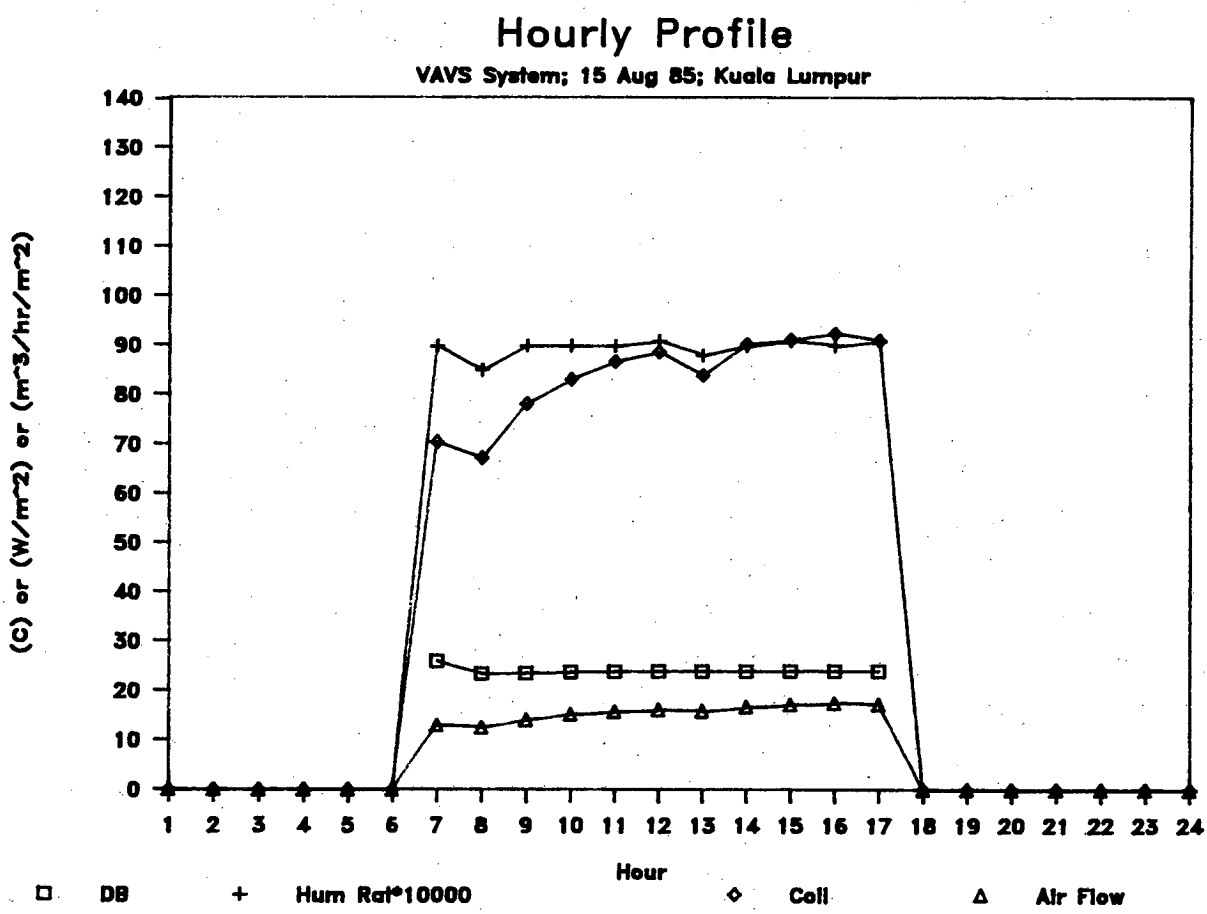

Figure 9-5. Hourly Profile for a Variable Air Volume (VAV) System showing return air humidity ratio and temperature and system air flow and cooling load on a peak day (15 August 1985).

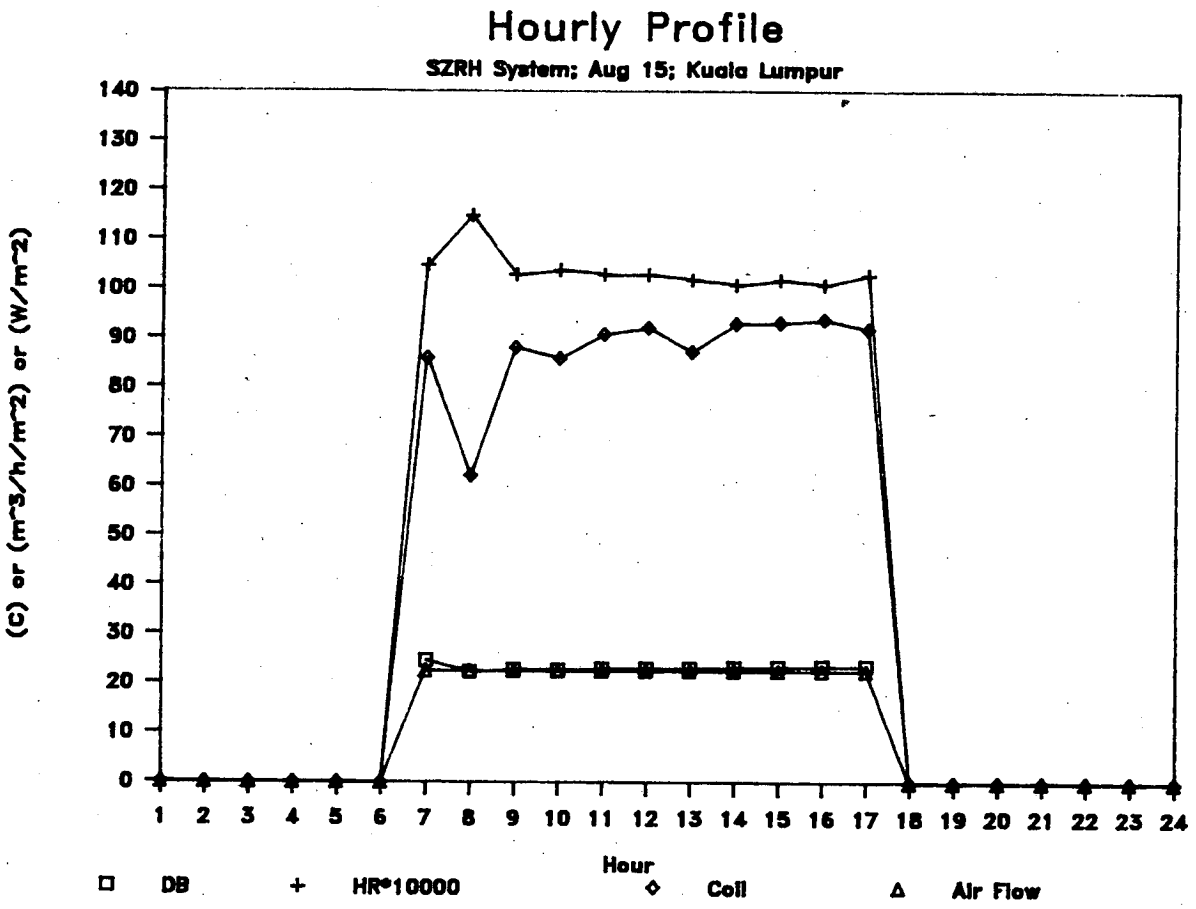

Figure 9-6. Hourly Profile for a Single Zone Reheat (SZRH) System showing return air humidity ratio and temperature and system air flow and cooling load on a peak day (15 August 1985).

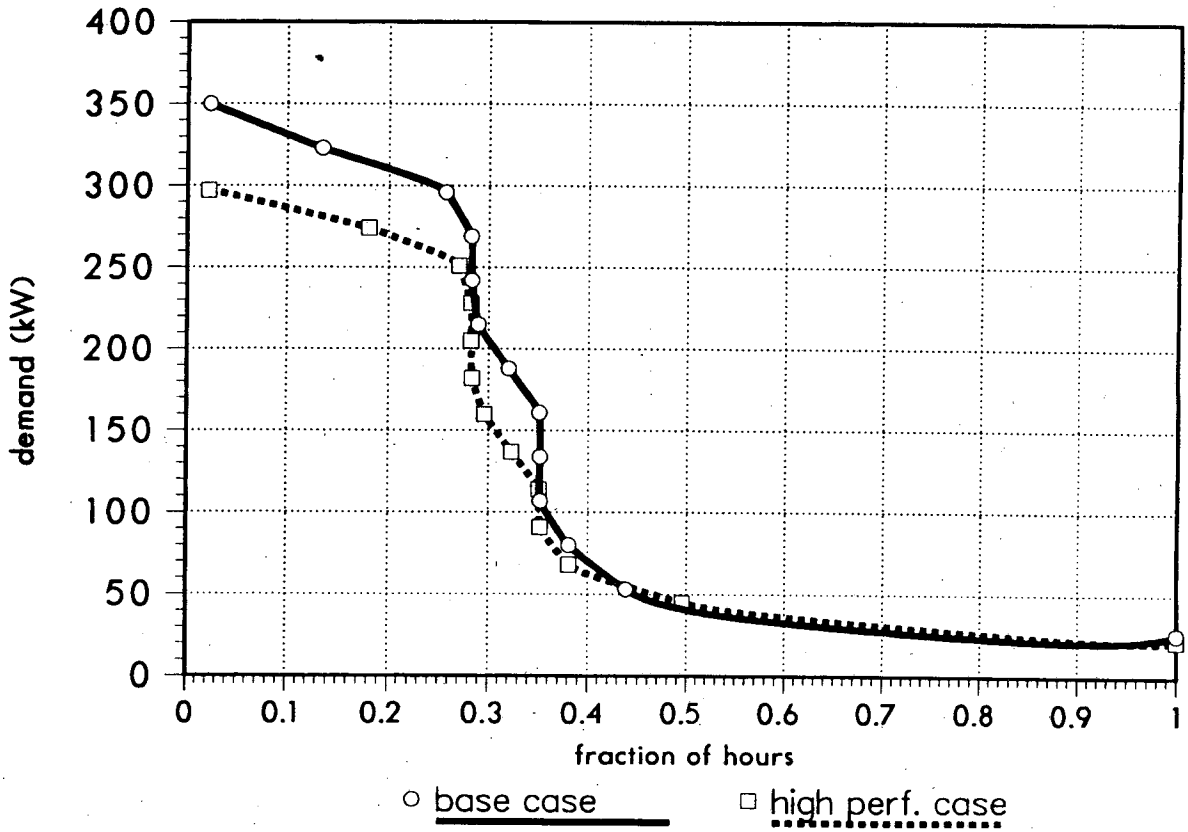

Figure 9-7. Load Duration Curves for Malaysian Commercial Building showing total electricity demand (kW) as a function of the fraction of annual hours for the base and high performance cases.

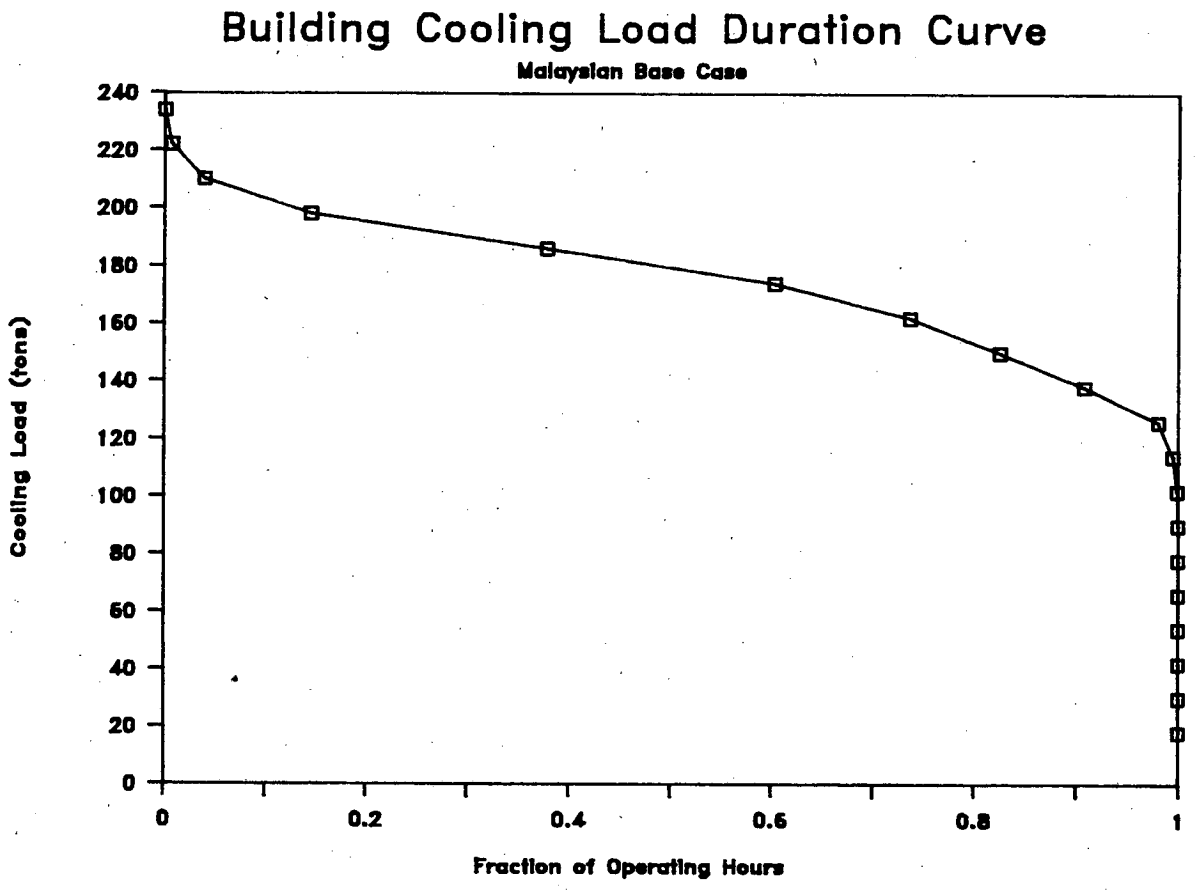

Figure 9-8. Cooling Duration Curves for Malaysian Commercial Building showing chiller cooling load (tons) as a function of the fraction of operating hours for the base case.

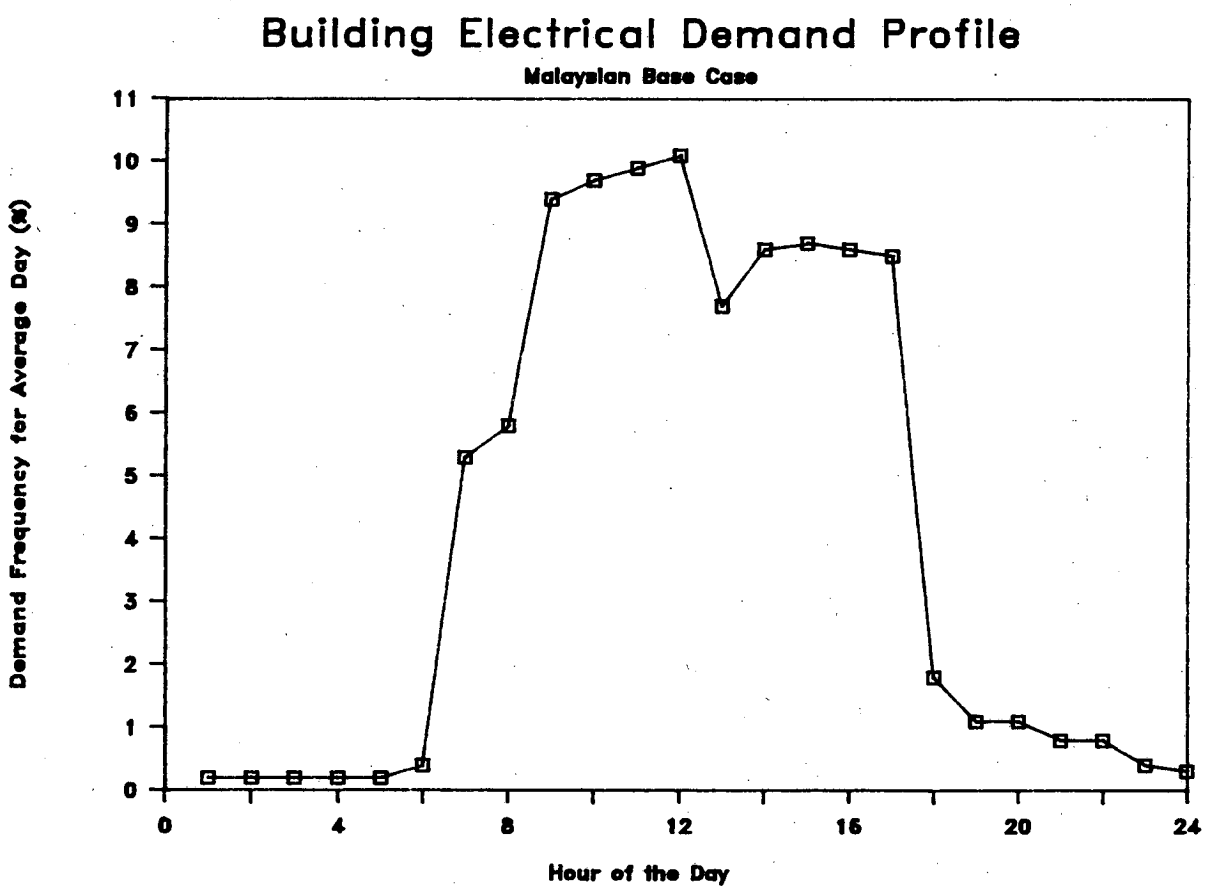

Figure 9-9. Average Annual Building Electrical Demand Profile showing demand frequency for the average day (%) as a function of the hour of the day for the Malaysian base case commercial building.

Table 9-1. Sensitivity Results from Base-Case VAV System*

CASE	FAN SAVINGS		CHILLER SAVINGS		BUILDING SAVINGS	
	Energy	Sizing	Energy	Sizing	Energy	Peak
Fan Control:						
Discharge Dampers	-38%	0	-4%	-1%	-7%	-2%
Inlet Vane (Base Case)	-	-	-	-	-	
Variable Speed	+13%	0	1%	0	+3%	0
Precooling:						
Precool 1 hr	-4%	0	-3%	+2%	-2%	+2%
Precool 2 hrs	-8%	0	-5%	+4%	-3%	+3%
Precool Monday 1 hr	0	0	0	+2%	0%	+2%
Supply Air Temperature:						
Tset 60F	-28%	-30%	0	0	-4%	-5%
Tset 55F (base Case)	-	-	-	-	-	-
Tset 50F	+17%	+17%	-1%	0	+2%	+4%
Tset 45F	+28%	+29%	-2%	0	+3%	+6%
Zone Temperature Setpoint:						
Tzone 75.2 (Base Case)	-	-	-	-	-	-
Tzone 77F	+9%	0	+4%	+3%	+3%	+4%
Tzone 79F	+15%	0	+9%	+8%	+6%	+8%
Tzone 81F	+19%	0	+13%	+12%	+8%	+12%
Lighting and Daylighting: sp .5						
2 W/ft^2 (base Case)	-	-	-	-	-	-
1 W/ft^2	+11%	+6%	+9%	+8%	+23%	+20%
4 W/ft^2	-24%	-12%	-18%	-14%	-47%	-38%
Continuous Dimming	+10%	+8%	-	+7%	+19%	+19%
Ventilation:						
10cfm/per (Base Case)	-	-	-	-	-	-
30cfm/per	-6%	0	-37%	-38%	-16%	-18%
Night Ventilation:	-68%	0	+4%	+3%	-9%	+3%
High Performance:	+58%	+29%	+13%	+11%	+14%	+16%

*Sign convention in Table 1: positive savings (+) means lower energy use and vice versa.

Table 9-2. Comparison of System Performance: *Energy*

System	Chiller (MWh)	Fans (MWh)	Lights (MWh)	Equip. (MWh)	Total (MWh)	Peak (kW)
VAVS	376	136	328	72	912	354
SZRH	391	209	328	72	1000	365
RHFS	401	210	328	72	1011	368
PIU	398	145	328	72	943	363
TPFC	315	56	328	72	771	291
TPIU	358	93	328	72	851	314
CBVAV	401	209	328	72	1010	362

Table 9-3. Comparison of System Performance: *Humidity*

	Return-Air Relative Humidity Hours						
System	81-100	71-80	61-70	51-60	41-50	31-40	0-30
VAVS	0	0	0	7	3077	0	0
SZRH	0	109	525	2126	324	0	0
RHFS	0	3	405	2346	330	0	0
PIU	0	0	0	0	3084	0	0
TPFC	0	180	716	2000	188	0	0
TPIU	0	0	0	22	3062	0	0
CBVAV	0	0	0	27	3057	0	0

CHAPTER 10: COGENERATION IN PHILIPPINE COMMERCIAL BUILDINGS

M.L. Soriano
Office of Energy Affairs
Republic of The Philippines

ABSTRACT

This paper summarizes a study conducted to determine the technical and economic feasibility of installing cogeneration systems in hotels and hospital buildings in Metro Manila. Various possible cogeneration configurations that could be applied at the sites under study were analyzed. It should be noted, however, that the evaluations produced only *preliminary* results, as the primary aim was only to estimate the investment cost and payback period for each possible cogeneration option prior to making a more detailed evaluation.

INTRODUCTION

The ever increasing cost of electrical energy has encouraged large electricity users to consider generating their own power. In terms of greater efficiency and realized cost savings, this option becomes more attractive if the possibility of utilizing the waste heat from power generation to meet heating and cooling needs is considered. The large heating, cooling, and electrical requirements of hotels and hospitals, which operate on a 24-hour basis, make these buildings potentially ideal sites for cogeneration. This study summarizes the results of two earlier case studies on the feasibility of implementing cogeneration at two existing sites in The Philippines [1,2]. It is hoped that the findings from these two specific applications in some sense represent the potential for cogeneration technology in Philippine commercial buildings in general.

Electric power can be produced from fuel-fired generators with the waste heat captured for heating by means of heat-recovery boilers, or for cooling by means of absorption chillers. These two modes of utilizing generator waste heat (i.e., for heating and cooling) were each analyzed. In conjunction with these two operating modes, four conceptual schemes for sizing the cogeneration plant were considered:

- Electrical Baseload. The prime mover capacity is based on the minimum electric power demand.
- Thermal Baseload. The prime mover capacity is based on the minimum thermal energy demand.
- Electrical Load Following. The prime mover capacity is based on the maximum electric power demand.
- Thermal Load Following. The prime mover capacity is based on the maximum thermal energy demand.

For the remainder of this paper, thermal energy demand refers to the requirements of the mode, either heating or cooling, under which the cogeneration system operates. In the following sections, the two buildings analyzed are briefly described. Lastly, summaries of the levels of technical and economic performance which the buildings would achieve if the optimal cogeneration configurations were installed are presented.

BUILDING DESCRIPTIONS

All of the information about the two buildings analyzed was gathered in the course of conducting building energy audits. Power demand of the building as a whole and thermal demands of the boilers were calculated using monthly energy bills. The estimated portion of total electricity demand devoted to chiller usage, which was 32% for both buildings, was determined through computer simulation of the buildings using the ASEAM-2 energy analysis program [3].

The Hotel

The hotel is a 14-story building located in Metro Manila. It has a gross floor area of 27,985 m^2. There are 390 air-conditioned guestrooms which occupy the top ten floors, an area equivalent to 15,300 m^2. About 20,000 m^2, or 71% of the total space, is air-conditioned. The thermal energy requirements are supplied by hotel boilers, and the steam generated is used for hot water and other heating processes. The hotel's air-conditioning requirements are supplied by three centrifugal chillers. One chiller has a capacity of 450 tons, while the other two each have a 200-ton capacity. The hotel's annual electricity consumption is about 6,989 MWh.

The Hospital

The hospital is a 12-story building located in Metro Manila. The heating requirements are presently met by boilers, and a centrifugal chiller provides centralized air-conditioning throughout the building. The air-conditioning load of the building averages 340 TR. The hospital consumes 8,102 MWh of electric power annually which is purchased from the utility. The total thermal requirements of the hospital are 8 TJ annually, an estimate based on the reported consumption and assuming an average boiler efficiency of 70%. The boiler operates for 16.5 hours per day.

TECHNICAL AND ECONOMIC FEASIBILITY ANALYSES

The technical and economic feasibility of cogeneration systems in the two building were evaluated for both modes of operation and for all conceptual sizing options. Not all of these options are reported here. Rather, this report only presents those results that yielded the greatest cost effectiveness for each building and operating mode combination.

Assumptions

- All prime mover capacities are "off-the-shelf" sizes.
- Both the gas turbines and diesel engines use industrial grade fuel oil.
- Zero inflation of energy prices.
- Fuel oil price is P2.82/liter.*
- Standby electricity costs are P54.00/kW/month.
- Depreciation over the project life is calculated as a straight line.

Heating Mode

In this option, the cogeneration waste heat is used for heating with the hot water boiler system. The most advantageous system in this mode is sized based on the minimum electricity demand of the buildings. The units would operate at maximum rated capacity at all times to supply the baseload electricity demand of the buildings. The rest of the electric power requirements would be purchased from the utility. The exhaust gases from the cogeneration units, which contain considerable amounts of energy, would be passed through a built-in waste heat recovery system to provide, depending on the performance of the system, part or all of the building's thermal requirements.

Tables 10-1 and 10-2 summarize the results of the technical and the economic and financial analyses, while Table 10-3 presents the detailed calculations of heating mode operation. The baseload power demands of the hotel and hospital would result in prime mover capacities of 550 and 750 kW_e respectively. The hotel has higher thermal requirements relative to its electrical requirements than does the hospital. It is this heat-to-power ratio which dictates the choice of prime mover technology: gas turbines in the hotel and diesel engines in the hospital. Both the recoverable heat rate and thermal energy utilization would be higher in the hotel than in the hospital. Thus, despite comparable investment costs and smaller electricity savings, the hotel's gas turbine cogeneration system would be more cost-effective than the diesel engine system in the

* The conversion rate used, as of June, 1990, was 22.885 Philippine pesos to 1 U.S. Dollar.

hospital because the former uses more of the waste heat from the boiler. Note that the proportion of debt acquired for the cogeneration system in the hotel would also be higher than that for the hospital. Higher debt to equity ratios generally enhance the economic attractiveness of the systems, but for the hospital system, 50% debt financing was the highest debt fraction considered.

Cooling Mode

Cogeneration systems can also be configured to utilize the recovered thermal energy for cooling. In this case, the cogeneration system includes a liquid absorption chiller that replaces the electric vapor-compression chiller. The optimum sizing of the cogeneration units is again based on the minimum electricity demand, excluding the electricity used by supplanted electric chiller units (i.e., electrical baseload).

Tables 10-4 and 10-5 summarize the results of the technical, and the economic and financial analyses, while Table 10-6 presents the detailed calculations of cooling mode operation. The heat-to-power ratios are generally higher in the cooling mode because of the large air-conditioning demand in tropical climates. However, the prime mover technologies remain the same for the respective buildings under this mode. In this case, a cogeneration system would be more cost-effective for the hospital than for the hotel, because the diesel generator in the hospital would reap greater savings (at comparable cost) than would the smaller gas turbine system of the hotel.

Overall, using a cogenerator to cool a building would be more cost-effective than to heat it. In the hospital, this configuration, sized to the baseload thermal demand, yielded a payback time of 1.8 years and a financial return of over 65%.

CONCLUSION

Cogeneration is a cost-effective energy conservation measure that should be considered for commercial buildings in the Philippines. Cogeneration systems installed in buildings that operate over a 24-hour period, such as hotels and hospitals, are more efficient when sized to meet the building's minimum electrical demands. This allows the generator to run at full capacity continuously and to direct exhaust heat to either water heating or space cooling demands. The overall optimal configuration, the diesel engine generator coupled with an absorption chiller and installed in a hospital, would yield a payback time of under two years and a return of over 60%.

The feasibility analysis indicates that, with sufficient third-party financing, a cogeneration project would pay off in a very short time (under four years for both building types and modes). The economic viability would be enhanced in the case of increased inflation. If cogeneration projects are implemented, however, it may be important to consider the installation of equipment for pollution control, since buildings of the types studied here are often situated within the confines of commercial and residential areas in Metro Manila.

REFERENCES

1. Soriano, M.L., "A Feasibility Study on Cogeneration at Makati Medical Center," Report of the Conservation Division, Office of the President, Office of Energy Affairs, Republic of The Philippines, March 1988.
2. Soriano, M.L., "Energy Audit Report: Hotel Intercontinental Manila," Report of the Conservation Division, Office of the President, Office of Energy Affairs, Republic of The Philippines, April 1988.
3. W.S. Fleming and Associates, Inc., *ASEAM 2-1: A Simplified Energy Analysis Method*, Albany, NY, 1987.

Table 10-1. Technical Data – Heating Mode

Building	Minimum Power Demand (kW)	Prime Mover Capacity (kW_e)	Heat-to-Power Ratio	Energy Prime Mover	Heating Requirement (TJ)	Type of Fuel
Hotel	560	550	1.4	Gas Turbine	21	Fuel Oil
Hospital	743	750	0.4	Diesel Engine	8	Fuel Oil

Table 10-2. Economic and Financial Data – Heating Mode

Building	Displaced Electricity (MWh)	Electricity Cost Savings (k.Pesos)	Cogen Unit Installed Cost (k.Pesos)	Loan Amount (%)	Payback Period (Yrs)	Internal Rate of Return (%)
Hotel	4722	9443	16208	75%	2.8	41.5%
Hospital	6441	12882	17205	50%	3.9	29.0%

Table 10-3. Cogeneration Feasibility Analysis: Heating Mode

	Units	Hotel	Hospital
A. Conceptual Design			
Minimum Electricity Demand	kW_e	560	743
Prime Mover Type	-	Gas Turbine	Diesel Engine
Prime Mover Capacity	kW_e	550	750
Cogen Plant Unit Cost	Pesos/kW_e	29470	22940
Installed Cost of Cogeneration Plant	k.Pesos	16208	17205
B. Energy Analysis (Annual Basis)			
Power Requirement	MWh	6979	8102
Power Production	MWh	4722	6439
Imported Power from the Grid	MWh	2257	1663
Prime Mover Gross Heat Rate	MJ/kW_e	17.3	10.1
Fuel Requirement of Cogeneration System	TJ	82	65
Thermal Energy Requirement	TJ	36	8
Prime Mover Recoverable Heat Rate	MJ/kW_e	10.3	3.4
Prime Mover Thermal Energy Production	TJ	49	22
Thermal Energy Utilized	TJ	42	10
Thermal Energy Dumped	TJ	7	12
C. Economic Analysis			
Debt/Equity Ratio	-	75/25	50/50
Interest on Loan	%	18.0	18.6
Loan Term	years	5	5
Project Life	years	15	20
Displaced Electricity	MWh	4722	6439
Cost of Purchased Electricity	Pesos/kWh	2	2
Savings in Electricity Cost	k.Pesos	9443	12877
Thermal Energy Displaced:			
Savings in Boiler Fuel Cost	k.Pesos	4115	806
Savings in Boiler O&M Cost	k.Pesos	136	23
Gross Savings Generated	k.Pesos	13694	13706
Cogeneration System Operating Cost:			
Fuel Cost	k.Pesos	5504	4400
O&M Cost (at 0.20 Peso/kWh)	k.Pesos	992	1288
Insurance (at 1% of equip. cost)	k.Pesos	125	132
Depreciation	k.Pesos	574	662
Amortized Loan	k.Pesos	3887	2425
Standby Electricity Charges	k.Pesos	356	486
Total Operating Cost	k.Pesos	11438	9393
Net Savings Before Taxes	k.Pesos	2256	4313
Income Tax (at 35%)	k.Pesos	790	1510
Net Savings After Taxes	k.Pesos	1466	2803
Net Cash Flow	k.Pesos	2040	3465
Cost of Money	%	20%	20%
Payback Period	years	2.8	3.8
Rate of Return on Investment	%	41.5%	29.0%

Table 10-4. Technical Data – Cooling Mode

Building	Minimum Power Demand (kW)	Prime Mover Capacity (kWe)	Heat-to-Power Ratio	Energy Prime Mover	Cooling Requirement (TR)	Type of Fuel
Hotel	358	350	1.9	Gas Turbine	400	Fuel Oil
Hospital	505	500	0.6	Diesel Engine	387	Fuel Oil

Table 10-5. Economic and Financial Data – Cooling Mode

Building	Displaced Electricity (MWh)	Electricity Cost Savings (k. Pesos)	Cogen Unit Installed Cost (k. Pesos)	Loan Amount (%)	Payback Period (Yrs)	Internal Rate of Return (%)
Hotel	4714	9427	12075	75%	2.7	42.8%
Hospital	6348	12697	12680	50%	1.9	62.6%

Table 10-6. Cogeneration Feasibility Analysis: Cooling Mode

	Units	Hotel	Hospital
A. Conceptual Design			
Minimum Electricity Demand	kW_e	350	505
Prime Mover Type	-	Gas Turbine w/ Absorp. Chiller	Diesel Engine w/Absorp. Chiller
Prime Mover Capacity	kW_e	350	500
Refrigeration Effect	TR	193	275
Cogen Plant Unit Cost	Pesos/kW_e	34500	25360
Installed Cost of Cogeneration Plant	k.Pesos	12075	12680
B. Energy Analysis (Annual Basis)			
Power Requirement	MWh	4453	6046
Power Production	MWh	3005	4292
Imported Power from Grid	MWh	1448	1754
Prime Mover Gross Heat Rate	MJ/kW_e	17.4	10.1
Fuel Requirement of Cogeneration System	TJ	52.2	43.5
Absorption Chiller Heat Rate	TR/kW_e	.55	.55
C. Economic Analysis			
Debt/Equity Ratio	-	75/25	50/50
Interest on Loan	%	18.0	18.6
Loan Term	years	5	5
Project Life	years	15	20
Displaced Electricity	MWh	4714	6348
Cost of Purchased Electricity	Pesos/kWh	2	2
Savings in Electricity Cost	k.Pesos	9427	12697
Gross Savings Generated	k.Pesos	9427	12697
Cogeneration System Operating Cost:			
Fuel Cost	k.Pesos	3519	2933
O&M Cost (at 0.20 Peso/kWh)	k.Pesos	601	858
Insurance (at 1% of equip. cost)	k.Pesos	93	98
Depreciation	k.Pesos	553	488
Amortized Loan	k.Pesos	2894	2053
Standby Electricity Charges	k.Pesos	227	324
Total Operating Cost	k.Pesos	7889	6754
Net Savings Before Taxes	k.Pesos	1539	5943
Income Tax (at 35%)	k.Pesos	539	2080
Net Savings After Taxes	k.Pesos	1000	3863
Net Cash Flow	k.Pesos	1553	4351
Cost of Money	%	20%	20%
Payback Period	years	2.7	1.9
Rate of Return on Investment	%	42.8%	62.6%

CHAPTER 11: THE FEASIBILITY OF COMMERCIAL BUILDING THERMAL ENERGY STORAGE IN ASEAN COUNTRIES

E. Wyatt*
Energy Analysis Program
Applied Science Division
Lawrence Berkeley Laboratory
Berkeley, CA USA

ABSTRACT

As an introductory analysis of the applicability of cool storage in commercial buildings for ASEAN countries (which include Indonesia, Malaysia, the Philippines, Thailand, and Singapore), this chapter presents a general overview of the technology and examines the relevant conditions in these nations. These conditions include electricity load curve shape, electrical demand growth rates, rate schedules, capital costs, operating costs, load factors, imported oil reliance, lead times, and transmission and distribution losses.

Using basic design calculations and assumptions made from these conditions, we have produced rough economic figures to demonstrate the cost-effectiveness of this technology. Based on these figures and the aforementioned electrical industry conditions, we conclude that in Singapore, Malaysia, and the Philippines, thermal energy storage is probably already economically viable. For Thailand and Indonesia, this technology is not yet practical, due to the influence of residential loads on the daily electrical demand curves. However, in the major *cities* of these countries, thermal energy storage is probably economically viable. With specific geographical and sectoral changes in electricity-use patterns, even in rural districts cool storage may eventually show cost-effectiveness.

THERMAL ENERGY STORAGE TECHNOLOGY FOR LARGE-BUILDING COOLING

Introduction

This paper offers a preliminary evaluation of the applicability of thermal energy storage technology to the Association of South-East Asian Nations (ASEAN). The nations of this organization are Indonesia, Malaysia, the Philippines, Thailand, and Singapore.

Although thermal energy storage is not a new technology, its use as an electrical peak-demand management strategy has risen only within the past several years. Thermal storage provides an opportunity to reduce building peak demand by shifting some of this load to off-peak hours, when utilities have excess capacity. The technology of thermal storage can be used in several ways, including heat storage (usually applied in regions with utilities facing winter peaking situations), seasonal storage (uncommon, but avoids the rapid cycles of daily storage), cool storage in industrial refrigeration processes, in churches, and both heat and cool storage in residential applications. But the widest use of thermal energy storage technology for cool storage is in commercial buildings. This latter application is the one with which we are concerned here. Instead of meeting the total cooling load instantaneously during the day, when electricity is expensive, the compressor is operated during off-peak hours (generally at night); this cooling energy is then *stored* using a medium (generally water or ice), to be used the next day during occupied hours, when electricity will again be expensive.

The technology benefits both building owners and managers who wish to lower their cooling costs, and electric utilities that generally want to increase their load factors and delay the need for new peak generating capacity. Countries facing the need for power plant construction can benefit from this technology by more effectively using their existing power generating facilities. Thermal storage further benefits building owners because first-cost savings on the cooling system, through

* Formerly with Lawrence Berkeley Laboratory, currently with the Association of Bay Area Governments, Oakland, CA.

smaller installed chiller capacity, can often pay for some or all of the costs of the storage. Its major operating savings are due to reductions in demand charges and, when there are time-differentiated electricity rates, lower energy costs.

This study is organized into four different sections, with two appendices. The first section provides an overview of thermal energy storage, presenting the principles of cool storage technology. In the second section, electric load conditions in the ASEAN countries are examined to determine the feasibility of thermal storage in these nations. Section three is an economic analysis of this technology on a fundamental level, using a typical commercial building as an example. Conclusions are presented in the fourth section. Finally, the two appendices offer a quick summary of experience with cool storage in the United States and a set of calculations for economic viability.

Cool Storage Technology

Thermal energy storage technology utilizes standard building cooling equipment in its operation. The heart of the refrigeration system is the chiller, which combines a compressor, condenser and evaporator. Three general types of chillers are manufactured: reciprocating, which is the type with the smallest capacity (less than 250 tons); centrifugal or screw compressors (most common in the United States), offering a medium-sized capacity (about 100-750 tons); and, finally, absorption chillers, which are the largest chillers made (100 tons on up). Thermal energy storage design requires three stages: choice of storage media, determination of operational strategy, and sizing calculations. Each of these criteria will be discussed.

Storage Media

The most common cool storage media today are water and ice, but other media, such as phase-change materials and clathrates, are also being developed (of course building mass has been used for heat storage for centuries). We will examine each type separately.

Chilled Water Systems:

Water is chilled at night to about 6°C by a conventional chiller, stored in a tank (generally made of concrete), and then circulated the following day through the cooling coils of the building. Advantages of chilled water systems include:

- There is a possibility, in retrofit applications, of using existing chillers. Chilled water is a readily available technology that engineers and technicians are more familiar with than other thermal storage systems.
- Large economies of scale for storage tanks larger than 2000 m^3 can reduce first costs.
- Chilled water storage systems operate at better efficiencies (energy output for a given energy input) than do other systems.

Water systems are not without disadvantages:

- Storage equipment is much larger and requires greater space than does ice storage. Water has a lower heat capacity than does ice because ice stores latent heat during the water-to-ice phase change; water must rely only on the specific heat of the liquid.
- Tank construction is not yet standardized or modular, so chilled water storage is less able to adjust to variations in cooling system sizing.
- The stringent standards met in factory-built construction of these tanks can not be applied to tanks built at the job site; water storage tanks are usually field built, and consequently there is a greater frequency of leakage than in modular ice tanks.
- Persistent technical difficulties in avoiding mixing of chilled water from the chiller and warmer return water have plagued water storage technology. Separation can be by temperature stratification or membrane, but each of these methods has encountered problems [1]. Both temperature stratification and diaphragms have allowed too much blending, and using an empty tank to fill or discharge water requires additional space.

- Thermal losses can be large. Losses can occur from the cold medium to its container as well as between the container and its environment. These losses can result in a 5-10% loss in performance. This type of thermodynamic phenomenon also occurs in ice storage, but it is usually higher for water because of the much greater surface-to-volume ratio for the tank(s).

As a general rule, chilled water tanks are used for large installations (greater than 400 tons of cooling). This tendency is mainly due to economies of scale; higher first costs for water in comparison to ice gradually disappear with increasing storage size. In the United States, chilled water storage has often been installed locally by companies not specializing in tank construction, or by small engineering companies, or designed by consultants. Currently, there seems to be no dominant manufacturer.

Water tanks can also store heat energy in winter for additional savings. Dual-season energy storage systems such as these can be economical under some time-of-use and seasonal rate schedules; most of these systems are installed for the purposes of peak shaving and heat recovery.

Ice Systems:

These can either be static or dynamic systems. Until recently, static systems have been the most widely used. In a static system, refrigerant is circulated in a coil inside a tank of water; ice then builds around this coil. To extract cooling later, water is circulated inside the tank, and pumped to the building's cooling coil. Although simple and available in a wide range of sizes (static systems are now sold off the shelf for capacity needs of 175 to 2400 kWh of storage), their evaporator surfaces are not easily accessible for maintenance, and they are subject to a rapid drop in efficiency as ice builds on the coils.

Dynamic systems, or ice harvesters, of which cafeteria ice-making machines are a type, build layers or cubes of ice. The ice is collected from the ice builder, crushed, and stored in a tank. Water is circulated in this tank to be used for cooling. A smaller compressor is required for the same ice-making capacity (in comparison with static systems), because it operates at a somewhat higher efficiency. Harvested ice is less dense than coil-built ice, so a larger storage space is needed. The volume of ice can be more easily measured with these systems, which do not depend on unreliable thickness sensors as do static systems. Ice systems in general have several advantages over chilled water storage:

- Ice systems have a larger cooling storage density. By taking advantage of the phase change of water (heat of fusion), a smaller storage volume will allow the same cooling capacity to be stored (only about 1/6 to 1/4 that of chilled water).
- The utilization of packaged systems carrying manufacturer's warranties usually means greater reliability, and it is relatively easy to identify and locate suppliers (at least in the United States).
- There are fewer design restraints, such as the need for stratification means in chilled water tanks.
- Thermal losses are smaller, due to a lower surface-to-volume ratio, even after accounting for the greater temperature difference over chilled water.
- A lower storage temperature translates into lower costs for pumping and air distribution, so pipes, ducts, pumps, and thermal equipment can be downsized.

Some disadvantages are present in ice systems as well, however:

- The necessity for lower chiller suction temperatures (around -5°C) often precludes compatibility with standard chillers. This adversely affects thermodynamic efficiency such that ice systems require 15-20% more electric energy. Thus chiller energy use by ice systems is often higher than by water systems.
- Some control problems exist, especially with static systems. Difficulty lies in measuring the quantity of ice built inside the storage tank as mentioned above.

- Because experience with ice systems is still limited, the technology is not yet widely accepted by all HVAC engineering firms. This acceptance is slowly growing in the United States, however, and may not be a problem in ASEAN nations as more experience is obtained with these systems.

Ice systems are often installed in small or medium-sized buildings. Lower first costs compared to water appear to be the main reason for this trend. Because chilled water is usually used for bigger systems, ice represents only 40% of the total installed cooling storage capacity. However, more buildings are using ice storage technology, especially small and medium-sized buildings; a recent survey shows that about 2/3 of the systems installed before 1985 use ice and about 1/3 use chilled water [2]. Storage space restrictions can favor ice systems in older buildings; nearly 40% of ice systems have been installed as retrofits [2].

Alternative Media:

Other media have recently been introduced for use in cool storage, such as salt storage media (clathrates) and phase-change materials. Phase-change materials incorporate benefits of both water and ice; they take advantage of the high heat of phase change (like ice), but do not require low suction temperatures as does ice. Current phase-change materials exhibit a heat of fusion in the range of 8-16°C and seem to be free of their initial technical problems of incongruous melting. However this medium has been, and continues to be, rather costly.

Clathrates are crystalline materials in which a noble gas is mixed within a structure of water molecules. The resulting compound raises the phase-change temperature of water to about 9°C and lowers the heat of fusion of ice by only 15%. The product is technically attractive, but still in the development stage. Success in the marketplace rests on reduction in its cost.

These products can be used with existing chillers and can result in higher chiller efficiencies (due to a higher phase-change temperature). Major shortcomings of alternative media include high first costs and unknown long-term performance. Space requirements are only slightly larger than those for ice systems.

Operating Strategies and Controls

The three basic operating strategies have been examined in the second section of this report, but will be briefly outlined here:

Strategies:

- A conventional cooling system, consisting of a chiller, and operating for 8-11 hours per day (during the occupied period). Under time-of-use rates, this is usually the time at which electricity is most expensive.
- A "full" storage system, where the chiller runs during off-peak (and/or partial-peak hours) to minimize the building's peak load. As previously discussed, this mode of operation requires a somewhat smaller chiller than the conventional system, but the largest storage of the three storage strategies as the peak cooling load must be met during the time at which the chiller is not operating.
- A "demand-limited" system, where the chiller runs during all periods *except* hours of maximum non-cooling demand. Both chiller and storage sizes are only slightly smaller than for full storage.
- A "partial" storage system, where the chiller is only a fraction of the size of a conventional chiller, and runs continuously. By operating 24 hours per day, the chiller allows the storage to be smaller than that for either full or demand-limited storage. The storage alone does not have to meet the peak demand for the day, as part of this demand is provided directly by the chiller.

Controls:

These strategies are not controlled with equal ease. For most efficient use of the chiller, full storage requires estimation of the cooling requirement for each subsequent day. Weather and internal loads must be accounted for and related to cooling needs. Instruments and controls used to determine cooling requirements include flow meters, differential temperature sensors, and storage measuring devices (ice thickness sensors and water temperature sensors). Demand-limited storage also requires the knowledge of the non-cooling load so that the chiller can be shut off during periods when this load is at its peak.

Two basic control options, relying on different principal cooling equipment, are available. *Chiller priority* is based on the chiller operating as much as possible. It is run any time there is load *or* when the storage needs charging and, consequently, operates at high efficiency. However, the storage is utilized only when the cooling demands exceed chiller capacity. Although this control method is very simple, it does not maximize demand reduction by fully using storage capabilities, so smaller utility cost savings will be realized.

Storage priority uses the storage to satisfy the cooling load, while the chiller runs only to maintain the minimum storage charge necessary. Utilization of storage energy is maximized in this mode, and by operating the chiller less often during the day, more of the load is shifted from these hours. The percentage of load shifted to off-peak hours using storage priority increases as the daily cooling load decreases (from design day to average-load day). Thus maximum demand reduction can be achieved using this control technique. Savings from utility charges shifted off-peak are usually greater than the increase in electrical use from running the chiller at reduced capacity. The difficulty in using storage priority control is that the status of storage must be known throughout the day— and balanced with chiller operation—to establish or maintain the necessary cooling in storage at each hour. Storage priority is less of a problem to implement if microprocessor controls are used.

System Sizing

Both chiller output and the combined capacity of chiller plus storage must be based on the maximum cooling demands of the building. Conventional refrigeration equipment is sized to meet the highest (instantaneous) cooling load of the year, so the chiller capacity alone must at least be equal to this maximum daily cooling demand.

For all storage modes, the sum of chiller output plus storage capacity must meet the total daily cooling load. In "partial" storage mode, the chiller runs continuously, so the cooling load is met over a the full day, and the chiller's size is reduced accordingly. With "full" or "demand-limited" storage systems, which require on and off control, the actual sizes of both the chiller and storage are dependent on the time-of-use schedule affecting that building. For full storage, the storage size must be large enough to completely meet the daily peak load without benefit of the building's chiller. Thus if the on-peak period is 10 hours, the storage must be fully charged to meet the cooling load over the remaining 14 hours. Storage sizing for both partial and demand-limited systems, however, must account for the occupancy schedule of the building.

Chiller capacity is generally given in tons (of refrigeration), a rate of cooling; storage capacity and cooling load are then expressed in ton-hours, an amount of cooling work. Energy input to the chiller is generally given in kilowatts, while the output of the device is in tons. One ton of refrigeration is defined as the rate of cooling equal to the melting of one ton of ice over 24 hours; based on the heat capacity of ice, this is equivalent to 12,000 BTU per hour. The efficiency of a chiller should be expressed by tons output per kW input; this parameter, however, is usually given in kW/ton.

A means of measuring the efficiency of a complete cooling system is by the coefficient of performance (COP). This parameter is simply the ratio of the desired energy (heat to be extracted from a space) to the energy needed to obtain this result (work). Many new systems may have a COP of about 4.0, but a more representative value, and one that we will use in this study, is 3.5.

Chiller Sizing:

All cooling systems utilize a chiller to meet the peak cooling load. The chiller installed with thermal storage will almost always have a smaller capacity than that of conventional systems, resulting in a smaller first cost for this component. Partial storage operation requires the smallest chiller, while full storage needs the largest (aside from a conventional system).

For all storage systems, the chiller must do two tasks—it must chill water when directly cooling the building, and it must produce ice or cold water when charging the storage. In the former mode, chiller operation generally occurs around design temperatures (for condenser and evaporator), so its average capacity is essentially the rated capacity [3]. For charging conditions, the evaporator temperature is about 10°C lower than the design temperature, reducing the actual capacity of the chiller to about 70% of its full value [3]. Chiller size is based on the *average* capacity, which accounts for its lower output when operating in ice building mode.

To properly size the chiller, its average capacity must be determined by adding the products of chiller output and number of hours at this level of operation, and then dividing the sum by the total number of operating hours. For partial storage, in which the chiller runs all the time, the average capacity would be given by:

[(1.00 * no. of hours serving bldg load) + (0.70 * no. of hours charging storage)] / 24 hours

The nominal sizing calculation is then based on the building load (in ton-hours) divided by the product of average capacity and the number of operating hours. Thus the chiller in a full storage system is sized by dividing the capacity-averaged number of non-peak hours into the daily load.

Storage Sizing:

Storage size depends on both chiller output, because the chiller's load is reduced when charging storage, and on the number of hours available for its charging. Full storage operation requires the largest storage size in order to meet the highest instantaneous load; a partial storage system requires the smallest.

This calculation relies on complete understanding of operational strategies. Both partial and full storage operation is simply based on the product of the nominal chiller capacity, the number of storage charging hours, and the chiller rating in storage mode (0.70). In the demand-limited case, the chiller meets some of the cooling load directly, while at the same time partially charging the storage. It ceases to operate when the baseload building demands rise. Thus the size of the storage equals the sum of the load it meets when the chiller is off *plus* the summation of the hourly differences between the cooling load and the nominal chiller capacity over all hours the load exceeds this capacity. The longer the on-peak period, the shorter the charging time; the storage must be charged in the remaining hours of the day. With this strategy, storage capacity is based on the summation of the difference between building load and chiller output over the hours this difference is positive. Sizing calculation examples are presented in Appendix 11-B.

ELECTRIC UTILITY LOADS AND RESOURCES IN ASEAN COUNTRIES

Introduction

In this section, key parameters relevant to cool storage feasibility will be examined for each of the ASEAN countries. These include utility load curves, load factors, rates, capital costs, operational costs, imported oil reliance, lead times, and transmission and distribution losses.

Load Curve

Because thermal storage is first and foremost a load management technology, the most important factor affecting its potential development in ASEAN countries is the shape of utility load curves. From the perspective of the utility, the irregularity of electricity demand across the day poses a capacity problem. To satisfy the highest demand, most utilities in these countries must build additional capacity, although some power companies have the option to purchase electricity, if available, from a neighboring utility. Both choices are expensive, so most utilities attempt to

avoid or minimize variations in daily peak load profile. Thermal energy storage is an excellent means, in the context of buildings, of leveling peak demand. Thus if a well-defined peak exists in a utility's daily load curves and this corresponds to the cooling load profile in commercial buildings, these buildings are good candidates for thermal storage. Load curve graphs for each country except Singapore follow.

For Malaysia (Figures 11-1 and 11-2) as well as Singapore, the daily utility load shapes show a peak from late morning to the late afternoon, with a "plateau" during this period. In the Philippines (Figures 11-5 and 11-6), a late morning peak occurs, but demand generally decreases through the afternoon, and an evening peak appears. The utility load in Thailand (Figures 11-7 and 11-8) is somewhat different, building through the day to a peak in the early evening. For all four countries, the level of peak demand is roughly 1.5 to 2 times higher than the minimum demand at night. Apparently, the evening "sub-peaks" (peak in Thailand) are driven by residential applications, while the daytime peak shape is primarily due to commercial and industrial demand.

Monthly patterns of electricity demand show little variation throughout the year. In Singapore, Malaysia, and Thailand, electricity demand tends to be relatively constant throughout the year. The highest level of demand generally remains only about 10% higher than for the month of lowest peak demand, with similar daily load shapes. The same trend in peak *levels* is visible in the Philippines. The "dual-peak" shape shifts slightly over *time*, however; the evening peak is generally the highest for nine months of the year while the noon peak is the maximum for the warmest three (generally the second quarter).

Indonesia presents a different situation (Figures 11-3 and 11-4). The electric generation system in that country faces a late afternoon/evening peak (about 4 P.M. -10 P.M.). Although only 15% of residences have electricity, the commercial and industrial sectors are very small and thus do not contribute significantly to the national demand for electric power. Indonesia's electric load is essentially seasonally invariant as well, due to relatively constant climatic conditions.

Assuming normal business hours (8 A.M.–5 P.M.), the commercial cooling loads occur during the utility's shoulder or off-peak periods. The only real concern to building owners in Indonesia, assuming time-differentiated rates, is to insure that cooling systems are turned off by 4:00 P.M. To maintain comfortable conditions after this time, overcooling in the morning and early afternoon may be necessary.

For three of these countries (Malaysia, the Philippines, and Singapore), the utilities' peak demand period occurs within some of the hours during which the cooling load of commercial buildings is present. This is the most important condition for thermal energy storage potential. In the remaining two countries (Thailand and Indonesia), however, this commercial cooling load does not contribute substantially to the utilities' daily peak, so the possibilities for significant cool storage development appear minimal. Within the jurisdiction of local urban utilities, such as the Manila Electric Company in the Philippines, the Metropolitan Electric Authority in (Bangkok) Thailand, and of course the Public Utilities Board in Singapore, the daily load profiles show a great deal of similarity to those of developed countries. (An example of this shape is shown as total energy sales in Figure 11-8.) For these utilities, thermal energy storage technology would probably be quite feasible.

In the future, Malaysia, and Indonesia in particular, expect relatively large growth in the industrial sector, especially in relation to the other ASEAN countries. All of the ASEAN countries with the exception of Thailand foresee a smaller percentage of peak capacity devoted to the residential sector and a relatively steady commercial sector growth. Thus it is likely that in the future, utility load shapes will shift from a residentially-driven peak to a larger, early afternoon peak, affected by greater commercial and industrial demand. Although there will likely also be substantial growth in residential electricity demand, the other two sectors are projected to grow even more quickly. Under these new conditions, thermal energy storage would be an important technology to consider in all of these countries.

Electric Demand Growth Rate

Compared to the experience of utilities in the United States, the electricity growth rate in the five ASEAN countries has been very high. Although this rate has slowed somewhat in recent years, it is still quite high.

The following tabulations show figures for *annual* electricity and peak demand growth rates:

Annual Electricity Growth Rates *

	Singapore	Malaysia	Indonesia	Philippines	Thailand	U.S.
Electricity (1975-80)	11.1%	12.2%	11.8%	8.4%	12.1%	3.7%
(1980-84)	7.6%	8.4%	16.1%	7.9%	10.5%	2.2%
(1985-2000, proj)	6.8%	8.2%	17.0%	8.5%	6.7%	2.7%

Annual Peak Demand Growth Rates *

	Singapore	Malaysia	Indonesia	Philippines	Thailand	U.S.
Peak Growth (1975-80)	9.3%	15.5%	17.7%	8.1%	11.1%	3.3%
(1980-84)	7.6%	8.6%	12.1%	6.0%	10.1%	2.4%
(1985-2000, proj)	6.9%	7.7%	16.8%	7.7%	7.5%	2.5%

Note: All data shown in this section are given in Tables 11-1 through 11-6.

Due to the rapid expansion in peak demand, large additions to the electric supply system will continue to be needed in the future. This expansion requires large capital outlays from the economies of these nations. Given the expected capacity need and the cost per kW for supplying that power, the total capital required in the year 2000 for plant construction alone will range from about $1.5 billion (Singapore) to $5.6 billion (Indonesia). However, these figures are in 1982 U.S. dollars; the nominal totals could very well be twice these by the end of the century. If thermal storage can reduce the need for additional generating capacity at lower expense and with equal reliability, then some of this capital could be used in other economic sectors. The higher the annual electricity and peak demand growth rates, the better the opportunities for thermal energy storage.

Malaysia and Indonesia in particular expect relatively large growth in the industrial sector, but all of the ASEAN countries with the exception of Thailand foresee a smaller percentage of peak capacity devoted to the residential sector. It is likely that in the future utility load shapes will shift from a residentially-driven peak to a larger, early afternoon peak caused by greater commercial and industrial demand. Although substantial growth in residential electricity demand is also likely, the other two sectors are projected to grow even more quickly. Under these new conditions, thermal energy storage would be an important technology to consider for commercial building application.

Commercial Growth:

Commercial electricity use is a significant portion of the total electricity consumption in all of the ASEAN countries. The following tabulation shows the percentage of total electrical use in each country that is devoted to this sector:

Commercial Electricity Consumption as a Percentage of Total Electricity Consumption *

	Singapore	Malaysia	Indonesia	Philippines	Thailand
% Commercial (1980)	41.4%	27.1%	29.4%	31.9%	27.2%
(1983)	36.4%	30%	20.9%	32%	26%
(2000, proj)	unknown	unknown	28%	unknown	19%

* Sources: Resources Systems Institute (1975-1980, 1985-2000 ASEAN data) [4]. Asian Electric Power Utilities Data Book (1980-1984 ASEAN data) [5]. Annual Energy Review 1985 (1975-1984 U.S. data) [6]. Electric Supply and Demand (U.S. Data, projected) [7].

These figures can be compared to the commercial sector electricity use in the United States in 1983 of approximately 25% [8].

Although not the largest factor in electricity growth rates (industrial use is), commercial electricity consumption has been growing rapidly. The following tabulation shows the annual growth rate in *commercial sector* electricity use:

Annual Commercial Sector Electricity Growth Rates *

	Singapore	Malaysia	Indonesia	Philippines	Thailand
Electricity (1975-80)	7.5%	14.1%	21.8%	~8%	11.2%
(1980-83)	2.9%	10.5%	3.0%	4.3%	5.9%
(1984-2000, proj)	unknown	unknown	18.1%	unknown	5.1%

While the growth rates in both total and commercial sector electrical demand have slowed in the most recent years, they are still large enough for concern. From electricity demand figures, both nationally and commercially, it is clear that high growth rates in all countries (especially Indonesia, Malaysia, and Thailand) indicate some potential for thermal storage as a socially beneficial technology.

Construction of new commercial buildings is also growing rapidly, as these countries attempt to expand their economies in the same manner as developed nations. Assuming that demand conditions warrant some examination of thermal storage as a viable technology, some entrepreneurs will take the initiative and install these systems in a certain percentage of new buildings. While thermal storage is not restricted to new buildings, it is more cost-effective when incorporated in them. The greater the growth rate of commercial building, the larger the number of energy storage systems that can be introduced.

Rate Schedules

Average utility rates for electricity consumption in these countries appear to be somewhat higher than those in the United States:

Average Utility Rates *(U.S. ¢ per kWh, 1982)*

[U.S.¢/kWh]	Singapore	Malaysia	Indonesia	Philippines	Thailand	U.S.
Utility rate, all sectors	8.5	8.6	8.6	6.9	7.9	~6.1
commercial sector	9.1	9.7	13.7	9.3	9.5	~6.9

To understand the significance of these rates, they can be compared to the 1982 gross national product (GNP) and GNP per capita, for each country, as given below [5].

Gross National Product and Gross National Product Per Capita *(1982 U.S. dollars)*

[U.S. $]	Singapore	Malaysia	Indonesia	Philippines	Thailand	U.S.
GNP (x$10^9)	16.6	27.8	87.1	40.4	39.4	3,070
GNP/capita	5,600	1,950	500	790	766	13,020

From the rates and income in the two tabulations above, the electricity charges appear particularly expensive to the average individual in an ASEAN country. Incentive to reduce at least individual electricity bills is undoubtedly greater in ASEAN countries than it would be in the U.S..

In addition to charges for electricity use, time-of-use demand charges are an important tool for any load management strategy, including thermal energy storage. The following tabulation

* Sources: Resources Systems Institute (1975-1980, 1985-2000 ASEAN data) [4]. Asian Electric Power Utilities Data Book (1980-1984 ASEAN data) [5].

shows the most recent demand charges, in U.S. dollars per kW (1982) [4]:

Demand Charge, Commercial Sector *(U.S. $ per kW, 1982)*

[U.S. $/kW]	Singapore	Malaysia	Indonesia	Philippines	Thailand	U.S.
Demand charge	1.40	4.60	varies w/kWh	1.48	4.25	wide range

Although all of these countries have some type of demand charges, there are variations in which customers are charged and at what rate. This type of charge is used by a utility to take into account additional capacity necessary to meet daily variations in electric loads. A utility demand charge should reflect, but rarely does, the marginal cost of supplying additional power at peak times. In Singapore, demand charges apply only to large, high voltage industrial and commercial customers. The other nations charge for demand, but the rate is not necessarily based on time of use.

While these figures by themselves cannot readily demonstrate how economical thermal storage may be in ASEAN countries, time-of-use rates would automatically provide some economic incentive to shift cooling loads off-peak. Other Asian nations, notably Korea, have shown that peak loads can be dramatically reduced by time-of-day pricing, especially for large electricity users [5]. Time-of-use rates are applied only to large industrial users in Singapore, Malaysia, and Thailand (not for commercial customers); in the Philippines they do not exist for any type of customer. It is only in Indonesia that time-differentiated rates apply to the commercial sector, with an on-peak rate about 60% higher than the off-peak rate. In fact, these tariffs were introduced to reflect the marginal costs of supply.

In general, electricity tariffs are not based on marginal costs, but are probably determined by some measure of average costs [5]. It seems that loan conditions imposed by international financial institutions (such as the World Bank) have raised costs of supplying new power and caused utility rates to be higher than would otherwise have occurred.

It is clear that if these countries were to institute time-of-use rates and raise or institute time-of-use demand charges, utility pricing would more accurately reflect utility costs, and thermal energy storage would have a greater economic potential.

Capital Costs

Due to such high growth rates in electric demand (as mentioned previously), there will be a need for the construction of many new power plants—especially with growth in peak demand. Financing new plants will place great strains on limited capital resources. Capital costs for new generating facilities vary with fuel type and have been estimated for each country, as shown in the following tabulation:

Capital Costs for Power Plant Construction (*U.S. $ per kW, 1982)*

[U.S. $/kW]	Singapore	Malaysia	Indonesia	Philippines	Thailand	U.S.
Oil plants	unknown	$680	$561	$989	$616	~ $500
Gas plants	no plants	$540	$254	no plants	$616	~ $250
Coal plants	no plants	$920	$667	$1100	$792	~ $1000

Thermal storage technology becomes more economically favorable as the financial commitment to new power capacity increases because it can replace some of the need for supplying additional demand more cheaply. A portion of this needed capacity—and thus required capital—can be avoided if some of the projected peak demand can be reduced or shifted to a period of excess capacity (off-peak) with cool storage. However, installing thermal energy storage systems shifts the financial burden from the central power authority (which typically has good access to capital) to the end user (who may have more difficulty raising capital).

Neither transmission nor distribution costs are included in these estimates, but these costs vary little among countries and by type of power plant. Between 1975 and 1983, transmission

investments in the Philippines amounted to 15% of total power expenses, approximately $50,000 to $100,000 per kilometer of distribution. In Indonesia, due to its island geography, these costs are somewhat greater.

Expenses for electricity generation are already 4-10% of annual gross domestic product in Thailand. In the Philippines, these expenses are growing at an annual rate of about 8.5%, while the annual gross domestic product is growing at only 7.6%. The result of this gap is that new power plants must be financed at up to 60% by foreign currency loans. This story is much the same in Malaysia, where both electricity and water use has been growing at 12% annually while the country's gross domestic product has been increasing at only a 7% annual rate [4]. Financial contributions to thermal storage technology are a more cost-effective method of meeting growth in electricity demand than is building new power plants. The role of capital costs will be made clearer in Appendix 11-B.

Utility Operating Costs

In all of the ASEAN countries, fuel costs make up a large percentage of electrical *generation* costs. Oil is the only fuel source common to all of these nations, and from the following tabulation we can observe that fuel costs are by far the largest component of generation costs for plants burning this fuel.

Oil & Fuel Costs as a Percentage of Electricity Generation Costs *(1982)*

	Singapore	Malaysia	Indonesia	Philippines	Thailand	U.S.
Oil costs (% of total)	71.3%	67.9%	unknown	70.0%	75.1%	unknown
Fuel costs (all fuels)	71.3%	66.0%	48.2%	78.6%	45.0%	~ 26%

Although the cost of oil is high relative to other fuels in all of these nations, oil (and its costs) makes up a large portion of total fuel costs. This suggests that for these countries which import much of their fuel, vulnerability to world fuel price changes is greater than for those that do not. As a result, ASEAN countries are attempting to shift to domestic fuel supplies for electricity production (gas in Malaysia and Thailand, coal in Indonesia, Thailand, and the Philippines). Long-term success of the plans depends on the indigenous quantities of these fuels in ASEAN countries and the rate of their exploitation. Thermal energy storage provides another method of reducing higher imported fuel costs by assisting these countries to minimize their operating costs (using less expensive domestic fuels).

Reliance on Imported Oil

A few of the ASEAN countries are heavily dependent on oil as the major fuel in the generation of electricity. Implementation of cool storage could avoid or delay reliance on an imported supply, as mentioned in the previous section. Singapore is most vulnerable, obtaining all of its energy from imported oil. The lowest rates of oil dependency of the five ASEAN nations are in Malaysia, with only 31% of its oil being imported, and Indonesia, with about 41% of its oil so obtained [4].

However, these figures do not specify the importance of oil in electricity production, as both Malaysia and Indonesia are net *exporters* of oil. These countries import oil that is either at a lower cost than domestically produced oil, or a higher grade of oil that is not found domestically. For the purposes of *electricity production*, these two countries are essentially independent from foreign sources.

Reliance on imported oil in the Philippines and Thailand appears even greater when focusing on the issue of imported oil used in electricity generation, because domestically produced oil in these two countries is mainly used for transportation.

Percentages of Oil Imported as a Primary Fuel *(1982)*

	Singapore	Malaysia	Indonesia	Philippines	Thailand	U.S.
% Oil Imported	100%	30.9%	40.8%	68.4%	57.1%	28%

Implementation of cool storage could minimize or delay the reliance on an imported fuel supply. Night electricity production tends to rely more on domestically produced baseload. Thailand, for example, uses its supply of lignite to generate baseload electricity. Malaysia generates its baseload with thermal plants (oil-fired now, with an attempt to shift to gas in the future), while in Indonesia this load is supplied with a combination of thermal plants and hydroelectricity. The overall policy for the future in all of these nations is to increase the use of domestically exploitable fuels and reduce imports. Switching commercial building cooling from daytime (on-peak) to nighttime (off-peak) can mean greater use of baseload capacity and thus a lower reliance on a foreign supply of fuel.

The fuel cost of a generated kilowatt-hour is about 70% of the total cost in these countries, indicating the smaller effect of capital costs in electricity production. Both lower capital costs and higher fuel costs are responsible for this trend. As a consequence, deferring the need for new power generation and avoiding associated capital costs will not produce the same effect as in the U.S., where typical fuel costs are only about 25% of the total [9]. Savings will more likely be from reduced operating (fuel) costs. Instead, increasing imported oil reliance provides another incentive for the introduction of thermal storage technology.

Load Factor

Utility load factor is defined as the ratio of average electrical demand to the highest demand for a given period. As electricity consumption is transferred from on-peak to off-peak periods, the load factor increases, and existing power plants will be used more effectively. Load factor tends to increase with a greater percentage of electrical energy devoted to industrial use. Power companies attempt to bring their load factors up as high as possible to better utilize generating capacity, so improving this parameter will continue to be a priority for the future.

Annual Load Factors *(1982)*

	Singapore	Malaysia	Indonesia	Philippines	Thailand	U.S.
Load Factor	67.5%	63.9%	59.8%	68%	67.7%	61.1%

With the exception of Indonesia, these figures are slightly higher than the average load factors in the U.S., which range from about 55% to 66% [7]. For two of these nations (Malaysia and Thailand), their utilities' load factor has declined slightly in recent years (by about 1-2%). In Thailand, this trend is expected to continue through the rest of this century.

Although it may be difficult to increase these figures dramatically, thermal energy storage can improve load factors in these countries by shifting demand from on-peak to off-peak periods.

Lead Times

Building new electrical capacity requires several years between initial planning and final connection to the power grid. This "lead time" in ASEAN countries is, at minimum, a 4-5 year period. Uncertainty in the world's economies affects industrial growth in each country, which in turn changes the growth rate of electricity demand. The greater this uncertainty, the higher the potential for errors by utility planners when lead time is taken into account; lead times can easily lengthen. Thermal energy storage becomes more favorable as lead times increase, because it can be added to building stock relatively quickly—allowing for much greater flexibility in responding to the need for power.

Lead Times for Construction of New Power Plants *(1982)*

	Singapore	Malaysia	Indonesia	Philippines	Thailand	U.S.
Lead Times (years)	unknown	4.5	7.5	6-8.5	6.5	various

Although there are also lead times for building design and construction, these are often shorter than the lead time for constructing power plants. Thus thermal storage offers utilities a means of more readily adapting to an expected change in electrical demand. It is likely, however, that thermal energy storage cannot be installed on the scale needed to eliminate all new peaking capacity needs.

Transmission and Distribution Losses

Because transmission and distribution losses can increase when there are swings in demand profiles, these losses become larger as utility load profiles display a large daily range (small load factors). These losses can be significant when considering the amount of electrical power generated [4]:

Transmission and Distribution Losses *(1982)*

	Singapore	Malaysia	Indonesia	Philippines	Thailand	U.S.
Losses	4.9%	8.8%	25.9%	14.2%	9.8%	unknown

Distribution losses are highest in Indonesia and the Philippines because they are island nations, and it is comparatively expensive to connect these geographic outposts to an electricity grid.

Additions to transmission and distribution systems are driven by peak demand, not energy; since thermal storage reduces peak demand, its use can reduce the growing need for new transmission and distribution facilities. By itself, thermal storage technology will not substantially reduce transmission and distribution losses, but reduction in peak loads due to energy storage installation avoids or delays additional generation, and thus transmission equipment. By inference this load reduction also avoids or delays losses within this system.

Tables 11-1 through 11-6 summarize the information presented thus far.

THERMAL ENERGY STORAGE COST-EFFECTIVENESS IN ASEAN COUNTRIES

Introduction

To fully evaluate the cost-effectiveness of thermal storage under ASEAN conditions, it is important to examine the components of cooling system economics. A brief discussion of engineering criteria will be included to understand the financial parameters of this technology.

Economic Analysis

The economic analysis is primarily dependent on both the applicable electric utility rate structure and on the sizing of the system; these in turn affect the economic parameters (costs of operation and capital costs).

Utility Rate Structure:

Thermal energy storage displaces energy from on-peak to off-peak, but does not necessarily save energy. Depending on building loads, energy use may be either higher, due to thermal losses (or poor control), or lower, because the chiller is used at full load (better efficiency). But energy savings, if they exist at all, will be small.

Utility rates are essential in the calculation of dollar savings. It is difficult to generalize on the point of rate schedules, because in the U.S. there are some 3000 electric utility companies. All have multiple rate schedules for different customer classes, depending on location, cost of fuels, operation mix, size, and regulatory policy. Increasingly, they offer seasonally adjusted

time-of-use rates, two or three periods per day, during which kWh and kW are charged at different rates. These types of rate schedules provide the best economic climate for thermal storage systems. An example of a typical time-of-use rate schedule for a U.S. utility is given in Appendix 11-B.

Strategies of Operation

As mentioned in the first section, three different storage strategies can be employed: partial storage, full storage, and demand-limited storage. Each approach will be discussed separately.

Partial Storage:

In this case, the chiller operates 24 hours per day. When the building is not occupied, the chiller is used to replenish cool energy in storage; during occupied (usually peak) hours, the cooling load is met by a combination of chiller operation (direct cooling) and storage output (indirect cooling). The chiller charges the storage when the cooling load is less than the rated chiller output. During occupied hours, the cooling load is greater than chiller output, so the energy from storage makes up this difference. During peak utility hours, cooling system demand (in kW) can be reduced by approximately 40-50%.

Full Storage:

This approach attempts to minimize a building's electrical demand during the utility peak demand period by providing the cooling requirements for the building directly from storage. To accomplish this, the chiller is not run during the peak period, when it would substantially increase the overall electric demand for that building. Thus the longer the on-peak period, the shorter the charging time; the storage must be charged in the remaining hours of the day. The peak cooling load can be reduced by 80-90% from the conventional cooling peak (the portion of the peak cooling load not reduced is from water and air distribution systems—fans and pumps). For situations in which on-peak cooling loads are of relatively short duration, full storage is the logical operational strategy.

Demand-Limited Storage:

By using more sophisticated controls, a demand-limited strategy is somewhat of a mix between partial and full storage. The objective is to minimize the cooling contribution to the building peak by ensuring that the non-cooling "baseload" building demand is never exceeded (similar to full storage), but that the chiller operates during all hours *other than* the hours at which baseload demands are at their peak. During some of the day, including some on-peak hours, the chiller can directly meet the cooling load while also charging the storage (as does partial storage). This strategy thus requires a smaller chiller than does full storage operation. It is also best suited for buildings with a large baseload demand and relatively short occupancy periods (to allow greater storage-charging time).

There are trade-offs for each strategy. Partial storage operation requires a smaller chiller and storage equipment than does full storage. This requires lower first costs, but also results in lower peak demand savings. Full storage has higher first costs, but also more significant peak demand savings. For demand-limited operation, both first costs and savings in reduced utility charges approach those of full storage. A demand-limited strategy requires the most complex set of controls, however; both the daily cooling *and* daily non-cooling loads must be known or accurately calculated in order to determine the proper hours and load of chiller operation.

In many cases, the lower initial costs of partial storage systems allow a rapid payback time, eliminating the need for utility payment programs. For a portion of *full storage* systems, utility-sponsored programs are often needed to reduce the payback time to an acceptably short period.

These operational strategies are presented graphically in Figures 11-9 through 11-12.

System Sizing

As discussed in the first section, both chiller output and the combined capacity of chiller plus storage must be based on the cooling demands of the building. Once the chiller and storage have been sized, the initial capital costs of the system can be calculated.

Economic Parameters

The two fundamental parameters to be studied are first-cost savings and annual operational costs. The first-cost savings from a cooling system in a building are the cost of all refrigeration equipment, including chiller(s) and storage, reduced by the savings over that of a conventional system. The level of savings depend on technology and strategy. For a conventional system, the first cost is simply the capital cost of the chiller; for the storage strategies, however, this cost includes both the chiller cost *and* the capital cost of the storage equipment. For the purposes of illustration, we will use U.S. capital cost data; these figures may be different in the ASEAN countries.

Chiller Cost:

The average installed chiller cost in 1985 was $336/ton [10]. In 1986, the City of Palo Alto (California) Utilities Department liberally estimated this cost to be $400/ton. For our analysis, we will consider this cost to be $400/ton.

Storage Cost:

For ice systems, basic storage cost is very size dependent, increasing by about 20% when transportation and installation are included. Current delivered costs of $1.20-$2.95/kg are widely accepted [11]. For a typical ice system, costs of storage would fall in the range of:

(12,660 [kJ/ton-hr] * 1.20-2.95 [$/kg])/ 335 [kJ/kg] = 45 to 111 [$/ton-hr]

Chilled water storage systems also exhibit economies of scale, although to a lesser extent than does ice storage. Large tanks, including pipes, pumps and controls, and installation costs, tend to be priced at costs of $0.55-$1.10/gallon ($0.15-$0.30/liter) [11]. Thus for a typical temperature difference in the tank of approximately 12°C, the storage cost would be:

(12,660 [kJ/ton-hr] * 0.15-0.30 [$/l]) / (4.19 [kJ/kg-°C] * 12 [°C] * 1.0 [kg/l]) = 38 to 76 [$/ton-hr]

Because the difference between ice and chilled water storage costs is more significant for small applications (higher costs per ton-hour), we will take the range of $50-$100/ton-hr to be representative of current storage costs.

Annual Operating Cost Savings:

For any given system, operating savings are dependent on rate schedules as the savings realized from cool storage are based on reductions in demand and in energy charges. We will discuss this figure in detail in Appendix 11-B.

Investment Analysis

Several basic parameters were used to analyze capital investment in the field of energy; simple payback time; net present value; and investment per peak kW saved.

- Simple payback time.

This variable indicates the period of time needed for a thermal storage system to realize operating savings equal to the increased capital investment over a conventional HVAC system. The payback period is calculated by simply dividing the capital cost difference (incremental first-cost) by the annual savings in operational costs.

Both the drawback and the advantage to this analysis is its simplicity. The time-value of savings, for example, is not considered. There is also an implicit assumption here that utility charges are fixed; however, any changes in utility rates will result in different savings and thus a different payback time. Yet the uncertainties in future costs of both equipment and utility rates are undoubtedly greater than those produced by the assumption of simple payback [3], especially for

relatively long time periods. For shorter time periods (3-5 years), lack of discounting does not pose a problem, and payback time provides an easy measure between two key parameters. Thus this method has wide acceptance.

- Net present value.

The concept of net present value expresses the worth of an investment's future values in current dollars based on an estimated discount rate. More specifically,

$$NPV = \Sigma \text{ (savings in Nth year / } (1 + r)^N) - \text{Initial investment cost}$$

It is clear that the discount rate, r, is very important in this analysis. As this rate increases, net present value approaches the current value, which corresponds to a short simple payback time. At low discount rates, the net present value increases (payback time lengthens), reducing the attractiveness of the investment. Simple payback is easier to calculate and thus more often used.

- Investment per peak kW saved.

This parameter is specifically useful to utilities which may be involved in the financing process. If some of the new peak demand can be met without having to build an expensive new plant or purchase energy from an adjacent power grid at a high price, the utility will be likely to pursue this course. Many utilities are willing to offer incentives for each kW saved, including that saved by thermal energy storage. Current examples of utility incentives in the U.S. range from $200/kW (Pacific Gas & Electric, California) to $400/kW (City of Palo Alto, California).

Example

At this point, we will examine a "typical" office building: the "Malaysian commercial office module" will be used as the case study. General daily load conditions are discussed in greater detail in Appendix 11-B.

Building Load = 800 ton-hours (2820 kWh)
Cooling peak = 92 tons
Chiller size = 100 tons (350 kW)
Building operating hours = 8 A.M. - 6 P.M. (10 hours)
On-peak hours = 10 A.M. - 6 P.M. (8 hours)

First-Cost Analysis:

All of the estimates for storage costs in this analysis will be based on the *average* of two costs: a typical case, with estimated U.S. figures for large storage equipment and operation of $50/ton-hr; and a conservative case, with high figures of $100/ton-hr. Of course, these figures are for illustrative purposes only—actual costs will vary.

Equipment	Cost
Chiller:	$400/ton
Storage:	$75/ton-hr

For a conventional system, the chiller size is about 350 kW (100 tons), and there is no storage.

$$100 \text{ [tons]} * \$400/\text{ton} = \$40{,}000$$

First costs for each storage mode based on this example building are calculated in Appendix 11-B.

The peak cost incurred by the installation of a thermal storage system can be compared to the cost of supplying an additional peak kW. In general, the cost per avoided peak kW tends to be lower for partial storage than are incremental supply (capital) costs. If we recall the 1982-based capital costs for new power facilities in ASEAN countries, we find these range from $540/kW to $1100/kW for all types of plants, with the one exception of $254 for gas plants in Indonesia. The cost for an avoided peak kW utilizing thermal storage in this example falls into the range of $213/kW to $523/kW. For this gas plant example, only the partial storage case demonstrates cost-effectiveness. But for all other plant construction, the avoided peak costs for *every* storage

case in this example are smaller.

From some *utilities'* perspectives, it makes better sense to offer subsidies (grants or rebates) for these types of load management techniques than to finance new peak load plant construction. However, estimated costs for all strategies are low enough not to *require* subsidies (grants or rebates); with subsidies, these strategies can show even greater cost-effectiveness.

Operational Cost Savings:

As we previously mentioned, the savings analysis is significantly dependent on the prevailing rate schedules of the local utility. Either a demand charge or time-of-use energy rates must be present for thermal energy storage to show any degree of cost-effectiveness.

The savings in annual operational costs are calculated by simple subtraction of the utility costs for each storage system from those of the conventional system. Finally, the simple payback time can be found by dividing the increased capital cost by these annual operating cost savings.

Applications to ASEAN Countries

Information on load shapes and rate schedules can be used with an example building to demonstrate the application of thermal energy storage under current conditions in ASEAN countries. Capital costs will be assumed as similar to those found in the United States. In each case, we will begin by analyzing capital costs for all four cooling system possibilities, then calculate operating costs and payback for the same systems. Theoretical cost-effective utility charges under these conditions are offered as well.

Malaysia:

Current load conditions show a utility peak from about 8:30 A.M. to 5:30 P.M., basically corresponding to business hours (9 hours). In the analysis, we will assume that this period will be considered on-peak for demand purposes. We also assume from the load curves that commercial building operation is from 7 A.M. to 6 P.M. (11 hours). Thus for demand-limited systems the chiller will operate for all but the period of peak building demand (10 A.M. - 4 P.M.); for full systems it will run from 5:30 P.M. to 8:30 A.M. the next day. Given this scenario, the chiller cost, storage cost, and total investment over a conventional system can be found by these methods, discussed in greater detail in the economics example of the next section, and are presented in the second tabulation below.

By subtracting operating costs for the storage cases from conventional system costs, the operating cost savings can be found. The ratio of the capital cost increase to annual operational savings is the payback time. Costs based on 1989 charges (demand charge of $4.40/kW and energy charge of $0.066/kWh for option 1 and demand charge of $6.96/kW and energy charge of $0.066/kWh on-peak, $0.029 off-peak, option 2) are shown in the third tabulation.

Payback times for all strategies under these conditions and assumptions for Malaysia are also listed below.

OPERATING SCHEDULES, MALAYSIA

	Conventional System	Partial Storage	Demand-Limited Storage	Full Storage
Averaged operating hours	11	18.42	12.58	10.50
On-peak hours of operation	8:30am-5:30pm	8:30-5:30	8:30-10, 4-5:30	none
Building cooling hours	11	8	0	0
Storage charging hours	0	13.5	13.5	15
Simultaneous operating hours	0	2.5	4.5	0

CAPITAL COSTS, MALAYSIA

	Conventional System	Partial Storage	Demand-Limited Storage	Full Storage
Effective chiller efficiency	1	0.77	0.70	0.70
Chiller capacity (tons)	100	43	64	76
Chiller capacity reduction (tons)	—	57	36	24
Chiller cost	$40,000	$17,375	$25,429	$30,476
Chiller cost reduction	—	$22,625	$14,571	$9,524
Storage size (ton-hrs)	0	478	666	800
Storage cost	—	$35,813	$49,950	$60,000
Capital cost increase	—	$13,187	$35,379	$50,476
Cooling peak reduction (tons)	—	57	36	24
Incremental capital cost	—	$233/ton	$971/ton	$2,120/ton
Cost per avoided peak kW	~$680/kW*	$26/kW	$110/kW	$241/kW

OPERATING COSTS, MALAYSIA

	Conventional	Partial	Demand-Limited	Full
† Option 1:				
Annual operational costs	$66,976.80	$56,464.30	$48,391.20	$48,391.20
Operational cost savings	—	$10,512.50	$18,585.60	$18,585.60
† Option 2:				
Annual operational costs	$72,857.80	$44,206.13	$25,784.20	$21,262.80
Operational cost savings	—	$28,651.68	$47,073.60	$51,595.00

PAYBACK, MALAYSIA

	Conventional	Partial	Demand-Limited	Full
Simple payback time (yrs)				
† Option 1:	—	1.3 yrs	1.9 yrs	2.7 yrs
† Option 2:	—	0.5 yrs	0.8 yrs	1.0 yrs

Next, operational economics can determine utility charges that would be cost-effective under Malaysian load conditions. Formulas are developed and presented in detail in Appendix 11-B. Demand charges and energy charge time differentials (peak charge – off-peak charge) can be calculated for each strategy for a three-year payback period. The following tabulation shows these calculated break-even rates.

---

* This figure is offered for comparison and is obtained from the data on capital costs of new power plants for the most common type of plant in each country, in U.S. $ per kW. In the case of Malaysia, this is the quoted cost for an oil-fired plant.

† Note that the following two options apply:

Option 1:		Option 2:	
Demand charge	$4.40 $/kW	Demand charge	$6.96 $/kW
Electricity charge	$0.066 $/kW	On-peak electricity charge	$0.066 $/kW
		Off-peak electricity charge	$0.029 $/kW

BREAK-EVEN RATES, MALAYSIA

	Conventional	Partial	Demand-Limited	Full
* Option 1:				
Demand charge	—	$2.40	$4.39	$5.23
Energy charge differential	—	$0.014	$0.025	$0.028

Indonesia:

Demand in Indonesia generally peaks between 5 P.M. and 11 P.M., but there are time-of-use rates for the period between 6 P.M. and 10 P.M.. We assume in this case that commercial building operation is from 7 A.M. to 6 P.M. This is an unusual condition for demand-limited systems, but since this type of system is designed to avoid adding to the building peak (not fundamentally concerned with the utility peak), we assume the building's non-cooling demand peaks for about six hours per day (10 A.M. - 6 P.M.). A full storage system will operate from 10 P.M. to 6 P.M. the next day. Chiller cost, storage cost, and total investment are found for Indonesian buildings in a similar manner as for the Malaysian example and are summarized in a tabulation below.

OPERATING SCHEDULES, INDONESIA

	Conventional System	Partial Storage	Demand-Limited Storage	Full Storage
Averaged operating hours	11	18.42	12.58	14.00
On-peak hours of operation	none	6-10pm	6-10pm	none
Building cooling hours	11	8	0	0
Storage charging hours	none	13.5	13.5	20
Simultaneous operating hours	none	2.5	4.5	none

CAPITAL COSTS, INDONESIA

	Conventional System	Partial Storage	Demand-Limited Storage	Full Storage
Effective chiller efficiency	1.0	0.77	0.70	0.70
Chiller capacity (tons)	100	43	64	57
Chiller capacity reduction (tons)	—	57	36	43
Chiller cost	$40,000	$17,375	$25,429	$22,857
Chiller cost reduction	—	$22,625	$14,571	$17,143
Storage size (ton-hrs)	0	478	666	800
Storage cost	—	$35,813	$49,950	$60,000
Capital cost increase	—	$13,187	$35,379	$42,857
Cooling peak reduction (tons)	—	57	36	43
Incremental capital cost	—	$233/ton	$971/ton	$1,000/ton
Cost per avoided peak kW	~$560/kW	$26/kW	$110/kW	$114/kW

* Note that the following two options apply:

Option 1:		Option 2:	
Demand charge	$4.40 $/kW	Demand charge	$6.96 $/kW
Electricity charge	$0.066 $/kW	On-peak electricity charge	$0.066 $/kW
		Off-peak electricity charge	$0.029 $/kW

OPERATING COSTS, INDONESIA

	Conventional	Partial	Demand-Limited	Full
* Option 1:				
Annual operational costs	$89,427.34	$64,590.31	$51,324.00	$43,992.00
Operational cost savings	—	$24,837.03	$38,103.34	$45,435.34
* Option 2:				
Annual operational costs	$105,338.69	$67,321.66	$38,126.40	$38,126.40
Operational cost savings	—	$38,017.02	$67,212.29	$67,212.29

PAYBACK, INDONESIA

	Conventional	Partial	Demand-Limited	Full
Simple payback time (yrs)				
* Option 1:	—	0.5 yrs	0.9 yrs	0.9 yrs
* Option 2:	—	0.3 yrs	0.5 yrs	0.6 yrs

BREAK-EVEN RATES, INDONESIA

	Conventional	Partial	Demand-Limited	Full
* Option 1:				
Demand charge	—	$2.40	$4.39	$5.92
Energy charge differential	—	$0.036	$0.072	not relevant

The Philippines:

The load curves for the Philippines indicate that a utility peak exists between about 9 A.M. and 8 P.M. Here we assume that normal commercial building operation is from 7 A.M. to 5 P.M. A demand-limited system would run between 4 P.M. and the following 9 A.M., and with these demand conditions a full storage system would operate for only 13 hours (8 P.M. to 9 A.M. the next day). Capital costs for each storage strategy follow.

Simple payback times are determined, and for a three-year payback, demand and differential energy charges are calculated.

OPERATING SCHEDULES, THE PHILIPPINES

	Conventional System	Partial Storage	Demand-Limited Storage	Full Storage
Averaged operating hours	10	18.19	11.19	9.10
On-peak hours of operation	9am-5pm	9am-8pm	4pm-8pm	none
Building cooling hours	10	7	0	0
Storage charging hours	none	14	14	13
Simultaneous operating hours	none	3	3	0

---

* Note that the following two options apply:

Option 1:		Option 2:	
Demand charge	$1.90 $/kW	Demand charge	$18.72 $/kW
On-peak electricity charge	$0.120 $/kW	Electricity charge	$0.052 $/kW
Off-peak electricity charge	$0.06 $/kW		

CAPITAL COSTS, THE PHILIPPINES

	Conventional System	Partial Storage	Demand-Limited Storage	Full Storage
Effective chiller efficiency	1.0	0.76	0.66	0.70
Chiller capacity (tons)	100	44	71	88
Chiller capacity reduction (tons)	—	56	29	12
Chiller cost	$40,000	$17,589	$28,589	$35,165
Chiller cost reduction	—	$22,411	$11,411	$4,835
Storage size (ton-hrs)	0	500	705	800
Storage cost	—	$37,475	$52,906	$60,000
Capital cost increase	—	$15,064	$41,495	$55,165
Cooling peak reduction (tons)	—	56	29	12
Incremental capital cost	—	$269/ton	$1,455/ton	$4,564/ton
Cost per avoided peak kW	~$1000/kW	$31/kW	$165/kW	$519/kW

OPERATING COSTS, THE PHILIPPINES

	Conventional	Partial	Demand-Limited	Full
Annual operational costs	$36,156.68	$34,097.76	$32,481.80	$32,481.80
Operational cost differential	—	$2,058.92	$3,674.88	$3,674.88

PAYBACK, THE PHILIPPINES

	Conventional	Partial	Demand-Limited	Full
Simple payback time (yrs)	—	7.3	11.3	15.0

BREAK-EVEN RATES, THE PHILIPPINES

	Conventional	Partial	Demand-Limited	Full
Demand charge	—	$2.70	$4.58	$4.95
Energy charge differential	—	$0.041	$0.085	$0.025

Thailand:

In Thailand, the load shape is skewed in comparison to Malaysia and the Philippines, peaking from about 2 P.M. to 10 P.M. This indicates a strong residential influence in daily peak loads, with Indonesia the only other country exhibiting a similar trend. By assuming building operation from 7 A.M. to 5 P.M., only the last three hours would fall into the peak period. The demand-limited case, concerned with not exceeding the non-thermal building load, again shows operation between 4 P.M. and the next 9 A.M. For full storage, the chiller is not run during this peak period, so it is run for 16 hours per day.

Simple payback times are also given below. Operational cost-effectiveness analysis for a three-year payback again offers estimated break-even demand and differential energy charges.

OPERATING SCHEDULES, THAILAND

	Conventional System	Partial Storage	Demand-Limited Storage	Full Storage
Averaged operating hours	10	18.19	11.19	11.20
On-peak hours of operation	2-5pm	2-10pm	4-10pm	none
Building cooling hours	10	7	0	0
Storage charging hours	none	14	14	16
Simultaneous operating hours	none	3	3	0

CAPITAL COSTS, THAILAND

	Conventional System	Partial Storage	Demand-Limited Storage	Full Storage
Effective chiller efficiency	1.0	0.76	0.66	0.70
Chiller capacity (tons)	100	44	71	71
Chiller capacity reduction (tons)	—	56	29	29
Chiller cost	$40,000	$17,589	$28,589	$28,571
Chiller cost reduction	—	$22,411	$11,411	$11,429
Storage size (ton-hrs)	0	500	705	800
Storage cost	—	$37,475	$52,906	$60,000
Capital cost increase	—	$15,064	$41,495	$48,571
Cooling peak reduction (tons)	—	56	29	29
Incremental capital cost	—	$269/ton	$1,455/ton	$1,700/ton
Cost per avoided peak kW	~$620/kW	$31/kW	$165/W	$193/kW

OPERATING COSTS, THAILAND

	Conventional	Partial	Demand-Limited	Full
Annual operational costs	$74,618.64	$52,940.81	$35,926.80	$35,926.80
Operational cost savings	—	$21,677.83	$38,691.84	$38,691.84

PAYBACK, THAILAND

	Conventional	Partial	Demand-Limited	Full
Simple payback time (yrs)	—	0.7	1.1	1.3

BREAK-EVEN RATES, THAILAND

	Conventional	Partial	Demand-Limited	Full
Demand charge	—	$2.70	$4.58	$5.37
Energy charge differential	—	$0.041	$0.085	$0.022

Singapore:

Load curves for Singapore are not available at this time, but it appears that its economy resembles an urbanized, developed economy more than one like Thailand or Indonesia. Thus it is assumed for the purposes of example that the utility load curve would peak between about 9 A.M. and 5 P.M., with building operation from 7 A.M. to 5 P.M. In this scenario, chiller operation for demand-limited storage would be from 4 P.M. to 10 A.M.; full storage operation would simply avoid the peak from 9 A.M. to 5 P.M.

OPERATING SCHEDULES, SINGAPORE

	Conventional System	Partial Storage	Demand-Limited Storage	Full Storage
Averaged operating hours	10	18.19	12.28	11.20
On-peak hours of operation	9am-5pm	9am-5pm	9-10am, 4-5pm	none
Building cooling hours	10	7	none	none
Storage charging hours	none	14	14	16
Simultaneous operating hours	none	3	4	none

CAPITAL COSTS, SINGAPORE

	Conventional System	Partial Storage	Demand-Limited Storage	Full Storage
Effective chiller efficiency	1.0	0.76	0.68	0.70
Chiller capacity (tons)	100	44	65	71
Chiller capacity reduction (tons)	—	56	35	29
Chiller cost	$40,000	$17,589	$26,066	$28,571
Chiller cost reduction	—	$22,411	$13,934	$11,429
Storage size (ton-hrs)	0	500	681	800
Storage cost	—	$37,475	$51,067	$60,000
Capital cost increase	—	$15,064	$37,133	$48,571
Cooling peak reduction (tons)	—	56	35	29
Incremental capital cost	—	$269/ton	$1,066/ton	$1,700/ton
Cost per avoided peak kW	unknown	$31/kW	$121/kW	$193/kW

OPERATING COSTS, SINGAPORE

	Conventional	Partial	Demand-Limited	Full
Annual operational costs	$54,822.33	$42,946.44	$32,880.85	$31,975.67
Operational cost savings	—	$11,875.89	$21,941.48	$22,846.67

PAYBACK, SINGAPORE

	Conventional	Partial	Demand-Limited	Full
Simple payback time (yrs)	—	1.3	1.7	2.1

BREAK-EVEN RATES, SINGAPORE

	Conventional	Partial	Demand-Limited	Full
Demand charge	—	$2.70	$4.50	$5.37
Energy charge differential	—	$0.041	$0.076	$0.022

CONCLUSIONS

Potential Impact of Cool Storage in ASEAN Countries

We will quickly summarize main points for each country and their relevance to thermal energy storage potential. Conditions of greatest importance in this discussion are those "inherent" to energy supply and demand in that country (load curve, electricity load curves, reliance on imported oil, and power plant construction costs—including lead times); of lesser weight

are those which can be most easily changed to respond to new conditions or desired policy (utility rates).

For Singapore, several of the previously outlined factors indicate at least some potential for using thermal energy storage. These include the general shape of the load curve (the exact shape is unavailable), the presence of a demand charge (although small), the overall costs of electricity generation, and reliance on imported oil. The commercial sector consumes a higher portion of electricity than in any of the other ASEAN countries. A few factors did not show favorable conditions for this technology—slowdown in the growth rate of electrical demand and low transmission losses, for example—but the most important factors are positive. Because Singapore is a bustling commerce center, an introduction of time-of-day rates and an increase in the demand charge would provide the conditions for expansion of cool storage technology.

In Malaysia, an attempt is being made to shift away from oil as the principal fuel source for the generation of electricity and toward the use of natural gas. The most important factors for demonstrating the potential of thermal energy storages are present, and these are load shape and the growth rate of electrical demand. In addition to these inherent conditions, a demand charge is present here also, increasing this potential. The hindering factors are low imported fuel reliance, low electricity prices (without commercial time-of-day rates), and low generation costs. Yet even with these drawbacks, some thermal storage potential does seem to exist; the load shape and electricity demand are dominating reasons.

Indonesia is a peculiar situation, because several factors are favorable to thermal storage (high capital costs, smaller load factors than other countries, high transmission losses, long lead time, and especially high electric demand growth rate), and the factor over which there is most control, utility rates, are already high enough to attract cool storage technology—but its load profile is not particularly favorable. Because the residentially-dominated utility load curve does not peak during all business hours, there is a smaller incentive for utilities to encourage this technology in Indonesia. Instead, by peaking in the evening hours, the load shape actually acts as a hindrance to thermal storage because chillers could not be run until later at night to build up the storage, reducing the necessary charging time. It appears that the industrial sector is expected to show the greatest growth for the remainder of the century. If this is the case, a more level daily load curve could result. Our conclusion is that for Indonesia, a change in the shape of the utility load curve to more closely resemble that of the commercial sector load curve would be the most promising occurrence for cool storage potential. With so many other very promising conditions present in Indonesia, utility load shape is really the limiting factor.

The Philippines is in a very good situation vis-à-vis thermal energy storage. The country's utility load shape is very conducive to the application of this technology, the growth rate in electrical demand is favorable, and commercial electricity use is a significant portion of all electricity demand. Capital costs (as well as lead times and transmission losses) are relatively high, especially those for coal and hydro; since the current plan in this country is to shift away from the use of oil as its main fuel in electricity production to other fuels, particularly coal, it may be quite expensive to build additional capacity in the future. Time-of-use rates are not present yet, but there is a demand charge (although small). Any policy that could reduce high oil dependency will be encouraged. Current conditions are somewhat favorable in the Philippines for the adoption of cool storage; commercial growth and introduction of time-of-day rates would increase this potential.

Lastly, Thailand also presents some conditions that are favorable to thermal energy storage, and several that are not. Although the load curve for the major commercial center (Bangkok) appears very appropriate to load management technology, the countrywide load curve indicates a residential bias during much of the year. As the nation becomes more developed and urbanized, demand conditions have been and will continue to move in the direction of more daytime load. Capital costs are relatively expensive, and imported oil reliance is high enough to cause concern. More importantly, growth in the use of electricity is high, and utility rates (particularly commercial rates and the presence of a reasonable demand charge) are favorable. Based on these conditions, thermal storage is specifically attractive in the urban center (Bangkok), but until the

nationwide load shape changes, it is not throughout the country.

While cool storage technology does appear to be cost-effective in all ASEAN countries for each storage strategy, it can be said that only in the *cities* of these nations—as commercial and industrial centers—is thermal energy storage probably already cost-effective; for rural utilities, inadequate incentives preclude standard operation of these systems. However, recall that it is precisely within the commercial setting that we are interested in the application of this technology.

Final Comments

We have determined that there is some potential for cool storage in ASEAN countries, but several points need to be examined more closely. Several pieces of data must be obtained to achieve stronger conclusions. These include more detailed load profiles, especially by sector and giving the end-use components of the daily peak; more detailed rate schedules, to give a more precise economic picture; a set of detailed simulations, to model system and building performance; and an expansion of this study to include other types of buildings. The next steps for consideration should be a more extensive technical analysis with utility rate scenarios, monitored demonstration buildings, and implementation strategies (such as guidelines for system design, operation management, rate adjustments, and utility rebate possibilities).

Although we cannot predict the future, we do have a good set of information on which to base a conclusion. We are confident that thermal energy storage is a load management technology that can be explored at this time in Malaysia, the Philippines, Singapore, and Thailand, and in Indonesia if and when the utility load curves favorably change. (Of course, uncertainties in future growth and costs will always exist, so that no unwavering conclusion can be made.) However, using partial storage operation, there is little reason *not* to use thermal energy storage—especially with similar first costs to a conventional system. We also believe that thermal storage should always be considered in conjunction with other load shifting or load reduction technologies, such as daylighting and efficient lighting.

Finally, the strongest incentive for the adoption of cool storage technology in ASEAN countries is to encourage all utilities to consider changing rate schedules to reflect actual generating costs.

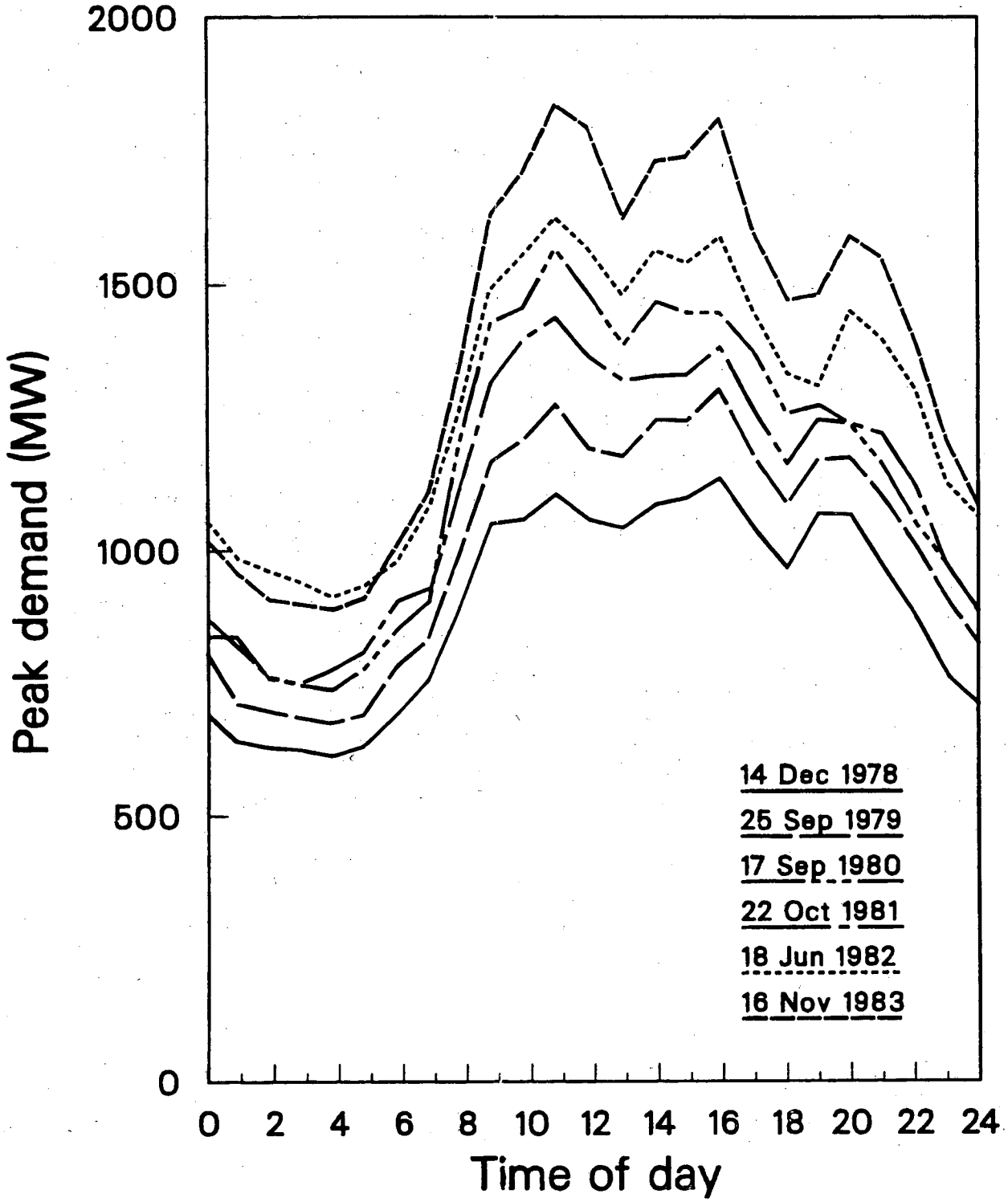

Figure 11-1. Typical Malaysian Daily Load Curves, 1982 [4]

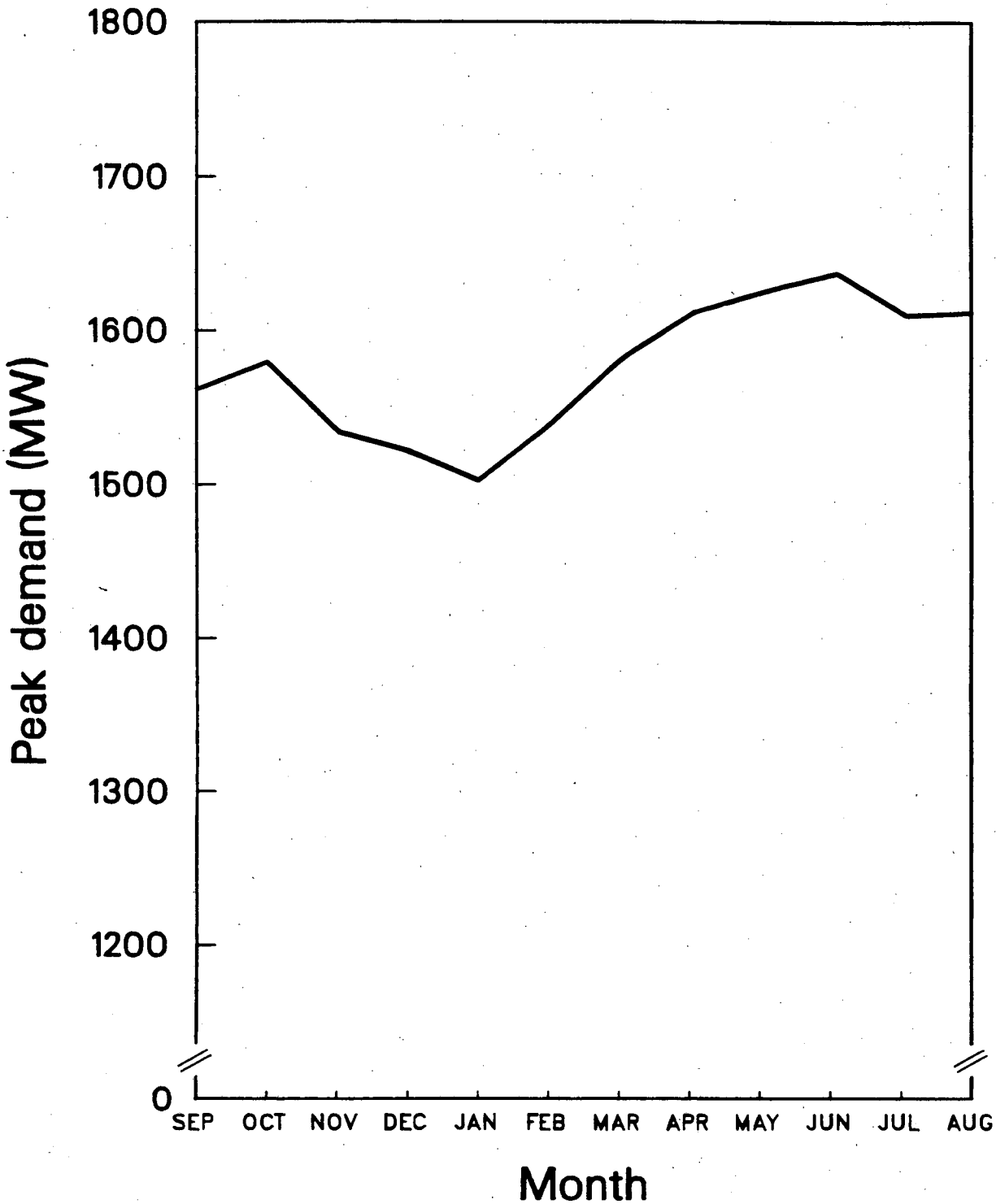

Figure 11-2. Seasonal Malaysian Load Curve, 1982 [5]

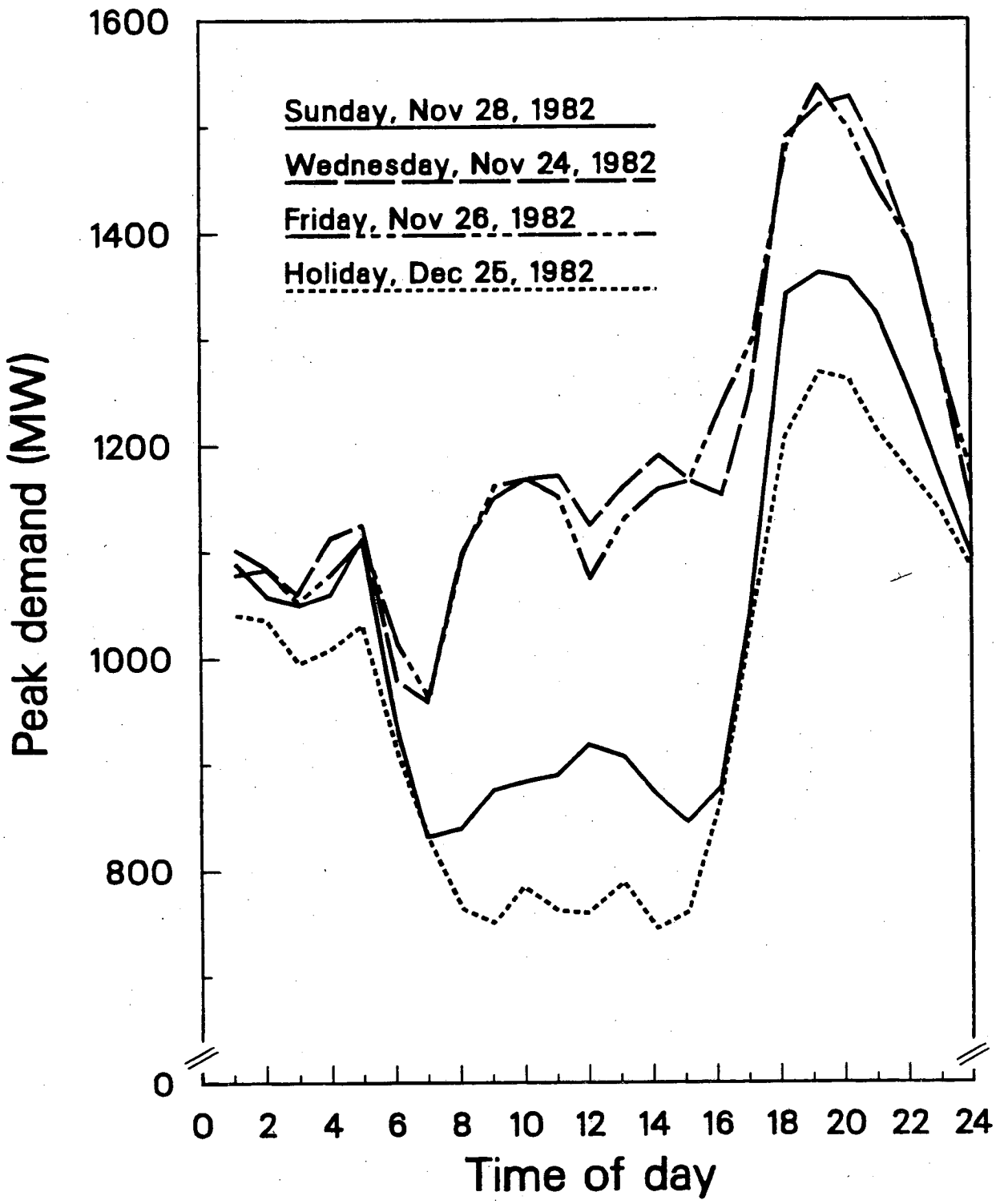

Figure 11-3. Typical Indonesian Daily Load Curves, 1982 [4]

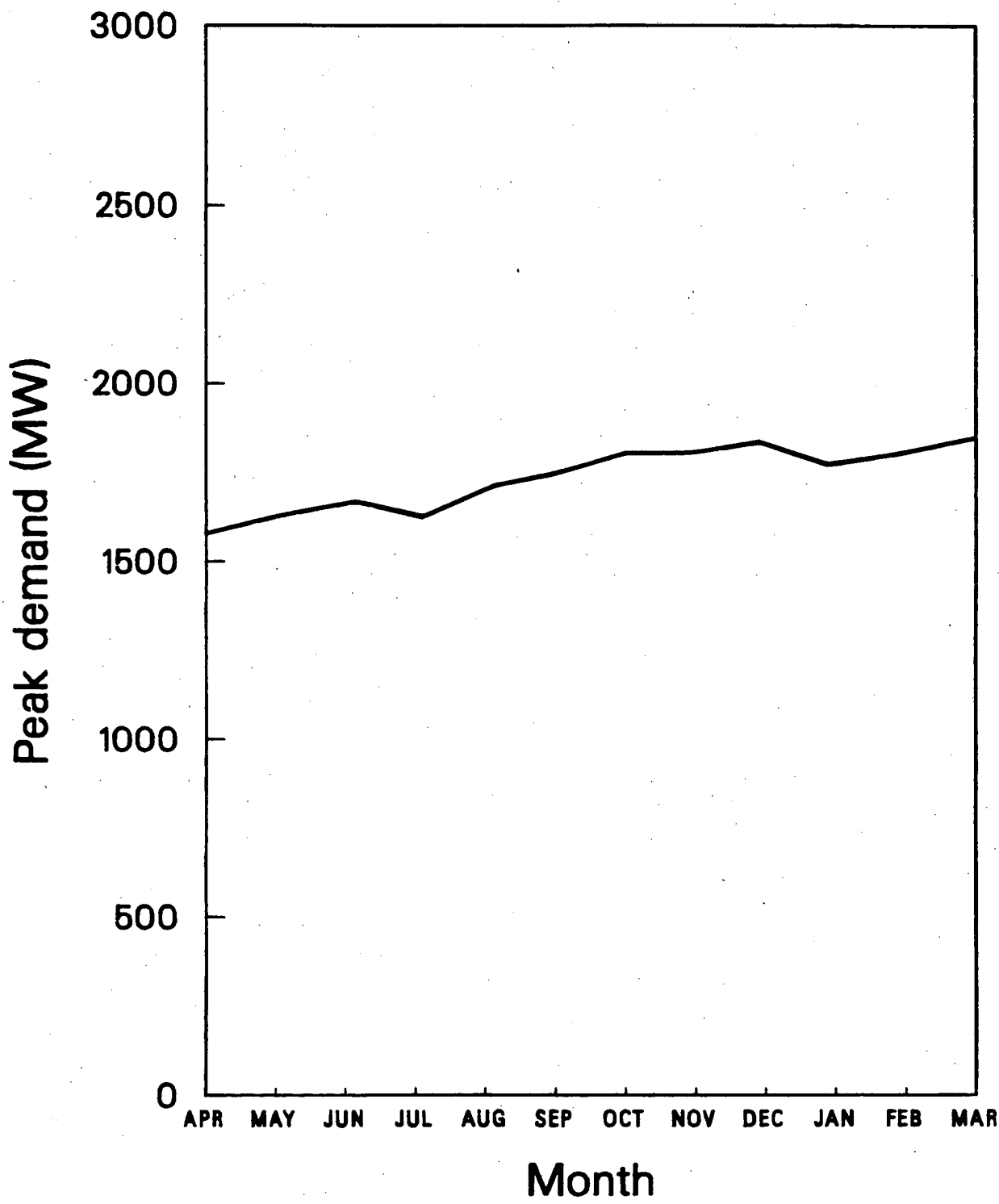

Figure 11-4. Seasonal Indonesian Load Curve, 1982 [5]

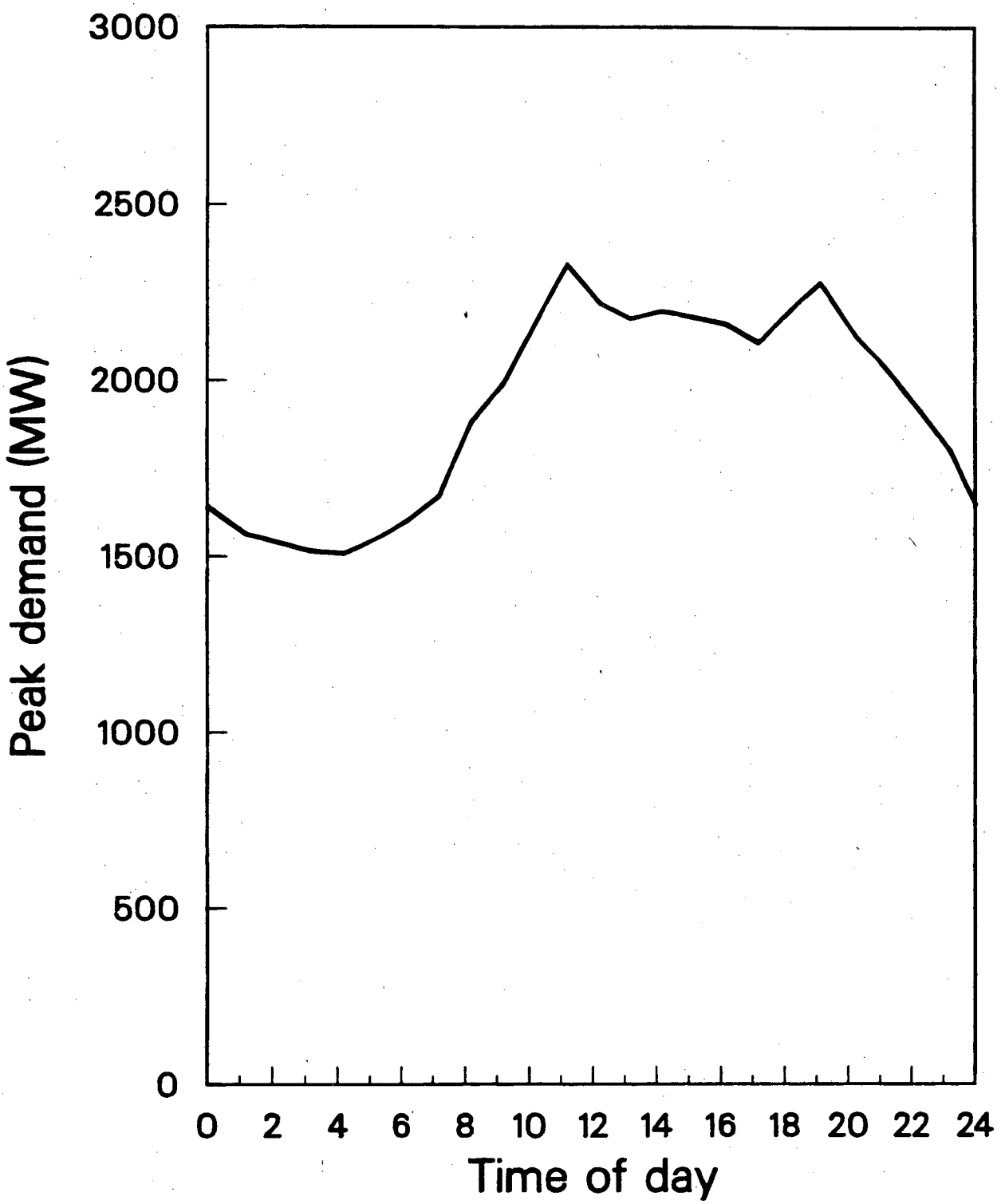

Figure 11-5. Typical Philippine Daily Load Curve, 1982 [4]

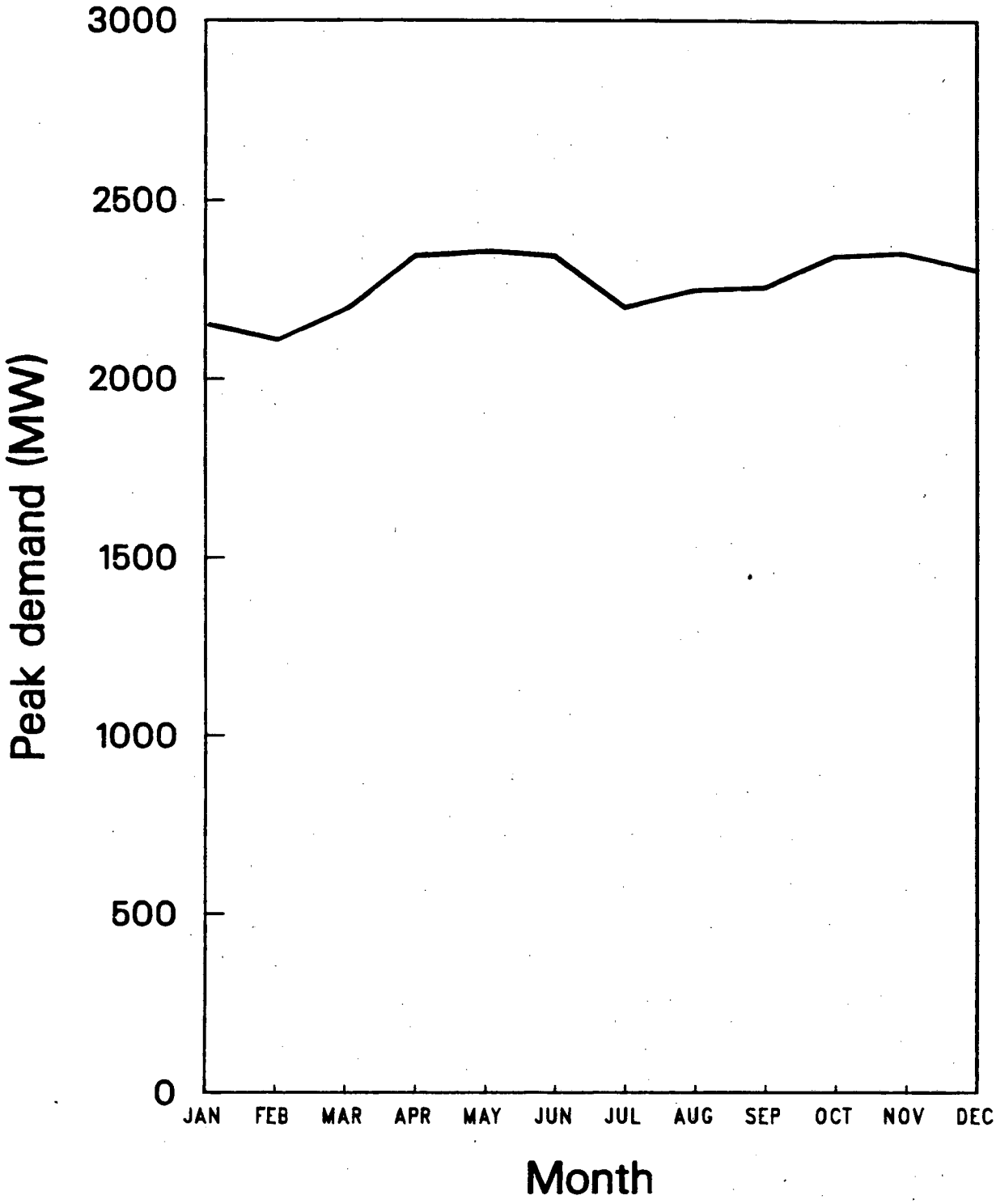

Figure 11-6. Seasonal Philippine Load Curve, 1982 [5]

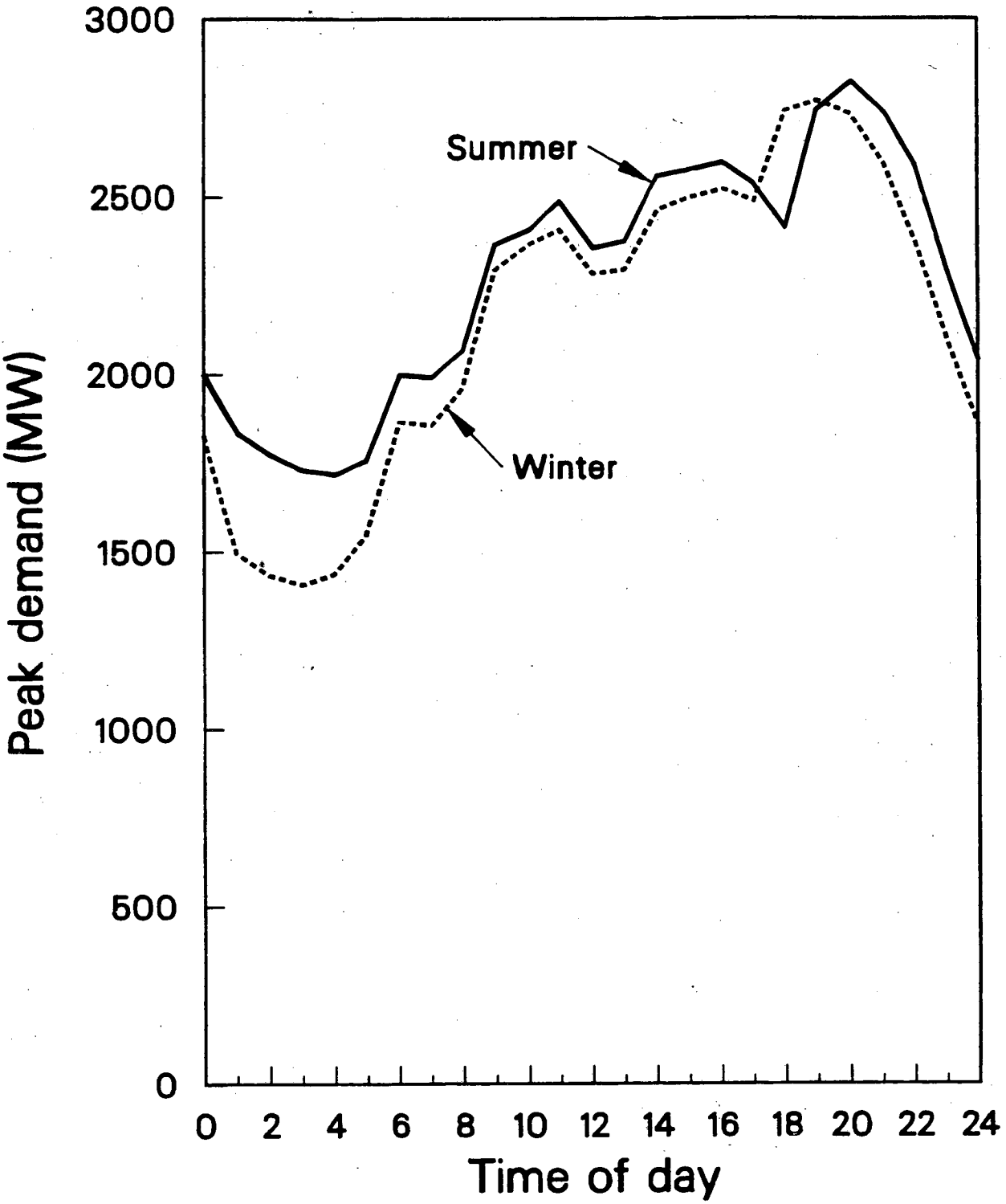

Figure 11-7. Typical Thailand daily load curve, 1982 [1].

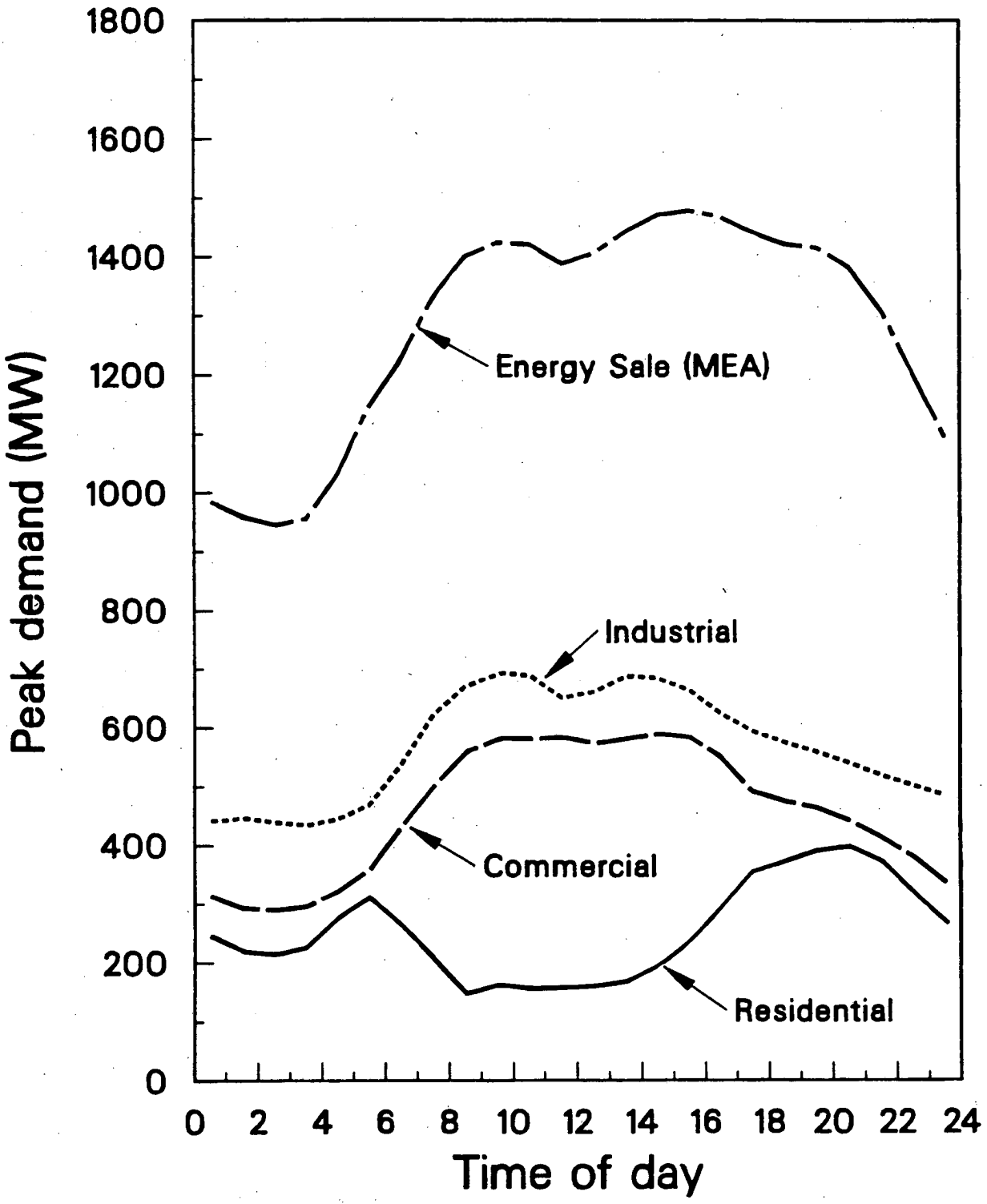

Figure 11-8. Typical Daily Load Curves by Sector, Bangkok, Thailand [4]

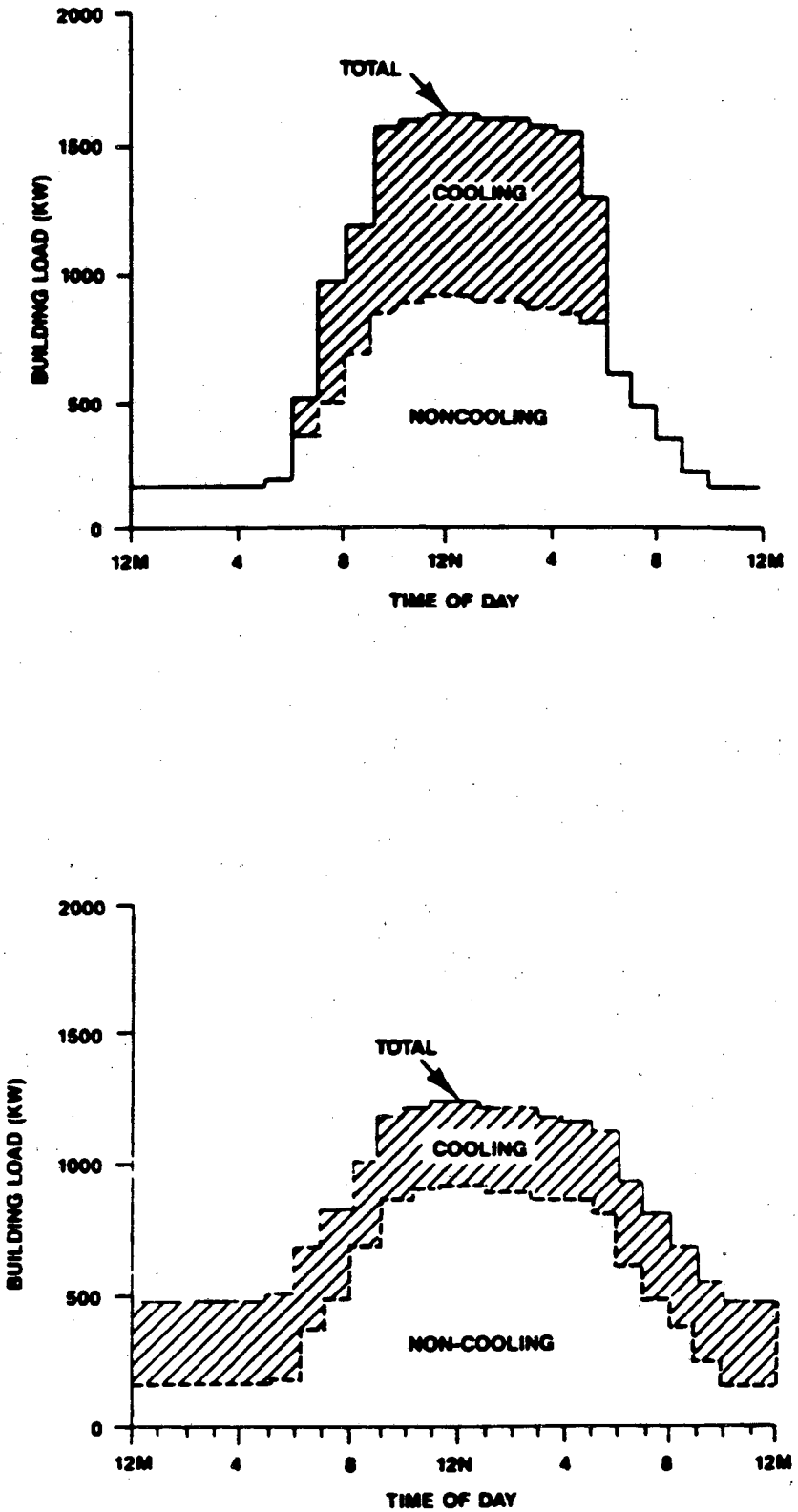

Figure 11-10. Hourly Load Profile for a Partial Storage System on the Same Day

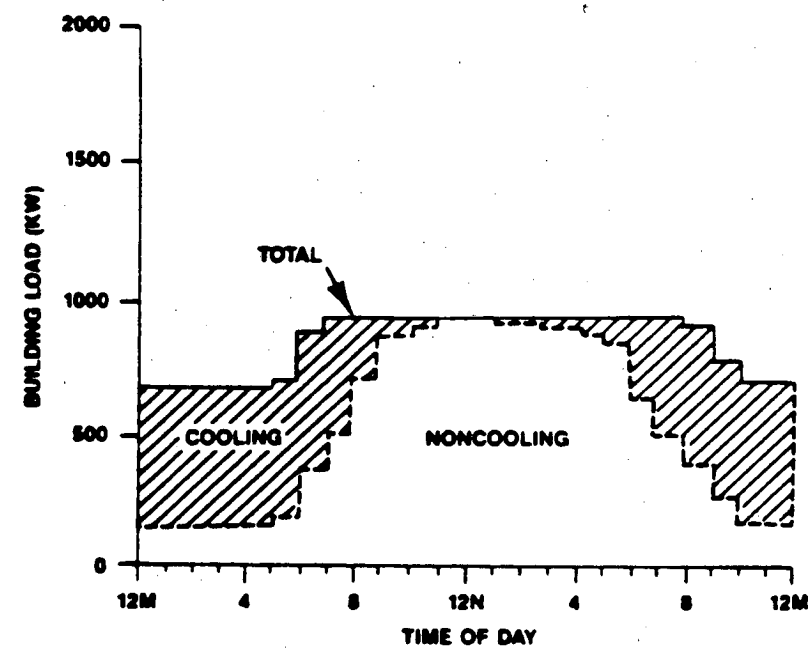

Figure 11-11. Design Day Load Profile using a Demand-Limited Operating Mode

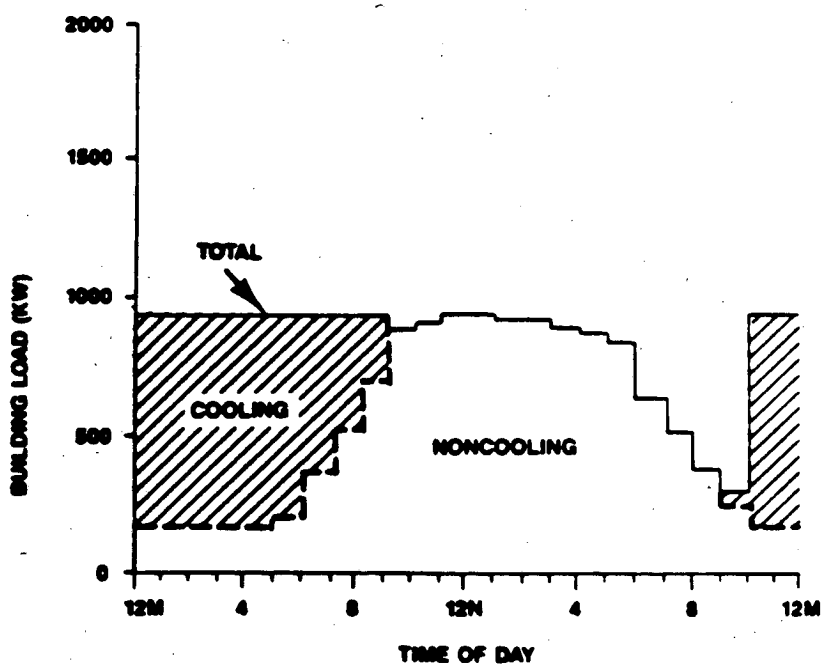

Figure 11-12. Hourly Load Profile under Full Storage Operation on the Design Day

Table 11-1. Electric Demand, Commercial Sector

Sector Totals:	Singapore	Malaysia	Indonesia	Philippines	Thailand
Annual electricity growth rate (1975-80)	7.5%	14.1%	21.8%	unknown	11.2%
Annual electricity growth rate (1980-82)	2.2%	8.2%	-2.2%	unknown	2.4%
Annual peak demand growth rate	7.5% (1981)	15.5% (1975-80)			
Electricity consumption, GWh; % of total (80)	2,569 (41.4%)	2,151 (24.7%)	1,915 (15.8%)	4,770 (31.8%)	3,541 (27.2%)
Electricity consumption, GWh; % of total (82)	2,683 (38.3%)	2,518 (27.6%)	unknown	unknown	3,712 (25.1%)
Electricity consumption, GWh; % (2000-proj.)	unknown	unknown	35,360	unknown	9,770 (19.0%)

Table 11-2. Economics, Commercial Sector

Sector Totals:	Singapore	Malaysia	Indonesia	Philippines	Thailand
Electricity prices, US$/kWh (1980)	$0.083	$0.076	$0.054	$0.079	$0.090
Electricity prices, US$/kWh (1982)	$0.091	$0.106	$0.095	$0.093	$0.137

Table 11-3. Electric Demand, National

Domestic Totals:	Singapore	Malaysia	Indonesia	Philippines	Thailand
Annual electricity growth rate (1975-80)	11.1%	12.2%	11.8%	8.4%	12.1%
Annual electricity growth rate (1980-82)	6.3%	6.9%	11.4%	6.1%	6.6%
Annual electricity growth rate (1985-2000, proj.)	6.2%	8.0%	14.7%	7.1%	6.6%
Peak demand growth rate (1975-80)	9.3%	15.5%	17.7%	8.1%	11.1%
Peak demand growth rate (1980-82)	6.8%	7.1%	15.5%	9.9%	7.9%
Peak demand growth rate (1985-2000, proj.)	6.1%	8.4%	14.4%	6.8%	6.6%
Electricity consumption, GWh (1980)	6,198	8,470	12,130	14,537	13,010
Electricity consumption, GWh (1982)	7,000	9,134	15,050	16,365	14,770
Electricity consumption, GWh (2000, proj.)	22,580	35,490	151,500	60,048	51,480
Peak capacity, MW (1980)	1,170	1,427	2,730	2,413	2,453
Peak capacity, MW (1982)	1,334	1,637	3,650	2,913	2,854
Peak capacity, MW (2000-proj.)	4,260	6,750	25,630	9,331	10,500
Imported fuel reliance, oil (1982)	100%	30.9%	40.8%	68.4%	57.1%

Table 11-4. Electric Supply, National

Domestic Totals:	Singapore	Malaysia	Indonesia	Philippines	Thailand
Electricity supplied, oil generated (1980)	100%	77.9%	82.1%	58.2%	78.8%
Electricity supplied, oil generated (1982)	100%	89.9%	85.8%	50.9%	33.8%
Electricity supplied, oil generated (2000-proj.)	unknown	40%	11.0%	11.5% (1995)	1.9%
Electricity supplied, hydro generated (1980)	---	14.3%	17.9%	22.4%	11.8%
Electricity supplied, hydro generated (1982)	---	13.4%	12.7%	21.2%	27.3%
Electricity supplied, hydro generated (2000-proj.)	unknown	10%	16.0%	28.3% (1995)	12.8%
Electricity supplied, diesel generated (1980)	---	7.8%	---	5.9%	---
Electricity supplied, diesel generated (1982)	---	6.7%	13.1%	1.3%	---
Electricity supplied, diesel generated (2000-proj.)	unknown	---	---	---	---
Electricity supplied, coal generated (1980)	---	---	---	0.3%	9.4%
Electricity supplied, coal generated (1982)	---	---	---	0.3%	10.1%
Electricity supplied, coal generated (2000-proj.)	unknown	7%	68.7%	28.4% (1995)	56.7%
Electricity supplied, gas generated (1980)	---	---	---	---	---
Electricity supplied, gas generated (1982)	---	---	---	---	28.8%
Electricity supplied, gas generated (2000-proj.)	unknown	42%	---	---	28.6%
Electricity supplied, geothermal (1980)	---	---	---	13.2%	---
Electricity supplied, geothermal (1982)	---	---	1.6%	20.3%	---
Electricity supplied, geothermal (2000-proj.)	unknown	---	4.3%	21.6% (1995)	---
Total electricity supplied/capita, kWh (1982)	2832	746	83.5	323	302

Table 11-5. Economics, National (1982)

Domestic Totals:	Singapore	Malaysia	Indonesia	Philippines	Thailand
Capital costs, oil plants, US$/kW	unknown	$680	$561 ('83)	$989	$616
Capital costs, gas plants, US$/kW	---	$540	$254 ('83)	---	$616
Capital costs, coal plants, US$/kW	---	$920	$667 ('83)	$1100	$792
Capital costs, hydro plants, US$/kW	---	---	---	$1184	---
Capital costs, geothermal plants, US$/kW	---	---	$770 ('83)	$539	---
Fuels costs, % of generation costs, oil	71.3%	67.9%	unknown	70.0%	75.1%
Fuels costs, %, gas	---	64.4%	unknown	---	70.9%
Fuels costs, %, coal	---	unknown	unknown	41.0%	55.3%
Fuels costs, %, geothermal	---	---	unknown	71.0%	---
Fuels costs, %, all fuels	71.3%	66.0%	48.2%	80.4%/69.4%	45.0%
Total costs, US$/kWh, oil plants	$0.077	$0.103	unknown	$0.069	$0.056
Total costs, US$/kWh, gas plants	---	$0.086	unknown	---	$0.048
Total costs, US$/kWh, coal plants	---	$0.085	unknown	$0.040	$0.043
Total costs, US$/kWh, hydro plants	---	---	---	$0.050	---
Total costs, US$/kWh, geothermal plants	---	---	unknown	$0.041	---
Total costs, US$/kWh, all plants	$0.0772	$0.0928	$0.0897	$0.0790/$0.0504	$0.0646
Electricity price, US$/kWh	$0.0854	$0.0940	$0.0855	$0.0800/$0.0503	$0.0792
Average power charges, US$/kW	$2.66-$3.00	$5.15	unknown	$1.51	$4.25

Table 11-6. Miscellaneous Data, National (1982)

Domestic Totals:	Singapore	Malaysia	Indonesia	Philippines	Thailand
Lead times, thermal plants, years	unknown	4.5	7.5	6-8.5	6.5
Transmission & distribution losses, %	4.9%	8.8%	25.9%	14.2%	9.8%
Load factor, %	67.5%	63.9%	59.8%	unknown	67.7%

APPENDIX 11-A

THERMAL ENERGY STORAGE IN THE UNITED STATES

APPENDIX 11-A

THERMAL ENERGY STORAGE IN THE UNITED STATES

INTRODUCTION

In the United States, thermal energy storage has primarily been installed in commercial buildings. This appendix presents some experience with these systems.

U.S. EXPERIENCE AND MARKET POTENTIAL

It is estimated that cooling of commercial buildings in the U.S. is responsible for about 30% of the peak electric demand, or about 150 GW out of 500 GW [10]. The growth in new commercial building construction is about 5% a year, and so cooling represents an annual increase in electric demand of about 7 GW.

The best application for thermal energy storage is in new construction, because installation costs are lower. Sixty-eight percent of present cool storage systems have been installed in new buildings [2]. Incorporation of cool storage into new construction enables the system and related components to be properly sized and designed for each particular building; thermal storage in retrofit construction often contends with an existing chiller that was not designed with storage in mind. Excessive capacity and/or related costs can be avoided, assuring the best application of this cooling technology. For example, a compressor runs most efficiently at rated capacity; maximum savings in operation will be realized if it is sized for the building load. Fans and ducts can be sized for storage loads and temperatures. However, reducing cooling costs in old buildings can still be possible with thermal storage.

A clear leader in the choice of operational mode has not yet appeared in the United States. The previously quoted survey [2] shows that existing systems are about evenly divided between partial and full storage operation, but with inexpensive and reliable microprocessor controls, there has been an increasing trend towards demand-limited operation.

The importance of investment in the development of energy storage is clearer when it is noted that electricity currently accounts for 70% of the energy bills of the U.S. commercial sector, with about ⅓ devoted to demand charges. In the U.S., a significant portion of public utilities have incorporated time-of-use rates (and/or demand rates) into their rate structures. A recent study by the Electric Power Research Institute (EPRI) estimates that by the end of this century, 25% of new construction and 15% of cooling system retrofits will have thermal storage [10]. Under these conditions, EPRI predicts that the market for thermal storage to be 25,000 buildings in 1990, increasing to 180,000 buildings by the year 2000 [11]. The savings in peak power would rise to 17 GW in that year from a savings of 2.5 GW in 1990. Market penetration has already begun.

Between 1982 and 1985, 14 office buildings with cool storage systems were built in Dallas, Texas, representing 15 million ft^2 and reducing peak growth by about 25 MW. In 1984, the penetration of cool storage in new construction was 38% of large office building in Dallas [12]. Texas, California, and Illinois have been the states where greatest efforts are being made in introducing load management technology, especially thermal energy storage, but the market is certainly not limited to these states. An important market for cool storage also exists in the industrial sector as process cooling, but because of its diversity, only in some industries (such as food processing) has this market has been penetrated.

MANUFACTURERS

The major U.S. manufacturers of ice systems are: Calmac, Baltimore Air Coil, Chester-Jensen, National Integrated Systems, Process Products, and the Turbo division of Aqua-Chem. Several other smaller companies also have a share of this market. Of all ice system manufacturers, Baltimore Air Coil has the highest total sales, but each manufacturer seems to have its own market niche. For example, Calmac has a good percentage of the retrofit market, because its system is compatible with most existing chillers. Rapid market expansion is taking place; almost

every month new products are introduced, particularly dynamic ice systems. Competition among manufacturers is increasing. These manufacturers generally install the systems on a turnkey basis and maintain the systems themselves. This profession has been gathering momentum, partly explaining why ice systems are taking over a growing part of the market from chilled water storage.

As mentioned previously, chilled water tanks are generally not factory-built, so there are few manufacturers of such equipment. The one major producer of chilled water systems, including tanks, insulation, instrumentation, and corrosion protection, is CBI Industries in Illinois.

There are several manufacturers of alternative storage media. Thermal Energy Storage, Inc., a developing company, has released its new product in the thermal storage market—clathrates. The most established company in the U.S. for systems using alternative media, Transphase, is using plastic containers filled with phase-change salts, which change phase at 8°C. Only a few percent of commercial buildings now use this technology. A French company, Christopia, produces a type of plastic ball containing eutectic salts with a similar phase-change temperature. Little experience can be found with this product in the U.S.

PERFORMANCE RESULTS

A recent study by Argonne National Laboratory systems examined the performance of 76 installed cool storage systems, but was inconclusive since too few buildings had submetered cooling systems [2]. Without this type of data, it is difficult to evaluate the performance of these systems, but a 1984 ASHRAE survey observed that 95% of thermal storage building owners and managers thought the systems in their buildings were performing satisfactorily after building operators became experienced with the systems. Very few maintenance problems were described.

To adequately analyze and evaluate system performance, detailed data for a number of thermal storage installations must be obtained by submetering. Although this level of detail has not been widely pursued, there have been some efforts to compile and analyze data that has been collected. The Buildings Energy Data Group at Lawrence Berkeley Laboratory has extended its Buildings Energy-use Compilation and Analysis (BECA) database with a compilation of cool storage buildings. The Electric Power Research Institute in Palo Alto, California, has undertaken a monitoring project for 1987. Preliminary results from these efforts indicate that thermal storage can work well if 1) the building's operating personnel has been properly trained with the system, 2) a "shakedown period" of at least two years is permitted, and of course 3) an equitable rate schedule that accurately reflects marginal costs of generation. As the experience with these systems grows, initial problems in both design and operation can be discovered and corrected to the benefit of future storage system users.

APPENDIX 11-B

ECONOMICS OF THERMAL STORAGE IN COMMERCIAL BUILDINGS

APPENDIX 11-B

ECONOMICS OF THERMAL STORAGE IN COMMERCIAL BUILDINGS

INTRODUCTION

This appendix compares the economics of the three storage options and presents all relevant calculations. In the third section of this paper, we introduced an example building module which was used to demonstrate the cost-effectiveness of cool storage technologies; the same module is used here to show calculations in more detail. Figures for ASEAN countries are determined using similar methods.

EXAMPLE BUILDING CALCULATIONS

The same building module characteristics and conditions from the example of the third section are presented here.

Building Daily Load = 800 ton-hours/day, or 2820 kWh/day
Cooling peak = 92 tons
Conventional chiller capacity = 100 tons, or 350 kW (nearest rating capacity to peak)
Building operating hours = 8 A.M. - 6 P.M. (10 hours)
On-peak hours = 10 A.M. - 6 P.M. (8 hours)
Partial Storage — chiller runs 24 hours/day, 14 hours off-peak;
- direct cooling (cools building), 5½ hours (10:30 A.M. - 4 P.M.)
- indirect cooling (charges storage), 15½ hours (5:30 P.M.-9 A.M.)
- simultaneous cooling (both), 3 hours (9 - 10:30 A.M., 4 - 5:30 P.M.)

Demand-Limited Storage — chiller runs 20 hours/day, 14 hours off-peak
- indirect cooling, 16 hours (6 P.M. - 10 A.M.)
- direct cooling, 0 hours
- simultaneous cooling, 4 hours (10 A.M. - 12 P.M., 4 P.M. - 6 P.M.)

Full Storage — chiller runs 16 hours/day, all of which is off-peak
- direct cooling, 0 hours
- indirect cooling, 16 hours (6 P.M. - 10 A.M.)
- simultaneous cooling, 0 hours

1) First costs:

Calculations for various parameters in each mode are as follows:

Averaged operating hours:	Σ (number of cooling hours * chiller efficiency)
Effective chiller efficiency:	averaged operating hours / total operating hrs
Chiller capacity [tons]:	bldg load [ton-hrs] / averaged operating hours
Chiller capacity reduction [tons]:	conventional capacity [tons] – new capacity [tons]
Chiller cost [$]:	chiller capacity [tons] * price per ton
Chiller cost reduction [$]:	conventional chiller cost – new chiller cost
Storage size [ton-hrs]:	chiller capacity [tons] * efficiency * storage charging hours, OR bldg load – (chiller capacity * efficiency * hrs supplying load)
Storage cost [$]:	storage size [ton-hrs] * price per ton-hr
Increased capital cost [$]:	storage cost – chiller cost reduction
Cooling peak reduction [tons]:	conventional peak [tons] – new chiller peak
Incremental capital cost [$/ton]:	increased capital cost / cooling peak reduction
Cost per avoided peak kW [$/kW]:	(incremental capital cost * COP) / 3.52 kW/ton

Capital costs will be based on the cost of chiller capacity ($400/ton) and on storage capacity ($75/ton-hour). Results of these calculations based on the assumptions and conditions of the

example building are summarized in the following tabulation:

	Conventional System	Partial Storage	Demand-Limited Storage	Full Storage
Effective chiller efficiency	1.0	0.81	0.66	0.7
Chiller capacity (tons)	100	41	60	71
Chiller capacity reduction (tons)	—	59	40	29
Chiller cost	$40,000	$16,400	$24,000	$28,400
Chiller cost reduction	—	$23,600	$16,000	$11,600
Storage size (ton-hrs)	0	460	725	800
Storage cost	—	$34,500	$54,400	$60,000
Capital cost increase	—	$10,900	$38,400	$48,400
Cooling peak reduction (tons)	—	51	92	92
Incremental capital cost	—	$214/ton	$417/ton	$526/ton
Cost per avoided peak kW	—	$213/kW	$415/kW	$523/kW

The actual calculations for each mode are as follows:

Conventional System:

Chiller size:	100 tons (given above)
Chiller cost:	100 * $400/ton = $40,000

Partial Storage:

Effective chiller efficiency:	(5½ hrs * 1.0 + (15½ hrs * 0.7) + (3hrs * 0.7 * ⅓) + (3hrs * ⅔)) / 24 hrs = 0.79
Chiller capacity:	800 ton-hrs / (24 * 0.77) = 43 tons
Chiller capacity reduction	100 tons – 43 tons = 57 tons
Chiller cost:	43 * $400/ton = $17,200
Chiller cost reduction:	$40,000 – $17,200 = $22,800
Storage size:	43 tons * (15½ + (3*⅓)) hrs * 0.7 = 500 ton-hrs
Storage cost:	500 * $75/ton-hr = $37,500
Capital cost increase:	$37,500 – $22,800 = $14,700
Cooling peak reduction:	92 tons – 43 tons = 49 tons
Incremental capital cost:	$14,700 / 49 tons = $300/ton
Cost per avoided peak kW:	($300/ton * 3.5 kW out/kW in) / 3.52 kW/ton = $298/kW

Demand-Limited Storage:

Effective chiller efficiency:	(16 hrs * 0.7 + 4 hrs * 0.7 * 0.7) / 20 hrs = 0.66
Chiller efficiency:	800 ton-hrs / (20 * 0.66) = 60 tons
Chiller capacity reduction:	100 tons – 60 tons = 40 tons
Chiller cost:	60 * $400/ton = $24,000
Chiller cost reduction:	$40,000 – $24,000 = $16,000
Storage size:	60 tons * (16 + 4*0.3) hrs * 0.7 = 725 ton-hrs
Storage cost:	725 * $75/ton-hr = $54,400
Capital cost increase:	$54,400 – $16,000 = $38,400
Cooling peak reduction:	92 tons – 0 tons = 92 tons
Incremental capital cost:	$38,400 / 92 tons = $417/ton
Cost per avoided peak kW:	($417/ton * 3.5) / 3.52 kW/ton = $415/kW

Note that for four hours the chiller operates at less than full load, which is reflected in the effective efficiency. Also, this scenario, reflects time-of-use demand charges, that is, only the peak that occurs during the on-peak rate period matters; if the daily peak occurs in the off-peak period, there is no penalty. The utility is unconcerned if it has plenty of capacity to meet this demand during

that time.

However, some utilities have a flatter load curve, with a finite off-peak capacity. In this case, the highest peak during *any* time of the day is the level determining billing demand. To avoid simply *shifting* demand to off-peak, this load can be *leveled* through the day. The resulting storage size would be slightly smaller than under the case just presented.

Full Storage:

Effective chiller efficiency:	(16 hrs * 0.7) / 16 hrs = 0.7
Chiller capacity:	800 ton-hrs / (16 * 0.7) = 71 tons
Chiller capacity reduction:	100 tons – 71 tons = 29 tons
Chiller cost:	71 * $400/ton = $28,400
Chiller cost reduction:	$40,000 – $28,400 = $11,600
Storage size:	71 tons * 16 hrs * 0.7 = 800 ton-hrs
Storage cost:	800 * $75/ton-hr = $60,000
Capital cost increase:	$60,000 – $11,600 = $48,400
Cooling peak reduction:	92 tons – 0 tons = 92 tons
Incremental capital cost:	$48,400 / 92 tons = $526/ton
Cost per avoided peak kW:	($526/ton * 3.5) / 3.52 kW/ton = $523/kW

This scenario also reflects time-of-use demand rates, but if the level of peak load at any hour was the basis of the monthly demand charge, the chiller would be smaller than the one calculated above. With greater chiller capacity saved, the incremental incurred cost would also be smaller and thus offer this storage mode better economic competitiveness.

2) Operating costs:

To illustrate the costs of the cooling system operation, an example set of utility rates can be used with this scenario.

As an example, SDG&E charges a peak-period rate in the summer between 11 A.M. and 6 P.M., a partial-peak rate between 6 and 11 A.M., and from 6 to 10 P.M., and an off-peak rate from 10 P.M. to 6 A.M.. During these periods, the kWh charges are about 12, 11, and 8 cents, respectively. Additionally, about $8 per month is billed for each kW of demand used during on-peak periods. The intent of thermal energy storage is to displace kWh to the off-peak rate and to avoid the on-peak kW charge. This cost can reach $20 per kW per month for some places in the U.S.

Grants and incentives offered by utilities also play a role, because these can effectively reduce the first cost of a thermal storage system. Some American utilities are faced with the problem of under-capacity, and construction of new power plants is expensive and risky. By offering a customer $300 per displaced kW for storage installation, utilities save a kW they would otherwise have to produce at a cost greater than $1500, at financial and technical risk.

As electricity consumption is transferred from on-peak to off-peak periods, utilities will more efficiently use their existing power plants by increasing their load factor. Strong interest by electric utilities should continue in the future.

Although many utilities have ratchet clauses and/or declining-block energy charges, these rate structure features do not need to be considered here to demonstrate the economics of thermal storage.

Case A:	Demand charge	$3.00/kW of billing demand (on-peak)
	Energy charge	$0.08/kWh of on-peak energy use
		$0.05/kWh of off-peak energy use
Case B:	Demand charge	$7.00/kW of billing demand (on-peak)
	Energy charge	$0.09/kWh of on-peak energy use
		$0.05/kWh of off-peak energy use

These rates determine operational costs for the four cooling cases in this example. Equal energy use for both the conventional system and the storage systems is assumed, meaning that lower operating efficiencies which occur when charging storage are not reflected. These calculations also assume that 260 operating days is a full operating year. Differences in annual operational savings are calculated by simple subtraction of the utility costs for each storage system from those for the conventional system. Calculations for example utility charges are summarized for a *conventional* cooling system are as follows:

Rate case A:

Demand charges:	100 tons * 3.52 kW/ton * $3/kW = $1060/month
On-peak energy:	2,820 kWh * (8 hrs/10 hrs) * $0.08/kWh = $180/day
Off-peak energy:	2,820 kWh * (2 hrs/10 hrs) * $0.05/kWh = $28/day
Annual charges:	($1060 * 12 mos) + ($180 + $28) * 260 days = $66,800.

Rate case B:

Demand charges:	100 tons * 3.52 kW/ton * $7/kW = $2,460/month
On-peak energy:	2,820 kWh * (8 hrs/10 hrs) * $0.09/kWh = $203/day
Off-peak energy:	2,820 kWh * (2 hrs/10 hrs) * $0.05/kWh = $28/day
Annual charges:	($2,460 * 12 mos) + ($203 + $28) * 260 days = $89,600.

For a partial storage system, these charges can be found in a similar manner:

Rate case A:

Demand charges:	43 tons * 3.52 kW/ton * $3/kW = $454/month
On-peak energy:	2,820 kWh * (8½ hrs/24 hrs) * $0.08/kWh = $80/day
Off-peak energy:	2,820 kWh * (15½ hrs/24 hrs) * $0.05/kWh = $91/day
Annual charges:	($454 * 12 mos) + ($80 + $91) * 260 days = $49,900.
Operational cost savings:	$66,800 — $49,900 = $16,900

Rate case B:

Demand charges:	43 tons * 3.52 kW/ton * $7/kW = $1060/month
On-peak energy:	2,820 kWh * (8.5 hrs/24 hrs) * $0.09/kWh = $90/day
Off-peak energy:	2,820 kWh * (15.5 hrs/24 hrs) * $0.05/kWh = $91/day
Annual charges:	($1060 * 12 mos) + ($90 + $91) * 260 days = $59,800.
Operational cost savings:	$89,600 — $59,800 = $29,800

Charges for a demand-limited system are calculated by:

Rate case A:

Demand charges:	0 tons * 3.52 kW/ton * $3/kW = $0/month
On-peak energy:	2,820 kWh * (4*0.7 hrs)/20 hrs * $0.08/kWh = $32/day
Off-peak energy:	2,820 kWh * (16 hrs/20 hrs) * $0.05/kWh = $113/day
Annual charges:	($0 * 12 mos) + ($32 + $113) * 260 days = $37,700.
Operational cost savings:	$66,800 — $37,700 = $29,100

Rate case B:

Demand charges:	0 tons * 3.52 kW/ton * $7/kW = $0/month
On-peak energy:	2,820 kWh * (4*0.7) hrs/20 hrs * $0.09/kWh = $36/day
Off-peak energy:	2,820 kWh * (16 hrs/20 hrs) * $0.05/kWh = $113/day
Annual charges:	($0 * 12 mos) + ($36 + $113) * 260 days = $38,700.
Operational cost savings:	$89,600 — $38,700 = $50,900

Finally, charges for a full storage system are as follows:

Rate case A:

Demand charges:	0 tons * 3.52 kW/ton * $3/kW = $0/month
On-peak energy:	0 kWh * $0.08/kWh = $0/day
Off-peak energy:	2,820 kWh * $0.05/kWh = $141/day
Annual charges:	($0 * 12 mos) + ($0 + $141) * 260 days = $36,700.
Operational cost savings:	$66,800 — $36,700 = $30,100

Rate case B:

Demand charges:	0 tons * 3.52 kW/ton * $7/kW = $0/month
On-peak energy:	0 kWh * $0.09/kWh = $0/day
Off-peak energy:	2,820 kWh * $0.05/kWh = $141/day
Annual charges:	($0 * 12 mos) + ($0 + $141) * 260 days = $36,700.
Operational cost savings:	$89,600 — $36,700 = $52,900

3) Simple Payback:

The payback time can be calculated by dividing the capital cost increase by operational cost savings.

Partial storage (rate A):

$14,700 / $16,900 = 0.87 years

Partial storage (rate B):

$14,700 / $29,800 = 0.49 years

Demand-limited storage (rate A):

$38,400 / $29,100 = 1.3 years

Demand-limited storage (rate B):

$38,400 / $50,900 = 0.75 years

Full storage (rate A):

$48,400 / $30,100 = 1.6 years

Full storage (rate B):

$48,400 / $52,900 = 0.92 years

This example shows the general trend that partial storage tends to have a faster payback time than full storage, especially with higher demand charges and/or on-peak energy costs (rate B). Of course, the length of this payback period will vary depending on the costs of both refrigeration and storage. Typically, payback times are longer than those calculated due to unforeseen capital costs and different rate structures. If this is indeed the case, utility rebates, as discussed previously, can make an important economic contribution.

4) Operational Economics:

General costs of operation can be developed, and utility charges determined, that would demonstrate cost-effectiveness in cases that are not economical. Although this case does not fall into that category, the example will still be made. In the following equations, "d" represents the demand charge (per peak kW), and "Δe" represents the difference between on-peak energy charges ("e_1") and off-peak energy charges ("e_2").

Conventional system:

Demand charges:	100 tons * 3.52 kW/ton * 12 mos * $d = $4,220d
On-peak energy:	2,820 kWh * 260 days * (8 hrs/10 hrs) * $$e_1$ = $587,000$e_1$
Off-peak energy:	2,820 kWh * 260 days * (2 hrs/10 hrs) * $$e_2$ = $147,000$e_2$
Total utility costs:	$4,220d + $587,000$\Delta e$ + $733,000$e_2$

Partial storage system:

Demand charges:	43 tons * 3.52 kW/ton * 12 mos * $d = $1,820d
On-peak energy:	2,820 kWh * 260 days * (8.5 hrs/24 hrs) * e_1$ = $260,000e$_1$
Off-peak energy:	2,820 kWh * 260 days * (15.5 hrs/24 hrs) * e_2$ = $474,000e$_2$
Total utility costs:	$1,820d + $260,000Δe + $733,000e$_2$
Operational cost savings:	$2,400d + $327,000Δe

Demand-limited storage system:

Demand charges:	0 tons * 3.52 kW/ton * 12 mos * $d = $0d
On-peak energy:	2,820 kWh * 260 days * (4*0.7) hrs/20 hrs * e_1$ = $103,000e$_1$
Off-peak energy:	2,820 kWh * 260 days * (16 hrs/20 hrs) * e_2$ = $587,000e$_2$
Total utility costs:	$103,000Δe + $689,000e$_2$
Operational cost savings:	$4,220d + $484,000Δe + $44,000e$_2$

Full storage system:

Demand charges:	0 tons * 3.52 kW/ton * 12 mos * $d = $0d
On-peak energy:	0 kWh * 260 days * e_1$ = $0e$_1$
Off-peak energy:	2,820 kWh * 260 days * e_2$ = $733,000e$_2$
Total utility costs:	$733,000e$_2$
Operational cost savings:	$4,220d + $587,000Δe

5) Break-even rates:

These mathematical expressions can be used to find the demand charge or energy price differential for a payback time of three years. Each of these hypothetical charges assume the other charge is zero.

Partial storage:

Demand charge:	$14,700 / $2,400d = 3; d = $2.04
Energy charge differential:	$14,700 / $327,000Δe = 3; Δe = $0.045

Demand-limited storage:

Demand charge:	$38,400 / $4,220d = 3; d = $3.03
Energy charge differential:	There are multiple solutions to this equation of two unknowns.

Full storage:

Demand charge:	$48,400 / $4,220d = 3; d = $3.82
Energy charge differential:	$48,400 / $587,000Δe = 3; Δe = $0.027

REFERENCES

1. Electric Power Research Institute, "Commercial Cool Storage Presentation Material, Volume 1," EPRI Report EM-4405, prepared by Engineering Interface, Ltd., Willowdale, Ontario, Canada, February, 1986.
2. Hersh, H., "Current Trends in Commercial Cool Storage," Argonne National Laboratory Project 2036-13, September, 1984.
3. Warren, M.L., "Impact of Operation and Control Strategy on the Performance of a Thermal Storage System," Lawrence Berkeley Laboratory Report LBL-20180, 1985.
4. Resources Systems Institute, East-West Center, Honolulu, HI, September, 1985.
   a. Kadir, A. and Kim, Y.H., "The Electric Future of Singapore."
   b. Rahman *et al.*, "The Electric Future of Malaysia."
   c. Kadir *et al.*, "The Electric Future of Indonesia."
   d. Herrera *et al.*, "The Electric Future of The Philippines."
   e. Aphaiphurminart *et al.*, "The Electric Future of Thailand."
5. Asian Development Bank, "Asian Electric Power Utilities Data Book," 1985.
6. U.S. Energy Information Agency, "Annual Energy Review 1985," DOE/EIA-0384(85).
7. North American Electric Reliability Council, "Electric Power Supply and Demand, 1985-1994," 1985.
8. Electric Power Research Institute, "Characteristics of Commercial Sector Buildings and Their Energy Use and Demand," EPRI Report RP1201-26, submitted by Enviro-Management and Research, Inc. and QLA, Inc., April, 1984.
9. Public Utilities Commission of Texas, "Energy and Power Conservation in Texas Buildings," 1986.
10. de la Moriniere, O., "The Attractive Economics of Thermal Storage in New Buildings," Lawrence Berkeley Laboratory Report LBL-19241, 1985.
11. Electric Power Research Institute, "Commercial Cool Storage Primer," EPRI Report EM-3371, prepared by RCF, Inc., Chicago, IL., January, 1984.
12. International Thermal Storage Advisory Council, San Diego, CA, "Technical Bulletin," July, 1986.
13. Electric Power Research Institute, "COMMEND Planning System: National and Regional Data Analysis," EPRI Report EM-4486, prepared by Georgia Institute of Technology, April, 1986.
14. Engineered Systems, Business News Publishing Co., "Movin' on up in Dallas," January/February, 1986.

CHAPTER 12: IMPLICATIONS OF DEMAND-SIDE MANAGEMENT TECHNOLOGY ON AN ELECTRIC UTILITY IN MALAYSIA

S. Sairan and A.H. Azit
Lembaga Letrik Negara
Kuala Lumpur, Malaysia

ABSTRACT

This report describes a research study on the implications of demand-side energy management and efficiency on the Lembaga Letrik Negara electric utility. Demand-side energy management generally implies more efficient utilization of energy through either new technology or improved operation of current technology. Consumers should receive immediate cost savings, while the utility should achieve more efficient dispatching of power plants.

Demand-side energy management could potentially reduce peak loads and improve system load factors. These improvements would invariably lead to lower production costs and improved reserve margins. In the long term, demand management could influence generation expansion plans by allowing for reduced capacity or deferment of installed generating units. Demand-side management, therefore, could benefit both consumers and the utility.

This study investigates the effects of introducing the new demand-side management technology: thermal energy storage. Thermal energy storage permits shifting the air-conditioning load from peak to off-peak hours. Hence, thermal energy storage both reduces the system peak and offers customers the savings of off-peak tariff rates. Wide application of thermal energy storage would certainly have an impact on the electricity demand profile, thus affecting the production costs of electricity.

The first part of this study attempted to quantify thermal energy storage's potential impacts on the electricity demand profile in terms of both supply and demand. An economic evaluation of total impact was also conducted. The second part of the study investigated the impacts that different levels of energy efficiency in the commercial sector would have on the utility. The four levels of energy efficiency examined are as close as possible to those stipulated in the *Guidelines for Energy Efficiency in Buildings* published by the Ministry of Energy, Telecommunication and Post.

One important aspect of the study was the compilation of a daily load profile for the commercial sector. Consumer class hourly demands, gathered from remote feeder reading facilities, were analyzed. The load research concluded that the building sectors contribute significantly to the peak demand. Energy audit reports indicate that air-conditioning forms the major load. Thermal energy storage therefore appears a viable demand-side management technology.

The study established several scenarios, assuming penetration rates of up to 50% thermal energy storage application by the year 2000. The projected building load after the transfer of electrical energy from peak to the off-peak hours was estimated.

The study examined how changes in the demand side would affect the supply side. Accordingly, changes in the demand profile resulting from thermal energy storage application were correlated to the overall system load profile. A typical weekly profile for each month was developed, as was another weekly profile representing the changes incurred due to thermal energy storage application.

A production cost model was used to determine and quantify the magnitude of thermal energy storage's impact on the supply side. The model, called UPLAN, was designed to study energy management in utilities. The system parameters investigated included peak reduction, load factor, reserve margin, and production cost.

Base-case demand and supply data were obtained for each year from 1990 to 2000. For each thermal energy storage penetration rate scenario, several simulations were made. This paper analyzed the simulation results.

The study also analyzed the financial effect that thermal energy storage implementation would have on the utility and the consumers. This was done by determining the benefit-cost ratio of the demand-side energy management program from the perspectives of both Lembaga Letrik Negara and consumers. The analysis showed that both the utility and its consumers would benefit from the demand-side energy management program. A sensitivity study then analyzed a possible demand-side energy-management marketing strategy whereby Lembaga Letrik Negara would subsidize—through incentives—the capital cost to consumers of installing a thermal energy storage system.

The study concluded that demand-side management technology would benefit both the utility and its customers. The success of such a program, however, would depend on both parties' commitment to achieving mutual benefits.

INTRODUCTION

Lembaga Letrik Negara

Lembaga Letrik Negara (LLN), along with the Sarawak Electric Supply Corporation (SESCO) and the Sabah Electric Board (SEB), are Malaysia's electric power utilities. LLN services the whole of Peninsular Malaysia, while SESCO and SEB service the states of Sarawak and Sabah, respectively. Figure 12-1 shows a map of Malaysia which indicates the service territories of the three utilities. The Ministry of Energy, Telecommunication and Posts coordinates the activities of the three utilities at the national level.

Broadly speaking, LLN has a statutory duty to generate, transmit, and distribute electricity for national development in Peninsular Malaysia. The utility must also supply electricity at the lowest possible cost and advise the Minister charged with the responsibility for electricity on all matters relating to electric power generation and use. LLN is required to manage and operate electrical installations acquired by, transferred to, or established by it. To enable LLN to carry out its duties, the utility is invested with wide powers to construct and operate supply lines and stations, to generate and sell electricity, to acquire electrical plants and property for such purposes, and, to a limited extent, to assemble and manufacture electrical plants and fittings.

LLN has the largest energy demand of the three utilities. Table 12-1 shows the utilities' total energy and peak demands for the year 1985. LLN's total sales in 1987 were 12,300 GWh, and its peak demand reached 2441 MW. Growth figures for the LLN integrated system were 10.4% for energy sent out, 9.97% for energy generated, and 7.62% for peak demand. The load factor based on energy generated was 68% [1].

LLN categorizes its customers into the following sectors: industrial, commercial, residential, mining, and public lighting. The first three sectors are considered to be the major sectors, based on their high total energy demand. In 1987, the industrial sector's total demand was about 42% of the system's total generation. Commercial, residential, mining, and public lighting sector energy demands were about 32%, 20%, 5%, and 1% of the system total respectively [2].

In 1986 LLN estimated that total installed capacity in 1990 would be on the order of 4900 MW, 26% coming from hydro and 74% from thermal [3]. In the long term, the future generation plan takes into consideration all possible future technologies (hydro plants, gas, and coal fired plants) in line with the national fuel strategy.

The above program has given the supply side sufficient "base" and "intermediate" plants for the immediate future. LLN has made efforts to reduce electricity production costs by improving efficiency and availability of power plants. On the demand side, however, many opportunities exist for implementing demand-side energy management (DSEM) to further reduce operating costs. Policy guidelines on DSEM are still lacking, especially since little effort is being made to study its possible implications.

In 1985 LLN introduced a tariff structure with different rates for peak and off-peak energy [4]. This new tariff structure should encourage consumers to review and change their consumption patterns in order to achieve the savings now possible. Also, this tariff structure could act as a

pivotal point around which LLN and its consumers would explore the advantages of DSEM.

The Potential Benefits of DSEM

DSEM concerns itself with all activities affecting patterns of energy consumption. Alternatively, the strategy could be defined as those utility activities designed to influence customer use of electricity in ways that will produce desired changes in the utility's load shape [5]. Treating loads as a partially controllable variable in the planning process rather than as a fundamental input to which one must react has already lent a new flexibility to management and could lead to significant benefits, not only for the utility, but also for its customers [6].

A dramatic increase in the uncertainty of key variables in the planning process has led LLN to DSEM. Unstable fuel costs, increasing competition between energy alternatives, and significant increases in construction costs for new power plants all challenge the planners. While DSEM is not a cure-all, it could provide utility management with alternatives to a host of utility activities.

Basically, DSEM introduces a new element into the planning framework by allowing the utility to deliberately change the load shape in order to pursue strategic objectives. DSEM activities are designed to help better utilize existing facilities, to reduce generation costs, and to help control rising energy prices. Combining DSEM with traditional supply-side alternatives in a resource-planning portfolio can greatly increase the flexibility and manageability of an electric power system.

What the traditional utility planning process produced as a least-cost plan is much more expensive than the plan that could be created if DSEM were incorporated into the planning process. DSEM would cut costs missed by traditional strategies. Most importantly, DSEM could reduce both the need for new generating facilities and the consumption of critical fuels, and could also allow better use of existing and planned facilities [7]. These savings would be achieved by significantly reducing energy and peak consumption, by implementing deliberate load growth programs, and by shifting loads to make greater use of more efficient generating units.

Advantages of DSEM

Most utilities in highly developed countries have increasingly turned to conservation and DSEM as alternatives to the construction of ever more costly electric generating facilities [8]. DSEM's chief appeal is that it has proven beneficial not only to the utility, but also to its customers. For the utility, DSEM can reduce operating costs, reduce or defer purchase of new generation sources, improve utility load characteristics, and optimize the reserve margin. Beside these obvious advantages, changing the system's load shape can permit adjustments in plant loading. This increases the load put on the more efficient plants and permits the use of less expensive and more domestically abundant energy sources.

Perhaps DSEM's greatest attraction is the increased flexibility it can bring to the planning process, especially in regards to load forecast revisions. In fact, some DSEM activities, like direct load controls, are specifically designed to match demand to available generation, transmission, and distribution resources nearly instantaneously. For consumers, DSEM can reduce electricity bills and provide the means to control future expenditures of electricity.

Making DSEM yet more attractive, past and future projection data show that the effective lifetime of underground energy resources is short. The projections show that oil will be exhausted in 35 years, natural gas in 56 years, high quality coal in 196 years, and uranium in 61 years [9]. Therefore, DSEM and conservation technology could help to improve energy efficiency and so prolong the remaining life of these natural resources.

Economic growth and development in newly developed countries like Malaysia and Singapore has brought parallel growth in energy use and electrification. As a result, these countries will face a shortage of electricity generating capacity until new plants can be constructed. The situation will force them to engage in ambitious and expensive construction programs to meet the high demand. As experience in developed countries shows, such problems could be solved by

considering DSEM as another alternative in the utility planning process [10]. Through DSEM, utilities could possibly defer the need for new supplies of electricity, thus providing more lead time to construct new generation plants.

The latest LLN generating expansion program shows that the construction program planned for the period until 1992 involves the installation of 2 x 300 MW coal units (in 1988 and 1989) and a 60 MW hydro unit (in 1992) [3]. From 1992 onward LLN plans to install many 300 MW combined cycle units which use gas as fuel. LLN has also focused on efficiency improvements in system operations, including plant rehabilitation, conversion from oil to gas/oil-firing, upgrading of the national load dispatch centre, establishment of regional control centres, and the introduction of computerized plant maintenance management systems.

Could DSEM improve the program mentioned above? Would DSEM help to improve operating efficiency? To answer these and other utility-related questions, this study investigated the impact of DSEM on LLN. This study is among the few preliminary attempts to investigate DSEM's impact. Though the study includes several uncertainties and assumptions, it still provides first-hand knowledge on DSEM's impact on the LLN system.

Thermal Energy Storage

One promising technology, thermal energy storage (TES), has potential for improving energy load management. TES is generally used to reduce on-peak electric demand (kW) by shifting operation of the air conditioner's compressor to off-peak hours when energy costs and demand charges are lower [11]. In TES, the compressor chills or freezes water during the night, and this cooling energy is then stored in a tank and used the next day during occupied peak hours. This strategy benefits building owners and managers, who wish to lower their electricity costs, and electric utilities, which generally want to increase load factors and delay the need for new peak generating capacity.

TES systems use mostly standard building cooling equipment, like chillers, which combine a compressor, condenser, and evaporator. Figure 12-2 is a schematic of an ice storage system, a basic example of a TES system. Fundamentally, designing TES systems involves choosing the storage media, the operational strategy, and the equipment size.

The most common storage media used in TES systems are water and ice [12], though the use of phase change materials is growing.

Basically, there are three different ways to control a TES system: "full storage," "partial storage," and "demand limited" systems. In a full storage system, the cooling requirements during peak period are met by the storage; the chiller is only used to charge the storage during off-peak hours. In the partial storage system, the cooling requirements during peak period cooling requirements are met by both the chiller and the storage. During off-peak hours the chiller will be used to charge the storage. Demand limited systems are operated somewhat in between the first two systems, the cooling requirements during peak period being met by the storage unless the non-cooling electric load is below some determined maximum demand, in which case the chiller is used. During the off-peak period the chiller is used to charge the storage. Figure 12-3 shows the three operational modes of TES in diagram form.

Equipment sizing for TES systems must be based on the building's maximum cooling demand. Depending on the control strategy employed, the chiller and storage are sized to meet different portions of the load. For all strategies, however, the combined cooling capacity must meet the maximum cooling load. The various advantages and disadvantages to each of the three operational modes depends on various aspects such as site specifications. This study investigated the full-storage system and its implications.

A Review of the Report

The next section of this report describes the research work performed on the demand side with respect to consumer consumption patterns and load management potential. The methodology used to perform the demand- and supply-side energy management study, along with the

results of the simulation runs, follow. The economic and financial analyses are subsequently illustrated, and then the implications to supply and demand sides are discussed in detail. Finally, the conclusions of the research study are presented.

DEMAND-SIDE ANALYSIS OF DSEM

Studying DSEM's impact on utility planning and operation requires a comprehensive analysis of the utility and its load patterns. This section presents the three most important areas for demand side: sectoral load shape analysis; impact of DSEM on end-use load shapes; and the overall impact of DSEM on utility load shapes.

Sectoral load shape analysis determined the most suitable load-shape changes to be made for the DSEM program. Once these changes and the end-uses and associated DSEM technology had been identified, the technology's impact on end-use load shapes was analyzed. Lastly, the impacts from wide-scale use of the technology were estimated.

Load Shape Analysis

The traditional planning process practiced by LLN normally requires an overall system load shape represented by the load duration curve. DSEM, however, requires detailed knowledge of consumers' load shapes. Information needed is commonly acquired by performing a load research survey. Such a survey is a big task and can take two to three years to obtain reliable results. This study developed an alternative approach to process the hourly load data taken from feeder readings.

From the point of view of our DSEM study, the accuracy of results obtained from this procedure was adequate. One obvious limitation to this procedure is that it cannot capture detailed end-use patterns, but these can be estimated from consumer survey data and energy audits [13]. Several energy audit reports for the commercial sector are already available.

Load Research by Feeder Readings:

Using facilities at the Regional Control Centre (BRCC), 76 feeders were selected and monitored for three consecutive months (February, March, and April 1988). Of these 76 feeders, 16 were used to monitor shop lots, 6 for hotels, 21 for offices, 14 for shopping complexes, 3 for hospitals, 7 for banks, 7 for industries, and 2 for residential buildings.

The hourly load readings for each feeder were collected, compiled using a micro-computer, and then screened and analyzed. Distorted hourly load readings, probably caused by distribution faults or malfunctioning of the recording instruments, were rejected. Non-distorted readings were used to generate typical weekly load shapes (Monday to Sunday) for each selected consumer type [14].

LLN Consumers' Typical Load Shapes:

In the load research survey, only industrial, residential, hotel, shopping complexes, office, and shop lots consumers were monitored.

Industrial consumers in Malaysia can be roughly grouped into three types, depending on how they schedule their factory operations. Some industrial consumers demand electricity continuously for three-shift operation. The second type practices a two-shift work schedule, running the factory for about two-thirds of the day (7 A.M. to 10 P.M.). The third group practice a single shift work schedule (7 A.M. to 2 P.M.).

This study grouped together all three types of industrial consumer because the feeders used to record the hourly loads actually supply to all three types (which all have similar energy consumption levels). Therefore, the recorded hourly loads actually reflect the overall industrial sector load shapes.

Residential consumers subdivide into urban and rural consumers. Since BRCC controls a wholly urban area, its recorded hourly residential loads reflect the load shapes for those consumers only. No information exists on the load shapes for rural residential load shape, but since their consumption is small, this study used the load shape of the urban residential consumers to

represent the total residential load shape.

Figures 12-4 and 12-5 show the typical peak day load shapes for the industrial and residential sectors.* These load shapes were obtained from the load research survey and the analysis subsequently conducted.

Our project studied the load profiles for the various types of commercial consumers in more detail. Hotels, shopping complexes, offices, and shop lots are the four major types of commercial consumers. Other types of commercial consumers are grouped together as "others."

This study monitored only the four major types of commercial consumers. Their load shapes were combined to form the overall commercial sector load shape shown in Figure 12-6.

The industrial sector load shape in Figure 12-4 showed an almost evenly distributed load throughout the day, with the exception of a valley occurring at 7:00 P.M. The load factor was about 0.82, which implies an average load of about 82% of the peak load.

The residential sector (see Figure 12-5) showed a dominant peak at about 10:00 P.M. The load, rising to small peaks at about 7:00 A.M. and 11:00 A.M., was low at the beginning of the day and almost constant until 5:00 P.M. At about 6:00 P.M. the load started to rise steeply, reaching its peak at about 10:00 P.M. It stayed at the peak for a short period of time before starting to decrease steeply. The low load factor was about 0.36.

The commercial sector load shown in Figure 12-6 had a plateau-like shape for the period 11:00 A.M. and 4:00 P.M., which falls well within the peak period. The load was low at the beginning of the day and remained almost constant until about 7:00 A.M., after which it started to rise steeply. It reached its peak at about 11:00 A.M. and stayed almost constant until 4:00 P.M., when it started to gradually decrease. It had a load factor of 0.59.

System Typical Load Shapes:

Analysis of overall system-demand behavior was an important step in the demand-side analysis. To accomplish this, one year of hourly system demand data was taken from the LLN National Load Dispatch Centre system log book. To stay consistent with the LLN financial planning year, data were taken for the period of September 1986 to August 1987. The hourly demand figures consisted of the MWs monitored from each generation unit, which include the system losses (transmission and distribution losses) and the energy used by the generating stations.

To input data for the simulation exercise, the hourly system demands were converted into typical weeks of hourly demands; twelve of these weeks represented a year of chronological loads (one for each month). In theory, there are many different ways to formulate typical weeks from the actual load profiles. Deciding on the best method required investigating the various system daily-load shapes in order to ensure that the typical shapes represented as closely as possible the actual load shapes (particularly the peak demands and the load factors).

The daily load shapes for various types of days, such as weekdays, peak days, weekends, half-working days, public holidays, and the day after public holidays, were determined. The term "weekend" stands for Sunday, while "half-working day" signifies Saturday. A public holiday is any weekday or Saturday declared a holiday.

In the load shape investigation process, a few factors, including peak demand, the time at which the peak occurred, the load factor, and the base-to-peak ratio were used as indicators. All these factors were calculated and compared (see Tables 12-2a to 12-2d). A number of important observations were made from these tables:

- The peaks for Sundays and public holidays always occurred between 10:00 P.M. and 11:00 P.M.
- The highest peaks for weekdays occurred either between 11:00 A.M. and 12:00 P.M. or between 3:00 P.M. and 4:00 P.M.

* The term "peak day" signifies the day when the highest load of the month occurs.

- The peaks for Saturdays occurred between 11:00 A.M. and 12:00 P.M.
- Public holiday load shapes did not behave like Sunday load shapes.
- No significant difference was observed among the weekday load patterns.
- No significant difference was observed between the load patterns for the normal weekdays and the peak day (Wednesday of the third week).
- Saturday had its own unique load shape.
- Sunday had its own unique load shape.

As an example, Figures 12-7a to 12-7g show the load shapes for all the days in September 1986. Similar analysis was done for all other months, but the results differed little from the findings for September. Significantly, monthly peaks occurred either between 11:00 A.M. and 12:00 P.M. or between 3:00 P.M. and 4:00 P.M. (see Table 12-3). Figure 12-8 shows the system typical week for September.

Determination DSEM Program - Load Shape Changes

The first part of the DSEM study determined the sectoral load shape changes most suitable for achieving the primary objective, system peak reduction. Each sector's load shape was compared to the overall system load shape. In this analysis, each sector's peak contribution factor (PCF) was determined. Each sector's load factor was also determined.

The sectors' typical load shapes were plotted on the same scale as the overall system load shapes, a task accomplished by fitting each sector's average daily energy consumption into its typical load shapes. The following equations describe the process.

Let the normalized sector's typical load shape be represented by N_i, where the subscript i denotes the hour (i.e., i = 1, 2, 3, ..., 24), and N denotes the normalized hourly demand (i.e., $1 \leq N \leq O$). The sector's average daily energy consumption, represented by E, was calculated as follows.

$$E = \frac{\text{Sector's annual energy consumption}}{365} \quad (1)$$

The next step was to calculate the total normalized energy consumption of the sector's typical load shape. This was done by summing the normalized hourly demands of the typical load shape:

$$A1 = \sum_{i=1}^{24}(N_i) \quad (2)$$

where A1 is the total normalized daily energy of the sector.

Next, the actual hourly demand was calculated:

$$H_i = \frac{E}{A1} \times N_i \quad (3)$$

where H_i is the sector hourly demand (in MW).

Figure 12-9 shows the plot of the overall system load profile and the sectors' peak-day load shapes. Note the curve called OTHERS in Figure 12-9 which constitutes the public lighting sector, mining sectors, and system losses. The peak contribution and load factors tabulated in Table 12-4 were determined from these load shapes.

Figure 12-9 shows the most suitable place to implement a load shift would be the commercial sector, since most of its energy consumption (more than 70%) is in the peak period. The industrial sector could also shift loads, but not on a wide scale if done in addition to commercial sector load shifting, since too much load would be shifted to the former off-peak period, thereby leaving the system load factor unchanged. This possible adverse effect of DSEM must be avoided.

The above information demonstrates that load shifting, especially in the commercial sector, would be a suitable load-management approach for LLN. The commercial sector in LLN's territory consists of many types of consumers with different energy consumption patterns. Therefore, a more detailed analysis of the commercial sector needs to be done.

Selection of End-Uses

The various classes of commercial-sector consumers (hotels, offices, shopping complexes, restaurants, etc.) each have their own consumption patterns. Thus it is necessary to identify each class's load-consumption pattern in order to target the class most appropriate for the load shift program. Since there are many classes of commercial consumers, only a selected few of them were analyzed.

Selecting Commercial Consumers:

Since TES applies to air-conditioning systems, only consumer classes with high electric consumption for air-conditioning were selected and analyzed. Based on this criterion, hotels, large offices, and shopping complexes were selected for further analysis. These consumers in general allocated more than 40% of their total energy consumption for air-conditioning. Furthermore, the total monthly energy consumption for these three classes was more than 50% of the total commercial sector's energy demand (see Table 12-5). This information was gathered from records on commercial consumers' energy consumption which are compiled monthly by the LLN commercial department. The records contain monthly information on large power commercial consumers sales, energy consumption, tariff group, maximum demand, load factor, and other related statistical information [15]. The records also show that each of the three classes included a small number of consumers who had very high energy consumption. This is an important factor to consider in a load management program. The overall findings from the analysis are summarized and tabulated in Tables 12-5, 12-6, and 12-7.

Note that the "other" category in these tables has a very large number of consumers (about 55% of all large power commercial consumers), as well as high monthly energy consumption (about 48% of the total large power commercial consumers energy consumption) compared to that of the other three classes. This distribution occurred because the "other" class is composed of many different types of commercial consumers such as restaurants, cinemas, entertainment centres, and educational centres.

Proceeding with the load-shape analysis for the three selected commercial consumer classes, their typical load shapes were determined from the load research survey discussed earlier. Figures 12-10, 12-11, and 12-12 show the typical load shapes for the three types of commercial consumers. The peak-day load shapes were superimposed on the overall commercial-sector load shape identified in the earlier section (see Figure 12-13). Important factors such as the peak coincidence factor and load factor were determined from the load shapes. Table 12-8 summarizes the findings.

According to the findings of the analysis, office consumers are the most suitable consumers for the DSEM program. The fact that office consumers had a low load factor (0.458), high energy consumption per consumer (especially for tariff classes C1 and C2, see Table 12-5), and high consumption of electricity for air-conditioning (i.e., about 55% to 65% of total building loads) all justify this conclusion. In addition, a large percentage of daily energy (more than 85%) was used well within the LLN peak period (8 A.M. to 10 P.M.). Furthermore, offices as a group contributed more than 26% to the system peaks at 11:00 A.M. and 4:00 P.M., a higher peak-contribution factor than came from either hotels or shopping complexes. The office class possessed more large power consumers than did any other group in tariff classes C1 and C2 (i.e., more than 2% of the total number of large power commercial consumers).

Impact of TES on Large Office Building Load Shapes

Software was developed specially to analyze TES's impact on consumer load shapes. TES simulations assumed an air-conditioning load of 40% of the total building load. Forty percent was

chosen since 15% of the total air-conditioning load (amounting to 55% of total electrical demand) was used for the air-handling units which must operate during peak hours in any case. Figure 12-14 shows the results of the simulations that were performed to find TES's impact on a typical large office building load shape.

Correlating Load Shape Changes Due to System Load Shape

The resulting impact of TES on typical large office building load shapes was then projected so as to simulate large-scale adoption of TES. The total impact was then correlated to the overall system load shape.

To project TES adoption in large office buildings, four scenarios were used. Each had a different set of TES penetration rates (Scenario 1 assured the highest penetration rate and Scenario 4, the lowest). TES penetration rate is simply the percentage of large office buildings that adopt TES. The penetration rates used started at 0% in 1990 and assumed the following rates by the year 2000:

- 50.0% penetration (Scenario 1)
- 37.5% penetration (Scenario 2)
- 25.0% penetration of TES (Scenario 3)
- 12.5% penetration (Scenario 4)

For each scenario in each year, a normalized form of the typical load shapes was translated into the actual load shape. This was done by apportioning the actual energy consumption onto the normalized typical load shapes. The typical load shapes were then correlated to the overall system load shape. This was a simple process, but required manipulating a large amount of data. A computer program called Load Shape Correlation (LSC) was developed to assist in the process. Figure 12-15 shows a flow chart of LSC.

One input important for LSC was the office sector energy, Unfortunately, this data not available to LLN, since relevant forecasting was only performed for the total system demand. A forecast of the sectoral energy was developed. Table 12-9 shows the result of this forecast.

SUPPLY-SIDE ANALYSIS OF DSEM

DSEM has direct implications for the utility demand profile, particularly for the peak demand and system load factors. In the short term, such changes could have immediate effects on unit commitments and cost of production. In the longer term, DSEM could affect the capacity expansion program, possibly resulting in reduced size for new plants or the deferment of plants.

Setting Up the Base Case Scenario

The base case scenario used in this analysis was the existing expansion program. The LLN Generation Planning Unit used the Wien Automatic System Planning (WASP) program to determine the future LLN generation mix. WASP, an optimization generation planning program developed in Vienna, Austria, is used by many utilities in developing countries.

The study used UPLAN, a production-cost model capable of analyzing the demand and supply side in a single environment. Before the model could be used to analyze the different scenarios, it had to be calibrated to SYSGEN, LLN's production-cost model.

The Base Case Scenario Calibration Process:

In the calibration process, UPLAN's base-case yearly production (GWh) outputs by fuel type were compared to SYSGEN's. This study performed the calibration process for each year from 1990 to 2000. UPLAN used the same supply-side input data as SYSGEN, and the demand-side inputs in UPLAN were taken from the same source as SYSGEN, but modeled differently. UPLAN modeled the demand-side input in the form of typical weeks, whereas SYSGEN used monthly load duration curves estimated with a fifth-order polynomial.

In order do the calibrations, a few adjustments were made to the supply-side data. These adjustments were necessary because UPLAN and SYSGEN used different approaches and techniques to modeling some of the system operational requirements (such as the approach UPLAN uses to determine the units to supply the reserve requirement). Some of the unit monthly capacity factors were also adjusted, as were other factors such as "block loading information" (where each unit can be forced into the required dispatch order) and "unit commitment level." The major parameters such as unit forced outage rate, maintenance schedules, operation and maintenance costs, and unit heat rates were not adjusted since these parameters are the same for both UPLAN and SYSGEN.

Setting Up Case Study Scenarios

The TES penetration rates used in the four scenarios were estimated by arbitrarily setting a maximum and minimum boundary for each each year and then assuming that this percentage would increase linearly throughout the planning period. The assumptions had to be made since no reliable information existed on consumer acceptance of TES in Malaysia.

The office sector's total energy demand for each year was estimated in order to determine the amount of office energy that would be shifted in each scenario. For each scenario in each year, the DSEM program's impact on the overall system load shape was determined. Tables 12-10a and 12-10b show the peak demand and load factors for the load shapes.

Results of the Case Study Scenarios Simulations

A summary of the simulation results is shown in Tables 12-11a to 12-11d and Tables 12-12a to 12-12g. Each table summarizes of the results for all the scenarios.

DSEM with TES would shift the peak-period load and reduce the system peak, as shown in Table 12-11a where peak reduction was achieved for every scenario. The degree of reduction merely depended on each scenario's penetration rate. Table 12-12b shows that DSEM decreased the total production costs for all years except 1991. In that year, the savings from reduced production costs during peak hours were less than the extra cost to produce the shifted energy during off peak hours plus the extra energy required by the DSEM program. In the latter years, as the peak reduction became larger, total production costs decreased.

The savings in production costs result from reduced use of expensive fuel oil. This can be shown by the increase of energy production in the intermediate plants. The energy output from the base load units, the Coal and Gas East resources units, would not change with DSEM because DSEM did not generally affect base load energy use. Diesel units would still play an important role in supplying energy for peak load (until they are put into retirement in 1997) because their small size (18 MW) caters to short periods of peak demand.

Table 12-11d shows that the DSEM program improved the system load factor, and the system reserve margin was found to increase with DSEM. In the year 2000 the reserve margin would be about 24% without DSEM and 28% with DSEM at the 50% penetration rate (Scenario 1) (see Table 12-11c). The improvement in reserve margin would help the system to improve unit availability.

ECONOMIC AND FINANCIAL ANALYSIS OF DSEM

This section describes economic aspects of TES introduction. The analysis considered both the consumer and utility perspectives, and though in a simplified form, provides some indications of DSEM's economic and financial viability.

Initially, the DSEM program was analyzed from an economic point of view. The analysis depicted the program as a black box with cost as the input and savings as the output. The DSEM case was compared to the base case. The existing system presently requires a total cost C. By introducing DSEM at an extra cost of ΔC, ΔS would be saved. The ΔC and ΔS can be described as the marginal cost and marginal savings incurred from introducing the new technology (DSEM) to the black box. DSEM would be economically viable if the marginal savings are greater than the

marginal costs.

The marginal cost in this case includes all costs related to the program such as the capital cost of TES and the program administrative cost. Likewise, the marginal savings include all the production cost savings and capacity cost savings, etc. Consumer-bill savings were not included in ΔS since they are cancelled by the utility's loss of revenue.

After showing DSEM to be economically viable, the study analyzed the benefit-cost ratio of the DSEM program from both the utility and consumer perspectives. Various benefits and costs incurred as a result of the DSEM program were identified.

Economic Analysis

Only capital costs of TES were considered when calculating ΔC. Information on typical office building was used to estimate the cost per installation, and the result was then projected for different penetration rates. The analysis assumed the standard office building to require power as follows:

- Building air-conditioning load: 5,000 kWh per day
- Air-conditioning cooling peak: 600 kW
- Air-conditioning operating hours: 7:00 A.M. to 5:00 P.M. (10 hours)

The following general facts were also used:

- System peak period: 8:00 A.M. to 10:00 P.M. (14 hours)
- Chiller costs: 284 M$/kW*
- Storage costs: 53 M$/kW

Capital costs of installing TES were calculated in the following steps:

- Chiller size was determined.
- The chiller size was determined by dividing the total air-conditioning load by the average operating hours. (Average operating hours is the total operating hours multiplied by a factor of 0.7.)
- Average operating hours = 10 [hrs] x 0.7 = 7 hrs
- Chiller size = 5000 [kWh] / 7 [hrs] = 714.29 kW ~ 750 kW

Chiller costs were calculated:

- Chiller cost = 750 [kW] x 284 [M$/kW] = M$ 213,000
- The storage size, equal to the chiller size times the average operating hours, was calculated.
- Storage size = 750 [kW] x 7 [hrs] = 5250 [kWh]

The storage costs were calculated:

- Storage cost = 5250 [kWh] x 53 [M$/kWh] = M$ 278,250

Other accessory costs (like refrigerant piping) were estimated to be about M$ 45,000.

The capital costs of installing TES were assumed to be the sum of chiller costs, storage costs, and other miscellaneous costs.

- Capital cost of TES = M$ 213,000 + M$ 278,250 + M$ 45,000 = M$ 536,250

As mentioned earlier, the program savings considered in the economic analysis were the production cost and capacity cost savings only. Production cost savings were found to come mostly from fuel cost savings. Table 12-13 shows the production cost savings from the four scenarios for each year. Capacity savings in this context refer to the savings gained from not

* The conversion rate used, as of June, 1990, was 2.7100 Malaysian Dollars to 1 US Dollar.

installing, generating, transmitting, and distributing a given amount of load. In other words, if the utility were able to reduce X MW of peak demand at a cost of Y M$/MW (where Y is the cost of installing, generating, transmitting, and distributing a MW of load), then the utility would be able to save X x Y M$ in capacity costs. Table 12-14 shows the costs for generating, transmitting, and distributing a kW of load. LLN planning engineers in the LLN Planning Unit determined these figures. The potential peak demand reductions determined earlier, along with the information contained in Table 12-14, were used to determine the capacity savings shown in Table 12-15.

Table 12-16 shows the marginal costs savings for each scenario. All present value calculations used a discount rate of 10%, and the amounts are expressed in 1990 Malaysian dollars. For all the scenarios, the results show a benefit-cost ratio of more than 1, meaning that ΔS is greater than ΔC. So, DSEM should be economically viable.

Financial Analysis - Utility Perspective

A utility involved in a demand-side program bears numerous costs. The most important cost is the loss in revenue, when energy previously used during the high (peak) rate period is shifted to the low (off-peak) rate period. Other costs, like administrative costs and subsidies to consumers for the installation of DSEM technology (also known as incentive costs), are incurred as well. Administrative costs related to the marketing program generally includes sales promotion, consumer liaison, advertising, and consumer education. The incentive costs could also be considered part of the marketing cost since they are paid by the utility to the consumers to subsidize the consumer capital costs for installing DSEM technology. This study omitted the program administrative costs from the analysis since no reliable information was available. The revenue losses were calculated each year for each scenario (see Table 12-17).

The benefits obtained by the utility from DSEM in the form of production and capacity cost savings were explained in earlier sections. Other benefits, such as improvements in the system reserve margin, improvements in the utilization of the generating units, transmission, and distributions system, and improvements in system reliability, were difficult to quantify in monetary terms, so they were omitted from this analysis.

Tables 12-18a to 12-18d show the costs and benefits of the demand-side program from the utility perspective.

Financial Analysis - Consumer Perspective

TES offers consumers reduced electricity bills for a similar amount of energy used. The cost borne by the consumer is merely the capital cost of installing TES. The utility could offer an incentive to help consumers reduce capital investment which would, consequently, shorten the payback period. Sample calculations of the cost of installing a TES system in a typical large office follow.

The Capital Cost of TES:

The capital cost of TES was calculated earlier, and the cost per installation for a typical large office building was found to be M$ 536,250.

Consumer Operating-Cost Savings:

The consumer's operating-cost savings derive from lower electricity bills. Assuming that the consumer is charged with tariff C1 before and tariff C2 after the installation of TES, the calculations are as follows:

- Demand charges:

  Tariff C1 = 600 [kW] x 12.00[M$/kW] = M$7,200

  Tariff C2 = 0 [kW] x 19.00 [M$/kW] = M$0

- On-peak energy charges:

  Tariff C1 = 5000 [kWh] x (9 [hrs] / 10 [hrs]) x 0.18 [M$/kWh] = M$810

  Tariff C2 = 0 [kWh] x 0.18 [M$/kWh] = M$0

- Off-peak energy charges:

  Tariff C1 = 500 [kWh] x (1 [hrs] / 10[hrs]) x 0.18 [M$/kWh] = M$90

  Tariff C2 = 500 [kWh] x 0.08 [M$/kWh] = M$400

- Total annual charges:

  Tariff C1 = (M$7,200 x 12 [month]) + (M$810 + M$90) x 260 [days] = 320,400M$/yr

  Tariff C2 = (M$400 x 260 [days]) = 104,000M$/yr

  Operational cost savings = 320,400 [M$/yr] – 104,000 [M$/yr] = 216,400M$/yr

  Payback period = 536,250 [M$] / 216,400 [M$/yr] = 2.5 years

The cost-benefit ratios from the consumer's perspective were determined from Table 12-19 which presents the yearly costs and benefits to the consumer.

DISCUSSION

Impact of DSEM on the Demand Side

The load shape analysis and past records of consumer energy consumption showed that large offices had a low load factor (0.458) and high energy consumption per building (831,600 kWh per month for tariff C2 and 389,179 kWh per month for tariff C1). The office sector also had high electricity consumption for air-conditioning (45% to 65% of the total building load) and used more than 85% of its energy during peak period. Consequently, offices constituted about 27% of the total commercial sector peak demand during the peak hours. The above information affirms that the office sector has great potential for energy load management and that TES seems an appropriate technology.

Commercial Consumers Load Shape - Large Office Buildings:

TES affects two load shape variables, peak demand and load factor. Table 12-20 shows the daily peak load for the typical large office building before and after TES. For each day except Sunday, where TES was not operated, the maximum peak reduction declined by 71%.

Changes in the consumer load pattern would change the load factor, a conclusion born out by Table 12-21, which depicts the daily load factor of a typical large office building before and after implementing TES. Table 12-21 shows that TES would improve the building load factor. The maximum load factor improvement, occurring on Saturday, was 61%.

Wide-Scale TES Penetration:

Wide-scale TES penetration in large office building air-conditioning systems was estimated. Table 12-22 shows the system peak demand for each scenario by year. The typical peak day system load shape was used in the analysis. It is clear from Table 12-22 that TES on a large scale would reduce system peak demand. The degree of potential reduction would depend on the penetration rate.

Table 12-22 shows that the maximum reduction in system peak would be achieved (each year) from Scenario 1, and the minimum reduction from Scenario 4. Figure 12-16, which plots the degree of potential peak reduction against various TES penetration rates, shows that percentage of peak reduction and penetration rate are linearly related. The gradient of the line, 0.0603, defines the relationship between them and can be used to determine the degree of peak reduction for various TES penetration rates. For example, a 75% penetration rate would result in a 4.523%

(i.e., .75 x 0.063) peak reduction. The maximum potential peak reduction would be about 6.03% (i.e., 1 x 0.0603)

Table 12-23 shows that, on a large scale, TES would also affect system load factor. The relationship between the percentage improvement in load factor and the TES penetration rate can be determined from the plot in Figure 12-17.

In Figure 12-17, the gradient of the line which relates the percentage improvement in load factor and the penetration rate is 0.0634. Therefore, the maximum potential improvement in the system load factor is 6.34% (i.e., 1 x 0.0634).

Impact of DSEM on the Supply-Side

TES's impact on the supply-side was analyzed with the production-costing program UPLAN. The potential reductions in production cost from load shifting are shown in Tables 12-25a and 12-25b, which present energy production aggregated by fuel type for the years 1992 and 1995. In general, all other years showed the same impacts: energy production from oil would decline; there would be no change in coal, hydro and gas east resource consumption; production in Gas West #1 would increase; and production in Gas West #2 would decrease.

Tables 12-25a and 12-25b clearly show that the avoided energy production from the most expensive resource would be replaced by production from the least expensive resource (Gas West #1). Energy production from the base load resources (i.e., coal, Gas East) and hydro resources would not be affected by TES. Therefore, TES would not influence base load unit production, affecting instead only the production from peak and intermediate units.

Several other impacts would result from the system peak load reduction. The system's reserve margin would improve, as would system reliability based on the reliability indicator LOLP. Figure 12-18 summarizes graphically the supply-side impacts of TES.

The overall economic analysis of DSEM showed that DSEM would be economically viable for all four scenarios. The internal rate of return (IRR) for all four was found to be about 50%. (IRR is the rate at which the cost is equal to the benefit.) IRR is usually used as an indicator to rank several projects: the higher the IRR, the higher a project's priority.

The benefit-cost analyses showed that both the consumer and utility would benefit from DSEM. For the high scenario, benefit-cost analysis from the utility perspective showed a benefit-cost ratio of about 1.348 at a 10% discount rate. From the consumer's perspective, the benefit-cost ratio was about 3.155 at a 10% discount rate. The IRR for the consumer was about 75%.

CONCLUSIONS

This report presented a study on DSEM's potential impact on the electric power utility LLN in Peninsular Malaysia. The technology analyzed was thermal energy storage; office buildings in the commercial sector were the target group. TES has the ability to shift air-conditioning loads from peak to off-peak hours.

The initial part of the study investigated the various consumers' consumption patterns, using remote feeder load-recording facilities. The commercial sector was identified as the most promising sector for load management, and office buildings were singled out because their air-conditioning load contributed substantially to the system peak.

Wide application of TES could significantly affect the system demand profile. On the demand side, the most significant implications are for the peak load and load factor of the large office sector. On a national scale, the system peak reduction depends on the rate of TES penetration. From simulation results, a penetration rate of 50% by the year 2000 would bring a peak reduction of about 192 MW.

For a typical large office building, the load factor would improve up to 17% on a normal weekday, and on a national level, the improvement on the system load factor would be from 0.61 to 0.71 by the year 2000, an improvement of about 3%.

The changes in peak demand and load factor would invariably affect the supply side. The expected savings for the year 2000 range from 2 to 7 million Malaysian dollars. For the reserve margin, the improvement could be up to about 4%.

Extending TES application to other types of commercial consumers, like hotels and shopping complexes, would result in additional benefits. The magnitude of savings would be less than from offices, though, since these consumer types use less energy.

The study provides information on the effects of TES in the LLN system, indicating that the introduction of TES would reduce the peak demand and take advantage of the off-peak tariff rates. Consumers would benefit directly from lower peak demand and energy charges. For the utility, benefits include lower electricity production costs and an improved system load factor.

The economic analysis performed found that introducing TES would be economically viable for both the utility and consumers. There is, therefore, a need to review and propose possible guidelines on DSEM, and if need be, some policy statements must be made to encourage and ensure DSEM's successful implementation.

REFERENCES

1. National Electricity Board, Development Planning Department, Malaysia, "Load Forecast, 1988 - 2010," Report PP(G) 1988/1, 31 December 1987.
2. National Electricity Board, Malaysia, "Highlands, 1986/87."
3. National Electricity Board, Development Planning Department, Malaysia, "Current Development Plans and Future Prospects," March 1988.
4. National Electricity Board, Malaysia, "LLN Tariff Structure," 1985.
5. Berkowitz, D.G. and Gellings, C.W., "Glossary of Terms Related to Load Management - Part I," *IEEE Transactions on Power Apparatus and Systems,* Vol. PAS-104, No. 9, September 1985, pp. 2387-2392.
6. Jackson, B.C., "Demand-Side Management: Treating electricity demands as partially controllable variables allows for more efficient planning," Report sponsored by NRECA & EPRI U.S., February 1986.
7. Bohlin, P., Edvinsson, M., Lindberg, G., and Lundqvist, C.G., "Successful Implementation of a Nation-Wide Load Management System," *IEEE Transactions on Power Apparatus and Systems,* Vol. PWRS-1, No. 4, November 1986, pp. 90-95.
8. Eto, J., Koomey, J., McMahon, J., and Chan, P., "Financial Impacts on Utilities of Load Shape Changes," Lawrence Berkeley Laboratory, Report LBL-21597, April 1986.
9. Yimsirikul, C., "Industrial Energy Saving: A Matter of Technology or Management?" *Energy Conservation in Industry Proceedings of a Regional Training Workshop,* Energy Research and Training Centre, Chulalongkorn University, Bangkok, Thailand, published by financial assistance of UNESCO, March 1986.
10. Rothkopf, M.H., Kahn, E.P., Teisberg, T.J., Eto, J., and Nataf, J.M., "Designing PURPA Power Purchase Auctions: Theory and Practice," Lawrence Berkeley Laboratory, Report LBL-23906, August 1987.
11. Piette, M.A., Wyatt, E., and Harris, J., "Technology Assessment: Thermal Cool Storage in Commercial Buildings," Lawrence Berkeley Laboratory, Report LBL-25521, January 1988.
12. Wyatt, E., "The Feasibility of Commercial Building Thermal Energy Storage in ASEAN Countries," Lawrence Berkeley Laboratory, December 1986. (Also published as Chapter 11 in this volume.)
13. Ministry of Energy, Telecommunications and Posts, Malaysia, "Energy Consumption in Buildings Study," Final Report Vol. 1 and 2, September 1985.
14. Azit, A.H., Sairan, S.B., and Jasmon, G.B., "Feeder Load Analysis for Utility Demand Side Management," *IEE Proceedings,* Vol. 136, Pt. C, No. 5, September 1989.
15. National Electricity Board, Malaysia, "Large Power Consumer Statistical Report," 1988.

Figure 12-1

Service Territories of Utilities in Malaysia

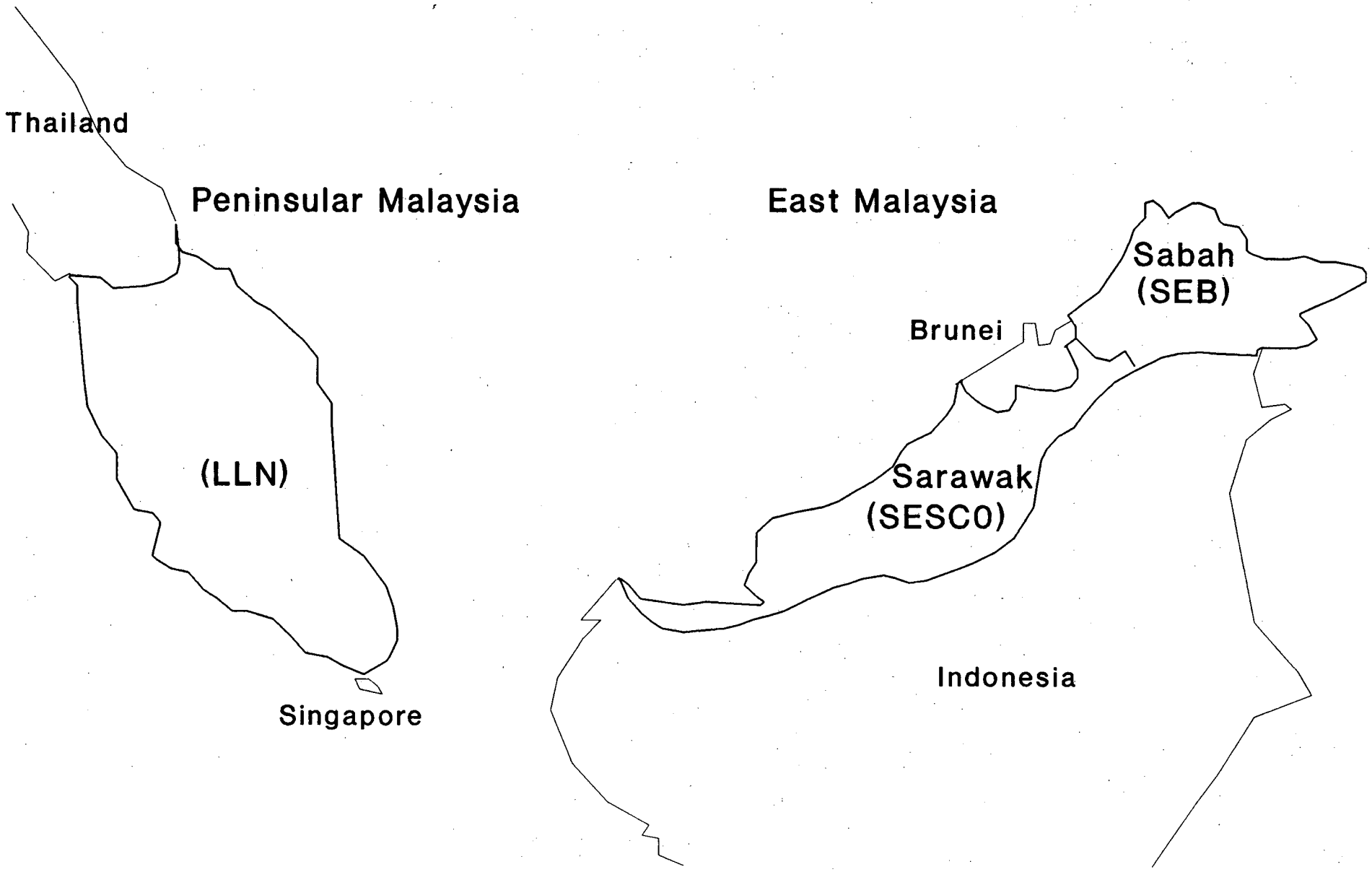

Figure 12-2
Ice Storage System

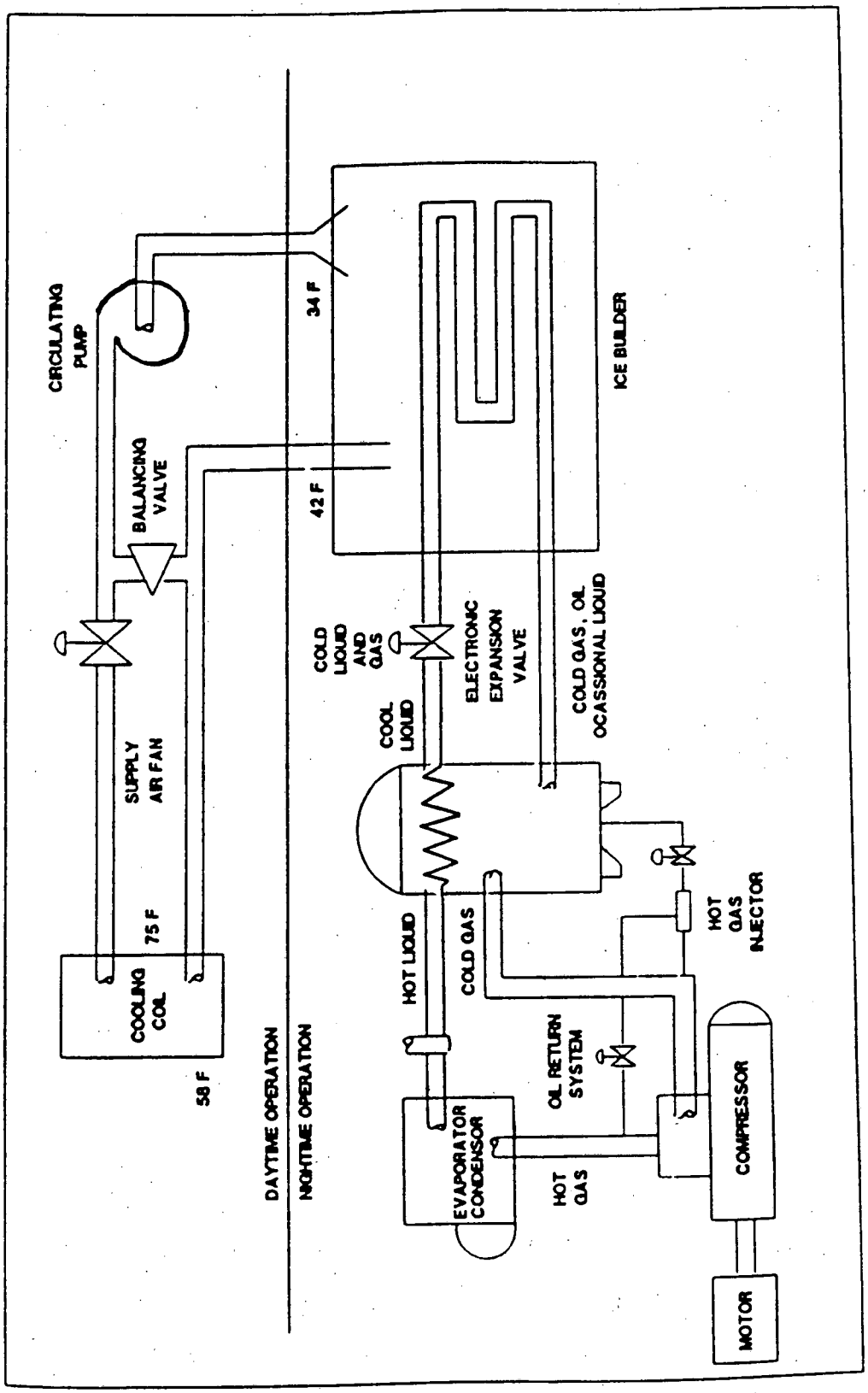

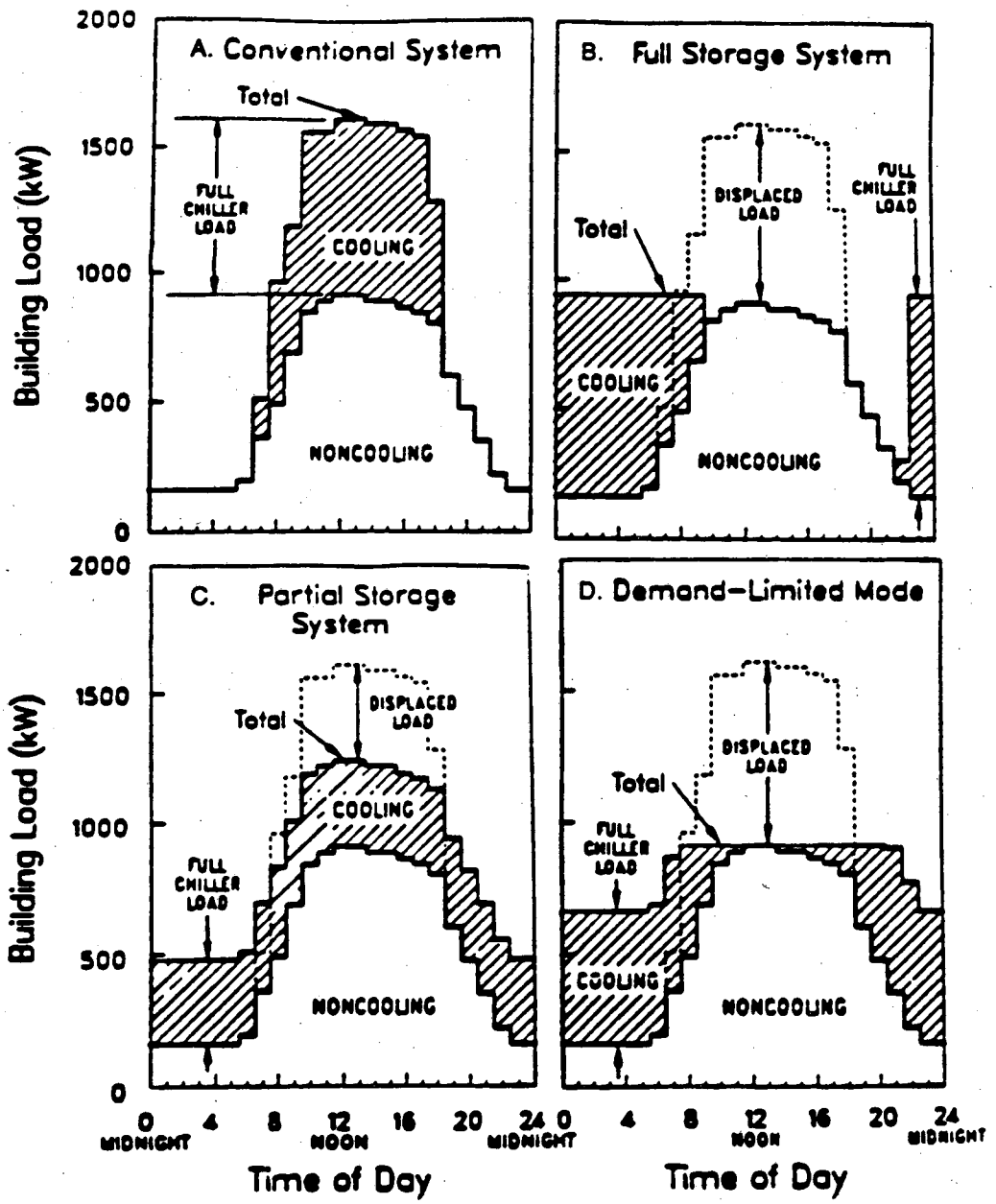

Figure 12-3
TES Operational Strategies

Figure 12-4

Typical Industrial Load Shape--Peak Day

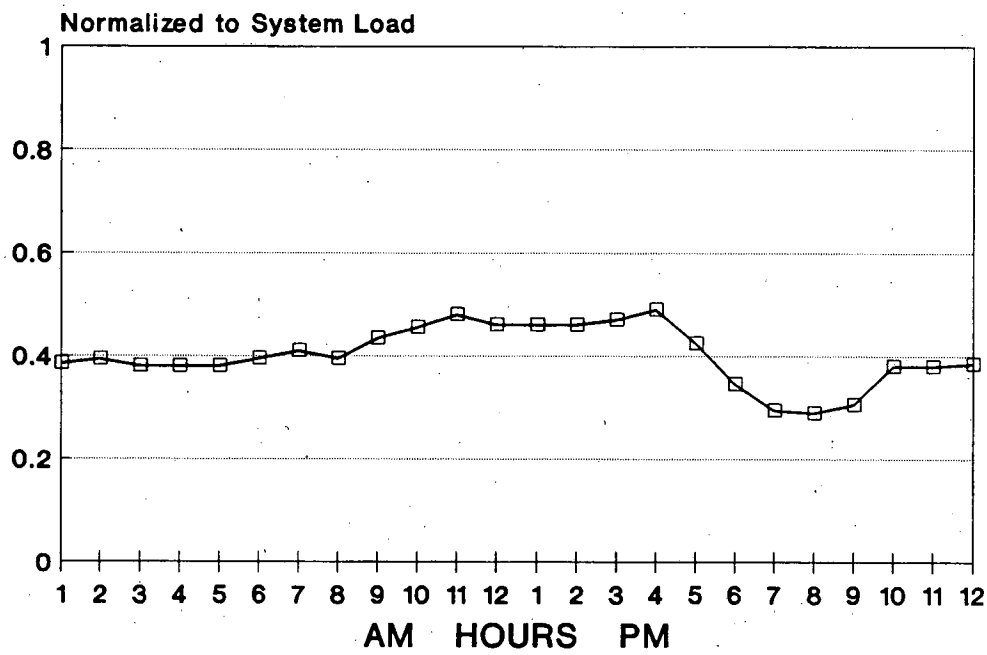

f04indpk.cc.9/90

Figure 12-5

Typical Residential Load Shape--Peak Day

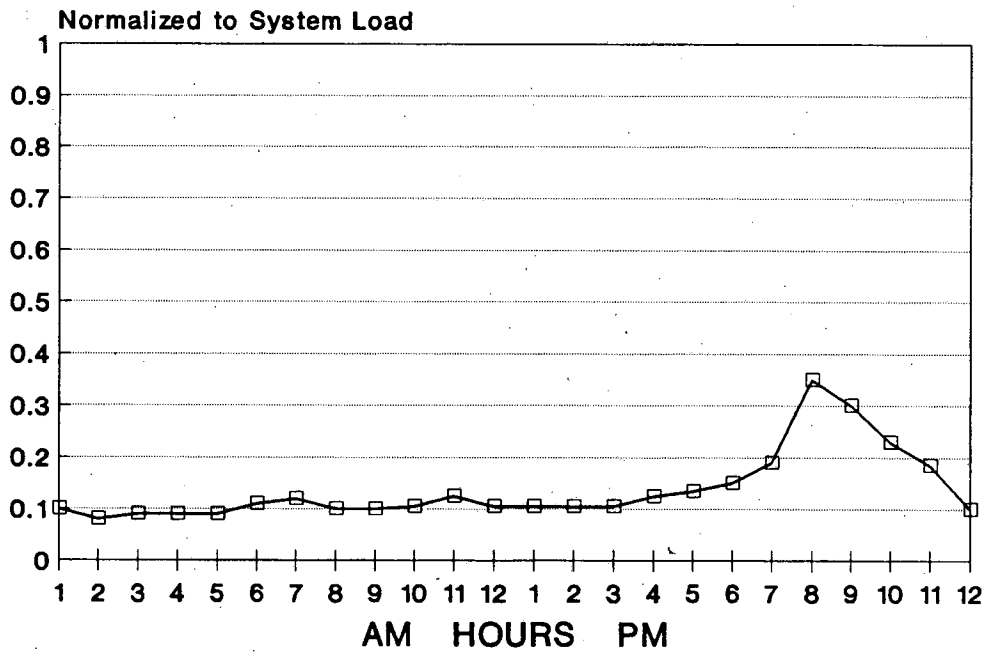

f06respk.cc.9/90

Figure 12-6

Typical Commercial Sector--Peak Day

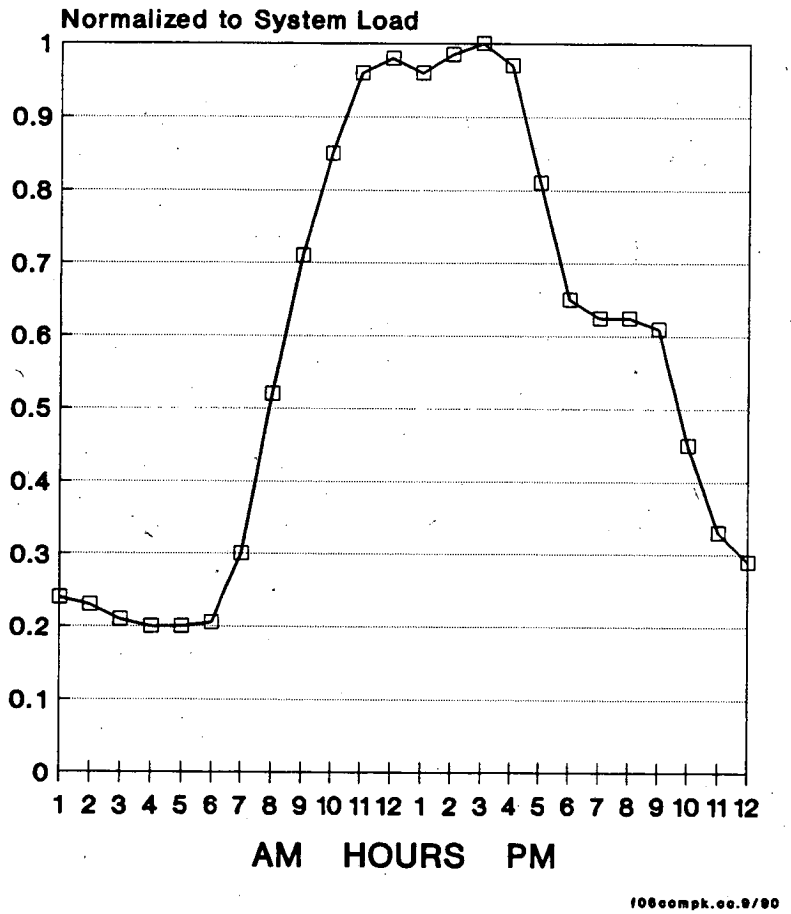

Figure 12-7
System Typical Daily Load Shape

Figure 12-7a SUNDAY

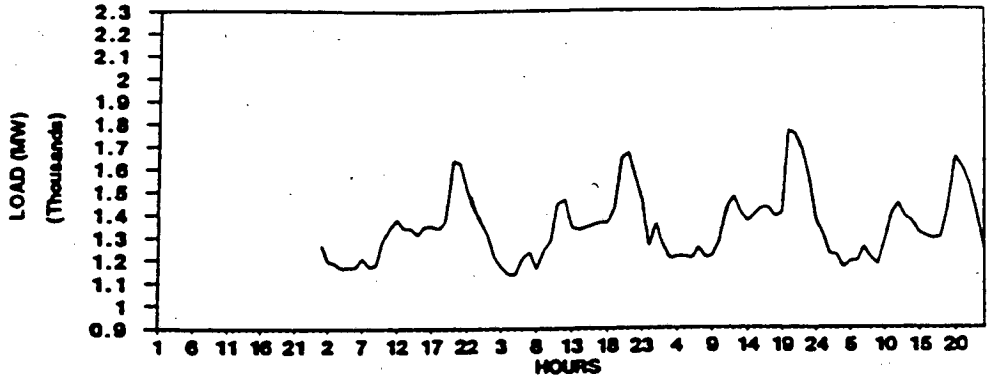

Figure 12-7b MONDAY

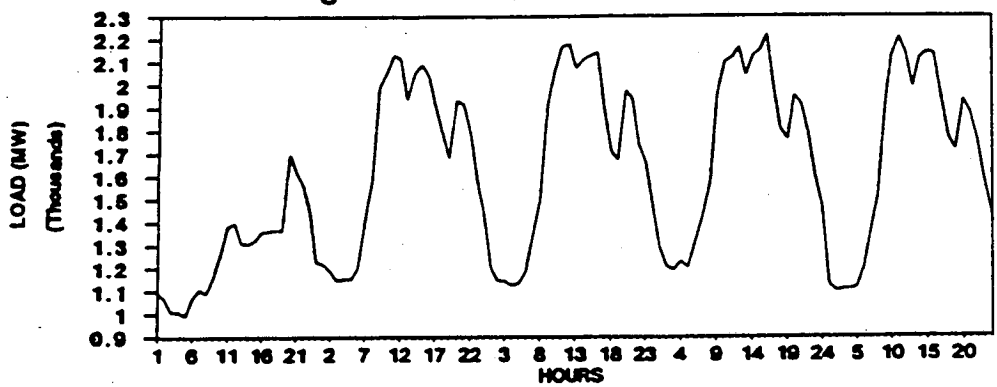

Figure 12-7c TUESDAY

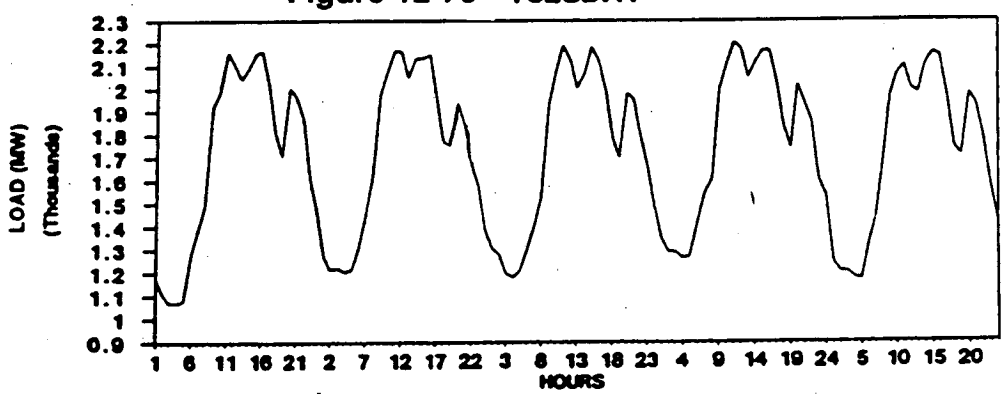

Figure 12-7d WEDNESDAY

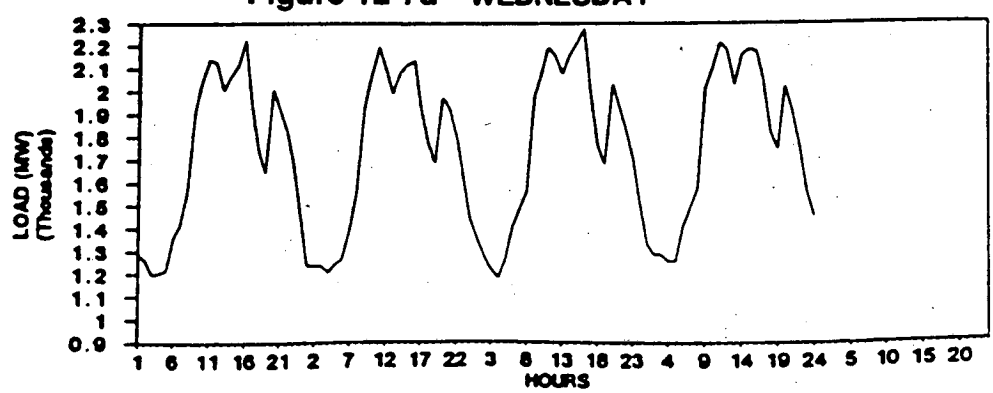

Figure 12-7e THURSDAY

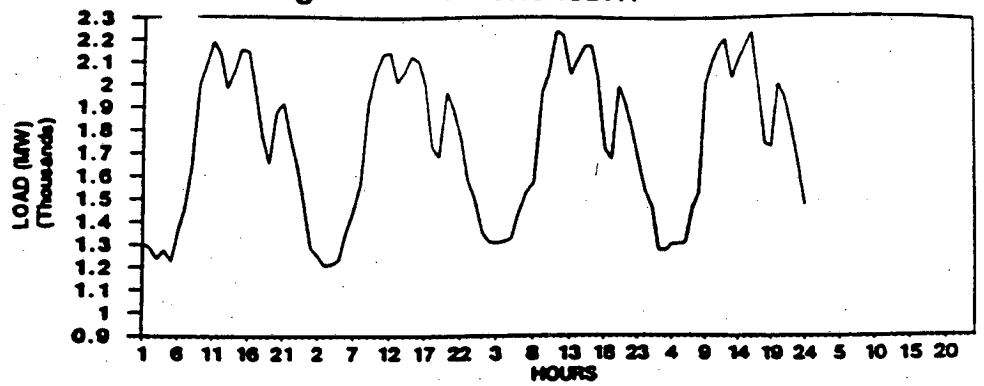

Figure 12-7f FRIDAY

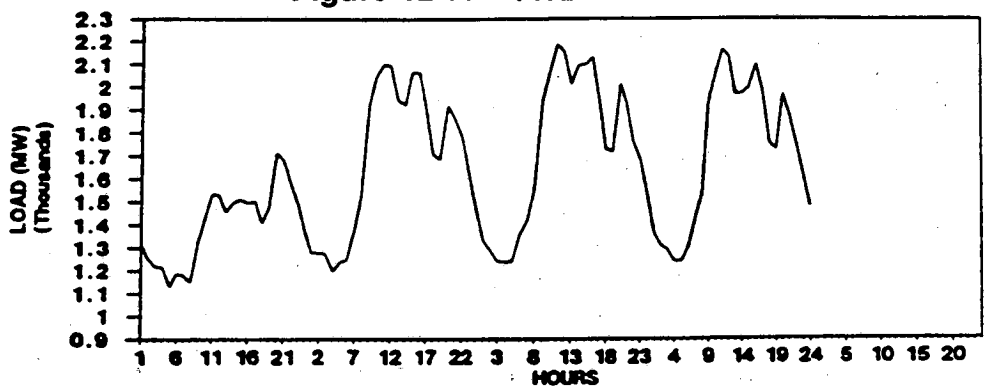

Figure 12-7g SATURDAY

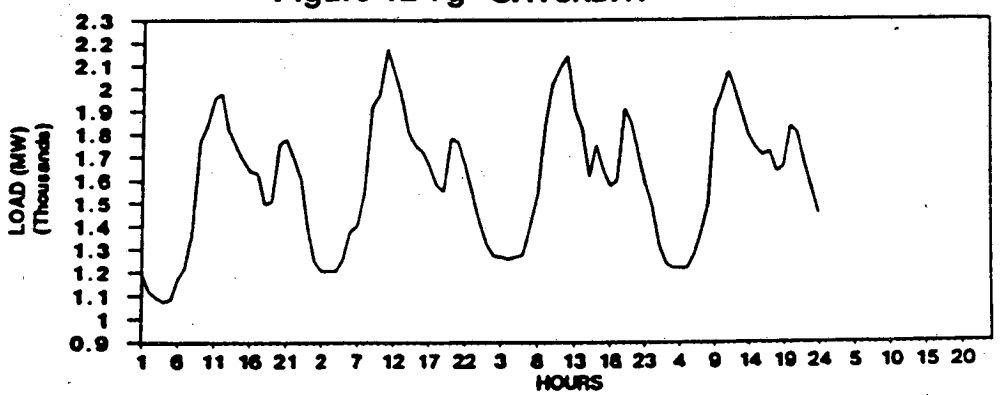

Figure 12-8
System Typical Weekly Load Shape

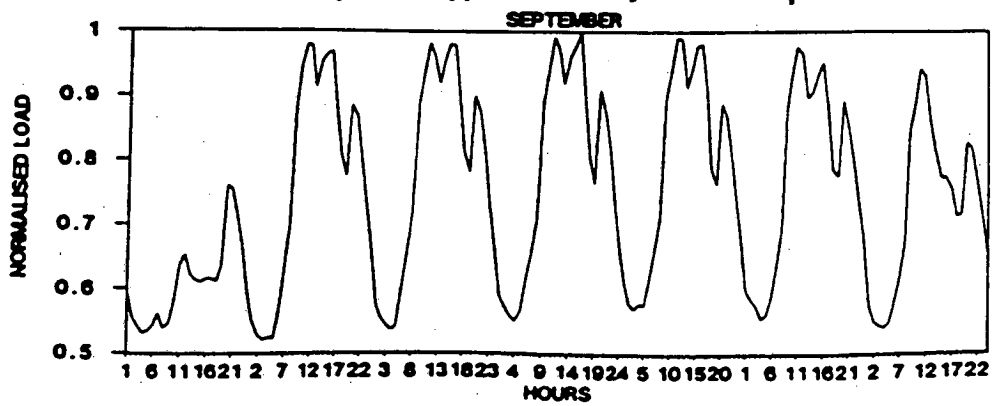

Figure 12-9

System and Its Sectors' Load Shapes

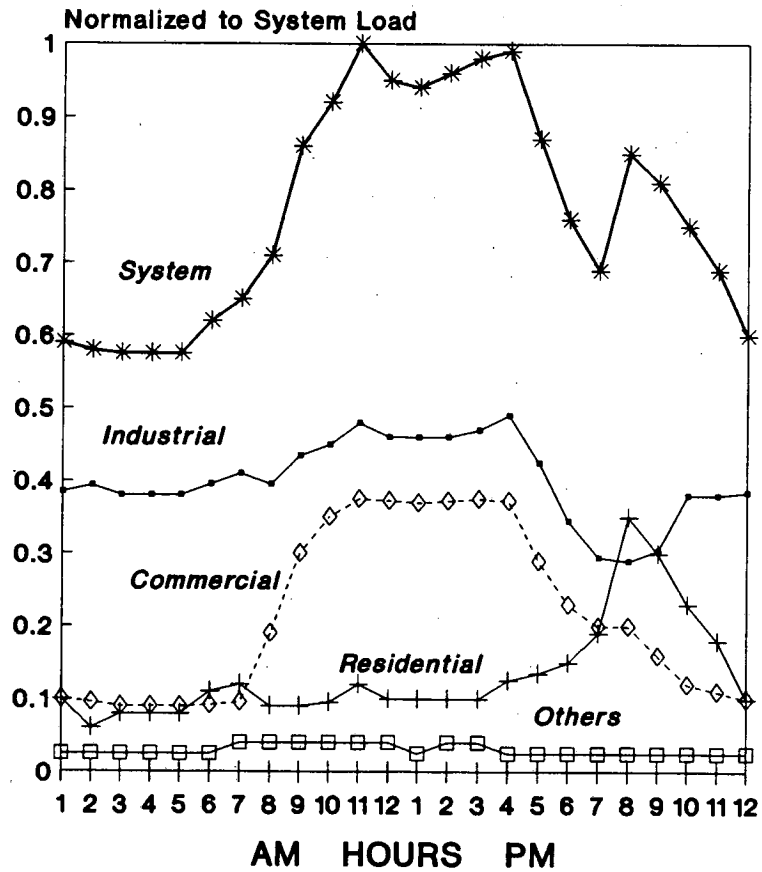

Figure 12-10a
Typical Weekday for Hotel

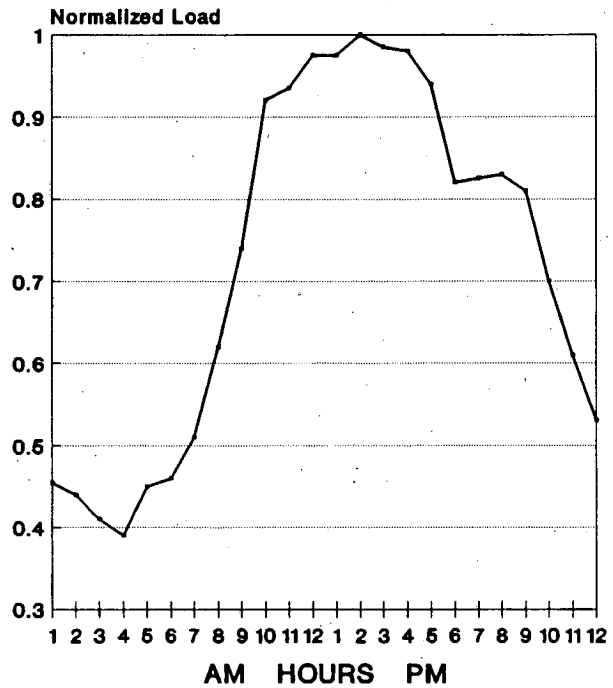

Figure 12-10b
Typical Saturday for Hotel

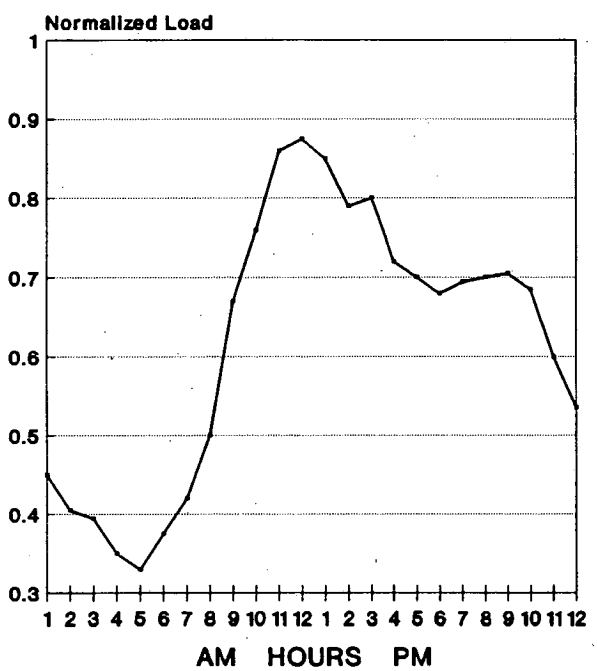

Figure 12-10c
Typical Sunday for Hotel

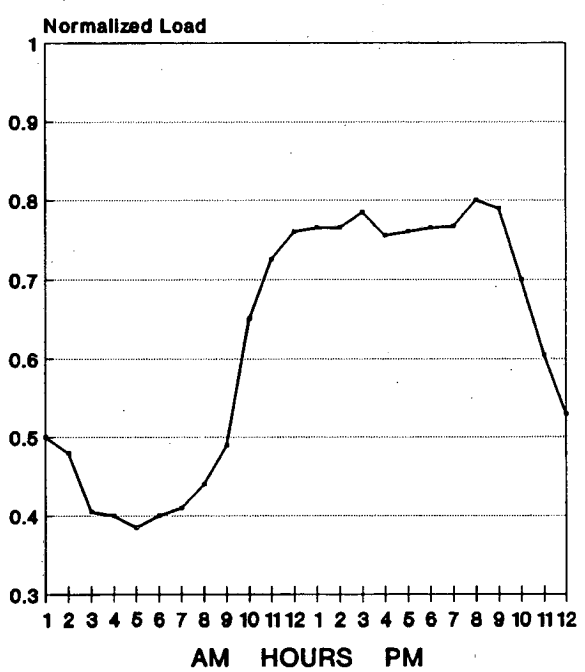

Figure 12-11a
Typical Weekday for Office

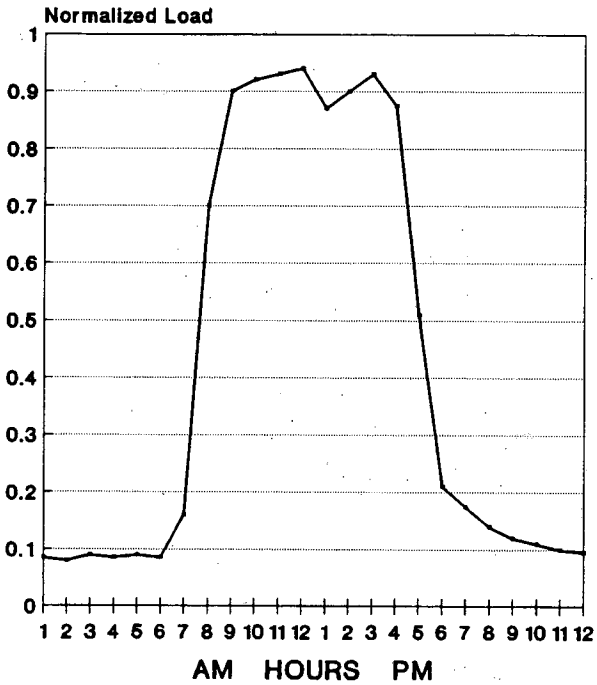

Figure 12-11b
Typical Saturday for Office

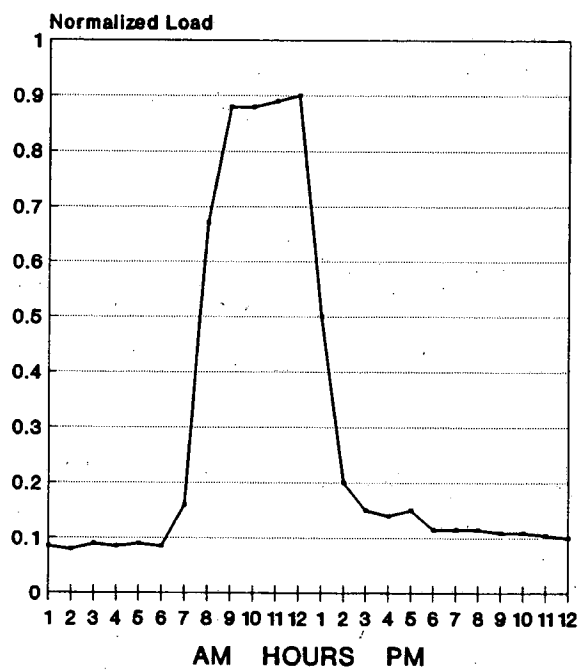

Figure 12-11c
Typical Sunday for Office

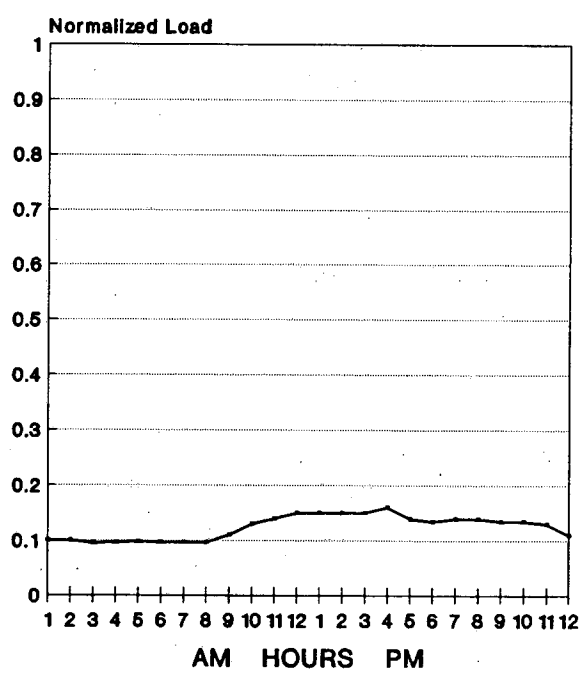

Figure 12-12
Typical Shopping Complex

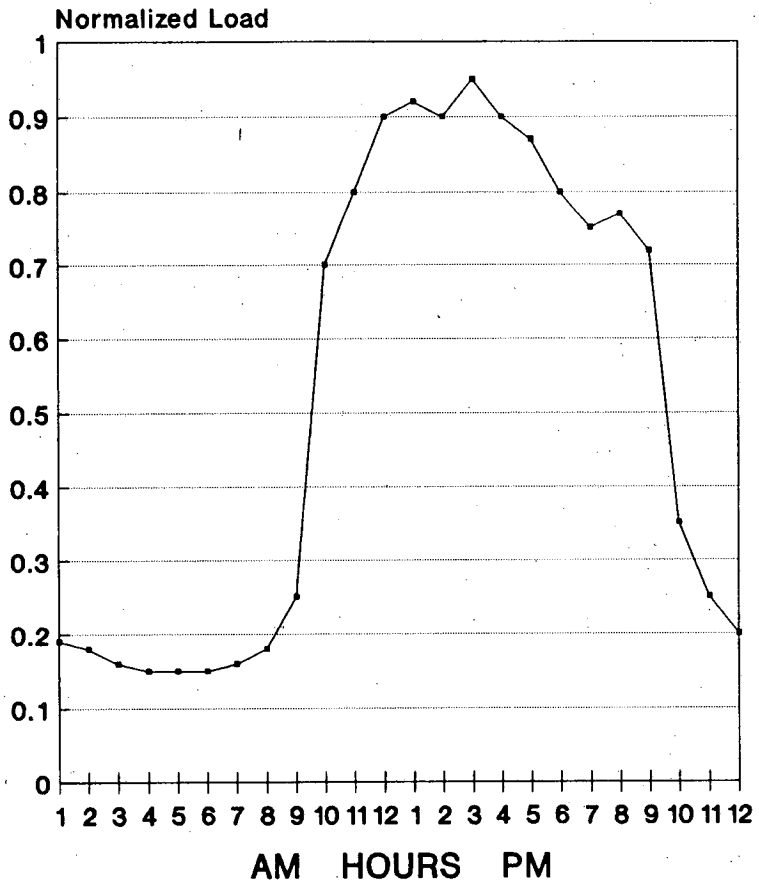

Figure 12-13
Commercial Consumers' Typical Load Shape

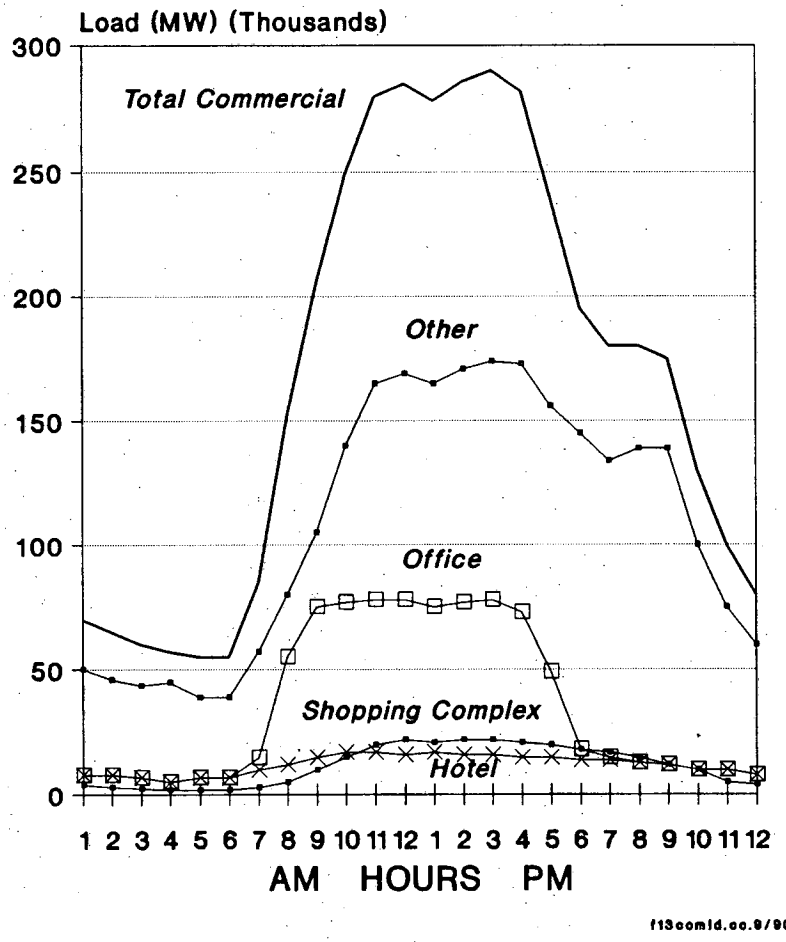

Typical Load Shapes Before and After TES

Figure 12-14a
Sunday

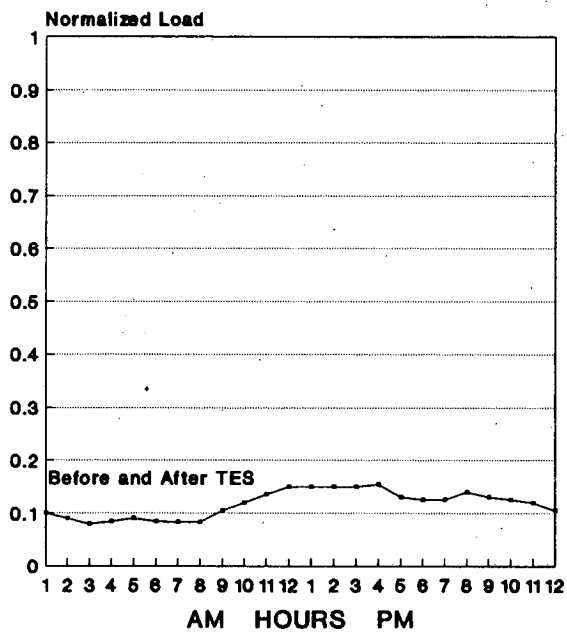

Figure 12-14b
Monday

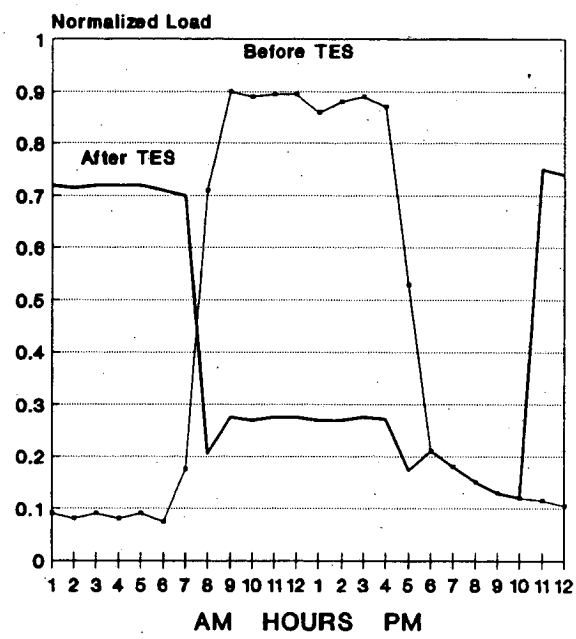

Figure 12-14c
Tuesday

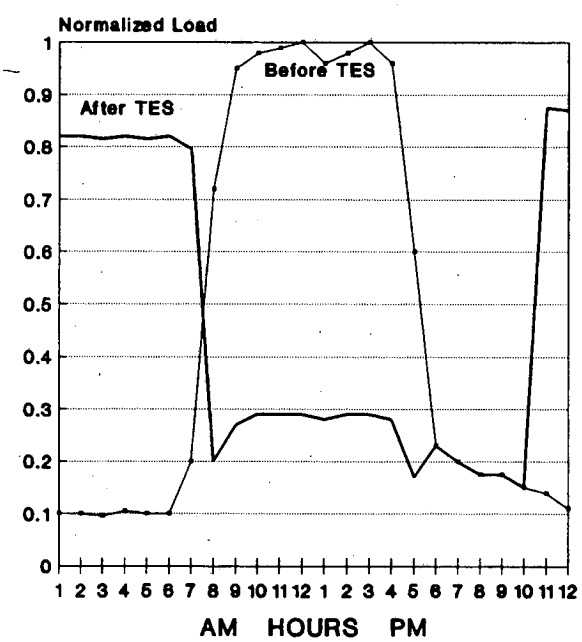

Figure 12-14d
Wednesday

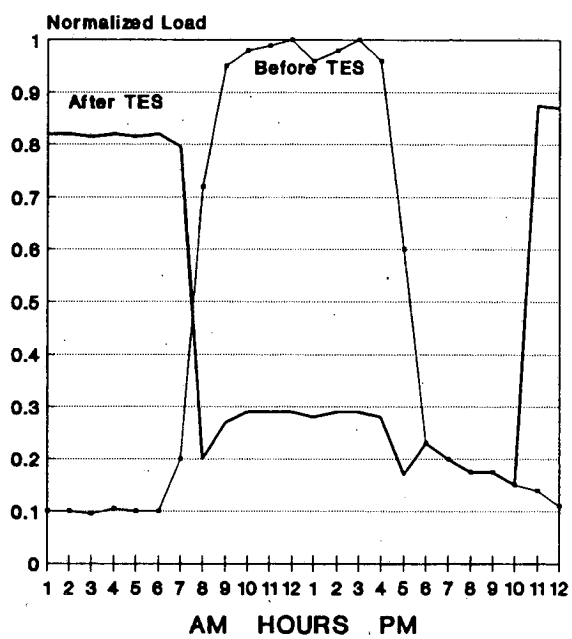

Typical Load Shapes Before and After TES

Figure 12-14e
Thursday

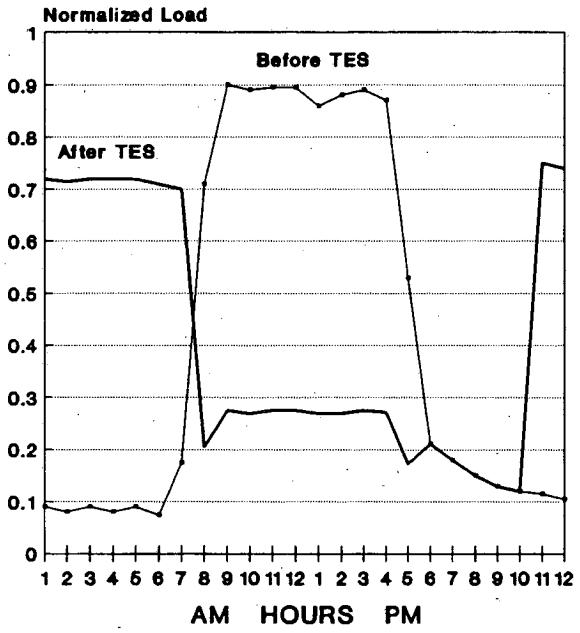

Figure 12-14f
Friday

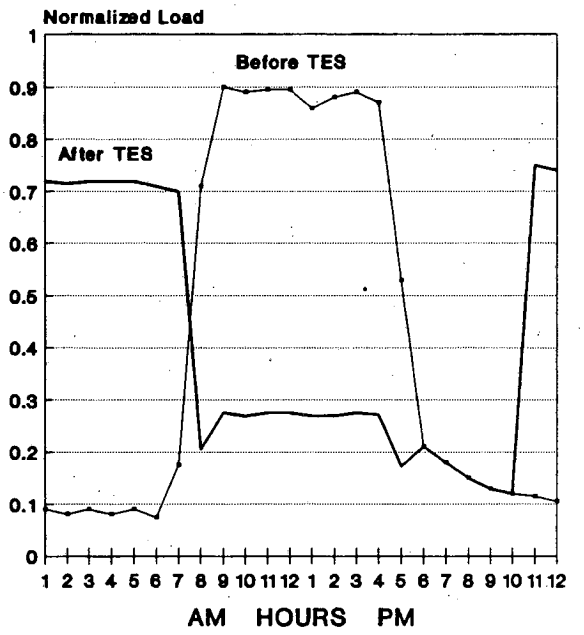

Figure 12-14g
Saturday

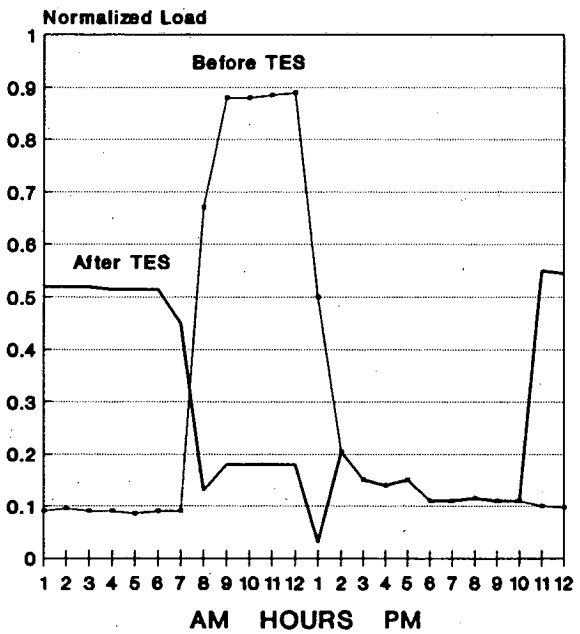

Figure 12-15

LSC Flow Diagram

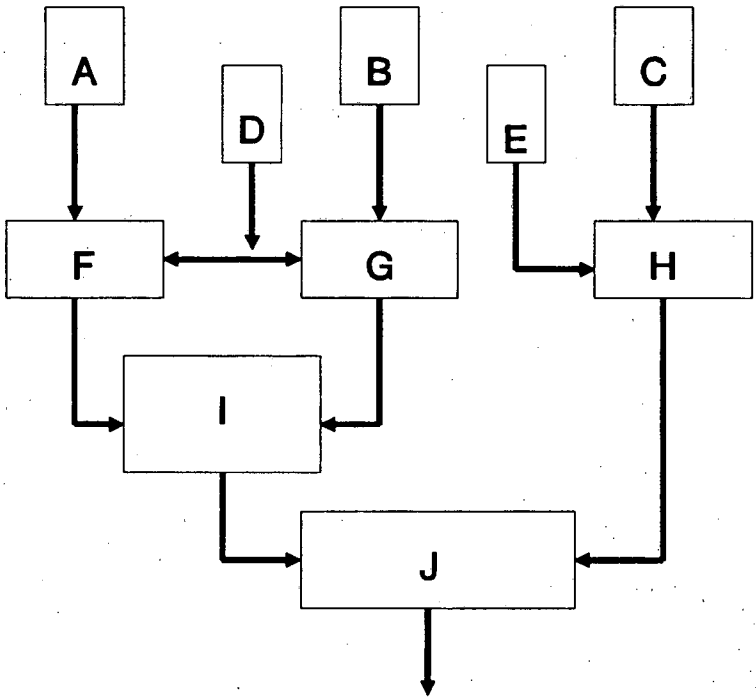

Final System Load Shape--Impact of TES

A Office Building Typical Week Without TES-Normalized Load

B Office Building Typical Week With TES-Normalized Load

C System Typical Week-Normalized Load

D Office Sector Monthly Energy

E System Monthly Energy

F Fitting a Month of Office Energy into the Load Shape

G Fitting a Month of Office Energy into the Load Shape

H Fitting a Month of System Energy into the Load Shape

I TES Load Shape Impact on Office Sector

J TES Load Shape Impact on Overall System Load Shape (C+I)

Figure 12-16
Peak Reduction
At Different TES Penetration Rates

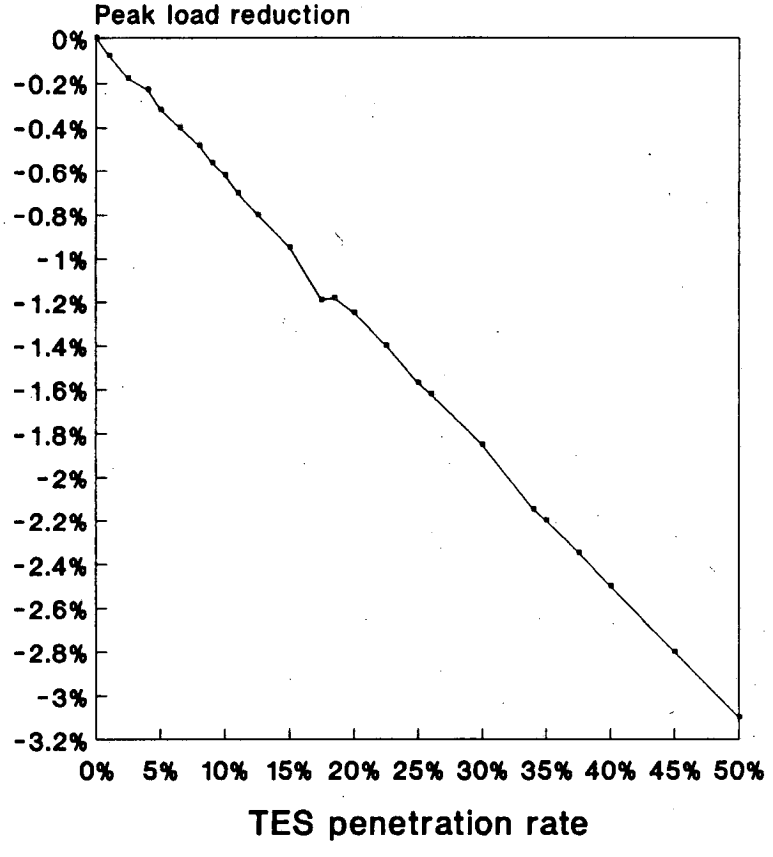

f16pkred.cc.9/90

Figure 12-17
Load Factor Improvement
At Different TES Penetration Rates

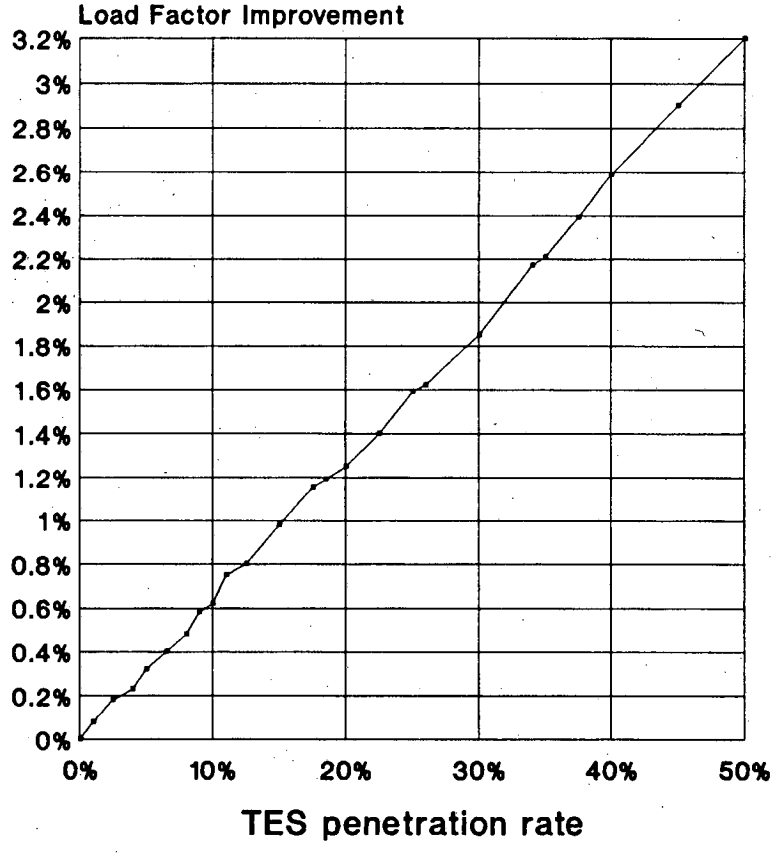

f17loadf.cc.9/90

Figure 12-18
Impact of DSEM

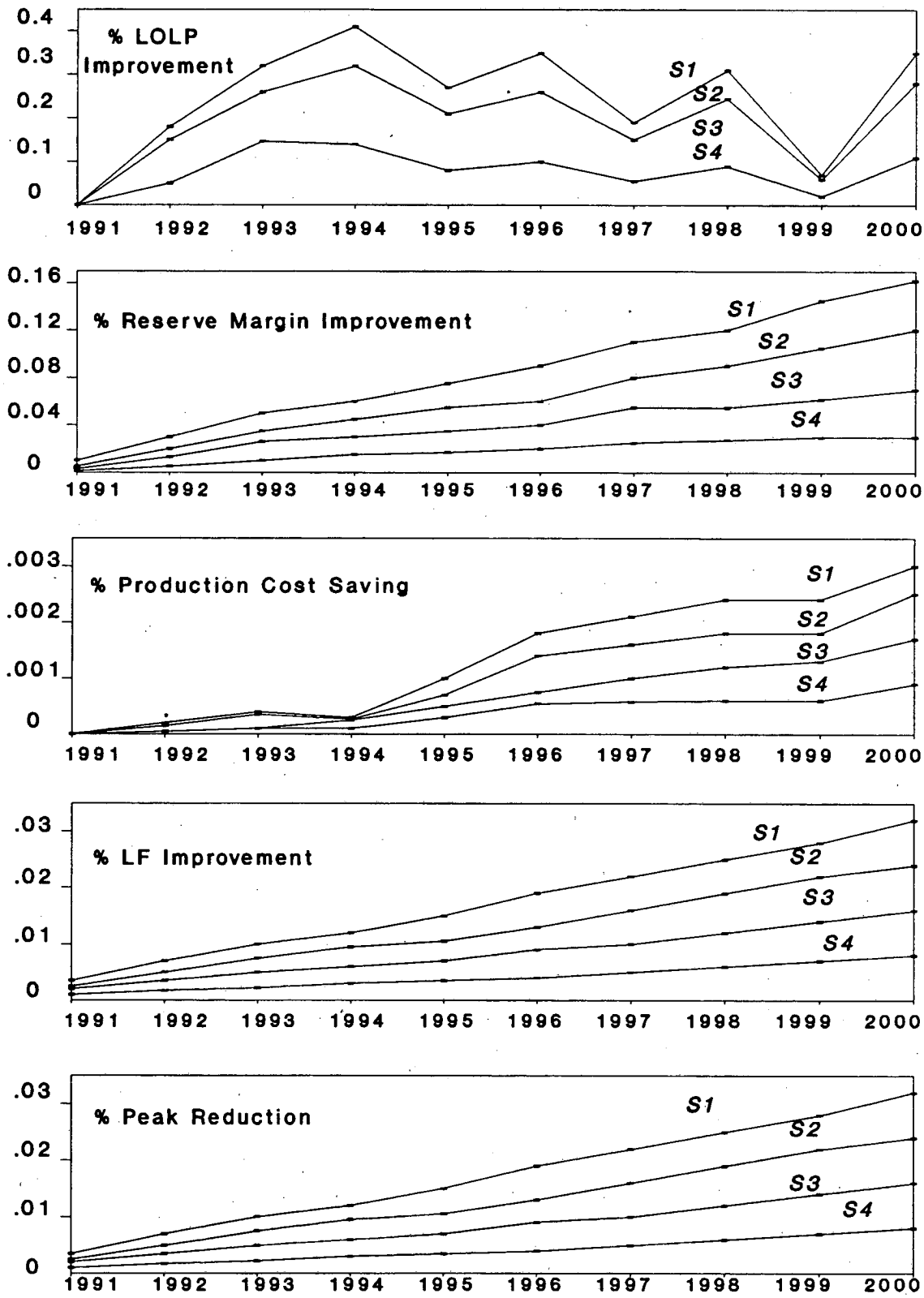

Table 12-1. LLN, SESCO, and SEB Electricity Demand In 1985

UTILITY	ENERGY DEMAND (GWh)	PEAK DEMAND (GWh)
LLN	12,200	2,120
SESCO	760	150
SEB	700	140

Table 12-2a. Base to Peak Ratio - September

WEEK	MON	TUE	WED	THU	FRI	SAT	SUN
1	0.642	0.493	0.537	0.559	0.658	0.542	-
2	0.536	0.555	0.548	0.563	0.569	0.555	0.710
3	0.516	0.538	0.518	0.581	0.564	0.586	0.682
4	0.536	0.572	0.567	0.567	0.572	0.587	0.681
5	0.498	0.543	-	-	-	-	0.704
AVERAGE	0.522	0.522	0.543	0.568	0.568	0.576	0.694

Table 12-2b. Time of Daily Peak - September

WEEK	MON	TUE	WED	THU	FRI	SAT	SUN
1	2000	1600	1600	1600	2000	2000	-
2	1100	1100	1100	1200	1100	1100	2000
3	1200	1100	1600	1100	1100	1200	2100
4	1600	1100	1100	1600	1100	1100	2000
5	1100	1500	-	-	-	-	2000

Table 12-2c. Daily Peak to Monthly Peak Ratio - September

WEEK	MON	TUE	WED	THU	FRI	SAT	SUN
1	0.747	0.854	0.977	0.962	0.963	0.870	-
2	0.937	0.953	0.965	0.940	0.922	0.955	0.720
3	0.957	0.963	1.000	0.984	0.962	0.942	0.733
4	0.786	0.976	0.968	0.973	0.984	0.911	0.786
5	0.970	0.949	-	-	-	-	0.724

Table 12-2d. Daily Load Factor - September

WEEK	MON	TUE	WED	THU	FRI	SAT	SUN
1	0.749	0.782	0.774	0.791	0.818	0.771	-
2	0.791	0.793	0.781	0.801	0.804	0.745	0.805
3	0.777	0.789	0.774	0.788	0.793	0.762	0.801
4	0.780	0.805	0.795	0.786	0.793	0.779	0.784
5	0.761B	0.793	-	-	-	-	-

Table 12-3. System Monthly Peak

MONTH	PEAK DEMAND (MW)	DAY IT OCCURS	TIME IT OCCURS
September '86	2272	Wednesday	1600 hrs
October '86	2271	Thursday	1100 hrs
November '86	2245	Wednesday	1100 hrs
December '86	2222	Tuesday	1200 hrs
January '87	2246	Wednesday	1100 hrs
February '87	2346	Wednesday	1100 hrs
March '87	2400	Thursday	1200 hrs
April '87	2396	Monday	1600 hrs
May '87	2370	Tuesday	1100 hrs
June '87	2457	Tuesday	1100 hrs
July '87	2412	Wednesday	1100 hrs
August '87	2397	Wednesday	1600 hrs

Table 12-4. Sectoral Peak Contribution and Load Factor

SECTOR	CONTRIBUTION FACTOR			LOAD FACTOR
	1100	1600	2000	
Industrial	0.47	0.49	0.32	0.82
Commercial	0.37	0.37	0.24	0.59
Residential	0.03	0.13	0.42	0.36
Others	0.03	0.02	0.02	0.80
System	1.00	1.00	1.00	0.75

Table 12-5. Monthly Average Energy Consumption (kWh) Per Consumer
(Large Power Commercial Consumer) [17]

TARIFF CLASS	SHOPPING	OFFICE	HOTEL	OTHERS
B	44,174	33,138	55,078	93,736
C1	252,544	389,179	11,424	991,194
C2	0	831,600	800,486	1,882,477

Table 12-6. Total Unit Consumed Per Month (MWh)
(Large Power Commercial Consumer) [14]

TARIFF CLASS	SHOPPING	OFFICE	HOTEL	OTHERS
B	14,754 (6.32%)	38,407 (16.50%)	12.007 (5.15%)	64,279 (27.50%)
C1	8,814 (3.78%)	33,080 (14.2%)	57 (0.02%)	34,854 (14.93%)
C2	0 (0%)	832 (0.36%)	13,608 (5.83%)	12,634 (5.41%)

Table 12-7. Number of Consumers By Consumer Type
(Large Power Commercial Consumer) [14]

TARIFF CLASS	SHOPPING	OFFICE	HOTEL	OTHERS
B	334 (8.09%)	1,159 (28.07%)	218 (5.28%)	2.194 (53.13%)
C1	25 (0.61%)	85 (2.06%)	5 (0.12%)	79 (1.91%)
C2	0 (0.00%)	1 (0.02%)	17 (0.41%)	12 (0.29%)

Table 12-8. Commercial Consumers' Peak Contribution and Load Factor

CONSUMER TYPE	PEAK CONTRIBUTION FACTOR 1100	1600	2000	LOAD FACTOR
S COMPLEX	7.08	7.40	9.86	0.545
OFFICE	27.67	26.40	7.38	0.458
HOTEL	6.02	6.05	8.28	0.727
OTHERS	59.23	60.16	74.47	0.622

Table 12-9. Office Sector Energy Forecast

YEAR	COMMERCIAL SECTOR	OFFICE SECTOR
1990	6319	885
1991	6973	976
1992	7603	1064
1993	8200	1148
1994	8796	1231
1995	9353	1309
1996	10097	1414
1997	10854	1519
1998	11793	1651
1999	12681	1775
2000	13441	1882

Table 12-10a. Load Shape Informations - Peak Demand (MW)

YEAR	BASE CASE	SCENARIO 1	SCENARIO 2	SCENARIO 3	SCENARIO 4
1990	2929	2929	2929	2929	2929
1991	3204	3293	3196	3198	3201
1992	3456	3433	3439	3445	3450
1993	3733	3698	3707	3715	3725
1994	4144	4092	4105	4118	4131
1995	4420	4351	4368	4385	4403
1996	4668	4133	4202	4357	4513
1997	5082	4972	5000	5063	5055
1998	5440	5304	5338	5372	5406
1999	5811	5647	5688	5729	5770
2000	6184	5993	6041	6089	6136

Table 12-10b. Load Shape Information - Load Factor

YEAR	BASE CASE	SCENARIO 1	SCENARIO 2	SCENARIO 3	SCENARIO 4
1990	0.6918	0.6918	0.6918	0.6918	0.6918
1991	0.6918	0.6941	0.6935	0.6930	0.6924
1992	0.6918	0.6964	0.6952	0.6941	0.6930
1993	0.6918	0.6986	0.6969	0.6952	0.6935
1994	0.6918	0.7006	0.6984	0.6962	0.6940
1995	0.6918	0.7028	0.7000	0.6973	0.6945
1996	0.6918	0.7052	0.7015	0.6983	0.6948
1997	0.6918	0.7072	0.7033	0.6994	0.6956
1998	0.6918	0.7096	0.7051	0.7006	0.6962
1999	0.6918	0.7119	0.7068	0.7017	0.6968
2000	0.6918	0.7139	0.7083	0.7027	0.6973

Table 12-11a. Peak Demand (MW)

YEAR	BASE CASE	SCENARIO 1	SCENARIO 2	SCENARIO 3	SCENARIO 4
1990	2929.0	2929.0	2929.0	2929.0	2929.0
1991	3203.6	3193.2	3195.8	3198.4	3201.0
1992	3455.6	3433.3	3438.9	3444.9	3449.9
1993	3733.9	3698.0	3707.0	3714.9	3724.9
1994	4144.1	4092.1	4105.2	4118.1	4131.1
1995	4419.7	4351.1	4368.3	4385.4	4402.5
1996	4667.9	4581.6	4603.1	4624.7	4646.3
1997	5082.4	4972.4	4999.7	5023.0	5054.8
1998	5440.2	5304.0	5338.1	5372.1	5406.2
1999	5810.9	5647.1	5688.3	5729.0	5770.0
2000	6184.3	5992.8	6040.7	6088.5	6136.4

Table 12-11b. Production Costs (M$)

YEAR	BASE CASE	SCENARIO 1	SCENARIO 2	SCENARIO 3	SCENARIO 4
1990	794.30	794.30	794.30	794.30	794.30
1991	902.31	902.38	902.32	902.33	902.31
1992	1005.15	1004.95	1005.02	1005.04	1005.10
1993	1088.12	1087.69	1087.82	1087.99	1087.98
1994	1227.68	1227.39	1227.46	1227.51	1227.60
1995	1342.56	1341.25	1341.55	1341.85	1342.21
1996	1412.26	1409.76	1410.36	1411.06	1411.56
1997	1629.93	1626.61	1627.43	1628.43	1629.01
1998	1759.16	1755.09	1756.14	1757.11	1758.12
1999	2054.81	2050.20	2051.28	2052.37	2053.58
2000	2338.95	2331.49	2333.28	2335.15	2336.95

Table 12-11c. Reserve Margin (%)

YEAR	BASE CASE	SCENARIO 1	SCENARIO 2	SCENARIO 3	SCENARIO 4
1990	63.00	63.00	63.00	63.00	63.00
1991	48.82	49.30	49.18	49.06	48.94
1992	27.76	28.59	28.38	28.18	27.97
1993	23.17	24.37	24.07	23.80	23.47
1994	24.19	25.77	25.37	24.98	24.58
1995	25.39	27.37	26.87	26.37	25.88
1996	26.30	28.70	28.00	27.50	26.85
1997	24.87	27.63	26.94	26.34	25.55
1998	26.55	29.80	28.97	28.15	27.35
1999	25.19	28.82	27.89	26.98	26.07
2000	24.38	28.36	27.34	26.34	25.35

Table 12-11d. Load Factor

YEAR	BASE CASE	SCENARIO 1	SCENARIO 2	SCENARIO 3	SCENARIO 4
1990	0.6918	0.6918	0.6918	0.6918	0.6918
1991	0.6918	0.6941	0.6935	0.6930	0.6924
1992	0.6918	0.6964	0.6952	0.6941	0.6930
1993	0.6918	0.6986	0.6969	0.6952	0.6935
1994	0.6918	0.7006	0.6984	0.6962	0.6940
1995	0.6918	0.7028	0.7000	0.6973	0.6945
1996	0.6918	0.7052	0.7015	0.6983	0.6948
1997	0.6918	0.7072	0.7033	0.6994	0.6956
1998	0.6918	0.7096	0.7051	0.7006	0.6962
1999	0.6918	0.7119	0.7068	0.7017	0.6968
2000	0.6918	0.7139	0.7083	0.7027	0.6973

Table 12-12a. Yearly Production (GWh)
(Year = 1991)

RESOURCE	BASE SCENARIO	SCENARIO 1	SCENARIO 2	SCENARIO 3	SCENARIO 4
COAL	4679	4679	4679	4679	4679
HYDRO	3517	3517	3517	3517	3517
OIL	4161	4163	4162	4162	4161
DIESEL	0	0	0	0	0
M OIL	0	0	0	0	0
GAS EAST	7059	7057	7058	7058	7058
TOTAL	19416	19416	19416	19416	19415

Table 12-12b. Yearly Production (GWh)
(Year = 1992)

RESOURCE	BASE SCENARIO	SCENARIO 1	SCENARIO 2	SCENARIO 3	SCENARIO 4
COAL	4191	4191	4191	4191	4191
HYDRO	3427	3427	3427	3427	3427
OIL	1772	1764	1766	1768	1770
DIESEL	0	0	0	0	0
M OIL	0	0	0	0	0
GAS EAST	6820	6820	6820	6820	6820
GAS WEST 1	4732	4740	4738	4736	4734
GAS WEST 2	0	0	0	0	0
TOTAL	20942	20942	20942	20942	20942

Table 12-12c. Yearly Production (GWh)
(Year = 1993)

RESOURCE	BASE SCENARIO	SCENARIO 1	SCENARIO 2	SCENARIO 3	SCENARIO 4
COAL	4190	4190	4190	4190	4190
HYDRO	3241	3241	3241	3241	3241
OIL	479	467	470	476	476
DIESEL	1	1	1	1	1
GAS EAST	6315	6315	6315	6315	6315
GAS WEST 1	6220	6240	6236	6228	6224
GAS WEST 2	2182	2174	2176	2178	2180
TOTAL	22628	22628	22629	22629	22627

Table 12-12d. Yearly Production (GWh)
(Year = 1994)

RESOURCE	BASE SCENARIO	SCENARIO 1	SCENARIO 2	SCENARIO 3	SCENARIO 4
COAL	4100	4100	4100	4100	4100
HYDRO	3448	3448	3448	3448	3448
OIL	508	514	513	511	510
DIESEL	0	0	0	0	0
GAS EAST	6823	6823	6823	6823	6823
GAS WEST 1	5994	6001	5999	5997	5991
GAS WEST 2	4242	4229	4233	4236	4240
TOTAL	25115	25115	25116	25115	25112

Table 12-12e. Yearly Production (GWh)
(Year = 1995)

RESOURCE	BASE SCENARIO	SCENARIO 1	SCENARIO 2	SCENARIO 3	SCENARIO 4
COAL	4191	4191	4191	4191	4191
HYDRO	3868	3868	3868	3868	3868
OIL	1093	1043	1055	1067	1081
DIESEL	4	3	3	3	4
GAS EAST	6421	6421	6421	6421	6421
GAS WEST 1	6977	7051	7034	7015	6995
GAS WEST 2	4211	4195	4199	4204	4208
TOTAL	26765	26772	26771	26769	26768

Table 12-12f. Yearly Production (GWh)
(Year = 1996)

RESOURCE	BASE SCENARIO	SCENARIO 1	SCENARIO 2	SCENARIO 3	SCENARIO 4
COAL	4191	4192	4192	4192	4191
HYDRO	3970	3970	3970	3970	3970
OIL	192	180	181	184	188
DIESEL	0	0	0	0	0
GAS EAST	6823	6824	6824	6824	6823
GAS WEST 1	4724	4589	4598	4624	4669
GAS WEST 2	8385	8534	8524	8495	8446
TOTAL	28285	28289	28289	28289	28287

Table 12-12g. Yearly Production (GWh)
(Year = 1997)

RESOURCE	BASE SCENARIO	SCENARIO 1	SCENARIO 2	SCENARIO 3	SCENARIO 4
COAL	4191	4191	4191	4191	4191
HYDRO	3725	3725	3725	3725	3725
OIL	422	403	405	421	415
GAS EAST	6421	6421	6421	642	6421
GAS WEST 1	4280	4217	4232	424	4266
GAS WEST 2	11725	11818	11798	11758	11749
TOTAL	30764	30775	30772	30765	30767

Table 12-12h. Yearly Production (GWh)
(Year = 1998)

RESOURCE	BASE SCENARIO	SCENARIO 1	SCENARIO 2	SCENARIO 3	SCENARIO 4
COAL	4191	4191	4191	4191	4191
HYDRO	3931	3931	3931	3931	3931
OIL	405	398	400	402	403
GAS EAST	6822	6822	6822	6822	6822
GAS WEST 1	3844	3725	3752	3780	3812
GAS WEST 2	13762	13894	13865	13832	13798
TOTAL	32955	32961	32961	32958	32957

Table 12-12i. Yearly Production (GWh)
(Year = 1999)

RESOURCE	BASE SCENARIO	SCENARIO 1	SCENARIO 2	SCENARIO 3	SCENARIO 4
COAL	4191	4191	4191	4191	4191
HYDRO	3893	3893	3893	3893	3893
OIL	468	471	469	467	467
GAS EAST	6421	6421	6421	6421	6421
GAS WEST 1	3265	3070	3114	3162	3214
GAS WEST 2	16850	17070	17021	16968	16910
TOTAL	35088	35116	35109	35102	35096

Table 12-12j. Yearly Production (GWh)
(Year = 2000)

RESOURCE	BASE SCENARIO	SCENARIO 1	SCENARIO 2	SCENARIO 3	SCENARIO 4
COAL	4191	4191	4191	4191	4191
HYDRO	3943	3943	3943	3943	3943
OIL	475	466	468	470	473
GAS EAST	6822	6822	6822	6822	6822
GAS WEST 1	3250	3058	3100	3147	3199
GAS WEST 2	18767	18984	18936	18883	18825
TOTAL	37448	37464	37460	37456	37453

Table 12-13. Production Cost Saving (M$)

YEAR	SCENARIO 1	SCENARIO 2	SCENARIO 3	SCENARIO 4
1991	$ -0.07	$ -0.01	$ -0.02	$ 0.00
1992	$ 0.20	$ 0.13	$ 0.11	$ 0.05
1993	$ 0.43	$ 0.30	$ 0.13	$ 0.14
1994	$ 0.29	$ 0.22	$ 0.17	$ 0.08
1995	$ 1.31	$ 1.01	$ 0.71	$ 0.35
1996	$ 2.50	$ 1.90	$ 1.20	$ 0.70
1997	$ 3.32	$ 2.50	$ 1.50	$ 0.92
1998	$ 4.07	$ 3.02	$ 2.05	$ 1.04
1999	$ 4.61	$ 3.53	$ 2.44	$ 1.23
2000	$ 7.46	$ 5.67	$ 3.80	$ 2.00

Table 12-14. Cost to Supply a kW of Load a Year

Generation Cost	193.92	$/kW/yr
Transmission Cost	146.30	$/kW/yr
Distribution Cost	229.40	$/kW/yr
TOTAL	569.62	$/kW/yr

Table 12-15. Capacity Savings (M$)

Year	PEAK REDUCTION (MW) S1	S2	S3	S4	CAPACITY SAVINGS (M$) S1	S2	S3	S4
1991	10.400	7.800	5.200	2.600	5.924	4.443	2.962	1.481
1992	22.300	16.700	10.700	5.700	12.703	9.513	6.095	3.247
1993	35.900	26.900	19.000	9.000	20.449	15.323	10.823	5.127
1994	52.000	38.900	26.000	13.000	29.620	22.158	14.810	7.405
1995	68.600	51.400	34.300	17.200	39.076	29.278	19.538	9.797
1996	86.300	64.800	43.200	21.600	49.158	36.911	24.608	12.304
1997	110.000	82.700	59.400	27.600	62.658	47.108	33.835	15.722
1998	136.200	102.100	68.100	34.000	77.582	58.158	38.791	19.367
1999	163.800	122.600	81.900	40.900	93.304	69.835	46.652	23.297
2000	191.500	143.600	95.800	47.900	109.082	81.797	54.570	27.285

Table 12-16. Benefit-Cost Analysis - An Economic View

Year	MARGINAL COST (ΔC) IN 1990 M$ S1	S2	S3	S4	MARGINAL SAVING (ΔS) IN 1990 M$ S1	S2	S3	S4
1991	7.038	5.278	3.519	1.759	5.854	4.433	2.942	1.481
1992	8.450	6.337	4.225	2.112	12.903	9.643	6.205	3.297
1993	9.578	7.183	4.789	2.394	20.879	15.623	10.953	5.267
1994	10.626	7.969	5.313	2.656	29.910	22.378	14.980	7.485
1995	11.979	8.984	5.990	2.995	40.386	30.288	10.147	10.147
1996	14.075	10.556	7.038	3.519	51.658	38.661	25.908	12.904
1997	15.640	11.730	7.820	3.910	65.978	49.738	35.535	16.552
1998	18.740	14.055	9.370	4.685	81.652	61.178	40.841	20.407
1999	20.138	15.103	10.069	5.034	97.914	73.365	49.092	24.527
2000	20.795	15.529	10.353	5.176	116.542	87.467	58.370	29.285

Table 12-17. Utility Revenue Losses (M$)

YEAR	S1	S2	S3	S4
1991	4.446	3.335	2.223	1.111
1992	9.696	7.272	4.848	2.424
1993	15.693	11.770	7.847	3.924
1994	22.344	16.758	11.172	5.586
1995	29.844	22.383	14.922	7.461
1996	38.656	28.992	19.328	9.664
1997	48.448	36.336	24.224	12.112
1998	60.180	45.135	30.090	15.045
1999	72.788	54.591	36.394	18.197
2000	85.751	64.313	42.875	21.438

Table 12-18a. Benefit - Cost Analysis - Utility Perspective
(Scenario 1)

YEAR	REVENUE LOSS (M$)	INCEN-TIVE (M$)	TOTAL COST (M$)	PROD COST SAVINGS (M$)	CAP COST SAVINGS (M$)	TOTAL BENEFITS (M$)	NET BENEFITS (M$)
1991	4.446	0.000	4.446	-0.070	5.924	5.854	1.408
1992	9.696	0.000	9.696	0.200	12.703	12.903	3.207
1993	15.693	0.000	15.693	0.430	20.449	20.879	5.187
1994	22.344	0.000	22.344	0.290	29.620	29.910	7.566
1995	29.844	0.000	29.844	1.310	39.076	40.386	10.542
1996	38.656	0.000	38.656	2.500	49.158	51.658	13.002
1997	48.448	0.000	48.448	3.320	62.658	65.978	17.530
1998	60.180	0.000	60.180	4.070	77.582	81.652	21.472
1999	72.788	0.000	72.788	4.610	93.304	97.914	25.126
2000	85.751	0.000	85.751	7.460	109.082	116.542	30.792
Net Present Value (10%)			196.324			264.743	68.41914
Benefit / Cost =			1.348501				

Table 12-18b. Benefit-cost Analysis - Utility Perspective
(Scenario 2)

YEAR	REVENUE LOSS (M$)	INCEN-TIVE (M$)	TOTAL COST (M$)	PROD COST SAVINGS (M$)	CAP COST SAVINGS (M$)	TOTAL BENEFITS (M$)	NET BENEFITS (M$)
1991	3.335	0.000	3.335	-0.010	4.443	4.433	1.098
1992	7.272	0.000	7.272	0.130	9.513	9.643	2.371
1993	11.770	0.000	11.770	0.300	15.323	15.623	3.853
1994	16.758	0.000	16.758	0.220	22.158	22.378	5.620
1995	22.383	0.000	22.383	1.010	29.278	30.288	7.905
1996	28.992	0.000	28.992	1.900	36.911	38.811	9.819
1997	36.336	0.000	36.336	2.500	47.108	49.608	13.272
1998	45.135	0.000	45.135	3.020	58.158	61.178	16.043
1999	54.591	0.000	54.591	3.530	69.835	73.365	18.775
2000	64.313	0.000	64.313	5.670	81.797	87.467	23.155
Net Present Value (10%)			147.243			198.569	51.32620
Benefit / Cost =			1.348581				

Table 12-18c. Benefit-cost Analysis - Utility Perspective
(Scenario 3)

YEAR (M$)	REVENUE LOSS (M$)	INCEN-TIVE (M$)	TOTAL COST (M$)	PROD COST SAVINGS (M$)	CAP COST SAVINGS (M$)	TOTAL BENEFITS (M$)	NET BENEFITS
1991	2.223	0.000	2.223	-0.020	2.962	2.942	0.719
1992	4.848	0.000	4.848	0.110	6.095	6.205	1.357
1993	7.847	0.000	7.847	0.130	10.823	10.953	3.106
1994	11.172	0.000	11.172	0.170	14.810	14.980	3.808
1995	14.922	0.000	14.922	0.710	19.538	20.248	5.326
1996	19.328	0.000	19.328	1.200	24.608	25.808	6.479
1997	24.224	0.000	24.224	1.500	33.835	35.335	11.112
1998	30.090	0.000	30.090	2.050	38.791	40.841	10.751
1999	36.394	0.000	36.394	2.440	46.652	49.092	12.698
2000	42.875	0.000	42.875	3.800	54.570	58.370	15.494
Net Present Value (10%)			98.162			133.912	35.75026
Benefit / Cost =			1.364196				

Table 12-18d. Benefit-Cost Analysis - Utility Perspective
(Scenario 4)

YEAR	REVENUE LOSS (M$)	INCEN-TIVE (M$)	TOTAL COST (M$)	PROD COST SAVINGS (M$)	CAP COST SAVINGS (M$)	TOTAL BENEFITS (M$)	NET BENEFITS (M$)
1991	1.111	0.000	1.111	0.000	1.481	1.481	0.370
1992	2.424	0.000	2.424	0.050	3.247	3.297	0.873
1993	3.924	0.000	3.924	0.140	5.127	5.267	1.343
1994	5.586	0.000	5.586	0.080	7.405	7.485	1.899
1995	7.461	0.000	7.461	0.350	9.797	10.147	2.686
1996	9.664	0.000	9.664	0.700	12.304	13.004	3.340
1997	12.112	0.000	12.112	0.920	15.722	16.642	4.530
1998	15.045	0.000	15.045	040	19.367	20.407	5.362
1999	18.197	0.000	18.197	0	23.297	24.527	6.331
2000	1.438	0.000	21.438	000	27.285	29.285	7.847
Net Present Value (10%)			49.081			66.534	17.45265
Benefit / Cost =			1.355588				

Table 12-19. Benefit-Cost Analysis - Consumer Perspective
(M$ 1000)

YEAR	CAPITAL COST	INCEN-TIVE	OPERATIONAL SAVINGS	TOTAL	NET BENEFIT
1991	491.25	0.00	216.00	216.00	(275.25)
1992			216.00	216.00	216.00
1993			216.00	216.00	216.00
1994			216.00	216.00	216.00
1995			216.00	216.00	216.00
1996			216.00	216.00	216.00
1997			216.00	216.00	216.00
1998			216.00	216.00	216.00
1999			216.00	216.00	216.00
2000			216.00	216.00	216.00
Net Present Value (10%) 446.59				1327.23	880.64
Benefit / Cost = 2.97					

Table 12-20. Typical Large Office Building Peak Load During the On-Peak Period

Day	No TES	With TES	% Reduction
Monday	1,017 kW	307 kW	69.81%
Tuesday	1,137 kW	330 kW	70.98%
Wednesday	1,137 kW	330 kW	70.98%
Thursday	1,017 kW	307 kW	69.81%
Friday	1,017 kW	307 kW	69.81%
Saturday	1,010 kW	193 kW	80.89%
Sunday	166 kW	166 kW	0.00%

Table 12-21. Typical Large Office Building Load Factor

Day	No TES	With TES	% Reduction
Monday	0.459	0.538	7.2%
Tuesday	0.458	0.525	14.6%
Wednesday	0.458	0.525	14.6%
Thursday	0.459	0.538	17.2%
Friday	0.459	0.538	17.2%
Saturday	0.313	0.504	61.0%
Sunday	0.745	0.745	0.0%

Table 12-22. System Peak Demand (MW)

YEAR	SCENARIO 1		SCENARIO 2		SCENARIO 3		SCENARIO 4		BASE CASE
1991	3193.2	0.32%	3195.8	0.24%	3198.4	0.16%	3201.0	0.08%	3203.6
1992	3433.3	0.64%	3438.9	0.48%	3444.9	0.30%	3449.9	0.16%	3455.6
1993	3698.0	0.96%	3707.0	0.72%	3714.9	0.50%	3724.9	0.24%	3733.9
1994	4092.1	1.25%	4105.2	0.93%	4118.1	0.62%	4131.1	0.31%	4144.1
1995	4351.1	1.55%	4368.3	1.16%	4385.4	0.77%	4402.5	0.38%	4419.7
1996	4581.6	1.84%	4603.1	1.38%	4624.7	0.92%	4646.3	0.46%	4667.9
1997	4972.4	2.16%	4999.7	1.62%	5023.0	1.16%	5054.8	0.54%	5082.4
1998	5304.0	2.50%	5338.1	1.87%	5372.1	1.25%	5406.2	0.62%	5440.2
1999	5647.1	2.81%	5688.3	2.10%	5729.0	1.40%	5770.0	0.70%	5810.9
2000	5992.8	3.09%	6040.7	2.32%	6088.5	1.54%	6136.4	0.77%	6184.3

Table 12-23. System Load Factor

YEAR	SCENARIO 1	SCENARIO 2	SCENARIO 3	SCENARIO 4	BASE CASE
1991	0.6941	0.6935	0.6930	0.6924	0.6918
1992	0.6964	0.6952	0.6941	0.6930	0.6918
1993	0.6986	0.6969	0.6952	0.6935	0.6918
1994	0.7006	0.6984	0.6962	0.6940	0.6918
1995	0.7028	0.7000	0.6973	0.6945	0.6918
1996	0.7052	0.7015	0.6983	0.6948	0.6918
1997	0.7072	0.7033	0.6994	0.6956	0.6918
1998	0.7096	0.7051	0.7006	0.6962	0.6918
1999	0.7119	0.7068	0.7017	0.6968	0.6918
2000	0.7139	0.7083	0.7027	0.6973	0.6918

Table 12-24. Energy Production Cost (M$) *

YEAR	SCENARIO 1	SCENARIO 2	SCENARIO 3	SCENARIO 4	BASE CASE
1991	902.38 (-0.01)	902.32 (-0.00)	902.33 (-0.00)	902.31 (0.00)	902.31
1992	1004.95 (0.02)	1005.02 (0.01)	1005.04 (0.01)	1005.10 (0.01)	1005.15
1993	1087.69 (0.04)	1087.82 (0.03)	1087.99 (0.01)	1087.98 (0.01)	1088.12
1994	1227.39 (0.02)	1227.46 (0.02)	1227.51 (0.01)	1227.60 (0.01)	1227.68
1995	1341.25 (0.10)	1341.55 (0.10)	1341.85 (0.10)	1342.21 (0.03)	1342.56
1996	1409.76 (0.18)	1410.36 (0.13)	1411.06 (0.09)	1411.56 (0.05)	1412.26
1997	1626.61 (0.20)	1627.43 (0.15)	1628.43 (0.10)	1629.01 (0.10)	1629.93
1998	1755.09 (0.20)	1756.14 (0.20)	1757.11 (0.12)	1758.12 (0.10)	1759.16
1999	2050.20 (0.22)	2051.28 (0.20)	2052.37 (0.12)	2053.58 (0.06)	2054.81
2000	2331.49 (0.32)	2333.28 (0.24)	2335.15 (0.20)	2336.95 (0.10)	2338.95

* All numbers in parenthesis represent respective percentage of production cost reduction.

Table 12-25a. Energy Production (GWh) - 1992

RESOURCE	SCENARIO 1	SCENARIO 2	SCENARIO 3	SCENARIO 4	BASE CASE
COAL	4191	4191	4191ct4	4191	4191
HYDRO	3427	3427	3427	3427	3427
OIL	1764	1766	1768	1770	1772
DIESEL	0	0	0	0	0
M OIL	0	0	0	0	0
GAS EAST	6820	6820	6820	6820	6820
GAS WEST 1	4740	4738	4736	4734	4732
	20942	20942	20942	20942	20942

Table 12-25b. Energy Production (GWh) - 1995

RESOURCE	SCENARIO 1	SCENARIO 2	SCENARIO 3	SCENARIO 4	BASE CASE
COAL	4191	4191	4191	4191	4191
HYDRO	3868	3868	3868	3868	3868
OIL	043	055	067	081	093
DIESEL	3	3	3	3	4
M OIL	0	0	0	0	0
GAS EAST	6421	6421	6421	6421	6421
GAS WEST 1	7051	7034	7015	6995	6977
GAS WEST 2	4195	4199	4204	4208	4211
	26772	26771	26769	26767	26765

Table 12-25c. Energy Production (GWh) - 1999

RESOURCE	SCENARIO 1	SCENARIO 2	SCENARIO 3	SCENARIO 4	BASE CASE
COAL	4191	4191	4191	4191	4191
HYDRO	3893	3893	3893	3893	3893
OIL	471	469	467	467	468
GAS EAST	6421	6421	6421	6421	6421
GAS WEST 1	3070	3114	3162	3214	3265
GAS WEST 2	17070	17021	16968	16910	16850
	35116	35109	35102	35096	35088

LAWRENCE BERKELEY LABORATORY
UNIVERSITY OF CALIFORNIA
TECHNICAL INFORMATION DEPARTMENT
BERKELEY, CALIFORNIA 94720